



**This electronic thesis or dissertation has been  
downloaded from Explore Bristol Research,  
<http://research-information.bristol.ac.uk>**

*Author:*

**Kivimaki, Anna-Liisa**

*Title:*

**Presence and activity of microbial populations in glaciers and their impact on rock  
weathering at glacial beds**

**General rights**

Access to the thesis is subject to the Creative Commons Attribution - NonCommercial-No Derivatives 4.0 International Public License. A copy of this may be found at <https://creativecommons.org/licenses/by-nc-nd/4.0/legalcode>. This license sets out your rights and the restrictions that apply to your access to the thesis so it is important you read this before proceeding.

**Take down policy**

Some pages of this thesis may have been removed for copyright restrictions prior to having it been deposited in Explore Bristol Research. However, if you have discovered material within the thesis that you consider to be unlawful e.g. breaches of copyright (either yours or that of a third party) or any other law, including but not limited to those relating to patent, trademark, confidentiality, data protection, obscenity, defamation, libel, then please contact [collections-metadata@bristol.ac.uk](mailto:collections-metadata@bristol.ac.uk) and include the following information in your message:

- Your contact details
- Bibliographic details for the item, including a URL
- An outline nature of the complaint

Your claim will be investigated and, where appropriate, the item in question will be removed from public view as soon as possible.





# **Presence and activity of microbial populations in glaciers and their impact on rock weathering at glacial beds**

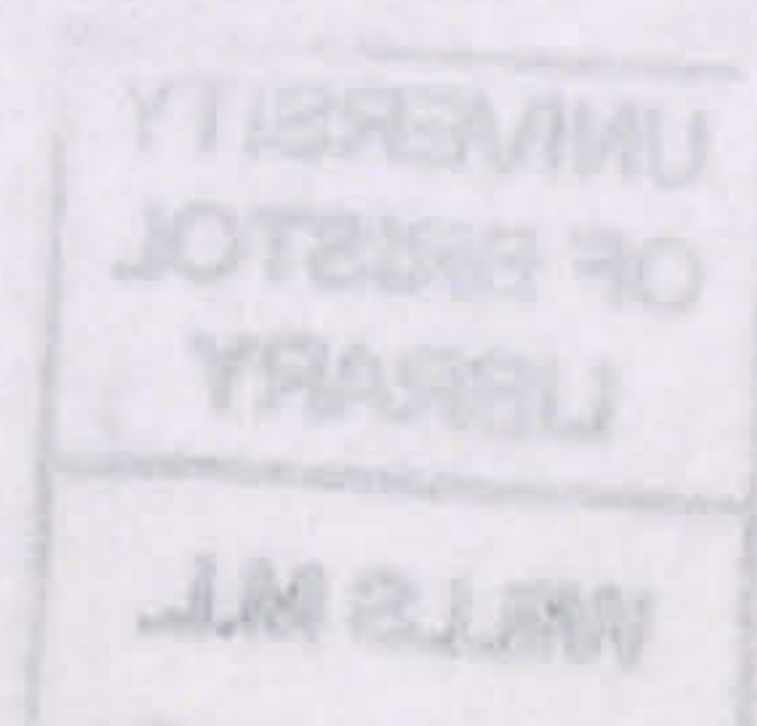
**Anna-Liisa Kivimäki**

A dissertation submitted to the University of Bristol in accordance with the  
requirements of the degree of Doctor of Philosophy (Ph.D.)  
in the Faculty of Science

Department of Earth Sciences

January 2005

46951 words





## ABSTRACT

In this research the presence and activity of bacterial populations in glacial drainage systems, especially in subglacial meltwaters, were studied. The three field sites represented glaciers with different characteristics: a warm-based ice cap in a maritime climate in Norway, a subarctic polythermal-based inland ice sheet in Greenland, and a polythermal-based valley glacier in a High Arctic climate in Svalbard. Lithologies ranged from Precambrian metamorphic gneisses and quartzites to Carboniferous and Permian sedimentary rocks. Low temperature weathering experiments in closed-system conditions lasting up to 10 months were conducted to determine *in situ* activity of subglacial micro-organisms, their energy and nutrient sources and their impact on the rate of chemical weathering.

The total number of bacteria in meltwaters ranged from 3.40 – 4.63 log<sub>10</sub> cells ml<sup>-1</sup> (from 2.51×10<sup>3</sup> to 4.27×10<sup>4</sup> cells ml<sup>-1</sup>). The different size and thermal regime of the glaciers did not have an effect on numbers of bacterial cells. Significantly higher numbers of bacteria in subglacial meltwaters were discovered at the very early phase of melt season, when melting was minimal and no dilution with snow and ice melt scarce in bacteria was occurring.

Obligate anaerobic bacteria, such as sulphate-reducing bacteria, were present in the meltwaters throughout the melt season from April to August. Sulphate-reducing bacteria were adapted to activity at constantly low temperatures from 0 to +4 °C, but their optimum temperature varied from +10 to +32 °C. After 25 weeks of incubation, activity was detected also at the subzero temperature of –0.6 °C.

Bacteria which originated from the subglacial drainage systems were active at the temperature range from +0.2 °C to +2.6 °C, when incubated with proglacial rock flour without any additional substrates. As a source of energy and nutrients, they used organic acids released from the rock flours, and oxidation of reduced inorganic constituents released from e.g. sulphide minerals. Oxygen or nitrate were utilised as electron acceptors. Microbial activity accelerated the release of alkali elements (K<sup>+</sup>, Na<sup>+</sup>) and earth alkaline elements (Mg<sup>2+</sup>, Ca<sup>2+</sup>), as well as sulphate (SO<sub>4</sub><sup>2-</sup>) from rock flours. Biologically mediated carbonate and silicate dissolution initiated after one month, whereas more than five months incubation was needed until oxidation of sulphides was occurring. The results of the weathering experiments demonstrated that both chemoorganotrophic and chemolithotrophic bacteria are able to grow in subglacial conditions, and their activity in the subglacial cavities during winter months can speed up chemical weathering. As a consequence, microbial activity has a marked impact on major ion concentrations in meltwaters in the early melt season, when discharge is low and dilution of subglacial meltwaters with snow and ice melt is minimal.







## **ACKNOWLEDGEMENTS**

This research was funded by a University of Bristol studentship to Anna-Liisa Kivimäki and supported by the following grants:  
Natural Environment Research Council (NERC) grant GCT/02/2204 to M. Tranter, J.L. Wadham, S.H. Bottrell, R. Hodgkins and R. Raiswell;  
NERC grant GR3/11689 to M. Tranter, S.H. Bottrell, R. Raiswell, P.W. Nienow and P.J. Statham;  
NERC grant GST/05/2192 (ARCICE thematic Programme) to T. Murray, M.J. Hambrey, A. Luckman and J.L. Wadham;  
The Leverhume Trust grant (F/00182/C) to H.M. Mader, J.L. Wadham, E. Wolff and J. Parkes.

Funding was also provided by the Finnish Environment Institute (SYKE), Kone Foundation (Koneen Säätiö) and the Finnish Cultural Foundation (Suomen Kulttuurirahasto).

The research was supervised by Professor John Parkes and Professor Martyn Tranter.

I wish to express special thanks to John Parkes and Martyn Tranter for giving me the opportunity to work on this project and for the guidance and encouragement that they have provided.

Jemma Wadham and Mark Skidmore gave me valuable help at several phases of the project. Their experience in glaciological research along with their supportive attitude was important to me.

I wish to thank everybody who worked in the Geomicrobiology Group at the University of Bristol. Not only did they help me with my work in the laboratory, but I also gained many good friends. Special thanks belong to Jenny Mills, who patiently gave me instruction and invaluable help with analytical equipment. Derek Martin kindly provided technical and logistical support, which I greatly appreciated. Peter Wellsbury as my mentor provided invaluable assistance through his good and critical comments regarding both technical and editorial issues.

A number of people including Linda Davies, Sari Lauri, Ian Mather, Violeta Palma Perez, Michala Pettitt, Francesco Senia, Karen Sheward, Luis Miguel Villaescusa Prada and Robert Watts made my time in Bristol more than an academic experience. They have left me with many joyful memories of our great times together.

I am grateful for the encouragement and support given by my colleagues at the Finnish Environment Institute in all stages of this project. I thank Sirkka Vuoristo for her kind assistance in graphic design of the thesis. I also highly appreciate the valuable help with statistical analyses given by Hannu Rita from the University of Helsinki.

Finally, I thank my family and friends in Finland. Throughout the three years in Bristol they gave support, for which I will always be grateful.







## DECLARATION

I declare that the work in this dissertation was carried out in accordance with the Regulations of the University of Bristol. I hereby declare that except where otherwise acknowledged this thesis is my own individual and original work. Furthermore, it has not been submitted for a degree at any other University for examination in the United Kingdom or overseas. The views expressed are those of the author and not of the University.



Anna-Liisa Kivimäki

January 2005







# CONTENTS

<b>ABSTRACT</b>	<b>i</b>
<b>ACKNOWLEDGEMENTS</b>	<b>iii</b>
<b>DECLARATION</b>	<b>v</b>
<b>CONTENTS</b>	<b>vii</b>
<b>LIST OF FIGURES</b>	<b>xiv</b>
<b>LIST OF TABLES</b>	<b>xxviii</b>
<b>CHAPTER I INTRODUCTION TO THE RESEARCH AREA</b>	<b>1</b>
1.1. Background and context for research	1
1.2. Research objectives	2
<b>CHAPTER II INTRODUCTION</b>	<b>4</b>
2.1. Glacial environment	4
2.1.1. Glaciated areas	4
2.1.2. Morphology of glaciers and glacier thermal regimes	5
2.1.3. Glacier hydrology	6
2.1.4. Development of drainage systems	8
2.2. Weathering in glacierized catchments	11
2.2.1. Glacial erosion	11
2.2.2. Biologically mediated weathering	12
2.2.3. Subglacial chemical weathering	13
2.3. Micro-organisms in cold environments	17
2.3.1. Presence and activity of micro-organisms in cold habitats	17
2.3.1.1. Deep sea water and sediments	18
2.3.1.2. Sea ice	19
2.3.1.3. Permafrost soils	19

2.3.1.4. Glaciers	20
2.3.2. Psychrophilic and psychrotrophic micro-organisms	23
2.3.3. Characteristics of microbes living at low temperatures	23
2.3.3.1. Cold-adapted enzymes	24
2.3.3.2. Structure and composition of cell membrane	25
2.3.4. Source of energy and nutrients in glacial environment	26
2.3.4.1. Bioavailability of energy	26
2.3.4.2. Physiological adaptation to oligotrophic environment	29
<b>CHAPTER III DESCRIPTION OF FIELD SITES</b>	<b>31</b>
<b>3.1. Criteria for selection of field sites</b>	<b>31</b>
<b>3.2. Akuliarusiarssuk Glacier and Manitsoq Glacier in Greenland</b>	<b>32</b>
3.2.1. Greenland Ice Sheet	32
3.2.2. Climate in Greenland	33
3.2.3. Geology of south-western Greenland	34
3.2.4. Glacier morphology and hydrology in Akuliarusiarssuk and Manitsoq Glaciers	34
<b>3.3. Jostedalsbreen Ice Cap in southern Norway</b>	<b>35</b>
3.3.1. Jostedalsbreen Ice Cap	35
3.3.2. Climate in Jostedalsbreen	36
3.3.3. Geology of Jostedalsbreen area	36
3.3.4. Glacier morphology and hydrology in four outlet glaciers of Jostedalsbreen ice cap: Bødalsbreen, Kjenndalsbreen, Nigardsbreen and Bergsetbreen	37
<b>3.4. Midre Lovénbreen and Finsterwalderbreen glaciers in Svalbard</b>	<b>39</b>
3.4.1. Glaciers in Svalbard	39
3.4.2. Climate in Svalbard	39
3.4.3. Geology of western Spitsbergen	40
3.4.4. Glacier morphology and hydrology in Midre Lovénbreen and Finsterwalderbreen	41



<b>CHAPTER IV</b>	<b>FIELD AND LABORATORY METHODOLOGY</b>	<b>44</b>
<b>4.1.</b>	<b>Field work</b>	<b>44</b>
4.1.1.	Design and preparation of sampling	44
4.1.1.1.	Akuliarusiarssuk Glacier and Manitsoq Glacier, Greenland ice sheet	44
4.1.1.2.	Jostedalsbreen ice cap, Norway	44
4.1.1.3.	Midre Lovénbreen and Finsterwalderbreen glaciers, Spitsbergen, Svalbard	45
4.1.1.4.	Preparation of the sampling before field trips	45
4.1.2.	Sampling methods	46
4.1.2.1.	Sampling water for microbiological analyses	46
4.1.2.2.	Sampling for water chemistry analyses	47
4.1.2.3.	Meltwater discharge in meltwater streams	48
4.1.2.4.	Sampling proglacial rock debris	48
4.1.3.	Transport and storage of samples	49
<b>4.2.</b>	<b>Laboratory experiments</b>	<b>49</b>
4.2.1.	Incubation of bacterial cultures	49
4.2.1.1.	Inoculating media with meltwater samples	52
4.2.2.	Thermal gradient experiments with enrichment cultures	53
4.2.3.	Weathering experiments	53
4.2.3.1.	Weathering experiment with proglacial rock debris and subglacial meltwater from Bødalsbreen, Norway	54
4.2.3.1.1.	Materials	54
4.2.3.1.2.	Sampling	55
4.2.3.2.	Long-term weathering experiment with proglacial rock debris from Norway and Svalbard, and meltwater from Bødalsbreen, Norway	56
4.2.3.2.1.	Materials	56
4.2.3.2.2.	Dispensing meltwater for aerobic biotic test vials	57
4.2.3.2.3.	Dispensing meltwater for anaerobic biotic test vials	57
4.2.3.2.4.	Dispensing meltwater for aerobic abiotic control vials	58
4.2.3.2.5.	Dispensing meltwater for anaerobic abiotic control vials	58
4.2.3.2.6.	Incubation of the biotic test vials and abiotic controls	58
4.2.3.2.7.	Water and gas sampling	59

4.2.3.2.8. Elemental composition of rock debris	59
4.2.3.3. Weathering experiment with proglacial rock debris from Norway and Svalbard, and meltwater from Svalbard	60
4.2.3.3.1. Materials	60
4.2.3.3.2. Water and gas sampling	60
<b>4.3. Laboratory analyses</b>	<b>60</b>
4.3.1. Suspended sediment concentration in meltwater samples	60
4.3.2. Chemical analyses of water samples	61
4.3.2.1. Major anions and cations in water by ion chromatography	61
4.3.2.2. Organic acids in water by ion chromatography	62
4.3.2.3. Dissolved organic carbon in meltwater	65
4.3.2.4. Ferrous iron concentration	65
4.3.2.5. Sulphide concentration	65
4.3.3. Determination of pH and oxygen concentration in water with microelectrodes	66
4.3.4. Determination of elemental composition of rock debris	67
4.3.4.1. Inductively coupled plasma-atomic emission spectrometry (ICP-AES)	67
4.3.4.2. X-ray fluorescence spectrometry (XRF)	69
4.3.5. Determination of mineralogical composition of rock debris	71
4.3.5.1. X-ray diffraction (XRD)	71
4.3.6. Determination of carbon, hydrogen, nitrogen and sulphur content in rock debris samples	72
4.3.6.1. Organic matter content	72
4.3.6.2. CHNS-analysis	72
4.3.7. Determination of grain size distribution	73
4.3.8. Headspace gas measurements	74
4.3.8.1. Oxygen and methane by gas chromatography	74
4.3.9. Microscopic methods	74
4.3.8.1. Total number of bacteria	74
4.3.8.2. Frequency of dividing and divided cells	75
4.3.8.3. Bacterial cells attached on particles	76
4.3.8.4. Doubling time of bacterial population	76



<b>4.4. Statistical analyses</b>	<b>76</b>
<b>CHAPTER V RESULTS I: BACTERIAL POPULATIONS IN MELTWATERS</b>	<b>77</b>
<b>5.1. Akuliarusiarssuk and Manitsoq glaciers in Greenland</b>	<b>77</b>
5.1.1. Meltwater discharge in the Manitsoq glacier	77
5.1.2. Bacterial populations in Greenland meltwaters	78
5.1.3. Growth of bacterial cultures at constantly low temperature	79
5.1.4. Temperature characteristics of sulphate-reducing bacteria in Greenland early and late melt season meltwaters	82
5.1.4.1. Sulphide production in Greenland SRB-cultures	82
5.1.4.2. Growth rate in Greenland SRB-cultures	88
5.1.5. Chemistry of Greenland meltwaters	91
<b>5.2. Jostedalsbreen ice cap in southern Norway</b>	<b>96</b>
5.2.1. Meltwater discharge in the Bødalsbreen outlet glacier	96
5.2.2. Bacterial populations in the Jostedalsbreen meltwaters	97
5.2.3. Growth of bacterial cultures at constantly low temperature	98
5.2.4. Temperature characteristics of sulphate-reducing bacteria in Jostedalsbreen early and mid melt season meltwaters	101
5.2.4.1. Sulphide production in Jostedalsbreen SRB-cultures	101
5.2.4.2. Growth rate in Jostedalsbreen SRB-cultures	106
5.2.5. Chemistry of Jostedalsbreen meltwaters	109
<b>5.3. Midre Løvenbreen glacier in Svalbard</b>	<b>113</b>
5.3.1. Initial melting before the actual melt season in the Midre Løvenbreen glacier	113
5.3.2. Bacterial populations in Midre Løvenbreen meltwaters	113
5.3.3. Growth of bacterial cultures at constantly low temperature	114
5.3.4. Temperature characteristics of sulphate-reducing bacteria in Midre Løvenbreen meltwater before the actual melt season	115
5.3.4.1. Sulphide production in Svalbard SRB-cultures	116
5.3.4.2. Growth rate in Svalbard SRB-cultures	117
5.3.5. Chemistry of Midre Løvenbreen meltwaters	120

<b>5.4. Discussion</b>	<b>124</b>
5.4.1. Total bacterial populations in glaciers in Greenland, Norway and Svalbard	124
5.4.2. Temperature characteristics of sulphate-reducing bacteria from different glaciers	128
 <b>CHAPTER VI RESULTS II: WEATHERING EXPERIMENTS</b>	 <b>133</b>
 <b>6.1. Weathering experiment with proglacial rock debris and subglacial meltwater from Bødalsbreen</b>	 <b>133</b>
6.1.1. <i>In situ</i> and laboratory experiment conditions	133
6.1.2. Grain size distribution of Bødalsbreen proglacial rock debris	133
6.1.3. Elemental composition of Bødalsbreen proglacial rock debris	135
6.1.4. Bacterial growth in Bødalsbreen meltwater	136
6.1.5. pH in Bødalsbreen meltwater	138
6.1.6. Major anions and cations in Bødalsbreen meltwater	141
 <b>6.2. Long-term weathering experiment with proglacial rock debris from Norway and Svalbard, and meltwater from Norway</b>	 <b>145</b>
6.2.1. <i>In situ</i> and laboratory experiment conditions	145
6.2.2. Grain size distribution of Bødalsbreen and Finsterwalderbreen rock flours	146
6.2.3. Elemental composition of Bødalsbreen and Finsterwalderbreen rock flours	147
6.2.4. Mineralogical composition of Bødalsbreen and Finsterwalderbreen rock flours	149
6.2.5. Bacterial growth in Bødalsbreen meltwater incubated with rock flours	150
6.2.6. Oxygen and methane in headspace	150
6.2.7. Dissolved oxygen and pH in Bødalsbreen meltwater incubated with rock flours	152
6.2.8. Major anions and cations in Bødalsbreen meltwater incubated with rock flours	158
6.2.9. Dissolved ferrous iron in meltwater incubated with rock flours	173



6.2.10. Organic acids in Bødalsbreen meltwater incubated with rock flours	173
<b>6.3. Weathering experiment with proglacial rock debris from Norway and Svalbard, and meltwater from Svalbard</b>	<b>177</b>
6.3.1. <i>In situ</i> and laboratory experiment conditions	177
6.3.2. Bacterial growth in Svalbard meltwater incubated with rock flours	177
6.3.3. Oxygen and methane in headspace	178
6.3.4. Dissolved oxygen and pH in Svalbard meltwater incubated with rock flours	179
6.3.5. Major anions and cations in Svalbard meltwater incubated with rock flours	180
6.3.6. Organic acids in Svalbard meltwater incubated with rock flours	185
<b>6.4. Discussion</b>	<b>187</b>
6.4.1. Rock debris as a source of energy and nutrients	187
6.4.2. Carboxylic acids as a source of carbon	191
6.4.3. Solute acquisition accelerated by microbial activity	192
<b>CHAPTER VII CONCLUSIONS</b>	<b>199</b>
<b>7.1. Presence of bacterial populations in meltwaters</b>	<b>199</b>
<b>7.2. Temperature characteristics of bacteria in meltwaters</b>	<b>200</b>
<b>7.3. Growth and activity of subglacial bacteria</b>	<b>202</b>
<b>REFERENCES</b>	<b>205</b>
<b>APPENDICES</b>	<b>225</b>

## LIST OF FIGURES

**Figure in the front page.** View to the Bødalsbreen outlet glacier of the Jostedalsbreen ice cap in June 2000

<b>Figure 2.1.</b> Development of the subglacial drainage system beneath a warm-based Alpine glacier	7
<b>Figure 2.2.</b> Routing of meltwater at a polythermal-based glacier	10
<b>Figure 2.3.</b> Structure of the cytoplasmic membrane in Bacteria	26
<b>Figure 3.1.</b> The Akuliarusiarssuk and Manitsoq Glaciers and their meltwater streams	32
<b>Figure 3.2.</b> Jostedalsbreen ice cap and the four outlet glaciers studied	37
<b>Figure 3.3.</b> Location of the Midre Lovénbreen and the Finsterwalderbreen glaciers in Spitsbergen	40
<b>Figure 4.1.</b> Sampling meltwater from the Nigardsbreen meltwater stream in June 2000	46
<b>Figure 4.2.</b> Inoculating growth media with supraglacial meltwater from the top of the Bødalsbreen outlet glacier in June 2000	47
<b>Figure 5.1.</b> Discharge in the main meltwater stream of the Manitsoq Glacier in the melt season 1999. S=meltwater sampling.	77
<b>Figure 5.2.</b> Total number of bacteria in meltwaters from the Manitsoq Glacier and the Akuliarusiarssuk Glacier in Greenland. The bars show the mean values of the three replicate counts and error bars show 95% confidence intervals for the means of three replicates. Sampling sites Manitsoq Glacier (solid bars) and Akuliarusiarssuk Glacier (bars with dots) as follows: 1 = subglacial meltwater, 22 June 1999; 2 = debris-poor supraglacial meltwater, 22 June 1999; 3 = debris-rich supraglacial meltwater,	79



22 June 1999; 4 = subglacial meltwater, 24 July 1999; 5 = debris-poor supraglacial meltwater, 24 July 1999; 6 = subglacial meltwater, 15 August 1999; 7 = subglacial meltwater, 27 July 1999; 8 = supraglacial meltwater, 27 July 1999.

**Figure 5.3.** Growth of sulphate-reducing bacteria from the early and late melt season subglacial meltwaters from the Manitsog Glacier. Cultures incubated in the thermal gradient system with a temperature range from 0 to +40 °C for 5 and 12 weeks. Growth measured as sulphide production (mM). 85

**Figure 5.4.** Growth of sulphate-reducing bacteria from the early and late melt season subglacial meltwaters from the Manitsog Glacier. Cultures incubated in the thermal gradient system with a temperature range from 0 to +40 °C for 32 and 42 weeks. Growth measured as sulphide production (mM). 86

**Figure 5.5.** Sulphate reduction rate at +4 °C, +17 °C and +25 °C in the early melt season culture of sulphate-reducing bacteria from the Manitsog Glacier. 87

**Figure 5.6.** Sulphate reduction rate at +4 °C, +17 °C and +25 °C in the late melt season culture of sulphate-reducing bacteria from the Manitsog Glacier. 87

**Figure 5.7.** Growth curves of bacterial populations in the early melt season SRB-enrichment cultures from the Manitsog Glacier at a range of incubation temperatures. Lines show the mean values of the three replicate counts. Blue line = +4 °C; brown line = +17 °C; red line = +25 °C. 89

**Figure 5.8.** Growth curves of bacterial populations in the late melt season SRB-enrichment cultures from the Manitsog Glacier at a range of incubation temperatures. Lines show the mean values of the three replicate counts. Blue line = +4 °C; brown line = +17 °C; red line = +25 °C. 89

<b>Figure 5.9.</b> Bacterial cells in the enrichment cultures of the early melt season sulphate-reducing bacteria from the Manitsoq Glacier incubated at +4 °C for 5 weeks.	90
<b>Figure 5.10.</b> Bacterial cells in the enrichment cultures of the early melt season sulphate-reducing bacteria from the Manitsoq Glacier incubated at +25 °C for 5 weeks.	90
<b>Figure 5.11.</b> Electrical conductivity (25 °C) in the bulk proglacial meltwater streams of the Manitsoq and Akuliarusiarssuk glaciers in the melt season 1999.	92
<b>Figure 5.12.</b> Dissolved organic carbon and nitrate concentrations in the bulk proglacial meltwater streams of the Manitsoq and Akuliarusiarssuk glaciers in the melt season 1999.	92
<b>Figure 5.13.</b> Major anion and cation concentrations in the bulk proglacial meltwater stream in the Manitsoq glacier in the melt season 1999.	93
<b>Figure 5.14.</b> Major anion and cation concentrations in the bulk proglacial meltwater stream in the Akuliarusiarssuk glacier in the melt season 1999.	93
<b>Figure 5.15.</b> Discharge in the main meltwater stream of the Bødalsbreen outlet glacier in the melt season 2000. S=meltwater sampling.	96
<b>Figure 5.16.</b> Total numbers of bacteria in meltwaters from four outlet glaciers of the Jostedalsbreen ice cap in the early melt season 2-7 June 2000 (dotted bars) and mid-melt season 19-28 July 2000 (solid bars). The bars show the mean values of the three replicate counts and error bars show 95% confidence intervals for the means of three replicates. Sampling sites as follows: 1-2 = Bødalsbreen subglacial meltwater; 3-4 = Bødalsbreen supraglacial meltwater; 5-6 = Kjenndalsbreen subglacial meltwater; 7-8 = Nigardsbreen subglacial meltwater; 9-10 = Bergsetbreen subglacial meltwater.	97



<b>Figure 5.17.</b> Growth of sulphate-reducing bacteria from the early (Kjenndalsbreen) and mid-melt (Bergsetbreen) season subglacial meltwaters. Cultures incubated in the thermal gradient system with a temperature range from $-0.6$ to $+40$ °C for 5 and 12 weeks. Growth measured as sulphide production (mM).	103
<b>Figure 5.18.</b> Growth of sulphate-reducing bacteria from the early (Kjenndalsbreen) and mid-melt (Bergsetbreen) season subglacial meltwaters. Cultures incubated in the thermal gradient system with a temperature range from $-0.6$ to $+40$ °C for 25 and 32 weeks. Growth measured as sulphide production (mM).	104
<b>Figure 5.19.</b> Growth of sulphate-reducing bacteria from the early (Kjenndalsbreen) and mid-melt (Bergsetbreen) season subglacial meltwaters. Cultures incubated in the thermal gradient system with a temperature range from $-0.6$ to $+40$ °C for 42 weeks. Growth measured as sulphide production (mM).	105
<b>Figure 5.20.</b> Sulphate reduction rate at $+5$ °C, $+16$ °C and $+25$ °C in the early melt season culture of sulphate-reducing bacteria from the Kjenndalsbreen glacier.	105
<b>Figure 5.21.</b> Sulphate reduction rate at $+5$ °C, $+16$ °C and $+25$ °C in the mid- melt season culture of sulphate-reducing bacteria from the Bergsetbreen glacier.	106
<b>Figure 5.22.</b> Growth curves of bacterial populations in the early melt season SRB-enrichment cultures from the Kjenndalsbreen glacier at a range of incubation temperatures. Lines show the mean values of the three replicate counts.. Blue line = $+5$ °C; brown line = $+16$ °C; red line = $+25$ °C.	108
<b>Figure 5.23.</b> Growth curves of bacterial populations in the mid-melt season SRB-enrichment cultures from the Bergsetbreen glacier at a range of temperatures. Lines show the mean values of the three replicate counts. Blue line = $+5$ °C; brown line = $+16$ °C; red line = $+25$ °C.	108



<b>Figure 5.24.</b> Electrical conductivity ( $\mu\text{S cm}^{-1}$ at 25 °C) in the bulk proglacial meltwater stream in the Bødalsbreen outlet glacier in the melt season 2000.	109
<b>Figure 5.25.</b> Major anion and cation concentrations in the bulk proglacial meltwater stream in the Bødalsbreen outlet glacier in the melt season 2000.	110
<b>Figure 5.26.</b> Dissolved organic carbon and nitrate concentrations in the bulk proglacial meltwater stream in the Bødalsbreen outlet glacier in the melt season 2000.	111
<b>Figure 5.27.</b> Total numbers of bacteria in meltwaters from the Midre Løvenbreen glacier before the actual melt season in spring 2001 (dotted bars) and 2002 (solid bars). The bars show the mean values of the three replicate counts and error bars show 95% confidence intervals for the means of three replicates. Sampling sites as follows: 1-2 = replicates from the same outflow; 3-6 = four different outflows located less than 10 m from each other.	114
<b>Figure 5.28.</b> Growth of sulphate-reducing bacteria from Midre Løvenbreen subglacial meltwater in May 2001. Cultures incubated in the thermal gradient system with a temperature range from $-0.6$ to $+40$ °C for 2.5 and 5 weeks. Growth measured as sulphide production (mM).	118
<b>Figure 5.29.</b> Growth of sulphate-reducing bacteria from Midre Løvenbreen subglacial meltwater in May 2001. Cultures incubated in the thermal gradient system with a temperature range from $-0.6$ to $+40$ °C for 12 and 25 weeks. Growth measured as sulphide production (mM).	119
<b>Figure 5.30.</b> Sulphate reduction rate at $+7$ , $+12$ and $+21$ °C in the cultures of sulphate-reducing bacteria from the Midre Løvenbreen glacier in May 2001.	120
<b>Figure 5.31.</b> Growth curves of bacterial populations in the SRB-enrichment cultures from the Midre Løvenbreen glacier (May 2001)	120



at a range of incubation temperatures. Lines show the mean values of the three replicate counts. Blue line = +7 °C; brown line = +12 °C; red line = +21 °C.

**Figure 5.32.** Scatterplot and linear regression test of suspended sediment concentration versus total number of bacteria in the meltwaters from Greenland ( $\log\text{AODC} = 4.03 + 0.09 \times \log\text{SSC}$ ,  $r^2 = 0.01$ ), Norway ( $\log\text{AODC} = 4.28 + 0.05 \times \log\text{SSC}$ ,  $r^2 = 0.01$ ) and Svalbard ( $\log\text{AODC} = 7.06 + 1.09 \times \log\text{SSC}$ ,  $r^2 = 0.13$ ).

**Figure 6.1.** Proportions of grain size fractions in the proglacial rock debris samples from the Bødalsbreen glacier (depths of 5 cm and 35 cm).

**Figure 6.2.** Grain size distributions of the fine-grained fractions (0-250  $\mu\text{m}$ ) of the proglacial rock debris from the Bødalsbreen glacier.

**Figure 6.3.** Growth curves of the total numbers of bacteria in meltwaters incubated at +7 °C with rock debris from the depths of 5 cm (■) and 35 cm (●), and frequency of dividing and divided cells (FDDC) over time. Subglacial meltwater and proglacial rock debris taken from the Bødalsbreen glacier. Lines and symbols show the mean values and error bars show 95% confidence intervals for the means of the three replicates ( $n=3$ ).

**Figure 6.4.** pH in meltwaters incubated at +7 °C with rock debris from the depths of 5 cm and 35 cm. Subglacial meltwater and proglacial rock debris taken from the Bødalsbreen glacier. Lines show the mean values and error bars show 95% confidence intervals for the means of the three replicates ( $n=3$ ). (●) = biotic test, depth of 5 cm; (▲) = biotic test, depth of 35 cm; (●) = abiotic control, depth of 5 cm; (▲) = abiotic control, depth of 35 cm.

**Figure 6.5.** Nitrate concentrations in meltwaters incubated at +7 °C with rock debris from the depths of 5 cm and 35 cm. Subglacial meltwater and proglacial rock debris taken from the Bødalsbreen glacier. Lines show the mean values and error bars show 95% confidence intervals for the means of the three replicates ( $n=3$ ). (●) = biotic test, depth of 5 cm;



(▲) = biotic test, depth of 35 cm; (●) = abiotic control, depth of 5 cm;

(▲) = abiotic control, depth of 35 cm.

**Figure 6.6.** Magnesium and calcium concentrations in meltwaters 142

incubated at +7 °C with rock debris from the depths of 5 cm and 35 cm.

Subglacial meltwater and proglacial rock debris taken from the Bødalsbreen glacier. Lines show the mean values and error bars show 95% confidence intervals for the means of the three replicates (n=3). (●) = biotic test, depth of 5 cm; (▲) = biotic test, depth of 35 cm; (●) = abiotic control, depth of 5 cm; (▲) = abiotic control, depth of 35 cm.

**Figure 6.7.** Potassium and sodium concentrations in meltwaters 143

incubated at +7 °C with rock debris from the depths of 5 cm and 35 cm.

Subglacial meltwater and proglacial rock debris taken from the Bødalsbreen glacier. Lines show the mean values and error bars show 95% confidence intervals for the means of the three replicates (n=3). (●) = biotic test, depth of 5 cm; (▲) = biotic test, depth of 35 cm; (●) = abiotic control, depth of 5 cm; (▲) = abiotic control, depth of 35 cm.

**Figure 6.8.** Sulphate concentrations in meltwaters incubated at 144

+7 °C with rock debris from the depths of 5 cm and 35 cm. Subglacial meltwater and proglacial rock debris taken from the Bødalsbreen glacier.

Lines show the mean values and error bars show 95% confidence intervals for the means of the three replicates (n=3). (●) = biotic test, depth of 5 cm; (▲) = biotic test, depth of 35 cm; (●) = abiotic control, depth of 5 cm; (▲) = abiotic control, depth of 35 cm.

**Figure 6.9.** Grain size distributions of the Bødalsbreen (solid line) 146

and Finsterwalderbreen (dotted line) rock flours.

**Figure 6.10.** Growth curves of the total numbers of bacteria in 151

meltwaters incubated at +1.6- +2.6 °C with rock flour, and frequency of dividing and divided cells (FDDC) over time. Subglacial meltwater taken from the Bødalsbreen glacier, and rock flour from Bødalsbreen, Norway and Finsterwalderbreen, Svalbard. Lines with symbols show the mean values and error bars show 95% confidence intervals for the means of the three



replicates (n=3). (■) = Norwegian rock flour, aerobic system; (●) = Norwegian rock flour, anaerobic system; (□) = Svalbard rock flour, aerobic system; (○) = Svalbard rock flour, anaerobic system.

**Figure 6.11.** Dissolved oxygen in Bødalsbreen meltwater incubated 154  
with rock flour from Bødalsbreen, Norway in aerobic and anaerobic  
conditions at a range of temperatures. Lines show the mean values and  
error bars show 95% confidence intervals for the means of the three replicates  
(n=3). (●) = biotic test at +1.6 - +2.6 °C; (⊗) = biotic test at +0.2 - +0.5 °C; (○)  
= biotic test at -1.2 - -1.0 °C; (●) = abiotic control at +1.6 - +2.6 °C;  
(⊗) = abiotic control at +0.2 - +0.5 °C; (○) = abiotic control at -1.2 - -1.0 °C.

**Figure 6.12.** pH in Bødalsbreen meltwater incubated with rock flour 155  
from Bødalsbreen, Norway in aerobic and anaerobic conditions at a range  
of temperatures. Lines show the mean values and error bars show 95%  
confidence intervals for the means of the three replicates (n=3).  
(●) = biotic test at +1.6 - +2.6 °C; (⊗) = biotic test at +0.2 - +0.5 °C; (○) = biotic  
test at -1.2 - -1.0 °C; (●) = abiotic control at +1.6 - +2.6 °C; (⊗) = abiotic  
control at +0.2 - +0.5 °C; (○) = abiotic control at -1.2 - -1.0 °C.

**Figure 6.13.** Dissolved oxygen Bødalsbreen meltwater incubated 156  
with rock flour from Finsterwalderbreen, Svalbard in aerobic and anaerobic  
conditions at a range of temperatures. Lines show the mean values and error  
bars show 95% confidence intervals for the means of the three replicates  
(n=3). (●) = biotic test at +1.6 - +2.6 °C; (⊗) = biotic test at +0.2 - +0.5 °C;  
(○) = biotic test at -1.2 - -1.0 °C; (●) = abiotic control at +1.6 - +2.6 °C;  
(⊗) = abiotic control at +0.2 - +0.5 °C; (○) = abiotic control at -1.2 - -1.0 °C.

**Figure 6.14.** pH in Bødalsbreen meltwater incubated with rock flour 157  
from Finsterwalderbreen, Svalbard in aerobic and anaerobic conditions  
at a range of temperatures. Lines show the mean values and error bars  
show 95% confidence intervals for the means of the three replicates (n=3).  
(●) = biotic test at +1.6 - +2.6 °C; (⊗) = biotic test at +0.2 - +0.5 °C; (○) = biotic  
test at -1.2 - -1.0 °C; (●) = abiotic control at +1.6 - +2.6 °C; (⊗) = abiotic  
control at +0.2 - +0.5 °C; (○) = abiotic control at -1.2 - -1.0 °C.



**Figure 6.15.** Nitrate concentrations in Bødalsbreen meltwater 160  
incubated with rock flour from Bødalsbreen, Norway in aerobic and  
anaerobic conditions at a range of temperatures. Lines show the mean  
values and error bars show 95% confidence intervals for the means of the  
three replicates (n=3). (●) = biotic test at +1.6 - +2.6 °C; (⊗) = biotic test at  
+0.2 - +0.5 °C; (○) = biotic test at -1.2 - -1.0 °C; (●) = abiotic control at +1.6 -  
+2.6 °C; (⊗) = abiotic control at +0.2 - +0.5 °C; (○) = abiotic control at -1.2 -  
-1.0 °C.

**Figure 6.16.** Nitrate concentrations in Bødalsbreen meltwater 161  
incubated with rock flour from Finsterwalderbreen, Svalbard in aerobic  
and anaerobic conditions at a range of temperatures. Lines show the mean  
values and error bars show 95% confidence intervals for the means of the  
three replicates (n=3). (●) = biotic test at +1.6 - +2.6 °C; (⊗) = biotic test at  
+0.2 - +0.5 °C; (○) = biotic test at -1.2 - -1.0 °C; (●) = abiotic control at +1.6 -  
+2.6 °C; (⊗) = abiotic control at +0.2 - +0.5 °C; (○) = abiotic control at -1.2 -  
-1.0 °C.

**Figure 6.17.** Magnesium concentrations in Bødalsbreen meltwater 162  
incubated with rock flour from Bødalsbreen, Norway in aerobic and  
anaerobic conditions at a range of temperatures. Lines show the mean  
values and error bars show 95% confidence intervals for the means of the  
three replicates (n=3). (●) = biotic test at +1.6 - +2.6 °C; (⊗) = biotic test at  
+0.2 - +0.5 °C; (○) = biotic test at -1.2 - -1.0 °C; (●) = abiotic control at +1.6 -  
+2.6 °C; (⊗) = abiotic control at +0.2 - +0.5 °C; (○) = abiotic control at -1.2 -  
-1.0 °C.

**Figure 6.18.** Calcium concentrations in Bødalsbreen meltwater 163  
incubated with rock flour from Bødalsbreen, Norway in aerobic and  
anaerobic conditions at a range of temperatures. Lines show the mean  
values and error bars show 95% confidence intervals for the means of the  
three replicates (n=3). (●) = biotic test at +1.6 - +2.6 °C; (⊗) = biotic test at  
+0.2 - +0.5 °C; (○) = biotic test at -1.2 - -1.0 °C; (●) = abiotic control at +1.6 -  
+2.6 °C; (⊗) = abiotic control at +0.2 - +0.5 °C; (○) = abiotic control at -1.2 -  
-1.0 °C.



**Figure 6.19.** Potassium concentrations in Bødalsbreen meltwater 164  
incubated with rock flour from Bødalsbreen, Norway in aerobic and  
anaerobic conditions at a range of temperatures. Lines show the mean  
values and error bars show 95% confidence intervals for the means of the  
three replicates (n=3). (●) = biotic test at +1.6 - +2.6 °C; (⊗) = biotic test at  
+0.2 - +0.5 °C; (○) = biotic test at -1.2 - -1.0 °C; (●) = abiotic control at +1.6 -  
+2.6 °C; (⊗) = abiotic control at +0.2 - +0.5 °C; (○) = abiotic control at -1.2 -  
-1.0 °C.

**Figure 6.20.** Sodium concentrations in Bødalsbreen meltwater 165  
incubated with rock flour from Bødalsbreen, Norway in aerobic and  
anaerobic conditions at a range of temperatures. Lines show the mean  
values and error bars show 95% confidence intervals for the means of the  
three replicates (n=3). (●) = biotic test at +1.6 - +2.6 °C; (⊗) = biotic test at  
+0.2 - +0.5 °C; (○) = biotic test at -1.2 - -1.0 °C; (●) = abiotic control at +1.6 -  
+2.6 °C; (⊗) = abiotic control at +0.2 - +0.5 °C; (○) = abiotic control at -1.2 -  
-1.0 °C.

**Figure 6.21.** Sulphate concentrations in Bødalsbreen meltwater 166  
incubated with rock flour from Bødalsbreen, Norway in aerobic and  
anaerobic conditions at a range of temperatures. Lines show the mean  
values and error bars show 95% confidence intervals for the means of the  
three replicates (n=3). (●) = biotic test at +1.6 - +2.6 °C; (⊗) = biotic test at  
+0.2 - +0.5 °C; (○) = biotic test at -1.2 - -1.0 °C; (●) = abiotic control at +1.6 -  
+2.6 °C; (⊗) = abiotic control at +0.2 - +0.5 °C; (○) = abiotic control at -1.2 -  
-1.0 °C.

**Figure 6.22.** Magnesium concentrations in Bødalsbreen meltwater 167  
incubated with rock flour from Finsterwalderbreen, Svalbard in aerobic  
and anaerobic conditions at a range of temperatures. Lines show the mean  
values and error bars show 95% confidence intervals for the means of the  
three replicates (n=3). (●) = biotic test at +1.6 - +2.6 °C; (⊗) = biotic test at  
+0.2 - +0.5 °C; (○) = biotic test at -1.2 - -1.0 °C; (●) = abiotic control at +1.6 -  
+2.6 °C; (⊗) = abiotic control at +0.2 - +0.5 °C; (○) = abiotic control at -1.2 -  
-1.0 °C.



**Figure 6.23.** Calcium concentrations in Bødalsbreen meltwater 168  
incubated with rock flour from Finsterwalderbreen, Svalbard in aerobic  
and anaerobic conditions at a range of temperatures. Lines show the mean  
values and error bars show 95% confidence intervals for the means of the  
three replicates (n=3). (●) = biotic test at +1.6 - +2.6 °C; (⊗) = biotic test at  
+0.2 - +0.5 °C; (○) = biotic test at -1.2 - -1.0 °C; (●) = abiotic control at +1.6 -  
+2.6 °C; (⊗) = abiotic control at +0.2 - +0.5 °C; (○) = abiotic control at -1.2 -  
-1.0 °C.

**Figure 6.24.** Potassium concentrations in Bødalsbreen meltwater 169  
incubated with rock flour from Finsterwalderbreen, Svalbard in aerobic  
and anaerobic conditions at a range of temperatures. Lines show the mean  
values and error bars show 95% confidence intervals for the means of the  
three replicates (n=3). (●) = biotic test at +1.6 - +2.6 °C; (⊗) = biotic test at  
+0.2 - +0.5 °C; (○) = biotic test at -1.2 - -1.0 °C; (●) = abiotic control at +1.6 -  
+2.6 °C; (⊗) = abiotic control at +0.2 - +0.5 °C; (○) = abiotic control at -1.2 -  
-1.0 °C.

**Figure 6.25.** Sodium concentrations in Bødalsbreen meltwater 170  
incubated with rock flour from Finsterwalderbreen, Svalbard in aerobic  
and anaerobic conditions at a range of temperatures. Lines show the mean  
values and error bars show 95% confidence intervals for the means of the  
three replicates (n=3). (●) = biotic test at +1.6 - +2.6 °C; (⊗) = biotic test at  
+0.2 - +0.5 °C; (○) = biotic test at -1.2 - -1.0 °C; (●) = abiotic control at +1.6 -  
+2.6 °C; (⊗) = abiotic control at +0.2 - +0.5 °C; (○) = abiotic control at -1.2 -  
-1.0 °C.

**Figure. 6.26.** Sulphate concentrations in Bødalsbreen meltwater 171  
incubated with rock flour from Finsterwalderbreen, Svalbard in aerobic  
and anaerobic conditions at a range of temperatures. Lines show the mean  
values and error bars show 95% confidence intervals for the means of the  
three replicates (n=3). (●) = biotic test at +1.6 - +2.6 °C; (⊗) = biotic test at  
+0.2 - +0.5 °C; (○) = biotic test at -1.2 - -1.0 °C; (●) = abiotic control at +1.6 -  
+2.6 °C; (⊗) = abiotic control at +0.2 - +0.5 °C; (○) = abiotic control at -1.2 -  
-1.0 °C.



**Figure 6.27.** Dissolved ferrous iron concentrations in Bødalsbreen 172  
meltwater incubated with rock flour from Bødalsbreen, Norway in aerobic  
and anaerobic conditions at a range of temperatures. Lines show the mean  
values and error bars show 95% confidence intervals for the means of the  
three replicates (n=3). (●) = biotic test at +1.6 - +2.6 °C; (⊗) = biotic test at  
+0.2 - +0.5 °C; (○) = biotic test at -1.2 - -1.0 °C; (●) = abiotic control at +1.6 -  
+2.6 °C; (⊗) = abiotic control at +0.2 - +0.5 °C; (○) = abiotic control at -1.2 -  
-1.0 °C.

**Figure 6.28.** Growth curves of the total numbers of bacteria in 178  
meltwaters incubated at +1.6 °C with rock flours for 96 days, and  
frequency of dividing and divided cells (FDDC) over time. Subglacial meltwater  
taken from the Midre Lovénbreen glacier, Svalbard and rock flour from  
Bødalsbreen, Norway and Finsterwalderbreen, Svalbard. Lines with symbols  
show mean values and error bars show 95% confidence intervals for means of  
two replicates (n=2). (●) = Norwegian rock flour; (◆) = Svalbard rock flour.

**Figure 6.29.** Dissolved oxygen concentrations in meltwaters 179  
incubated at +1.6 °C with rock flours for 96 days. Subglacial meltwater  
taken from the Midre Lovénbreen glacier, Svalbard and rock flour from  
Bødalsbreen, Norway and Finsterwalderbreen, Svalbard. Symbols show  
values of two replicates (n=2). (●) = biotic test with Norwegian rock flour;  
(●) = abiotic control with Norwegian rock flour; (◆) = biotic test with Svalbard  
rock flour; (◆) = abiotic control with Svalbard rock flour.

**Figure 6.30.** pH in meltwaters incubated at +1.6 °C with rock flours 180  
for 96 days. Subglacial meltwater taken from the Midre Lovénbreen glacier,  
Svalbard and rock flour from Bødalsbreen, Norway and Finsterwalderbreen,  
Svalbard. Symbols show values of two replicates (n=2). (●) = biotic test with  
Norwegian rock flour; (●) = abiotic control with Norwegian rock flour; (◆) =  
biotic test with Svalbard rock flour; (◆) = abiotic control with Svalbard rock  
flour.

**Figure 6.31.** Nitrate concentrations in meltwaters incubated 182  
at +1.6 °C with rock flours for 96 days. Subglacial meltwater taken from



the Midre Lovénbreen glacier, Svalbard and rock flour from Bødalsbreen, Norway and Finsterwalderbreen, Svalbard. Symbols show values of two replicates ( $n=2$ ). (●) = biotic test with Norwegian rock flour; (●) = abiotic control with Norwegian rock flour; (◆) = biotic test with Svalbard rock flour; (◆) = abiotic control with Svalbard rock flour.

**Figure 6.32.** Magnesium concentrations in meltwaters incubated at  $+1.6\text{ }^{\circ}\text{C}$  with rock flours for 96 days. Subglacial meltwater taken from the Midre Lovénbreen glacier, Svalbard and rock flour from Bødalsbreen, Norway and Finsterwalderbreen, Svalbard. Symbols show values of two replicates ( $n=2$ ). (●) = biotic test with Norwegian rock flour; (●) = abiotic control with Norwegian rock flour; (◆) = biotic test with Svalbard rock flour; (◆) = abiotic control with Svalbard rock flour.

**Figure 6.33.** Calcium concentrations in meltwaters incubated at  $+1.6\text{ }^{\circ}\text{C}$  with rock flours for 96 days. Subglacial meltwater taken from the Midre Lovénbreen glacier, Svalbard and rock flour from Bødalsbreen, Norway and Finsterwalderbreen, Svalbard. Symbols show values of two replicates ( $n=2$ ). (●) = biotic test with Norwegian rock flour; (●) = abiotic control with Norwegian rock flour; (◆) = biotic test with Svalbard rock flour; (◆) = abiotic control with Svalbard rock flour.

**Figure 6.34.** Potassium concentrations in meltwaters incubated at  $+1.6\text{ }^{\circ}\text{C}$  with rock flours for 96 days. Subglacial meltwater taken from the Midre Lovénbreen glacier, Svalbard and rock flour from Bødalsbreen, Norway and Finsterwalderbreen, Svalbard. Symbols show values of two replicates ( $n=2$ ). (●) = biotic test with Norwegian rock flour; (●) = abiotic control with Norwegian rock flour; (◆) = biotic test with Svalbard rock flour; (◆) = abiotic control with Svalbard rock flour.

**Figure 6.35.** Sodium concentrations in meltwaters incubated at  $+1.6\text{ }^{\circ}\text{C}$  with rock flours for 96 days. Subglacial meltwater taken from the Midre Lovénbreen glacier, Svalbard and rock flour from Bødalsbreen, Norway and Finsterwalderbreen, Svalbard. Symbols show values of two replicates ( $n=2$ ). (●) = biotic test with Norwegian rock flour; (●) = abiotic control with Norwegian rock flour; (◆) = biotic test with Svalbard rock flour;



(♦) = abiotic control with Svalbard rock flour.

**Figure 6.36.** Sulphate concentrations in meltwaters incubated at +1.6 °C with rock flours for 96 days. Subglacial meltwater taken from the Midre Lovénbreen glacier, Svalbard and rock flour from Bødalsbreen, Norway and Finsterwalderbreen, Svalbard. Symbols show values of two replicates (n=2). (●) = biotic test with Norwegian rock flour; (●) = abiotic control with Norwegian rock flour; (◆) = biotic test with Svalbard rock flour; (♦) = abiotic control with Svalbard rock flour.

**Figure 6.37.** Images of bacteria cells growing in meltwater incubated with (a) Norwegian rock flour and (b) Svalbard rock flour.

**Figure 6.38.** Scatterplot of  $\text{Ca}^{2+}$  and  $\text{Mg}^{2+}$  versus  $\text{SO}_4^{2-}$  in meltwaters incubated with (a) Norwegian rock flour and (b) Svalbard rock flour at a range of temperatures (n=24). (●) = biotic test at +1.6 - +2.6 °C; (⊗) = biotic test at +0.2 - +0.5 °C; (○) = biotic test at -1.2 - -1.0 °C; (●) = abiotic control at +1.6 - +2.6 °C; (⊗) = abiotic control at +0.2 - +0.5 °C; (○) = abiotic control at -1.2 - -1.0 °C.



## LIST OF TABLES

<b>Table 2.1.</b> Climatic changes and the response level of glaciers	5
<b>Table 2.2.</b> Phases of the melt season	9
<b>Table 2.3.</b> The main geochemical weathering reactions in subglacial environments	15
<b>Table 3.1.</b> Change in the position of the terminus of the Jostedalsbreen outlet glaciers from autumn 1999 to autumn 2000	38
<b>Table 4.1.</b> Analytical columns used in Dionex DX500 ion chromatography	61
<b>Table 4.2.</b> Precision and accuracy (min and max of 26 runs) of the Dionex DX500 ion chromatography system used to analyse major anions and cations	63
<b>Table 4.3.</b> Standards and precision of the Dionex DX600 gradient analysis using KOH as an eluent used to analyse major organic acids	64
<b>Table 4.4.</b> Final concentrations (ppm) of calibration standards in ICP-AES analyses.	68
<b>Table 4.5.</b> Detection limits and relative errors for aqueous solutions of single elements in ICP-AES analyses with Spectrometer JY 24 Sequential ICP.	69
<b>Table 4.6.</b> SPECTRO X-LAB detection limits and relative errors for major elements.	70
<b>Table 4.7.</b> Standard sample values and relative mean errors in CHNS-analysis.	73

**Table 5.1.** Growth of cultures of nitrate-reducing bacteria from the Manitsok Glacier. Incubation at +4 °C. 0=no change in colour nor turbidity, no precipitates; 1= colour turned from deep purple to pale violet, slightly turbid, yellow precipitates, growth; 2= colour yellow-grey, turbid, lot of precipitates, strong growth. Figures show growth in two replicates: culture A / culture B. 80

**Table 5.2.** Growth of cultures of nitrate-reducing bacteria from the Akuliarusiarssuk Glacier. Incubation at +4 °C. 0=no change in colour nor turbidity, no precipitates; 1= colour turned from deep purple to pale violet, slightly turbid, yellow precipitates, growth; 2= colour yellow-grey, turbid, lot of precipitates, strong growth. Figures show growth in two replicates: culture A / culture B. 81

**Table 5.3.** Growth of cultures of sulphate-reducing bacteria from the Manitsok Glacier. Incubation at +4 °C. 0=no sign of growth; 1=culture turning cloudy, dark grey precipitates, growth; 2=black precipitates, strong growth. Figures show growth in two replicates: culture A / culture B. 81

**Table 5.4.** Growth of cultures of sulphate-reducing bacteria from the Akuliarusiarssuk Glacier. Incubation at +4 °C. 0=no sign of growth; 1=culture turning cloudy, dark grey precipitates, growth; 2=black precipitates, strong growth. Figures show growth in two replicates: culture A / culture B. 81

**Table 5.5.** Estimated doubling times of the total number of cells in cultures of sulphate-reducing bacteria from the Manitsok Glacier in the early and late melt season during exponential growth, and the frequency of dividing and divided cells (FDDC) after 35 days incubation at a range of high sulphide production temperatures. 88

**Table 5.6.** Chemical composition of the meltwaters in the Manitsok and Akuliarusiarssuk glaciers at the early melt season (22-23 June), mid-melt season (24-27 July) and late melt season (15-16 August) in 1999. SS = suspended sediment concentration. Anion and cation concentration unit is  $\mu\text{eq l}^{-1}$ . 95



**Table 5.7.** Growth of cultures of nitrate-reducing bacteria 99  
from the Jostedalsbreen outlet glaciers in the early melt season (2.-7.6.2000).  
Incubation at +2 °C. 0=no change in colour nor turbidity, no precipitates;  
1= colour turned from deep purple to pale violet, slightly turbid, yellow  
precipitates, growth; 2= colour yellow-grey, turbid, lot of precipitates, strong  
growth. Figures show growth in two replicates: culture A / culture B.

**Table 5.8.** Growth of cultures of sulphate-reducing bacteria 99  
from the Jostedalsbreen outlet glaciers in the early melt season (2.-7.6.2000).  
Incubation at +2 °C. 0=no sign of growth; 1=culture turning cloudy, dark grey  
precipitates, growth; 2=black precipitates, strong growth. Figures show growth  
in two replicates: culture A / culture B.

**Table 5.9.** Growth of cultures of nitrate-reducing bacteria 100  
from the Jostedalsbreen outlet glaciers in mid-melt season meltwaters  
(19.- 28.7.2000). Incubation at +2 °C. 0=no change in colour nor turbidity, no  
precipitates; 1= colour turned from deep purple to pale violet, slightly turbid,  
yellow precipitates, growth; 2= colour yellow-grey, turbid, lot of precipitates,  
strong growth. Figures show growth in two replicates: culture A / culture B.

**Table 5.10.** Growth of cultures of sulphate-reducing bacteria 100  
from the Jostedalsbreen outlet glaciers in mid-melt season meltwaters  
(19.-28.7.2000). Incubation at +2 °C. 0=no sign of growth; 1=culture turning  
cloudy, dark grey precipitates, growth; 2=black precipitates, strong growth.  
Figures show growth in two replicates: culture A / culture B.

**Table 5.11.** Estimated doubling times of the total number of cells in 107  
cultures of sulphate-reducing bacteria in the early (Kjenndalsbreen) and  
mid-melt (Bergsetbreen) season during exponential growth, and the frequency  
of dividing and divided cells (FDDC) after 35 days of incubation at a range of  
high sulphide production temperatures.

**Table 5.12.** Chemical composition of the meltwaters in the four 112  
outlet glaciers of Jostedalsbreen at the early (2-7 June) and the mid-melt



(19-28 July) season in summer 2000. Figures of one early and one mid-melt sampling from each outlet glacier. SS = suspended sediment concentration. Anion and cation concentration unit is  $\mu\text{eq l}^{-1}$ .

**Table 5.13.** Growth of cultures of sulphate-reducing bacteria 115  
from Midre Løvenbreen meltwater before the actual melt season in May 2001 and April 2002. Incubation at +2 °C. 0=no sign of growth; 1=culture turning cloudy, dark grey precipitates, growth; 2=black precipitates, strong growth. Figures show growth in two replicates: culture A / culture B. (30/45 = 35 ml of sample inoculated to 15 ml of SRB-medium; 10/40 = 10 ml of sample inoculated to 30 ml of SRB-medium; 1/40 = 1 ml of sample inoculated to 39 ml of SRB-medium; 0.1/40 = 0.1 ml of sample inoculated to 39.9 ml of SRB-medium).

**Table 5.14.** Estimated doubling times of the total number of cells 119  
in cultures of sulphate-reducing bacteria from the Midre Løvenbreen glacier during exponential growth, and the frequency of dividing and divided cells (FDDC) after 35 days at a range of high sulphide production temperatures.

**Table 5.15.** Chemical composition of meltwaters in the Midre 122  
Løvenbreen before the actual melt season in 2001 (2 May) and 2002 (10 April) (Wadham, unpublished data). SS = suspended sediment concentration. Anion and cation concentration unit is  $\mu\text{eq l}^{-1}$ .

**Table 5.16.** Summary of total bacterial populations in meltwaters 123  
of glaciers in Greenland, Norway and Svalbard, suspended sediment concentrations and frequency of bacterial cells attached to mineral grains suspended in meltwater. Figures are mean values of three replicates. Man= Manitsoq glacier; Aku= Akuliarusiarssuk glacier; Bødal= Bødalsbreen glacier; Kjenndal= Kjenndalsbreen glacier; Nigard= Nigardsbreen glacier; Bergset= Bergsetbreen glacier.

**Table 5.17.** Summary of bacterial populations and concentrations of 127  
dissolved organic carbon in early melt season subglacial meltwaters from Greenland (1999), Norway (2000) and Svalbard (2002).



<b>Table 6.1.</b> Elemental composition of the rock debris from the depths of 5 cm and 35 cm at the beginning and at the end of the experiment. Percentages of major elements analysed by ICP-AES / XRF. If there are two figures presented, the first one is by ICP/AES, and the second one is by XRF. nd= not determined.	135
<b>Table 6.2.</b> Results of the t-tests (independent samples pooled-variance and separate-variance t-test) for equality of means (three replicates) of pH and major anions and cations in Bødalsbreen meltwater incubated at +7 °C with rock debris from the depths of 5 cm (table A) and 35 cm (table B). Comparisons between biotic tests and abiotic controls at the end of incubation (t=98 days).	139
<b>Table 6.3.</b> Results of the t-tests of pH and major anions and cations in Bødalsbreen meltwater incubated at +7 °C with rock debris from the depths of 5 cm and 35 cm. Comparisons between biotic tests with rock debris from depths of 5 cm and 35 cm at the end of incubation (t=98 days).	140
<b>Table 6.4.</b> Elemental composition of the rock debris from the Bødalsbreen proglacial outwash plain, at the beginning and at the end of the experiment. Incubation temperature +1.6 - +2.6 °C. Percentages of major elements analysed by XRF.	147
<b>Table 6.5.</b> Elemental composition of the rock debris from the Finsterwalderbreen proglacial outwash plain, at the beginning and at the end of the experiment. Incubation temperature +1.6- +2.6 °C. Percentages of major elements analysed by XRF.	148
<b>Table 6.6.</b> The crystalline minerals identified in Bødalsbreen (Norway) and Finsterwalderbreen (Svalbard) rock flour. Identification is based on comparison of X-ray diffractograms with the diffraction patterns in the MacDiff (version 4.2.5) reference database.	149
<b>Table 6.7.</b> Organic acids detected in Bødalsbreen meltwater incubated with the Norwegian rock flour. Figures presented are the mean values of the two replicates. Incubation for 298 days at	174



temperature of +1.6 – +2.6 °C.

<b>Table 6.8.</b> Organic acids detected in Bødalsbreen meltwater incubated with the Svalbard rock flour. Figures presented are the mean values of the two replicates. Incubation for 298 days at temperature of +1.6 – +2.6 °C.	175
<b>Table 6.9.</b> Results of the separate-variance t-tests (equal variances not assumed) for equality of means (two replicates) of pH and major anions and cations in Midre Lovénbreen meltwater incubated at +1.6 °C with rock flours from Bødalsbreen, Norway (table A) and Finsterwalderbreen, Svalbard (table B). Comparisons between biotic tests and abiotic controls after 63 days of incubation.	181
<b>Table 6.10.</b> Organic acids detected in Midre Lovénbreen meltwater incubated with the Norwegian rock flour. Figures presented are the mean values of the two replicates. Incubation for 96 days at temperature of +1.6 °C.	186
<b>Table 6.11.</b> Organic acids detected in Midre Lovénbreen meltwater incubated with the Svalbard rock flour. Figures presented are the mean values of the two replicates. Incubation for 96 days at temperature of +1.6 °C.	186
<b>Table 6.12.</b> Basic nutrients in the rock flours from the proglacial outwash plains in Norway and Svalbard.	189
<b>Table 6.13.</b> Incubation times needed at a range of temperatures to detect the first signs of impact of microbial activity on solute concentrations in the meltwater mixed with the rock flour originating from quartzo-feldspathic gneiss from Bødalsbreen, Norway .	193
<b>Table 6.14.</b> The major cations and anions in Bødalsbreen meltwater (a) after 300 days of laboratory incubation in aerobic conditions with microbes deriving energy and nutrients from the rock flour at +1.6 to +2.6 °C ; (b) after 300 days abiotic incubation with the rock flour (sterile controls) at +1.6 to +2.6 °C and (c) after a long residence time in the subglacial drainage system (sampling at the early melt season from the bulk meltwater stream).	194



Comparison of equality of means between biotic (a) and abiotic (b) systems with the pooled-variance t-test.

**Table 6.15.** Partial pressure of carbon dioxide  $p(\text{CO}_2)$  in the rock flour -meltwater mixture at the beginning and the end of incubation at +1.6 to +2.6 °C. Figures show the mean values and standard deviations of the three replicates. Calculations based on the following equation:  $\log p(\text{CO}_2) = \log(\text{HCO}_3^-) - \text{pH} + p\text{KCO}_2 + p\text{K}_1$ , where  $p\text{KCO}_2 = 1.12$  and  $p\text{K}_1 = 6.58$ . 198



## CHAPTER I INTRODUCTION TO THE RESEARCH AREA

### 1.1. Background and context for research

Studies in the variety of permanently cold glacial environments have demonstrated that viable and active microbial populations can be found on the top of glaciers in surface snow and firn (Carpenter et al. 2000, Sæther et al. 2001); at various depths of ice sheets (Abyzov 1993, Abyzov et al. 1998, Prisco et al. 1999); in glacier runoff and basal ice (Sharp et al. 1999, Skidmore et al. 2000a and 2000b) as well as in sediments in proglacial



extensive consequences that was earlier assumed (Tranter et al. 1994 and 1997). Furthermore, the results suggested that at glacier beds microbial activity has a significant effect on the rate of oxidation of sulphide minerals such as pyrite (Tranter et al. 2002), and microbially mediated oxidation of organic carbon may be a significant proton source beneath glaciers (Brown 2002). Sharp et al. (1999) confirmed that widespread bacterial populations are present at glacier beds. The positive correlation between population size and microbial respiration rates in ice and meltwater samples suggested that subglacial bacteria at the ice/bed interface derive energy from the oxidation of reduced minerals or organic carbon within the fine-grained rock flour. However, incubation experiments by Sharp et al. (1999) were conducted at 4 °C with the maximum incubation time of two months, while the in situ



# **CHAPTER I INTRODUCTION TO THE RESEARCH AREA**

## **1.1. Background and context for research**

Studies in the variety of permanently cold glacial environments have demonstrated that viable and active microbial populations can be found on the top of glaciers in surface snow and firn (Carpenter et al. 2000, Sattler et al. 2001); at various depths of ice sheets (Abyzov 1993, Abyzov et al. 1998, Priscu et al. 1999); in glacier runoff and basal ice (Sharp et al. 1999; Skidmore et al. 2000a and 2000b) as well as in sediments in proglacial forefields (Gounot 2001; Welker et al. 2002; Sigler and Zeyer 2002). Psychrophilic or psychrotolerant micro-organisms from these environments have shown metabolic activity at the temperature range from +3 °C (Priscu et al. 1999) and +0.3 °C (Skidmore et al. 2000a) to –12 to –17 °C (Carpenter et al. 2000). Typically these micro-organisms have been heterotrophs which use particulate or dissolved organic carbon as a source of energy and carbon (Ward and Priscu 1997; Priscu et al. 1999; Sharp et al. 1999; Carpenter et al. 2000; Price 2000; Skidmore et al. 2000a; Gounot 2001; Welker et al. 2002; Campen et al. 2003).

Previous studies on geochemistry of subglacial meltwaters showed variations in nitrate concentration, which implied that microbial processes including denitrification take place in the subglacial drainage systems with more extensive consequences than was earlier assumed (Tranter et al. 1994 and 1997). Furthermore, the results suggested that at glacier beds microbial activity has a significant effect on the rate of oxidation of sulphide minerals such as pyrite (Tranter et al. 2002), and microbially mediated oxidation of organic carbon may be a significant proton source beneath glaciers (Brown 2002). Sharp et al. (1999) confirmed that widespread bacterial populations are present at glacier beds. The positive correlation between population size and sediment concentrations in ice and meltwater samples suggested that subglacial bacteria at the ice-till interface derive energy from the oxidation of reduced minerals or organic carbon within the fine-grained rock flour. However, weathering experiments by Sharp et al. (1999) were conducted at +4 °C with the maximum incubation time of two months, while the *in situ*-



temperature at the base of the glacier is ca. 0 °C (Skidmore et al. 2000), and in subglacial meltwater streams from +0.5 to +2.5 °C (Brown et al. 1994a).

The limitation of some other earlier studies on potential microbial activity in the permanently cold regions has been incubation of micro-organisms at higher than their *in situ*-temperatures for short periods, as well as addition of easily bioavailable nutrients such as acetate and glucose. Also, most of the laboratory experiments on water-rock interactions in glacial environments have been conducted in free contact with the atmosphere, giving results which are not directly applicable to subglacial isolated cavities or distributed drainage systems (Brown 2002). Therefore, further studies on subglacial bacterial populations and their interactions with rock flour in closed-system conditions at near-zero temperature were essential to confirm the role of microbial activity in subglacial chemical weathering.

## **1.2. Research objectives**

The specific objectives of the research were:

- 1) to determine the size and distribution of bacterial populations in meltwaters from a range of glaciers covering a spectrum of glacier size and thermal regime, and of bedrock type.
- 2) to quantify the presence of a range of different bacterial metabolic groups in each glacier system, as well as to determine their temperature characteristics.
- 3) to conduct weathering experiments to determine the impact of bacteria on the rate of low temperature chemical weathering.
- 4) to determine the *in situ* activity of subglacial bacteria and their potential energy and nutrient sources.

The three field sites represented glaciers with different characteristics: a warm-based ice cap with several outlet glaciers in a maritime climate; a



subarctic polythermal-based inland ice sheet; and a polythermal-based valley glacier in a high arctic climate. Lithologies ranged from Precambrian granitic rocks of crystalline basement and Precambrian metamorphic gneisses and quartzites to Carboniferous and Permian sedimentary rocks.

The laboratory experiments on water-rock interactions were designed to simulate a highly oligotrophic environment in subglacial cavities during winter months, when melting is minimal. Hence, low temperature experiments in closed-system conditions with no other substrates but rock flour, lasting up to 10 months were conducted.



## **CHAPTER II INTRODUCTION**

### **2.1. Glacial environment**

#### **2.1.1. Glaciated areas**

Glaciers cover approximately 10% ( $14.9 \times 10^6 \text{ km}^2$ ) of the Earth's land area. Besides the massive ice sheets and glaciers of the South and North Polar regions, covering in total  $12.6 \times 10^6 \text{ km}^2$  and  $2.1 \times 10^6 \text{ km}^2$  respectively, a variety of ice caps and smaller glaciers can be found in high altitudes in North America (Alaska), South America, Europe (Scandinavia, Alps, Caucasus), Asia (Himalaya, K'un Lun chains, Khunjerab ranges), Africa and the Pacific region (including New Zealand) (Sugden and John 1976, Flint 1971). The vital variables influencing the spatial distribution of glaciers are precipitation, temperature, latitude, altitude and bedrock topography. In high latitudes, glacierization occurs down to sea-level, whereas in low latitudes, glacier can exist only at high altitudes. For example, most of the glaciers in the western Alps are located at altitude greater than 2000 m a.s.l. (Sugden and John 1976).

A substantial part of the Arctic and Antarctic ice covered areas are bodies of sea ice. Sea ice is an approximately 3 - 4 metre thick layer of ice on the ocean surface, formed by the freezing of seawater. Especially massive sea ice can be found at the North Pole, floating on the Arctic Ocean. On the Antarctic continent, the ice sheet with a maximum thickness of 4300 metres buries the South Pole. Sea ice may also contain drifting icebergs with thicknesses of 100 m, derived from glaciers (Sharp 1988).

The total areas of glaciers fluctuate as a result of global and local changes in climate. Currently, a matter of great concern is the continuing melting of ice masses. For example, glaciers and ice-sheets covering the Arctic landscape are shrinking by 0.5 to 5 % per year (Welker et al. 2002). The High Arctic is particularly sensitive to climatic change (Glasser and Hambrey 2001), and changes in the Earth's climate are expected to occur first in the Arctic glaciers with a maritime influence (Fleming et al. 1997). For example, in the Kongsfjorden area in Svalbard, all the glaciers have retreated in the last



hundred years (Liestøl 1990). Conversely, in some regions, particularly in Scandinavia, the annual net balance of the small outlet glaciers has recently been positive, and the glaciers have advanced (Kjøllmoen 2001). Hence, glacier volume fluctuation is a complicated issue, and the response rate of glaciers to climate change is a function of glacier type (see table 2.1).

**Table 2.1.** Climatic changes and the response level of glaciers (after Sugden and John 1976).

<i>Climatic change</i>	<i>Approximate time scale (years)</i>	<i>Glacier type affected</i>
long term fluctuations	100000-10000	ice sheets
medium term fluctuations	10000-1000	ice caps, ice fields and larger valley glaciers
medium term fluctuations	1000-100	smaller valley glaciers
short term fluctuations	100-10	cirque glaciers
high frequency, low magnitude fluctuations	10-1	small firn fields and snow beds

### 2.1.2. Morphology of glaciers and glacier thermal regimes

Glaciers can be categorized on the basis of geometry and internal temperature regime. Ice sheets, such as ice sheets of Antarctica and Greenland, occupy broad areas of gentle landscape, and they generally flow outward in all directions. Ice caps are masses of glacier ice, of less than 50000 km<sup>2</sup>, capping upland and spreading out radially. Ice streams flowing down outward from the margins of ice domes are called either outlet glaciers or valley glaciers (Sharp 1988). The difference between outlet and valley glaciers is that valley glaciers are constrained by topography, whereas an outlet glacier may occupy a shallow, rather irregular, depression. Valley glaciers, usually 10-30 km in length, flow in a valley on a steep bedrock slope, and are overlooked by rock cliffs. Outlet glaciers are common around ice caps, such as Icelandic Vatnajökull and Norwegian Jostedalsbreen (Sugden and John 1976).

Based on the thermal regime, glaciers can be classified as warm-based and cold-based, also called temperate and polar glaciers, respectively. The basis



of these categories is the location of the pressure melting point. Increasing pressure lowers the freezing point of water at a rate of 0.0072 °C per atmosphere. Thus, for example, at the base of a glacier 1500 metres thick, the pressure is high enough to lower the melting point to –1 °C. By definition, a warm-based glacier has basal ice at the pressure melting point. This also usually means that water can exist throughout the glacier. In contrast, a cold-based glacier has a basal temperature below the melting point of ice. Consequently, a cold-based glacier usually contains no liquid water, neither internally nor at the base (Sharp 1988). In reality, thermal systems of large glaciers are hardly ever this simple, and polythermal glaciers, also called subpolar glaciers, with an inner warm-based region surrounded by a cold-based margin are common (Tranter et al. 1996).

### **2.1.3. Glacier hydrology**

Two main sources of glacier meltwater can be recognized: from surface melting and basal melting. Surface supplies usually reach a peak in late summer, whereas basal supplies fluctuate less noticeably and usually exist throughout the year (Sugden and John 1976). The bulk runoff from glaciers is composed of three main components, mixed in different ratios at different phases of the melt season. Supraglacial meltwater is surficial meltwater flowing in streams on the surface of a glacier (Sharp 1988, Sharp et al. 1999). Subglacial meltwater is the component routed slowly near or at the bed, and has elevated sediment and solute loads due to increased contact with bedrock, percolation through moraine debris and interaction with sediment-loaded basal ice. Englacial meltwater is the dilute and almost sediment-free component routed quickly through the glacier body (Richards et al. 1996). Subglacial water can be distinguished from englacial water on the basis of the concentration of aerosol and sea salt derived species (nitrate, chloride) leached from the snowpack. Concentrations are high in subglacial waters which are fed by snowmelt, and low in englacial waters dominated by ice melt (Richards et al. 1996).

The above mentioned definitions are generalized, since the hydrological pathways of the components are complex and interconnected. Moreover, the structure of a drainage system changes throughout a melt season (Sharp et



al. 1995, Nienow et al. 1998), as shown in figure 2.1. An alternative basis for distinguishing between drainage components is the residence time of meltwaters at the glacier bed, resulting in components called delayed flow and quick flow (e.g. Tranter et al. 1993, Sharp et al. 1995). Early in the ablation season, bulk runoff is dominated by delayed flow, and discharge and suspended sediment concentrations are low. As the ablation season progresses, the dominance of quick flow increases, along with suspended sediment concentrations (Tranter et al. 1993).

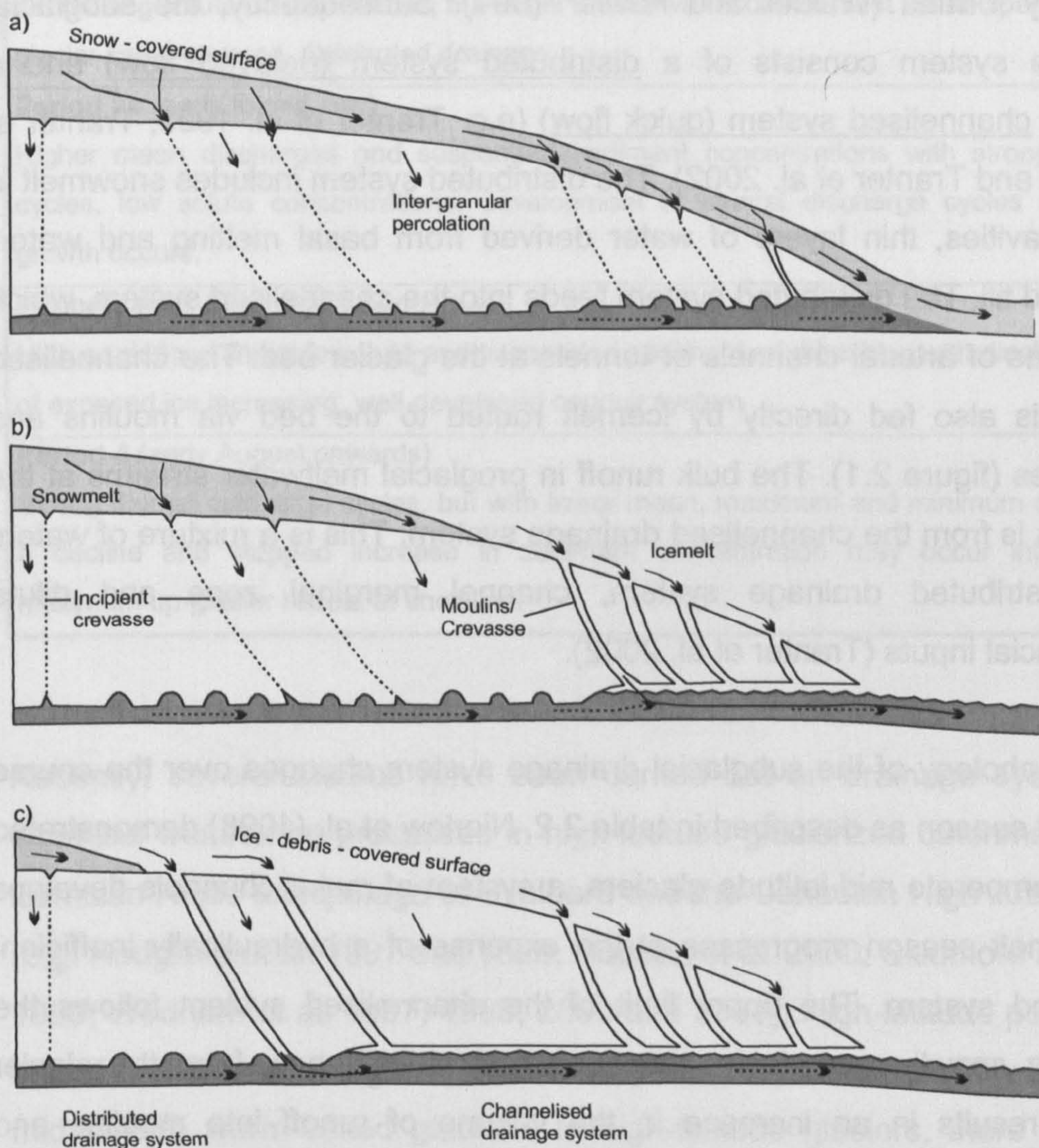


**Figure 2.1.** Development of the subglacial drainage system beneath a warm-based Alpine glacier (after Brown 2002 and Tranter et al. 1994).



#### **2.1.4. Development of drainage systems**

Most glaciers are underlain by a deformable bed of glacial till, which acts as a confined aquifer as long as it is much more permeable than the underlying bedrock (Fountain and Walder 1998). If the discharge is low, flow through the till will be sufficient to drain all meltwaters, but as discharge increases the till pore-water pressure will increase until a water film forms at the ice-till interface (Walder and Fowler 1994). This film accommodates little water flux but affects water chemistry (Fountain and Walder 1998). Due to the instability of the sheet flow, a network of drainage conduits - canals and channels - is gradually formed (Walder and Fowler 1994). Subsequently, the subglacial drainage system consists of a distributed system (delayed flow) and a discrete channelised system (quick flow) (e.g. Tranter et al. 1993, Tranter et al. 1997 and Tranter et al. 2002). The distributed system includes snowmelt in linked cavities, thin layers of water derived from basal melting and water-saturated till. The distributed system feeds into the channelised system, which is a series of arterial channels or tunnels at the glacier bed. The channelised system is also fed directly by icemelt routed to the bed via moulins and crevasses (figure 2.1). The bulk runoff in proglacial meltwater streams at the terminus is from the channelised drainage system. This is a mixture of waters from distributed drainage system, channel marginal zone and dilute supraglacial inputs (Tranter et al. 2002).

The morphology of the subglacial drainage system changes over the course of a melt season as described in table 2.2. Nienow et al. (1998) demonstrated that in temperate mid-latitude glaciers, a system of major channels develops as the melt season progresses at the expense of a hydraulically inefficient distributed system. The upper limit of the channelised system follows the retreating snowline up-glacier, because removal of snow from the glacier surface results in an increase in the volume of runoff into moulins and crevasses (figure 2.1) and short-term storage of large volumes of water. This induces high water pressures within the distributed drainage system, which causes it to evolve rapidly into a channelised system (Nienow et al. 1998). Similar evolution of drainage systems occurs in polythermal high Arctic glaciers, where approximately 40% of supraglacially-derived meltwater has



been found to route subglacially to the glacier snout (Nienow et al., submitted).

**Table 2.2.** Phases of the melt season (after Richards et al. 1996).

<p><b>Period 1</b> (early to mid-June)</p> <p>Low air temperatures, low flows and suspended sediment concentrations, high solute concentrations, glacier surface snow-covered, no conduits, distributed drainage over glacier bed.</p>
<p><b>Period 2a</b> (mid to late June)</p> <p>Gradual increase in discharge; suspended sediment concentrations relatively stable, decreasing solute concentrations, but larger diurnal variations of most solute species, glacier snow-covered, distributed drainage.</p>
<p><b>Period 2b</b> (early to mid July)</p> <p>Higher mean discharges and suspended sediment concentrations with stronger diurnal cycles, low solute concentrations, development of diurnal discharge cycles as conduit growth occurs.</p>
<p><b>Period 3</b> (mid July to early August)</p> <p>High peak flow, unstable solute and suspended sediment relationships with discharge, area of exposed ice increasing, well-developed conduit system</p>
<p><b>Period 4</b> (early August onwards)</p> <p>Strong diurnal discharge cycles, but with lower mean, maximum and minimum discharges, a decline and stepped increase in sediment concentration may occur intermittently, maximum up-glacier retreat of snowline.</p>

Recently, several studies have been carried out on drainage systems and chemical weathering processes in high-latitude glacierized catchments in the Eurasian Arctic archipelago of Svalbard and the Canadian High Arctic islands (e.g. Hodgkins et al. 1997 and 1998; Hodson et al. 2000; Skidmore and Sharp 1999; Wadham et al. 1997, 1998, 2000 and 2001). High-latitude polythermal-based and cold-based glaciers have very different meltwater flow paths from mid-latitude warm-based glaciers. In high-latitude glaciers, there is often a thick layer of cold englacial ice restricting the penetration of surficial meltwaters to the subglacial environment (Hodson et al. 2000). In cold-based glaciers, there is no subglacial drainage system, and meltwater routes via ice-marginal flow paths. Also, the occurrence of crevasses and moulins is limited by the slow rate of ice deformation, the low rate of glacier activity and the formation of superimposed ice (Hodgkins et al. 1998). Superimposed ice



forms at the base of the snowpack, where percolating meltwater refreezes on contact with underlying cold ice (Woodward et al. 1997).

Water stored beneath the warm-based core of polythermal glaciers may also escape through the cold-based snout via fissures in sediments beneath the permafrost layer, and emerge as a high-pressure upwelling (Wadham et al. 1998, Rippin et al. 2003). Other potential routes are fractures within basal ice (figure 2.2) or the ice-bed interface (Rippin et al. 2003). As a part of the drainage system evolution, at the early stage of melt season there is often a sudden and brief outburst of subglacially stored meltwater, blocked previously by a cold ice dam. This outburst usually has a high concentration of suspended sediments (Wadham et al. 2001, Skidmore and Sharp et al. 1999).

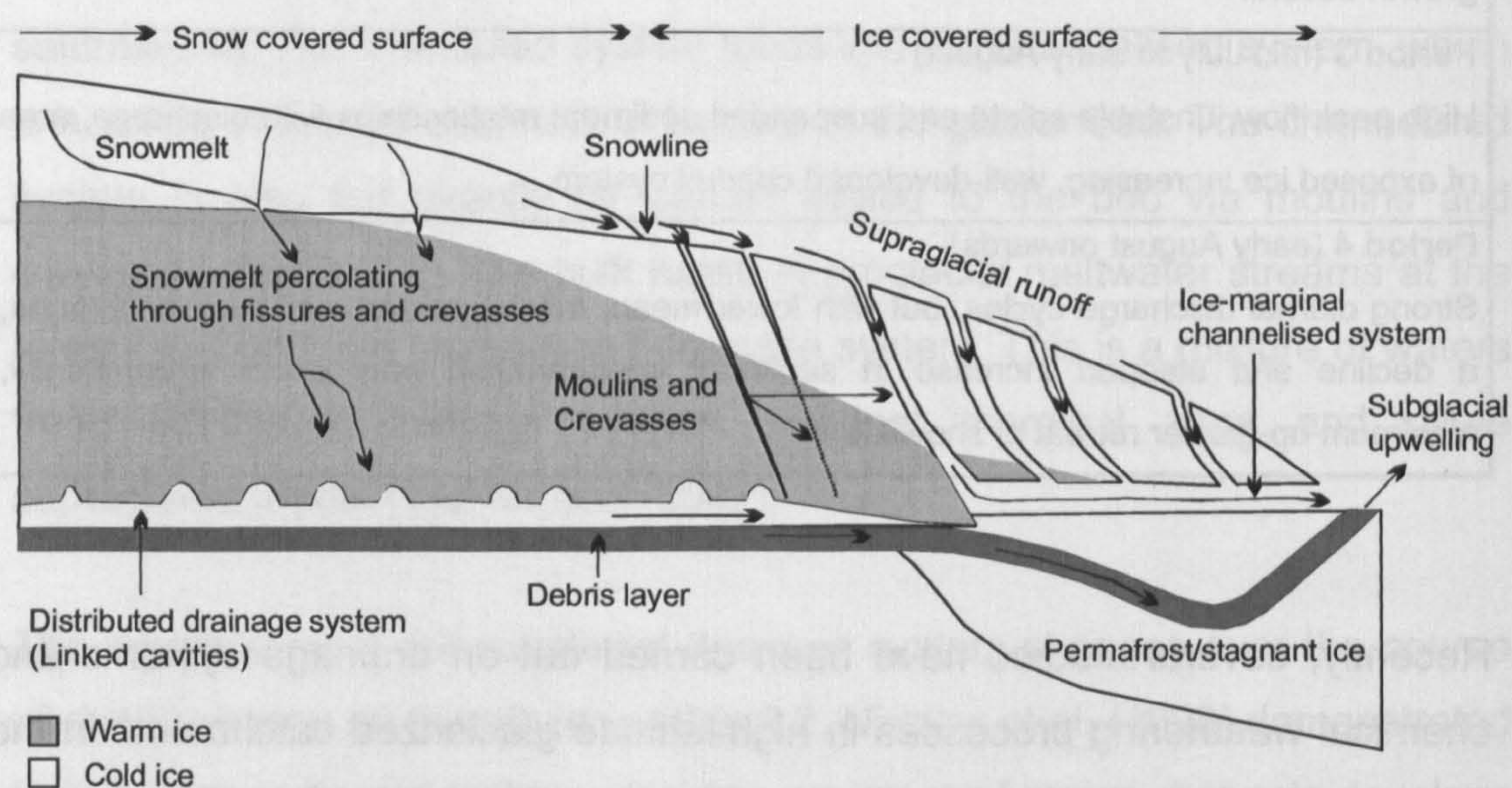


**Figure 2.2.** Routing of meltwater at a polythermal-based glacier (after Wadham et al. 1998).

Characteristic for high Arctic glaciers is the formation of proglacial icings, also called aufeis or naled (Hodgkins et al. 1997, Wadham et al. 2000). The proglacial icing is formed during winter by refreezing of meltwater, stored at the glacier bed at the end of the melt season, and continuing to emerge from the glacier during winter. Icings accumulate in the basin between the glacier terminus and the end moraine, and they play an important role in the solute budget, releasing ions such as  $\text{Na}^+$ ,  $\text{HCO}_3^-$  and  $\text{SO}_4^{2-}$  at the very start of the



melt season. Interstitial liquid water from icings usually has very high concentrations of solutes. There are several reasons for this. The long residence time, lasting all through the winter season, allow slow chemical reactions to add solute to the meltwater. Moreover, freezing of meltwater concentrates the residual interstitial water in the icing and increases the partial pressure of CO<sub>2</sub>, which dissociates to provide protons that promote further chemical weathering (Hodgkins et al. 1997).

## **2.2. Weathering in glacierized catchments**

### **2.2.1. Glacial erosion**

By definition, weathering is a process whereby rock is broken into smaller particles and eventually into constituent minerals. The whole process of weathering, which is largely a result of chemical alteration, also involves physical and biological processes (Ehrlich 1981).

Physical weathering processes in glacierized catchments include abrasion, fracturing and grinding, resulting in debris composed of rock fragments and fine-grained rock flour. In abrasion, bedrock is scored by debris carried in the sliding basal ice. Fractures may form along lines of bedrock weakness by the force of the overriding ice and the contained rock debris (Sugden and John 1976), or due to freezing and thawing of water in cracks (Ehrlich 1981). Rock flour with an average grain size less than 100 µm is the result of grinding at the ice-rock interface (Sugden and John 1976), and thus provides plenty of fresh reactive mineral surfaces on which biological and chemical processes take place.

The efficiency of physical glacial erosion is dependent on the bedrock composition and characteristics of glacier system. The lithology of the underlying bedrock determines the type and quantity of basal debris, whereas the thermal regime of the glacier, basal ice velocity and ice thickness are important glacier system variables. Abrasion and meltwater transport are most effective beneath warm-based ice, while freeze-thaw is significant when temperatures at the bed fluctuate around the pressure melting point. Basal ice



velocity and basal water pressure affects the amount of debris dragged across the glacier bed. High basal water pressure reduces friction between a glacier and its bed, thus weakening abrasion. Ice thickness has the opposite effect on friction; the thicker the ice the greater the potential for abrasion and rock fracture (Sugden and John 1976).

### **2.2.2. Biologically mediated weathering**

Biological processes play an important role in the weathering of surface soil layers. The interaction of microbes with inorganic compounds can be distinguished between enzymatic (direct) and nonenzymatic (indirect) interactions. Examples of enzymatic interactions include the oxidation or reduction of sulphur, iron and manganese compounds, the breakdown of chelates of inorganic compounds, and the hydrolysis of inorganic polymers, such as phosphate esters and polyphosphates. Nonenzymatic interactions include the deposition of inorganic compounds on a cell surface, and the reactions of metabolic end products of microbes with inorganic compounds, leading to precipitation, solution, chelation or structural alteration of insoluble inorganic compounds (Ehrlich 1981).

In subsurface and glacial environments, lack of carbon, nitrogen and phosphorus may limit microbial growth and metabolism. Bacterial cells often form microcolonies on particles in order to derive nutrients concentrated on their surface (Ehrlich 1981). Bacteria attach to sites of high surface energy, such as etches, pits, grooves and steps (Edwards et al. 1999). As a part of their metabolism, microbes produce  $\text{NH}_3$ ,  $\text{HNO}_3$ ,  $\text{H}_2\text{SO}_4$ ,  $\text{CO}_2$ , oxalic, citric and gluconic acids (Ehrlich 1981), as well as extracellular enzymes (Bennett et al. 2001). These metabolic products, especially polyfunctional organic acids, speed up the dissolution of minerals, releasing, for example, phosphorus and iron (Bennett et al. 2001). By forming complexes with metal cations on mineral surface or by decreasing the pH of solution, carboxylic acids are capable of increasing dissolution of aluminosilicates, carbonates, quartz and barite (Prapaipong et al. 1999). The dissolution rate depends upon the complexation structure formed between the organic ligand and the surface hydroxyl groups (Duckworth and Martin 2001).



Edwards et al. (1999) found in their pyrite dissolution experiments that in the presence of micro-organisms, oxidised Fe and S compounds (iron oxides and polysulphides) rapidly formed on the surfaces of pyrite crystals, whereas abiotic samples remained free of surface deposits. Bennett et al. (2001) have suggested that subsurface colonized feldspars containing trace nutrients necessary for micro-organisms weather very quickly, leaving behind a clay residue and feldspars without nutritive value. Colonized minerals were found to contain iron and phosphate as minor constituents, while the barren minerals were typically aluminium-rich, but without nutrient potential (Bennett et al. 2002). Thus, microbial activity may significantly alter weathering patterns as bacteria trying to survive in oligotrophic environment search for limiting nutrients.

### **2.2.3. Subglacial chemical weathering**

Basal thermal regime is a key factor controlling chemical weathering rates beneath glaciers (Wadham et al. 1997). Chemical weathering at warm-based glaciers mostly occurs in distributed drainage systems, due to long residence times and the continuous supply of freshly comminuted rock flour with reactive mineral surfaces (Tranter et al. 1993). At cold-based glaciers, the majority of weathering takes place in ice-marginal and supraglacial channels (Hodgkins et al. 1997). Comparison of the estimated chemical weathering rate at glaciers of different thermal regimes demonstrates the importance of a well-developed distributed drainage system. In studies by Wadham et al. (1997), the mean annual weathering rate at a polythermal-based high Arctic glacier was estimated to be  $330 \text{ meq}\Sigma^+\text{m}^{-2} \text{ year}^{-1}$ , whereas at a cold-based glacier it was only  $160 \text{ meq}\Sigma^+\text{m}^{-2} \text{ year}^{-1}$  (Hodgkins et al. 1997), and at a variety of warm-based glaciers ranged from 450 to  $1000 \text{ meq}\Sigma^+\text{m}^{-2} \text{ year}^{-1}$  (Wadham et al. 1997, Hodgkins et al. 1997).

A supply of protons is required for chemical weathering. In subglacial environment, protons may be generated by slow diffusion of atmospheric  $\text{CO}_2$  into solution (table 2.3, equation 1), oxidation of sulphides such as pyrite (equation 2), or dissolution of acid sulphate or nitrate aerosols precipitated or dry-deposited on to the glacier surface (equation 3) (Tranter et al 1993).



Moreover, CO<sub>2</sub> can also be released into solution from bubbles in glacier ice, englacial voids or microbial oxidation of organic carbon (e.g. Tranter et al. 1997, 2002). Protons are rapidly removed from solution by surface exchange and slower dissolution of the mineral lattice, and are replaced by base cations (e.g. Ca<sup>2+</sup>, Mg<sup>2+</sup>, K<sup>+</sup>, Na<sup>+</sup>) from rock-flour surfaces (Tranter et al. 1993). In catchments underlain predominantly by igneous and metamorphic bedrock, the dominant cation in bulk glacial outflow is Ca<sup>2+</sup>, with lesser quantities of Mg<sup>2+</sup>, Na<sup>+</sup> and K<sup>+</sup>, whereas the dominant anions are HCO<sub>3</sub><sup>-</sup> and SO<sub>4</sub><sup>2-</sup> (Brown 2002). The reason for the elevated Ca<sup>2+</sup> concentration is that CaCO<sub>3</sub> dissolves much more rapidly than silicates. Therefore, CaCO<sub>3</sub> dissolution may often be the main process of solute acquisition even when calcite is present in low concentrations (Thomas and Raiswell 1984).

The main mechanism by which rock minerals are weathered is acid hydrolysis, especially hydrolysis of carbonates (equation 4), aluminosilicates (equation 5) and silicates (equation 6) (Raiswell 1984). These reactions are the initial chemical weathering reactions also in subglacial environments, along with cation exchange of divalent ions for monovalent ions on surface exchange sites. Subsequently, carbonation reactions (equations 7 and 8) and coupled reactions of sulphide oxidation and carbonate dissolution (equation 9) take place (Tranter et al. 1993, 2002).

Assuming that CO<sub>2</sub> dissolution is the main source of H<sup>+</sup>, solute acquisition in the glacial system may follow two distinct chemical pathways: a closed-system pathway or an open-system pathway (Thomas and Raiswell 1984). High rates of weathering usually result in closed system conditions in subglacial cavities, where there is no dissolution of gaseous CO<sub>2</sub> to replace the H<sub>2</sub>CO<sub>3</sub>+CO<sub>2</sub>(aq) used in weathering. This is in contrast with open systems, where there is unrestricted transport of CO<sub>2</sub> between gas and water phases (Raiswell and Thomas 1984). As a consequence, the p(CO<sub>2</sub>), a measure of the pressure of dissolved CO<sub>2</sub>, goes below the atmospheric value of 10<sup>-3.5</sup> bar. Further closed-system weathering is limited in extent because the initial concentration of H<sub>2</sub>CO<sub>3</sub>+CO<sub>2</sub>(aq) can only supply an equivalent concentration of H<sup>+</sup>. Once this H<sup>+</sup> has been consumed, weathering by acid hydrolysis is restricted, unless other weathering reactions supply H<sup>+</sup> (table 2.3). However, when subglacial water from closed-system mixes with the



englacial component near the glacier terminus, undissociated  $\text{H}_2\text{CO}_3 + \text{CO}_2(\text{aq})$  available may initiate further solute acquisition, if reactive mineral particles are available (Raiswell 1984).

**Table 2.3.** The main geochemical weathering reactions in subglacial environments (after Tranter et al. 1993, 2002).

<b>Equation 1: Dissociation of dissolved carbon dioxide</b> $\text{CO}_2(\text{aq}) + \text{H}_2\text{O}(\text{aq}) \rightleftharpoons \text{H}^+(\text{aq}) + \text{HCO}_3^-(\text{aq})$
<b>Equation 2: Oxidation of pyrite</b> $4\text{FeS}_2(\text{s}) + 15\text{O}_2(\text{aq}) + 14\text{H}_2\text{O}(\text{aq}) \rightleftharpoons 16\text{H}^+(\text{aq}) + 4\text{Fe}(\text{OH})_3(\text{s}) + 8\text{SO}_4^{2-}(\text{aq})$
<b>Equation 3: Dissolution of acids</b> $\text{H}_2\text{SO}_4(\text{s}) \rightleftharpoons 2\text{H}^+(\text{aq}) + \text{SO}_4^{2-}(\text{aq})$ $\text{HNO}_3(\text{s}) \rightleftharpoons \text{H}^+(\text{aq}) + \text{NO}_3^-(\text{aq})$
<b>Equation 4: Carbonate hydrolysis</b> $\text{Ca}_{1-x}(\text{Mg}_x)\text{CO}_3(\text{s}) + \text{H}_2\text{O}(\text{l}) \rightleftharpoons (1-x)\text{Ca}^{2+}(\text{aq}) + x\text{Mg}^{2+}(\text{aq}) + \text{HCO}_3^-(\text{aq}) + \text{OH}^-(\text{aq})$
<b>Equation 5: Feldspar hydrolysis</b> $\text{KAlSi}_3\text{O}_8(\text{s}) + \text{H}_2\text{O}(\text{l}) \rightleftharpoons \text{HAlSi}_3\text{O}_8 + \text{K}^+(\text{aq}) + \text{OH}^-(\text{aq})$
<b>Equation 6: Pyroxene hydrolysis</b> $\text{Mg}_2\text{Si}_2\text{O}_6(\text{s}) + 6\text{H}_2\text{O}(\text{l}) \rightleftharpoons 2\text{Mg}^{2+}(\text{aq}) + 4\text{OH}^-(\text{aq}) + 2\text{H}_4\text{SiO}_4(\text{aq})$
<b>Equation 7: Carbonation of feldspar surfaces</b> $\text{CaAl}_2\text{Si}_2\text{O}_8(\text{s}) + 2\text{CO}_2(\text{aq}) + 2\text{H}_2\text{O}(\text{l}) \rightleftharpoons \text{Ca}^{2+}(\text{aq}) + 2\text{HCO}_3^-(\text{aq}) + \text{H}_2\text{Al}_2\text{Si}_2\text{O}_8(\text{s})$
<b>Equation 8: Carbonation of carbonate</b> $\text{Ca}_{1-x}(\text{Mg}_x)\text{CO}_3(\text{s}) + \text{CO}_2(\text{aq}) + \text{H}_2\text{O}(\text{l}) \rightleftharpoons (1-x)\text{Ca}^{2+}(\text{aq}) + x\text{Mg}^{2+}(\text{aq}) + 2\text{HCO}_3^-(\text{aq})$
<b>Equation 9: Sulphide oxidation coupled to carbonate dissolution</b> $4\text{FeS}_2(\text{s}) + 16\text{Ca}_{1-x}(\text{Mg}_x)\text{CO}_3(\text{s}) + 15\text{O}_2(\text{aq}) + 14\text{H}_2\text{O}(\text{l}) \rightleftharpoons$ $16(1-x)\text{Ca}^{2+}(\text{aq}) + 16x\text{Mg}^{2+}(\text{aq}) + 16\text{HCO}_3^-(\text{aq}) + 8\text{SO}_4^{2-}(\text{aq}) + 4\text{Fe}(\text{OH})_3(\text{s})$
<b>Equation 10: Oxidation of sulphide by ferric ions</b> $\text{FeS}_2(\text{s}) + 14\text{Fe}^{3+}(\text{aq}) + 8\text{H}_2\text{O}(\text{l}) + 16\text{CaCO}_3(\text{s}) \rightleftharpoons$ $15\text{Fe}^{2+}(\text{aq}) + 16\text{Ca}^{2+}(\text{aq}) + 2\text{SO}_4^{2-}(\text{aq}) + 16\text{HCO}_3^-(\text{aq})$
<b>Equation 11: Oxidation of organic carbon</b> $\text{C}_{\text{org}}(\text{s}) + \text{O}_2(\text{aq}) + \text{H}_2\text{O}(\text{l}) \rightleftharpoons \text{CO}_2(\text{aq}) + \text{H}_2\text{O}(\text{l}) \rightleftharpoons \text{H}^+(\text{aq}) + \text{HCO}_3^-(\text{aq})$



Sulphide oxidation occurs rapidly if freshly comminuted rock flour and oxidising agents are present. Hence, it is likely that reactive sulphides will be exhausted within the distributed system, and are largely absent from rock flour transported from the distributed system into the channelised system (Tranter et al. 1993). Generally, the rate of sulphide oxidation is controlled by the dissolved oxygen content, pH, temperature, surface area and the concentrations of  $\text{Fe}^{2+}$  and  $\text{Fe}^{3+}$ . Recent studies by Sharp et al. (1999) and Tranter et al. (2002) suggest that in subglacial environments, microbial activity also has a significant effect on the rate of sulphide oxidation. It has been estimated that sulphate yield from pyrite oxidation in abiotic system is two orders of magnitude less than from microbially mediated oxidation at +3 °C (Sharp et al. 1999). In addition, microbially mediated oxidation of organic carbon (table 2.3, equation 11) may be a significant proton source beneath glaciers. This would lessen the importance of atmospheric  $\text{CO}_2$  (table 2.3, equation 1) in acid hydrolysis reactions at the ice-bedrock interface (Brown 2002).

The concentration of dissolved oxygen in meltwater may be low in isolated subglacial cavities. The main reactions depleting dissolved oxygen are sulphide oxidation and microbial respiration. For example, in studies at Alpine glacier by Brown et al. (1994b), the percentage dissolved oxygen saturation ranged from 33 to 82%. After oxygen depletion,  $\text{NO}_3^-$  concentrations may also drop to zero in closed subglacial drainage system, even though nitrate is present in the initial supraglacial snowmelt (Tranter et al. 1994, Richards et al. 1996).

Concentrations of suspended sediment vary greatly throughout the ablation season from June to August. Early season runoff from the distributed system transports minimum amounts of suspended sediments, and the concentration increases along with increase in meltwater discharge. For example, at an Alpine warm-based glacier, the suspended sediment concentration in the ablation season 1989 ranged from  $0.1 \text{ g l}^{-1}$  in early June to  $6.0 \text{ g l}^{-1}$  at the end of July (Brown et al. 1994a). In the distributed system, rock-water ratios may be significantly higher than values detected in bulk runoff. Also, water passing through the distributed system may flow through immobile sediments without transporting them further due to the low flow velocity (Brown et al. 1994a).



Brown et al. (1994a) suggest that a significant proportion of the solute load of bulk meltwaters is derived from post-mixing reactions with suspended sediment. Post-mixing chemical reactions take place after the two components of meltwaters, dilute quickflow and concentrated delayed flow, are mixed. This proportion may reach 70% under high discharge conditions in August. On the other hand, so far most of the laboratory experiments on water-rock interactions in glacial environments have been conducted in free contact with the atmosphere, so called "free-drift" conditions (Brown 2002). The results of these experiments are not directly applicable to isolated cavities, distributed drainage systems or channel marginal zone. Therefore Brown (2002) emphasizes that further extended laboratory experiments are essential to investigate solute acquisition in closed-system conditions.

### **2.3. Micro-organisms in cold environments**

#### **2.3.1. Presence and activity of micro-organisms in cold habitats**

Metabolism of micro-organisms can be distinguished into three states: active, rest and anabiosis. The long-term survival at subzero conditions is commonly explained to be based on remaining in the state of anabiosis, in which the metabolic activity of cells is minimal (Vorobyova et al. 2001). Transition to the dormant state is a complicated process of structural changes in the cell, and thus differentiation of microbial communities into deep rest includes different levels of metabolic activity. Micro-organisms trapped in liquid veins of ice or unfrozen pores of permafrost sediments are dormant, but they remain alive if they are preadapted to subzero conditions (Gounot 2001). As soon as liquid water is present, metabolic activity becomes possible.

Water covers approximately 70% of the Earth's surface and the majority of this is marine. More than 90% by volume of the marine environment is at a temperature of +5 °C or less (Herbert 1986). In addition to the marine environment, polar regions, constituting some 14% of the Earth's surface, are at very low ambient temperature (Herbert 1986). Micro-organisms from polar



regions permanently face temperatures ranging from +2 to –35 °C (Feller et al. 1997, Deming 2002).

#### **2.3.1.1. Deep sea water and sediments**

Generally, temperatures in the deep sea water range from –1 to +4 °C (Deming 2002). In Arctic and Antarctic seawater and sediment, the temperature is approximately –1 °C, but still densities of bacterial cells as high as  $7.0 \log_{10} \text{ cells ml}^{-1}$  are present (Gerday et al. 2000).

In cold marine sediments, substantial anaerobic biodegradation of organic matter takes place, including a significant contribution by bacteria which use sulphate as an electron acceptor (Isaksen and Jørgensen 1996). Although sulphate reduction is considered to be the most important process of organic material degradation on the continental shelf (Jørgensen 1982), its importance in permanently cold environments along with the role of oxygen and nitrate has only recently been demonstrated (Sagemann et al. 1998). In Arctic sediments around Svalbard, the sulphate reduction rates accounted for 28% to 42% of the total benthic mineralization (Sagemann et al. 1998). Nedwell et al. (1993) estimated that 32% of the mineralization of organic material in Antarctic coastal sediment takes place through sulphate reduction.

Sulphate-reducing bacteria from Arctic marine sediments have been found to grow at temperatures as low as –1.7 °C (Knoblauch et al. 1999). In general, sulphate-reducing bacteria can be divided into two major groups: those that oxidise the carbon source completely to CO<sub>2</sub>, and those that oxidise the carbon source incompletely to acetate (Sahm et al. 1999; Knoblauch et al. 1999). Sulphate-reducing bacteria from Arctic marine sediments (Knoblauch et al. 1999) use volatile fatty acids (acetate, propionate, butyrate), as well as lactate and hydrogen, as substrates, although only one strain was able to oxidise fatty acids completely to CO<sub>2</sub>.



### **2.3.1.2. Sea ice**

Brine inclusions and the ice-water interface in sea ice provide microhabitats that support rich microbial populations (Palmisano and Garrison 1993). In sea ice, internal fluids remain liquid even at the wintertime temperature of  $-35\text{ }^{\circ}\text{C}$  (Deming 2002). Previously, Russell (1990) stated that there is no evidence of microbial growth at temperatures below  $-12\text{ }^{\circ}\text{C}$ , and according to Rothschild and Mancinelli (2001), the lowest recorded temperature for active microbial communities is  $-18\text{ }^{\circ}\text{C}$ . However, in recent studies respiratory activity has been detected in sea ice in the brine-filled veins between ice crystals at temperature as low as  $-20\text{ }^{\circ}\text{C}$  (Junge et al. 2001). Also, in the Antarctic dry valleys, endolithic microbial communities capable of growing between the crystals of porous rocks at 0 to  $-15\text{ }^{\circ}\text{C}$  have been found (Friedmann 1982).

A variety of morphological types of bacteria, including rods, cocci, straight and branching filamentous, have been found in association with sea ice (Palmisano and Garrison 1993; Sullivan and Palmisano 1984). Bacteria in sea ice are generally larger than those found in the seawater, indicating that the nutrient concentration is higher in the ice. As for a source of carbon and energy, both photoheterotrophic and chemoautotrophic bacteria have been detected. The main energy source, however, is dissolved organic material. (Palmisano and Garrison 1993).

### **2.3.1.3. Permafrost soils**

In permafrost soils, 0.5 - 3% of water is unfrozen, thus enabling survival of microbial populations. The upper layer from 0.5 to 1 m freezes and thaws every year. At a depth of 14 m below the surface, temperature remains at around  $-10\text{ }^{\circ}\text{C}$  throughout a year, and the thickness of unfrozen water layers at the substrate-ice interface may be 50 nm (Shi et al. 1997). Viable micro-organisms ranging from 2 to  $8\log_{10}\text{ cells g}^{-1}$  have been found in several sites in Siberian permafrost (e.g. Shi et al. 1997, Khlebnikova et al. 1990). Culturable aerobic and anaerobic bacteria growing at  $+4\text{ }^{\circ}\text{C}$  have been detected down to depths of 7.5 m (Gounot 2001). Viable anaerobic micro-organisms cultured from buried permafrost sediments include denitrifiers,



acetoclastic methanogens, hydrogenotrophic methanogens, iron(III)-reducers and sulphate-reducers (Rivkina et al. 1998). Sulphate-reducing bacteria from these sediments produced sulphide after six months of incubation at +4 °C, but potential activity at subzero temperatures was not tested (Rivkina et al. 1998). Acidophilic autotrophs and heterotrophs capable of iron solubilisation using FeS<sub>2</sub> as an electron donor even at 0 °C have been detected in exposed sulphide ore material in Greenland (Langdahl and Ingvorsen 1997).

#### **2.3.1.4. Glaciers**

In glacierized regions, micro-organisms can live in the full spectrum of subsystems, from snowpack in the accumulation area on the top of the glacier, through glacial ice, subglacial and supraglacial meltwaters and sediment beneath the ice, to proglacial moraine.

Micro-organisms found in remote glacial ice can be either locally derived or dispersed airborne long distances and deposited in the snow covering the ice (Abuzov 1993, Willerslev et al. 1999). Microbial populations from 2.3 to 3.7 log<sub>10</sub> cells ml<sup>-1</sup> have been found in Antarctic surface snow and firn (Carpenter et al. 2000), whereas in Alpine mountain ridges, bacterial abundance of 4.0 log<sub>10</sub> cells ml<sup>-1</sup> was found in surface snow to a depth of 10 cm (Sattler et al. 2001). Low levels of metabolic activity (<sup>3</sup>H-thymidine and <sup>3</sup>H-leusine incorporation) of micro-organisms in snow were detected at temperatures from -12 to -17 °C. The potential sources of energy for these bacteria are allochthonous marine microbes and other organic matter in snowfall (Carpenter et al. 2000).

Several deep core drilling expeditions have been conducted in Antarctica to study the distribution of viable micro-organisms at various depths within the ice sheet (e.g. Abyzov 1993, Abyzov et al. 1998, Priscu et al. 1999). Viable micro-organisms have been found in ice layers from 10000 to 13000 years old. Among the micro-organisms isolated are representatives of both non-spore-forming and spore-forming bacteria, non-spore-bacteria being prevalent in the younger surface layers (Abyzov 1993). In central Antarctica, microbial cells have been found to depths of 2405 and 2750 m (Abyzov 1993, Abyzov



et al. 1998). The total number of cells was  $2.9 - 4.0 \log_{10} \text{ cells ml}^{-1}$ , of which some were still viable, after 110000 - 240000 years of anabiosis (Abyzov et al. 1998). Furthermore, Priscu et al. (1999) detected microbial cells ( $3.4 - 4.6 \log_{10} \text{ cells ml}^{-1}$ ) in ice from a depth of 3590 m in central Antarctica. When incubating the ice melts with  $^{14}\text{C}$ -labeled acetate and glucose at  $+3^\circ\text{C}$ , production of  $\text{CO}_2$  was detected indicating the presence of metabolically active cells. Ice at this depth represents refrozen water from the subglacial Lake Vostok accreted to the bottom of the glacial ice. Thus the finding implies that Lake Vostok, which is kept liquid by the pressure of the ice overburden and possibly by geothermal heating, may support a microbial population, despite more than 1000000 years of isolation from the atmosphere (Priscu et al. 1999).

The recent finding of Campen et al. (2003) demonstrated anomalously high concentrations of  $\text{CO}_2$ ,  $\text{N}_2\text{O}$  and  $\text{CH}_4$  within a low-latitude South American mountain glacier, suggesting a presence of metabolizing micro-organisms within the ice. Campen et al (2003) stated that the high length/diameter ratio of veins along three-grain-junctions, described also by Price (2000), restricts oxygen diffusion and allows slow metabolism to exhaust oxygen and other electron acceptors, finally resulting in methanogenesis. According to Mulvaney et al. (1988), polar ice consists of solid ice grains with air bubbles and grain boundaries filled with liquid veins. One major component in these veins is sulphuric acid (Mulvaney et al. 1988), which remains liquid at glacial ice temperature of  $-5^\circ\text{C}$  (Deming 2002). Higher concentrations of solutes in veins will also prevent the fluid network from freezing. In addition, on freezing bacteria may be preferentially partitioned into the vein network (Pettitt and Parkes, personal communication). Price (2000) suggests that in these veins energy and carbon are provided for bacteria. Methanosulphonic acid ( $\text{HCH}_3\text{SO}_3$ ), formic acid ( $\text{HCOOH}$ ) and acetic acid ( $\text{CH}_3\text{COOH}$ ) can be sources of energy and carbon, and aqueous sulphuric acid and nitric acid are the main electron acceptors. In Antarctic glacial ice, the above mentioned organic acids have been detected with concentrations of  $0.084 \mu\text{M}$ ,  $0.020 \mu\text{M}$  and  $0.013 \mu\text{M}$ , respectively (Price 2000).

Viable and active microbial populations have been found in glacier runoff and basal ice in several glacial systems (Sharp et al. 1999; Skidmore et al. 2000a



and 2000b). In Alpine valley glaciers (Sharp et al. 1999), the total number of bacterial cells in meltwaters ranged from 4.7 to 5.7 log<sub>10</sub>cells ml<sup>-1</sup>, whereas in debris-rich basal ice the number of cells was 7.0 log<sub>10</sub>cells ml<sup>-1</sup>, supporting the finding also stated by Skidmore et al. (2000a) that bacterial populations are positively correlated with sediment concentrations. From 5 to 24% of the cells counted were dividing or had just divided, suggesting that part of the population was active (Sharp et al. 1999).

Furthermore, viable aerobic and anaerobic bacteria were enriched at +0.3 to +4.0 °C from thawed basal ice from a polythermal Canadian High Arctic glacier (Skidmore et al. 2000a). Strictly anaerobic methane-producing microorganisms were present in the basal ice, demonstrating that within the unfrozen basal sediments there are anaerobic microenvironments that have the potential to generate methane subglacially (Skidmore et al. 2000a). Earlier, Souchez et al. (1995) measured very low oxygen concentrations (3%) in basal ice from central Greenland, indicating that oxidation of organic matter underneath the ice may drive conditions anoxic and thus stimulate anaerobic bacterial activity.

Organic detritus originated from ice also accumulates at the front of the glacier. Aerobic heterotrophic bacteria have been found in these proglacial sediments from the Canadian Rocky Mountains, the Alps and Norwegian Lapland. The number of viable bacteria growing on soil extract agar plates at +2 °C ranged from 4.8 to 6.6 log<sub>10</sub> cells per g dry weight (Gounot 2001).

Welker et al. (2002) detected considerable microbial activity in the soils adjacent (< 0.10 m) to glaciers in the Canadian Arctic and Greenland. Microbial populations in soils that have just become ice-free were actively decomposing ancient soil organic matter and releasing detectable levels of CO<sub>2</sub>. Rates of soil CO<sub>2</sub> efflux increased with distance from the ice, reaching a maximum of 3.5 g CO<sub>2</sub> m<sup>-2</sup> d<sup>-1</sup> at a site that had been deglaciated for 5000 years. This is consistent with findings of Sigler and Zeyer (2002) in two Alpine glacial forefields, where activity (measured by assays of dehydrogenase activity and fluorescein diacetate hydrolysis activity) in soil was as low as 2.00 µg TTC reduced g<sup>-1</sup> soil h<sup>-1</sup> next to the glacier terminus, but increased steadily as distance increased. According to Welker et al. (2002), indigenous microbial



populations adapted to permanently cold environment were already present and active under the ice before being released by the receding glacier. This explanation is supported by findings by Skidmore et al. (2000a) on active microbial populations beneath a Canadian High Arctic glacier.

### **2.3.2. Psychrophilic and psychrotrophic micro-organisms**

Cold-adapted micro-organisms that may grow at 0 °C are called either psychrophiles or psychrotrophs. Psychrophilic organisms have an optimum growth temperature < +15 °C and an upper cardinal temperature around +20 °C, whereas psychrotrophs have an optimum growth temperature > +15 °C and an upper cardinal temperature > +20 °C, although they are able to multiply close to 0 °C (Morita 1975). Mesophilic species that are able to acclimatize at low temperatures are called psychrotolerants (Feller and Gerday 1997). Surprisingly, in permanently cold environments such as polar regions and deep-sea waters, the psychrotrophs are relatively more abundant than the psychrophiles (Feller et al. 1996). Also, among Antarctic marine sulphate-reducing bacteria, psychrotrophic bacteria rather than truly psychrophiles appear to be predominant (Isaksen and Jørgensen 1996). On the other hand, the majority of true psychrophiles that has been isolated are from marine environments. Compared with permafrost, marine environments provide bacteria with stable temperature and an easy access to water and nutrients, resulting in a higher metabolic activity and division rate (Shi et al. 1997).

### **2.3.3. Characteristics of microbes living at low temperatures**

Adaptation of micro-organisms to the glacial environment is a result of the survival mechanism triggered by several factors, the main ones being constantly low temperature, lack of nutrients and cycles of freezing-thawing. However, when an organism is challenged by one set of conditions, cross-protection may occur against other stresses. For instance, stress of starvation causing natural desiccation and the formation of stress proteins which cross-protect also against low temperature (Morita 2000).



Temperature influences the response of microbes either directly by its effect on growth rate, enzyme activity, cell membrane composition and nutritional requirements, or indirectly through its effect on the solubility of solute molecules, ion transport and diffusion, osmotic effects on membranes, surface tension, density and many colloidal properties of matter in aqueous systems (Oppenheimer 1970; Herbert 1986). Cold-adapted micro-organisms have evolved a mixture of mechanisms to compensate for these effects of low temperature on cell metabolism.

#### **2.3.3.1. Cold-adapted enzymes**

The lower temperature limit of life is commonly defined as the freezing point of cellular water. In freezing-thawing cycles, cells can be damaged by two mechanisms, the formation of ice crystals inside the cell and the increase in solute concentrations due to water crystallisation (Gounot 2001). In cold-adapted micro-organisms, synthesis of antifreeze glycoproteins and peptides depress the freezing point of cellular water (Feller and Gerday 1997). The antifreeze is also concealed outside the cell, hence protecting efficiently the bacterial cell against possible damages caused by the freezing of the surrounding water (Gerday et al. 1997).

Bacteria are particularly vulnerable to cold-shock while they are dividing and when they are initiating DNA replication. Psychrophilic bacteria produce cold-shock proteins in response to a drop in temperature, and also cold-acclimation proteins during continuous growth at low temperatures. Low temperatures reduce the viscosity of lipid cell membrane, impairing transport and other functions. The membrane bound enzymes that use intact acyl lipids for membrane formation are part of the mechanism for introducing double bonds into fatty acids, thus maintaining the optimum membrane lipid composition and fluidity (Russell 1997).

Generally, biochemical reactions display a reaction rate 2 - 3 times lower when the temperature is decreased by 10 °C (Feller and Gerday 1997). Sattler et al. (2001) stated that snow and ice bacteria showed a 1.5 fold



increase in growth rates if temperature was increased from 0 °C to +5 °C. Micro-organisms that are adapted to the cold environment produce enzymes which have high specific activity or turnover number, compensating for the effect of low temperature with catalytic rate (Feller and Gerday 1997; Feller et al. 1997). The higher specific activity can be explained by a lower activation energy resulting from an easier accommodation of the macromolecular substrates at low temperatures. This in turn is a consequence of a more flexible structure reducing the cost of the conformational changes required to interact with the substrate (Feller et al. 1996).

The flexible crystal structure of the psychrophilic enzymes is caused by a decreased number of hydrogen-bonding networks (Aghajari et al. 1998) and improved solvent interactions with a hydrophilic surface via additional charged side chains (Feller et al. 1997). Other structural features observed in cold-adapted enzymes are a lower hydrophobicity of the hydrophobic clusters forming the core of the protein, and a looser coordination of  $\text{Ca}^{2+}$  ions. The looser ion coordination can be a consequence of their folding flexibility (Feller et al. 1997).

#### **2.3.3.2. Structure and composition of cell membrane**

The cytoplasmic membrane is a highly selective barrier that surrounds the prokaryotic cell (figure 2.3). It has a structure of a phospholipid bilayer, containing both highly hydrophobic and hydrophilic (glycerol) moieties (Madigan et al. 1997). The hydrophobic fatty acids in Bacteria may be straight chain saturated, straight chain unsaturated, branched chain or cyclopropane acids (Herbert 1986). Lipids in Archaea (e.g. methanogens) lack fatty acids, and instead have side chains composed of repeated units of the hydrocarbon molecule isoprene (Madigan et al. 1997).

Dynamically, the lipid bilayer is anisotropic: the interior of a bilayer is mostly well-organized, and only a small region in the middle is liquid-like (Driesen et al. 1996). Fatty acid composition affects the viscosity of the membrane lipids. In microbes adapted to low temperature environments, the most common feature is an increased proportion of unsaturated membrane lipids, and a



decreased proportion of branched chain lipids compared to mesophiles or thermophiles (Nedwell 1999).

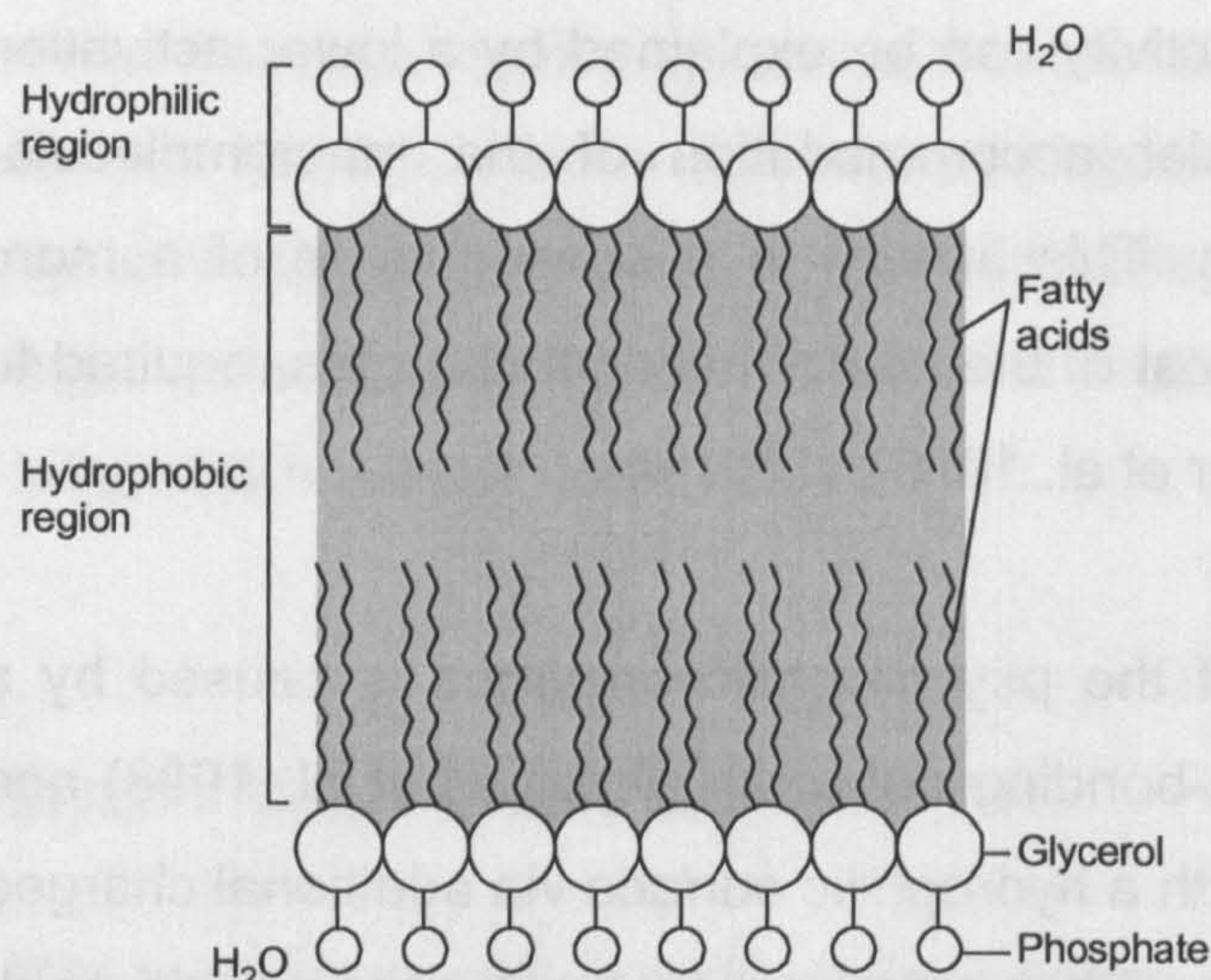


**Figure 2.3.** Structure of the cytoplasmic membrane in Bacteria (after Madigan et al. 1997).

The minimum temperature for the growth of microbes is largely controlled by the low temperature inhibition of solute transport processes into the cell at near-zero temperatures (Herbert 1986). Liquid-crystalline state is characterized by a fairly loosely packed, fluid and permeable structure. Transition from gel to liquid-crystalline state enhances solute transport, the assembly of transport proteins and the activity of membrane-bound enzymes (Herbert 1986). The previously mentioned changes in fatty acid composition produce membranes with a lower gel to liquid-crystalline transition temperature, thereby maintaining membrane mobility (Herbert 1986).

#### 2.3.4. Source of energy and nutrients in glacial environment

##### 2.3.4.1. Bioavailability of energy

Growth of micro-organisms in nature, especially in oligotrophic environments, is generally sporadic. Within a given microbial population, only a small portion of the cells may be growing while the others are in a no-growth state or in a



starvation-survival state, which is a physiological state resulting from an insufficient level of bioavailable nutrients or energy (Morita 1988). In nutrient-limited environments, survival of micro-organisms depends upon the ability of a species to compete over sparse resources of nutrients. Active transport of substrates by transporter proteins in the cell membrane depends upon the affinity of the micro-organisms for the substrates (Nedwell 1999). In glacial environment, affinity for substrates is severely lowered due to stiffening of the lipids of the membranes.

In extreme environments, microbial populations with extraordinarily slow growth rates have been found. The doubling time of the organisms may be months (Morita 1988). Novitsky and Morita (1977) found that marine vibrio starved at +5 °C were still viable after one year of starvation. In the deep sea, long-term survival periods as long as several decades without nutrients have been reported (Morita 1985). The recent findings have demonstrated that halophilic micro-organisms have survived 250 to 425 millions of years in fluid inclusions of halite (NaCl) (Vreeland et al. 2000, Fish et al. 2002). Halophilic Archaea have also been cultured from ancient brines, although they do not form protective spores. The long-term survival of these micro-organisms may be possible due to slow movement of fluid inclusions through rock salt, which supplies organic substrates and nutrients (Parkes 2000).

It has been suggested that in glacial systems the source of utilizable organic carbon may be derived from bedrock, soils or plant material overridden during glacial advance and from inwashing from the glacier surface (Sharp et al. 1999). Skidmore et al. (2000a and 2000b) reported that concentrations of particulate organic carbon in the debris-rich basal ice from a High Arctic polythermal glacier were 0.53 to 0.97 M of carbon, compared with 34  $\mu$ M in the glacier ice. Given that dissolved organic concentration as low as 0.2 to 1.7 mM in subglacial Antarctic lake provides sufficient organic substrates for bacteria (Ward and Priscu 1997), it is likely that debris-rich basal ice maintains enough carbon source readily available for bacterial metabolism. The Antarctic soils without vegetation contain approximately 0.05 to 1.5 % organic carbon (Vishniac 1993). As for the composition of bedrock, shales deposited during the Cretaceous period have been found to include high enough contents of organic carbon (TOC from 0.75 to 1.5 % w/w) to maintain



activity of heterotrophic micro-organisms, although a fraction of organic matter is recalcitrant (Morita 2000).

Readily utilizable carbon is severely limited in soil and subsurface sedimentary rocks. Much of the organic matter in soils is resistant to decomposition, and is in the form of humic substances, tannins and lignins (Morita 1988). The recalcitrant polymeric compounds require energy to synthesize the necessary exoenzymes to degrade it into monomers so that the organic matter can be transported into the cell (Morita 2000). In addition, the bioavailability of organic substrates, such as polysaccharides, protein, peptides, amino acids, nucleic acids and nucleotides, is reduced when adsorbed to clay minerals in soils and sediments (Morita 1988).

The resistance of organic matter to degradation may be a mechanism of organic matter preservation so that it can be utilised slowly as a source of energy for maintenance over a long period of time. In aquatic environments, in addition to threshold levels of organic matter, alternative sources of energy such as methane, carbon monoxide, hydrogen and other reduced gases can be used (Morita 1986).

As a survival mechanism, many species of Bacteria produce dormant endospores, which are differentiated cells that are very resistant to extreme temperatures and also to other harmful agents such as drying, radiation and acids. Bacterial sporulation does not occur when cells are dividing exponentially but only when growth ceases due to exhaustion of an essential nutrient. An endospore may remain dormant but viable for at least several decades, maybe even millions of years, but it can convert back to a vegetative cell fairly rapidly. Sporulation requires that the synthesis of some proteins involved in vegetative cell functions cease and that specific spore proteins be made. The core of a mature endospore contains only 10-30% of the water content of the vegetative cell, and thus the consistency of the core cytoplasm is that of a gel (Madigan et al. 1997).



#### **2.3.4.2. Physiological adaptation to oligotrophic environment**

For microbes living in polar environments, physiological adaptation for growth both in cold and low nutrient and energy environment is vital. Studies on Antarctic marine bacteria demonstrated that the organism which normally grew morphologically as a rod-shaped cell responded to starvation by fragmenting to produce large numbers of ultramicrobacteria, able to pass through a 0.45  $\mu\text{m}$  pore size filter (Novitsky and Morita 1976; Morgan and Dow 1986). Also, aquatic bacteria passing through a 0.2  $\mu\text{m}$  filter have been isolated (Morita 1988). Microbial coccoid cells with a diameter of 0.1 to 0.4  $\mu\text{m}$  have been found in the deep ice core from Antarctica (Karl et al. 1999).

Ultramicrocells have generally a very slow growth rate (Morita 1986), and only a small fraction seems to be capable of forming colonies (Morita 1988). On inoculation of starved ultramicrobacteria into fresh medium, recovery normally occurs after an initial lag period proportional to the starvation period, due to a possible relationship between the period of starvation and the time taken for the ultramicrobacteria to attain a size suitable for cell division (Amy et al. 1983; Morgan and Dow 1986). Generally, the longer the starvation period, the longer the lag phase of the starved cells when placed in a nutrient rich environment (Morita 1988). Also Christner et al. (2000) suggest that aged dormant bacterial cells preserved in glacial ice need time to synthesize enzymes to repair cell damage before they can grow. Christner et al. (2000) found that when starved cells from glacial ice were plated on low nutrient media, they grew well since damaged cells had sufficient time for cell repair before initiating growth, whereas cells plated on rich nutrient media attempted to grow before they had repaired all the cell damage.

In oligotrophic environments, there is a limited supply of carbon and also other nutrients. However, studies on starvation for either carbon, nitrogen or phosphorus have revealed that only a lack of carbon allows for the development of stress resistant ultramicrocells that are able to immediately initiate an upshift and regrowth response by addition of nutrients (Kjelleberg et al. 1993a; Holmquist and Kjelleberg 1993). Nitrogen and phosphorus starved cells did not develop cross-protection against a variety of stress conditions (Kjelleberg et al. 1993a), but they formed filaments or swollen rods



with large inclusion bodies of poly- $\beta$ -hydroxy-butyrate (PHB) (Holmquist and Kjelleberg 1993). PHB is one of the most common carbon storage polymers occurring as inclusion bodies within prokaryotic cells (Madigan et al. 1997).

During the early phase of starvation there is an intense metabolic activity while the cells are increasing in number and fragmenting into small cells (Morita 1988). Even after fragmentation, the cells may continue to reduce in size (Morita 1986). Also, lipids, PHB, and carbohydrates disappear from the cells after being used as endogenous substrates (Morita 1988). At the later phase of starvation, cells utilize all the biosynthetic enzymes as well as other enzymes not necessary for the purpose of obtaining energy from the environment. Through the whole starvation-survival process, the genome remains intact and when sufficient nutrients are present, all the cellular enzymes are synthesized again (Morita 1988).



## **CHAPTER III DESCRIPTION OF FIELD SITES**

### **3.1. Criteria for selection of field sites**

Field sites were chosen on three main criteria:

- 1) the thermal regime of the glacier,**
- 2) the size of the glacier, and**
- 3) the composition of bedrock and rock debris in the catchment area**

The thermal regime of the glacier determines whether or not water flows in subglacial meltwater conduits (Patterson 1994). Since the main goal of this research was to study processes in meltwater and rock flour beneath ice, warm or polythermal thermal conditions were the primary criterion for site selection. Three field sites were chosen in Greenland, Norway and Svalbard. The two field sites in the subarctic coastal area of Greenland were chosen to represent two different sizes of outlet glaciers of polythermal inland ice (Weidick 1976; Weidick et al. 1992). The four outlet glaciers around Jostedalsbreen ice cap are warm-based, and located in southern Norway in warmer maritime climate (Bickerton and Matthews 1993). Thirdly, the glaciers in a High Arctic climate of Svalbard are polythermal-based valley glaciers, with complicated drainage systems, and in some marginal areas the glacier is frozen to the bed (Wadham 1997; Ødegård et al. 1997; Glasser and Hambrey 2001; Rippin 2001). No purely cold-based glaciers were included in this research, since generally they lack subglacial drainage systems.

A final criterion was the mineralogical composition of bedrock in the catchment area of the glacier. Oxidation of inorganic compounds and organic carbon in rock flour is a potential source of energy for micro-organisms living in subglacial cavities (Sharp et al. 1999). The aim was to take samples from sites with different bedrock compositions, and thus also meltwaters with varying chemical compositions. In the Greenland and Norway sites, bedrock consists mainly of Precambrian gneisses (Escher and Watt 1976; Oftedahl 1980). In Norway, part of the glacier lies on an area of metasedimentary rocks, including mica schists (Austrheim and Mørk 1988). The Svalbard sites are located in an area consisting primarily of Precambrian phyllites and mica schists with dolomitic and calcareous limestones and quartzite beds, although



Carboniferous to Jurassic carbonates, quartzitic sandstones, siltstones and shales can also be found (Hjelle 1993; Dallmann et al. 1990).

### 3.2. Akuliarusiarssuk Glacier and Manitsoq Glacier in Greenland

#### 3.2.1. Greenland Ice Sheet

The two glaciers are located on the south-western margin of the Greenland Ice Sheet ( $67^{\circ}18' \text{ N}$ ,  $49^{\circ}57' \text{ W}$ ), east from the Nordre Isortoq fjord (figure 3.1). The glaciers did not have any official names prior to the field expedition (Weidick et al. 1992), so they were named Akuliarusiarssuk and Manitsoq Glaciers (Jones 2002).

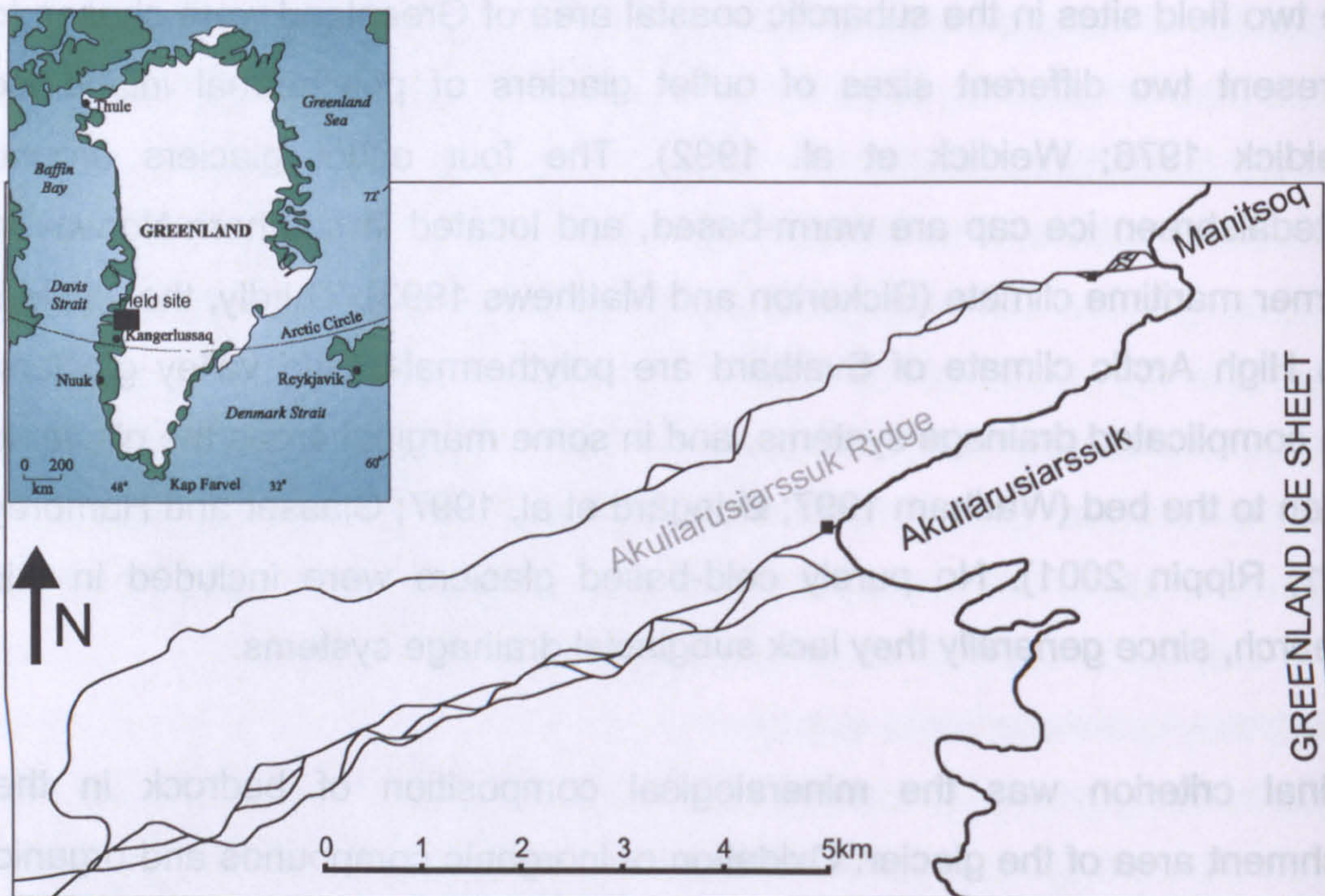


**Figure 3.1.** The Akuliarusiarssuk and Manitsoq Glaciers and their meltwater streams. (Figure prepared by Ian Jones, modified by Amy Jackson).

The total area of Greenland is  $2186000 \text{ km}^2$ , of which approximately 80 % is covered by inland ice (Escher and Watt 1976). The inland ice was initially formed during the first glaciation around 3 Ma ago, and the maximum was reached 0.4-0.2 Ma ago, during the Illinoian-Saale glacial stages. The main postglacial recession of the inland ice margin - at places up to 20 km - took



place 10000-6000 years BP, and 6000-5000 years BP the inland ice reached its present stability. During historical time, the glacier lobes have retreated gradually since 1920 (Weidick 1976). However, during recent decades, the glacier margin in the south-western slope of the inland ice has slightly advanced, mainly at the higher altitudes of the ice margin (Weidick et al. 1992).

The average thickness of the Greenland Ice Sheet is 1500 m. The southern part of the inland ice lies on a mountainous base approximately 1000 m a.s.l., and the ice forms a close-fitting cap with a maximum thickness of 850 m. The profile of the ice is steeper in the south than in the northern part of the ice sheet, resulting in more dynamically active conditions. The ice reaches its greatest thickness in the central and northern parts: bedrock is at sea level or up to 400 m below, and ice thickness is 3200-3400 m. In the eastern coast of Greenland, ice is cut off from the coast by high mountain chains. Consequently, any strong ablation to the east is prevented, whereas lower lying areas and the occurrence of subglacial valley systems in the western coast direct drainage to the west (Fristrup 1966).

### **3.2.2. Climate in Greenland**

Greenland has an arctic to subarctic climate (Jones 2002), the annual mean temperature on the different parts of the ice sheet varying from -6 °C to -30 °C (Fristrup 1966). Climatic records from the western coast and the centre of the inland ice show a distinct temperature difference. The July mean temperature ranges from +10 °C (coast) to -10 °C (inland). Coastal precipitation in the Nordre Isortoq region is 350 mm a<sup>-1</sup>, whereas inland it is 200 mm a<sup>-1</sup> (Weidick et al. 1992). On average, the annual snow accumulation on the ice sheet is 1 m (Jones 2002). Lower precipitation in some of the inland areas is due to the rain shadow effect of the coastal highlands (Weidick et al. 1992).



### **3.2.3. Geology of south-western Greenland**

The major part of Greenland consists of crystalline rocks of the Precambrian shield, in which four major structural provinces are recognised. The Nordre Isortoq fjord and glaciers draining to it are part of the province called the Nagssugtoqidian mobile belt. In this area bedrock consists mainly of Precambrian gneisses which were deformed about 2700 Ma ago (Escher and Watt 1976). In the study area, the basement is composed of granulite facies gneisses, containing plagioclase, quartz, hyperstene, biotite and hornblende as principal minerals. Also magnetite is present in most places. Supracrustal rocks, composed mainly of garnet-biotite-sillimanite gneisses, form thin belts, interlayered and deformed together with the basement gneisses. In places, there may occur horizons of graphite and marble (Escher et al. 1976).

The Holocene deposits of Greenland are found as thin, scattered occurrences of moraine on the bedrock. Thicker layers occur in valleys. The ice-free hilly uplands are covered largely by ground moraine. Signs of the ancient ice margin, such as terminal and marginal moraines, kame terraces, along with valley trains, can be found. In general, the clay fraction is scarce, both in the moraine matrix and glaciofluvial sediments. The slow production of organic material in arctic areas means that soil and peat deposits are thin and uncommon (Weidick 1976).

### **3.2.4. Glacier morphology and hydrology in Akuliarusiarssuk and Manitsoq Glaciers**

By definition, the main feature of the inland ice is a form which, apart from a narrow marginal zone, is independent of the subglacial topography (Weidick et al. 1992). In places, it is difficult to distinguish if the glacier is a marginal ice dome or a marginal sector of the inland ice. The field sites were chosen to represent outlet glaciers of the actual inland ice, to minimise valley glacier characteristics.

The Akuliarusiarssuk and Manitsoq outlet glaciers are part of the same marginal sector of the inland ice. The total area of the sector (for those parts



below 1800 m a.s.l.) is 1565 km<sup>2</sup>. The major supply for these slightly advancing lobed glaciers is snow and drift snow (Weidick et al. 1992). The Akuliarusiarssuk and Manitsoq glacier catchments are separated by the Akuliarusiarssuk mountain range. According to Jones (2002), the Akuliarusiarssuk and Manitsoq catchment areas are 55 km<sup>2</sup> and 16.5 km<sup>2</sup>, respectively.

The Akuliarusiarssuk glacier discharge system consists of a group of meltwater streams flowing through a wide valley (width approximately 800 m). Most of the meltwaters from the Akuliarusiarssuk glacier run south-west, but there is also a tributary river flowing to the south of the glacier snout. Apart from a small braided region in the glacier forefield, the Manitsoq glacier meltwaters drain along a single channel, which enters the main meltwater stream of the Akuliarusiarssuk glacier about 13 km south-west from the snout. Eventually, waters discharge into the Nordre Isortoq fjord (Jones 2002).

### **3.3. Jostedalsbreen Ice Cap in southern Norway**

#### **3.3.1. Jostedalsbreen Ice Cap**

Jostedalsbreen is a plateau ice cap located in southern Norway (61°30' - 61°53' N, 6°40' - 7°30' E). Covering an area of 486 km<sup>2</sup>, it is the largest ice cap on the European continent, with approximately 50 outlet glaciers descending from the plateau into surrounding valleys. The altitude at the highest point of Jostedalsbreen is 1960 m a.s.l., and the maximum ice thickness is approximately 500 m (Norske Statens kartverk 1995).

The last ice age in northern Europe finished about 9000 years ago, and glaciers in Jostedalsbreen area melted away. The current ice cap started forming 5000-2500 years ago, when the climate cooled. The ice cap extended to its latest maximum around 1750. Since then, most of the outlet glaciers have continually retreated, although there have been some short periods of advance (Norske Statens Kartverk 1995).



### **3.3.2. Climate in Jostedalsbreen**

The Jostedalsbreen ice cap is characterised by a maritime climate and a high annual rate of precipitation. The annual precipitation may exceed 2500 mm over much of the plateau (Bickerton and Matthews 1993); for example, in Nigardsbreen the annual precipitation is 2300 mm (Oerlemans 1992). Precipitation is lower in the valleys, glacier forelands receiving 1000-2000 mm a<sup>-1</sup> (Bickerton and Matthews 1993). Air temperatures also vary greatly in different parts of the ice cap. In 2000, in the upper parts of the glacier (1630 m a.s.l.), the daily mean air temperature for the summer season (June-September) was +2.0 °C, whereas it was +11.8 °C in the Jostedalen valley (324 m a.s.l.) (Kjøllmoen 2001). Mean annual temperatures in the forelands vary from +2 to +4 °C (Bickerton and Matthews 1993).

### **3.3.3. Geology of Jostedalsbreen area**

Norway consists of two major geological provinces, the Precambrian and the Caledonian. The age of the Younger Precambrian rocks is 570 Ma, but formation and metamorphism of supracrustal gneisses in the coastal area took place 1700 Ma ago. However, the Caledonian orogeny (main phase 435 Ma ago) affected large areas of Precambrian granitic rocks along the western coast of Norway (Oftedahl 1980).

The Jostedalsbreen ice cap is located in the southern Precambrian province, the Namsos-Bergen coastal gneiss area. South of 62° N, two major complexes can be identified in bedrock: the Jostedal Complex and the Fjordane Complex. The Jostedal Complex consists of strongly folded migmatized gneisses, whereas the overlying Fjordane Complex consists of a heterogeneous sequence of folded gneisses with layers of augen gneiss, schists, amphibolites, and metasedimentary rocks including quartzites, meta-anorthosites, eclogites and peridotites (Oftedahl 1980). Most of the Jostedalsbreen ice cap lies on the crystalline basement, but the southwestern part of the glacier reaches the geological setting of Western Gneiss Region which consists of middle and lower allochthonous metasedimentary



rocks, such as mica-schist, quartzo-feldspathic schists, marbles, calc-silicate gneisses and quartzites (Austrheim and Mørk 1988).

### 3.3.4. Glacier morphology and hydrology in four outlet glaciers of Jostedalsbreen ice cap: Bødalsbreen, Kjenndalsbreen, Nigardsbreen and Bergsetbreen

Field studies were carried out at four temperate outlet glaciers: two of them - Bødalsbreen and Kjenndalsbreen - are located at the north-western border of the ice cap; and two - Nigardsbreen and Bergsetbreen - at the south-eastern border (figure 3.2). In 2000, the glacier front at the north-western border was more or less stagnant, whereas at the south-eastern border the outlet glaciers advanced (table 3.1).

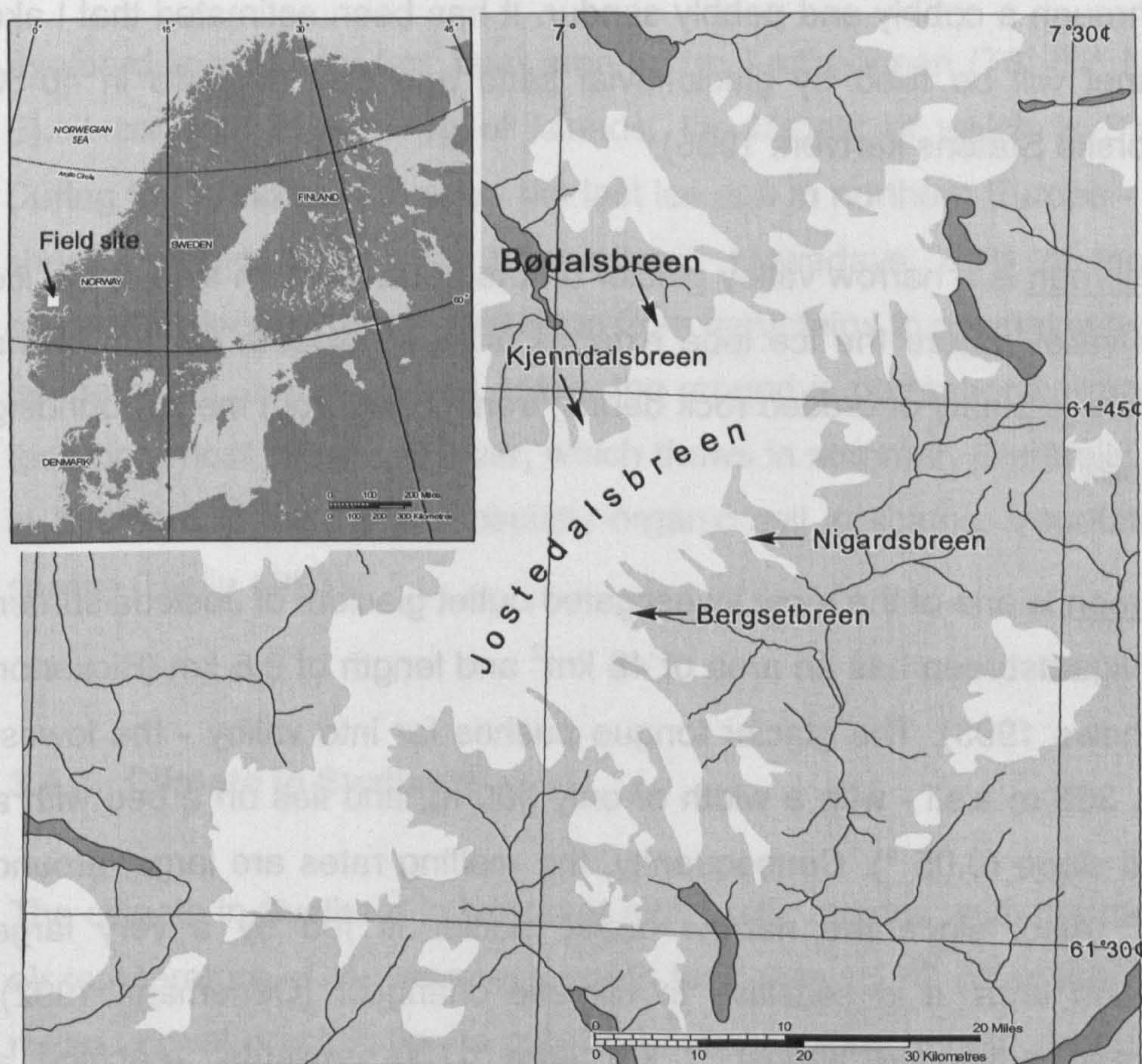


**Figure 3.2.** Jostedalsbreen ice cap and the four outlet glaciers studied. (Figure prepared by Mark Skidmore).



**Table 3.1.** Change in the position of the terminus of the Jostedalsbreen outlet glaciers from autumn 1999 to autumn 2000 (Kjøllmoen 2001). Positive value= advance, negative value=retreat.

Outlet glacier	Change (m)
Bødalsbreen	4
Kjenndalsbreen	-1
Nigardsbreen	23
Bergsetbreen	9

Bødalsbreen is a steep outlet glacier with surface area of about 8 km<sup>2</sup>, and length of 6.5 km. The altitude ranges from 740 to 1990 m a.s.l. (Bickerton and Matthews 1993). The proglacial Lake Sætrevatnet is located 500 m downstream from the glacier snout, fed by a network of meltwater streams flowing through a cobbly and pebbly sandur. It has been estimated that Lake Sætrevatnet will be filled by glaciofluvial sand and clay deposits in 40-50 years (Norske Statens kartverk 1995).

Kjenndalsbreen is a narrow valley glacier on the north-western side of the ice cap. The valley where the ice lobe extends is steep sloped. On top of the glacier there is plenty of eroded rock debris, transported from the surrounding rocky slopes.

Nigardsbreen is one of the most investigated outlet glaciers of Jostedalsbreen ice cap. Nigardsbreen has an area of 48 km<sup>2</sup> and length of 9.6 km (Bickerton and Matthews 1993). The glacier tongue pushes far into valley - the lowest altitude is 355 m a.s.l - with a width of only 500 m, and lies on a bed with a very small slope (0.05 °). Consequently, the melting rates are large, around 10 m a<sup>-1</sup>. Also, since the narrow outlet glacier is fed by a very large accumulation area, it is sensitive to climatic changes. (Oerlemans 1992). Nigardsbreen advanced almost 3 km from 1700 onwards, reaching a neoglacial maximum in 1748. After that, a steady retreat took place, and by 1987 the total retreat of the snout was 4.5 km (Norske Statens kartverk 1995, Oerlemans 1997). Since 1988, Nigardsbreen has advanced about 260 m. In 1999, due to the advance of the glacier front position, the meltwater drainage



system changed from one main river to several smaller channels (Kjøllmoen 2001). Nowadays, the glacier terminus overlies gneissic bedrock. All glaciofluvial deposits are flushed downstream to the proglacial lake and sandur. The current distance of Lake Nigardsbrevatnet from the glacier snout is about 500 m.

Bergsetbreen has an area of 8 km<sup>2</sup> and length of 10.5 km. It ranges from 1960 m a.s.l. to 560 m a.s.l. Due to the steep valley sides, extensive alluvial and colluvial fans have developed. The terminal moraines in the valley are composed largely of fine-grained sediments.

### **3.4. Midre Lovénbreen and Finsterwalderbreen glaciers in Svalbard**

#### **3.4.1. Glaciers in Svalbard**

Svalbard is a 63 000 km<sup>2</sup> land area in the Arctic ocean (76°-81° N, 11°-13 ° E). It consists of a group of islands, the largest of which is Spitsbergen. During the Weichsel ice age - the last ice age in northern Europe - a thick ice sheet covered large parts of Svalbard. Nowadays, 60% of land area is covered by local glaciers, stretching from mountains to coastal outwash plains by the fjords. In the ice-free areas, the ground is permanently frozen, except the uppermost 1.5 m soil layer, which thaws in summer. Generally, soil cover in Svalbard is thin, and especially organic soil is scarce. Vegetation is also sparse (Hjelle 1993).

#### **3.4.2. Climate in Svalbard**

The climate in Svalbard is typical of high arctic regions, with the mean annual air temperature of the warmest month less than +5 °C (Wadham 1997). The mean annual precipitation is only 300 mm, resulting in cold desert conditions (Hjelle 1993).



### 3.4.3. Geology of western Spitsbergen

The two field sites studied in this research are located on the western coast of Spitsbergen (figure 3.3). Roughly, bedrock in this region is composed of sedimentary and metamorphic rocks. In the vicinity of the coast line, there is a zone of thrust faults running from south-east to north-west. Along this fault zone occurs the contact of late Palaeozoic-Mesozoic sedimentary rocks and early Palaeozoic basement rocks (Hjelle 1993).

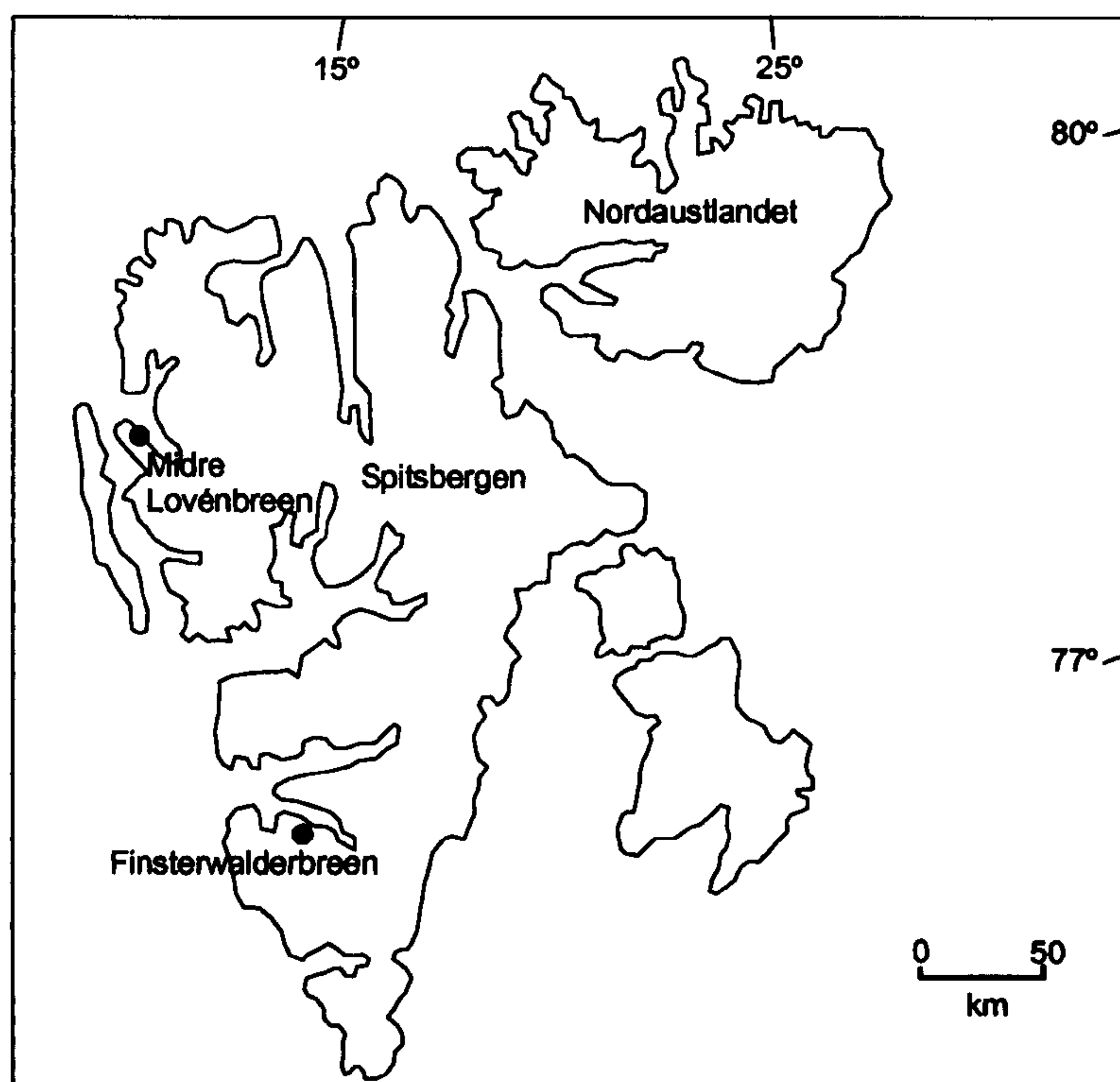


**Figure 3.3.** Location of the Midre Lovénbreen and the Finsterwalderbreen glaciers in Spitsbergen.

Midre Lovénbreen is located in north-western Spitsbergen, south of Kongsfjorden. Most of the catchment area is dominated by basement rocks, consisting of Proterozoic phyllites and mica schists with carbonate and quartzite beds. At the snout of the glacier, Carboniferous and Permian sedimentary rocks, such as sandstones, together with calcareous and dolomitic beds, underlie the proglacial end moraines (Hjelle 1993). The immediate proglacial forefield is covered by streamlined ridged moraine and a



moraine-mould complex. The uppermost layer down to 0.5-1.0 m consists of supraglacial gravel, glaciofluvial muddy-sandy gravel, and clast-rich muddy basal till. Pebbles, cobbles and boulders in this layer include both Proterozoic and Carboniferous lithologies (Glasser and Hambrey 2001).

Finsterwalderbreen is located in south-western Spitsbergen; between Recherchefjorden and VanKeulenfjorden. At the highest and southernmost part, the Finsterwalderbreen catchment reaches the basement zone, where bedrock consists of Proterozoic dolomitic and calcareous limestones, along with quartzite/gneissose. In places, limestones contain layers rich in the iron minerals magnetite and hematite (Hjelle 1993). Further north, at lower elevations, the bedrock composition is dominated by Carboniferous to Jurassic carbonates, quartzitic sandstones, siltstones and shales (Dallmann et al. 1990).

#### **3.4.4. Glacier morphology and hydrology in Midre Lovénbreen and Finsterwalderbreen**

Midre Lovénbreen is a small polythermal-based valley glacier 5.95 km<sup>2</sup> in area and 4.2 km long (Glasser & Hambrey 2002). The altitude ranges from 0 to 700 m a.s.l. (Fleming et al. 1997). The ice thickness is up to 180 m (Hodson et al. 2000). Midre Lovénbreen is a subpolar type glacier: it is frozen to the bed at the snout and margins, but has a warm basal layer up to 50 m thick beneath the central part (Glasser and Hambrey 2001). Since large areas of the glacier are at a higher altitude, formation of superimposed ice is significant. Superimposed ice makes up 10-30 % of the total mass balance (Fleming et al. 1997).

The mass balance (winter accumulation minus summer ablation) of Midre Lovénbreen has been negative almost continuously over the last 40 years, resulting in constant shrinkage of the glacier (Liestøl 1990). Midre Lovénbreen has retreated almost 1 km since a maximum ca. 1890 (Glasser & Hambrey 2002). Glasser and Hambrey (2001) suggest that, along with recession and thinning, the glacier's thermal structure is in a process of



transition from predominantly wet-based (Neoglacial maximum) through partly frozen (current phase) to completely frozen.

Since the glacier is frozen to the bed at the snout, no efficient subglacial drainage system at the terminus can develop. Nevertheless, both winter and summer drainage take place in Midre Lovénbreen. In the winter, proglacial icings are formed as a result of slow winter seepage through permeable sediments beneath a permafrost layer. In the summer, subglacial meltwater is stored at the boundary between cold and temperate ice. When water pressure becomes high enough, water is released and passes through the cold snout at the ice/bed interface. As a result, subglacial drainage emerges mostly in the form of a pressurised upwelling in the proglacial region (Rippin 2001).

The actual melt period takes place from late June until mid-September. During the high melt season, meltwaters drain through two main routes: the eastern pressurised proglacial upwelling, or the western conduit. High water pressures are required for water to break through to the west, and in most years pressures are too low for that (Rippin 2001). For example, field studies in summer 1999 proved that 76 % of the total proglacial discharge drained to the east, while 24 % flowed to the western proglacial stream. Proglacial discharge peaked in mid-July, the maximum discharge in eastern outlet being 4.0 to 4.5 m<sup>3</sup>s<sup>-1</sup>. Turbidity in the eastern outlet rose rapidly with increasing discharge, whereas in the western stream the change in turbidity was minor. This indicated that the eastern stream was mostly fed by the subglacial component, rich in sediments, but the western stream carried mainly supraglacial discharge (Rippin 2001; Hodson, unpublished data).

Finsterwalderbreen is 44 km<sup>2</sup> in area, 11 km long, and ice thickness ranges from 30 m to 200 m. It is a polythermal-based valley glacier with a two-layered thermal structure: the glacier is at the pressure melting point over most of its bed, but in the accumulation area, temperate ice is overlain by a 25-170 m thick cold layer (Wadham 1997, Ødegård et al 1997). Finsterwalderbreen can also be classified as a surge-type glacier: since a warm-based thermal structure is dominant, the basal drainage system is well-developed, resulting in build up for a potential major surge. A surging glacier



undergoes rapid increase in flow velocity of 10 to 200 fold (Wadham 1997). The last surge of Finsterwalderbreen took place between 1898 and 1920, when the glacier front advanced by 1.5 km and thickened by up to 100 m. Since 1920, the terminus of the glacier has thinned and retreated to the same dimensions as in 1898 (Nuttall et al. 1997).

Several supraglacial streams seep into Finsterwalderbreen via moulins and crevasses. At the terminus, the glacier is drained by three outflows: a basal conduit and a subterranean upwelling of water on the western margin, and an ice-marginal stream on the eastern margin. The two western outflows contribute 90 % of bulk runoff, the streams flowing parallel to the glacier terminus for 1 km, until they form a proglacial lake (Wadham 1997, Wadham et al. 1997).

There are distinct seasonal variations in the discharge of Finsterwalderbreen subglacial meltwater streams. Discharge is usually at its highest from mid-July until early August (Wadham et al. 1997). The meltwater flow peak often starts with a sudden outburst of subglacially stored concentrated meltwaters rich in suspended sediments (Wadham et al. 2001).



## **CHAPTER IV FIELD AND LABORATORY METHODOLOGY**

### **4.1. Field work**

Field work was carried out in 1999-2002 in Greenland, southern Norway and Svalbard during the melt season, from April to August. Sampling was focused on subglacial meltwaters but samples of supraglacial meltwaters, proglacial till and subglacially derived fine-grained rock flour were also taken.

#### **4.1.1. Design and preparation of sampling**

##### **4.1.1.1. Akuliarusiarssuk Glacier and Manitsoq Glacier, Greenland Ice sheet**

Subglacial and supraglacial meltwater samples were taken in the Greenland Ice Sheet in summer 1999 from June to August to determine the size of bacterial populations. Samples were also inoculated into growth media to detect the presence of culturable bacteria. Media used for iron-oxidising, nitrate-reducing and sulphate-reducing bacteria were inoculated with meltwater. A time course of samples were taken at the beginning of the melt season (June), during high discharge melt period (July) and at the end of melt season (August) to study temporal variation in microbial biomass.

##### **4.1.1.2. Jostedalsbreen ice cap, Norway**

Meltwater samples were taken from four outlet glaciers in different parts of ice cap twice in summer 2000 to determine the size of bacterial populations as well as seasonal and spatial variations of bacterial populations. Samples of subglacial and supraglacial meltwaters were taken in early melt period (early June) and during peak flow period (July). Again, samples were inoculated into growth media for nitrate-reducers and sulphate-reducers to quantify the presence of a range of different metabolic groups. In addition to meltwater samples, rock debris samples from the northern border of the Jostedalsbreen ice cap were taken before the melting period.



#### **4.1.1.3. Midre Lovénbreen and Finsterwalderbreen glaciers, Spitsbergen, Svalbard**

Subglacial meltwater samples were collected from Svalbard in early May 2001 and April 2002. The aim was to sample meltwater before the actual melt season, thus obtaining waters with a long residence time at the glacier bed. Meltwater samples were collected from Midre Lovénbreen.

The proglacial till and rock flour debris to be used in weathering experiments were taken from the Finsterwalderbreen outwash plain.

#### **4.1.1.4. Preparation of the sampling before field trips**

Both non-fixed and fixed meltwater samples were taken. 1000 ml polypropylene bottles were used for fresh non-fixed meltwater samples. Bottles were sterilised by autoclaving for 30 minutes at 121°C. For fixed meltwater samples, 250 ml DURAN-bottles were used. Bottles were sterilised by heating overnight at 550 °C. The plastic screw caps of the bottles were autoclaved at 121 °C for 30 minutes. As a fixing reagent, 25 ml of 0.2 µm filter-sterilised formaldehyde (38% w/w) was dispensed to the bottles.

Polypropylene boxes (volume of 2.2 litres) for proglacial till samples were autoclaved for 30 minutes at 121 °C with the lid loosely on.

Modified media for iron oxidisers, nitrate- and sulphate-reducers were prepared in the laboratory just before field trip. Liquid medium was dispensed into crimp vials, sealed with butyl septa and aluminum crimps. The recipes of the media used are given in the section 4.2.1.

Bottles for water chemistry samples were rinsed three times with milli-Q-water and dried overnight in a drying cabinet. Glass vials for DOC-samples were furnaceed overnight at 550 °C.



#### 4.1.2. Sampling methods

##### 4.1.2.1. Sampling water for microbiological analyses

Subglacial meltwater samples were taken from meltwater streams as close to the glacier margin as possible, the distance from ice margin varying from  $<10$  to 50 m (figure 4.1). Bottle was soaked in the meltwater stream upstream until filled full to the brim. Bottles were sealed under the water, to avoid air bubbles in the sample. While sampling, vinyl gloves swiped with ethanol were worn to avoid contamination. Supraglacial meltwater samples were taken from the trickles flowing on the top of the glacier following the same method.



**Figure 4.1.** Sampling meltwater from the Nigardsbreen meltwater stream in June 2000.

Water samples for inoculating growth medium vials *in situ* were taken from the meltwater streams with sterile 50 ml syringes, and injected to the crimp vials using sterile 0.4 x 40 mm needles (figure 4.2). Neoprene septa were wiped with ethanol before injection.





**Figure 4.2.** Inoculating growth media with supraglacial meltwater from the top of the Bødalsbreen outlet glacier in June 2000.

#### 4.1.2.2. Sampling for water chemistry analyses

Samples for analysing water chemistry were taken concurrently with the water samples for microbiological analyses.

FeSO <sub>4</sub> ·7H <sub>2</sub> O	0.50 g	taken
MgSO <sub>4</sub> ·7H <sub>2</sub> O	2.50 g	taken
Rosazurin 0.1 % w/v (redox indicator)	1.00 ml	taken
NaHCO <sub>3</sub> (sterile aqueous solution)		taken



#### **4.1.2.3. Meltwater discharge in meltwater streams**

Meltwater discharge in the meltwater streams was measured in the Manitsoq glacier (Greenland) and the Bødalsbreen glaciers (Norway) throughout the melt season. The gauging station was composed of pressure transducer, temperature sonde, conductivity probe and fluorometer. Discharge calculations were based on a pressure transducer time series recorded using a Druck PDCR1830 Pressure Transducer (Jones 2002).

#### **4.1.2.4. Sampling proglacial rock debris**

Samples of proglacial rock debris were taken in June and July 2000 in the Jostedalsbreen field site in southern Norway. Rock debris samples were taken in the forefield of Bødalsbreen outlet glacier, as close to the glacier terminus as possible.

In June, two test pits were dug. The first pit was dug 2 m from ice/snow front, and the second 100 m downstream, towards the proglacial lake. Samples were taken horizontally from two depths with a flame sterilised stainless steel scoop into sterile plastic bags or sterile polypropylene boxes.

Test pit 1: samples from the depth of 5-10 cm and 35 cm

Test pit 2 : samples from the depth of 5-10 cm and 15 cm

In July, rock debris samples were taken again at the two distances from the ice margin. Samples of fine-grained sediment slurry were taken from a small shallow pool of subglacial meltwater, 30 m from the snout. In the bottom of the pool, there was a 5-10 cm thick layer of sediment. A sample was taken from the surface layer of this deposit. 100 m downstream, rock debris sample from the bottom of the meltwater stream, from the depth of 0-10 cm, was taken.



**4.1.3. Transport and storage of samples**

In the field, water samples were stored refrigerated at +4 °C. Samples were transported to the laboratory in cool boxes with ice/ice blocks. In the laboratory, meltwater and proglacial rock debris samples were stored in cooled incubators at +2 °C.

**4.2. Laboratory experiments**

**4.2.1. Incubation of bacterial cultures**

In order to culture different metabolic groups of subglacial bacteria, the following growth media were used:

- SRB - medium for sulphate-reducing bacteria  
acetate and lactate as substrates, sulphate as an electron acceptor
- NRB medium for nitrate-reducing bacteria  
nitrate as an electron acceptor
- FeO medium for ferrous iron-oxidising bacteria

**SRB-medium (based on Postgate 1984)**

KH <sub>2</sub> PO <sub>4</sub>	0.50 g
NH <sub>4</sub> Cl	1.00 g
Sodium acetate (anhyd.)	0.90 g
Sodium lactate (60% lactic acid syrup)	1.92 g
Yeast extract	0.10 g
Ascorbic acid	0.10 g
CaSO <sub>4</sub>	1.00 g
FeSO <sub>4</sub> ·7H <sub>2</sub> O	0.50 g
MgSO <sub>4</sub> ·7H <sub>2</sub> O	2.00 g
Resazurin 0.1 % w/v (redox indicator)	1.00 ml
NaHCO <sub>3</sub> (sterile anaerobic solution)	30 ml



Thioglycollic acid	143 $\mu$ l
Deionised water	1000 ml

The medium was made with anoxic water. The pH was adjusted to 7.5 with 1 M NaOH before dispensing into 50 ml/100 ml/125 ml vials in an anaerobic cabinet, to be sealed with neoprene septa and aluminium crimp caps, and autoclaved at 121 °C for 40 minutes.

NRB-medium (based on Cragg et al. 1990)

Nutrient Broth (Difco, without NaCl)	25.00 g
KNO <sub>3</sub>	1.01 g
Resazurin 0.1 % w/v (redox indicator)	1.00 ml
Bromocresol purple (pH indicator)	1.00 ml
Deionised water	1000 ml

The medium was made with anoxic water. The pH was adjusted to 7.5 with 1 M NaOH before dispensing into 50 ml/100 ml/125 ml vials in the laminar flow cabinet. After dispensing and sealing the medium was autoclaved at 121 °C for 40 minutes.

FeO-medium (based on DSMZ medium 70: *Thiobacillus ferrooxidans* medium with ferrous sulphate)

(NH <sub>4</sub> ) <sub>2</sub> SO <sub>4</sub>	0.40 g
KH <sub>2</sub> PO <sub>4</sub>	0.40 g
MgSO <sub>4</sub> ·7H <sub>2</sub> O	0.40 g
H <sub>2</sub> SO <sub>4</sub> 0.1 M	900 ml
Sterile ingredients	
FeSO <sub>4</sub> ·7H <sub>2</sub> O	33.30 g dissolved in 100 ml water
Vitamin solution	3.00 ml
Trace elements	3.00 ml
Deionised water	1000 ml



The basic ingredients were added in 0.1 M H<sub>2</sub>SO<sub>4</sub>-solution, pH was adjusted to 3.0 with NaOH-pellets and then medium was autoclaved at 121 °C for 40 minutes. After cooling down the medium in the laminar flow cabinet, filter-sterilised (0.2 µm) ferrous-sulphate solution and sterile vitamins and trace elements were added. Finally, medium was dispensed under air into autoclaved 50 ml/125 ml vials.

Vitamin solution

4-aminobenzoic acid	0.004 g
D Biotin	0.001 g
Thiamine-HCl	0.010 g
Folic acid	0.002 g
Pyridoxine-HCl	0.010 g
Riboflavin	0.005 g
Nicotinic acid	0.005 g
DL calcium pantothenate	0.005 g
Lipoic acid (thiotic acid)	0.005 g
Cyanocobalamine	0.005 g
Anoxic water	300 ml

5 ml vials were sealed in anaerobic cabinet and autoclaved at 121 °C for 30 minutes. Solution was made with anoxic water and dispensed under O<sub>2</sub>-free N<sub>2</sub>-gas and sterilised with 0.2 µm-filter attached to syringe. To keep the sealed vials anaerobic, solution was dispensed into 5 ml vials with sterile OFN-flushed syringe and needle, with a sterile needle vent.

Trace elements

FeCl <sub>2</sub> ·4H <sub>2</sub> O	1.50 g in 10 ml 25% HCl
CoCl <sub>2</sub> ·6H <sub>2</sub> O	0.190 g
MnCl <sub>2</sub> ·4H <sub>2</sub> O	0.100 g
ZnCl <sub>2</sub>	0.070 g
H <sub>3</sub> BO <sub>3</sub>	0.062 g
Na <sub>2</sub> MoO <sub>4</sub> ·2H <sub>2</sub> O	0.036 g
NiCl <sub>2</sub> ·6H <sub>2</sub> O	0.024 g
CuCl <sub>2</sub> ·2H <sub>2</sub> O	0.017 g



Trace element solution was made up to 1000 ml with deionised water, autoclaved at 121 °C for 30 minutes and dispensed into 5 ml vials.

#### **4.2.1.1. Inoculating media with meltwater samples**

Media were inoculated in duplicate with meltwater samples either *in situ* immediately after sampling (Greenland and Norway samples), or in the laboratory after 2-6 days storage in the fridge at +4 °C (Svalbard 2001 samples). Because of potentially low numbers of viable micro-organisms in the highly oligotrophic glacial meltwater, the inoculation ratio of 2:1 was used:

Greenland cultures            60 ml of meltwater to 30 ml of medium;

Norway cultures              30 ml of meltwater to 15 ml of medium;

Svalbard 2001 cultures      30 ml of meltwater to 15 ml of medium.

With Svalbard 2002 samples, SRB medium was inoculated with fresh meltwater with three inoculation ratios, each in duplicate:

Svalbard 2002 cultures      10 ml of meltwater to 30 ml of medium;

   1 ml of meltwater to 39 ml of medium;

   0.1 ml of meltwater to 39.9 ml of medium.

Cultures were incubated at +2 °C, and subcultured once every 2-4 months using freshly prepared medium. Cultures were examined once a week or once in two weeks. Both NRB and SRB media produce a colour change indicating growth of bacteria which can be detected by visual examination. In SRB-cultures, production of a black iron monosulphide precipitate demonstrated growth of sulphate-reducing bacteria. Classification of degree of FeS precipitation was: 0=no change, hence no growth; 1=culture turning cloudy, dark grey precipitates indicating growth; 2=black precipitates indicating strong growth. In NRB-cultures, changes in colour and turbidity along with occurrence of precipitates indicated growth of nitrate-reducing bacteria. Categories of growth were: 0=no change in colour nor turbidity, no precipitates, hence no growth; 1= colour turned from deep purple to pale violet, slightly turbid, yellow precipitates indicating growth; 2= colour yellow-grey, turbid, lot of precipitates indicating strong growth. Visual estimation of growth was confirmed with acridine orange direct count.



#### **4.2.2. Thermal gradient experiments with enrichment cultures**

Thermal gradient experiments with enrichment cultures were conducted to determine the temperature characteristics of sulphate-reducing bacteria in meltwaters. The temperature gradient system described by Isaksen and Jørgensen (1994) with slight modifications (Barnes et al. 1998) was used. The system consists of an insulated aluminium block with a series of four rows of 47 wells for 5-10 ml crimp-top vials. The temperature gradient used was from -0.6 to +42.0 °C, the temperature difference between each row being 1.9 - 2.1 °C.

Before the thermal gradient experiment, cultures of sulphate-reducing bacteria were incubated at +2 °C, and subcultured once every 2-4 months. In the thermal gradient experiment, enrichment cultures after two subculturing were used.

The same SRB-medium used for culturing sulphate-reducing bacteria was prepared and dispensed into 5-10 ml vials. 5 ml of medium was inoculated with 0.25 ml of subculture. Enrichment cultures were then incubated in the temperature gradient system. At the beginning of the experiment, the vials were examined visually once a week. Uninoculated medium incubated at 0, +4 and +15 °C were used as a control. Samples for measuring sulphide production were fixed with 10 % w/v zinc acetate solution, 500 µl of sample to 125 µl ZnAc. Samples for acridine orange direct count were fixed with formaldehyde (0.25 ml of sample to 2.25 ml of 4% formaldehyde solution). Sulphide samples were stored frozen, and AODC samples at + 7 °C.

#### **4.2.3. Weathering experiments**

Three low-temperature weathering experiments were conducted with proglacial rock debris from Jostedalsbreen and Finsterwalderbreen, and meltwaters from Jostedalsbreen and Midre Lovénbreen:

- (1) Incubation of rock debris-meltwater mixture from Jostedalsbreen at +7 °C for 100 days
- (2) Incubation of meltwater from Jostedalsbreen and rock debris



from Jostedalsbreen and Finsterwalderbreen at a temperature range from  $-1.2$  to  $+2.6$  °C for 300 days

- (3) Incubation of meltwater from Midre Lovénbreen and rock debris from Jostedalsbreen and Finsterwalderbreen at  $+1.6$  °C for 100 days.

The earlier studies on bacterial populations and activity in meltwaters and debris-rich basal ice (Sharp et al. 1999) have demonstrated that in subglacial environment fine-grained rock flour provides a favourable substrate for microbial activity. While the initial DOC concentration in the Bødalsbreen meltwater was only  $6-12$   $\mu\text{M}$  and in the the Midre Lovénbreen  $400-450$   $\mu\text{M}$ , the potential major source of substrate during the several months incubation was the rock debris, i.e. organic and inorganic compounds released from the rock debris. This was the postulation in all the weathering experiments conducted.

#### **4.2.3.1. Weathering experiment with proglacial rock debris and subglacial meltwater from Bødalsbreen, Norway**

The objective of the first weathering experiment was to study whether glacial microbes can use fine-grained rock debris as an energy source at low temperatures and have an effect on rock weathering. The temperature in the sandy layers on the surface of the Bødalsbreen proglacial field ranged from  $+2.8$  to  $+8.8$  °C. Moreover, the first results from thermal gradient experiments showed that after five weeks incubation subglacial bacteria grew at the temperature range from  $+7$  to  $+30$  °C. Hence, the first weathering experiment was conducted at  $+7$  °C.

##### **4.2.3.1.1. Materials**

- Proglacial rock debris from Bødalsbreen, Norway
- Early melt season subglacial meltwater from Bødalsbreen, Norway.

Rock debris samples were crushed with mortar and pestle to maximise the area of reactive mineral surfaces. Porcelain mortar and pestle were sterilised



by heating before using. While crushing, samples were handled in the constant temperature room at +7 °C. Subsamples (1.0 g) were taken for analysing the final grain size distribution with a laser scattering based particle sizer (Mastersizer Micro, Malvern Instruments Inc., Southborough MA, USA).

Rock debris and meltwater were dispensed to sterile 5 ml crimp vials in the laminar flow cabinet: 0.5 g of rock debris and 5 ml of meltwater into each vial (rock/water ratio 100 g l<sup>-1</sup>). Vials with the headspace of air were sealed with neoprene septa and aluminium crimp caps. Rock debris-water mixtures for controls were sterilized by autoclaving at 121°C for 40 min to terminate the biological activity.

The biotic test vials and abiotic controls were incubated on a rocking table (Luckham 4RT Rocking Table) at the constant temperature of +7 °C.

#### **4.2.3.1.2. Sampling**

Gas and water samples were taken in triplicate after 1, 3, 7, 14, 28, 56 and 98 days incubation. First, gas samples from headspace of the three replicates of the biotic test vials and abiotic control vials were taken to measure oxygen and/or methane by gas chromatography. Water samples were taken for analysing anions (Cl<sup>-</sup>, NO<sub>3</sub><sup>-</sup>, SO<sub>4</sub><sup>2-</sup>), cations (Na<sup>+</sup>, K<sup>+</sup>, Mg<sup>2+</sup>, Ca<sup>2+</sup>), pH and total number of bacteria. Samples for anion-cation analyses were filtered through 0.45 µm membrane filter and stored at +2 °C for determination by ion chromatography. pH was measured immediately after sampling with a pH-microprobe at the room temperature.

Elemental composition (P<sub>2</sub>O<sub>5</sub>, Al<sub>2</sub>O<sub>3</sub>, Fe<sub>2</sub>O<sub>3</sub>, MnO, MgO, TiO<sub>2</sub>, CaO, Na<sub>2</sub>O, K<sub>2</sub>O) of the rock debris at the beginning and the at the end of the experiment was analysed by inductively coupled plasma-atomic emission spectrometry (ICP-AES).



#### **4.2.3.2. Long-term weathering experiment with proglacial rock debris from Norway and Svalbard, and meltwater from Bødalsbreen, Norway**

The objective of the experiment was to determine the effect of microbial activity on weathering at near-zero and sub-zero temperatures. An additional aim was to test the adaptation of glacial bacteria to the different geochemical environment. Therefore, microbes from Norway meltwater were incubated with rock debris both from Norway and Svalbard. The experiment was set up to simulate early melt season ice-bedrock interface, that is suboxic and anoxic subglacial cavities, where the subglacial water is mainly composed of long-residence time waters (Brown et al 1994a). At the base of a glacier, crushing produces sediment of particle size  $> 0.5$  mm and abrasion fine-grained rock flour  $< 0.5$  mm (Brown et al. 1996; Boulton 1978). The concentration of dissolved oxygen may be low in the distributed system where there is plenty of freshly ground rock material and hence reactive sulphide mineral surfaces, and access to an atmospheric source of oxygen is limited because linked cavities may be full of water (Brown et al. 1994b). Temperature at the base of the glacier is ca.  $0^{\circ}\text{C}$  (Skidmore et al. 2000), and in subglacial meltwater streams from  $+0.5$  to  $+2.5^{\circ}\text{C}$  (Brown et al. 1994a).

##### **4.2.3.2.1. Materials**

- Proglacial rock debris from Bødalsbreen, Norway
- Proglacial rock debris from Finsterwalderbreen, Svalbard
- Mid melt season subglacial meltwater from Bødalsbreen, Norway
- Mid melt season supraglacial meltwater from Bødalsbreen, Norway
- Subglacial meltwater-sediment slurry from Bødalsbreen, Norway

Proglacial fine-grained rock debris from Bødalsbreen, Norway and Finsterwalderbreen, Svalbard, was dried overnight at  $105^{\circ}\text{C}$  before grinding and homogenizing with an automatic mortar grinder "Pulverisette 2" (Fritsch GmbH, Idar-Oberstein, Germany). The agate (99.9 %  $\text{SiO}_2$ ) mortar and pestle were cleaned with milli-Q-water and acetone before using.



In the first weathering experiment abiotic controls were sterilised by autoclaving rock debris-water mixture at 121 °C for 40 minutes. However, autoclaving caused difference in the initial water composition between heated controls and non-heated test vials. Therefore, all the rock debris used in this experiment was sterilised by dry heat. Dry heat sterilisation requires higher temperatures and longer heating periods than does sterilisation with steam, but heating at 140 °C for 4 hours is adequate for most purposes (Norris and Ribbons 1969). Rock debris (6 g) was dispensed into 10 ml vials in the laminar flow cabinet. Vials were covered with tin foil, and then dry heat sterilised at 120 °C for 8 hours. Higher temperature was not used in order to avoid oxidation of bioavailable compounds in rock debris. Dry heat sterilising was repeated the day before the experiment started.

Meltwater (3700 ml) with no suspended sediments was mixed with 300 ml of meltwater-sediment slurry to maximise the number of active glacial bacteria, and stored at +7 °C until dispensed. The bottles were kept in ice in the laminar flow cabinet during the dispensing procedure.

#### **4.2.3.2.2. Dispensing meltwater for aerobic biotic test vials**

Meltwater (6 ml) was added to 6 g of rock debris in 10 ml vials. The vials were sealed with sterile butyl septa and aluminium crimp caps. Time-zero samples were taken from three separate vials immediately after dispensing. Biotic test vials and abiotic control vials were then moved to cooled incubators.

#### **4.2.3.2.3. Dispensing meltwater for anaerobic biotic test vials**

Meltwater was flushed with N<sub>2</sub>-gas overnight, bottle kept in the laminar flow cabinet in crushed ice. 2 l DURAN bottle with gas tubing system and dispensing hood was used when dispensing the water under OFN-gas into the vials. After filling the vials, air was released from the pores of the fine-grained rock flour. Therefore, before sealing, the water and headspace in vials (approximately 1 ml) was flushed with OFN-gas for 15-30 seconds.



Again, after sealing the time-zero sampling from three replicates was carried out immediately.

#### **4.2.3.2.4. Dispensing meltwater for aerobic abiotic control vials**

The meltwater for aerobic abiotic controls was filter-sterilised. First suspended solids were removed by prefiltering the water through pre-furnaced glass microfibre filters GF/C (pore size 1.2  $\mu\text{m}$ ). Water was filtered first through a 0.2  $\mu\text{m}$  filter unit, and then through a 0.1  $\mu\text{m}$  filter. After filter-sterilising the water was stored at +7 °C until dispensed in the laminar flow cabinet.

#### **4.2.3.2.5. Dispensing meltwater for anaerobic abiotic control vials**

Filter-sterilised meltwater was flushed overnight with N<sub>2</sub> -gas. 2 l DURAN bottle with gas tubing system and dispensing hood was used when dispensing the water under OFN-gas into 10 ml vials. Subsamples from the water were taken immediately for measuring time zero oxygen and pH. Before sealing, water and headspace in the vials was flushed with OFN-gas for 15-30 seconds.

#### **4.2.3.2.6. Incubation of the biotic test vials and abiotic controls**

The biotic test vials and abiotic controls were incubated in cooled incubators at three temperatures: -1.2- -1.0 °C ; +0.2 - +0.5 °C and +1.6 - +2.6 °C. All the vials were mixed manually using a Whirlmixer once a week.

Gas samples and water samples were taken from three separate aerobic and anaerobic biotic test vials and three separate aerobic and anaerobic abiotic control vials after 4, 17, 34, 63, 133, 203 and 298 days incubation.



#### **4.2.3.2.7. Water and gas sampling**

(1) 1 ml of gas sample from headspace was taken using a gas sampling syringe to measure oxygen and/or methane concentrations by gas chromatography. Before taking the sample the septum was wiped with ethanol and flame sterilised.

(2) 0.25 ml of water sample was fixed with 4 % formaldehyde solution for determining the total number of bacteria (0.25 of sample in 2.25 ml of formaldehyde solution).

(3) 0.2 ml of water sample was filtered through 0.45  $\mu\text{m}$  filter and fixed with 0.8 ml of 0.5 M HCl to analyse ferrous iron concentration. Samples were stored in the freezer.

(4) Dissolved oxygen content in water/rock flour mixture was measured directly with a microelectrode.

(5) 1 ml of water sample was filtered through 0.45  $\mu\text{m}$  filter for measuring pH with a microelectrode.

(6) 2 ml of water sample was filtered through 0.45  $\mu\text{m}$  filter for analysing anions ( $\text{Cl}^-$ ,  $\text{NO}_3^-$ ,  $\text{SO}_4^{2-}$ ), cations ( $\text{Na}^+$ ,  $\text{K}^+$ ,  $\text{Mg}^{2+}$ ,  $\text{Ca}^{2+}$ ) and organic acids. Samples were stored in a freezer and analysed by ion chromatography.

#### **4.2.3.2.8. Elemental composition of rock debris**

Grain size distribution of the rock flour was analysed with Mastersizer laser light scattering-particle sizing system. At the beginning and at the end of the experiment samples from rock flour were taken for CHNS-analysis and XRF (X-ray fluorescence spectrometer).



#### **4.2.3.3. Weathering experiment with proglacial rock debris from Norway and Svalbard, and meltwater from Svalbard**

Complementary weathering experiment was conducted with proglacial debris from Norway and Svalbard, and subglacial meltwater from Svalbard to verify results of the previous long-term weathering experiment. The incubation temperature was +1.6 °C.

##### **4.2.3.3.1. Materials**

- Proglacial rock debris from Bødalsbreen, Norway
- Proglacial rock debris from Finsterwalderbreen, Svalbard
- Early melt season subglacial meltwater from Midre Løvenbreen, Svalbard

The rock debris and meltwater (6 g of rock debris and 6 ml of water) were dispensed into 10 ml vials as described in the section 4.2.3.2. Meltwater was dispensed under air and the headspace in the sealed vials was air.

##### **4.2.3.3.2. Water and gas sampling**

Sampling procedure was identical with the long-term weathering experiment described in the section 4.2.3.2.7. Samples from two replicate biotic test vials and two replicate abiotic control vials after 32, 63 and 96 days incubation.

#### **4.3. Laboratory analyses**

##### **4.3.1. Suspended sediment concentration in meltwater samples**

Whatman GF/F 47mm filter papers were placed in a drying furnace at 100 °C for 30 minutes and were then allowed to cool in a desiccator. The papers were weighed individually on a five-figure balance. A filter paper was placed in a Millipore funnel filtration apparatus setup and the paper was washed with 100 ml of deionised water. 100 ml of the sample was measured out in a



volumetric flask and poured into the funnel. The flask was rinsed twice with deionised water and poured into the funnel. The funnel was then rinsed with deionised water to ensure that all suspended particles were on the filter paper. The filter paper was removed and dried in a drying furnace for 60 minutes. The filter papers were again placed in a desiccator and reweighed. This was repeated until the weights remained unchanged to ensure all the water had evaporated and the increase in weight was due to the suspended solid only.

### 4.3.2. Chemical analyses of water samples

#### 4.3.2.1. Major anions and cations in water by ion chromatography

Anion and cation concentrations in water samples were analysed by ion chromatography (Dionex DX 500) with micromembrane suppressor and conductivity detector (Hodgins et al. 1997). Guard columns IonPac®AG11-HC and IonPac®CG12 were used for preventing contamination of the separator. Both anions and cations were analysed with one run using a system of 4-mm analytical columns. The volume of the water sample dispensed into the autosampler vials was 800  $\mu$ l. Specifications for analytical columns are in the table 4.1. Precision and accuracy of the system are described in the table 4.2. Due to the high number of samples, numerous runs were done, and precision may have varied from one run to another. Hence, relative standard deviations for each run have been calculated, based on analysis of medium standard concentration after every tenth sample in the run. Minimum and maximum relative standard deviation of 26 runs is presented.

**Table 4.1.** Analytical columns used in Dionex DX500 ion chromatography.

	Anions (Cl <sup>-</sup> , NO <sub>3</sub> <sup>-</sup> , SO <sub>4</sub> <sup>2-</sup> )	Cations (Na <sup>+</sup> , K <sup>+</sup> , Mg <sup>2+</sup> , Ca <sup>2+</sup> )
column	IonPac®AS11-HC	IonPac®CS12A
injection loop volume	25 $\mu$ l	100 $\mu$ l
eluent	30 mM NaOH	20 mM MSA*
eluent flow rate	1.25 ml min <sup>-1</sup>	1.0 ml min <sup>-1</sup>

\* MSA = methanesulfonic acid



#### 4.3.2.2. Organic acids in water by ion chromatography

The Dionex DX 500 ion chromatography system with an IonPac®AS11-HC analytical column, which was used for analysing anion concentrations, was not designed for identification organic acids. However, the chromatograms showed the presence or absence of organic anions, such as lactate ( $\text{CH}_3\text{CH}(\text{OH})\text{COO}^-$ ), acetate ( $\text{CH}_3\text{COO}^-$ ), propionate ( $\text{CH}_3\text{CH}_2\text{COO}^-$ ), formate ( $\text{HCOO}^-$ ) and butyrate ( $\text{C}_3\text{H}_7\text{COO}^-$ ), as a combined peak with the shortest retention time, before the peaks of the common anions, such as chloride, sulphate and nitrate. These organic acids were separated and identified by high performance ion chromatography (Dionex DX600) gradient analysis using KOH as an eluent with concentration range from 1.5 to 40 mM. IonPac AG11-HC was used as a guard column and AS11-HC as a separator column, and continuous electrolytic suppression was accomplished with the ASRS-ULTRA suppressor. Standard solutions and precision of the system are described in the table 4.3.



**Table 4.2.** Precision and accuracy (min and max of 26 runs) of the Dionex DX500 ion chromatography system used to analyse major anions and cations.

Ion	Standard solutions (std1-std5 µeq l <sup>-1</sup> )	Correlation coefficient (%) (linear 5 point calibration curve) min-max	<u>Accuracy</u>		<u>Precision</u>	
			Std (µeq l <sup>-1</sup> )	Mean; n=6 (µeq l <sup>-1</sup> )	Relative mean error (%)	Check std conc. (µeq l <sup>-1</sup> ) Relative SD (%) min-max
Cl <sup>-</sup>	5-200 / 50-1000	99.9207-99.9998	17.29	18.16	5.05	250 0.58-6.66 (1 failed run 11.53)
			85.31	85.35	0.25	
SO <sub>4</sub> <sup>2-</sup>	2-250 / 10-1000	99.8909-100.0000	63.92	65.15	1.92	250 0.09-6.46 (1 failed run 11.61)
			315.48	325.37	3.14	
NO <sub>3</sub> <sup>-</sup>	0.5-50 / 1-200	99.6627-99.9987	33.21	37.08	11.67	50 0.91-6.54 (1 failed run 12.09)
			163.90	174.63	6.55	
Na <sup>+</sup>	10-500	99.9876-99.9999	179.56	175.60	2.20	250 0.20-3.68
K <sup>+</sup>	1-200 / 10-500	99.9861-99.9999	267.30	269.01	0.64	100 0.71-3.27
Mg <sup>2+</sup>	1-200 / 10-1000	99.6449-99.9999	459.42	465.92	1.41	100 0.30-2.53
Ca <sup>2+</sup>	10-500 / 50-1000	99.7531-100.0000	546.19	516.12	5.50	250 0.66-2.76



**Table 4.3.** Standards and precision of the Dionex DX600 gradient analysis using KOH as an eluent used to analyse major organic acids.

Monocarboxylic and dicarboxylic organic anions	Standard solutions (std1-std5 $\mu\text{mol l}^{-1}$ )	Correlation coefficient (%) (linear 5 point calibration curve)	Precision Check std conc. ( $\mu\text{mol l}^{-1}$ )	Relative SD (%)
formate $\text{HCOO}^-$	10-100	99.9771	50	2.32
acetate $\text{CH}_3\text{COO}^-$	10-100	99.8366	50	11.90
lactate $\text{CH}_3\text{CH(OH)COO}^-$	10-100	99.9754	50	3.20
propionate $\text{CH}_3\text{CH}_2\text{COO}^-$	10-100	99.7769	50	3.29
butyrate $\text{C}_3\text{H}_7\text{COO}^-$	10-100	99.8877	50	1.33
glutarate $\text{HOOCCH}_2\text{CH}_2\text{CH}_2\text{COO}^-$	10-100	99.3598	50	1.19
malate $\text{HOOCCH(OH)CH}_2\text{COO}^-$	10-100	99.8129	50	5.11
sorbate $\text{CH}_3\text{-CH=CH-CH=CH-COO}^-$	10-100	99.7833	50	20.49
succinate $\text{HCOOHC=CHCOO}^-$	10-100	70.4704	50	48.37



#### **4.3.2.3. Dissolved organic carbon in meltwater**

Dissolved organic carbon (DOC) in meltwaters was determined as described in Lafrenière and Sharp (2002). The concentration of dissolved organic carbon was measured as non-purgeable organic carbon (NPOC) by high temperature combustion (680 °C) with a Shimazu TOC 5000A analyzer equipped with a high sensitivity platinum catalyst.

#### **4.3.2.4. Ferrous iron concentration**

The following reagents were used in the preparation of meltwater samples for measuring ferrous iron by spectrophotometry (method based on Stookey 1970):

**0.5 M HCl:** 43 ml concentrated HCl made up to 1 litre with milli-Q-water.

**Fe<sup>2+</sup> standard solution:** 0.050 g of ferrous sulphate in 50 ml of 1.2 M HCl.

**Ferrozine reagent:** 0.5 g Ferrozine dissolved in 500 ml of 50 mM HEPES buffer (Buffer: 5.958 g HEPES in 500 ml milli-Q-water, pH adjusted to 7.0 with 1M NaOH).

Ferrozine reagent (5 ml) was added to a 0.5 ml aliquot of the acidified sample and standard solutions. Colour was allowed to develop for 30 minutes before measuring absorbance by spectrophotometer (CECIL Instruments CE292) with the wavelength of 562 nm.

#### **4.3.2.5. Sulphide concentration**

The following reagents were used when preparing samples for determination of sulphide production with spectrophotometer (method based on Cline 1969):

**10% (w/v) zinc acetate solution**

**Sulphide standard solution:** 0.075g Na<sub>2</sub>S • 9H<sub>2</sub>O in 100ml milli-Q-water.

**Colour complex reagent:** 10 ml of 0.22 M FeCl<sub>3</sub> (anhydrous) in 50%, and 10 ml of 0.17M *N-N*-dimethyl-*p*-phenylenediamine sulphate in 50% HCl.



Colour was allowed to develop for 50 minutes before measuring absorbance by spectrophotometer (CECIL instruments CE292) using wavelength of 670 nm. The concentration of sulphide in the samples was calculated from the absorbance-sulphide concentration calibration curve, based on linear spectrophotometric response with seven standard solutions, concentrations ranging from 0 to 0.623 mM. Effect of dilution with zinc acetate when fixing the samples was corrected by multiplying the concentration by 1.25.

#### **4.3.3. Determination of pH and oxygen concentration in water with microelectrodes**

Oxygen concentration and pH in the meltwater mixed with glacial rock flour were measured as described by Sagemann et al. (1999), using needle electrodes (768-20R oxygen needle electrode and 811 combination pH needle electrode, Diamond General, Ann Arbor, USA).

Oxygen concentrations were measured using a gold-plated platinum electrode with a built in Ag/AgCl reference electrode, and covered with an oxygen-permeable membrane. These electrodes were linked to a chemical polarographic microsensor system (Diamond General, Ann Arbor). The oxygen electrode was calibrated in milli-Q-water at +15 °C: 100% O<sub>2</sub> saturation calibration was performed by immersing the electrode in air-saturated water, and 0% O<sub>2</sub> saturation in water deoxygenated by flushing with OFN-gas for 15-30 minutes. While measuring oxygen concentration, vials were kept in the water bath at the temperature of +15 °C. Readings were taken after 60 seconds. The effect of temperature was eliminated by correcting the result, based on values of solubility of oxygen in water at different temperatures (European Standard EN 25814:1992).

Water samples were filtered through 0.45 µm filter to prevent rapid pH changes and fast pH dependent solid-aqueous reactions after samples were taken from the closed system and were exposed to the atmosphere. pH was measured using a 0.5 mm diameter needle electrode which is set in 1.25 mm



diameter stainless steel tube together with a capillary glass reference electrode (reference electrolyte 20% glycerol in 2.5M KCl solution), and linked to a pH-meter (Orion, Boston, USA). Calibration was done with standard low ionic strength buffers pH 4.10; 6.97 and 9.15. (Orion Research Inc., USA) at +15 °C. While measuring pH, vials were kept in the water bath at the temperature of +15 °C. The readings were taken after 90 seconds, when reading was stable.

#### **4.3.4. Determination of elemental composition of rock debris**

##### **4.3.4.1. Inductively coupled plasma-atomic emission spectrometry (ICP-AES)**

Acid soluble major elements in the rock debris in the first low temperature weathering experiment, conducted at +7 °C, were determined by inductively coupled plasma-atomic emission spectrometry (ICP-AES). The instrument used was Spectrometer JY 24 Sequential ICP (Jobin Yvon). Inductively Coupled Plasma (ICP) analysis involves introducing the elements to be analysed into an argon plasma induced by a high frequency, where temperature is in the order of 8000 °K. The sample, in the form of an aerosol, is introduced into the plasma via a "torch", where it is excited. Each excited element furnishes a characteristic spectrum whose light intensity is directly proportional to the quantity of that element present in the sample (Jobin Yvon, 1989).

Before preparation of samples, the mortar and pestle and all the glassware and plasticware were soaked overnight in 10 % v/v nitric acid, washed three times in milli-Q-water and dried. Three replicates of the rock debris, 0.5 g each, were combined and homogenised. Rock debris was crushed and ground to fine-grained powder and then dried overnight at 110 °C before acid digestion.

200 mg of dried rock powder was placed into a 50 ml P.T.F.E beaker and moistened with 1-2 ml of milli-Q-water. 10 ml of 40% v/v hydrofluoric acid and



2.5 ml of concentrated nitric acid were added. Rock powder and acids were heated on a hot plate at 100 °C for 2 hours until hydrofluoric acid was evaporated. Then the temperature was increased to 230 °C and samples were heated to dryness. After cooling, 20 ml of 1% v/v nitric acid was added and the solution was heated on a hot plate for 5 minutes. Again, solution was cooled down before transferring it to 100 ml volumetric flask, and the volume was made to 100 ml with 1% v/v nitric acid. Thus, the final solution of the samples was a 500-1 dilution of the original rock powder. Samples were run with five calibration standards (table 4.4) and six known reference standards (table 4.5) for calculating a drift factor and errors. The final results after drift correction are given as wt%. JY 24 detection limits for aqueous solutions of elements are specified in the table 4.5.

**Table 4.4.** Final concentrations (ppm) of calibration standards in ICP-AES analyses.

	<b>Std1</b>	<b>Std2</b>	<b>Std3</b>	<b>Std4</b>	<b>Std5</b>	<b>r<sup>2</sup>-value</b>
<b>Na</b>	10	20	30	40	50	0.9993
<b>Mg</b>	20	40	60	80	100	0.9999
<b>Al</b>	20	40	60	80	100	1.0000
<b>P</b>	2	4	6	8	10	0.9997
<b>K</b>	10	20	30	40	50	0.9993
<b>Ca</b>	20	40	60	80	100	0.9998
<b>Ti</b>	5	10	15	20	25	0.9998
<b>Mn</b>	5	10	15	20	25	0.9995
<b>Fe</b>	20	40	60	80	100	1.0000



**Table 4.5.** Detection limits and relative errors for aqueous solutions of single elements in ICP-AES analyses with Spectrometer JY 24 Sequential ICP.

<b>Element</b>	<b>Detection limit (<math>\mu\text{g g}^{-1}</math>)</b>	<b>Relative mean error (%)</b>
Na <sub>2</sub> O	0.005	3.21
MgO	0.00007	15.17
Al <sub>2</sub> O <sub>3</sub>	0.005	6.33
P <sub>2</sub> O <sub>5</sub>	0.013	3.00
K <sub>2</sub> O	0.020	4.02
CaO	0.007	8.57
TiO <sub>2</sub>	0.004	10.87
MnO	0.0002	7.71
Fe <sub>2</sub> O <sub>3</sub>	0.001	5.84

**4.3.4.2. X-ray fluorescence spectrometry (XRF)**

Elemental composition of the rock flour used in the weathering experiments was analysed by X-ray fluorescence spectrometry, SPECTRO X-LAB 200 system (SPECTRO Analytical Instruments UK Ltd, United Kingdom). This method gave elemental composition also for non-soluble residue, consisting mainly of silicates, which was not dissolved in acid when preparing samples for ICP-AES (Szalóki et al. 1999). Energy-dispersive X-ray fluorescence (ED-XRF) analysis is based on the characteristic X-ray radiation emitted from the atoms excited in a samples. The energy levels of the individual electron levels and therefore the energy differences between them are specific to the atoms. The radiation from the sample is examined for its energetic composition in an energy dispersive spectrometer. A frequency distribution of the energies of the absorbed x-ray photons is obtained from an impulse height analysis of the signals from the detector. This is the spectrum of the emitted radiation (SPECTRO 1999).



6.0 g samples of the rock flour were dried overnight at 105 °C. The dried rock flour samples were homogenised and 1.5000 g of the rock flour from each sample was used for preparing glass beads for analysing major elements. Samples were ignited at 980 °C for 30 minutes to burn away organic carbon. After ignition, 0.4700-0.6300 g of sample was mixed with lithium-metaborate-flux in acid-washed crucible, and heated at 980 °C for 20 minutes until melted. Then flux-rock flour-melt was poured to the glass bead press, and glass beads were left to cool down on the hot plate for 3-6 hours.

**Table 4.6.** SPECTRO X-LAB detection limits and relative errors for major elements.

<b>Element</b>	<b>Detection limit (<math>\mu\text{g g}^{-1}</math>)</b>	<b>Relative mean error (%)</b>
Na <sub>2</sub> O	2000	6.46
MgO	1000	13.62
Al <sub>2</sub> O <sub>3</sub>	600	0.95
SiO <sub>2</sub>	300	0.73
P <sub>2</sub> O <sub>5</sub>	120	9.88
K <sub>2</sub> O	150	6.17
CaO	80	1.30
TiO <sub>2</sub>	25	2.76
MnO	1.5	4.17
Fe <sub>2</sub> O <sub>3</sub>	15	2.07

Three international sediment standards (MAG-1, NBS98a, TILL-1) and three rock standards (ACE/D, GA/D, SY2/D) were used to determine errors when analysing the samples, and the laboratory's internal standard 3570 was used to verify the results. The sensitivity of the system (SPECTRO 1999) for detecting major elements is specified in the table 4.6.



#### **4.3.5. Determination of mineralogical composition of rock debris**

##### **4.3.5.1. X-ray diffraction (XRD)**

Mineralogical composition of the rock debris was analysed by x-ray diffraction, PW1800 Automatic Powder Diffractometer System (Philips, The Netherlands). Powder diffraction measurements are made by causing a beam of X-radiation to fall onto a specimen and measuring the angles at which a specific characteristic X-ray wavelength  $\lambda$  is diffracted. The diffraction angle  $\theta$  can be related to the interplanar spacing  $d$ , by the Bragg law:  $n\lambda = 2d \sin\theta$ . X-ray detector then converts the individual X-ray photons into voltage pulses that are counted and integrated to diffractograms indicating X-ray intensity (Jenkins 1989). Thus, powder diffraction can be used for the identification and characterization of crystalline substances, but amorphous phases are not detected. (Reynolds 1989). Also, presence of amorphous component gives rise to scattering in the diffraction pattern, significantly increasing background (Bish and Reynolds 1989).

To achieve sufficient sample strength, the sample was ground very fine to achieve a grain size of 5-25  $\mu\text{m}$  (Philips 1989). Grinding was done with mortar and pestle, washed with milli-Q-water and acetone before using. After grinding, rock flour was mixed a few drops of acetone. Mixture of rock flour and acetone was pipetted onto a glass slide, and spread evenly on the slide. After the sample on the slide had dried, the edges of the slide were wiped clean and all surplus loose powder was removed. Three replicates of each sample were analysed.

The HT generator is the part of a diffractometry system which generates the high voltage required for the x-ray tube, and controls the tube current. X-ray powder diffractograms were obtained with  $\text{CuK}\alpha$  radiation generated at 40 mA and 45 kV. Specimens were step scanned from  $2^\circ$  to  $70^\circ$   $2\theta$  at  $0.02$ - $0.05^\circ$   $2\theta$  steps integrated at the rate of 1.0 s per step. Various crystalline minerals present in the samples were identified comparing X-ray diffractograms with the diffraction patterns in the MacDiff (version 4.2.5) reference database.



#### **4.3.6. Determination of carbon, hydrogen, nitrogen and sulphur content in rock debris samples**

##### **4.3.6.1. Organic matter content**

Ignition of the rock debris samples was the first step when preparing glass beads for XRF. Simultaneously, weight loss also gave an approximate value for content of organic matter in rock debris (e.g. Wellsbury et al. 1996).

Ignition loss was determined from selected rock debris samples by heating them at 980°C for 30 minutes, following the standard procedure of XRF sample preparation. Thus the ignition temperature was higher than normally used for loss of ignition (550 °C for 2 hours), and loss of structural water from clay minerals was possibly contributing to changes in mass. Ignition loss was calculated with the following equation:

$$\text{LOI (\%)} = [(ds - ir) / ds] \times 100$$

ds = mass of dry rock flour, dried overnight at 105 °C

ir = mass of ignition residue, heated for 30 min at 980 °C.

##### **4.3.6.2. CHNS-analysis**

Rock debris samples were taken during weathering experiments before and after long-time incubation. CHNS-analysis was performed using a Leco CHNS-analyser (University of Leeds, Department of Earth Sciences). The rock flour samples were homogenised and 1.00000 g of the rock flour from each sample was used for preparing glass beads for analysis. For calculating the final results as % of dry weight, loss of weight was determined by drying the rock flour overnight at 105 °C. For organic carbon analysis, samples were soaked in 10 % HCl for 24 hours to remove carbonates.



**Table 4.7.** Standard sample values and relative mean errors in CHNS-analysis.

<b>Element</b>	<b>Std sample value (%)</b>	<b>Relative mean error (%)</b>
total-C	3.69	3.60
H	0.60	11.43
N	0.40	60.00
S	1.32	7.12

**4.3.7. Determination of grain size distribution**

Grain size distribution of the mineral material used in the weathering experiments was determined with laser scattering based particle sizer (Mastersizer Micro, Malvern Instruments Inc., Southborough MA, USA). The system is capable of analysing grain sizes ranging from 0.3 to 300  $\mu\text{m}$ . The results of particle size distributions are volume based, and all the particles are assumed to be spherical. Thus, the distribution is expressed in terms of the volumes of equivalent spheres.

Rock debris samples were dried overnight at 105 °C and sieved through 500  $\mu\text{m}$  and 250  $\mu\text{m}$  sieves. Fractions of < 250  $\mu\text{m}$ ; 250-500  $\mu\text{m}$  and >500  $\mu\text{m}$  were weighed. Grain size distribution of the finest fraction was then analysed with scattering based particle sizer.

Sample of rock flour was added in the beaker containing milli-Q-water. Amount of sample dispersed was represented by the obscuration display - the relative amount of light scattered, or absorbed, by the particles. To achieve a good signal, the obscuration value had to be 5-10% at the minimum. Rock flour was kept suspended with ultrasonic stirring. A pump circulated suspended sample to the measurement cell, and the light from a low power Helium-Neon laser was used to form a monochromatic beam of light. The diffraction pattern of scattered light was measured with the Fourier optics composed of focusing lens and detectors (Mastersizer Reference Manual).



#### **4.3.8. Headspace gas measurements**

##### **4.3.8.1. Oxygen and methane analysis by gas chromatography**

Gas chromatography was used to determine oxygen and/or methane concentration in headspace (Skidmore et al. 2000). In the weathering experiments, samples were incubated in 10 ml vials sealed with gas-impermeable butyl septa. Gas samples from the headspace were taken with a 1 ml gas syringe (Hamilton Co. Gastight® #1001, Reno, USA) and sterile 0.5 x 16 mm needles. The volume of the sample injected was 1 ml. Flow rate of carrier gas (nitrogen) was 20 ml min<sup>-1</sup>. Molecular Sieve column (Supelco) was used to separate gases. The concentrations were determined by Perkin Elmer GC8500 gas chromatograph with thermal conductivity detector (oxygen) or flame ionisation detector (methane), linked to Hewlett-Packard 3392A and Spectra-Physics Chrom-Jet integrators, respectively. The calibration curve, peak area plotted against gas concentration, was based on three injections of different volumes (0.2 ml; 0.5 ml and 1.0 ml) of the Supelco 2-2562 standard gas (1.00 % methane, 1.00 % oxygen).

#### **4.3.9. Microscopic methods**

##### **4.3.9.1. Total number of bacteria**

Water samples taken for determining the total number of bacteria were fixed in 4% formaldehyde saline solution: 100 ml of 38% formaldehyde and 35 g of sodium chloride was dissolved in 1 litre of milli-Q-water. Formaldehyde solution was filtered through 0.1 µm VacuCap 60 bottle-top vacuum filter unit (Gelman Sciences) to be furnace-dried (at 450 °C for 2 hours) DURAN-bottles, then autoclaved at 121 °C for 15 minutes, and stored at +7 °C. Before fixing the water samples, formaldehyde solution was once again filter-sterilised using Anotop 0.1 µm syringe filters. The ratio water sample/fixing solution was 1:10. For slide preparation, 2% formaldehyde saline solution was prepared following the same protocol as when preparing 4% formaldehyde solution. For counting bacterial cells, samples were stained with acridine orange, which is



fluorescent dye staining DNA and RNA of living cells (Fry 1988). Slides for direct counting were prepared as described in Sharp et al. (1999). Fixed samples were vortex mixed, and a 100 - 500  $\mu$ l subsample was added to 10 ml of 2% filter-sterilised (0.1  $\mu$ m) formaldehyde solution. 50  $\mu$ l of 1 g l<sup>-1</sup> acridine orange solution was added, resulting in the final concentration of 5 mg l<sup>-1</sup>. After 3 minutes, the solution was filtered through a 25-mm-diameter Nucleopore black polycarbonate membrane with 0.2  $\mu$ m pore size. The filter was rinsed with a further 10 ml of 2% filter-sterilised formaldehyde, and mounted in paraffin oil under a coverslip. 200 fields of view or a minimum of 400 cells per slide were counted. Slides were viewed with a Zeiss Axioskop microscope fitted with a 50 W mercury-vapor lamp, a wide-band interference filter set for blue excitation, a 100x Plan Neofluar objective lens, and 10x eyepieces.

From the field samples of Greenland, Norway and Svalbard meltwaters, three independent replicates from each meltwater sample of 250 ml were counted. In the thermal gradient experiments counts were done in triplicate. In the weathering experiments, one membrane from each replicate 10 ml vial was prepared and counted, giving three replicate membranes in the first two weathering experiments and two replicate membranes in the third weathering experiment.

#### **4.3.8.2. Frequency of dividing and divided cells**

Acridine orange direct count is mainly a means of determining the total number of intact bacterial cells in the sample, but an estimation about bacterial cell production can also be gained. According to Wellsbury et al. (1996) and Sharp et al. (1999), direct microscopic determination of number of dividing/divided cells of the total number of bacteria gives an index of bacterial growth rate. Especially when estimating bacterial productivity in water samples, results of the frequency-of-dividing-cells (FDC) method correlate strongly with [<sup>3</sup>H]thymidine method (Newell and Fallon 1982).

The frequency of cells which were dividing or divided was determined. Bacterial cells exhibiting a clear invagination were counted as dividing cells,



as one cell in both the total count and dividing cell count. Bacterial cells appearing as closely adjacent identical cells with a visible gap between them were classified as two divided cells, and were counted as two cells in the total count.

#### **4.3.8.3. Bacterial cells attached on particles**

Frequency of cells attached on surface of mineral particles in meltwater samples was also determined by direct count. Cells were counted as on-particle if they were apparently attached to the upper surface of a particle. Cells attached to the side of a particle where black membrane was visible on three sides of the cell were counted as off-particle.

#### **4.3.8.4. Doubling time of bacterial population**

Doubling times of exponentially growing bacterial populations were estimated from semilogarithmic growth curve graphs, in which total numbers of bacteria on a logarithmic scale ( $\log_{10}$ ) were plotted versus incubation time (Madigan et al. 1997). The doubling time of the exponentially growing population was read directly from the straight line of the semilogarithmic graph.

### **4.4. Statistical analyses**

Statistical analysis were done using SPSS for Windows version 11.5. In Chapter V and studies on bacterial populations in meltwaters from the three field sites, analysis of variance was used to test significant differences (F-test in ANOVA-table) and multiple comparison technique called Tukey's HSD-test (honestly significant difference test) was used to further detect homogenous subgroups and analyse the differences. Bivariate non-parametric correlation tests and linear regression tests were also done. In Chapter VI and reporting the results of the weathering experiments, independent samples t-test, one-way analysis of variance, two-way univariate ANOVA with interactions and post hoc multiple comparisons were used.



**CHAPTER V RESULTS I: BACTERIAL POPULATIONS  
IN MELTWATERS**

**5.1. Akuliarusiarssuk and Manitsok glaciers in Greenland**

**5.1.1 Meltwater discharge in the Manitsok glacier**

The actual melt period in summer 1999 started in late June in the Manitsok Glacier (figure 5.1). At the beginning of the melt season, the meltwater stream was confined to a single channel. Later on, after runoff increased significantly, the meltwater stream system developed from a one-channel to a two-channel system (Jones 2002). Two peaks in discharge in the proglacial bulk stream were documented: the first at the beginning of July, and the second at the beginning of August. The discharges at these times increased from less than  $10 \text{ m}^3 \text{ s}^{-1}$  to  $28 \text{ m}^3 \text{ s}^{-1}$  and  $33 \text{ m}^3 \text{ s}^{-1}$ , respectively (Grust, Skidmore and Tranter, unpublished data).

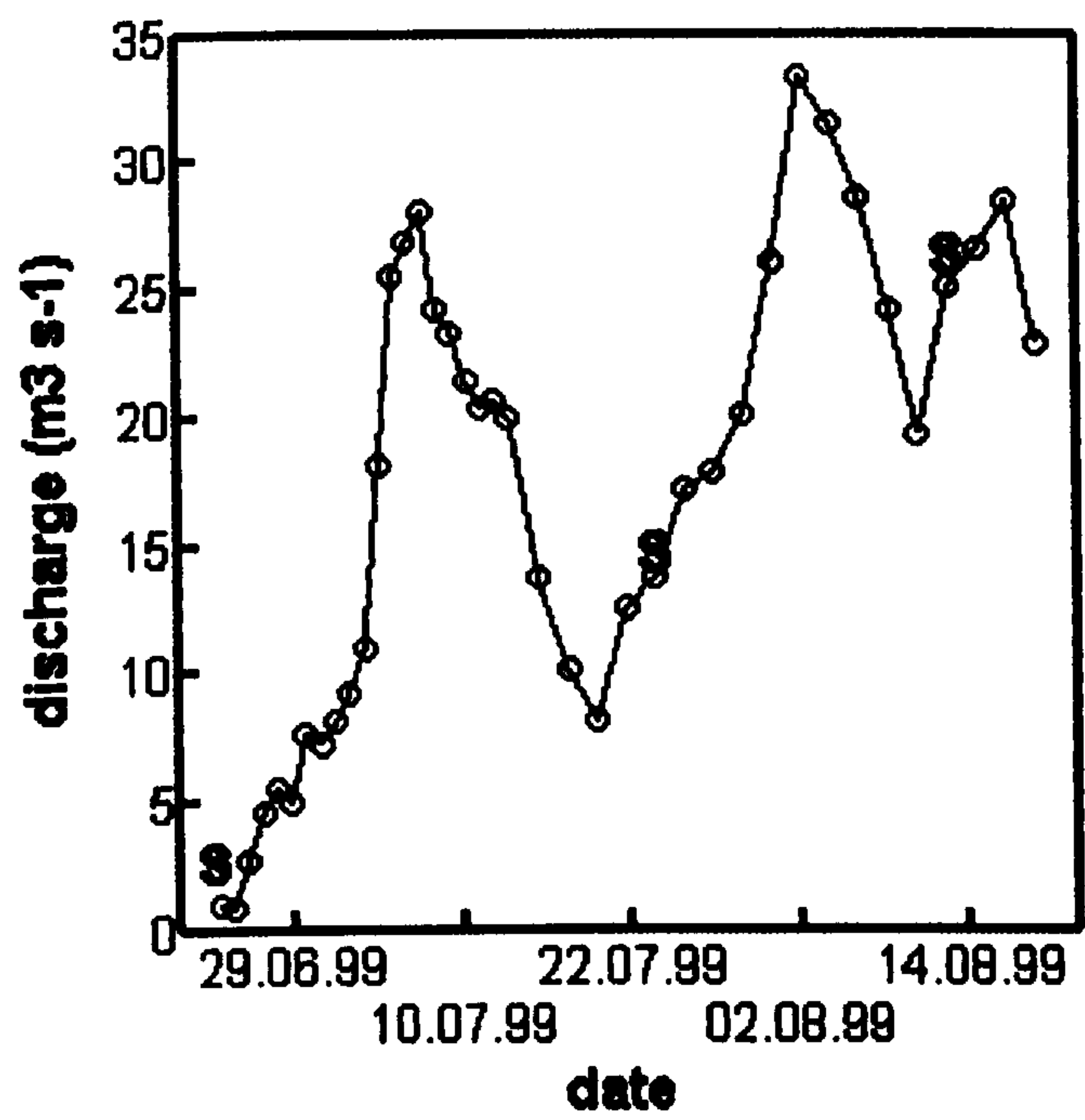


**Figure 5.1.** Discharge in the main meltwater stream of the Manitsok Glacier in the melt season 1999 (Grust, Skidmore and Tranter, unpublished data). S=meltwater sampling.



No discharge measurements were made in the Akuliarusiarssuk meltwater stream, but discharges are estimated to be at least an order of magnitude greater than those in Manitsoq glacier (Jones 2002).

### **5.1.2. Bacterial populations in Greenland meltwaters**

The total numbers of bacteria in subglacial and supraglacial meltwaters from the Manitsoq Glacier were  $3.83 - 4.54 \log_{10} \text{ cells ml}^{-1}$  and  $3.62 - 4.21 \log_{10} \text{ cells ml}^{-1}$ , respectively (Fig.5.2). The maximum number of bacteria was detected in subglacial meltwater at the beginning of the melt season when discharge in the proglacial bulk stream was still low. Total number of bacteria in this early melt season subglacial meltwater was significantly higher than in the other samples (Tukey's HSD test, appendix 2). Later in the mid and late melt season, there were no significant changes in bacterial populations in subglacial or supraglacial meltwaters.

In the Akuliarusiarssuk Glacier meltwater, the total number of bacteria was approximately the same as in the Manitsoq Glacier: in subglacial meltwater  $3.91 \log_{10} \text{ cells ml}^{-1}$ , and in supraglacial meltwater  $3.40 \log_{10} \text{ cells ml}^{-1}$  (Fig. 5.2). In both glaciers and in every stage of the melt season, the number of bacteria was higher in the subglacial than supraglacial meltwaters, but statistically the difference was not significant (appendix 2). Bacterial cells were coccus or rod shaped, but so small ( $< 1 \mu\text{m}$ ) that it was not possible to distinguish reliably whether or not cells were dividing.



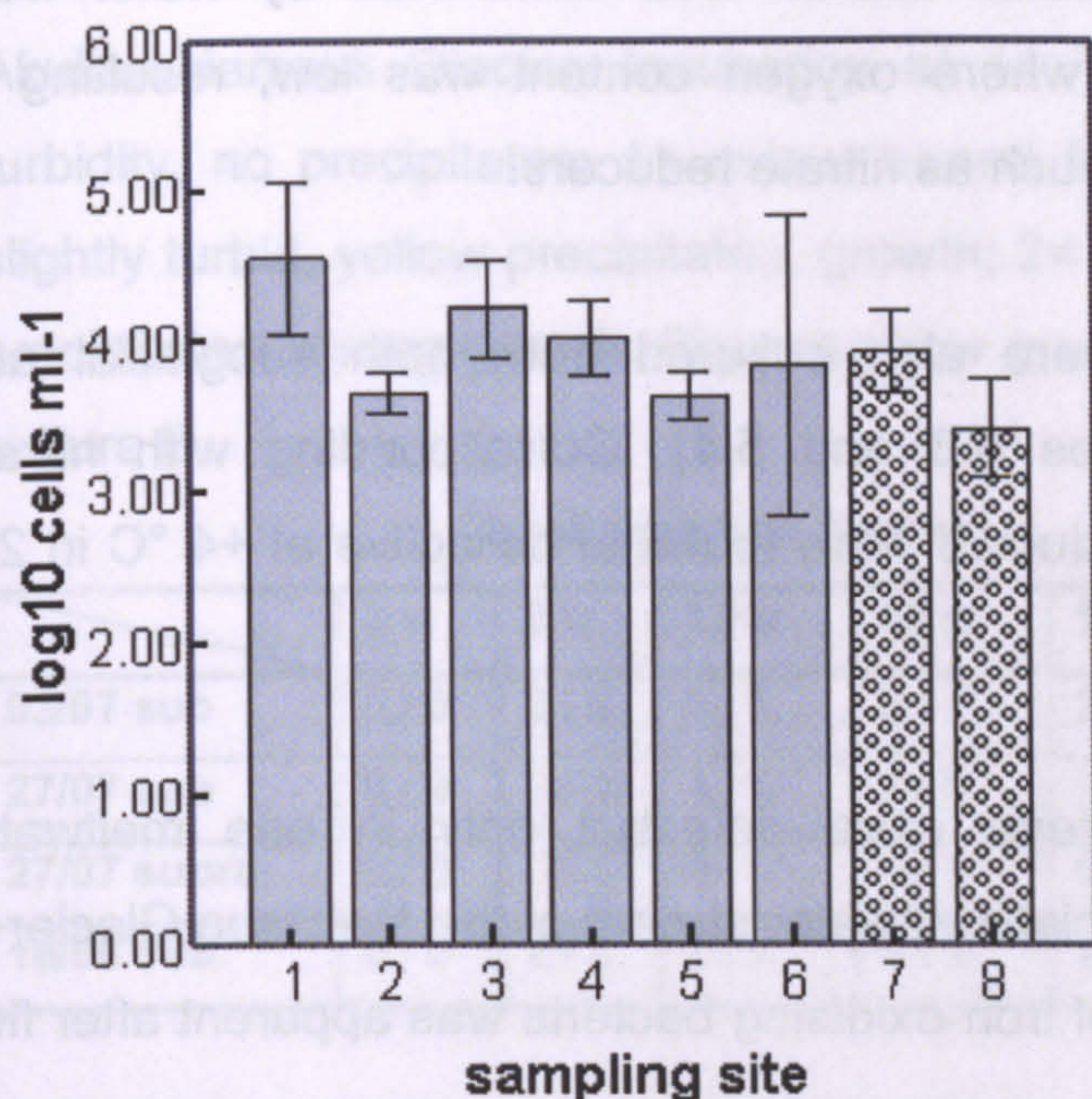


**Figure 5.2.** Total number of bacteria in meltwaters from the Manitsoq Glacier and the Akuliarusiarsuk Glacier in Greenland. The bars show the mean values of the three replicate counts and error bars show 95% confidence intervals for the means of three replicates. Sampling sites Manitsoq Glacier (solid bars) and Akuliarusiarsuk Glacier (bars with dots) as follows: **1** = subglacial meltwater, 22 June 1999; **2** = debris-poor supraglacial meltwater, 22 June 1999; **3** = debris-rich supraglacial meltwater, 22 June 1999; **4** = subglacial meltwater, 24 July 1999; **5** = debris-poor supraglacial meltwater, 24 July 1999; **6** = subglacial meltwater, 15 August 1999; **7** = subglacial meltwater, 27 July 1999; **8** = supraglacial meltwater, 27 July 1999.

### 5.1.3. Growth of bacterial cultures at constantly low temperature

Nitrate- and sulphate-reducing bacteria were cultured at +4 °C from both the Greenland glaciers. Visual assessment of bacterial growth was confirmed by direct counts of enrichment cultures after four months' incubation.

Nitrate-reducing bacteria were cultured from both subglacial and supraglacial meltwaters (tables 5.1 and 5.2). Incubation times as long as 2-4 months were needed before evident growth took place, except in the early melt season (22 June) cultures which grew in less than three weeks. At the very beginning of



the melt season, bulk meltwater stream was dominated by water from subglacial discharge system where oxygen content was low, resulting in activity of anaerobic bacteria, such as nitrate reducers.

Sulphate-reducing bacteria were also cultured from both subglacial and supraglacial meltwaters (tables 5.3 and 5.4). Corresponding with nitrate reducing bacteria, sulphate-reducers were found to be active at +4 °C in 2-4 months.

Culturable iron-oxidising bacteria were detected only in one meltwater sample, taken from the subglacial meltwater stream of the Manitsog Glacier in the late melt season. Growth of iron-oxidising bacteria was apparent after five weeks incubation.

**Table 5.1.** Growth of cultures of nitrate-reducing bacteria from the Manitsog Glacier. Incubation at +4 °C. 0=no change in colour nor turbidity, no precipitates; 1= colour turned from deep purple to pale violet, slightly turbid, yellow precipitates, growth; 2= colour yellow-grey, turbid, lot of precipitates, strong growth. Figures show growth in two replicates: culture A / culture B.

Incubation time (weeks)								
	3 w	8 w	12 w	16 w	17 w	18 w	19 w	20 w
<b>22/06 sub</b>	2 / 2	2 / 2	2 / 2	2 / 2	2 / 2	2 / 2	2 / 2	2 / 2
<b>22/06 supra</b>	0 / 0	0 / 0	0 / 0	0 / 0	1 / 0	2 / 0	2 / 0	2 / 0
<b>24/07 sub</b>	0 / 0	0 / 0	0 / 0	1 / 1	2 / 2	2 / 2	2 / 2	2 / 2
<b>24/07 supra</b>	0 / 0	0 / 0	0 / 0	1 / 0	1 / 0	1 / 0	1 / 0	1 / 0
<b>15/08 sub</b>	0 / 0	0 / 0	1 / 0	2 / 0	2 / 0	2 / 0	2 / 0	2 / 0
<b>15/08 supra</b>	0 / 0	0 / 0	0 / 2	0 / 2	0 / 2	0 / 2	0 / 2	0 / 2



**Table 5.2.** Growth of cultures of nitrate-reducing bacteria from the Akuliarusiarssuk Glacier. Incubation at +4 °C. 0=no change in colour nor turbidity, no precipitates; 1= colour turned from deep purple to pale violet, slightly turbid, yellow precipitates, growth; 2= colour yellow-grey, turbid, lot of precipitates, strong growth. Figures show growth in two replicates: culture A / culture B.

Incubation time (weeks)								
	3 w	8 w	12 w	16 w	17 w	18 w	19 w	20 w
03/07 sub	0 / 0	0 / 0	0 / 0	2 / 1	2 / 1	2 / 1	2 / 1	2 / 1
27/07 sub	0 / 0	0 / 0	1 / 0	2 / 0	2 / 0	2 / 0	2 / 0	2 / 0
27/07 supra	0 / 0	0 / 0	0 / 1	0 / 1	0 / 1	0 / 1	0 / 1	0 / 1
16/08 sub	0 / 0	2 / 2	2 / 2	2 / 2	2 / 2	2 / 2	2 / 2	2 / 2

**Table 5.3.** Growth of cultures of sulphate-reducing bacteria from the Manitsog Glacier. Incubation at +4 °C. 0=no sign of growth; 1=culture turning cloudy, dark grey precipitates, growth; 2=black precipitates, strong growth. Figures show growth in two replicates: culture A / culture B.

Incubation time (weeks)								
	3 w	8 w	12 w	16 w	17 w	18 w	19 w	20 w
22/06 sub	0 / 0	0 / 0	0 / 0	2 / 2	2 / 2	2 / 2	2 / 2	2 / 2
22/06 supra	0 / 0	0 / 0	0 / 0	0 / 0	0 / 0	0 / 0	1 / 1	1 / 1
24/07 sub	0 / 0	0 / 0	0 / 0	1 / 1	1 / 1	1 / 1	1 / 1	1 / 1
24/07 supra	0 / 0	0 / 0	0 / 0	1 / 1	1 / 1	1 / 1	1 / 1	1 / 1
15/08 sub	0 / 0	1 / 1	2 / 2	2 / 2	2 / 2	2 / 2	2 / 2	2 / 2
15/08 supra	0 / 0	1 / 0	2 / 0	2 / 0	2 / 0	2 / 0	2 / 0	2 / 0

**Table 5.4.** Growth of cultures of sulphate-reducing bacteria from the Akuliarusiarssuk Glacier. Incubation at +4 °C. 0=no sign of growth; 1=culture turning cloudy, dark grey precipitates, growth; 2=black precipitates, strong growth. Figures show growth in two replicates: culture A / culture B.

Incubation time (weeks)								
	3 w	8 w	12 w	16 w	17 w	18 w	19 w	20 w
03/07 sub	0 / 0	2 / 2	2 / 2	2 / 2	2 / 2	2 / 2	2 / 2	2 / 2
27/07 sub	0 / 0	0 / 0	0 / 0	2 / 2	2 / 2	2 / 2	2 / 2	2 / 2
27/07 supra	0 / 0	0 / 0	0 / 0	0 / 0	0 / 0	0 / 0	0 / 0	0 / 0
16/08 sub	0 / 0	2 / 2	2 / 2	2 / 2	2 / 2	2 / 2	2 / 2	2 / 2



#### **5.1.4. Temperature characteristics of sulphate-reducing bacteria in Greenland early and late melt season meltwaters**

A thermal gradient experiment was conducted with the enrichment cultures of sulphate-reducing bacteria from the Manitsog Glacier. The temperature characteristics of the following four cultures were studied:

- (1)** Meltwater from the bulk proglacial stream in the early melt season (22 June 1999), dominated by subglacial meltwater;
- (2)** Meltwater from the bulk proglacial stream in the late melt season (15 August 1999), fed by subglacial and supraglacial melting.

##### **5.1.4.1. Sulphide production in Greenland SRB-cultures**

Enrichment cultures of sulphate-reducing bacteria after two subculturing were inoculated to Postgate's (1984) SRB-medium. The ratio of numbers of dividing cells to the total number of bacteria (FDC) in the cultures was 21-35 %. Cultures were incubated at temperatures from 0 to +42 °C, with 2.1 °C intervals. The first sampling was done when sulphide production also at the lowest temperatures was taking place. Based on earlier experiments with enrichment cultures of Arctic marine sulphate reducers (Knoblauch et al. 1999), sulphide production at near zero temperatures was expected to start after four weeks. At the beginning of the experiment, the cultures were studied visually every other day, and growth of bacteria was detected by formation of dark grey or black iron monosulphide (FeS) precipitates. After only one week incubation, FeS was produced at temperatures from +15 to +23 °C. After two weeks, visible growth took place from +6 °C to +23 °C (appendix 3).

Sulphide production measured after 5, 12, 32 and 42 weeks incubation in the thermal gradient system revealed the presence of several populations with different temperature characteristics and activities at different phases of melt season (figures 5.4 and 5.5). Sulphate-reducing bacteria from the early melt season subglacial meltwater were more active than late melt season bacteria. Maximal sulphide production after five weeks incubation was 4.1 mM in early melt season culture, and 1.7 mM in late melt season culture (figure 5.3). The



sulphate production rate after five weeks in the early melt season culture was 14.9 - 115.2  $\mu\text{M d}^{-1}$ , whereas in late season it was 19.8 - 48.5  $\mu\text{M d}^{-1}$  (figures 5.5 and 5.6).

In early melt season meltwater, optimum growth temperature was +17 to +30 °C (figures 5.3 and 5.4). Activity in the early melt season was thus dominated by mesophilic and psychrotolerant organisms (figure 5.5), whereas in the late melt season meltwater psychrophilic organisms were dominant (figures 5.4 and 5.6). It may be that true psychrophiles survive better in the drainage system further from glacier terminus, and thus they were released to the meltwater stream only later in the melt season. At +4 °C sulphate-reducers grew slowly, but finally reduced sulphate effectively. After 42 weeks incubation, the maximum sulphide production - 3.0-3.2 mM - took place at +4 °C and +9 °C (figure 5.4).

Several distinct peaks of sulphate production at different temperatures (+4 °C, +9 °C, +16 - 19 °C, +23 - 25 °C) both in early and late melt season meltwaters (figures 5.3 and 5.4) indicated the presence of several bacterial populations with different temperature characteristics. The decrease of FeS in the early melt season culture at temperature of +19 °C to +30 °C after the first sampling may be due to chemical oxidation. The SRB-medium used was strictly anaerobic, and when samples were taken, oxygen-free N<sub>2</sub> gas was used to replace the volume of the sample taken out. Even so, there was a risk of oxygen contamination during sampling. If air seeps into the medium, and the population of facultative aerobic bacteria in the enrichment culture of mixed populations is in the lag or the death phase, oxygen will not be consumed. Therefore, rapid chemical oxidation of sulphide precipitates back to sulphate may have happened. Since the sulphate-reducing bacteria are obligate anaerobic organisms, they can survive only very limited exposure to air, from < 3 to 72 hours (Battersby 1988). The continuous presence of lots of S<sup>2-</sup> in fast-growing cultures of sulphate reducing bacteria prevented oxygen exposure. Oxygen contamination, however, may have caused death of slow-growing sulphate-reducers, as little or no S<sup>2-</sup> was present for protection. Unfortunately, because of the limited number of rows in thermal gradient system, a new replicate per sampling to avoid oxygen contamination could not be used. Therefore, this flaw in experiment set up remained in the



subsequent thermal gradient experiments with cultures from Norway and Svalbard, influencing the results of slow growing populations (see chapters 5.2 and 5.3).

Activity of sulphate-reducing bacteria at near zero temperatures was the focus of thermal gradient experiments. Hence it was highly important to avoid oxygen contamination of slowly growing low temperature SRB-cultures in the lag phase. This was the reason why the first sampling in each thermal gradient experiment was done after visual signs of growth also at near zero temperatures were detected, i.e. colour of medium turned cloudy and dark grey precipitates were formed (see appendices 3, 6 and 8). The possibility of partially missing the exponential growth phase, especially in case of psychrotolerant and mesophilic cultures, was acknowledged and considered when interpreting the results.



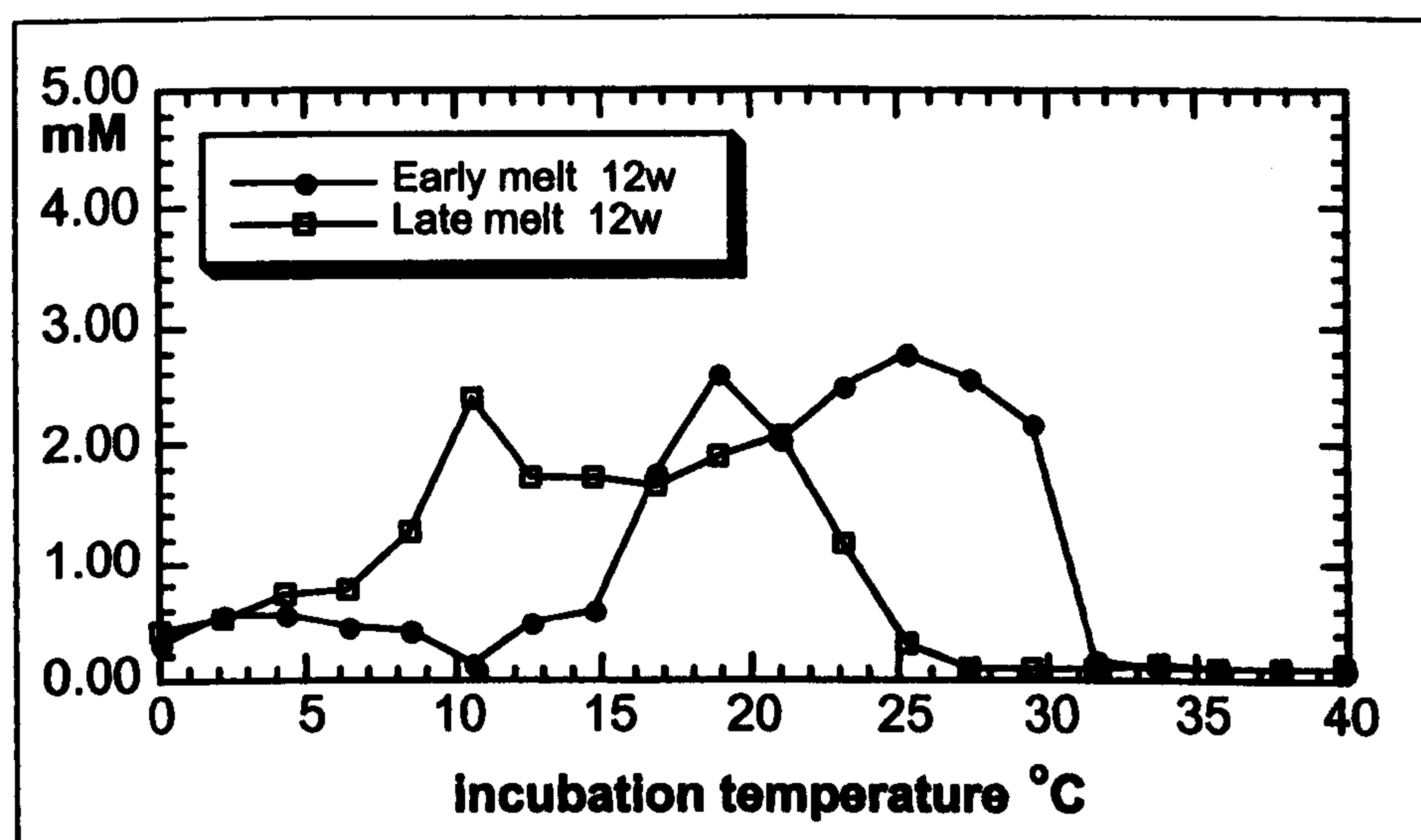
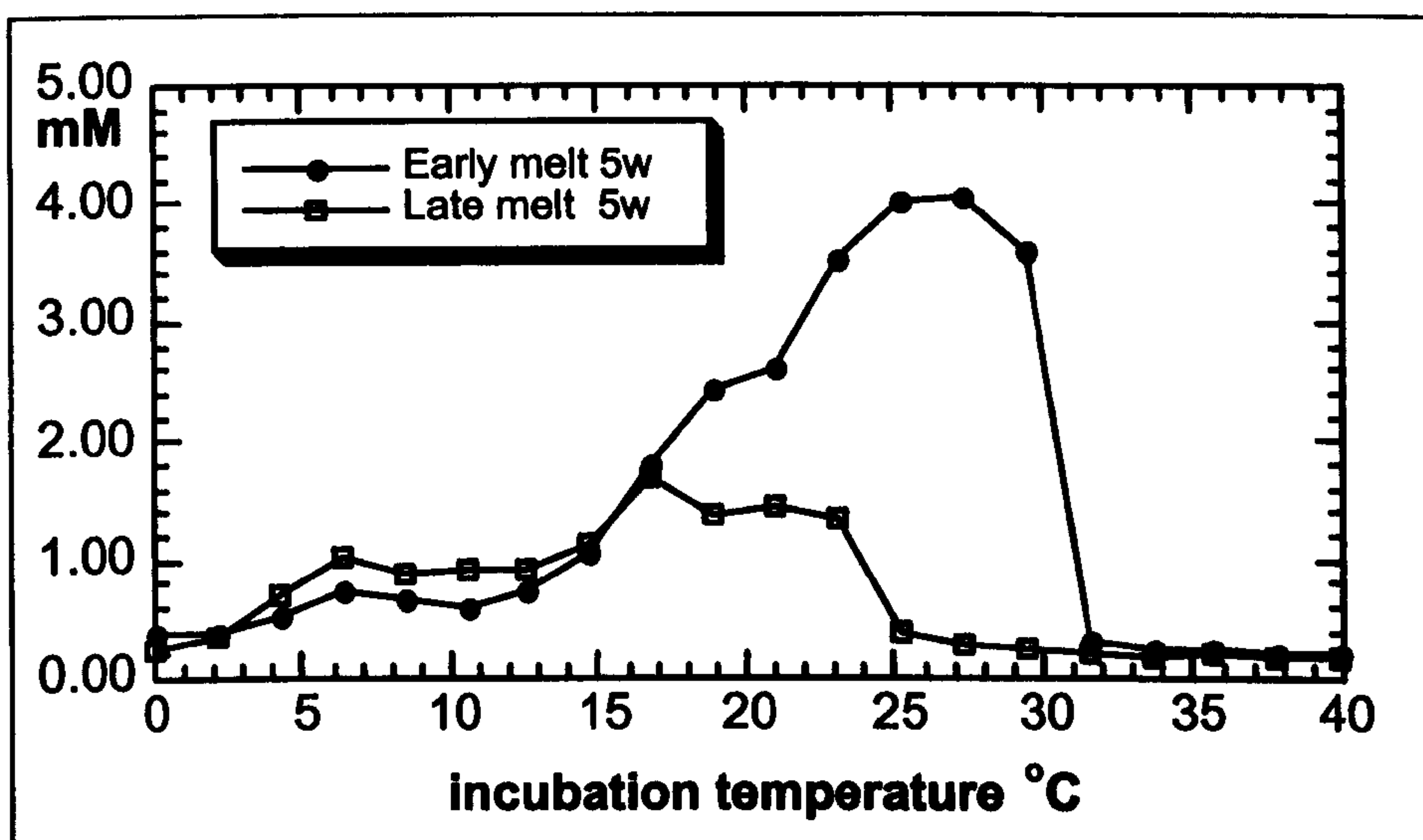


**Figure 5.3.** Growth of sulphate-reducing bacteria from the early and late melt season subglacial meltwaters from the Manitsog Glacier. Cultures incubated in the thermal gradient system with a temperature range from 0 to +40 °C for 5 and 12 weeks. Growth measured as sulphide production (mM).



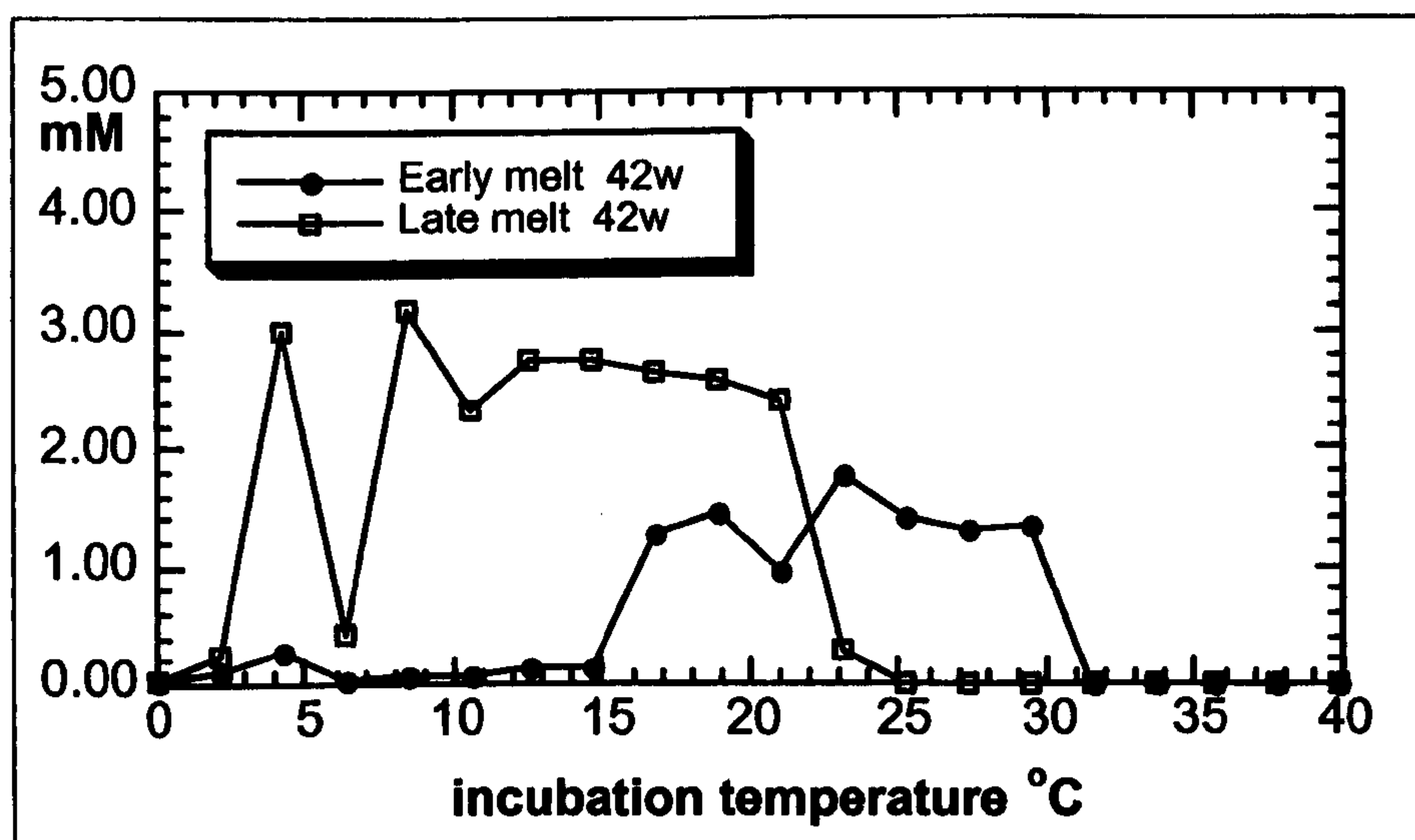
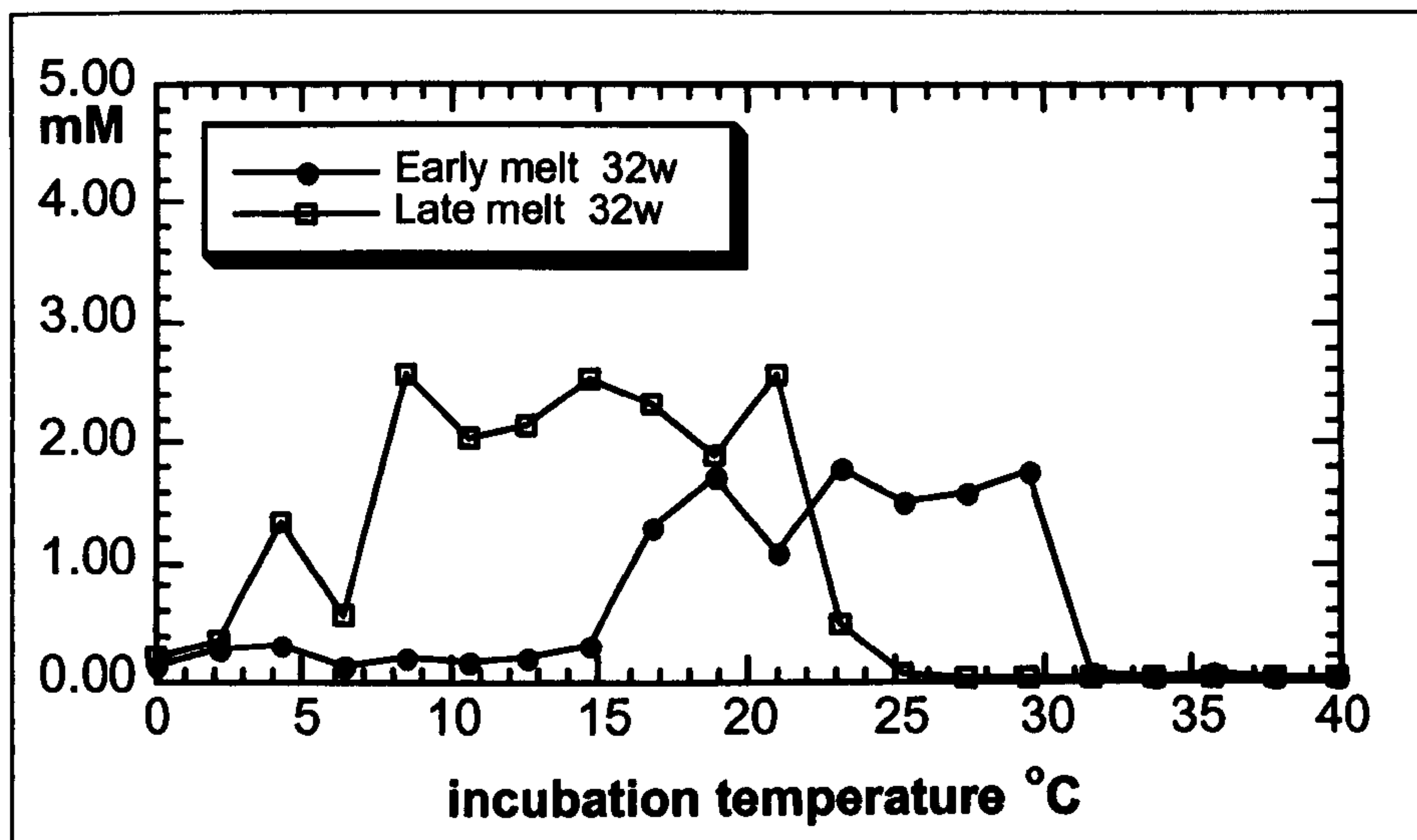


**Figure 5.4.** Growth of sulphate-reducing bacteria from the early and late melt season subglacial meltwaters from the Manitsog Glacier. Cultures incubated in the thermal gradient system with a temperature range from 0 to +40 °C for 32 and 42 weeks. Growth measured as sulphide production (mM).



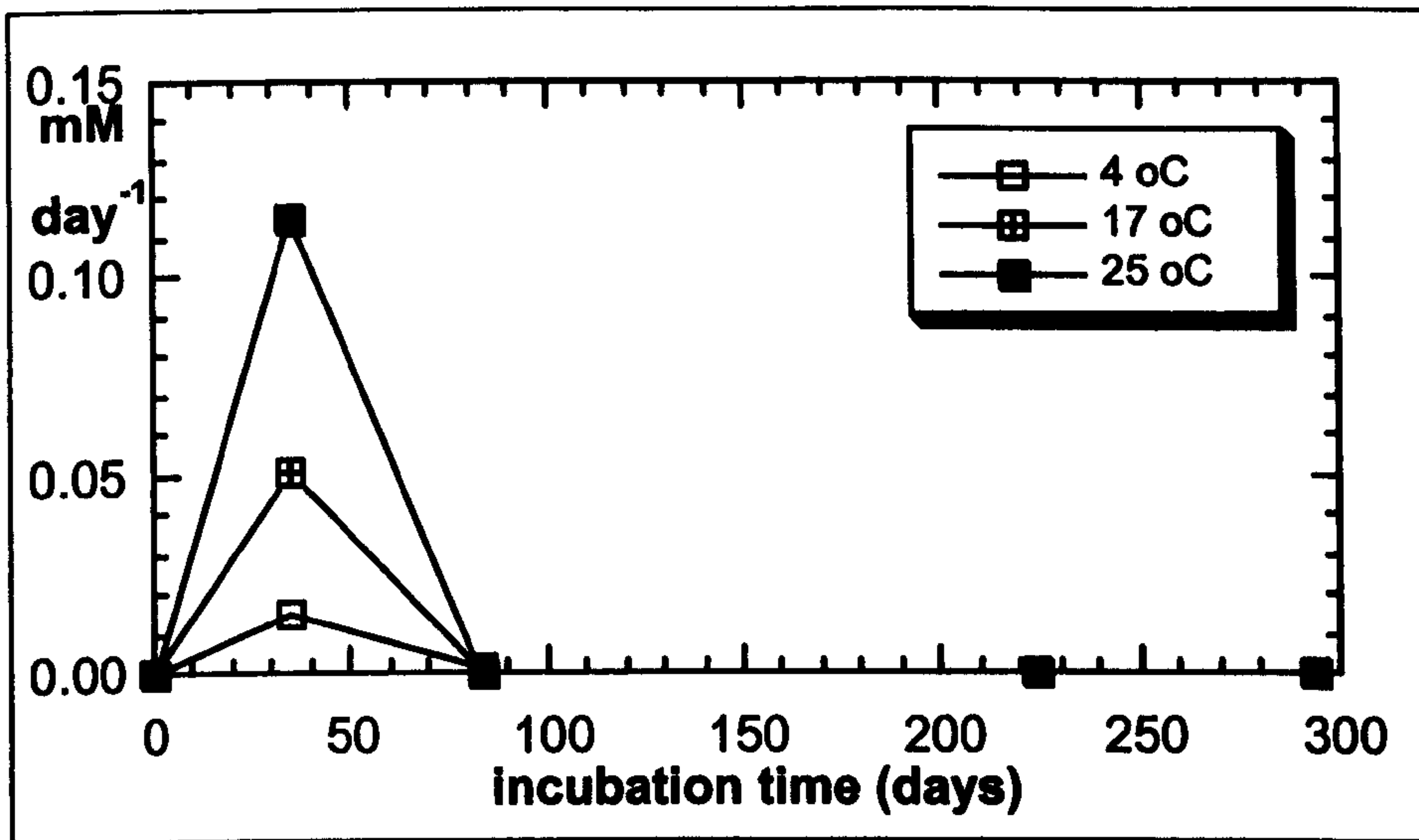


**Figure 5.5.** Sulphate reduction rate at +4 °C, +17 °C and +25 °C in the early melt season culture of sulphate-reducing bacteria from the Manitsoq Glacier.

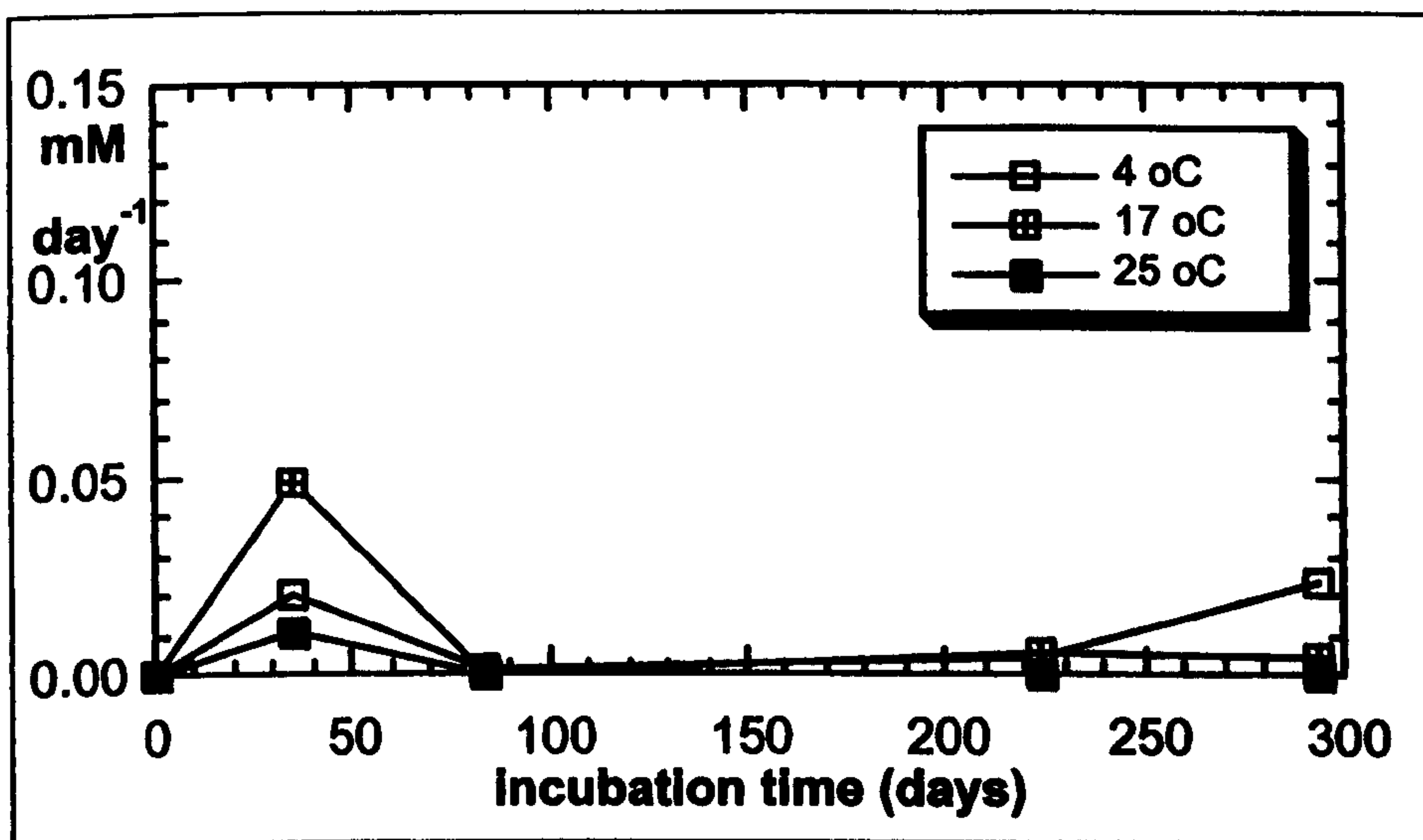


**Figure 5.6.** Sulphate reduction rate at +4 °C, +17 °C and +25 °C in the late melt season culture of sulphate-reducing bacteria from the Manitsoq Glacier.



5.1.4.2. Growth rate in Greenland SRB-cultures

Cultures of psychrophilic, psychrotolerant and mesophilic sulphate-reducing bacteria with high sulphide production (figures 5.3 and 5.4) were chosen for estimating differences in growth rates. By 35 days bacterial populations in both early and late melt season cultures had rapidly increased throughout the temperature range, giving a maximum doubling time of 7 to 8.5 days (table 5.5, figures 5.7 and 5.8). In the late melt season culture, however, the growth was slightly slower at +4 °C than at +17 °C and +25 °C. Since the first sampling was done only after 35 days, the rate of exponential growth during the first weeks of incubation may have been higher, resulting in shorter doubling times. Therefore, the estimates of minimum and maximum doubling times are given in the table 5.5 (see appendix 4 for semilogaritmik graph method used for estimating the doubling times). For estimating the minimum doubling time it was assumed that stationary phase was reached after 20 days, instead of > 35 days (see figure 5.31 and growth curves with the first sampling after 18 days incubation). As a comparison, if bacterial numbers in the early melt season cultures (figure 5.7) had peaked by 20 days of incubation, doubling time would have been ~ 4 days, instead of 7.5 days.

**Table 5.5.** Estimated doubling times of the total number of cells in cultures of sulphate-reducing bacteria from the Manitsog Glacier in the early and late melt season during exponential growth, and the frequency of dividing and divided cells (FDDC) after 35 days incubation at a range of high sulphide production temperatures.

		+4 °C	+17 °C	+25 °C
Early melt season	DT (days)	4 - 7.5	4 - 7.5	4 - 7.5
	FDDC (%)	51.8	51.6	37.5
Late melt season	DT (days)	5 - 8.5	3.5 - 7	3.5 - 7
	FDDC (%)	51.6	44.8	39.1

After 35 days, the frequency of dividing and divided cells was lower at +25 °C than at +4 °C. Again, as also the shapes of the growth curves (figures 5.7 and 5.8) suggest, we may have missed the point when populations incubated at high temperatures reached stationary phase. Probably at high temperatures



cells divided faster than estimated, whereas at near zero temperatures the growth curve more likely reflects the real growth rate of bacterial populations.

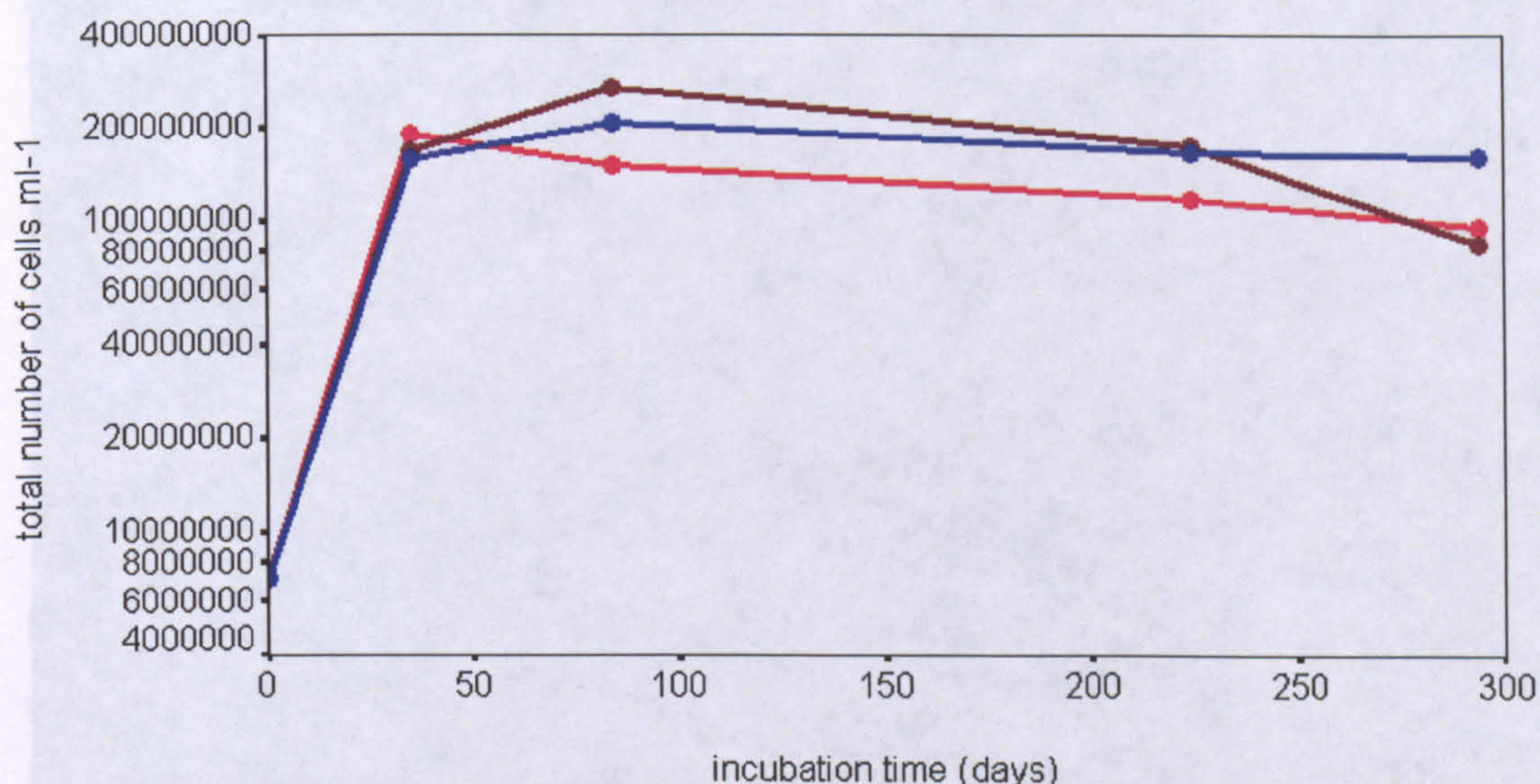


**Figure 5.7.** Growth curves of bacterial populations in the early melt season SRB-enrichment cultures from the Manitsoq Glacier at a range of incubation temperatures. Lines show the mean values of the three replicate counts. Blue line = +4 °C; brown line = +17 °C; red line = +25 °C.

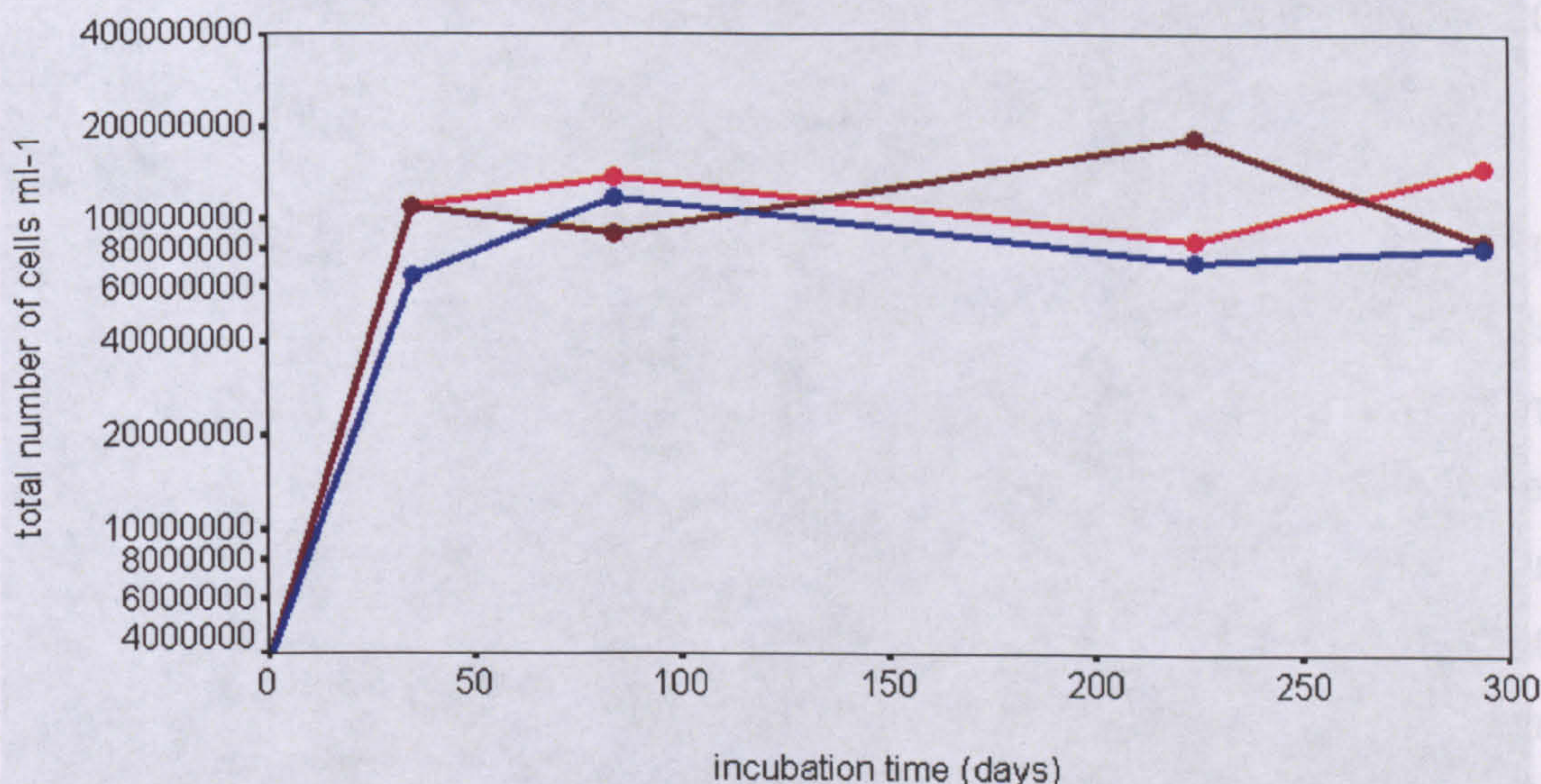


**Figure 5.8.** Growth curves of bacterial populations in the late melt season SRB-enrichment cultures from the Manitsoq Glacier at a range of incubation temperatures. Lines show the mean values of the three replicate counts. Blue line = +4 °C; brown line = +17 °C; red line = +25 °C.



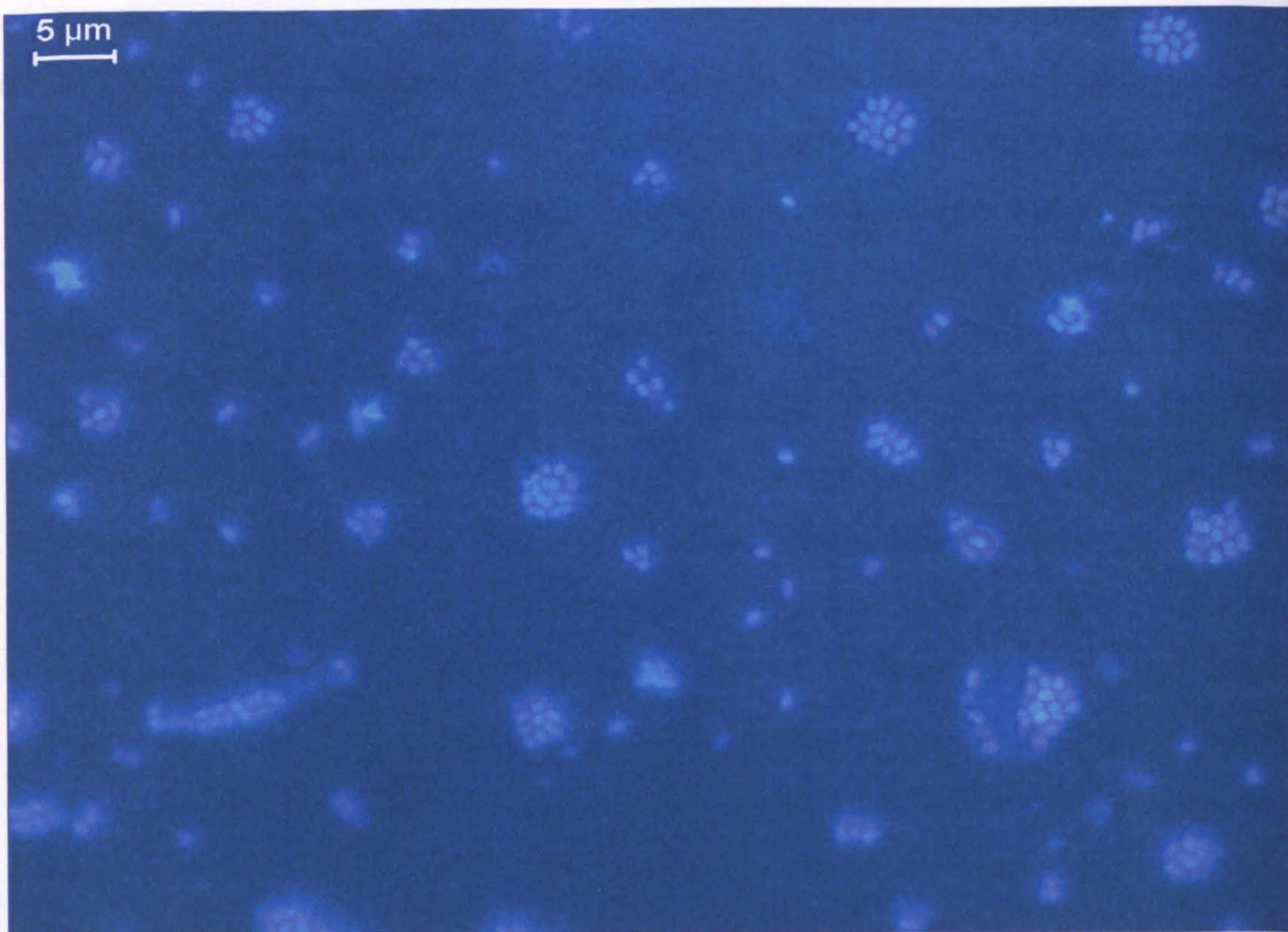


**Figure 5.9.** Bacterial cells in the enrichment cultures of the early melt season sulphate-reducing bacteria from the Manitsog Glacier incubated at +4 °C for 5 weeks.

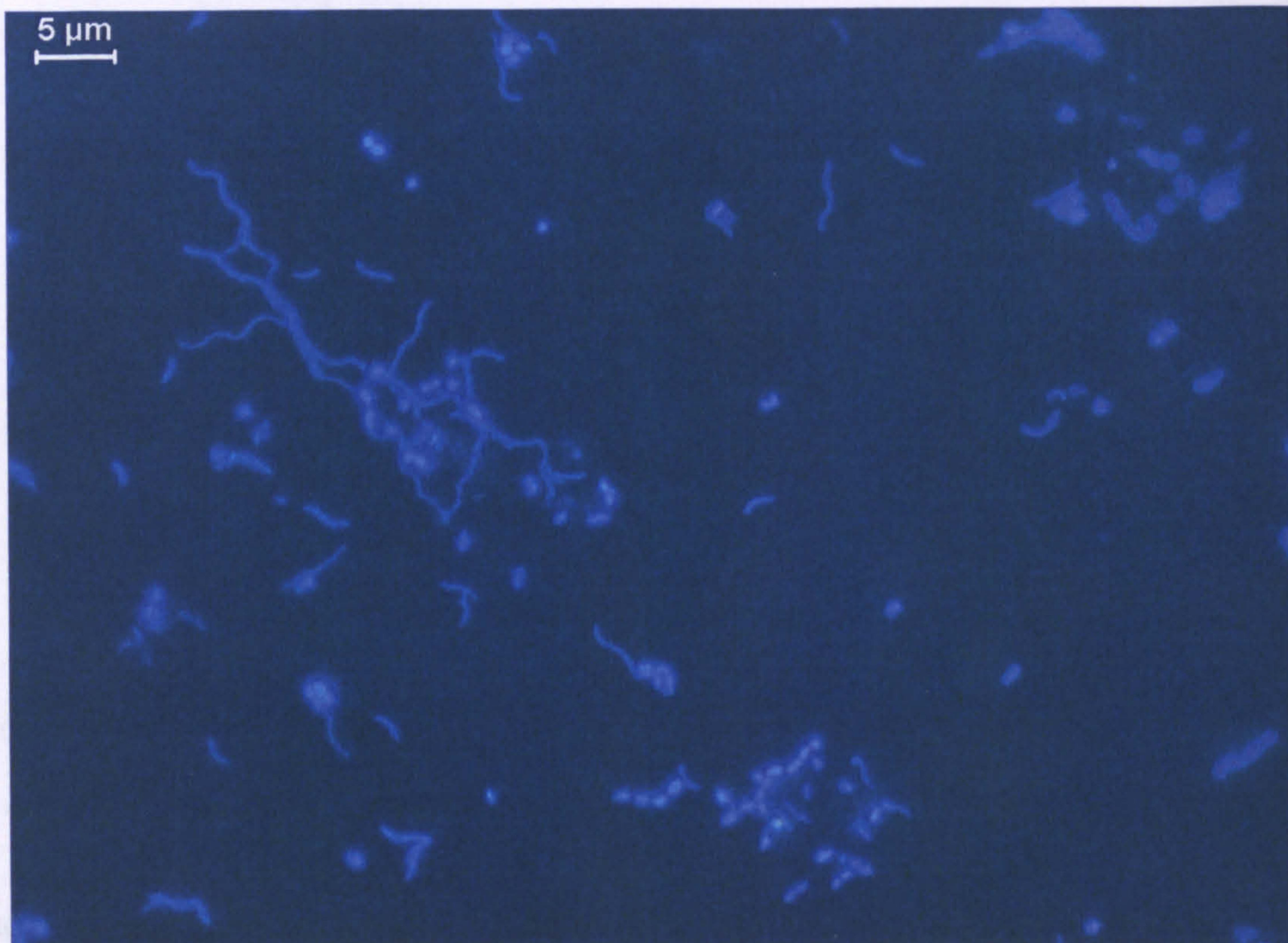


**Figure 5.10.** Bacterial cells in the enrichment cultures of the early melt season sulphate-reducing bacteria from the Manitsog Glacier incubated at +25 °C for 5 weeks.



There were also morphological differences between low and high temperature populations in the early melt season meltwater. In the cultures at +4 °C, coccus-shaped cells ~ 1  $\mu\text{m}$  in diameter grew in clusters (figure 5.9). At +25 °C, populations of spirillum-shaped and filamentous cells were dominant. Length of spirillum-shaped cells was approximately 3  $\mu\text{m}$ . Also, rod-shaped cells ~ 2  $\mu\text{m}$  in length grew at the temperature of + 25 °C (figure 5.10).

#### **5.1.5. Chemistry of Greenland meltwaters**

Electrical conductivity in the bulk meltwater stream of the Manitsoq glacier was at its highest, 46  $\mu\text{S cm}^{-1}$ , at the early stage of the melt season, indicating release of long-residence time meltwaters with high solute concentrations (figure 5.11). By early July, concurrent with the first discharge peak, electrical conductivity decreased to the level of 5 - 10  $\mu\text{S cm}^{-1}$ , and remained low until the end of the melt season (Skidmore and Tranter, unpublished data).

Electrical conductivity in the Akuliarusiarssuk meltwater followed a similar trend to the Manitsoq meltwater stream, except in the late melt season when electrical conductivity in Akuliarusiarssuk meltwater suddenly increased to 20 - 25  $\mu\text{S cm}^{-1}$  (Skidmore and Tranter, unpublished data).

Suspended sediment concentration was at its highest in mid-July (table 5.6) and thus followed the pattern of melt season phases presented by Richards et al. (1996), showing higher discharges and suspended sediment concentrations from early to mid July (see table 2.2). On the whole, concentration of suspended sediments remained surprisingly low throughout the melt season, compared to suspended sediment range from 0.1  $\text{g l}^{-1}$  to 6.0  $\text{g l}^{-1}$ , recorded at an Alpine warm-based glacier (Brown et al. 1994a, Brown 2002) and a range from 0.5  $\text{g l}^{-1}$  to 6.7  $\text{g l}^{-1}$ , recorded at a High Arctic polythermal glacier (Hodgkins et al. 1997).



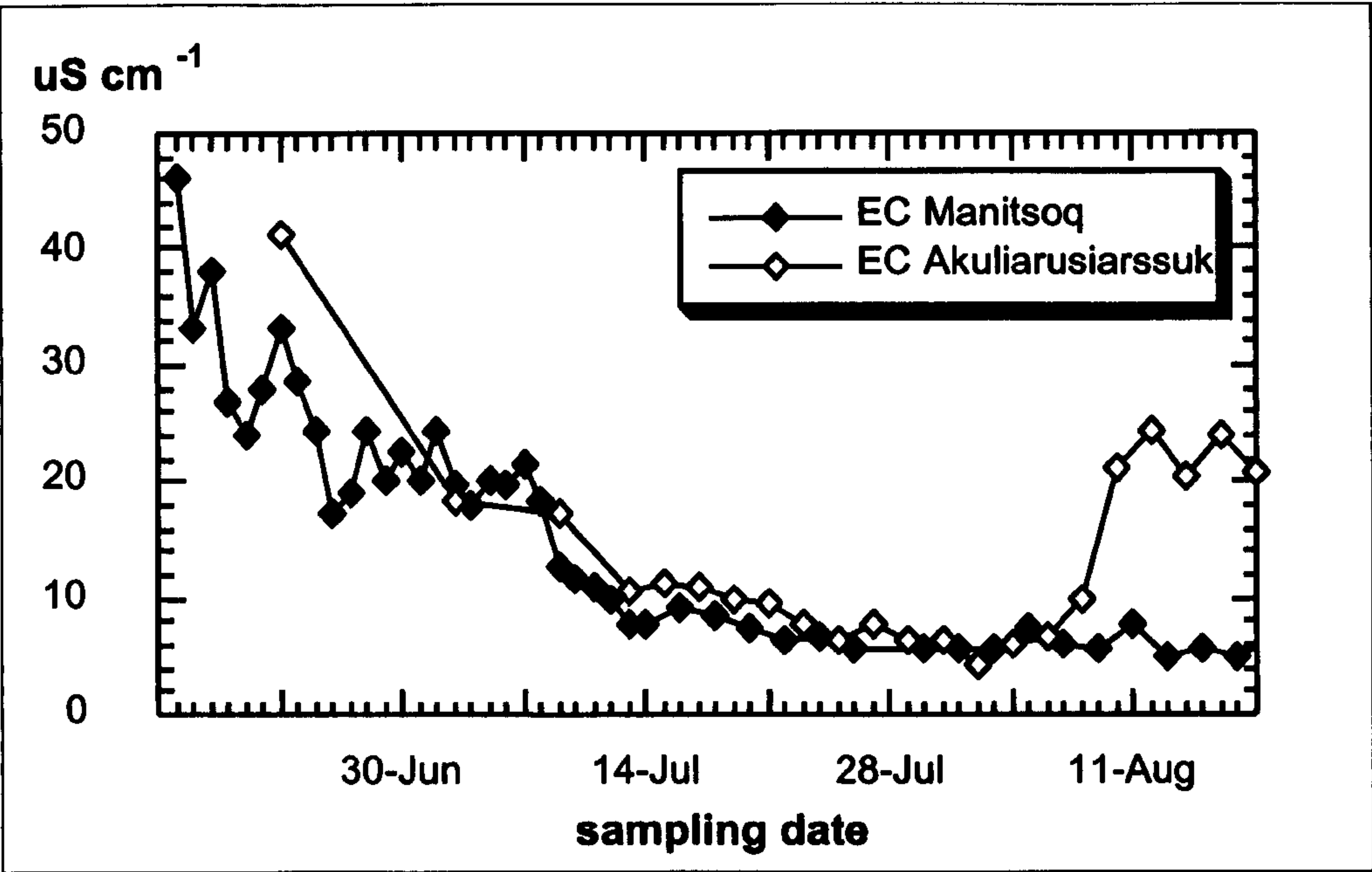


**Figure 5.11.** Electrical conductivity (25 °C) in the bulk proglacial meltwater streams of the Manitsoq and Akuliarusiarsuk glaciers in the melt season 1999 (Skidmore and Tranter, unpublished data).

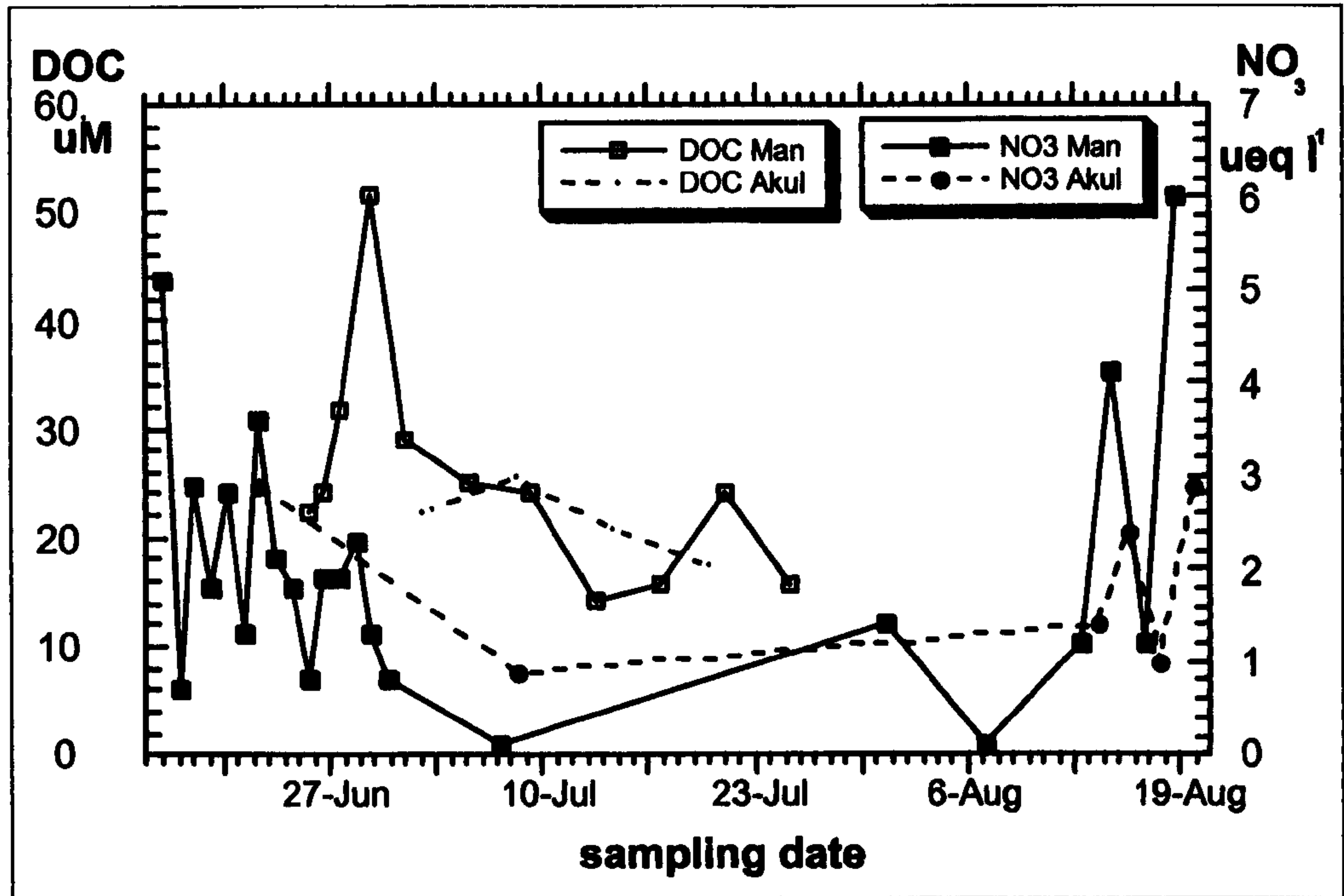


**Figure 5.12.** Dissolved organic carbon and nitrate concentrations in the bulk proglacial meltwater streams of the Manitsoq and Akuliarusiarsuk glaciers in the melt season 1999 (Skidmore and Tranter, unpublished data).



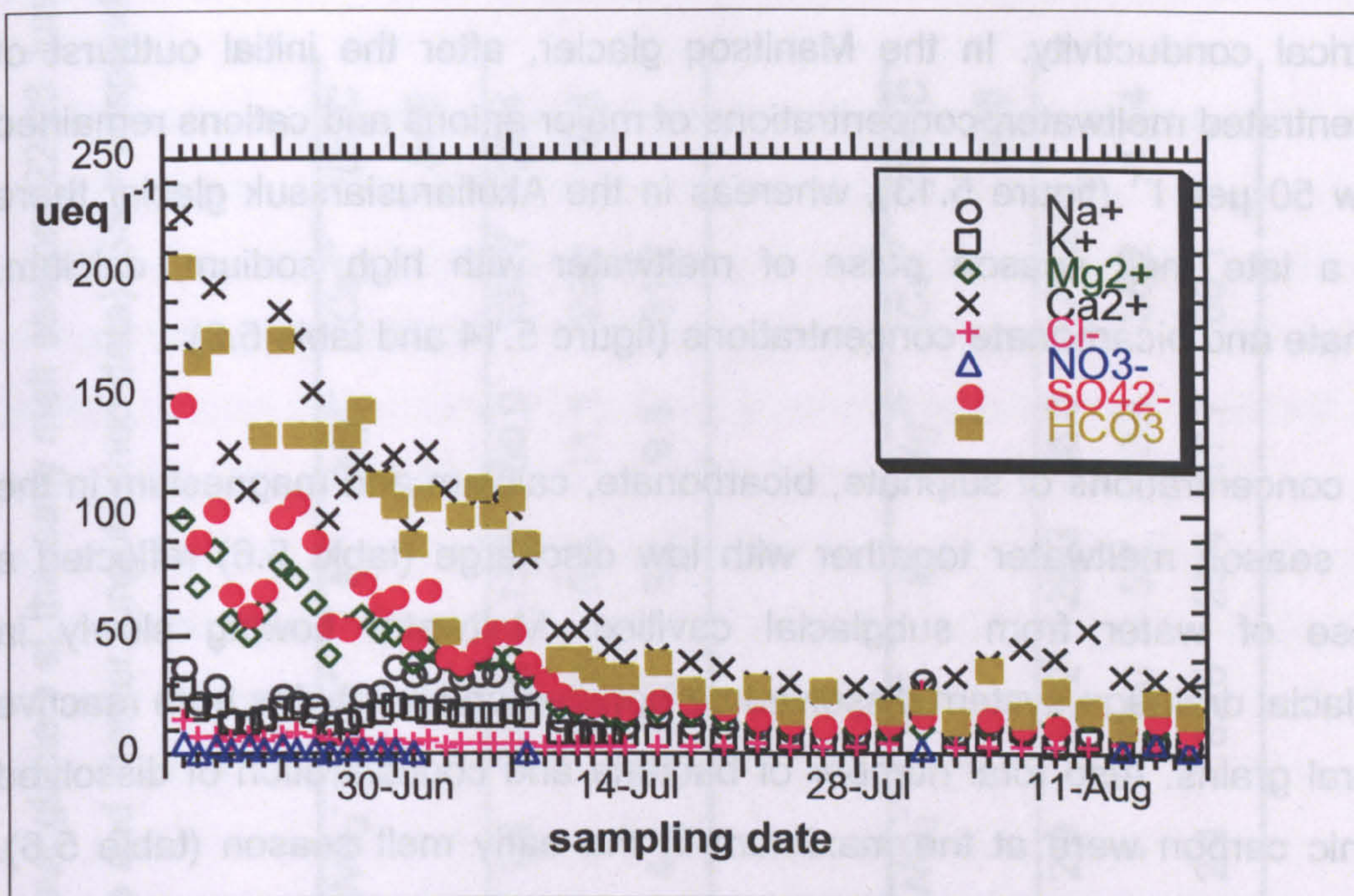


**Figure 5.13.** Major anion and cation concentrations in the bulk proglacial meltwater stream in the Manitsog glacier in the melt season 1999 (Skidmore and Tranter, unpublished data).

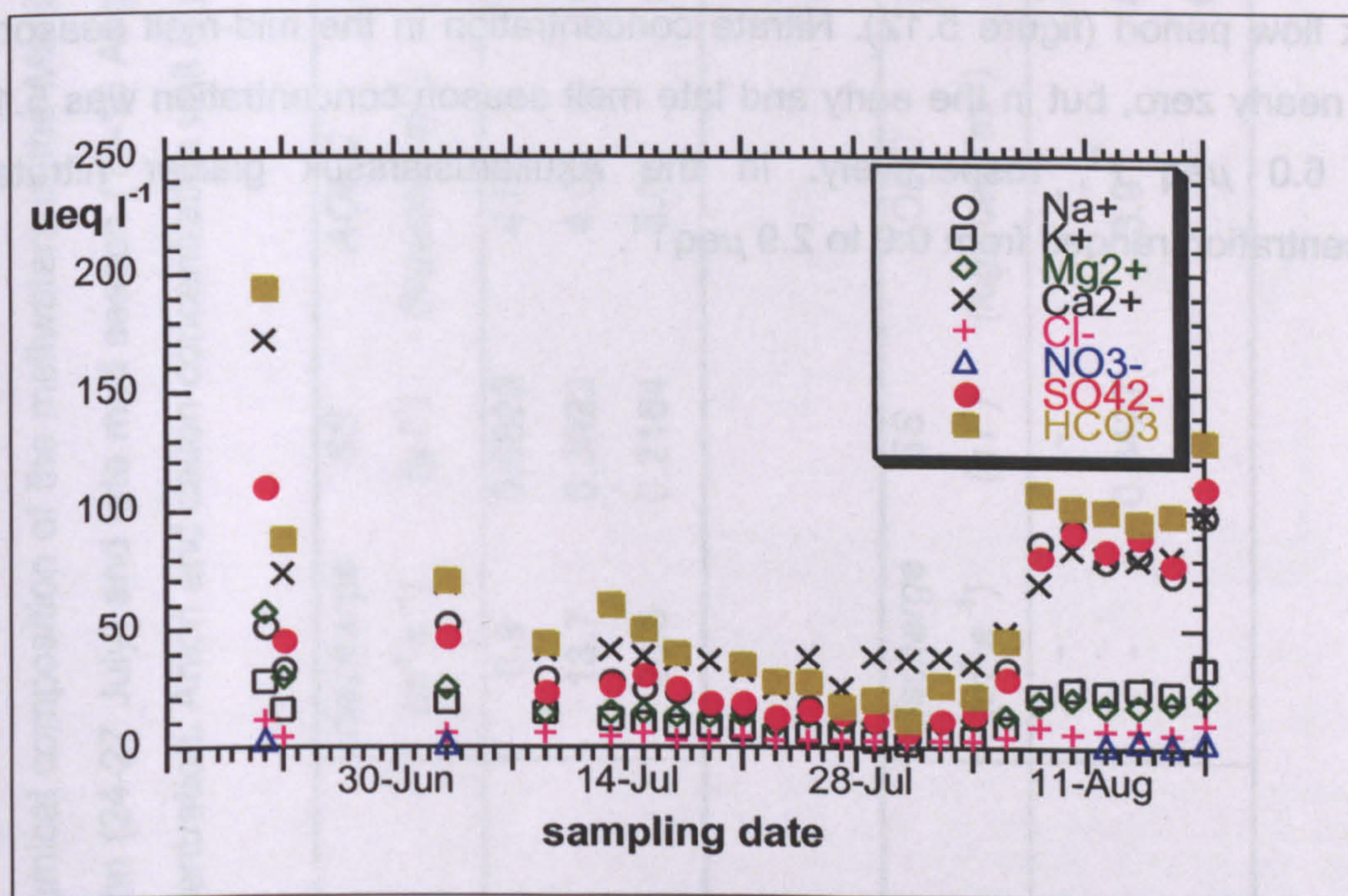


**Figure 5.14.** Major anion and cation concentrations in the bulk proglacial meltwater stream in the Akuliarusiarssuk glacier in the melt season 1999 (Skidmore and Tranter, unpublished data).



Sulphate, calcium and bicarbonate concentrations followed a similar trend to electrical conductivity. In the Manitsoq glacier, after the initial outburst of concentrated meltwater, concentrations of major anions and cations remained below  $50 \mu\text{eq l}^{-1}$  (figure 5.13), whereas in the Akuliarusiarssuk glacier there was a late melt season pulse of meltwater with high sodium, calcium, sulphate and bicarbonate concentrations (figure 5.14 and table 5.6).

High concentrations of sulphate, bicarbonate, calcium and magnesium in the early season meltwater together with low discharge (table 5.6) reflected a release of water from subglacial cavities. Meltwater flowing slowly in subglacial drainage system dissolved carbonates and sulphides from reactive mineral grains. Also total number of bacteria and concentration of dissolved organic carbon were at the maximum in the early melt season (table 5.6). Later on, when discharge and dilution with supraglacial meltwaters in the bulk meltwater stream increased, bacterial population densities decreased.

The concentration of dissolved organic carbon (DOC) in meltwaters from both glaciers remained low in the mid-melt season. The maximum concentration ( $51.6 \mu\text{M}$ ) was detected in the Manitsoq glacier at the end of June, before the peak flow period (figure 5.12). Nitrate concentration in the mid-melt season was nearly zero, but in the early and late melt season concentration was  $5.1$  and  $6.0 \mu\text{eq l}^{-1}$ , respectively. In the Akuliarusiarssuk glacier nitrate concentration ranged from  $0.9$  to  $2.9 \mu\text{eq l}^{-1}$ .



**Table 5.6.** Chemical composition of the meltwaters in the Manitsoq and Akuliarussarsuk glaciers at the early melt season (22-23 June), mid-melt season (24-27 July) and late melt season (15-16 August) in 1999 (Skidmore and Tranter, unpublished data). SS = suspended sediment concentration. Anion and cation concentration unit is  $\mu\text{eq l}^{-1}$ .

Manitsoq	discharge ( $\text{m}^3 \text{ s}^{-1}$ )	SS ( $\text{g l}^{-1}$ )	AODC ( $\log_{10}\text{cells ml}^{-1}$ )	pH	Cl	$\text{SO}_4^{2-}$	$\text{NO}_3^-$	$\text{Na}^+$	$\text{K}^+$	$\text{Mg}^{2+}$	$\text{Ca}^{2+}$	DOC ( $\mu\text{M}$ )
22/06	0.9	0.0828	4.54	7.6	6.6	68.9	1.3	16.0	15.0	60.0	133.7	22.4
24/07	13.7	0.3922	4.02	6.6	3.9	14.2	-	10.3	5.5	11.1	29.4	15.8
15/08	26.5	0.2164	3.83	6.6	3.0	14.7	4.1	6.6	3.1	9.8	31.7	-

Akuliaru-siarssuk	discharge ( $\text{m}^3 \text{ s}^{-1}$ )	SS ( $\text{g l}^{-1}$ )	AODC ( $\log_{10}\text{cells ml}^{-1}$ )	pH	Cl	$\text{SO}_4^{2-}$	$\text{NO}_3^-$	$\text{Na}^+$	$\text{K}^+$	$\text{Mg}^{2+}$	$\text{Ca}^{2+}$	DOC ( $\mu\text{M}$ )
23/06	-	-	-	7.3	11.6	110.1	2.9	52.2	28.3	58.0	172.2	-
27/07	-	0.9427	3.91	6.8	2.8	16.9	-	18.0	5.7	13.4	38.2	17.4
16/08	-	-	-	6.9	7.7	90.4	2.4	82.5	25.4	17.7	80.1	-



5.2. Jostedalsbreen ice cap in southern Norway

5.2.1. Meltwater discharge in the Bødalsbreen outlet glacier

In summer 2000, meltwater discharge measurements in the north-western margin of the Jostedalsbreen ice cap started at the beginning of June. By then, melting had already started. In Bødalsbreen outlet glacier, tracer experiments suggested that at the beginning of June the subglacial drainage system was in a phase of hydraulically inefficient, distributed system (Grust et al. 2002). Discharge in the main meltwater stream at the early melt season was  $2.6 \text{ m}^3 \text{ s}^{-1}$  and suspended sediment concentration was  $0.014 \text{ g l}^{-1}$  (figure 5.15 and table 5.12). From then on, discharge varied between 2 and  $4 \text{ m}^3 \text{ s}^{-1}$ , but there were noticeable peaks at the beginning and at the end of July. The maximum discharge measured was  $6.5 \text{ m}^3 \text{ s}^{-1}$  (Skidmore and Tranter, unpublished data).

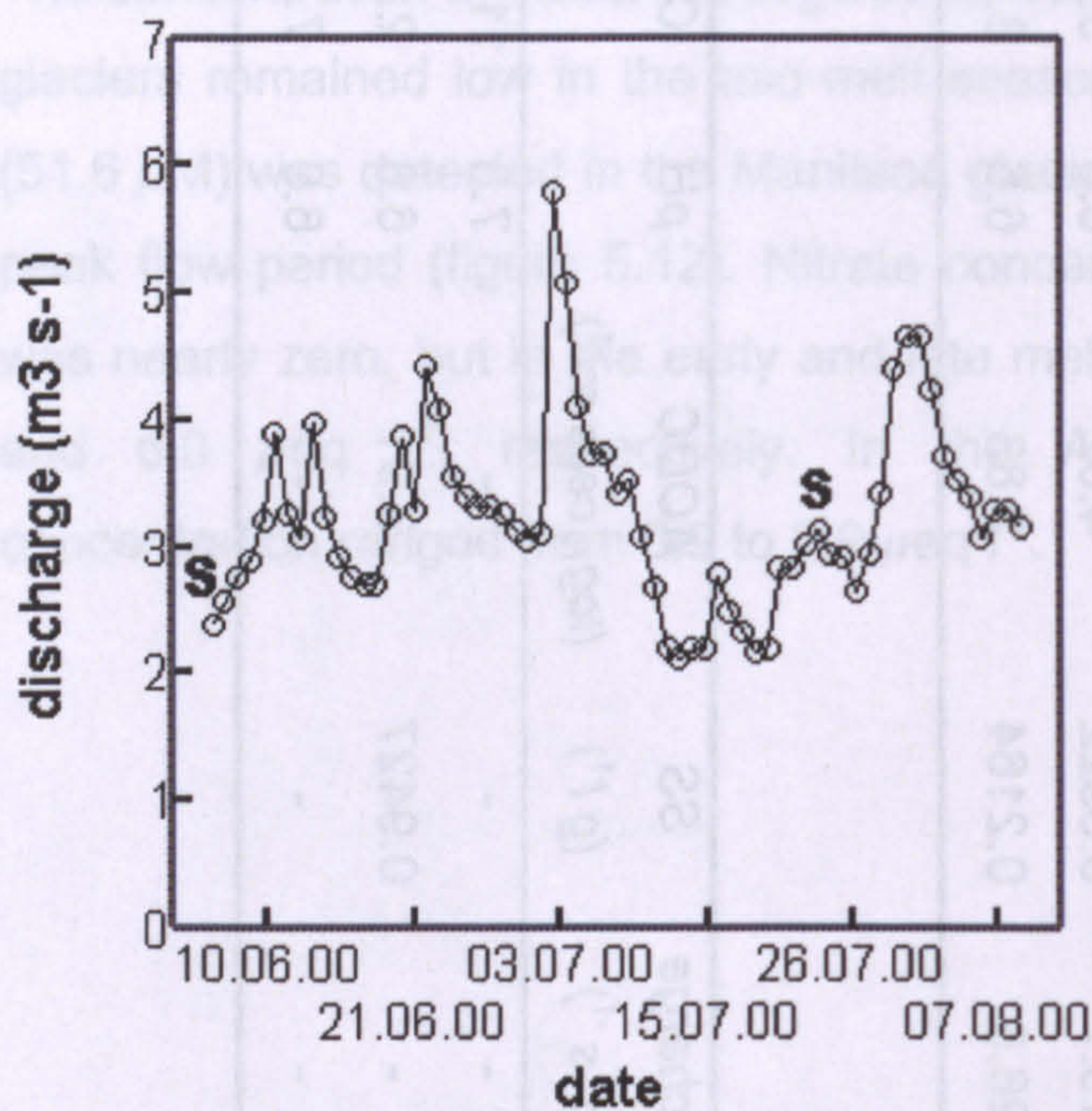


**Figure 5.15.** Discharge in the main meltwater stream of the Bødalsbreen outlet glacier in the melt season 2000 (Grunt, Skidmore and Tranter, unpublished data). S=meltwater sampling.



### 5.2.2. Bacterial populations in Jostedalsbreen meltwaters

In the early melt season, the total number of bacteria in meltwaters of the four outlet glaciers of the Jostedalsbreen ice cap ranged from 3.87 to 4.18  $\log_{10}$  cells  $\text{ml}^{-1}$ , and after the high discharge peak 4.24 - 4.36  $\log_{10}$  cells  $\text{ml}^{-1}$ . There were only slight spatial and temporal variations, and no statistical significant differences in meltwaters around the ice cap were detected (figure 5.16 and appendix 5). In multiple comparison test, early melt season subglacial meltwater from the Bødalsbreen outlet glacier stood out with lower numbers of bacterial cells than the other meltwaters. However, no evidence for obvious seasonal trend in numbers of bacterial cells in meltwaters from early to mid melt season was found (statistical test for homogeneous subsets in appendix 5).

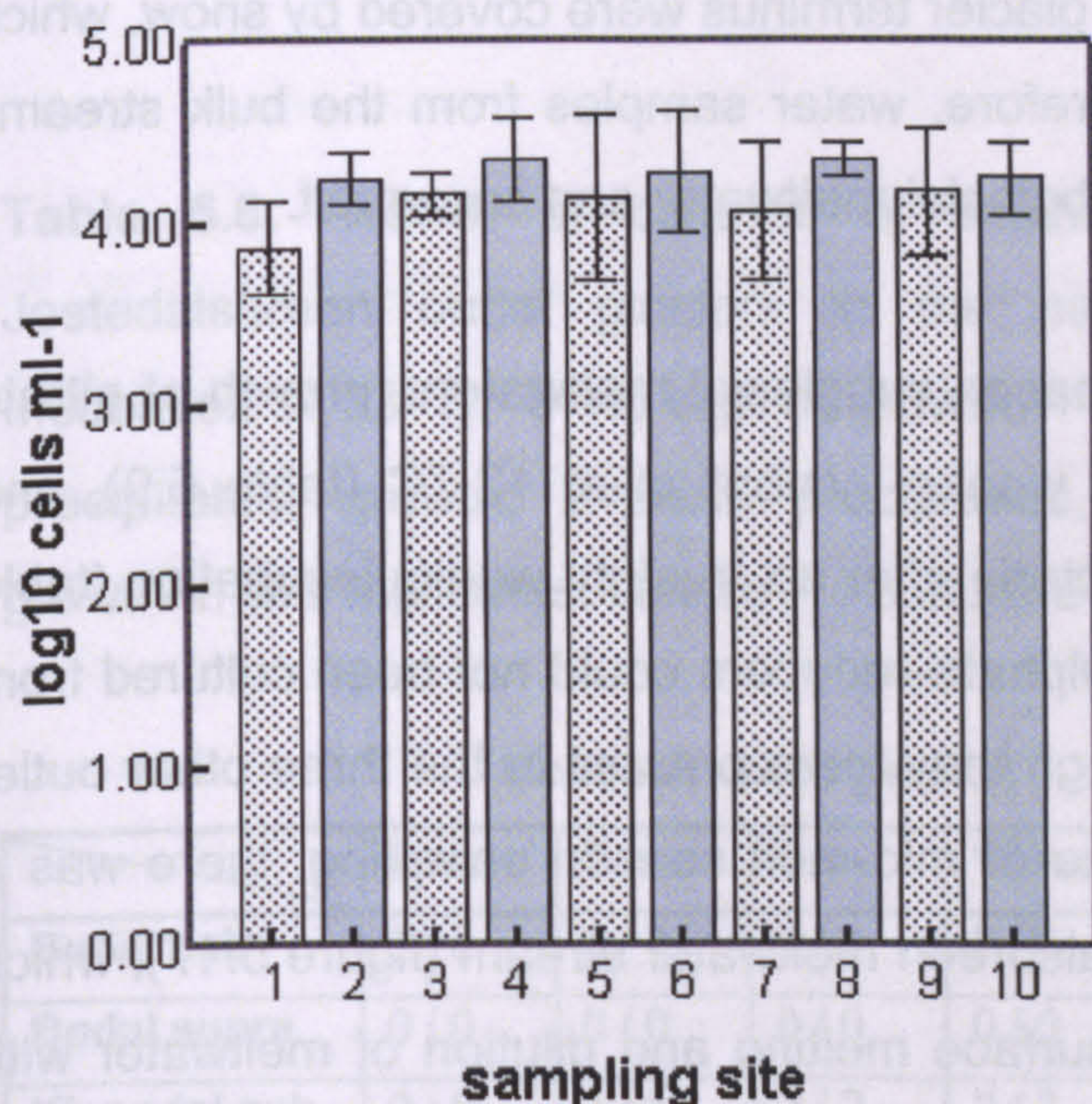


**Figure 5.16.** Total numbers of bacteria in meltwaters from four outlet glaciers of the Jostedalsbreen ice cap in the early melt season 2-7 June 2000 (dotted bars) and mid-melt season 19-28 July 2000 (solid bars). The bars show the mean values of the three replicate counts and error bars show 95% confidence intervals for the means of three replicates. Sampling sites as follows: **1-2** = Bødalsbreen subglacial meltwater; **3-4** = Bødalsbreen supraglacial meltwater; **5-6** = Kjenndalsbreen subglacial meltwater; **7-8** = Nigardsbreen subglacial meltwater; **9-10** = Bergsetbreen subglacial meltwater.



### **5.2.3. Growth of bacterial cultures at constantly low temperature**

Nitrate-reducing bacteria and sulphate-reducing bacteria were cultured from the early melt season subglacial meltwaters, but not from the supraglacial meltwater (tables 5.7 and 5.8). Visible growth of both nitrate reducers and sulphate reducers was detected after five weeks incubation at +2 °C. Bacteria with different growth characteristics were found in the various outlet glaciers. In the early melt season cultures from the Bødalsbreen and Bergsetbreen glaciers, no growth of sulphate-reducing bacteria was detected even after 24 weeks incubation, whereas growth of sulphate-reducers in cultures from the Kjenndalsbreen glacier was more rapid than in all the other outlet glaciers (table 5.8). The absence of sulphate-reducing bacteria in the Bødalsbreen and Bergsetbreen glaciers in the early melt season can be explained with the effect of snowpack. At the time of early melt season sampling, the glaciers and proglacial field close to the glacier terminus were covered by snow, which was rapidly melting away. Therefore, water samples from the bulk streams were likely to be a mixture of subglacial meltwater and snowmelt.

In cultures from the mid-melt season subglacial meltwaters, growth of nitrate reducers was evident after six weeks incubation at +2 °C (table 5.9), and growth of sulphate-reducing bacteria after six to eight weeks incubation (table 5.10). Surprisingly yet again, sulphate-reducers could not be cultured from Bødalsbreen meltwaters, although they were present in the three other outlet glaciers (table 5.10). At the time of mid-melt season sampling, there was a slight peak in discharge of Bødalsbreen meltwater stream (figure 5.17), which may be a sign of increase in surface melting and dilution of meltwater with waters from the top of the glacier.



**Table 5.7.** Growth of cultures of nitrate-reducing bacteria from the Jostedalsbreen outlet glaciers in the early melt season (2.-7.6.2000). Incubation at +2 °C. 0=no change in colour nor turbidity, no precipitates; 1= colour turned from deep purple to pale violet, slightly turbid, yellow precipitates, growth; 2= colour yellow-grey, turbid, lot of precipitates, strong growth. Figures show growth in two replicates: culture A / culture B.

Incubation time (weeks)								
	2 w	5 w	8 w	12 w	14 w	16 w	20 w	24 w
<b>Bødal sub</b>	0 / 0	1 / 1	1 / 1	1 / 1	1 / 1	1 / 1	1 / 1	1 / 1
<b>Bødal supra</b>	0 / 0	0 / 0	0 / 0	0 / 0	0 / 0	0 / 0	0 / 0	0 / 0
<b>Kjenndal sub</b>	0 / 0	1 / 1	1 / 1	1 / 1	1 / 1	1 / 1	1 / 1	1 / 1
<b>Nigard sub</b>	0 / 0	1 / 1	1 / 1	1 / 1	1 / 1	1 / 1	1 / 1	1 / 1
<b>Bergset sub</b>	0 / 0	1 / 1	1 / 1	1 / 1	1 / 1	1 / 1	1 / 1	1 / 1

**Table 5.8.** Growth of cultures of sulphate-reducing bacteria from the Jostedalsbreen outlet glaciers in the early melt season (2.-7.6.2000). Incubation at +2 °C. 0=no sign of growth; 1=culture turning cloudy, dark grey precipitates, growth; 2=black precipitates, strong growth. Figures show growth in two replicates: culture A / culture B.

Incubation time (weeks)								
	2 w	5 w	8 w	12 w	14 w	16 w	20 w	24 w
<b>Bødal sub</b>	0 / 0	0 / 0	0 / 0	0 / 0	0 / 0	0 / 0	0 / 0	0 / 0
<b>Bødal supra</b>	0 / 0	0 / 0	0 / 0	0 / 0	0 / 0	0 / 0	0 / 0	0 / 0
<b>Kjenndal sub</b>	0 / 0	1 / 1	2 / 2	2 / 2	2 / 2	2 / 2	2 / 2	2 / 2
<b>Nigard sub</b>	0 / 0	1 / 1	1 / 1	1 / 1	1 / 1	1 / 1	1 / 1	1 / 1
<b>Bergset sub</b>	0 / 0	0 / 0	0 / 0	0 / 0	0 / 0	0 / 0	0 / 0	0 / 0



**Table 5.9.** Growth of cultures of nitrate-reducing bacteria from the Jostedalsbreen outlet glaciers in mid-melt season meltwaters (19.-28.7.2000). Incubation at +2 °C. 0=no change in colour nor turbidity, no precipitates; 1= colour turned from deep purple to pale violet, slightly turbid, yellow precipitates, growth; 2= colour yellow-grey, turbid, lot of precipitates, strong growth. Figures show growth in two replicates: culture A / culture B.

Incubation time (weeks)					
	6 w	8 w	12 w	17 w	21 w
Bødal sub	1 / 1	1 / 1	1 / 1	1 / 1	1 / 1
Bødal supra	1 / 1	1 / 1	1 / 1	1 / 1	1 / 1
Kjenndal sub	1 / 1	1 / 1	1 / 1	1 / 1	1 / 1
Nigard sub	1 / 1	1 / 1	1 / 1	1 / 1	1 / 1
Bergset sub	1 / 1	1 / 1	1 / 1	1 / 1	1 / 1

**Table 5.10.** Growth of cultures of sulphate-reducing bacteria from the Jostedalsbreen outlet glaciers in mid-melt season meltwaters (19.-28.7.2000). Incubation at +2 °C. 0=no sign of growth; 1=culture turning cloudy, dark grey precipitates, growth; 2=black precipitates, strong growth. Figures show growth in two replicates: culture A / culture B.

Incubation time (weeks)					
	6 w	8 w	12 w	17 w	21 w
Bødal sub	0 / 0	0 / 0	0 / 0	0 / 0	0 / 0
Bødal supra	0 / 0	0 / 0	0 / 0	0 / 0	0 / 0
Kjenndal sub	1 / 1	1 / 2	1 / 2	2 / 2	2 / 2
Nigard sub	0 / 0	1 / 0	2 / 1	2 / 1	2 / 1
Bergset sub	0 / 1	1 / 2	2 / 2	2 / 2	2 / 2



#### **5.2.4. Temperature characteristics of sulphate-reducing bacteria in Jostedalsbreen early and mid-melt season meltwaters**

The enrichment cultures with strong growth from both early melt season and mid-melt season (tables 5.8 and 5.10) were chosen for further studies on temperature characteristics of sulphate-reducing bacteria. Cultures from the Kjenndalsbreen subglacial early season meltwater and the Bergsetbreen subglacial mid-melt season meltwater were studied. The incubation temperature ranged from -0.6 °C to +40.0 °C, with 1.9 °C intervals. The frequency of dividing cells in the cultures at the beginning of the experiment was 28 - 33%.

##### **5.2.4.1. Sulphide production in Jostedalsbreen SRB-cultures**

After one week incubation, black precipitates appeared at temperatures from +12 °C to +29 °C in the early melt season cultures, and from +12 °C to +34 °C in the mid-melt season cultures. After two and five weeks, the minimum temperature for visible growth was +7 °C and +3 °C, respectively (appendix 6).

In the early melt season cultures, the maximum sulphide production after five weeks was 2.95 mM, and the optimum temperature was +13 - +16 °C, although there was another sulphide production peak at +25 – +29 °C (figure 5.17). After 12 weeks, high concentration of sulphide (1.88 mM) was produced also at +5 °C. From then onwards, psychrotolerant and psychrophilic organisms were dominant. After 25 weeks, sulphide-reducing bacteria were growing even at the lowest temperature of -0.6 °C, resulting in sulphide production of 1.01 mM (figure 5.18). Due to the oxygen contamination during sampling (see chapter 5.1.4.1), sulphate-reducers which grew extremely slowly at subzero temperature died and chemical oxidation of  $S^{2-}$  took place. Hence, sulphide was not found at -0.6 °C after 32 or 42 weeks.



In the mid-melt season culture, there was no growth of sulphate-reducing bacteria below +7 °C (figures 5.17 - 5.18). Sulphide production activity was dominated by mesophilic and psychrotolerant organisms. After 5 and 12 weeks, the optimum temperature was +32 °C, but there was secondary sulphide production at +12 - +16 °C (figures 5.17 and 5.18). Later on, the activity of psychrotrophs was negligible, and only mesophilic sulphate-reducers remained active until the end of 42 weeks incubation, with the maximum sulphide production at +24 °C (figure 5.18). Uncommonly, sulphide production rate at +24 - +25 °C reached a maximum only after 32 weeks incubation. In contrast, cultures incubated at +5 °C and +16 °C peaked by about 5 weeks (figure 5.20).

Sulphate reduction rates were clearly higher in the early melt season cultures than in the mid-melt season cultures. After five weeks the rates were 3.8 - 83.7  $\mu\text{M d}^{-1}$  and 0.03 - 22.2  $\mu\text{M d}^{-1}$ , respectively (figure 5.20 and 5.21). However, sulphate reduction rate at +5 °C reached the maximum only after 25 weeks incubation (figure 5.18). Although sulphate reducers grew slowly at 0 - +5 °C and it took several months to reach the maximum sulphide production rate, they finally produced sulphide equally with the fast-growing mesophiles.



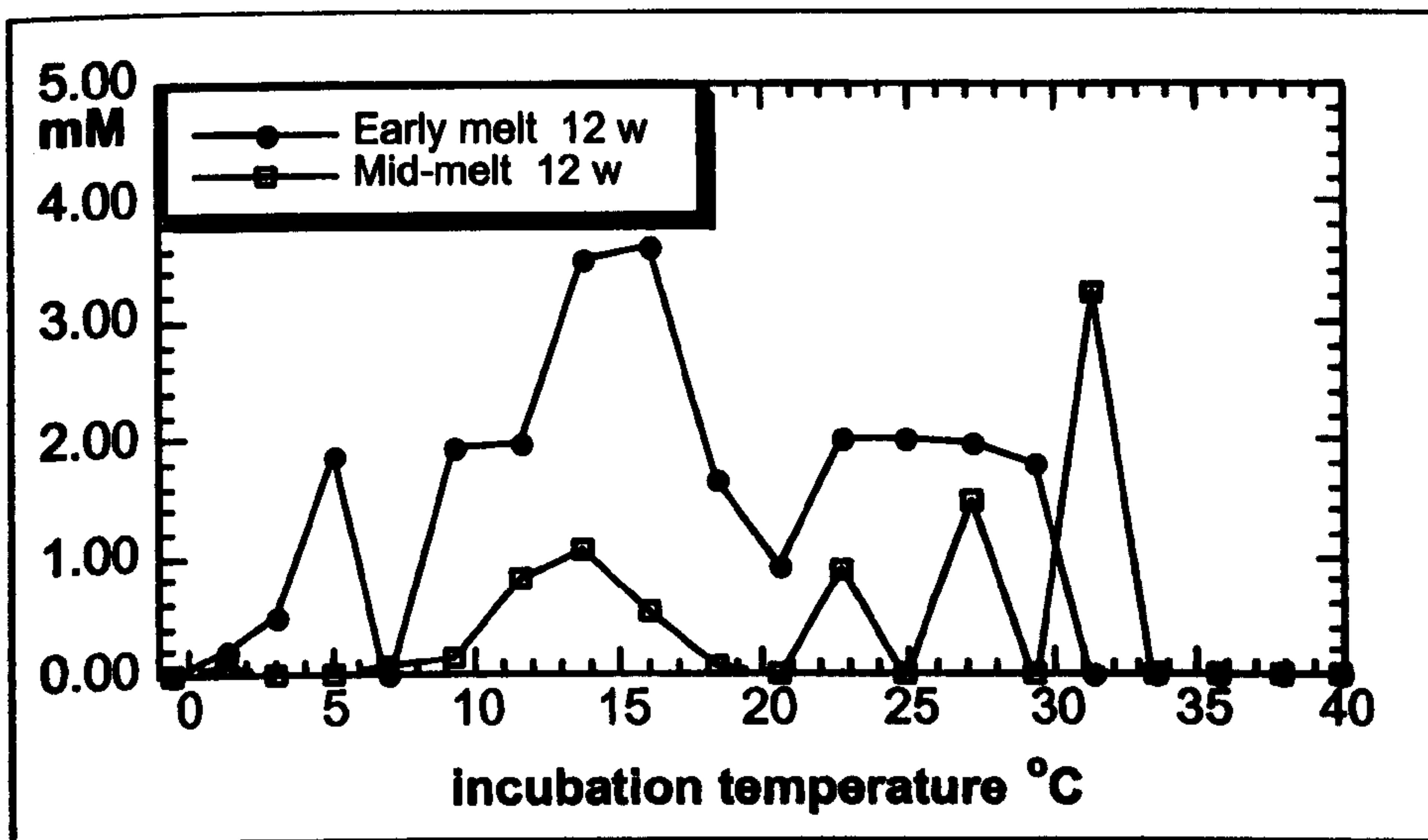
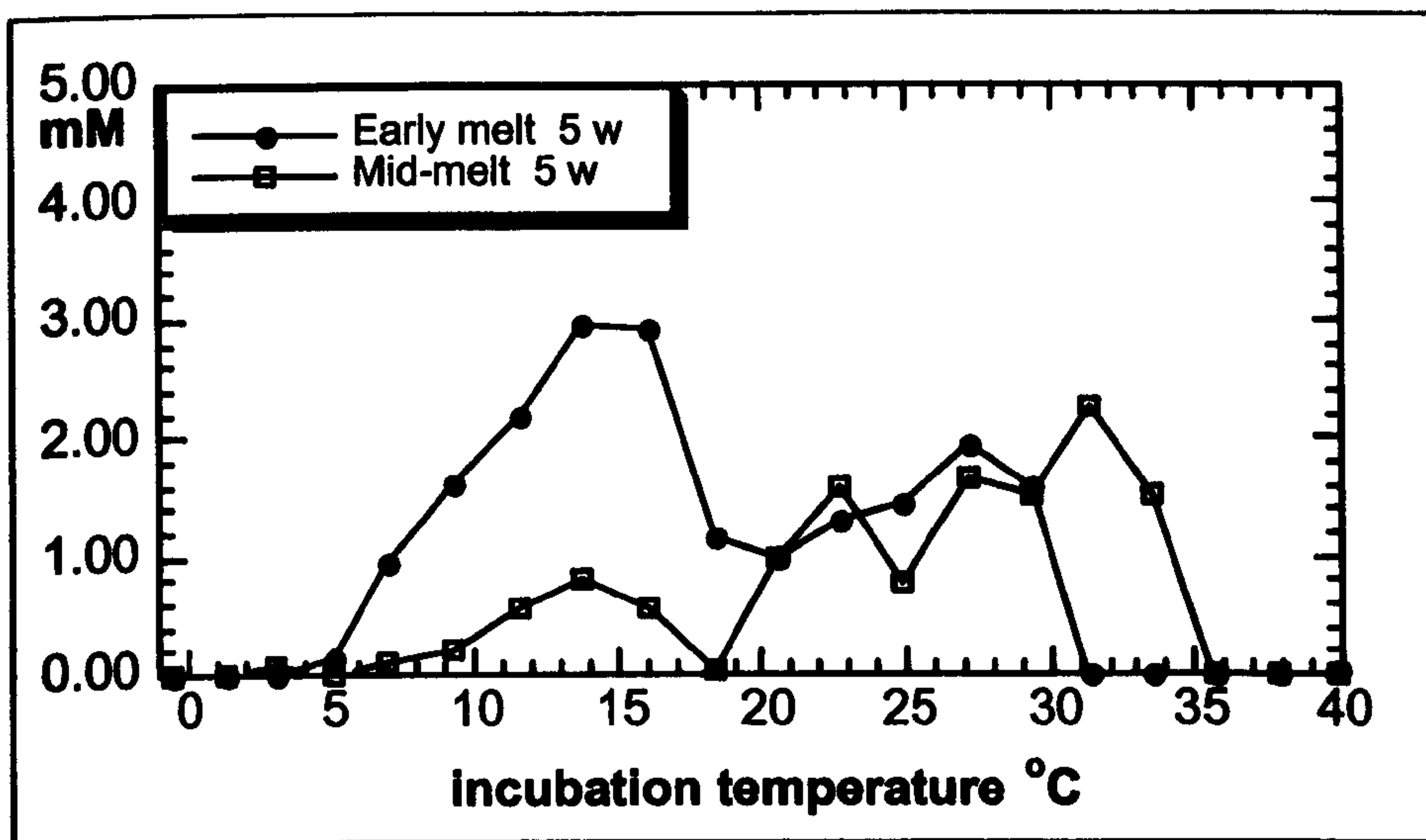


**Figure 5.17.** Growth of sulphate-reducing bacteria from the early (Kjenndalsbreen) and mid-melt (Bergsetbreen) season subglacial meltwaters. Cultures incubated in the thermal gradient system with a temperature range from  $-0.6$  to  $+40$  °C for 5 and 12 weeks. Growth measured as sulphide production (mM).



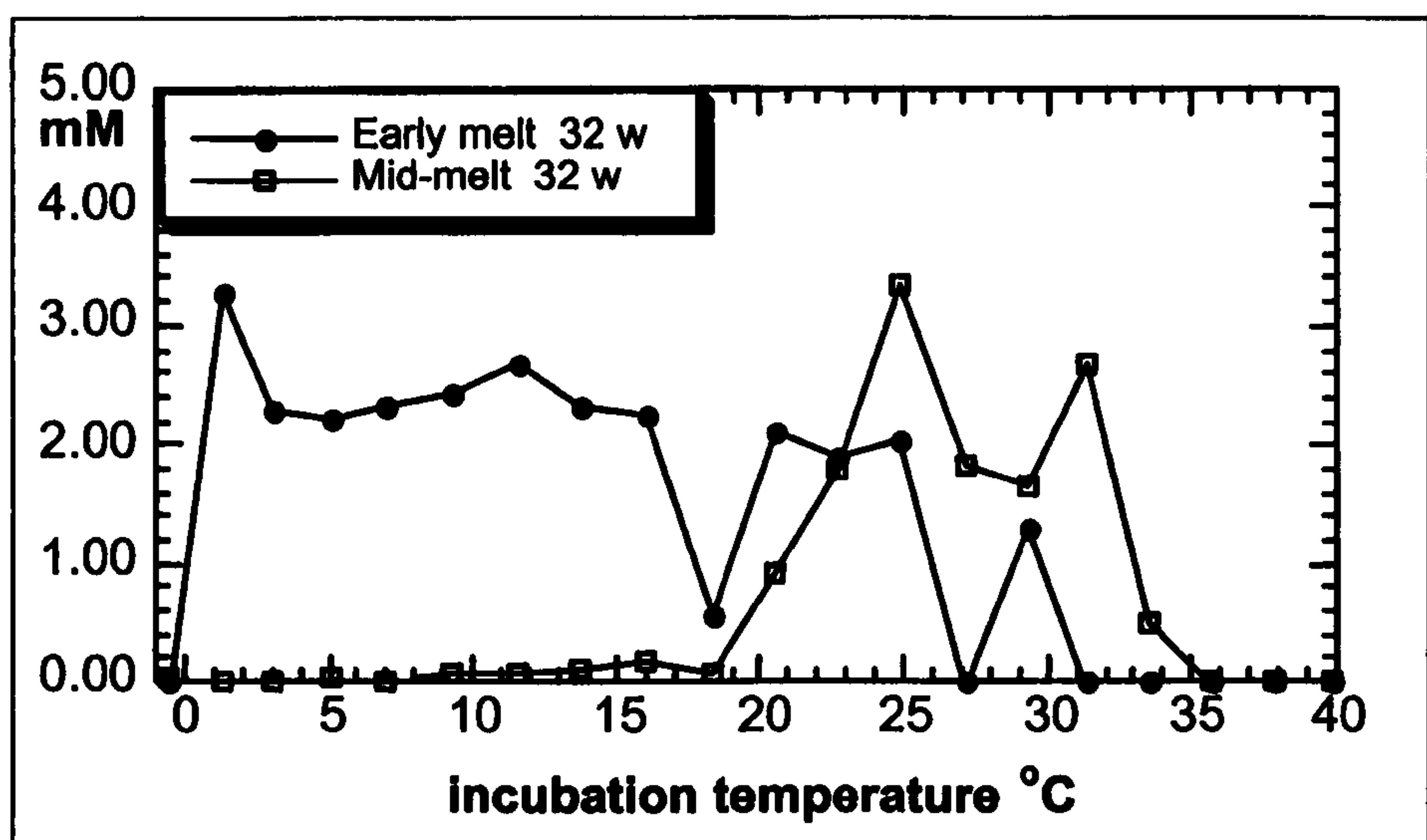
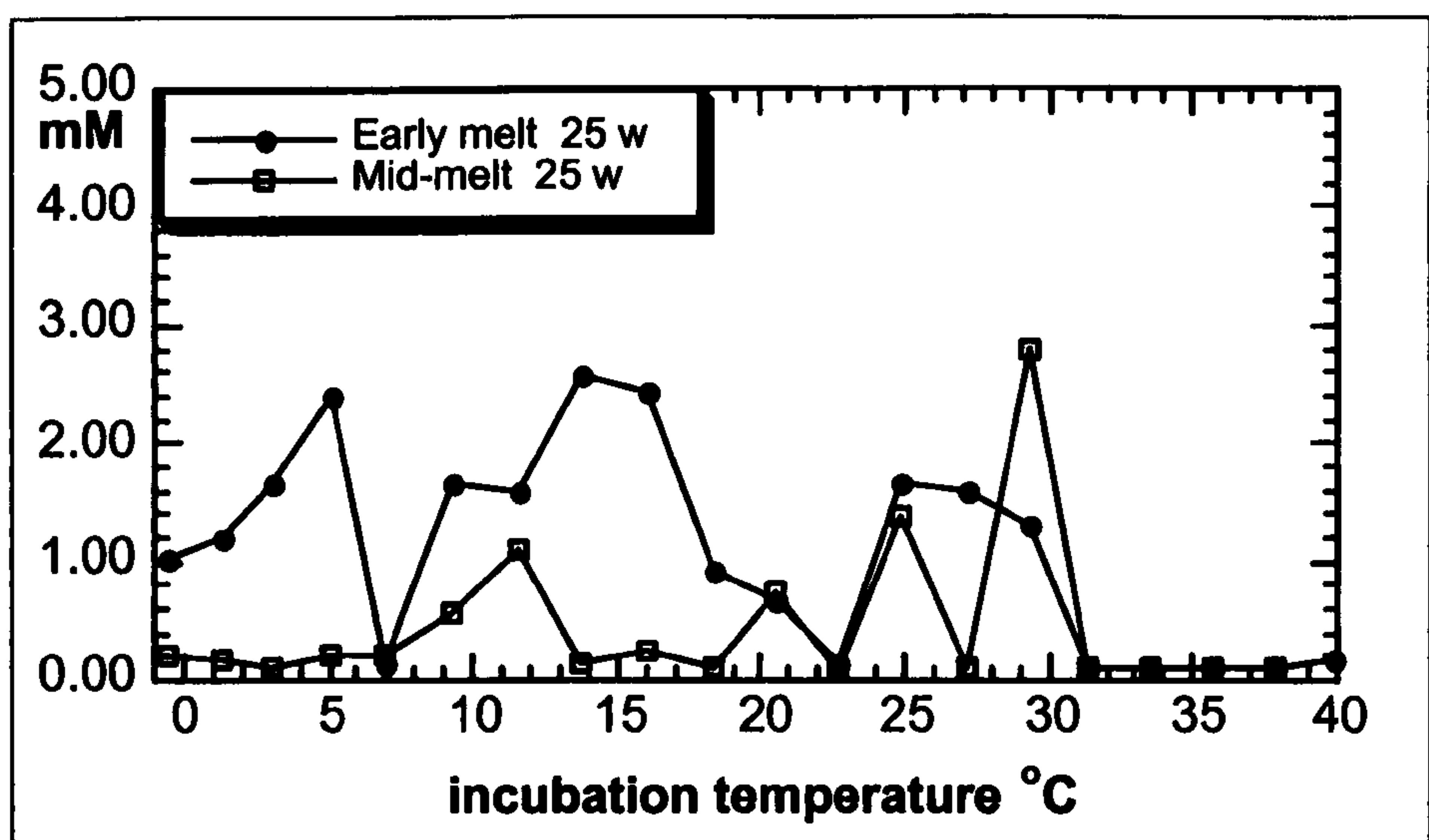


**Figure 5.18.** Growth of sulphate-reducing bacteria from the early (Kjenndalsbreen) and mid-melt (Bergsetbreen) season subglacial meltwaters. Cultures incubated in the thermal gradient system with a temperature range from  $-0.6$  to  $+40$  °C for 25 and 32 weeks. Growth measured as sulphide production (mM).



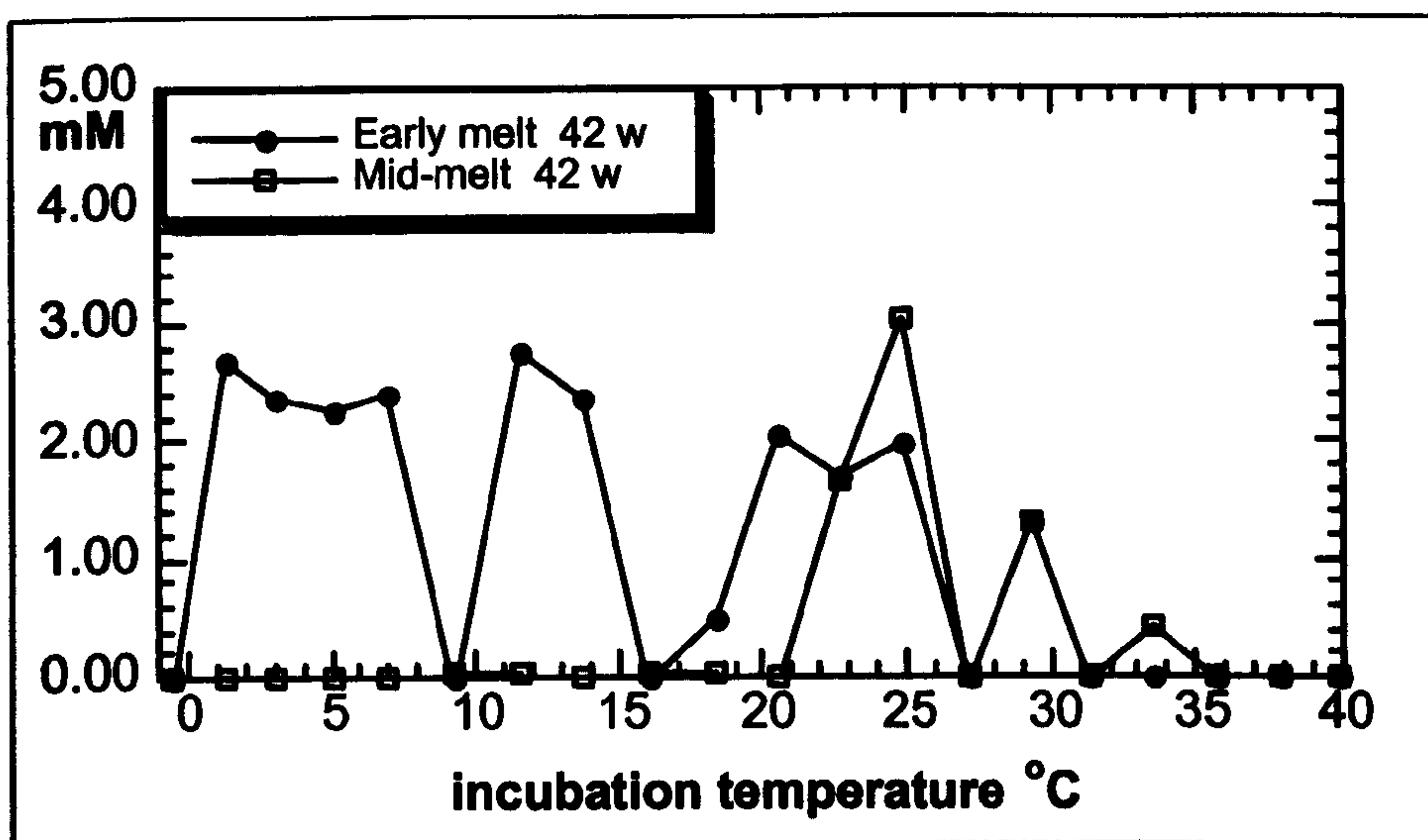


**Figure 5.19.** Growth of sulphate-reducing bacteria from the early (Kjenndalsbreen) and mid-melt (Bergsetbreen) season subglacial meltwaters. Cultures incubated in the thermal gradient system with a temperature range from  $-0.6$  to  $+40$  °C for 42 weeks. Growth measured as sulphide production (mM).

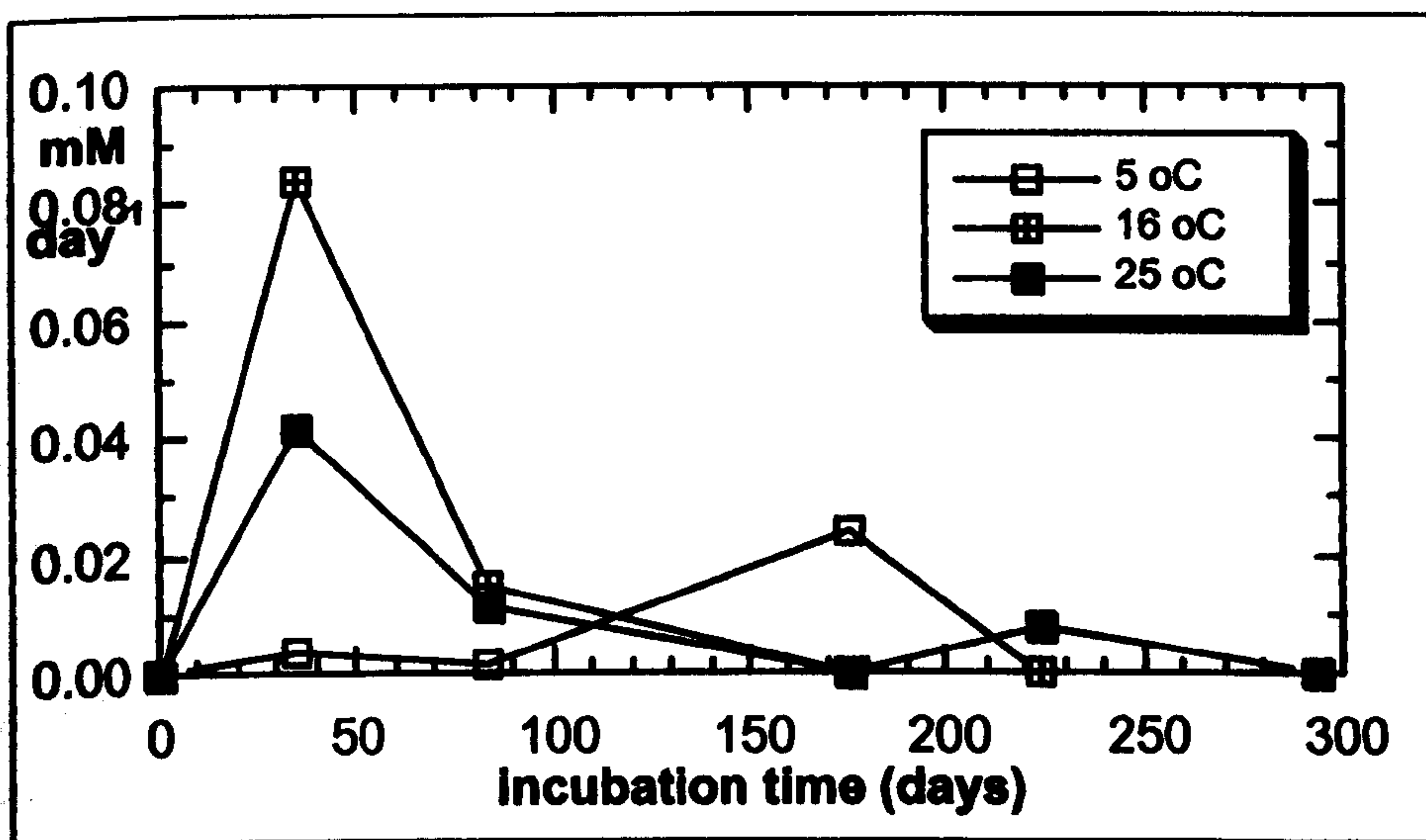


**Figure 5.20.** Sulphate reduction rate at  $+5$  °C,  $+16$  °C and  $+25$  °C in the early melt season culture of sulphate-reducing bacteria from the Kjenndalsbreen glacier.



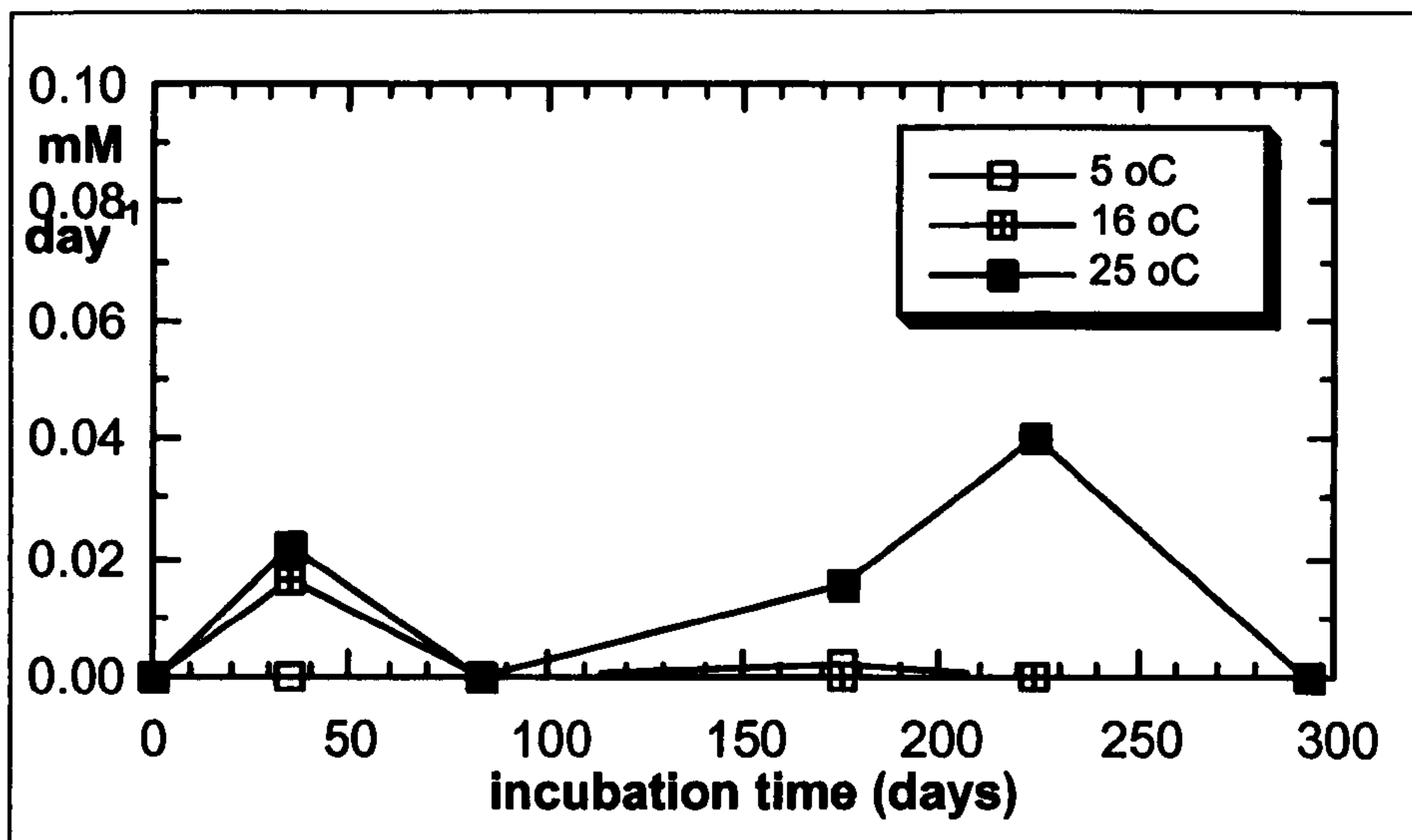


**Figure 5.21.** Sulphate reduction rate at +5 °C, +16 °C and +25 °C in the mid- melt season culture of sulphate-reducing bacteria from the Bergsetbreen glacier.

#### 5.2.4.2. Growth rate in Jostedalsbreen SRB-cultures

In the early melt season cultures, the estimated maximum doubling time of bacterial populations at the beginning of the exponential phase of growth was 7.5 to 8.5 days (table 5.11). The stationary phase was reached after 35 days throughout the temperature range (figure 5.22). Towards the end of the 300 days incubation period there was an increase in total cells at +5 °C and +16 °C. Differences in growth rate at high and low temperatures were more noticeable in the mid-melt season cultures (figure 5.23). The maximum doubling time ranged from 6 to 12 days (table 5.11), and at +16 °C the stationary phase was reached only after more than 100 days, compared to 35 days at +5 °C and +25 °C (figure 5.23). Soon after this, the number of bacteria at +16 °C decreased dramatically, indicating a rapid death phase (figure 5.23), different from the smooth and gradual death of populations incubated at other temperatures.

Frequency of dividing and divided cells after 35 days of incubation was higher at +5 °C, compared to +16 °C and +25 °C (table 5.11, early melt season sample from Kjenndalsbreen). As in the thermal gradient experiment with



Greenland cultures, bacterial growth at the very beginning of incubation may have been much faster at high temperatures, and exponential growth may have ended before the first sampling. Values of FDDC in mid-melt season samples at different temperatures (table 5.11) together with growth curves (figure 5.23) support this explanation. The FDDC values of slowly growing populations at +5 °C and +16 °C after 35 days were comparable (37.5% and 34.9%), whereas at +25 °C populations were already in a gradual death phase and FDDC had dropped to 22.2%.

As for morphology of the cells, at low temperatures cells were mostly thick rods or cocci, approximately 1 μm in diameter. At the temperature of +25 °C, the average diameter of the rod-shaped single cells was 2 - 4 μm.

**Table 5.11.** Estimated doubling times of the total number of cells in cultures of sulphate-reducing bacteria in the early (Kjenndalsbreen) and mid-melt (Bergsetbreen) season during exponential growth, and the frequency of dividing and divided cells (FDDC) after 35 days of incubation at a range of high sulphide production temperatures.

		+5 °C	+16 °C	+25 °C
<b>Early melt (Kjenndalsbreen)</b>	DT (days)	4 - 7.5	4.5 – 8.5	4 - 7.5
	FDDC (%)	40.8	24.4	22.7
<b>Mid melt (Bergsetbreen)</b>	DT (days)	4 - 8	6 - 12	3.5 - 6
	FDDC (%)	37.5	34.9	22.2



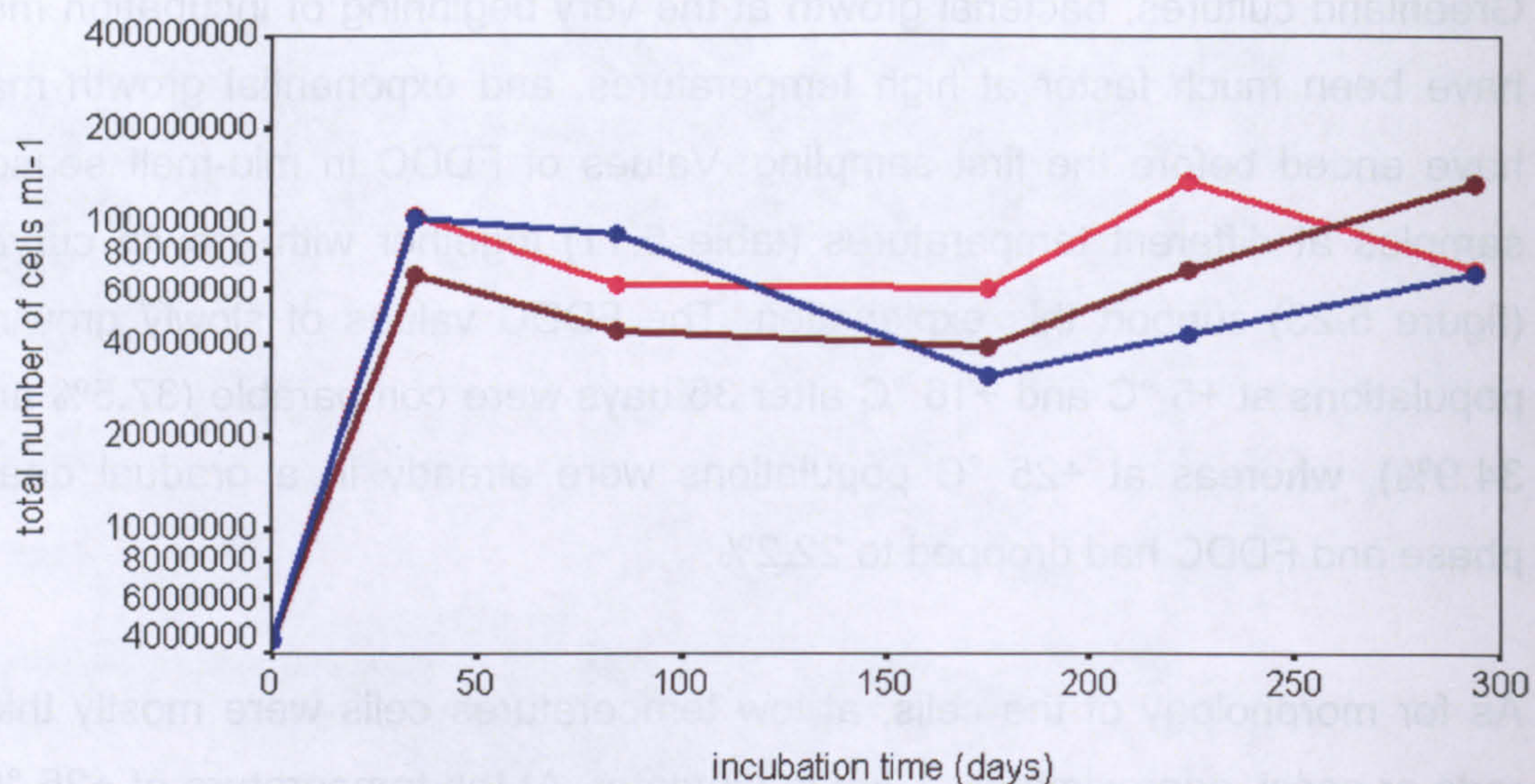


**Figure 5.22.** Growth curves of bacterial populations in the early melt season SRB-enrichment cultures from the Kjenndalsbreen glacier at a range of incubation temperatures. Lines show the mean values of the three replicate counts.. Blue line = +5 °C; brown line = +16 °C; red line = +25 °C.

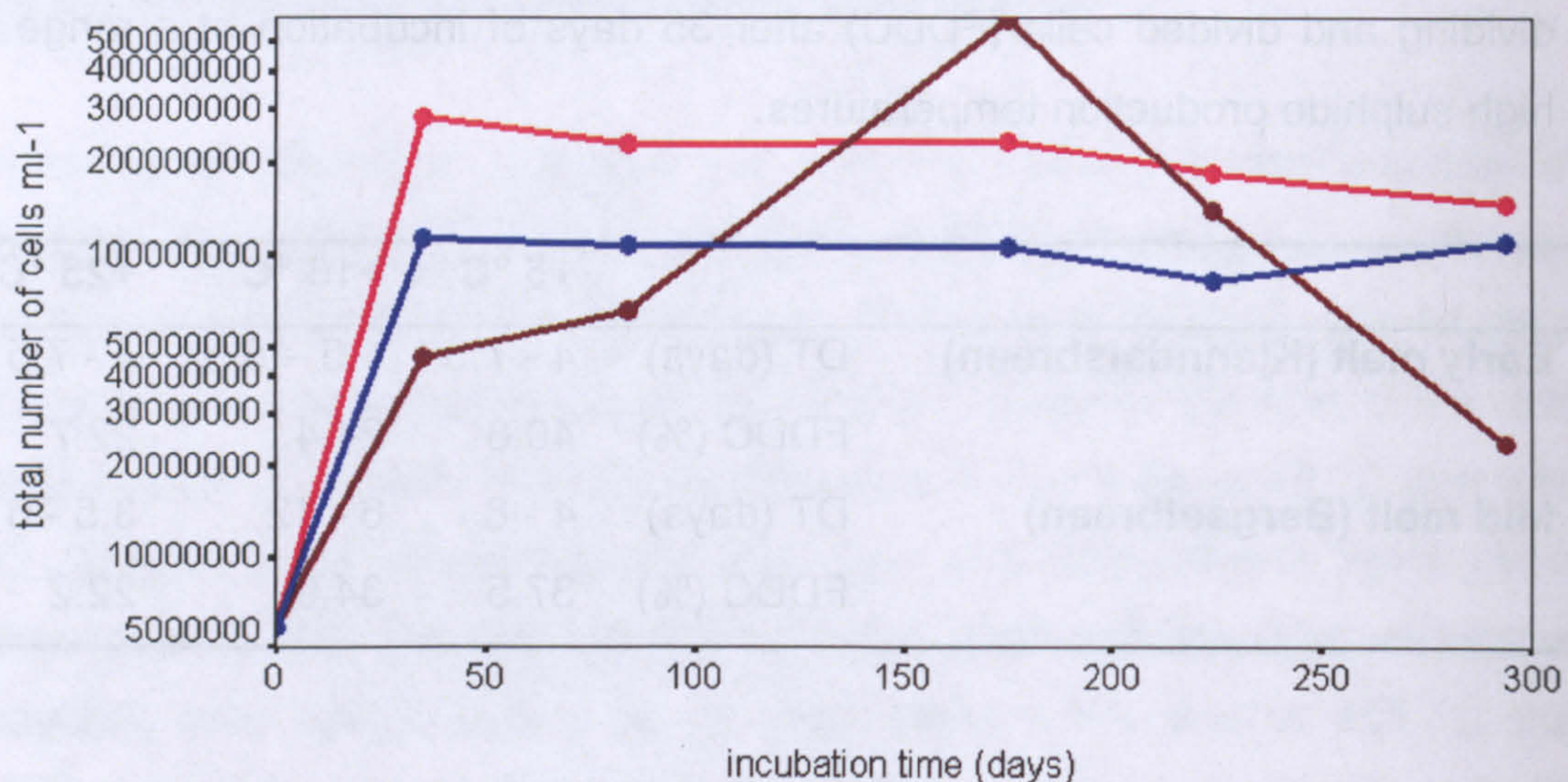


**Figure 5.23.** Growth curves of bacterial populations in the mid-melt season SRB-enrichment cultures from the Bergsetbreen glacier at a range of temperatures. Lines show the mean values of the three replicate counts. Blue line = +5 °C; brown line = +16 °C; red line = +25 °C.



### 5.2.5. Chemistry of Jostedalsbreen meltwaters

Monitoring of water chemistry in melt season 2000 was focused on meltwaters from the Bødalsbreen outlet glacier: water samples for analysing major anions and cations were taken daily throughout the melt season. Water quality at the three other outlet glaciers was analysed twice during the early melt season and the mid-melt season (table 5.12). The water temperature in the bulk meltwater streams at the time of sampling was  $+0.3 - +0.6$  °C. In a proglacial bulk meltwater stream in the Bødalsbreen outlet glacier, there was a rapid increase in electrical conductivity in mid-June reflecting outburst of the subglacially stored waters (figure 5.24). At the end of June there was another peak from  $7.8$  to  $16.5 \mu\text{S cm}^{-1}$ , followed by quick change to lower solute concentration of the typical high melt season diluted meltwaters. This reduction of solutes, as well as another sudden decrease at the end of July, were concurrent with the peaks in discharge in the main meltwater stream (figure 5.15).

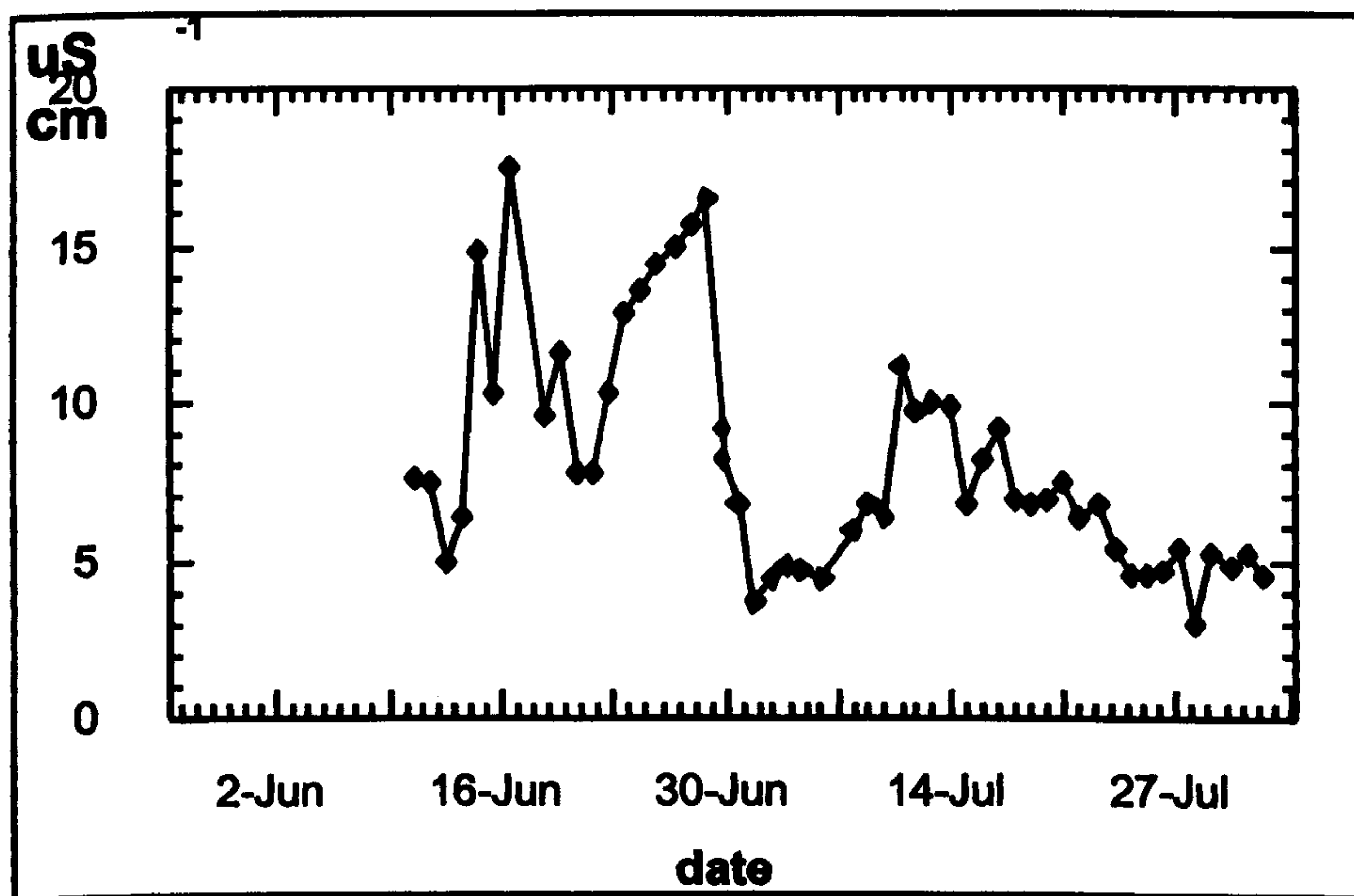


**Figure 5.24.** Electrical conductivity ( $\mu\text{S cm}^{-1}$  at  $25$  °C) in the bulk proglacial meltwater stream in the Bødalsbreen outlet glacier in the melt season 2000 (Skidmore and Tranter, unpublished data).



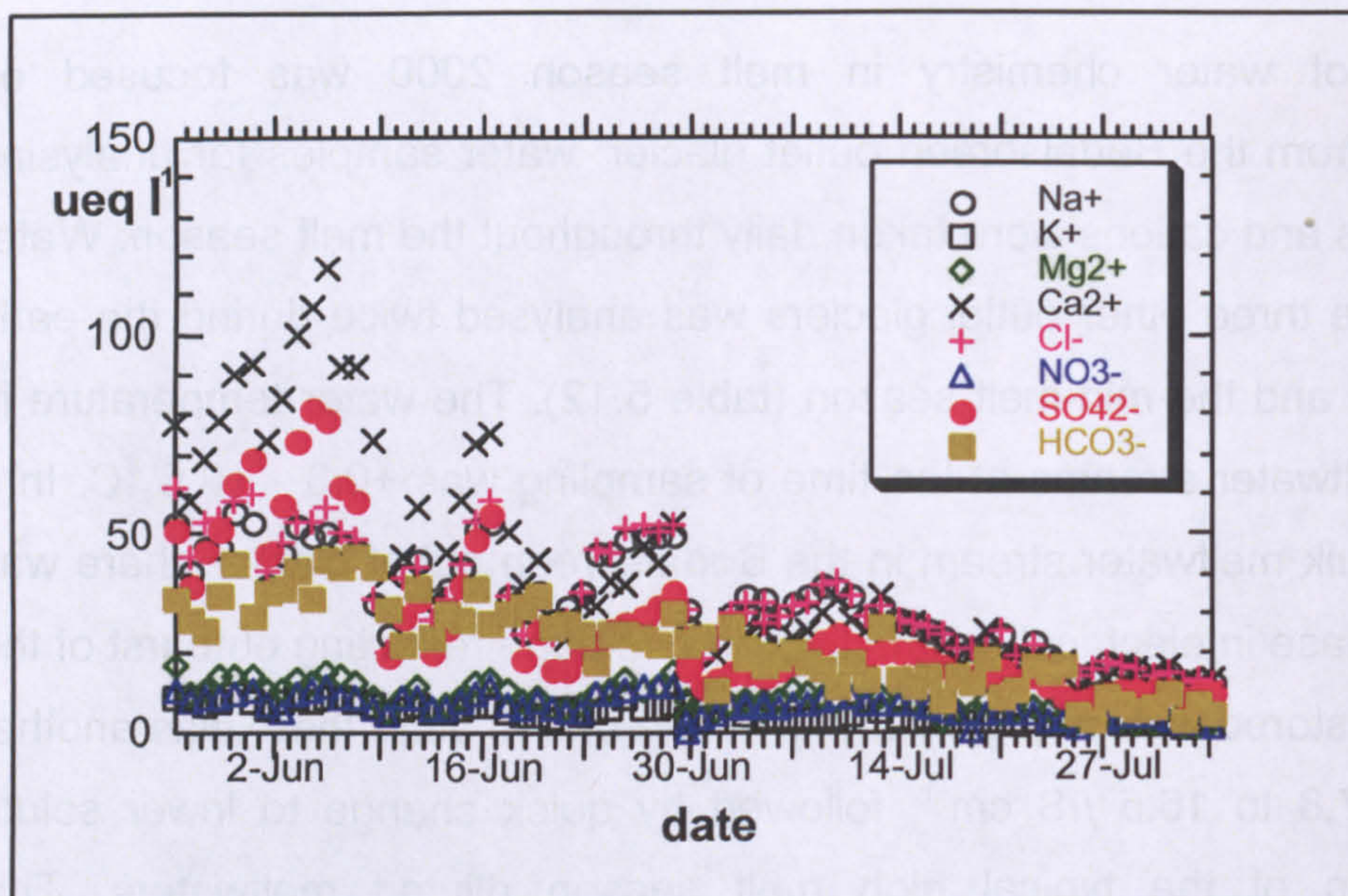


**Figure 5.25.** Major anion and cation concentrations in the bulk proglacial meltwater stream in the Bødalsbreen outlet glacier in the melt season 2000 (Skidmore and Tranter, unpublished data).

After the initial outburst of meltwaters with high cation and anion concentrations, there was a gradual decrease in ion concentrations in all of the four outlet glaciers around the ice cap. In the Bødalsbreen glacier, notable increase of calcium (maximum  $116.2 \mu\text{eq l}^{-1}$ ) and sulphate (maximum  $81.2 \mu\text{eq l}^{-1}$ ) took place at the beginning of June, followed by gradual decrease (table 5.12 and figure 5.25). The other three outlets followed a similar trend, the maximum calcium and sulphate concentrations at the beginning of melt season being  $47.7 - 93.9 \mu\text{eq l}^{-1}$  and  $32.6 - 65.3 \mu\text{eq l}^{-1}$ , respectively. Supraglacial meltwater in the Bødalsbreen glacier had very low concentrations of solutes throughout the melt season.



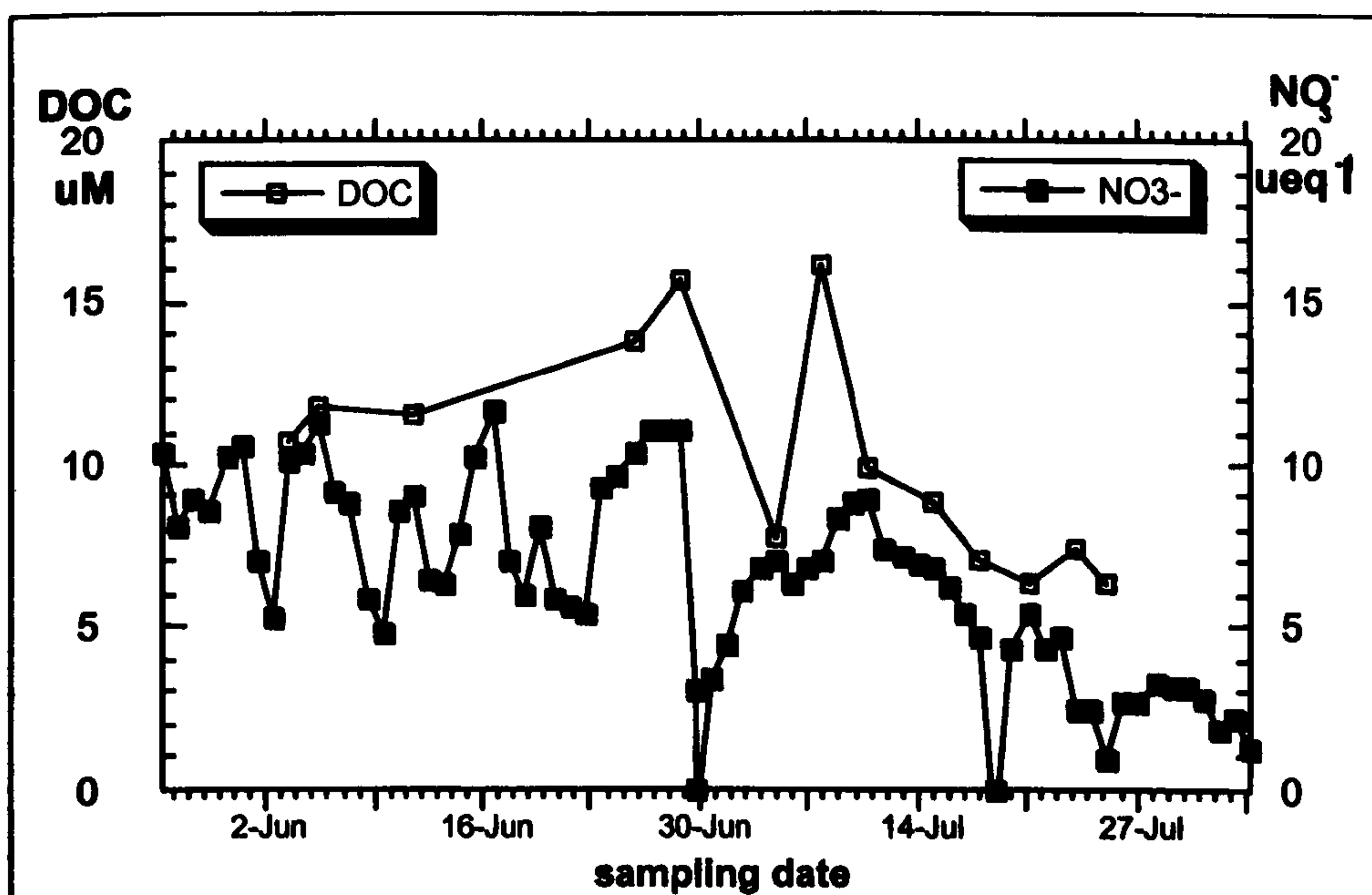


**Figure 5.26.** Dissolved organic carbon and nitrate concentrations in the bulk proglacial meltwater stream in the Bødalsbreen outlet glacier in the melt season 2000 (Skidmore and Tranter, unpublished data).

Dissolved organic carbon content was low throughout the melt season: from 6.4 to 16.1  $\mu\text{M}$  in subglacial meltwater, and even lower in supraglacial meltwater (4.3  $\mu\text{M}$ ). Variations in nitrate and DOC-concentrations were to some extent similar ( $\text{NO}_3 = 0.77955 \times \text{DOC} + 0.27983$ ,  $r^2 = 0.7172$ ), suggesting a potential for degradation of organic carbon by heterotrophic nitrate reducing organisms (figure 5.26). However, decrease in concentrations of nitrate and DOC was concurrent with high flow rates in bulk meltwater stream (figure 5.15), reflecting increased dilution with supraglacial meltwater with zero nitrate concentration and low DOC (table 5.12).



**Table 5.12.** Chemical composition of the meltwaters in the four outlet glaciers of Jostedalsgreen at the early (2-7 June) and the mid-melt (19-28 July) season in summer 2000. Figures of one early and one mid-melt sampling from each outlet glacier (Skidmore and Tranter, unpublished data). SS = suspended sediment concentration. Anion and cation concentration unit is  $\mu\text{eq l}^{-1}$ .

Early	discharge ( $\text{m}^3 \text{ s}^{-1}$ )	SS ( $\text{g l}^{-1}$ )	AODC ( $\log_{10}\text{cells ml}^{-1}$ )	pH	Cl	$\text{SO}_4^{2-}$	$\text{NO}_3^-$	$\text{NH}_4^+$	$\text{Na}^+$	$\text{K}^+$	$\text{Mg}^{2+}$	$\text{Ca}^{2+}$	DOC ( $\mu\text{M}$ )
Bødal sub	2.6	0.0139	3.87	6.3	50.3	61.7	9.2	0.9	47.4	8.9	14.4	92.1	11.8
Bødal supra	-	0.0064	4.17	5.7	4.8	1.9	0.0	0.0	4.1	0.0	0.0	0.0	-
Kjenndal sub	-	0.0060	4.14	6.4	33.6	36.4	7.3	5.3	35.2	4.7	8.6	57.1	11.9
Nigard sub	-	0.0220	4.07	6.1	32.7	32.6	12.0	2.2	34.9	5.3	13.0	47.9	-
Bergset sub	-	0.0173	4.18	6.2	24.3	65.3	6.9	1.7	30.7	6.7	5.8	93.9	-

Mid	discharge ( $\text{m}^3 \text{ s}^{-1}$ )	SS ( $\text{g l}^{-1}$ )	AODC ( $\log_{10}\text{cells ml}^{-1}$ )	pH	Cl	$\text{SO}_4^{2-}$	$\text{NO}_3^-$	$\text{NH}_4^+$	$\text{Na}^+$	$\text{K}^+$	$\text{Mg}^{2+}$	$\text{Ca}^{2+}$	DOC ( $\mu\text{M}$ )
Bødal sub	3.1	0.0299	4.25	6.1	15.7	8.5	2.7	0.6	14.1	1.5	2.1	11.1	6.4
Bødal supra	-	0.0070	4.36	5.7	3.8	1.9	0.0	6.0	1.3	2.9	4.7	0.0	4.3
Kjenndal sub	-	0.0269	4.29	6.4	16.3	8.1	0.3	2.1	15.5	1.2	2.5	15.7	-
Nigard sub	-	0.0225	4.35	5.7	20.7	10.8	5.3	3.6	20.0	2.9	7.2	11.5	-
Bergset sub	-	0.0152	4.25	6.2	10.8	11.3	2.2	2.6	10.8	3.3	9.4	18.5	-



### **5.3. Midre Løvenbreen glacier in Svalbard**

#### **5.3.1. Initial melting before the actual melt season in the Midre Løvenbreen glacier**

The hydrochemistry of the Midre Løvenbreen glacier was studied in spring 2001 and 2002 before the actual melt season. Hence, there were no real meltwater streams, and the samples were taken from spring-type outflows from the surface of the icing. The sampling point was located approximately 50 m from the terminus of the glacier near the eastern proglacial upwelling. At the time of sampling, air temperature was close to zero, and surface melting of snowpack did not occur. Meltwater samples collected were composed of basal melt and water stored in cavities from the previous melt season (Wadham, pers.comm.). In May 2001, samples were taken from one outflow running on the surface of the icing, whereas in April 2002 samples were taken from four different outflows located less than 10 m from each other.

#### **5.3.2. Bacterial populations in Midre Løvenbreen meltwaters**

The total number of bacteria in the Midre Løvenbreen meltwater before the actual melt season in spring 2001 and 2002 was  $4.03 - 4.20 \log_{10}\text{cells ml}^{-1}$  and  $4.32 - 4.63 \log_{10}\text{cells ml}^{-1}$ , respectively (figure 5.27). In 2002, numbers of bacteria in the three separate outflows formed homogeneous subgroup (subset homogeneity p-value = 0.695, appendix 7). Significantly higher numbers in April 2002 compared with the previous year (Tukey's HSD test, appendix 7) may be due to catching the slow winter seepage water with long residence time and contact with mineral material beneath the glacier, whereas in May 2001 dilution of subglacial meltwater with minor melting of snowpack may have taken place.



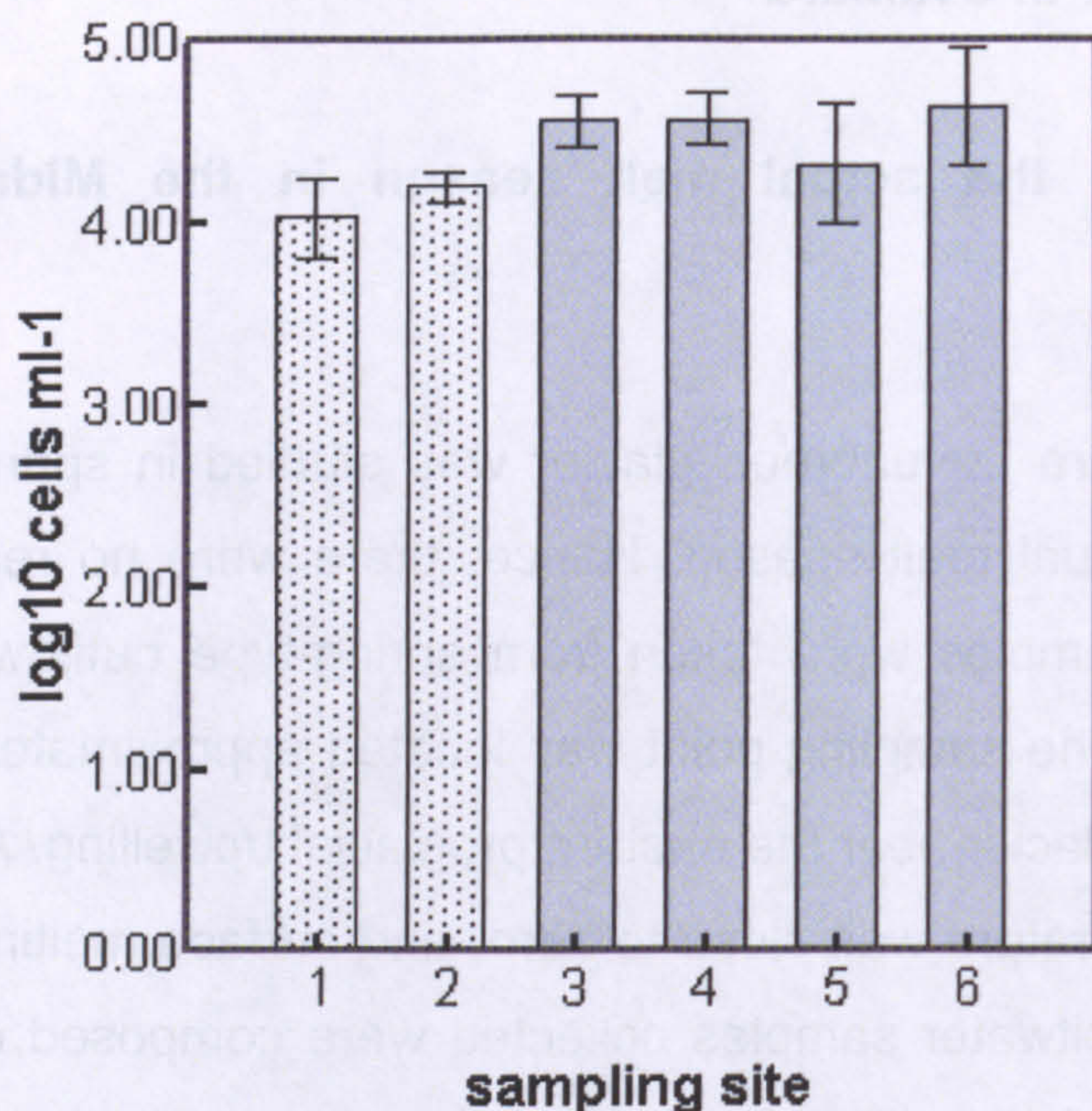


**Figure 5.27.** Total numbers of bacteria in meltwaters from the Midre Løvenbreen glacier before the actual melt season in spring 2001 (dotted bars) and 2002 (solid bars). The bars show the mean values of the three replicate counts and error bars show 95% confidence intervals for the means of three replicates. Sampling sites as follows: **1-2** = replicates from the same outflow; **3-6** = four different outflows located less than 10 m from each other.

### 5.3.3 Growth of bacterial cultures at constantly low temperature

Sulphate-reducing bacteria were cultured from meltwater in both May 2001 and April 2002. The cultures were incubated at +2 °C. Sulphide production took place in six weeks in all samples (table 5.13). Bacterial cells growing in the enrichment cultures were rod-shaped with a thickness of 1  $\mu\text{m}$  and 4-6  $\mu\text{m}$  long.



**Table 5.13.** Growth of cultures of sulphate-reducing bacteria from Midre Løvenbreen meltwater before the actual melt season in May 2001 and April 2002. Incubation at +2 °C. 0=no sign of growth; 1=culture turning cloudy, dark grey precipitates, growth; 2=black precipitates, strong growth. Figures show growth in two replicates: culture A / culture B. (30/45 = 35 ml of sample inoculated to 15 ml of SRB-medium; 10/40 = 10 ml of sample inoculated to 30 ml of SRB-medium; 1/40 = 1 ml of sample inoculated to 39 ml of SRB-medium; 0.1/40 = 0.1 ml of sample inoculated to 39.9 ml of SRB-medium).

	1 w	2 w	4 w	6 w	8 w	11 w	13 w
<b>2001 outflow 1A 30 / 45</b>	0 / 0	0 / 0	0 / 0	1 / 1	1 / 1	2 / 2	2 / 2
<b>2001 outflow 1B 30 / 45</b>	0 / 0	0 / 0	0 / 0	1 / 1	1 / 1	2 / 1	2 / 2
<b>2002 outflow 1 10 / 40</b>	0 / 0	0 / 0	0 / 0	1 / 1	1 / 1	1 / 1	2 / 2
<b>2002 outflow 2 10 / 40</b>	0 / 0	0 / 0	0 / 0	1 / 1	1 / 1	1 / 1	1 / 1
<b>2002 outflow 2 1 / 40</b>	0 / 0	0 / 0	0 / 0	1 / 1	1 / 1	1 / 1	1 / 1
<b>2002 outflow 2 0.1 / 40</b>	0 / 0	0 / 0	0 / 0	0 / 0	0 / 0	0 / 0	0 / 0
<b>2002 outflow 3 10 / 40</b>	0 / 0	0 / 0	0 / 0	1 / 1	1 / 1	1 / 1	2 / 1
<b>2002 outflow 4 10 / 40</b>	0 / 0	0 / 0	0 / 0	1 / 1	1 / 1	1 / 1	2 / 1

#### **5.3.4. Temperature characteristics of sulphate-reducing bacteria in Midre Løvenbreen meltwater before the actual melt season**

The enrichment cultures of sulphate-reducing bacteria from meltwater in May 2001 were incubated at -0.6 °C to +40.0 °C in the thermal gradient system. Initially the frequency of dividing cells was 23 - 31%. The cultures 1A and 1B incubated were replicates, inoculated with meltwater samples 1A and 1B, respectively, both taken from the same outflow running on the surface of the icing.



#### **5.3.4.1. Sulphide production in Svalbard SRB-cultures**

After one week incubation, definite growth of sulphate reducing bacteria was detected at +12 °C to +16 °C. After two weeks, the minimum temperature for sulphide production was +3 °C (appendix 8).

Since the cultures incubated were replicates from one sampling point, it was expected that temperature characteristics of the sulphate-reducing bacteria in both cultures would be more or less identical. Interestingly, there were some differences in sulphide production at different temperatures between the two replicates. After 18 days, the culture A showed two distinct sulphide production peaks, 6.21 mM at +14 °C and 6.84 mM at +21 °C, whereas in the culture B a mesophilic community with the broad temperature range from +11 to +21 °C was growing, resulting in sulphide production from 5.43 mM to 7.32 mM (figure 5.28). Oxygen contamination in some of the test vials explains the difference. Presence of oxygen in the culture A at the very beginning of experiment prevented the initial growth of sulphate-reducers at +12 °C and +16 - +18 °C (appendix 8). After 5 weeks incubation, the maximum sulphide concentration of 5.75 - 6.13 mM in both cultures was detected at +7 - +9 °C, along with two secondary sulphide production peaks at +14 °C and +21 °C. Surprisingly, sulphide peak at +14 °C in a culture A gradually disappeared during 12 weeks of incubation. This suggests that some bacteria in mixed cultures simply stopped growing while the other populations took over. Bacteria at +14 °C grew fast and produced sulphide already after one weeks incubation, but after five weeks the medium had turned slightly pink, indicating oxygen contamination during the first sampling (after 2.5 weeks) and minimal growth in the culture (appendix 8).

Sulphate reduction rate at +12 °C and +21 °C during the first weeks of incubation was as high as 0.406 mmol l<sup>-1</sup> d<sup>-1</sup> (figure 5.30). In contrast, samples incubated at +3 - +7 °C had an initial sulphate reduction rate of < 0.04 mmol l<sup>-1</sup> d<sup>-1</sup>, but after five weeks at +7 °C the reduction rate was 0.299 mmol l<sup>-1</sup> d<sup>-1</sup>.



Although the optimal temperature range for sulphide production throughout the 25 weeks incubation was more or less identical in cultures 1A and 1B, the different distinct peaks showed heterogeneity of bacterial populations in the samples taken from the same outflow at the same sampling time. After 25 weeks incubation, however, both replicates had sulphide production peaks at two separate temperature ranges, +4 – +9 °C and +18 – +23 °C (figure 5.29). Moreover, in both samples activity of psychrophilic sulphate-reducing bacteria was dominant.

#### **5.3.4.2. Growth rate in Svalbard SRB-cultures**

The estimated doubling time of bacterial populations at the beginning of exponential growth was 3 - 4 days, with growth at +21 °C being slower than at either +7 °C or +12 °C (table 5.14). Results of the previous thermal gradient experiments with cultures from Greenland and Norway (chapters 5.1.4.2 and 5.2.4.2) indicated that growth rate at the very beginning was faster than was estimated. Therefore, in the experiment with cultures from Svalbard the first sampling was done already after 2.5 weeks incubation, in order to get more reliable estimate of the exponential growth phase. Hence it is likely that the doubling times given in the table 5.14 are close to the true doubling times. The shape of growth curves and increasing total numbers of cells from time zero to 35 days (figure 5.31) supports this assumption. Despite a similar estimated growth rate during exponential growth at temperatures of +7 °C and +12 °C, after five weeks incubation frequency of dividing and divided cells was lower at +12 °C than at +7 °C (36.3% and 41.6%, respectively). This is consistent with the trend in growth curves: at +7 °C bacterial population kept on growing after five weeks, whereas at + 12 °C number of cells gradually decreased (figure 5.31).



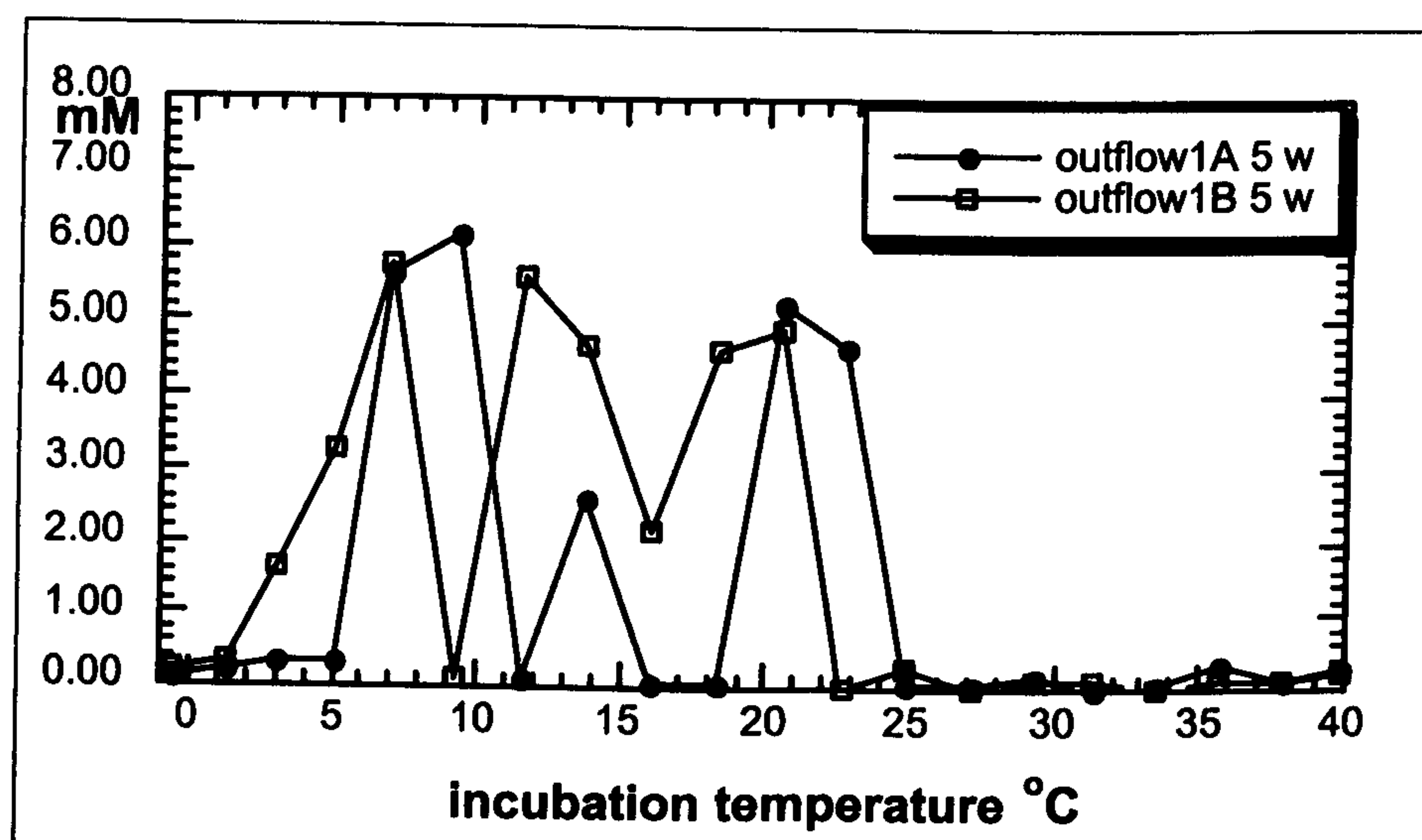
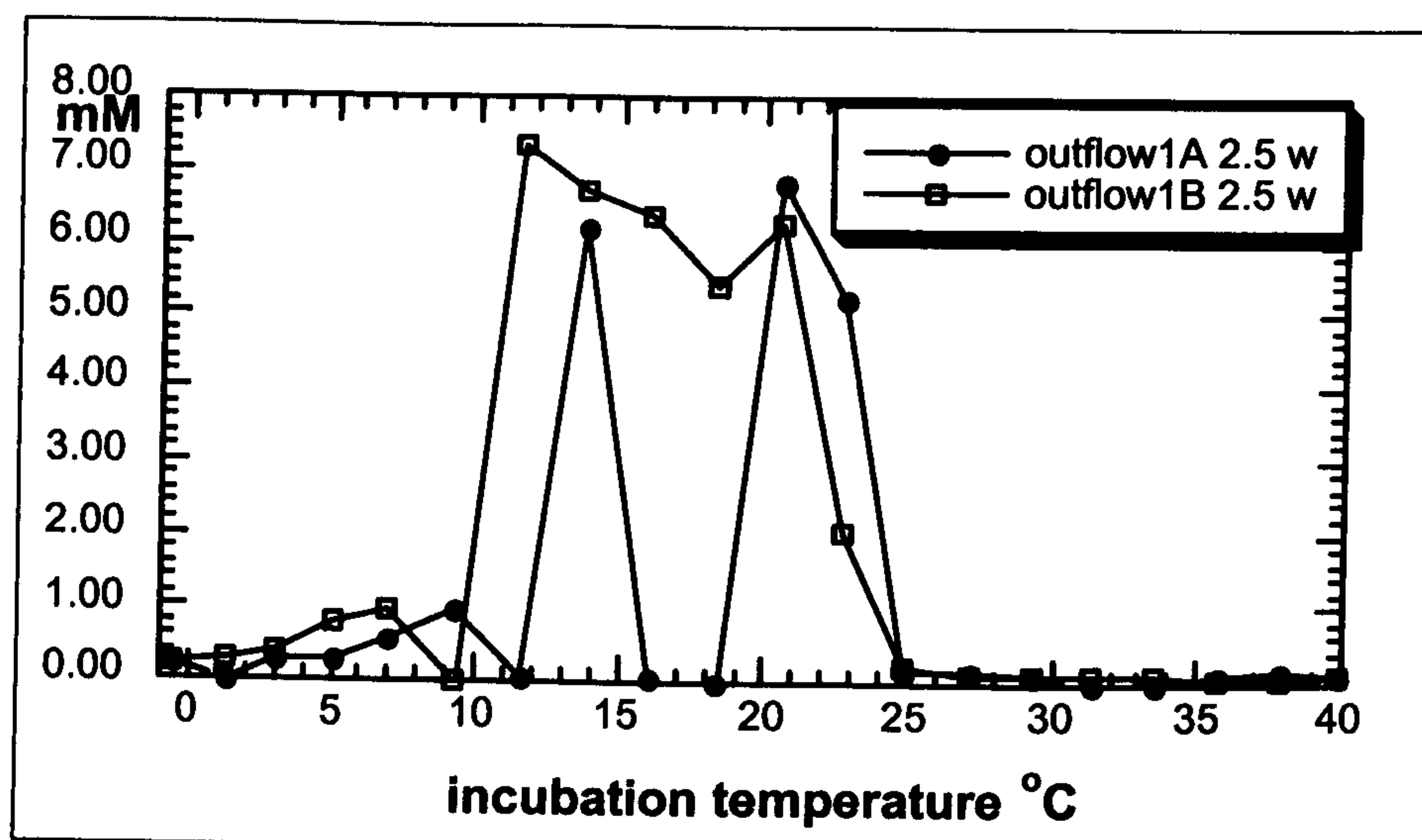


**Figure 5.28.** Growth of sulphate-reducing bacteria from Midre Løvenbreen subglacial meltwater in May 2001. Cultures incubated in the thermal gradient system with a temperature range from  $-0.6$  to  $+40$  °C for 2.5 and 5 weeks. Growth measured as sulphide production (mM).



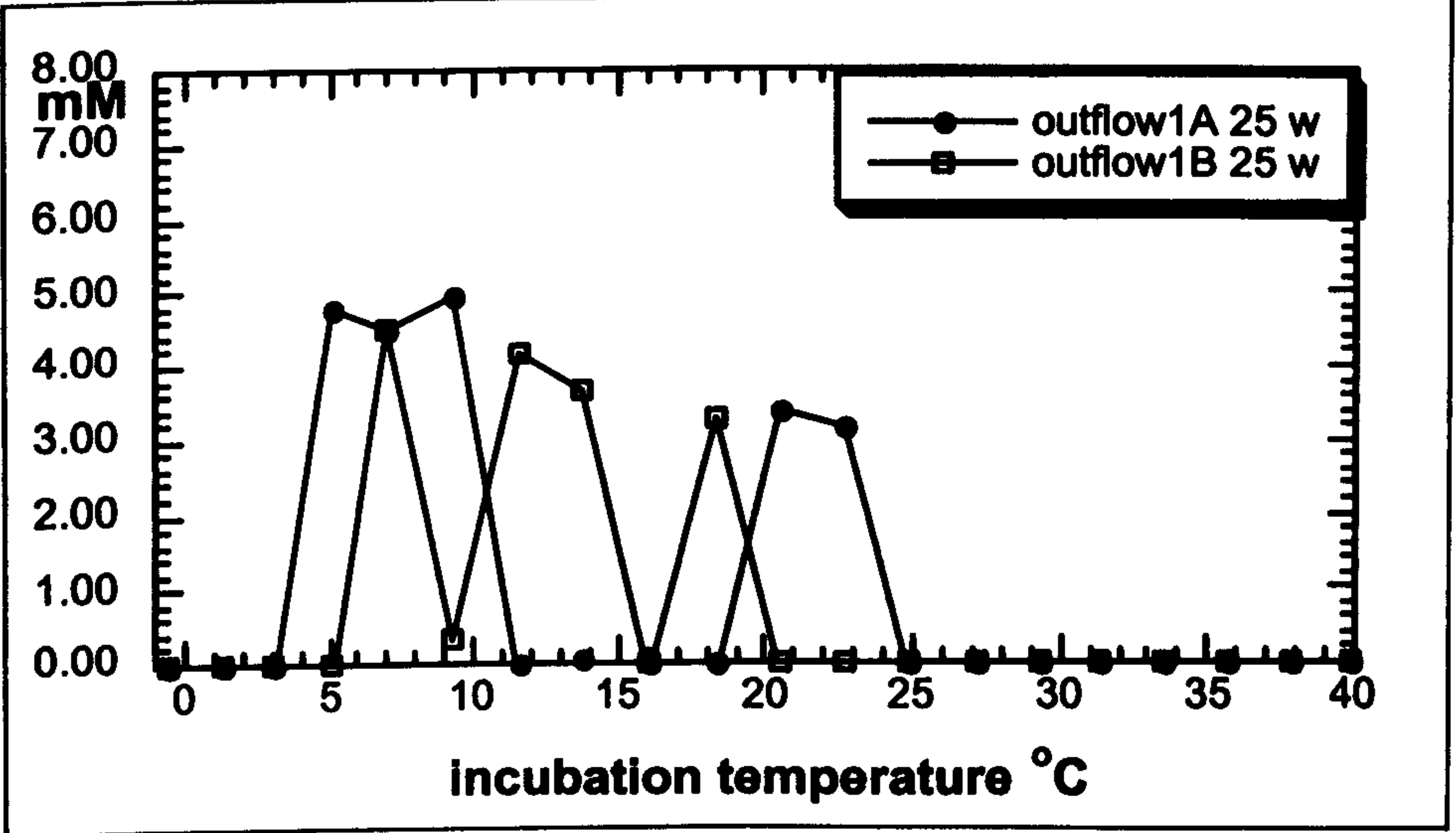
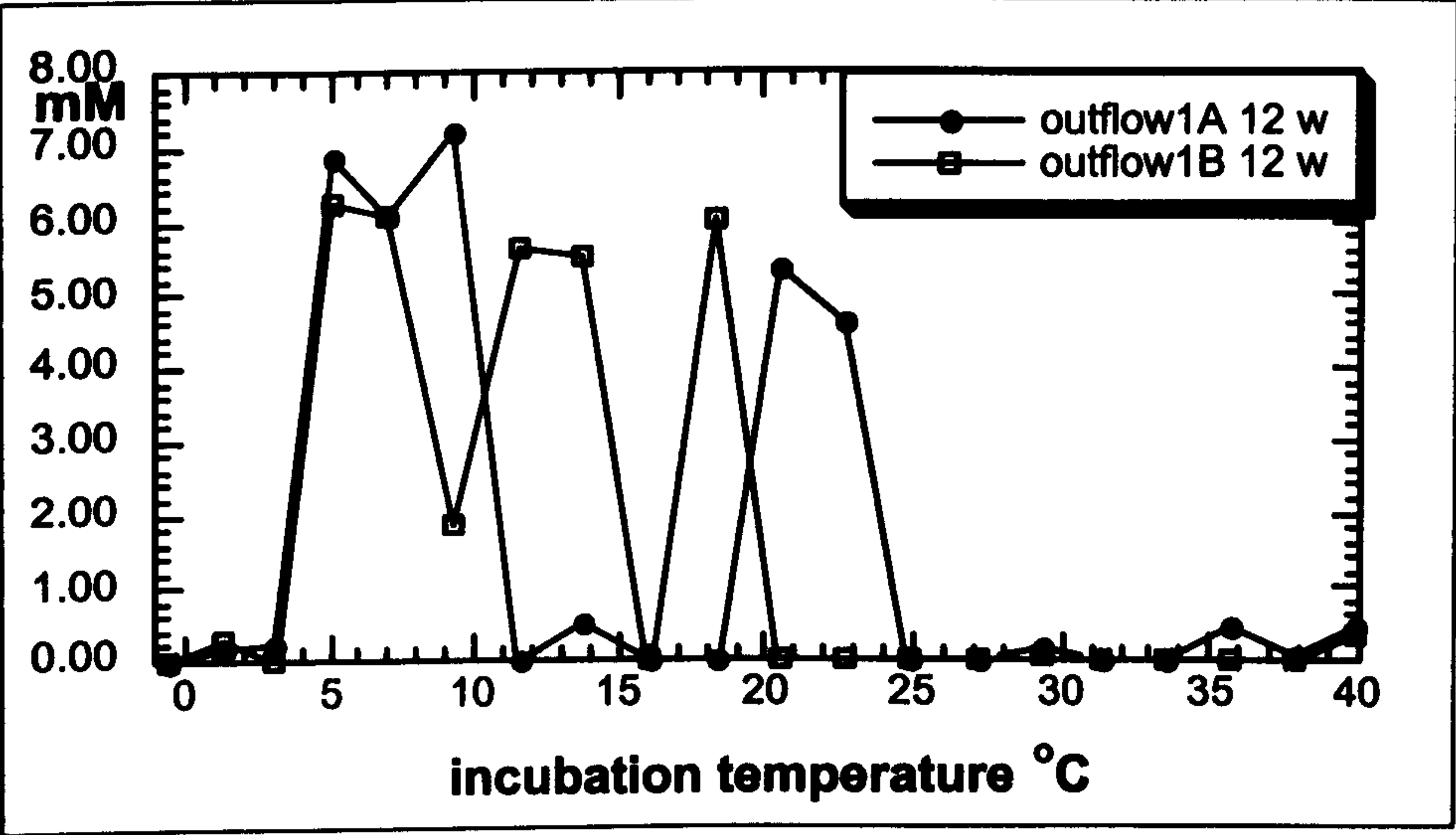


**Figure 5.29.** Growth of sulphate-reducing bacteria from Midre Løvenbreen subglacial meltwater in May 2001. Cultures incubated in the thermal gradient system with a temperature range from –0.6 to +40 °C for 12 and 25 weeks. Growth measured as sulphide production (mM).

**Table 5.14.** Estimated doubling times of the total number of cells in cultures of sulphate-reducing bacteria from the Midre Løvenbreen glacier during exponential growth, and the frequency of dividing and divided cells (FDDC) after 35 days at a range of high sulphide production temperatures.

		+7 °C	+12 °C	+21 °C
Midre Løvenbreen (May 2001)	DT (days)	3	3	4
	FDDC (%)	41.6	36.3	39.0



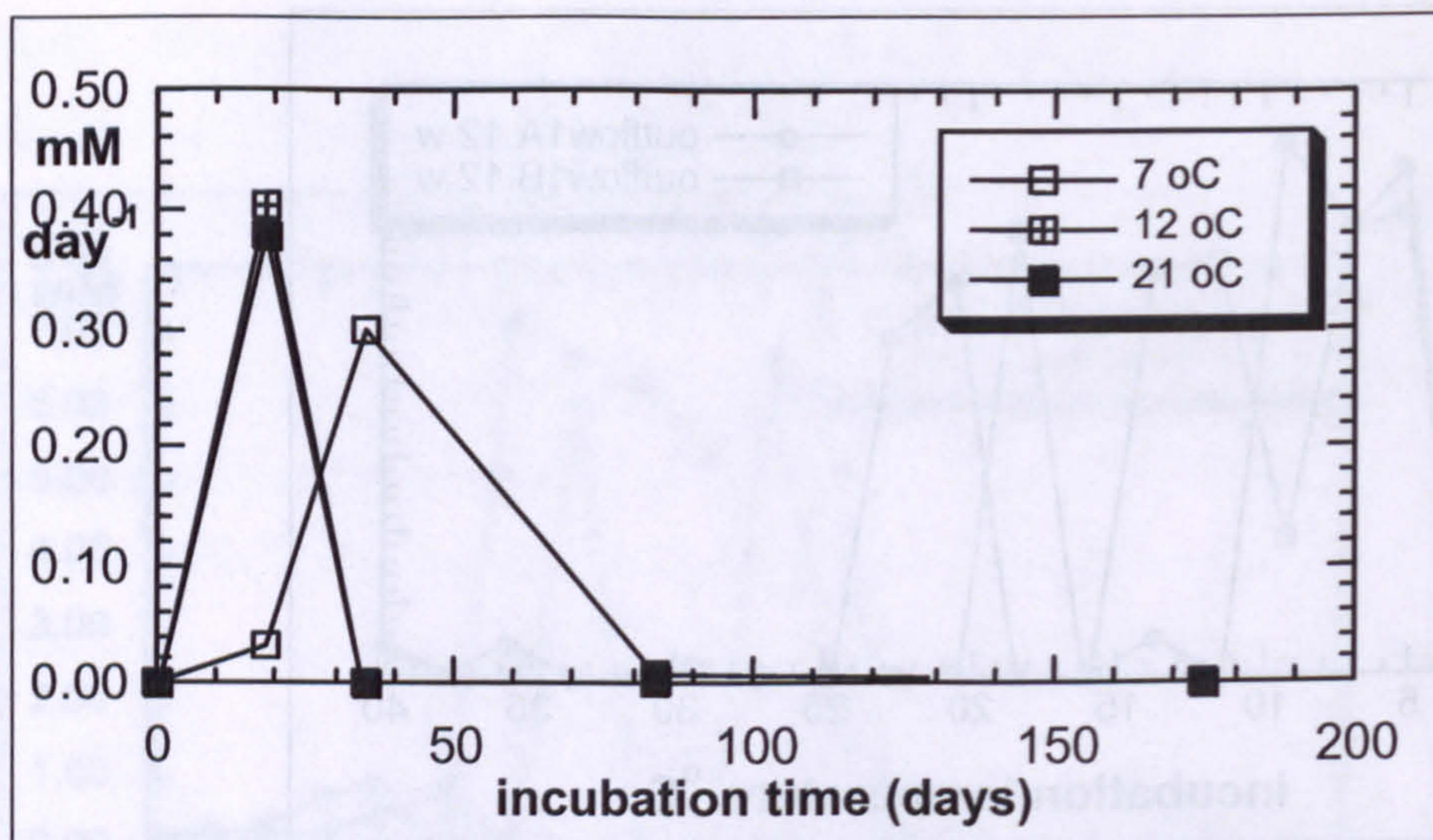


**Figure 5.30.** Sulphate reduction rate at +7, +12 and +21 °C in the cultures of sulphate-reducing bacteria from the Midre Løvenbreen glacier in May 2001.

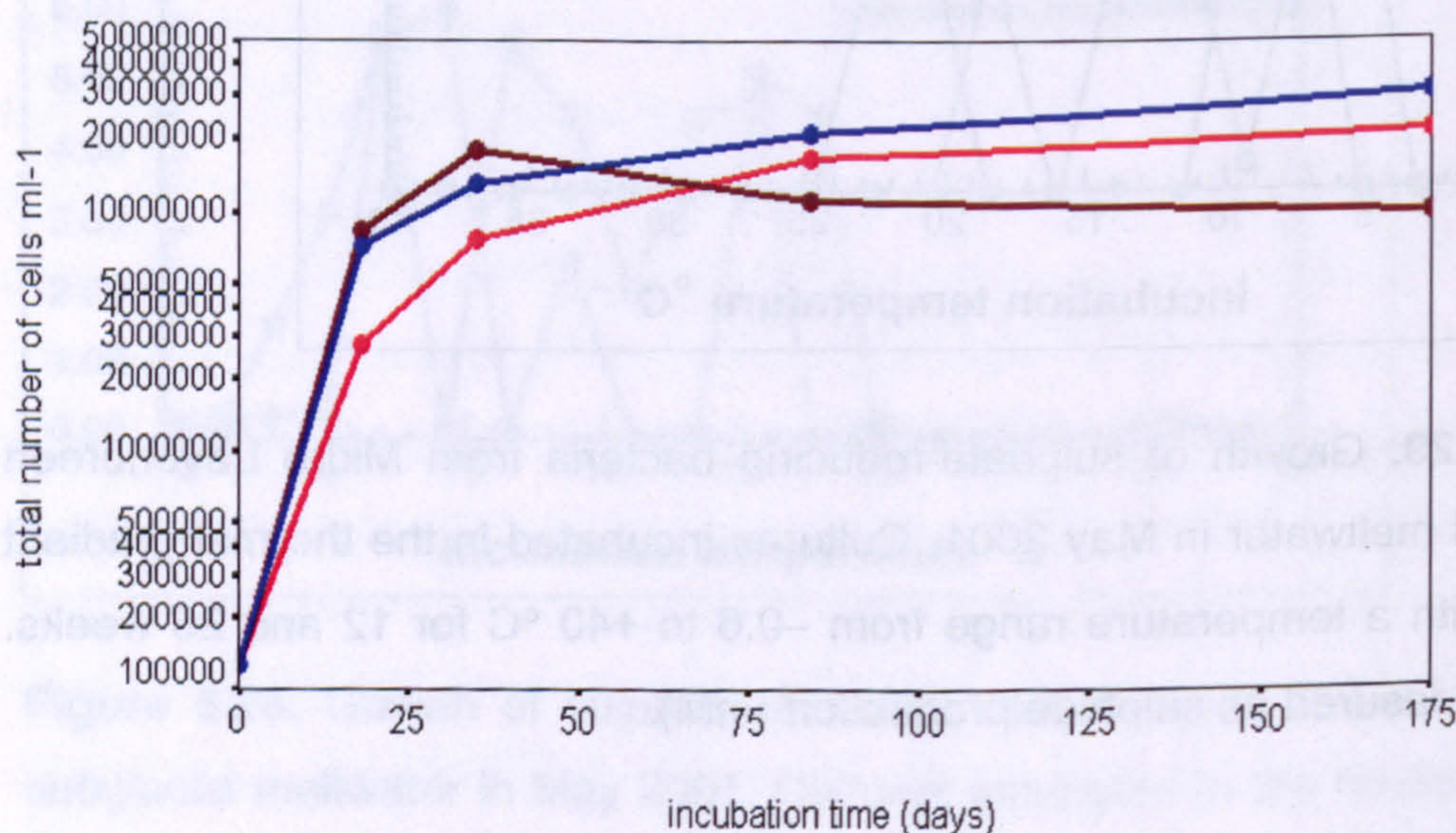


**Figure 5.31.** Growth curves of bacterial populations in the SRB-enrichment cultures from the Midre Løvenbreen glacier (May 2001) at a range of incubation temperatures. Lines show the mean values of the three replicate counts. Blue line = +7 °C; brown line = +12 °C; red line = +21 °C.



### **5.3.5. Chemistry of Midre Løvenbreen meltwaters**

Temperature and oxygen saturation in the meltwater at the time of sampling were  $< +1$  °C and 15 - 54 %, respectively (Wadham, pers.comm.). Low dissolved oxygen concentrations indicate that the meltwater collected was purely a product of subglacial basal melt, not diluted with supraglacial meltwaters.

The concentrations of dissolved ions in meltwaters were high, especially  $\text{SO}_4^{2-}$ ,  $\text{Ca}^{2+}$  and  $\text{Mg}^{2+}$  (table 5.15). Solute concentrations were typical of concentrated proglacial icings (frozen winter outflows of subglacial water) (Hodgkins et al. 1997). Moreover, the dissolved organic carbon concentration was surprisingly high - from 400 to 450  $\mu\text{M}$  (DOC analysed only for 2002 samples). Nitrate was present in only trace quantities. Low nitrate concentration is consistent with low dissolved oxygen concentration. Nitrate may have been consumed during winter storage by nitrate-reducing organisms which use organic carbon as an energy source, and this may have caused activation of sulphate-reducing bacteria.

Major anion and cation concentrations in the meltwaters were higher in April 2002 than in May 2001. Also, total number of cells was higher in the latter year (table 5.15). Since the melt season had not started yet, samples in April 2002 represented water stored in subglacial cavities from the previous melt season. Long residence time resulted in high concentrations of ions dissolved from minerals, and consequently also higher numbers of bacteria.



**Table 5.15.** Chemical composition of meltwaters in the Midre Løvenbreen before the actual melt season in 2001 (2 May) and 2002 (10 April) (Wadham, unpublished data). SS = suspended sediment concentration. Anion and cation concentration unit is  $\mu\text{eq l}^{-1}$ .

2001	SS (g l <sup>-1</sup> )	AODC (log <sub>10</sub> cells ml <sup>-1</sup> )	pH	Cl <sup>-</sup>	SO <sub>4</sub> <sup>2-</sup>	NO <sub>3</sub> <sup>-</sup>	tot-N	Na <sup>+</sup>	K <sup>+</sup>	Mg <sup>2+</sup>	Ca <sup>2+</sup>	DOC ( $\mu\text{M}$ )
outflow 1A	0.0028	4.03	8.3	132	1049	-	-	418	91	739	1500	-
outflow 1B	0.0042	4.20	8.1	132	1042	-	-	418	88	737	1499	-

2002	SS (g l <sup>-1</sup> )	AODC (log <sub>10</sub> cells ml <sup>-1</sup> )	pH	Cl <sup>-</sup>	SO <sub>4</sub> <sup>2-</sup>	NO <sub>3</sub> <sup>-</sup>	tot-N	Na <sup>+</sup>	K <sup>+</sup>	Mg <sup>2+</sup>	Ca <sup>2+</sup>	DOC ( $\mu\text{M}$ )
outflow 1	0.0029	4.56	8.0	186	1294	0.2	-	750	110	810	1574	453
outflow 2	0.0044	4.57	8.2	150	1145	0.0	9.7	670	88	714	1396	407
outflow 3	0.0033	4.33	8.3	176	1272	0.0	-	740	100	804	1548	-
outflow 4	0.0040	4.63	8.3	240	1610	0.0	-	960	120	1030	1974	-



**Table 5.16.** Summary of total bacterial populations in meltwaters of glaciers in Greenland, Norway and Svalbard, suspended sediment concentrations and frequency of bacterial cells attached to mineral grains suspended in meltwater. Figures are mean values of three replicates. Man= Manitsoq glacier; Aku= Akuliarusiarssuk glacier; Bødal= Bødalsbreen glacier; Kjenndal= Kjenndalsbreen glacier; Nigard= Nigardsbreen glacier; Bergset= Bergsetbreen glacier.

	<i>Total number of bacteria (log<sub>10</sub>cells ml<sup>-1</sup>)</i>	<i>Suspended sediment concentration (g l<sup>-1</sup>)</i>	<i>Frequency of cells attached to mineral grains (%)</i>
<b>GREENLAND (1999)</b>			
Man-sub-early melt	4.54	0.0828	3.3
Man-supra-early melt	3.65	0.0891	51.3
Man-sub-mid melt	4.02	0.3922	7.8
Man-supra-mid melt	3.62	0.0888	0.0
Man-sub-late melt	3.83	0.2164	4.0
Aku-sub-mid melt	3.91	0.9427	23.9
Aku-supra-mid melt	3.40	0.0196	76.7
<b>NORWAY (2000)</b>			
Bødal-sub-early melt	3.87	0.0139	0.0
Bødal-supra-early melt	4.17	0.0064	38.5
Kjenndal-sub-early melt	4.14	0.0060	10.1
Nigard-sub-early melt	4.07	0.0220	0.0
Bergset-sub-early melt	4.18	0.0173	26.6
Bødal-sub-mid melt	4.25	0.0299	13.9
Bødal-supra-mid melt	4.36	0.0070	19.9
Kjenndal-sub-mid melt	4.29	0.0269	32.8
Nigard-sub-mid melt	4.35	0.0225	44.3
Bergset-sub-mid melt	4.25	0.0152	21.0
<b>SVALBARD</b>			
outflow 1A (2001)	4.03	0.0028	0.0
outflow 1B (2001)	4.20	0.0042	10.0
outflow 1 (2002)	4.56	0.0029	61.7
outflow 2 (2002)	4.57	0.0044	38.1
outflow 3 (2002)	4.33	0.0033	31.5
outflow 4 (2002)	4.63	0.0040	50.2



## **5.4 Discussion**

### **5.4.1. Total bacterial populations in glaciers in Greenland, Norway and Svalbard**

The total number of bacteria in meltwaters from the glaciers in Greenland, Norway and Svalbard ranged from  $3.40 \log_{10} \text{ cells ml}^{-1}$  to  $4.63 \log_{10} \text{ cells ml}^{-1}$  (table 5.16). At Greenland and Norway field sites, meltwater samples were taken at the early, mid and late phases of the melt season, and no significant temporal variations were detected (appendix 2 and 5). However, multiple comparisons of numbers of bacterial cells in meltwaters from the three field sites at the very beginning of the melt season (appendix 9) showed some noticeable regional differences (ANOVA table,  $F=10.03$  with significance level of 0.004). Numbers of bacterial cells in meltwaters from Norway in June 2000 and from Svalbard in May 2001 were indistinguishable, but markedly lower than in Greenland in June 1999. Interestingly, significantly higher numbers of bacteria were discovered in the meltwaters from the Midre Løvenbreen glacier in Svalbard in April 2002 (appendix 9, Tukey's HSD-test). At that time, the actual melt season had not started yet. Melting was minimal and no meltwater streams had formed. Hence, meltwater represented pure subglacial water, stored in subglacial cavities and not diluted with snow and ice melt scarce in bacteria. Total number of bacteria in snowpack in the field sites was not determined, but in the earlier studies, bacterial concentrations found in surface snow in glaciated areas have ranged from  $2.30\text{-}3.70 \log_{10} \text{ cells ml}^{-1}$  (Carpenter et al. 2000).

Meltwater discharge in the meltwater streams was measured in the Manitsoq glacier (Greenland) and the Bødalsbreen glacier (Norway) throughout the melt season, whereas in Svalbard field studies were done at the very beginning of the melt season when melting was negligible, so there was no discharge measurements. When changes in discharge rates (tables 5.6 and 5.12) are considered, the total microbial biomass in the studied meltwater streams from early to mid-melt season in the Manitsoq glacier and the Bødalsbreen glacier ranged from  $10.50$  to  $11.16 \log_{10} \text{ cells s}^{-1}$  and from  $10.28$  to  $10.73 \log_{10} \text{ cells s}^{-1}$ , respectively. Although meltwaters were more diluted



with snow and ice melt in the mid melt season, enhanced flushing of the subglacial sediments increased the total microbial biomass at both glaciers.

Concentration of suspended sediments in meltwaters was low throughout the melt season at all the field sites (table 5.16). In the early melt season samples from Greenland and Norway field sites, and in all the samples from Svalbard this was expected, since the aim was to sample meltwater at the very beginning of melt season when discharge was minimal. The highest suspended sediment concentration of  $0.94 \text{ g l}^{-1}$  was detected in the mid-melt season at the Greenland field site (table 5.16), in the meltwater stream flowing through a wide valley. Given that July was supposed to be the high melt season, the maximum suspended sediment load was surprisingly low, compared to suspended sediment range from  $0.1 \text{ g l}^{-1}$  to  $6.0 \text{ g l}^{-1}$ , recorded at an Alpine warm-based glacier (Brown et al. 1994a, Brown 2002) and a range from  $0.5 \text{ g l}^{-1}$  to  $6.7 \text{ g l}^{-1}$ , recorded at a High Arctic polythermal glacier (Hodgkins et al. 1997). The relatively low suspended sediment load in the Greenland field site may be due to glacier hydrology and bedrock composition. Discharge in the proglacial meltwater stream of the Manistoq glacier at the time of sampling was  $13 \text{ m}^3 \text{ s}^{-1}$ , and thus the sampling time did not hit the maximum discharge of  $33 \text{ m}^3 \text{ s}^{-1}$  in the main meltwater stream (figure 5.1). Moreover, bedrock is mainly composed of Precambrian gneisses, containing minerals resistant to physical glacial erosion. Fine-grained clay fraction also in the moraine matrix and glaciofluvial deposits around the glacier margin is scarce (Weidick 1976).

In another study on meltwaters in bulk runoff from the low latitude Alpine valley glacier (Sharp et al. 1999), suspended sediment concentration ranged from  $0.2 \text{ g l}^{-1}$  to  $1.4 \text{ g l}^{-1}$ . Concurrently, bacterial populations ranged from  $4.94 \log_{10} \text{ cells ml}^{-1}$  (at the time of minimum discharge of  $2.6 \text{ m}^3 \text{ s}^{-1}$ ) to  $5.74 \log_{10} \text{ cells ml}^{-1}$  (at the time of maximum discharge of  $4.4 \text{ m}^3 \text{ s}^{-1}$ ), showing distinct variation at different times of the melt season (Sharp et al. 1999). Moreover, Sharp et al. (1999) found that bacterial populations were positively correlated with sediment concentrations in meltwater samples ( $\log\text{AODC} = 7.67 + 0.59 \times \log\text{SSC}$ ,  $r^2 = 0.68$ ,  $p < 0.001$ ). No such strong correlation was found in meltwater samples from Greenland, Norway and Svalbard (figure 5.32 and appendix 10). Occurrence of datapoints of the three field sites in separate



clusters (figure 5.32) demonstrates that sediment load in meltwaters varied greatly from one field site to another, but it did not directly affect the total number of bacteria. It has to be kept in mind that all the meltwaters studied had very low sediment concentrations (ranging from 0.003 g l<sup>-1</sup> to 0.94 g l<sup>-1</sup>) and several bacterial cells detected were ultramicrobacteria, with coccus-shaped cells smaller than 0.5 µm. Starved ultramicrobacteria become non-attachable and therefore tend to remain suspended (Cullimore 1993) and have limited ability to form colonies (Morita 1988). Also, variable nutrient potential of suspended mineral grains was likely to affect the occurrence of attached and non-attached bacterial cells. Therefore, frequency of cells attached to mineral grains in meltwaters varied widely (table 5.16).

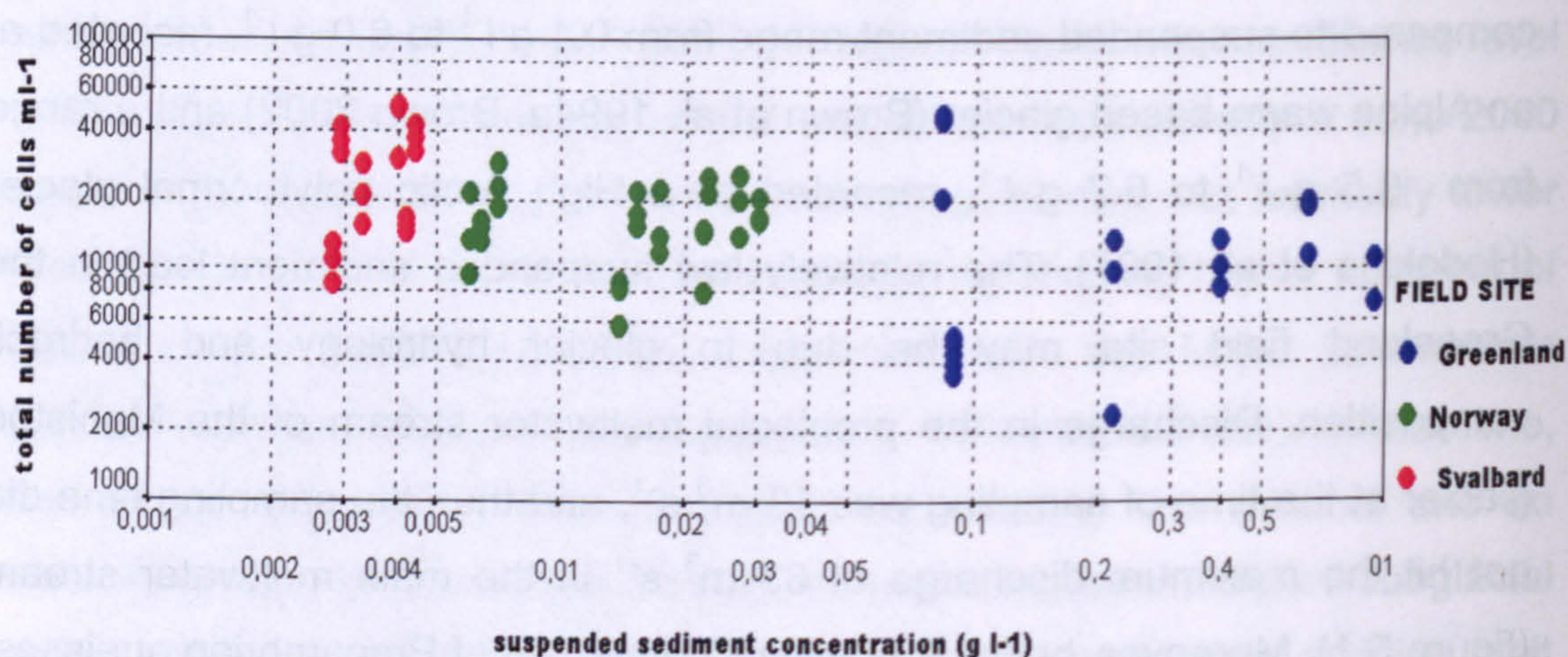


**Figure 5.32.** Scatterplot and linear regression test of suspended sediment concentration versus total number of bacteria in the meltwaters from Greenland ( $\log AODC = 4.03 + 0.09 \times \log SSC$ ,  $r^2 = 0.01$ ), Norway ( $\log AODC = 4.28 + 0.05 \times \log SSC$ ,  $r^2 = 0.01$ ) and Svalbard ( $\log AODC = 7.06 + 1.09 \times \log SSC$ ,  $r^2 = 0.13$ ).

The concentration of dissolved organic carbon in meltwaters from the glaciers in Greenland was low (14 - 52 µM) (figure 5.12). Data on DOC from the melt season 1999 is too sporadic for testing correlation with factors indicating potential microbial degradation of organic matter. Content of DOC in meltwaters from the glacier in Norway was also very low (table 5.12 and figure 5.26). At the early melt season it was 12 µM, followed by a 50% decrease by the mid-melt season. A simultaneous decrease of nitrate



concentration and DOC may indicate degradation of organic carbon by heterotrophic nitrate-reducing bacteria. However, variations in discharge of meltwater stream causing dilution make this interpretation unreliable.

**Table 5.17.** Summary of bacterial populations and concentrations of dissolved organic carbon in early melt season subglacial meltwaters from Greenland (1999), Norway (2000) and Svalbard (2002).

	DOC ( $\mu\text{M}$ )	Median AODC ( $\log_{10}\text{cells ml}^{-1}$ )
Greenland	22-52	4.65
Norway	12-16	3.96
Svalbard	407-453	4.57

The concentration of dissolved organic carbon in meltwater from Midre Løvenbreen in Svalbard was over an order of magnitude higher than at other glaciers studied (table 5.17), due to the different bedrock composition. Bedrock in the Midre Løvenbreen catchment area is composed of sedimentary rocks such as sandstones with calcareous and dolomitic beds (Hjelle 1993), whereas in the field sites in Greenland and Norway, bedrock consists mainly of Precambrian gneisses (Escher and Watt 1976; Oftedahl 1980). Generally, the content of inorganic carbon plus organic matter in calcareous sedimentary rocks can be as high as 24 – 100 %, whereas in igneous granitic rocks content of carbon is less than 0.05 % (Hitchon et al. 1999). Despite the vast difference in content of dissolved organic carbon between Svalbard meltwater (407 – 453  $\mu\text{M}$ ) and Greenland and Norway early melt season meltwaters (22-52  $\mu\text{M}$  and 12-16  $\mu\text{M}$ , respectively), response of total bacterial populations was not parallel. In the early melt season, the median total number of bacteria in Svalbard meltwater was four times as high as in Norway meltwater, but less than in Greenland meltwater (table 5.17).

Previous studies in other glaciated areas have proved that cold-adapted heterotrophic bacteria can grow in low nutrient environments. In a high arctic Canadian glacier, Skidmore et al. (2000) detected DOC concentrations of 100



$\mu\text{M}$  in the basal ice at the glacier bed, and  $24 \mu\text{M}$  in non-basal glacier ice, confirming that there was elevated organic carbon available beneath glacier to facilitate subglacial microbial metabolism. When ice cores were drilled from above the subglacial Lake Vostok in Antarctica, DOC concentration of  $43 \mu\text{M}$  and bacterial abundance from  $3.45$  to  $4.56 \log_{10}\text{cells ml}^{-1}$  were detected in ice cores from  $3590 \text{ m}$ . It was estimated that in the water of Lake Vostok DOC concentration was approximately  $100 \mu\text{M}$ , adequate to support on the order of  $5 - 6 \log_{10}\text{cells ml}^{-1}$  of heterotrophic micro-organisms (Priscu et al. 1999). Abyzov et al. (1998) have detected  $2.90 - 4.03 \log_{10}$  bacteria  $\text{ml}^{-1}$  from deep ice cores in Central Antarctica. The existence of the above mentioned heterotrophic microbial populations in deep ice support our finding that heterotrophic bacteria survive also in subglacial cavities, although organic carbon concentration may be minimal. Given that glaciers cover  $\sim 10\%$  of the Earth's land area (Sugden and John 1976), widespread subglacial bacterial populations, including also heterotrophic bacteria, are likely to have greater impact on biogeochemical processes and global carbon cycle than has earlier been anticipated.

#### **5.4.2. Temperature characteristics of sulphate-reducing bacteria from different glaciers**

Nitrate- and sulphate-reducing bacteria growing at  $+4^\circ\text{C}$  were cultured from both of the Greenland glaciers, although incubation times as long as  $60 - 120$  days were needed to reach maximum growth (tables 5.1-5.4). Presence of nitrate- and sulphate-reducers suggest that oxygen content beneath glaciers is reduced, or conditions are truly anaerobic. In earlier studies (e.g. Nedwell et al. 1993; Isaksen and Jørgensen 1996) it has been demonstrated that in permanently cold marine environments, anaerobic biodegradation of organic matter takes place mainly by microbes which use sulphate as an electron acceptor. Moreover, studies on subglacial drainage systems (Brown et al. 1994b, Tranter et al. 1994 and Richards et al. 1996) have demonstrated that oxygen and nitrate concentrations may drop to zero in closed subglacial drainage system, due to a combination of limited access to atmospheric oxygen and oxidation of sulphide minerals in freshly ground rock material beneath glacier. This is consistent with the discovery of very low oxygen



concentration (3%) in Greenland basal ice by Souchez et al (1995), which was explained to be a result of oxidation of organic matter underneath the ice. Field studies on meltwater chemistry in Greenland indicated that oxygen and nitrate concentrations in subglacial meltwater were depleted (figure 5.12 and table 5.6). Therefore it was concluded that sulphate is a likely electron acceptor for obligate anaerobes also in subglacial conditions, and further experiments focused on sulphate-reducing bacteria. Successful culturing of bacteria growing in the strictly anaerobic SRB-medium confirmed that viable mixed populations of anaerobic bacteria were present constantly from June to August. However, active sulphate-reducing bacteria were detected only in meltwaters dominated by waters from the subglacial drainage system, which confirms that there was no oxygen or limited amount of oxygen present in subglacial cavities.

Temperature characteristics and growth rates of mixed cultures of sulphate-reducing bacteria from the Greenland glacier revealed apparent changes in bacterial populations from early to late melt season. In the early melt season bulk meltwater, sulphate reduction activity in enrichment culture was dominated by mesophilic and psychrotolerant organisms (figures 5.3 and 5.4), and the maximum sulphate reduction rate of  $115.2 \mu\text{M d}^{-1}$  was reached within 35 days at  $+25^\circ\text{C}$  (figure 5.5). In the late melt season meltwater, psychrophilic organisms were dominant (figures 5.3 and 5.4). Growth was slow at  $+4^\circ\text{C}$ , and sulphate reducing bacteria remained active until the end of the incubation period of almost 300 days. The doubling time in the early exponential phase ranged from 3.5 to 8.5 days, which is comparable with a doubling time of 7 days at  $+10^\circ\text{C}$  for psychrophilic sulphate-reducing bacteria from Arctic sediments (Knoblauch and Jørgensen, 1999).

Although the *in situ*-temperature of the Greenland meltwater bacteria was below  $+1^\circ\text{C}$ , the optimum temperature for sulphate reduction in early melt season samples was  $+17$  to  $+30^\circ\text{C}$  (figures 5.3 and 5.4). In similar temperature-gradient incubations, Sagemann et al. (1998) found that although the *in situ*-temperature was from  $-1.7$  to  $+7.0^\circ\text{C}$ , the optimum temperature for these sulphate-reducing organisms was  $+23$  -  $+30^\circ\text{C}$ . Also, Nedwell (1989) reported a similar difference between *in situ* and optimum temperature for sulphate reduction in Antarctic sediments ( $-1.5^\circ\text{C}$  *in situ*,  $+21$



°C optimum). Sagemann et al. (1998) remark that sulphate-reducing bacteria are well adapted to low temperatures, but they are more dependent on substrate concentration at low than at high temperatures. The SRB-medium (based on Postgate 1984) used in our experiments included sufficient substrates for bacteria (sodium acetate 0.90 g l<sup>-1</sup>, sodium lactate 1.92 g l<sup>-1</sup>). Therefore, there was no lack of nutrients limiting growth or metabolic activity of bacteria. Similar growth rates and total sulphide production (table 5.5, figures 5.5, 5.9 and 5.10) at +4 °C compared to +17 °C or 25 °C proved adaptation of sulphate-reducing bacteria to permanently low temperature.

Anaerobic sulphate-reducing bacteria growing at +2 °C were cultured also from the subglacial meltwaters from the Jostedalsbreen ice cap (Norway) but not from the supraglacial meltwaters (tables 5.7 – 5.10). Samples of supraglacial meltwaters were taken from the trickles flowing on the top of the glacier, so it is understandable that obligate anaerobes did not survive in that environment. Growth of sulphate-reducing bacteria from the bulk proglacial stream dominated by subglacial meltwater was evident after 5 - 6 weeks incubation at +2 °C (tables 5.8 and 5.10). Thus the rate of sulphide production was equivalent to that reported in permanently cold Arctic marine sediments. Enrichment cultures of Arctic marine sulphate reducers started to produce sulphide at +4 °C after 4 weeks if lactate was used as carbon source, and after 8 - 10 weeks if acetate or propionate was used (Knoblauch et al. 1999). The medium for sulphate-reducing bacteria used in our experiment included both lactate and acetate (Postgate 1984).

Again, like in the Greenland glacier, there were differences in the temperature characteristics of sulphate-reducing bacteria (figures 5.17 - 5.19) and sulphate reduction rates (figures 5.20 and 5.21) in the early and mid melt season meltwaters from the Jostedalsbreen ice cap. In the early melt season, the optimum temperature for sulphide production after 5 and 12 weeks was +13 - +16 °C, reflecting the presence of psychrotolerant and psychrophilic sulphate-reducers. Interestingly, after 25 weeks incubation sulphate-reducing bacteria showed activity also at -0.6 °C, with a sulphate reduction rate of 5.79  $\mu\text{mol l}^{-1} \text{ d}^{-1}$  (figure 5.18). Sagemann et al. (1998) also detected activity of sulphate-reducing bacteria in sediments of the Arctic Ocean at subzero temperatures from -5 to 0 °C. The sulphate reduction rate after short



incubation of only five hours was  $0.003 - 0.008 \mu\text{mol l}^{-1} \text{d}^{-1}$ . Moreover, Knoblauch et al. (1999) have isolated several strains of psychrophilic bacteria from cold Arctic marine sediments which grew well at a temperature of  $-1.8^\circ\text{C}$  although the optimum growth temperature was up to  $20^\circ\text{C}$  higher.

The dominance of psychrophilic bacteria in the early melt season meltwater from Jostedalsbreen ice cap reflects the permanently cold conditions of subglacial drainage system. Conversely, in the mid melt season meltwater, no sulphate reduction took place below  $+7^\circ\text{C}$  (figures 5.17 – 5.19 and 5.21) and the optimum temperature for sulphate reducers after 5 and 12 weeks was  $+32^\circ\text{C}$  (figure 5.17). The decrease in concentrations of dissolved ions (figure 5.25) shows that meltwater at the mid melt season was diluted with vast quantities of ice melt originating partly from melting of a glacier surface, where temperature variations are wider, providing suitable conditions for mesophilic bacteria. Mesophiles may have survived all the way through moulins and crevasses to the base of glacier, and finally been brought in the bulk meltwater. Surprisingly, in Greenland meltwaters the early melt season seemed to favour mesophilic bacteria, and psychrophilic bacteria dominated later in the melt season. Differences in climate and glacier morphology between the two glaciers may explain this. Greenland has an arctic climate (Jones 2002) and coastal precipitation in the Nordre Isortoq region is  $350 \text{ mm a}^{-1}$ , whereas Jostedalsbreen has a warmer maritime climate and the annual precipitation of  $1000 - 2000 \text{ mm a}^{-1}$  (Bickerton and Matthews 1993). Greenland glacier represents marginal sector of the extensive inland ice, with catchment area of  $16.5 \text{ km}^2$  and drainage along the single channel (Jones 2002), whereas Jostedalsbreen is a plateau ice cap with an area of  $486 \text{ km}^2$  and numerous outlet glaciers extending to steep-sloped valleys (Norske Statens Kartverk 1995). During the sampling season, the maximum discharge in the main meltwater stream in Greenland was  $28 - 33 \text{ m}^3 \text{ s}^{-1}$ , whereas in an outlet glacier in Norway it was as low as  $6 \text{ m}^3 \text{ s}^{-1}$ . Hence, the development of the drainage system in these two glaciers may have differed, and appearance of mixed populations with different temperature characteristics was thus possible.

Sulphate reduction rate in Svalbard enrichment culture was 12 - 20 times as high as in Greenland and Norway cultures (figures 5.5, 5.20 and 5.30).



According to Knoblauch and Jørgensen (1999), cell-specific sulphate reduction rates are highest in the early exponential growth phase and decrease rapidly as the culture approaches the stationary growth phase. The cultures used in these experiments were approximately at the same growth phase (FDDC in Greenland culture 21 - 35%, Norway 28 - 31%, Svalbard 23 - 31%), proving that remarkable difference in sulphate reduction rate was not a result of different growth phase. When using a medium with plenty of substrates (lactate, acetate), bacterial populations in enrichment cultures from Svalbard high nutrient environment had lower doubling times (3 - 4 days, table 5.14) than cultures from oligotrophic meltwaters from Greenland (3.5 – 8.5 days, table 5.5) and Norway (4 – 12 days, table 5.11), suggesting that the medium used was more suitable for sulphate-reducing bacteria whose initial habitat provided similar substrates.

In Midre Løvenbreen, chemical composition revealed that meltwater from the outflows around proglacial icings was truly subglacial meltwater, the product of basal melt. High pH, high concentrations of dissolved ions (table 5.15) as well as very low dissolved oxygen concentrations confirmed this. Long residence time resulted in high concentrations of ions dissolved from minerals, and consequently also higher numbers of bacteria. High solute concentrations detected in the Midre Løvenbreen glacier were consistent with composition of pre-melt season meltwater analysed from other High Arctic glaciers. Hodgins et al. (1997) have also demonstrated that proglacial icing is a highly concentrated store of weathering products from the winter season, and yields solutes to meltwater early in the melt season.



**6.1. Weathering experiment with proglacial rock debris and subglacial meltwater from Bødalsbreen**

**6.1.1. *In situ* and laboratory experiment conditions**

Proglacial rock debris for the first weathering experiment was taken from the forefield of the Bødalsbreen outlet glacier, 100 m from the terminus of the glacier. Rock debris from the surface layer (depth 5 cm) and from a depth of 35 cm was used to study whether microbial activity in the proglacial forefield in two different depths varied. The temperature profile at the time of sampling was:

air temperature	+10.4 °C
5 cm below surface	+8.8 °C
10 cm	+6.1 °C
15 cm	+3.6 °C
25 cm	+2.9 °C
45 cm	+2.8 °C

Meltwater for the first experiment was taken from a subglacial meltwater stream of the Bødalsbreen glacier. At the time of sampling, the water temperature was +0.3 °C and the electrical conductivity was 13.3  $\mu\text{S cm}^{-1}$ . Meltwater and rock debris samples were transported from the field site to the laboratory in 16 hours, packed in cooler boxes, and thereafter stored at +2 °C for four weeks. Biotic test vials and abiotic controls were incubated at +7 °C for 100 days.

**6.1.2. Grain size distribution of Bødalsbreen proglacial rock debris**

The rock debris used was mostly composed of silicates rich in quartz and feldspars (table 6.1), which are more resistant to mechanical stress and weathering than other silicate minerals (Hitchon et al. 1999, Bowen's reaction series in Faure 1991). Rock debris samples were ground manually with mortar and pestle to simulate the subglacial crushing of bedrock and to release fresh mineral surfaces which may act as suitable substrates for



microbial activity. There were several grain size fractions in each ground sample (figure 6.1). Only 45 weight-% and 40 weight-% of the samples from 5 cm and 35 cm, respectively, were composed of the fraction of 0-250  $\mu\text{m}$ . In this finest fraction,  $d_{50}$ -values were 110  $\mu\text{m}$  (surface layer) and 86  $\mu\text{m}$  (deeper layer) (figure 6.2).

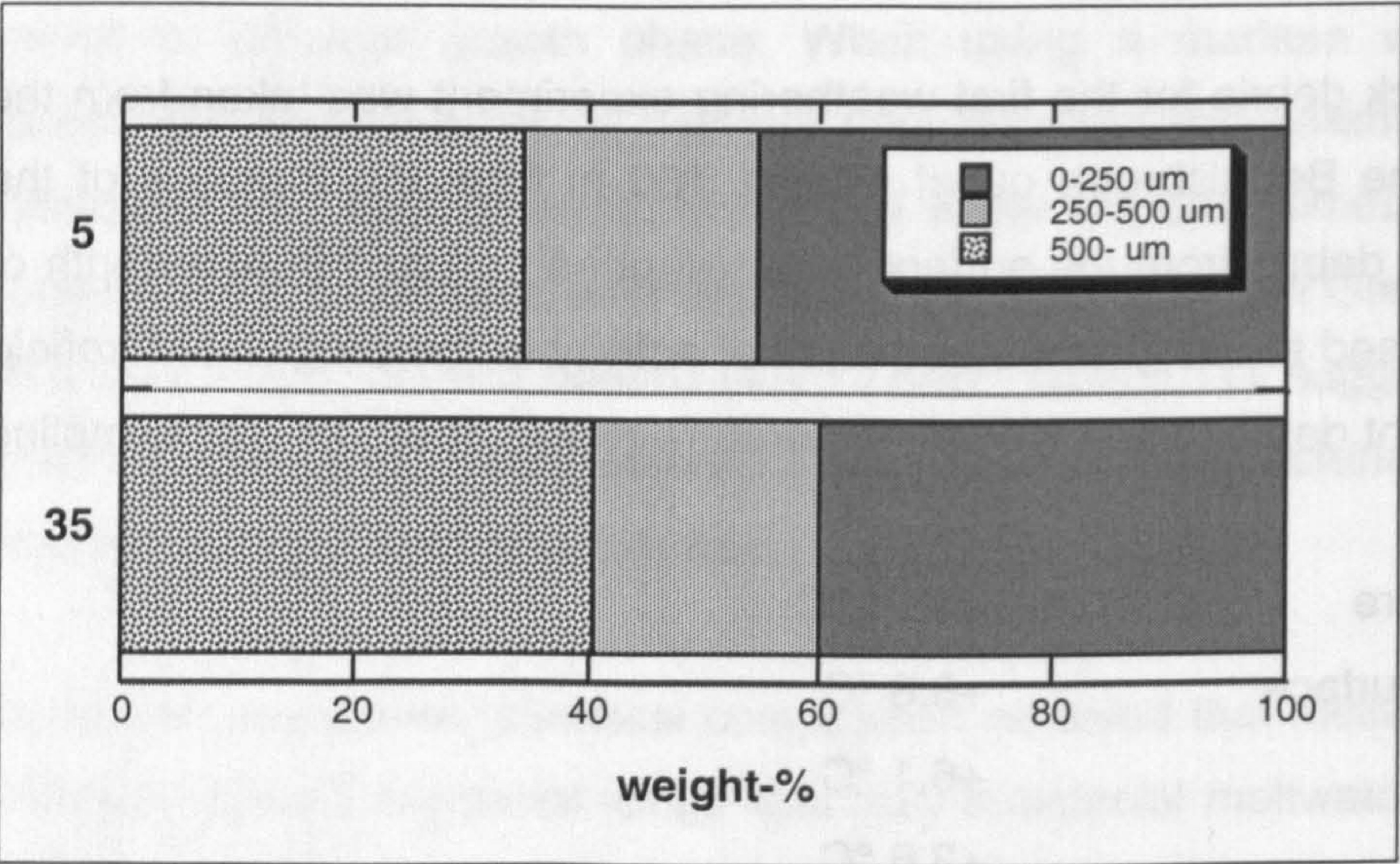


**Figure 6.1.** Proportions of grain size fractions in the proglacial rock debris samples from the Bødalsbreen glacier (depths of 5 cm and 35 cm).

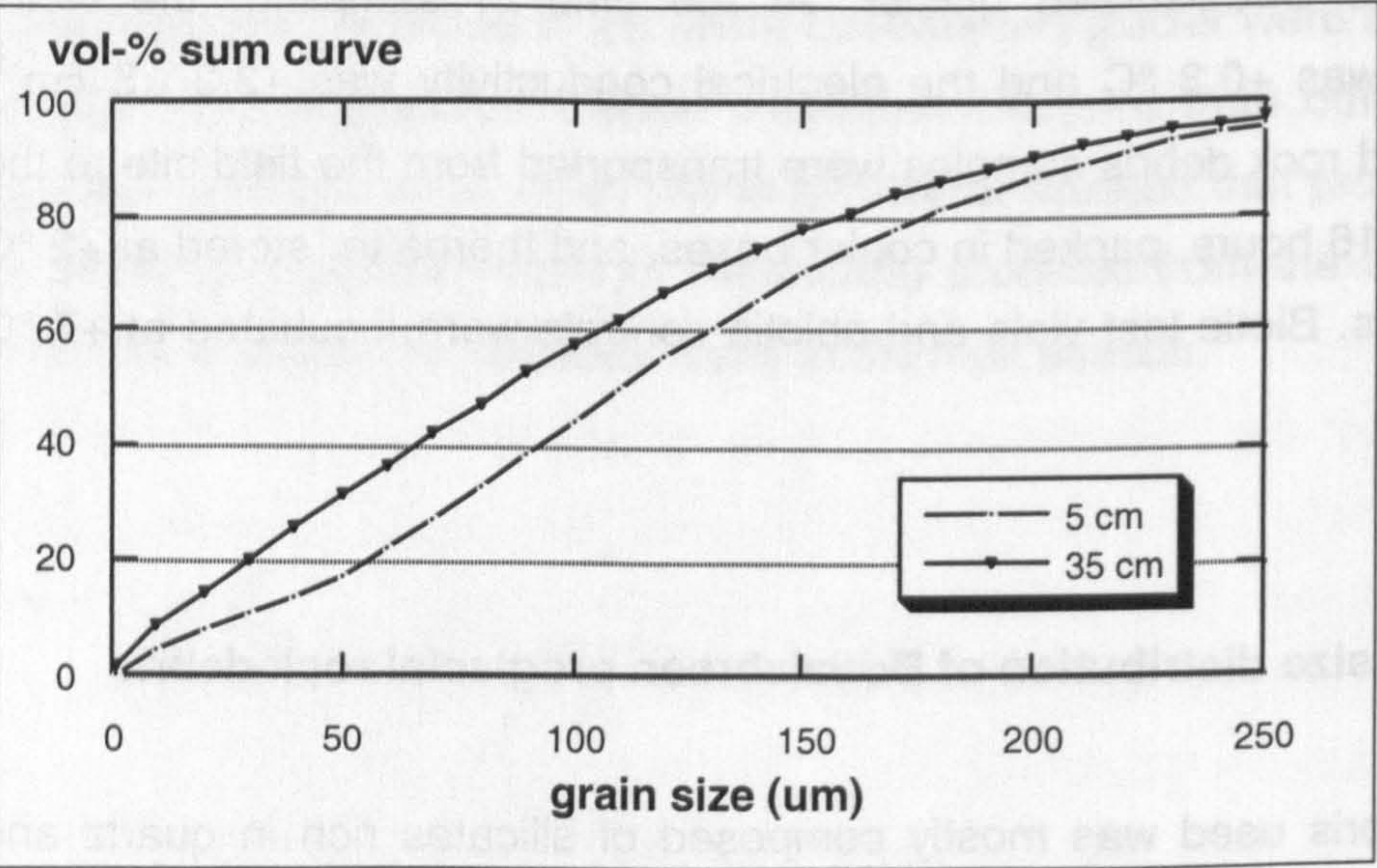


**Figure 6.2.** Grain size distributions of the fine-grained fractions (0-250  $\mu\text{m}$ ) of the proglacial rock debris from the Bødalsbreen glacier.



### 6.1.3. Elemental composition of Bødalsbreen proglacial rock debris

The elemental composition at the beginning of experiment was analysed both by inductively coupled plasma-atomic emission spectrometry (ICP-AES) and x-ray fluorescence spectrometry (XRF). Results were comparable (table 6.1), although XRF gave slightly higher values, the maximum difference being 1.25 %, with  $\text{Al}_2\text{O}_3$ . The elemental composition of the rock debris at the two depths of 5 cm and 35 cm were identical (table 6.1). High contents of  $\text{SiO}_2$ ,  $\text{Al}_2\text{O}_3$ ,  $\text{K}_2\text{O}$  and  $\text{Na}_2\text{O}$  are typical of granite and gneiss, with quartz, feldspar and mica being the main minerals. Only negligible amounts of organic carbon, carbonate and sulphate were found.

**Table 6.1.** Elemental composition of the rock debris from the depths of 5 cm and 35 cm at the beginning and at the end of the experiment. Percentages of major elements analysed by ICP-AES / XRF. If there are two figures presented, the first one is by ICP/AES, and the second one is by XRF. nd= not determined.

	depth 5 cm start of exp	depth 35 cm start of exp	depth 5 cm end of exp	depth 35 cm end of exp
<b>LOI % (980 °C)</b>	0.5	0.5	1.1	1.2
<b>org-C %</b>	0.03	0.01	nd	nd
<b>CO<sub>3</sub>-C %</b>	0.00	0.01	nd	nd
<b>H %</b>	0.00	0.01	nd	nd
<b>N %</b>	0.00	0.40	nd	nd
<b>S %</b>	0.03	0.02	nd	nd
<b>Na<sub>2</sub>O %</b>	3.5 / 3.6	3.2 / 3.2	3.3 /	3.7 /
<b>MgO %</b>	1.0 / 0.8	1.1 / 1.1	0.9 /	1.1 /
<b>Al<sub>2</sub>O<sub>3</sub> %</b>	12.7 / 14.0	13.3 / 14.5	12.5 /	13.5 /
<b>SiO<sub>2</sub> %</b>	/ 70.6	/ 69.0		
<b>P<sub>2</sub>O<sub>5</sub> %</b>	0.2 / 0.2	0.2 / 0.2	0.2 /	0.2 /
<b>K<sub>2</sub>O %</b>	4.2 / 4.4	4.2 / 4.5	4.2 /	4.2 /
<b>CaO %</b>	2.2 / 2.4	2.4 / 2.8	2.2 /	2.6 /
<b>TiO<sub>2</sub> %</b>	0.5 / 0.5	0.5 / 0.5	0.5 /	0.5 /
<b>MnO %</b>	0.1 / 0.1	0.1 / 0.1	0.1 /	0.1 /
<b>Fe<sub>2</sub>O<sub>3</sub> %</b>	2.5 / 2.6	3.1 / 3.3	2.4 /	3.0 /
<b>major elements</b>	<b>27.0 / 99.3</b>	<b>28.6 / 99.7</b>	<b>26.3 /</b>	<b>28.9 /</b>
<b>sum %</b>				



It is most likely that the sensitivities of the methods were not high enough for detecting changes in elemental composition at the beginning and at the end of experiment. Due to limited amount of rock debris sample in each test vial, three replicates of each sample were not analysed. Hence, the data presented in table 6.1 is inadequate for testing statistically whether there were significant differences in elemental composition before and after incubation.

#### **6.1.4. Bacterial growth in Bødalsbreen meltwater**

Bacterial populations from rock debris and subglacial meltwater were incubated in 5 ml vials, with freshly ground rock debris as a potential substrate, and with a rock/water ratio of 0.10 g ml<sup>-1</sup>. Vials with the headspace of air were sealed with neoprene septa and aluminium crimp caps. At +7 °C, bacterial growth started immediately without any lag phase, and exponential growth continued for the first 14 days (figure 6.3). The deeper layer rock debris gave rise to lower numbers of bacteria in water during the initial stage of incubation, but after two weeks of exponential growth, the total number of bacteria was above 7.00 log<sub>10</sub> cells ml<sup>-1</sup> in both systems (figure 6.3).

The frequency of dividing and divided cells was at its highest during the first week of incubation (figure 6.3). Thereafter, it remained below 10% until the end of incubation. In both systems, the population remained in the stationary phase throughout the 14 weeks of incubation, and did not reach the death phase by the end of the experiment.



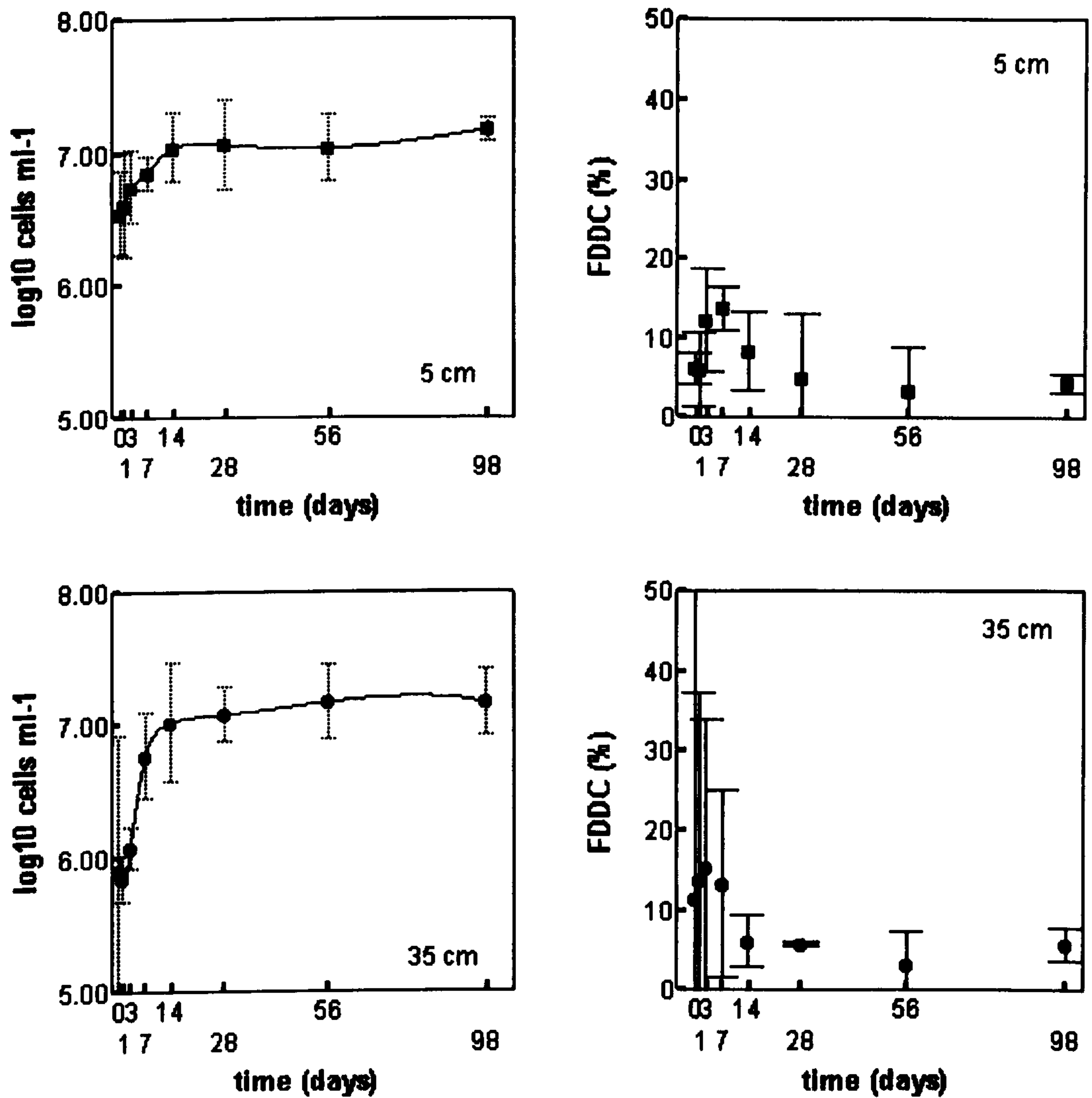


**Figure 6.3.** Growth curves of the total numbers of bacteria in meltwaters incubated at +7 °C with rock debris from the depths of 5 cm (■) and 35 cm (●), and frequency of dividing and divided cells (FDDC) over time. Subglacial meltwater and proglacial rock debris taken from the Bødalsbreen glacier. Lines and symbols show the mean values and error bars show 95% confidence intervals for the means of the three replicates (n=3).



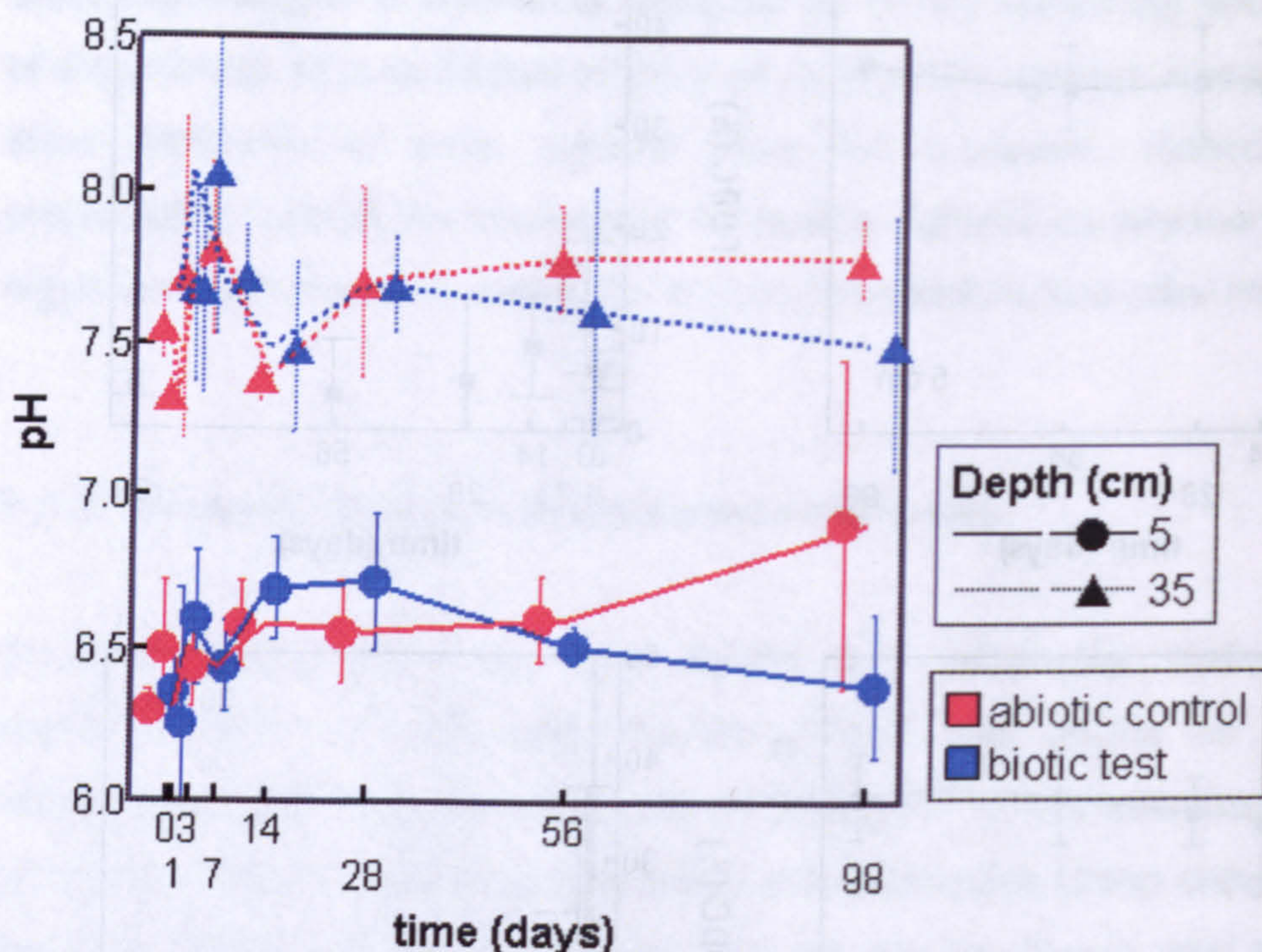


**Figure 6.4.** pH in meltwaters incubated at +7 °C with rock debris from the depths of 5 cm and 35 cm. Subglacial meltwater and proglacial rock debris taken from the Bødalsbreen glacier. Lines show the mean values and error bars show 95% confidence intervals for the means of the three replicates (n=3). (●) = biotic test, depth of 5 cm; (▲) = biotic test, depth of 35 cm; (●) = abiotic control, depth of 5 cm; (▲) = abiotic control, depth of 35 cm.

#### 6.1.5. pH in Bødalsbreen meltwater

In the meltwater incubated with surface layer rock debris, the initial pH was 1.3 units lower than in the meltwater incubated with deeper layer rock debris (pH of 6.4 and 7.7, respectively) (figure 6.4). The reason for such a distinct difference may have been due to organic matter attached to the mineral particles in surficial layer, and production of organic acids through gradual biodegradation during storage. Moreover, there were less carbonates present in the surface layer (table 6.1), due to the preceding dissolution of minerals on the top of the outwash plain. However, variations in pH throughout the 98 days incubation followed an analogous pattern in both systems. During the first weeks of the incubation, pH varied correspondingly in biotic and abiotic vials, indicating that rapid chemical dissolution reactions occurred. After 4 - 8



weeks, pH gradually decreased in biotic test vials, as a result of the production of CO<sub>2</sub> into meltwaters, whereas in abiotic control vials pH remained relatively stable. At the end of 14 weeks incubation, the difference in pH between biotic tests and abiotic controls of the surface layer rock debris was noticeable (figure 6.4 and table 6.2).

**Table 6.2.** Results of the t-tests (independent samples pooled-variance and separate-variance t-test) for equality of means (three replicates) of pH and major anions and cations in Bødalsbreen meltwater incubated at +7 °C with rock debris from the depths of 5 cm (table A) and 35 cm (table B). Comparisons between biotic tests and abiotic controls at the end of incubation (t=98 days).

<b>TABLE A</b>	Test for equality of variances F	Test for equality of variances p	t-test for equality of means / t	t-test for equality of means / p
pH	4.041	0.115	-3.872	0.036
NO <sub>3</sub> <sup>-</sup>	6.323	0.066	-2.835	0.101
Mg <sup>2+</sup>	0.354	0.584	2.690	0.055
Ca <sup>2+</sup>	0.504	0.517	-0.041	0.969
Na <sup>+</sup>	0.966	0.398	-2.884	0.063
K <sup>+</sup>	2.416	0.195	-1.469	0.236
SO <sub>4</sub> <sup>2-</sup>	0.777	0.428	2.385	0.076

<b>TABLE B</b>	Test for equality of variances F	Test for equality of variances p	t-test for equality of means t	t-test for equality of means p
pH	3.084	0.154	-2.813	0.088
NO <sub>3</sub> <sup>-</sup>	6.526	0.063	-4.785	0.029
Mg <sup>2+</sup>	1.687	0.264	8.274	0.001
Ca <sup>2+</sup>	0.035	0.861	2.115	0.102
Na <sup>+</sup>	1.313	0.335	0.120	0.912
K <sup>+</sup>	8.848	0.041	-3.403	0.076
SO <sub>4</sub> <sup>2-</sup>	2.980	0.159	2.282	0.085



**Table 6.3.** Results of the t-tests of pH and major anions and cations in Bødalsbreen meltwater incubated at +7 °C with rock debris from the depths of 5 cm and 35 cm. Comparisons between biotic tests with rock debris from depths of 5 cm and 35 cm at the end of incubation (t=98 days).

	Test for equality of variances <b>F</b>	Test for equality of variances <b>p</b>	t-test for equality of means <b>t</b>	t-test for equality of means <b>p</b>
pH	0.891	0.399	-10.085	0.001
NO <sub>3</sub> <sup>-</sup>	0.694	0.452	0.648	0.552
Mg <sup>2+</sup>	0.770	0.430	-5.780	0.004
Ca <sup>2+</sup>	5.292	0.083	-13.815	0.003
Na <sup>+</sup>	22.819	0.017	-6.350	0.077
K <sup>+</sup>	5.300	0.083	-14.323	0.005
SO <sub>4</sub> <sup>2-</sup>	0.683	0.455	1.429	0.226

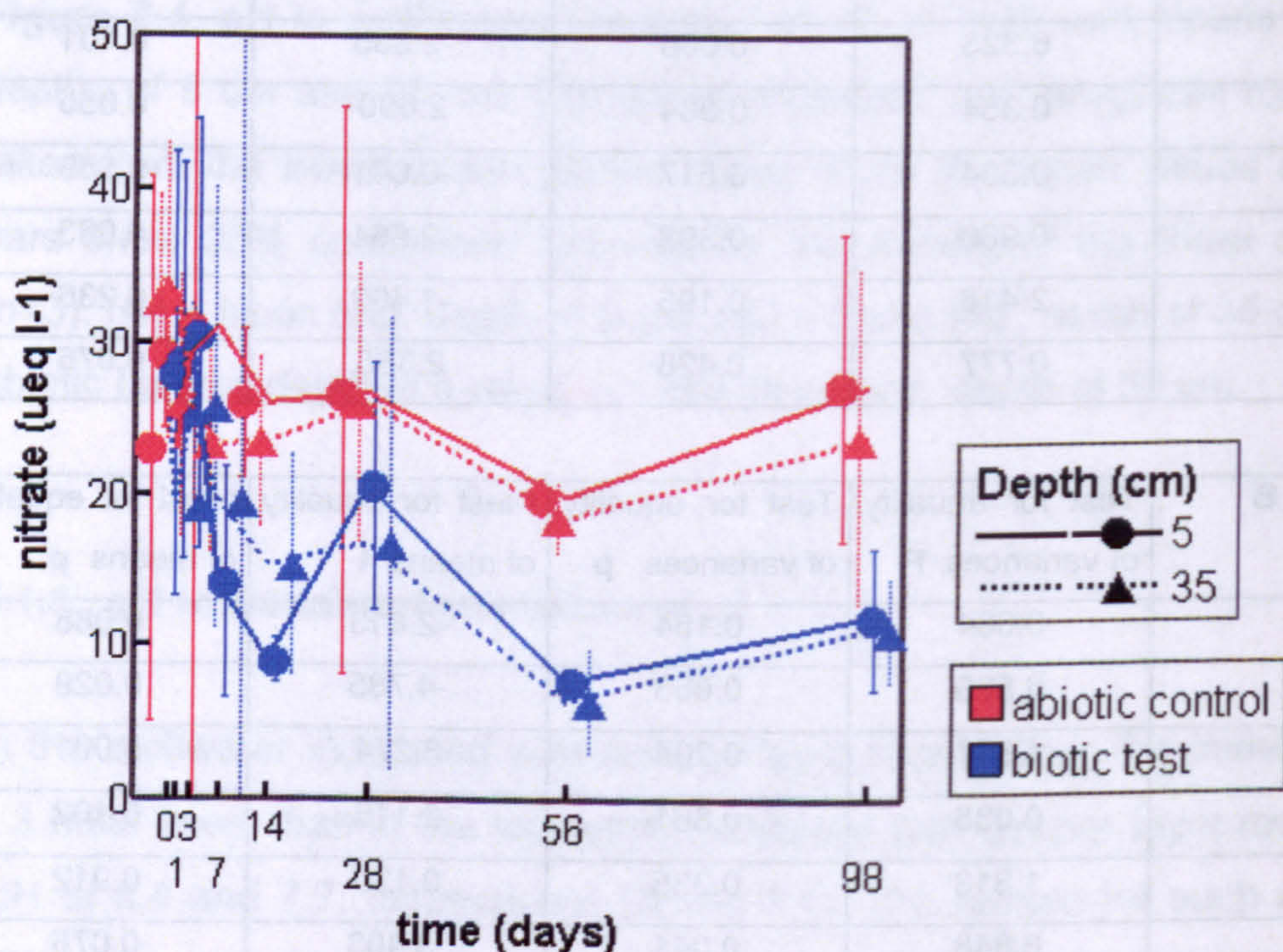


**Figure 6.5.** Nitrate concentrations in meltwaters incubated at +7 °C with rock debris from the depths of 5 cm and 35 cm. Subglacial meltwater and proglacial rock debris taken from the Bødalsbreen glacier. Lines show the mean values and error bars show 95% confidence intervals for the means of the three replicates (n=3). (●) = biotic test, depth of 5 cm; (▲) = biotic test, depth of 35 cm; (●) = abiotic control, depth of 5 cm; (▲) = abiotic control, depth of 35 cm.



### 6.1.6. Major anions and cations in Bødalsbreen meltwater

Although the elemental composition of the rock debris at the depths of 5 cm and 35 cm were identical (table 6.1), markedly higher concentrations of  $\text{Mg}^{2+}$ ,  $\text{Ca}^{2+}$  and  $\text{K}^{+}$  were released to meltwater from the deep layer rock debris (figures 6.6 and 6.7 and table 6.3). The likely explanation is that before sampling the rock debris on the top of the outwash plain (depth of 5 cm) had been more exposed to weathering and dissolution of minerals. Moreover, since the rock debris from the depth of 35 cm was originally more coarse-grained than the top layer material, crushing and grinding produced more grains with fresh mineral surfaces than in the rock debris from the depth of 5 cm.

As early as after 7-14 days of incubation, there was reduction in concentration of  $\text{NO}_3^-$  (figure 6.5) in the biotic test vials, indicating that microbial nitrate respiration was taking place. In the abiotic controls, nitrate concentrations remained higher throughout the incubation (figure 6.5). Due to the high relative error in  $\text{NO}_3^-$  analysis (relative mean error 6.55 - 11.67 %, table 4.2 and error bars in figure 6.5), statistical tests (table 6.2) did not demonstrate strong evidence for differences between biotic and abiotic systems. Nevertheless, difference between biotic and abiotic system at the end of incubation was significant ( $p < 0.05$ ) in meltwater mixed with rock debris from the depth of 35 cm (table 6.2).

Microbial activity elevated release of  $\text{Mg}^{2+}$  (figures 6.6 and table 6.2), whereas there was no impact on  $\text{Ca}^{2+}$ ,  $\text{Na}^{+}$  and  $\text{K}^{+}$  concentrations (figures 6.6 and 6.7 and table 6.2). Elevated concentration of  $\text{Mg}^{2+}$  was noticeable after two weeks, especially in the water incubated with the rock debris from the depth of 35 cm. As for  $\text{SO}_4^{2-}$  concentration, there was slight increase in biotic systems after 14 weeks incubation (figure 6.8), but statistically the difference compared to abiotic systems was not significant (table 6.2). The results indicated (figures 6.6 to 6.8) that in order to convincingly study the impact of glacial micro-organisms on subglacial weathering, longer than 100 days incubation times at the *in situ* temperature range from 0 to +2 °C ( Skidmore et al. 2000 and Brown et al. 1994b) would be essential.



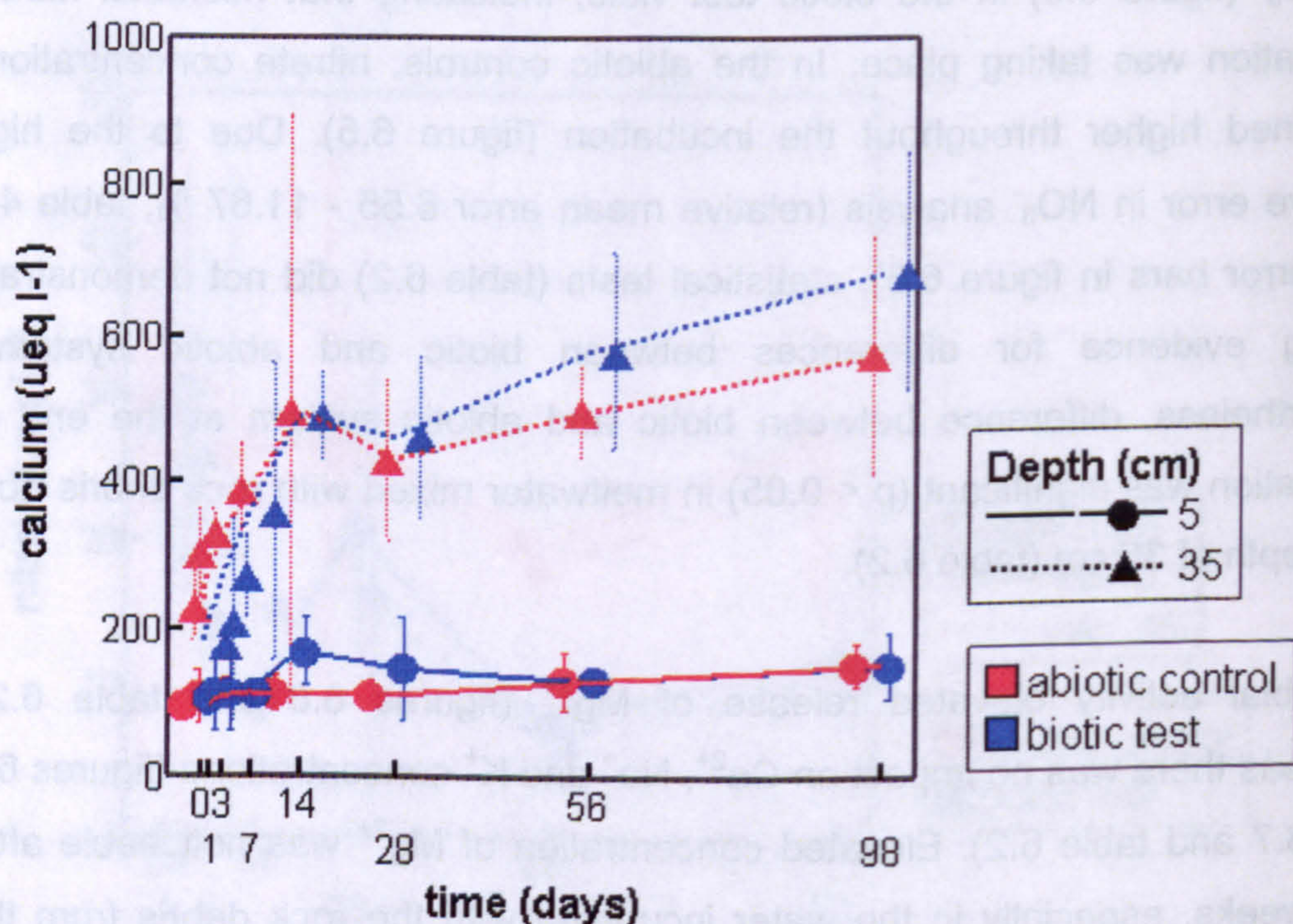
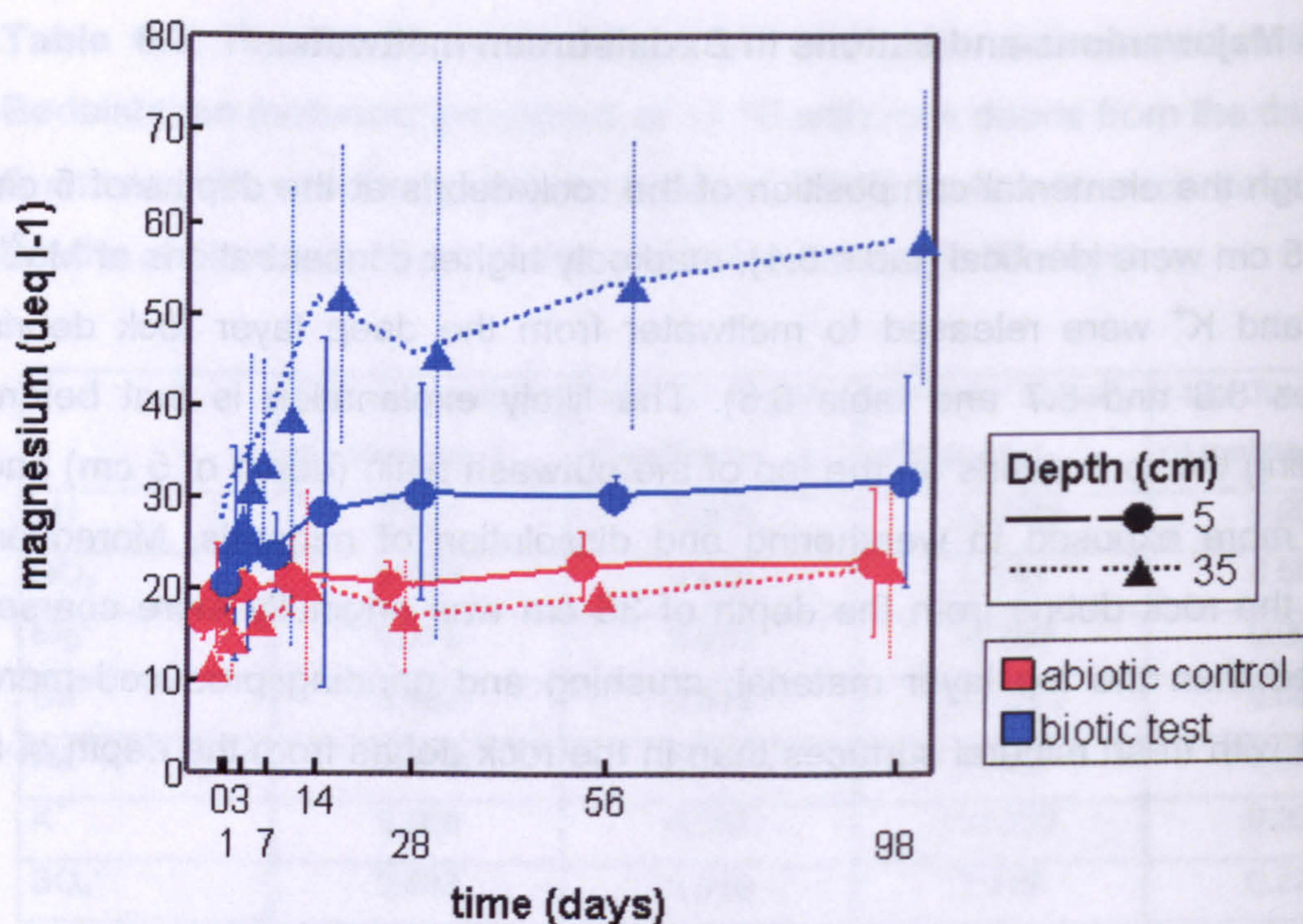


**Figure 6.6.** Magnesium and calcium concentrations in meltwaters incubated at +7 °C with rock debris from the depths of 5 cm and 35 cm. Subglacial meltwater and proglacial rock debris taken from the Bødalsbreen glacier. Lines show the mean values and error bars show 95% confidence intervals for the means of the three replicates ( $n=3$ ). (●) = biotic test, depth of 5 cm; (▲) = biotic test, depth of 35 cm; (●) = abiotic control, depth of 5 cm; (▲) = abiotic control, depth of 35 cm.



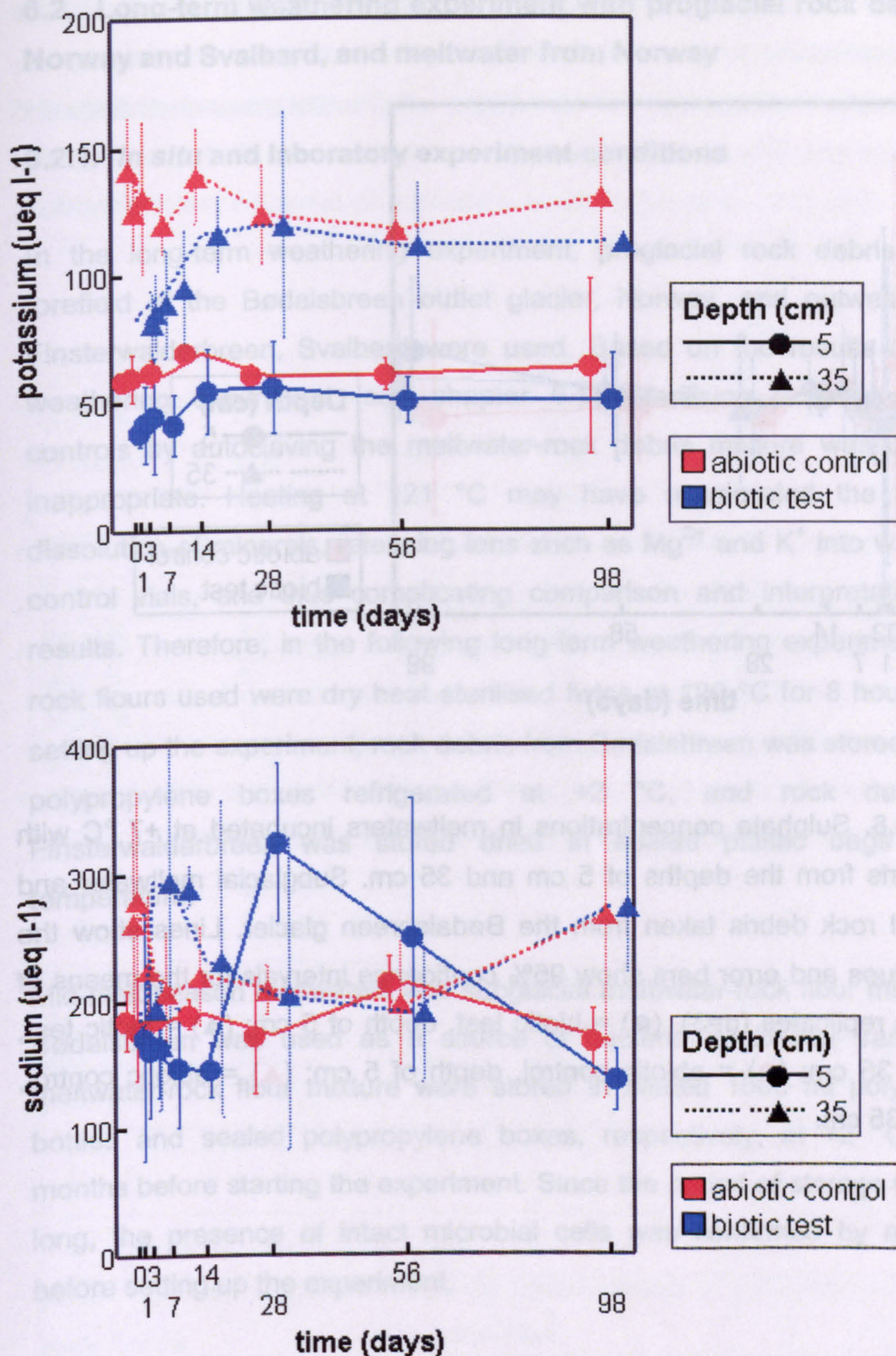


**Figure 6.7.** Potassium and sodium concentrations in meltwaters incubated at +7 °C with rock debris from the depths of 5 cm and 35 cm. Subglacial meltwater and proglacial rock debris taken from the Bødalsbreen glacier. Lines show the mean values and error bars show 95% confidence intervals for the means of the three replicates (n=3). (●) = biotic test, depth of 5 cm; (▲) = biotic test, depth of 35 cm; (●) = abiotic control, depth of 5 cm; (▲) = abiotic control, depth of 35 cm.



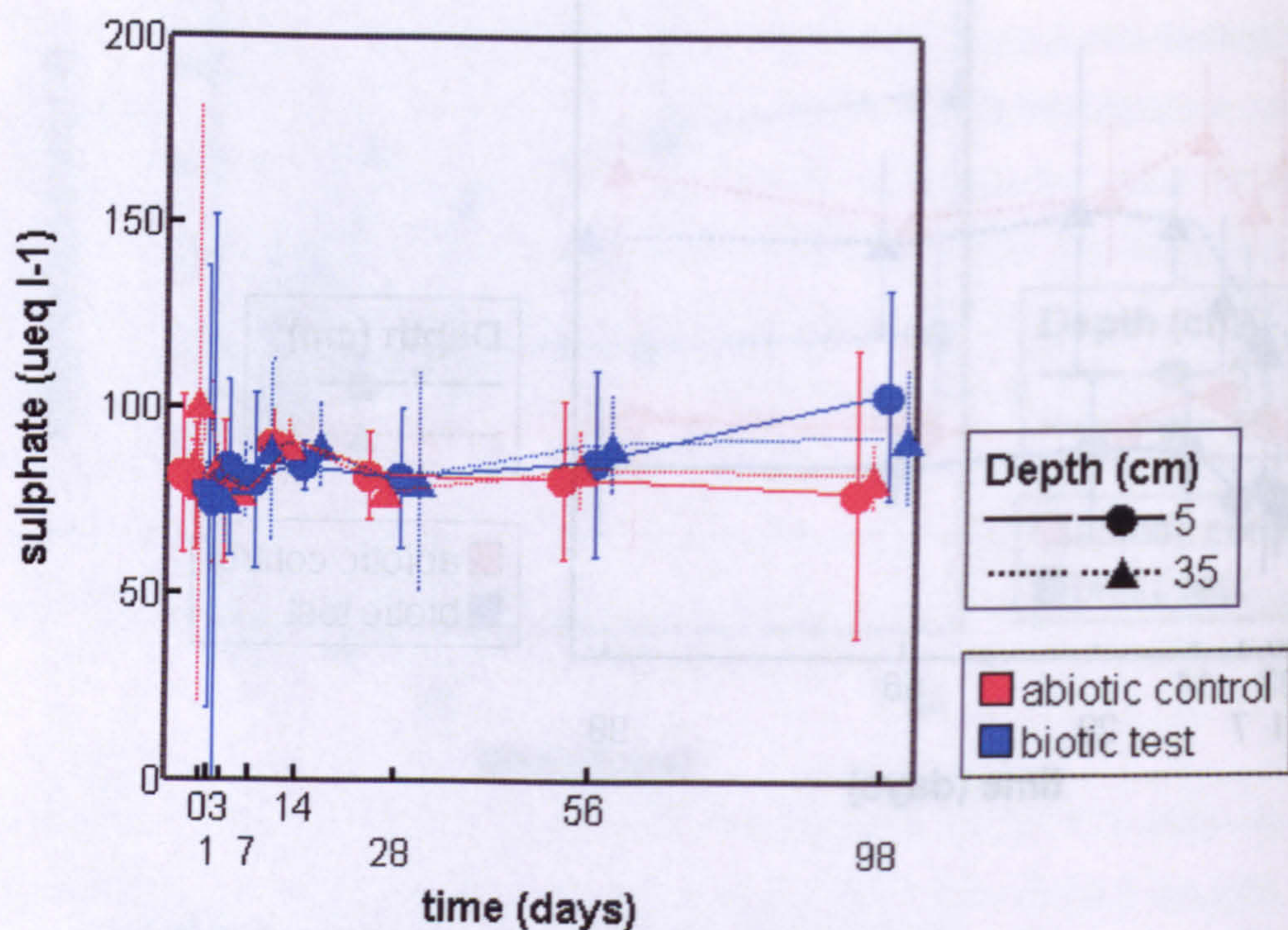


**Figure 6.8.** Sulphate concentrations in meltwaters incubated at +7 °C with rock debris from the depths of 5 cm and 35 cm. Subglacial meltwater and proglacial rock debris taken from the Bødalsbreen glacier. Lines show the mean values and error bars show 95% confidence intervals for the means of the three replicates ( $n=3$ ). (●) = biotic test, depth of 5 cm; (▲) = biotic test, depth of 35 cm; (●) = abiotic control, depth of 5 cm; (▲) = abiotic control, depth of 35 cm.



## **6.2. Long-term weathering experiment with proglacial rock debris from Norway and Svalbard, and meltwater from Norway**

### **6.2.1. *In situ* and laboratory experiment conditions**

In the long-term weathering experiment, proglacial rock debris from the forefield of the Bødalsbreen outlet glacier, Norway, and outwash plain of Finsterwalderbreen, Svalbard were used. Based on the results of the first weathering experiment (see chapter 6.1), sterilising to produce abiotic controls by autoclaving the meltwater-rock debris mixture was considered inappropriate. Heating at 121 °C may have accelerated the immediate dissolution of minerals, releasing ions such as  $\text{Mg}^{2+}$  and  $\text{K}^+$  into water in the control vials, and thus complicating comparison and interpretation of the results. Therefore, in the following long-term weathering experiment, all the rock flours used were dry heat sterilised twice at 120 °C for 8 hours. Before setting up the experiment, rock debris from Bødalsbreen was stored in sealed polypropylene boxes refrigerated at +2 °C, and rock debris from Finsterwalderbreen was stored dried in sealed plastic bags at room temperature.

Mid-melt season meltwaters and subglacial meltwater-rock flour mixture from Bødalsbreen was used as a source of bacteria. Meltwater samples and meltwater-rock flour mixture were stored in sealed 1000 ml polypropylene bottles and sealed polypropylene boxes, respectively, at +2 °C for nine months before starting the experiment. Since the period of storage was rather long, the presence of intact microbial cells was confirmed by microscopy before setting up the experiment.

Mixture of rock flour and meltwater was incubated in 10 ml vials, with a rock/water ratio of 1.00 g ml<sup>-1</sup>. The vials were sealed with butyl septa and aluminium crimp caps, with the headspace of air (aerobic systems) or oxygen-free nitrogen (anaerobic systems) (for detailed description see chapter 4.2.3.2). The biotic test vials and abiotic controls – three parallel sets of both – were incubated in cooled incubators at –1.2 - -1.0 °C, +0.2 - +0.5 °C and +1.6 - +2.6 °C for 300 days. According to the manufacturer, the average variation of temperature in the incubators was +/- 0.5 °C, and



fluctuations of 0.1 °C only should occur with average workload. However, the temperature setting in the cooled incubators was found not to be accurate, and temperature differences from the upper shelf to the lower shelf were 2.6 °C at maximum. The temperature in the incubators was readjusted and the vials moved to two – instead of three – shelves to minimize the temperature variation.

### 6.2.2. Grain size distribution of Bødalsbreen and Finsterwalderbreen rock flours

After grinding rock debris samples from Bødalsbreen and Finsterwalderbreen with an automatic mortar grinder, the grain size of the samples was  $\leq 300 \mu\text{m}$ , representing abraded fine-grained rock flour at the base of glaciers. Although an identical method was used when grinding both of the samples, mineralogical differences caused differences in the grain size distribution. Finsterwalderbreen rock flour was more fine-grained than that of Bødalsbreen (figure 6.9), and  $d_{50}$ -values were  $37 \mu\text{m}$  and  $66 \mu\text{m}$ , respectively.

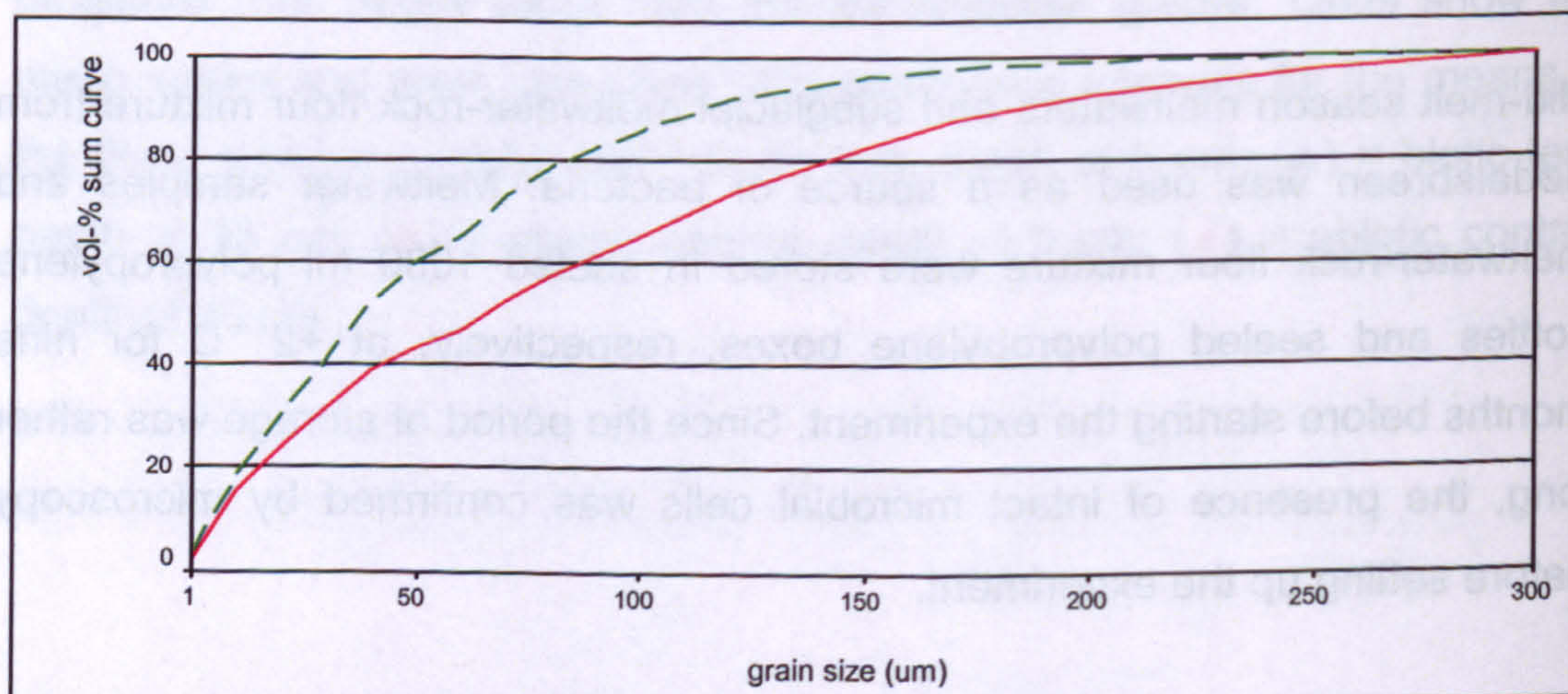


**Figure 6.9.** Grain size distributions of the Bødalsbreen (red solid line) and Finsterwalderbreen (green dotted line) rock flours.



**Table 6.4.** Elemental composition of the rock debris from the Bødalsbreen proglacial outwash plain, at the beginning and at the end of the experiment. Incubation temperature +1.6 - +2.6 °C. Percentages of major elements analysed by XRF.

	start of exp	end of exp aerobic	end of exp anaerobic	end of exp aerobic control	end of exp anaerobic control
<b>LOI % (980 °C)</b>	0.4	0.4	0.3	0.4	0.3
<b>org-C %</b>	0.01	0.00	0.00	0.00	0.00
<b>CO<sub>3</sub>-C %</b>	0.00	0.00	0.00	0.00	0.00
<b>H %</b>	0.00	0.00	0.00	0.00	0.00
<b>N %</b>	0.00	0.03	0.00	0.00	0.03
<b>S %</b>	0.03	0.02	0.02	0.10	0.02
<b>Na<sub>2</sub>O %</b>	3.9	7.1	3.4	3.6	3.4
<b>MgO %</b>	0.7	0.8	0.8	0.8	0.8
<b>Al<sub>2</sub>O<sub>3</sub> %</b>	13.7	13.3	13.8	13.9	13.8
<b>SiO<sub>2</sub> %</b>	71.8	69.3	72.2	71.8	72.1
<b>P<sub>2</sub>O<sub>5</sub> %</b>	0.2	0.1	0.1	0.1	0.1
<b>K<sub>2</sub>O %</b>	4.7	4.6	4.7	4.7	4.7
<b>CaO %</b>	2.1	2.1	2.2	2.2	2.2
<b>TiO<sub>2</sub> %</b>	0.3	0.3	0.4	0.4	0.3
<b>MnO %</b>	0.0	0.0	0.0	0.0	0.0
<b>Fe<sub>2</sub>O<sub>3</sub> %</b>	1.9	1.9	1.9	1.9	1.9
<b>major elements</b>	<b>99.3</b>	<b>99.6</b>	<b>99.5</b>	<b>99.5</b>	<b>99.4</b>
<b>sum %</b>					

**6.2.3. Elemental composition of Bødalsbreen and Finsterwalderbreen rock flours**

Elemental composition as determined by x-fluorescence spectrometry (tables 6.4 and 6.5), did not show any significant changes in rock flours from the beginning to the end of the experiment. As mentioned in the chapter 6.1.3, the sensitivities of the methods were not high enough for detecting changes in elemental composition in rock flours from the beginning to the end of experiment. However, lithological differences between catchments were evident. In Bødalsbreen, pebbles and cobbles in the proglacial plain were



mainly gneissose rocks, with high contents of SiO<sub>2</sub>, Al<sub>2</sub>O<sub>3</sub>, K<sub>2</sub>O and Na<sub>2</sub>O (table 6.4). Organic carbon was negligible, and no carbonate was detected. In Finsterwalderbreen rock debris (table 6.5), the alkali elements (Na<sub>2</sub>O and K<sub>2</sub>O) were less abundant, whereas higher contents of alkaline earth elements (CaO and MgO) and carbonate indicated the presence of dolomite, CaMg(CO<sub>3</sub>)<sub>2</sub>. Also, loss on ignition was significantly higher, due to the organic carbon and content of shale. Proportions of iron and sulphur were higher, and hence the pyrite (FeS<sub>2</sub>) may be higher, too.

**Table 6.5.** Elemental composition of the rock debris from the Finsterwalderbreen proglacial outwash plain, at the beginning and at the end of the experiment. Incubation temperature +1.6- +2.6 °C. Percentages of major elements analysed by XRF.

	start of exp	end of exp aerobic	end of exp anaerobic	end of exp aerobic control	end of exp anaerobic control
LOI % (980 °C)	7.2	7.0	7.2	7.1	7.1
org-C %	0.70	0.69	0.69	0.44	0.72
CO <sub>3</sub> -C %	1.42	1.28	1.23	1.54	1.26
H %	0.12	0.13	0.11	0.10	0.06
N %	0.04	0.13	0.05	0.00	0.00
S %	0.45	0.50	0.42	0.51	0.44
Na <sub>2</sub> O %	0.8	0.8	*	0.8	0.8
MgO %	2.4	2.5	*	2.6	2.5
Al <sub>2</sub> O <sub>3</sub> %	7.4	7.2	*	7.4	7.0
SiO <sub>2</sub> %	71.0	71.3	*	70.8	71.4
P <sub>2</sub> O <sub>5</sub> %	0.2	0.2	*	0.2	0.2
K <sub>2</sub> O %	1.5	1.5	*	1.5	1.5
CaO %	4.8	4.8	*	4.9	4.8
TiO <sub>2</sub> %	0.6	0.6	*	0.6	0.6
MnO %	0.1	0.1	*	0.1	0.1
Fe <sub>2</sub> O <sub>3</sub> %	3.2	3.3	*	3.4	3.2
major elements	94.7	95.0	*	94.9	94.6
sum %					

\* Glass bead for XRF-run broke. Not enough sample to prepare a new one.



6.2.4. Mineralogical composition of Bødalsbreen and Finsterwalderbreen rock flours

The mineralogical composition of the rock debris samples was analysed by XRD. Table 6.6 shows the main crystalline minerals identified in the samples. Although the elemental composition (table 6.5) showed the presence of sulphur in Finsterwalderbreen rock flour, no sulphur- bearing crystalline minerals were identified. The source of sulphur is likely to be amorphous gypsum ( $\text{CaSO}_4 \cdot 2\text{H}_2\text{O}$ ), which is an evaporite mineral occurring widespread across the surface of the Finsterwalderbreen proglacial zone (Cooper et al. 2002). There is no gypsum in the underlying bedrock (Dallmann et al. 1990), so ultimately sulphate must be derived from the oxidation of sulphides present in shales and carbonates (Cooper et al. 2002).

**Table 6.6.** The crystalline minerals identified in Bødalsbreen (Norway) and Finsterwalderbreen (Svalbard) rock flour. Identification is based on comparison of X-ray diffractograms with the diffraction patterns in the MacDiff (version 4.2.5) reference database.

Bødalsbreen (Norway) rock flour	Finsterwalderbreen (Svalbard) rock flour
<i>quartz</i> $\text{SiO}_2$ <i>albite</i> $(\text{Na,Ca})\text{Al}(\text{Si,Al})_3\text{O}_8$ (plagioclase feldspar) <i>anorthoclase</i> $(\text{Na}_2\text{K})(\text{Si}_3\text{Al})\text{O}_8$ (alkali feldspar) <i>microcline</i> $\text{KAlSi}_3\text{O}_8$ (potassium feldspar) <i>biotite</i> $\text{K}(\text{Mg,Fe})_3(\text{Si}_3\text{Al})\text{O}_{10}(\text{OH})_2$ (trioctahedral mica)	<i>quartz</i> $\text{SiO}_2$ <i>albite</i> $(\text{Na,Ca})\text{Al}(\text{Si,Al})_3\text{O}_8$ (plagioclase feldspar) <i>dolomite</i> $\text{CaMg}(\text{CO}_3)_2$ <i>biotite</i> $\text{K}(\text{Mg,Fe})_3(\text{Si}_3\text{Al})\text{O}_{10}(\text{OH})_2$ (trioctahedral mica)

Analysis of the elemental composition of single mineral particles with scanning electron microscope and electron microanalysis detector confirmed the dominance of silicates identified by XRD (table 6.6). Moreover, in mineral grains of Finsterwalderbreen rock flour, trace elements such as titanium (Ti) and molybdenum (Mo) were detected, indicating the presence of accessory minerals characteristic for schists.



### **6.2.5. Bacterial growth in Bødalsbreen meltwater incubated with rock flours**

Bacteria originating from Bødalsbreen meltwater grew better when incubated at +1.6- +2.6 °C with rock debris from Bødalsbreen (figure 6.10, N-aerobic and N-anaerobic), compared with growth with Svalbard rock flour (figure 6.10, S-aerobic and S-anaerobic). When incubated with Norwegian Bødalsbreen rock flour, there was a 10-fold increase in total number of bacteria in 17 days. The total number of  $7.25 \log_{10}$  cells  $\text{ml}^{-1}$  was gained in both aerobic and anaerobic systems, although the initial bacterial population was clearly lower in anaerobic meltwater.

Incubation with Svalbard rock flour resulted in a gradual growth of the bacterial population, but with lower total numbers, and in anaerobic system only after one months lag phase (figure 6.10, S-anaerobic). After 17 days, the total number of bacteria in aerobic Svalbard system was only third of total number gained when incubated with Norwegian rock flour.

### **6.2.6. Oxygen and methane in headspace**

The oxygen content in the headspace of the sealed vials decreased during the 300 days of incubation, from the atmospheric value of 21 vol.% to 7.5 vol.% (when incubated with Norwegian rock flour) and 2.5 vol.% (when incubated with Svalbard rock flour). At the end of the incubation, there was still some oxygen left in headspace, even in the anaerobic vials. Thus, conditions were not suitable for the survival of obligate anaerobes, such as methanogens, and no methane was detected in the headspace.



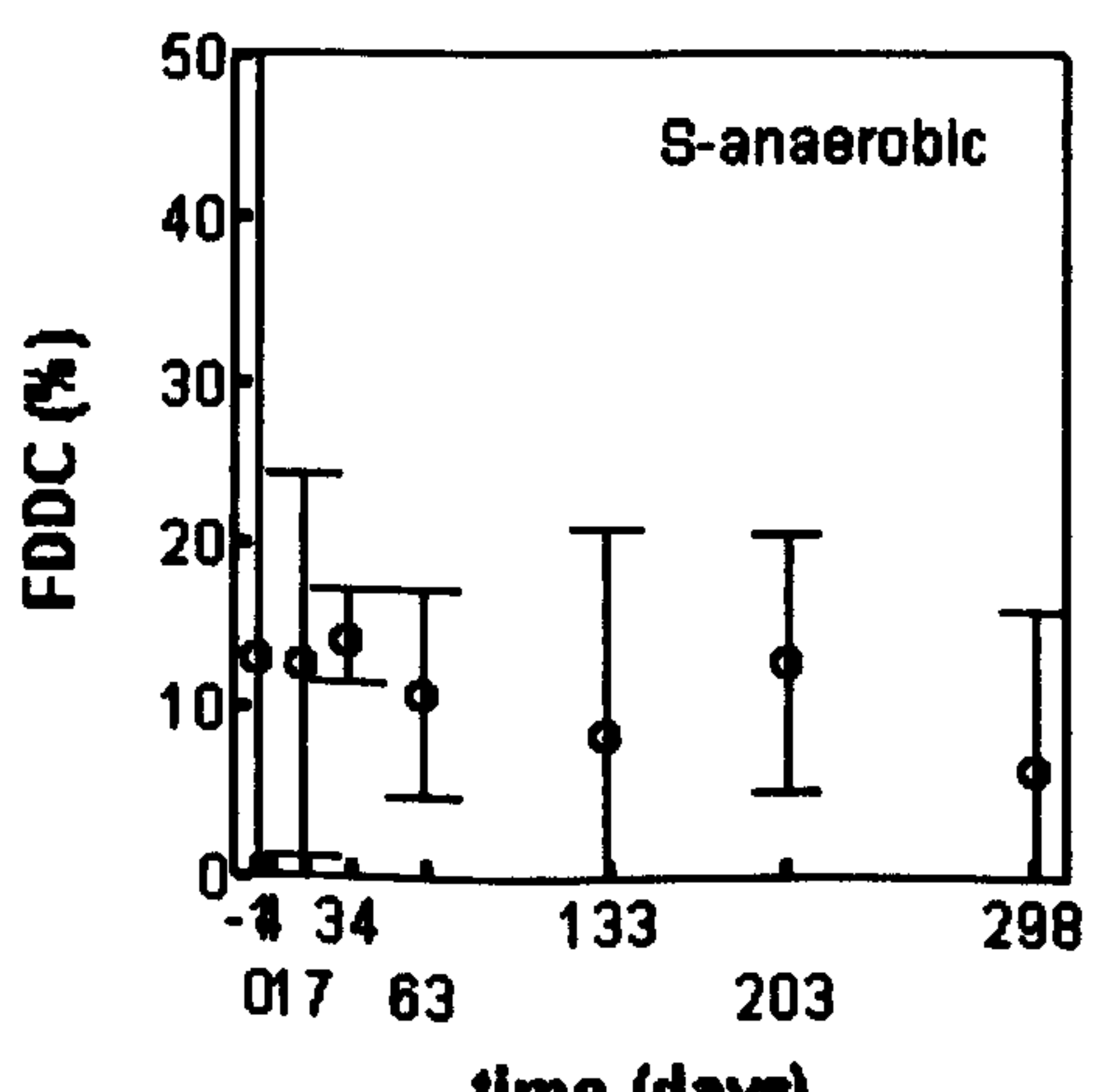
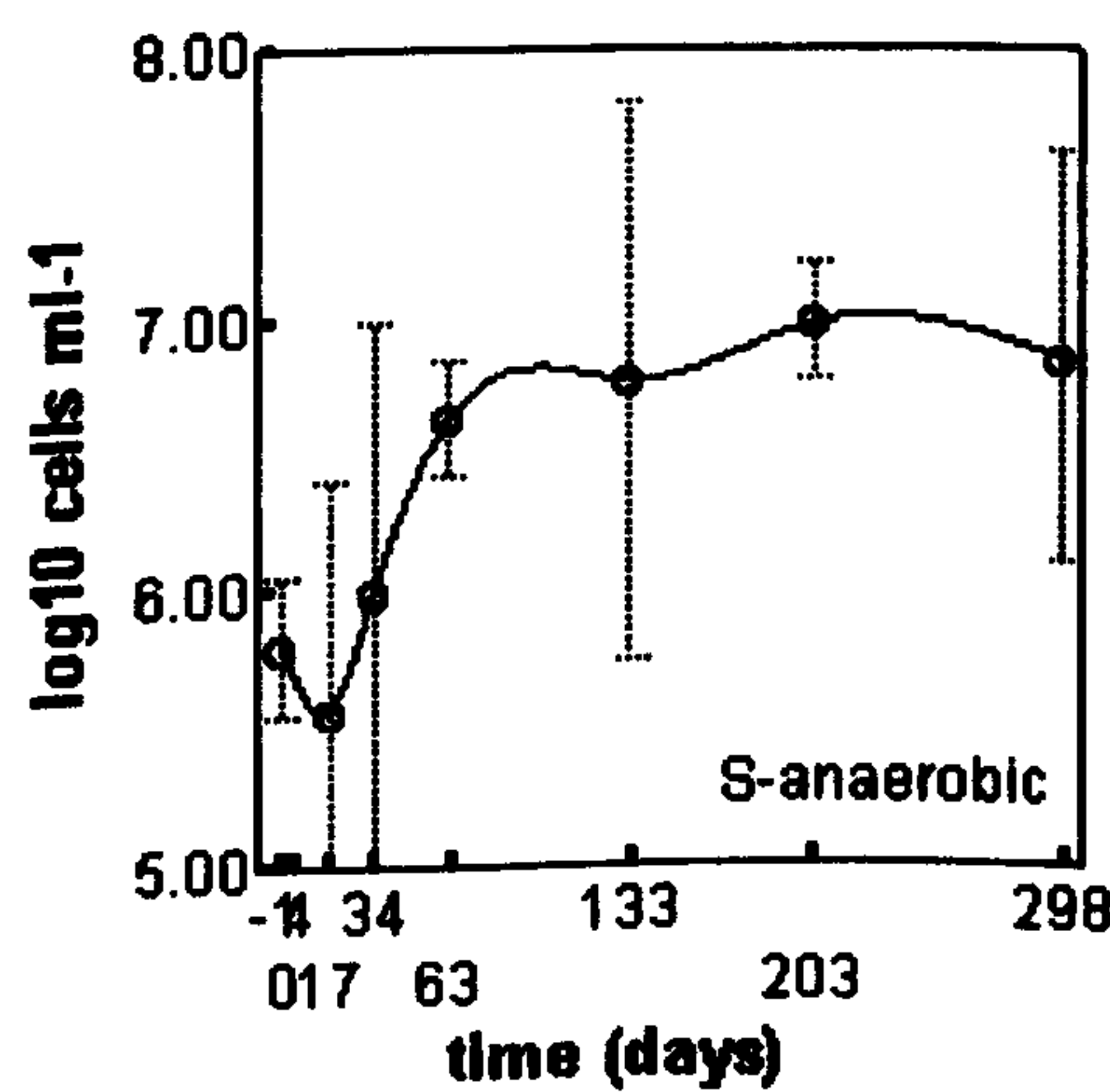
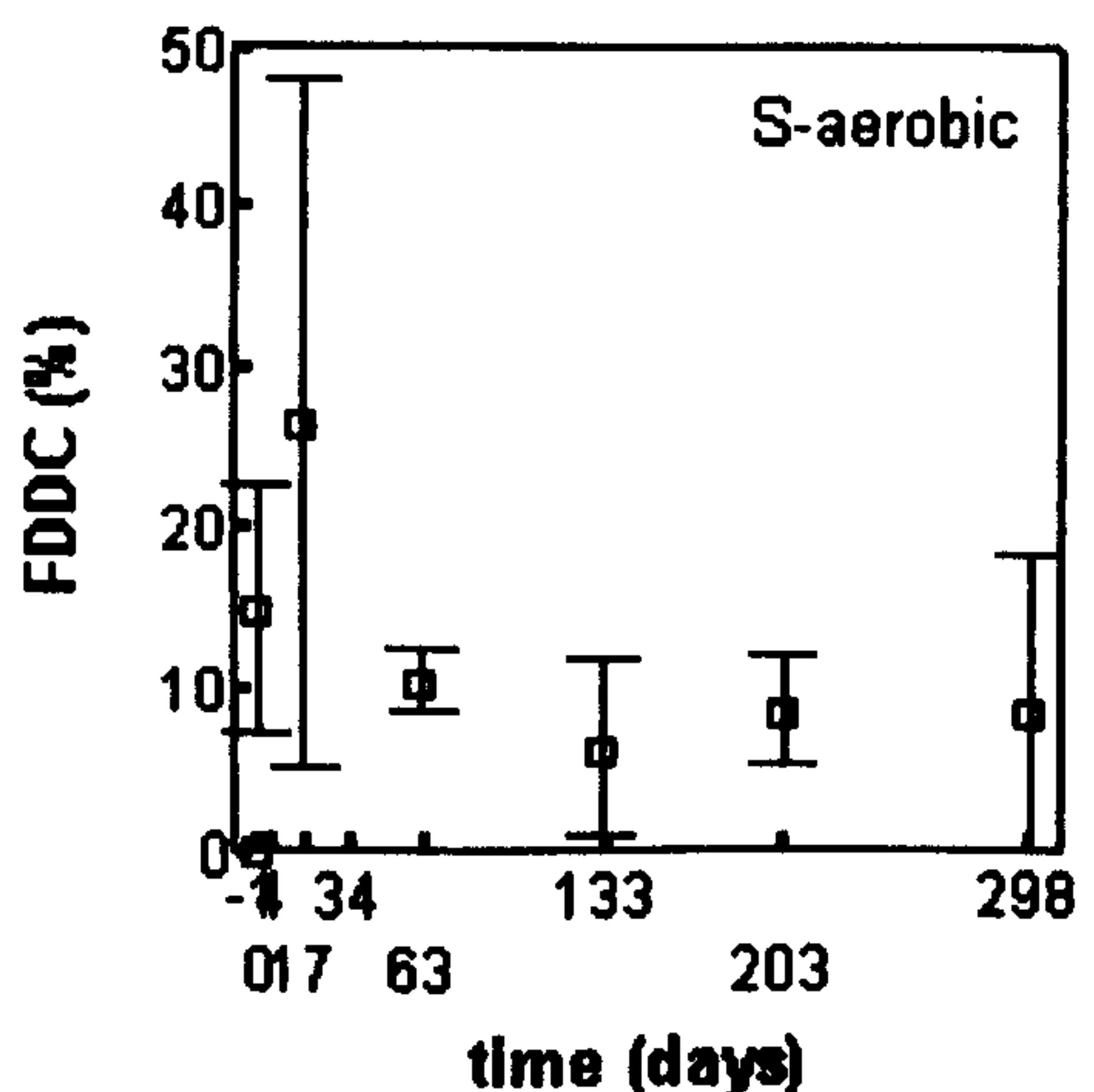
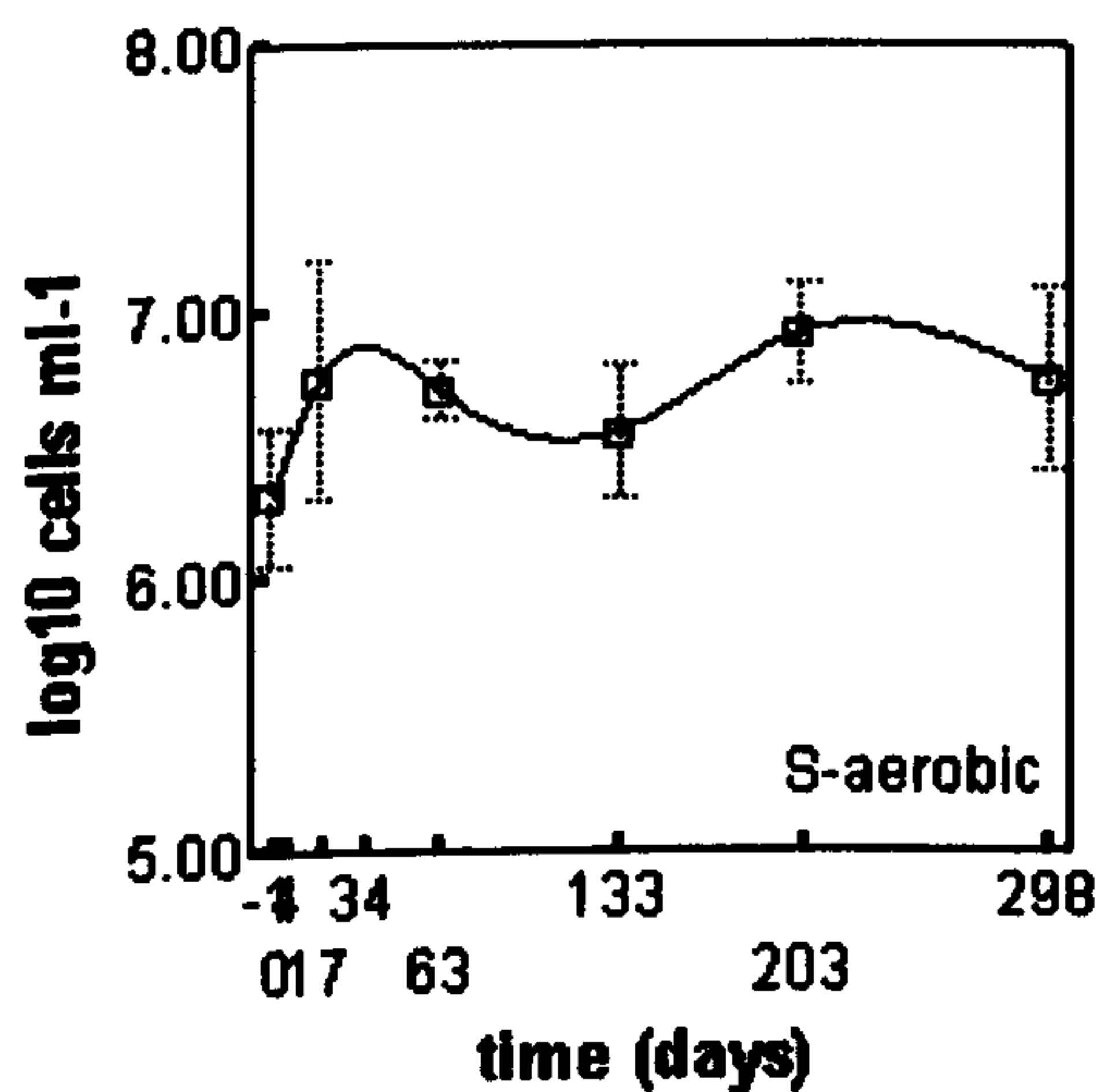
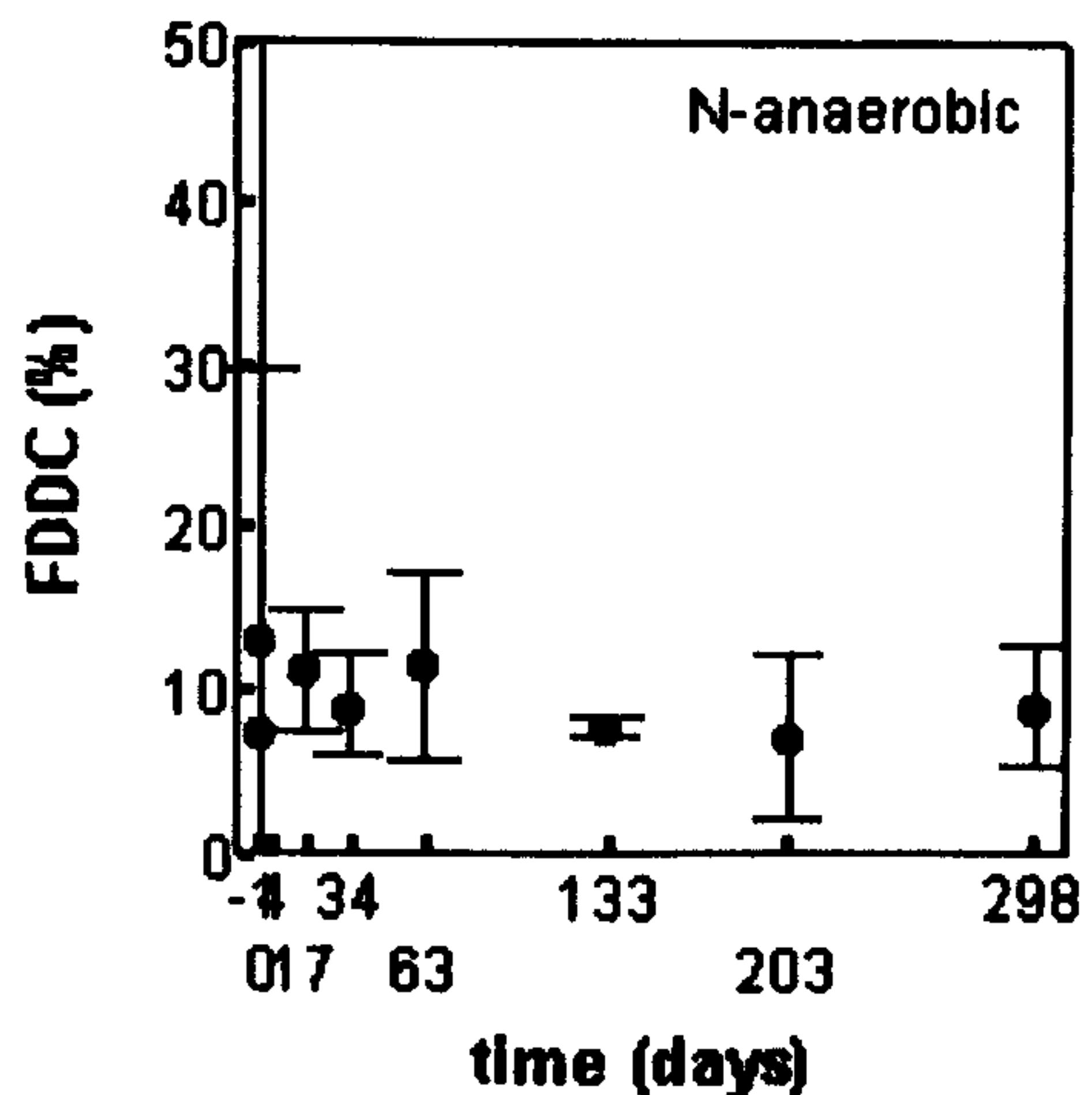
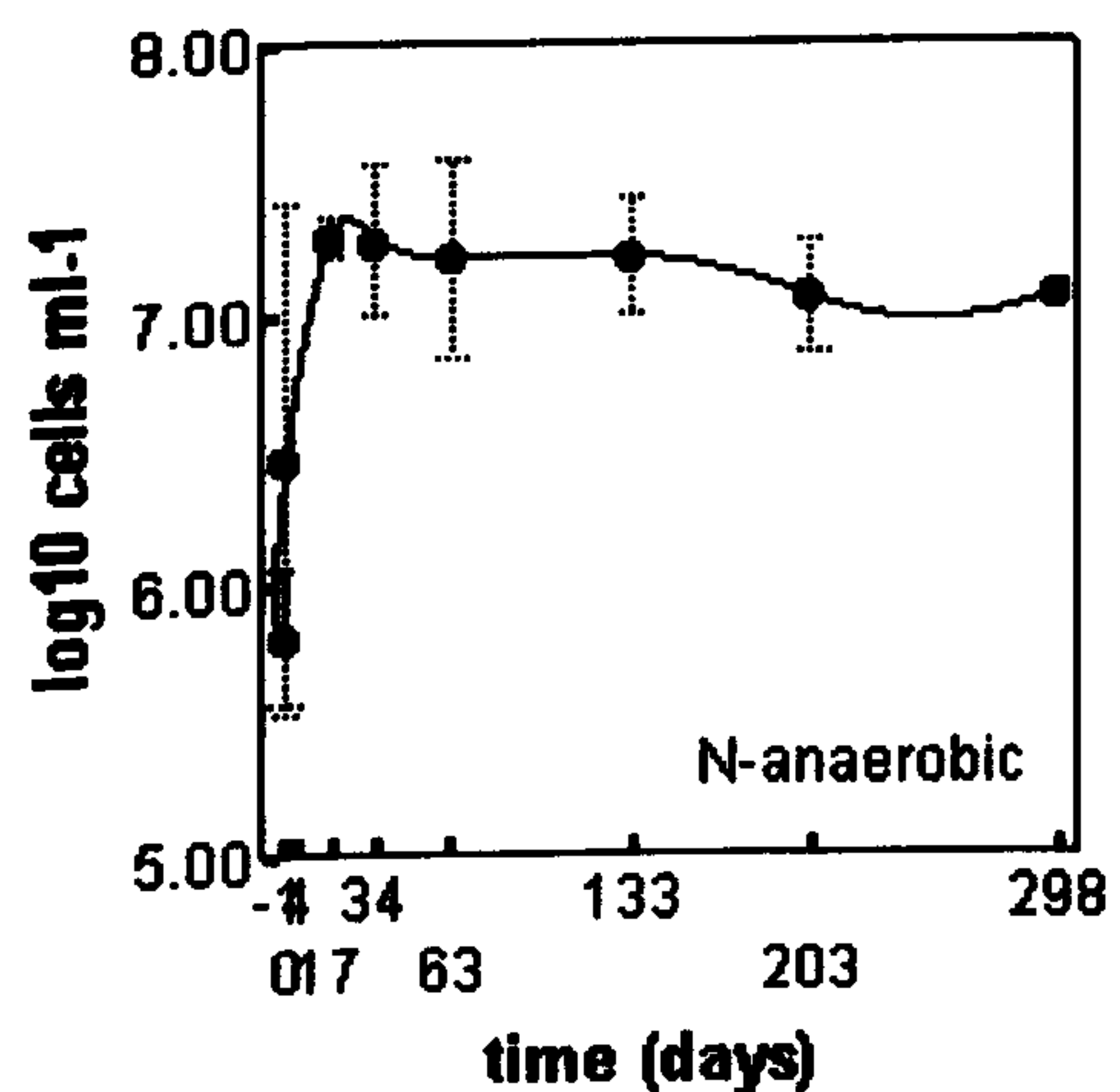
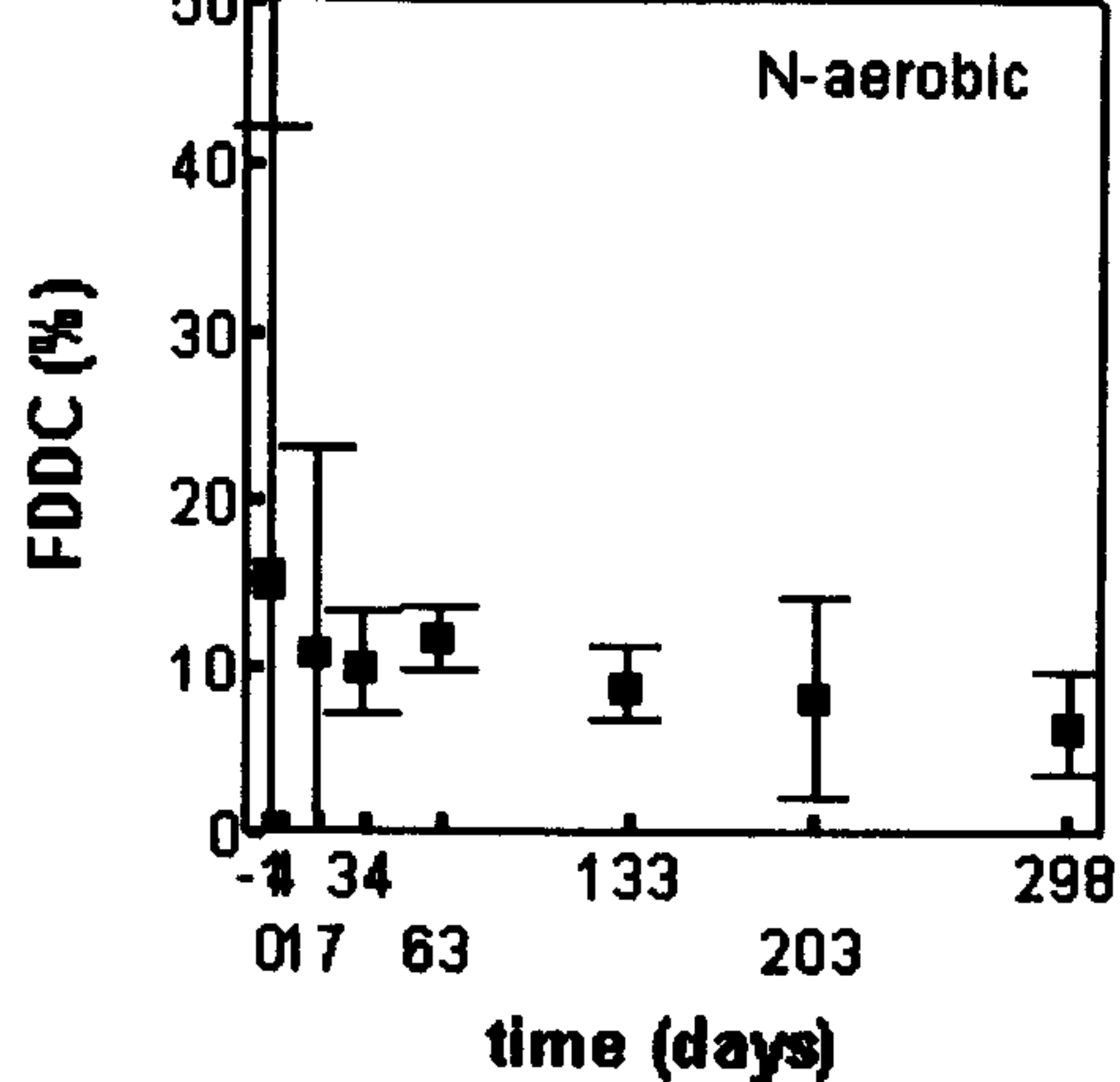
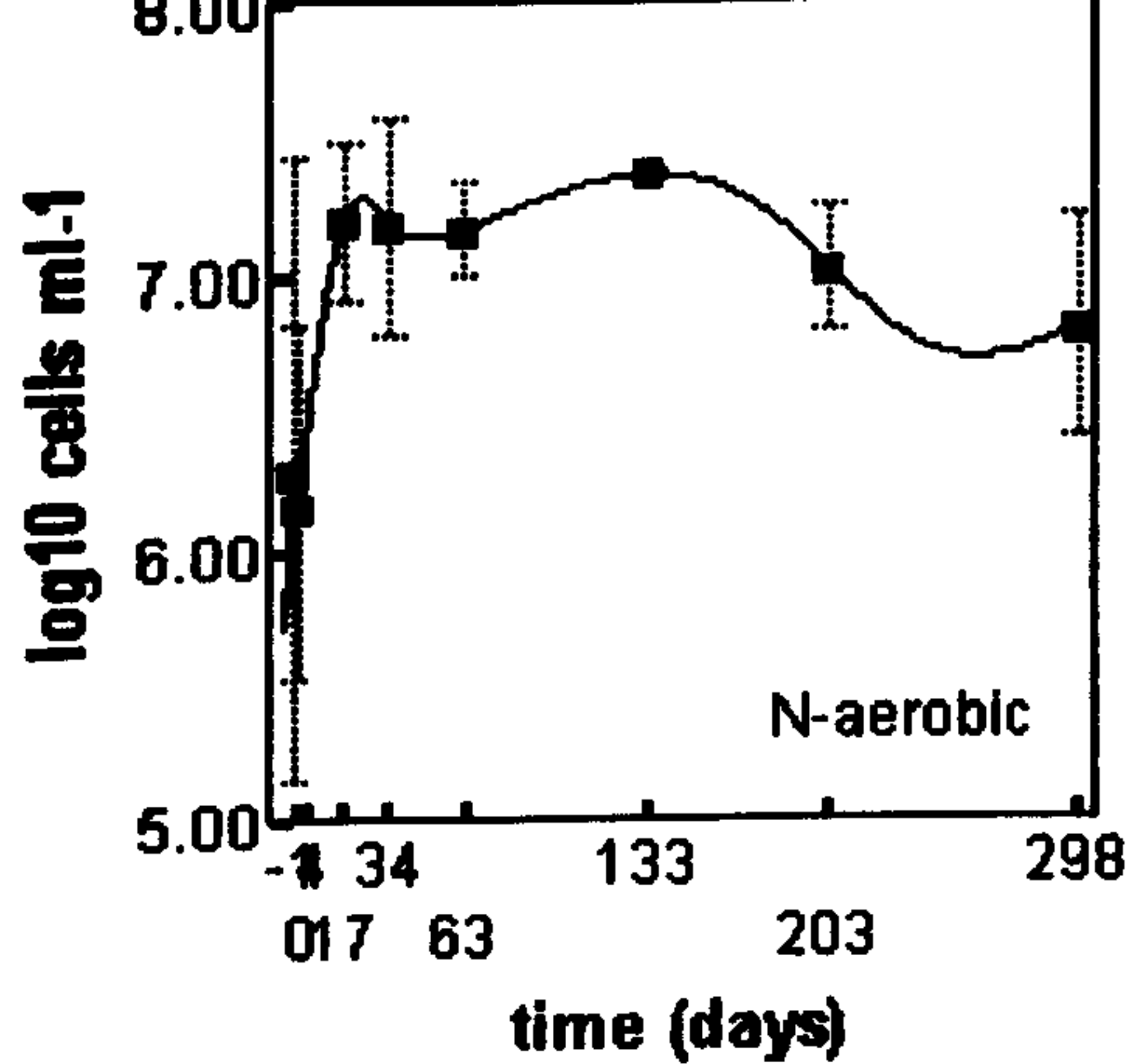




**Figure 6.10. (previous page).** Growth curves of the total numbers of bacteria in meltwaters incubated at +1.6- +2.6 °C with rock flour, and frequency of dividing and divided cells (FDDC) over time. Subglacial meltwater taken from the Bødalsbreen glacier, and rock flour from Bødalsbreen, Norway and Finsterwalderbreen, Svalbard. Lines with symbols show the mean values and error bars show 95% confidence intervals for the means of the three replicates (n=3). (■) = Norwegian rock flour, aerobic system; (●) = Norwegian rock flour, anaerobic system; (□) = Svalbard rock flour, aerobic system; (○) = Svalbard rock flour, anaerobic system.

#### **6.2.7. Dissolved oxygen and pH in Bødalsbreen meltwater incubated with rock flours**

Dissolved oxygen concentrations in the meltwaters increased in all the vials at the very beginning of incubation (figures 6.11 and 6.13), because air trapped in the pores of the rock flour was released into the meltwater. Thus, also the alleged anaerobic vials with initial meltwater containing no dissolved oxygen and an N<sub>2</sub>-headspace, had some oxygen present. However, after two months incubation, microbial activity at +0.2 - +2.6 °C had consumed most of the oxygen dissolved. In the aerobic abiotic controls, incubated with Norwegian rock flour, dissolved oxygen concentration remained around 0.30 - 0.40 mmol l<sup>-1</sup>, whereas in the biotic systems it dropped to < 0.10 mmol l<sup>-1</sup> (figure 6.11). In the anaerobic biotic test vials incubated at +0.2 to +2.6 °C, dissolved oxygen concentration remained continually below 0.10 mmol l<sup>-1</sup>. Statistical tests (appendix 11) showed that presence of micro-organisms had an effect on dissolved oxygen concentration (F-value 86.71, p< 0.05, partial r<sup>2</sup>-value 0.77). Statistical tests were run with the data gathered at incubation time of 203 days. This incubation time of 6-7 months represented time equivalent to winter period inbetween melt seasons in glaciated areas, and simulated slow reactions occurring in subglacial isolated cavities.

The rock flour from Svalbard was much more chemically reactive, resulting in rapid consumption of some of dissolved oxygen even in abiotic controls (figure 6.13). So much so, that temperature was more important factor than



presence of viable microbes (partial  $r^2$  values and observed power values 0.78 / 1.00 and 0.001 / 0.05, respectively, appendix 11) affecting dissolved oxygen concentration in meltwater.

Due to the differences in the elemental composition of the rock flours (tables 6.4 and 6.5), the initial pH in meltwater was much higher when incubated with Norwegian rock flour (mean pH in aerobic system 9.75), compared to Svalbard rock flour (mean pH 8.41). However, equilibrium was achieved after four months incubation at all the incubation temperatures, and from then on pH remained at a value of 7.5 in all the systems (figures 6.12 and 6.14).



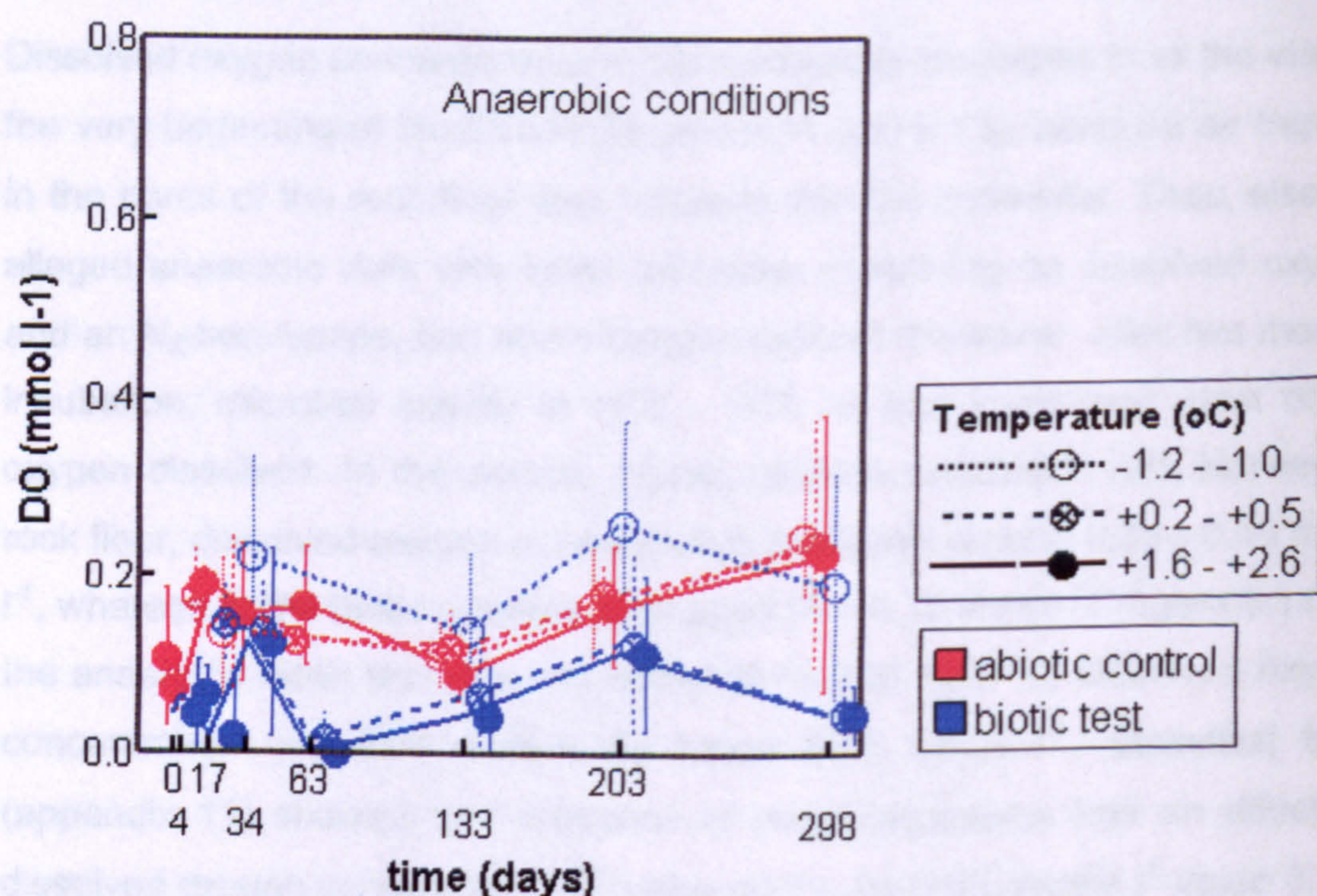
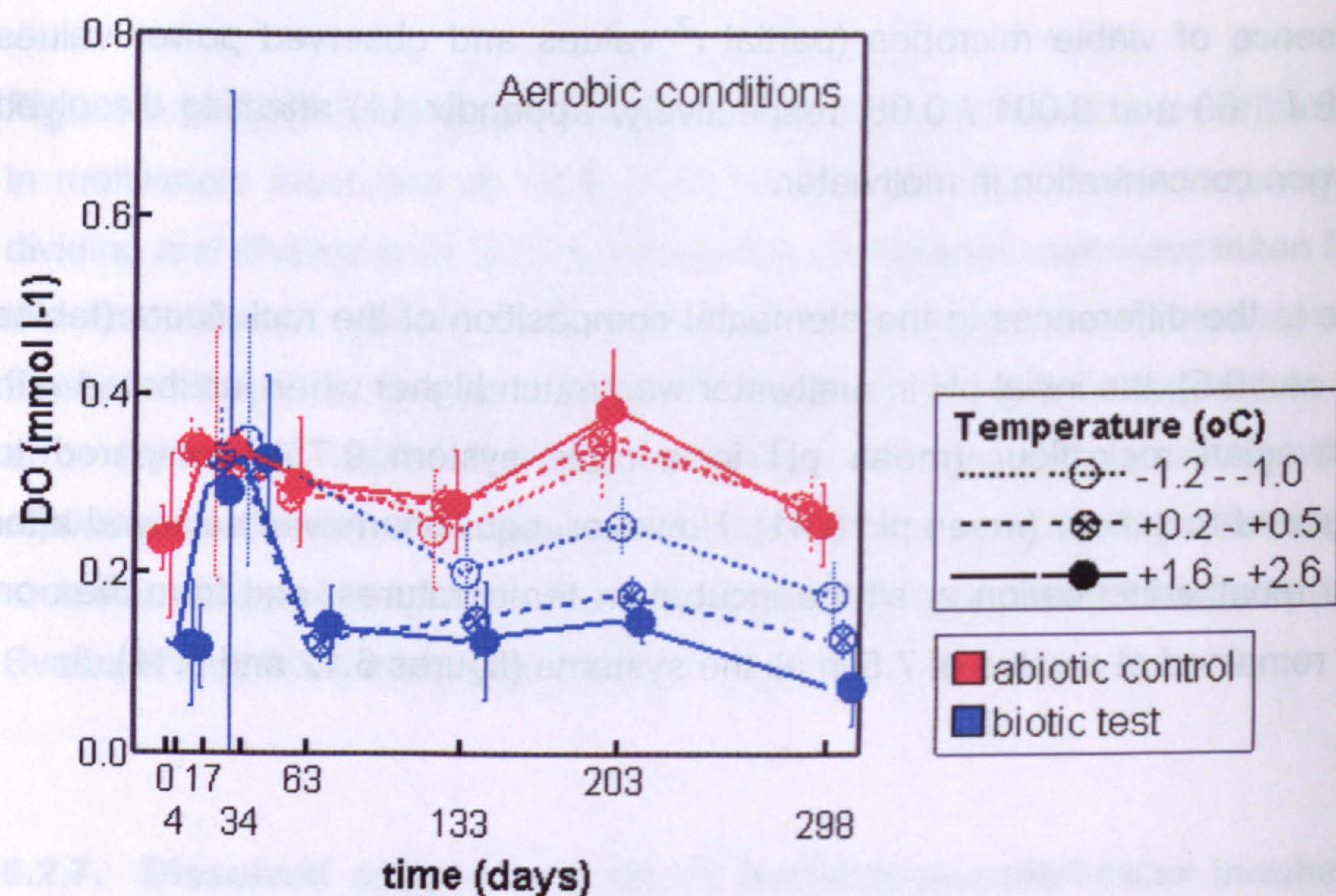


**Figure 6.11.** Dissolved oxygen in Bødalsbreen meltwater incubated with rock flour from Bødalsbreen, Norway in aerobic and anaerobic conditions at a range of temperatures. Lines show the mean values and error bars show 95% confidence intervals for the means of the three replicates ( $n=3$ ). (●) = biotic test at +1.6 - +2.6 °C; (⊗) = biotic test at +0.2 - +0.5 °C; (○) = biotic test at -1.2 - -1.0 °C; (●) = abiotic control at +1.6 - +2.6 °C; (⊗) = abiotic control at +0.2 - +0.5 °C; (○) = abiotic control at -1.2 - -1.0 °C.



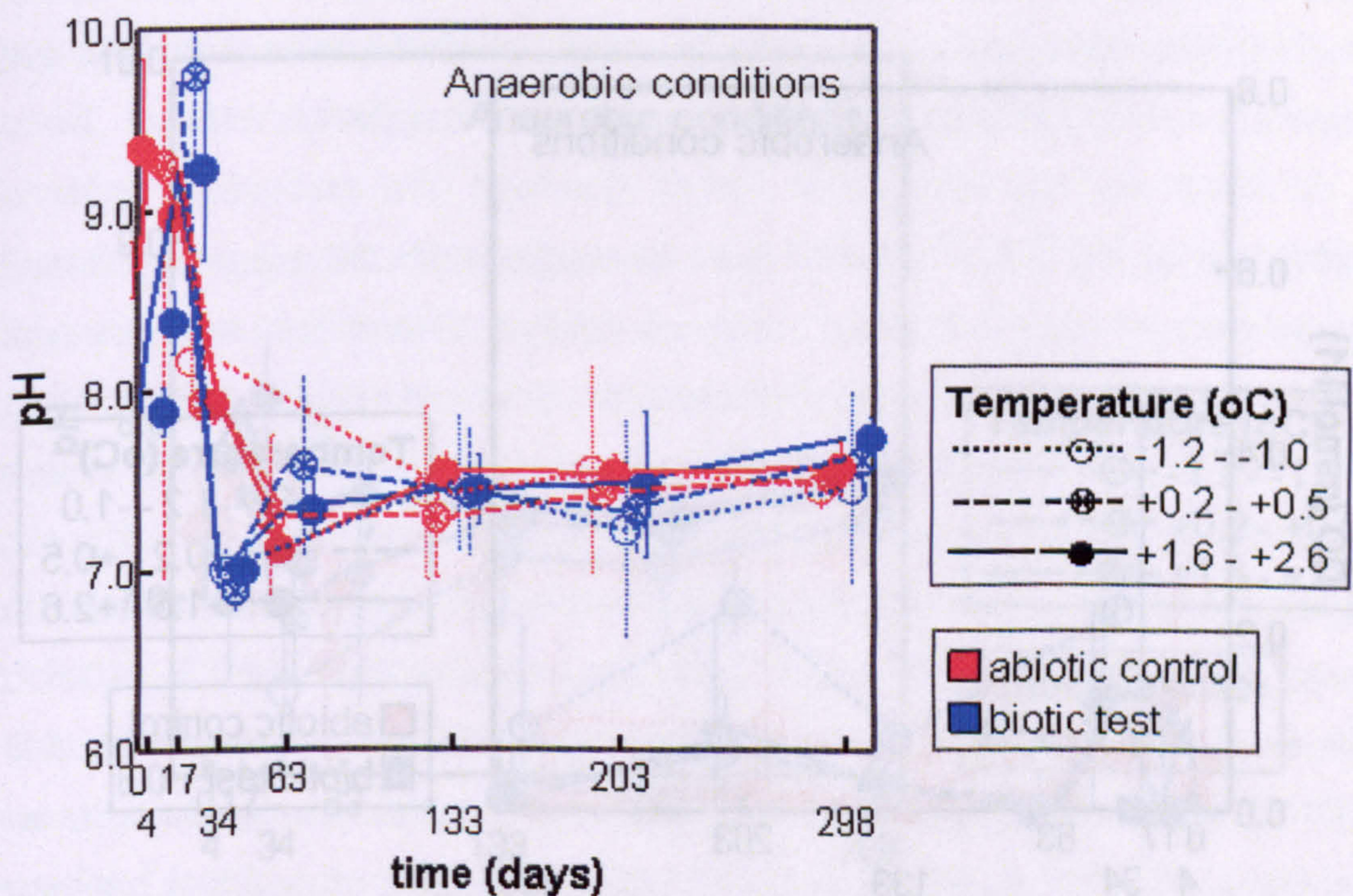
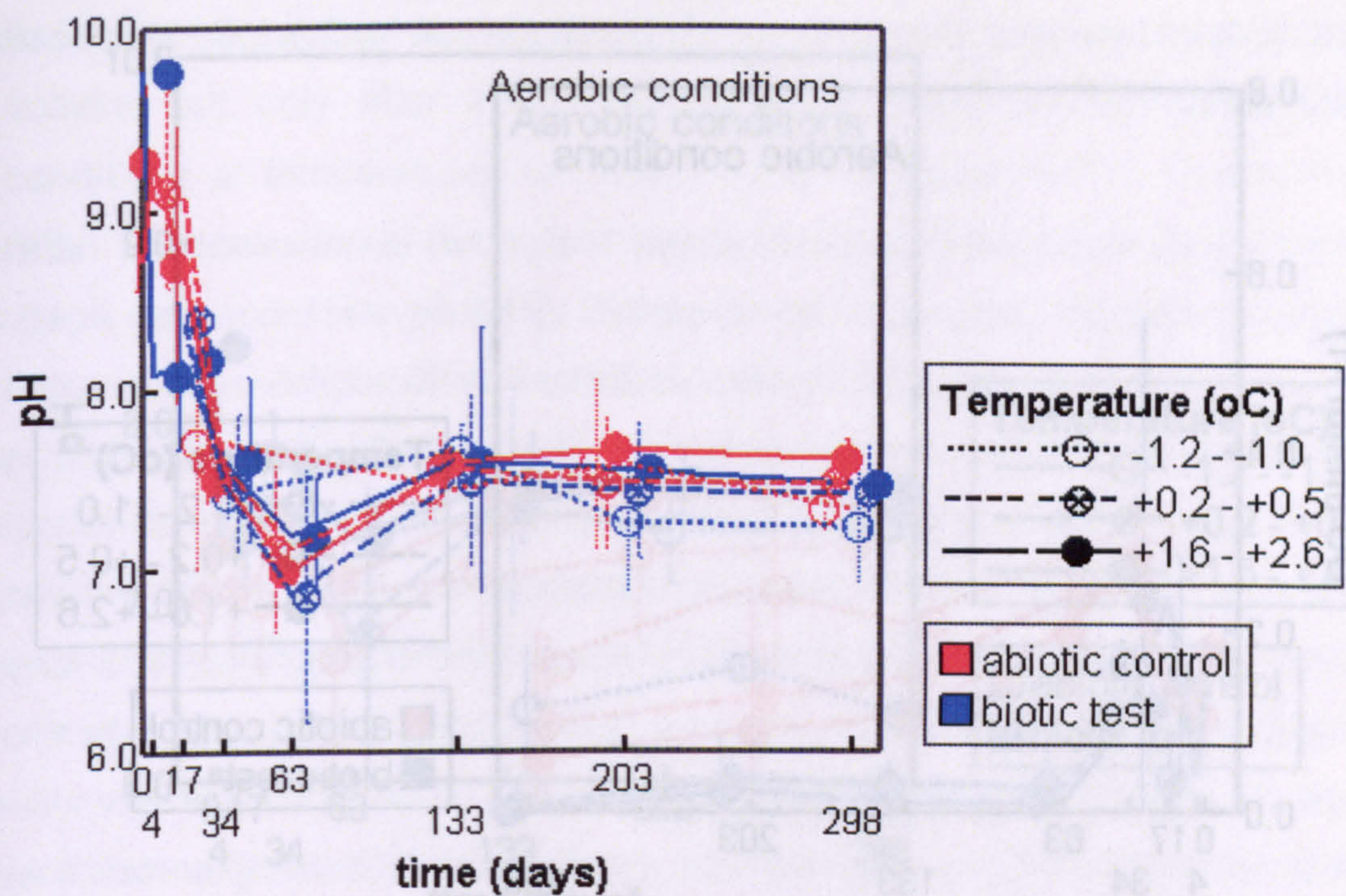


**Figure 6.12.** pH in Bødalsbreen meltwater incubated with rock flour from Bødalsbreen, Norway in aerobic and anaerobic conditions at a range of temperatures. Lines show the mean values and error bars show 95% confidence intervals for the means of the three replicates ( $n=3$ ). (●) = biotic test at +1.6 - +2.6 °C; (⊗) = biotic test at +0.2 - +0.5 °C; (○) = biotic test at -1.2 - -1.0 °C; (●) = abiotic control at +1.6 - +2.6 °C; (⊗) = abiotic control at +0.2 - +0.5 °C; (○) = abiotic control at -1.2 - -1.0 °C.



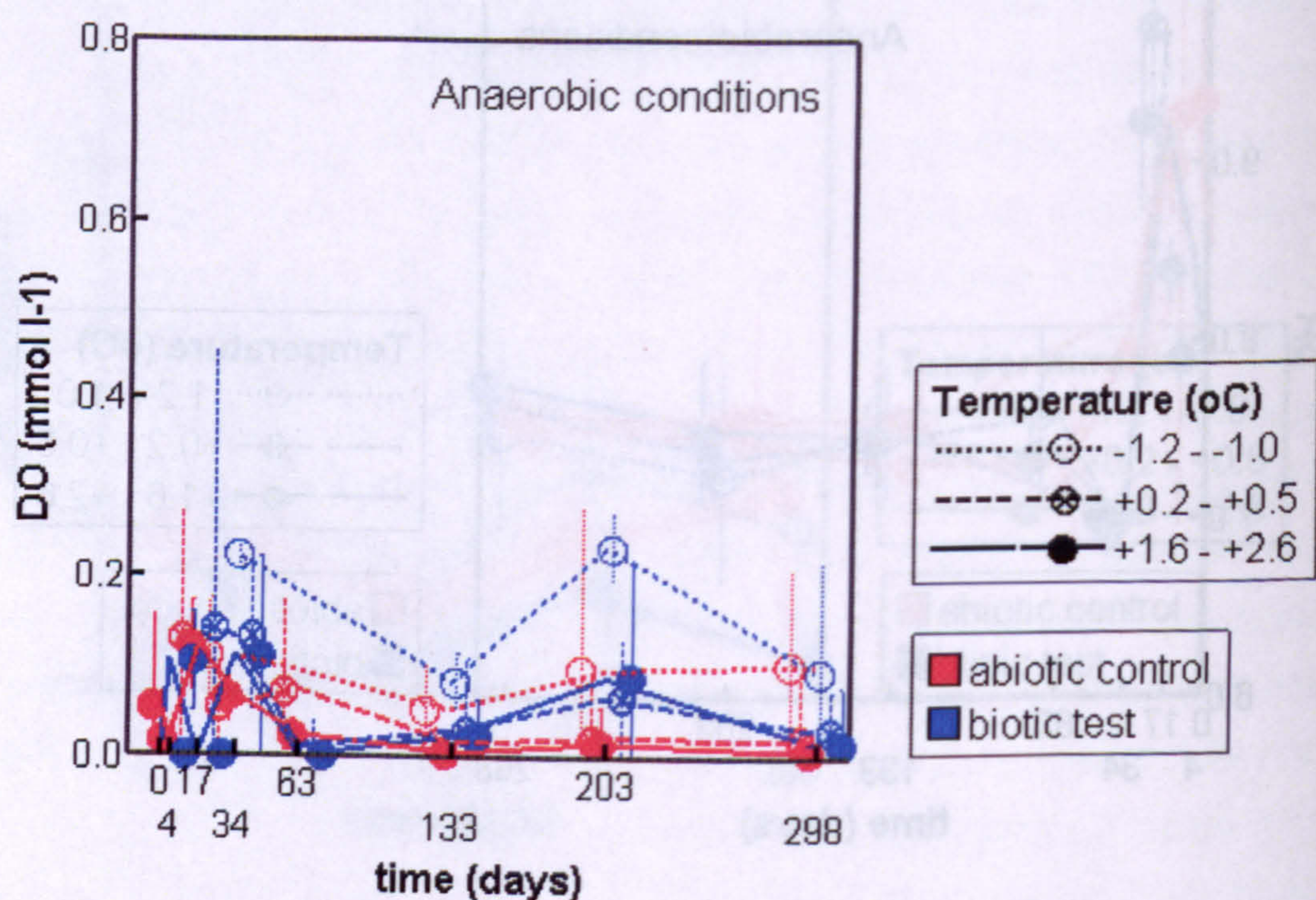
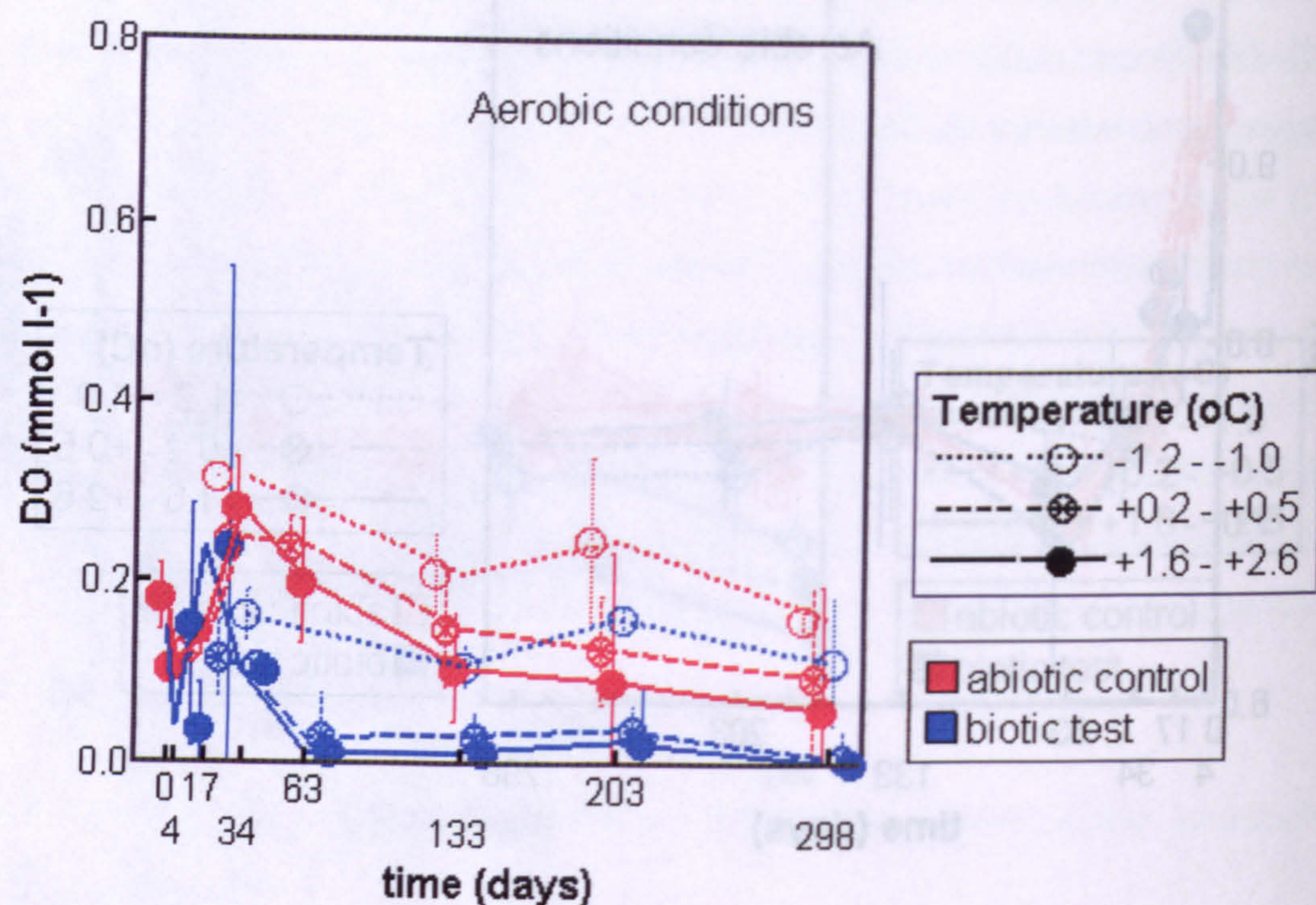


**Figure 6.13.** Dissolved oxygen Bødalsbreen meltwater incubated with rock flour from Finsterwalderbreen, Svalbard in aerobic and anaerobic conditions at a range of temperatures. Lines show the mean values and error bars show 95% confidence intervals for the means of the three replicates ( $n=3$ ). (●) = biotic test at +1.6 - +2.6 °C; (⊗) = biotic test at +0.2 - +0.5 °C; (○) = biotic test at -1.2 - -1.0 °C; (●) = abiotic control at +1.6 - +2.6 °C; (⊗) = abiotic control at +0.2 - +0.5 °C; (○) = abiotic control at -1.2 - -1.0 °C.



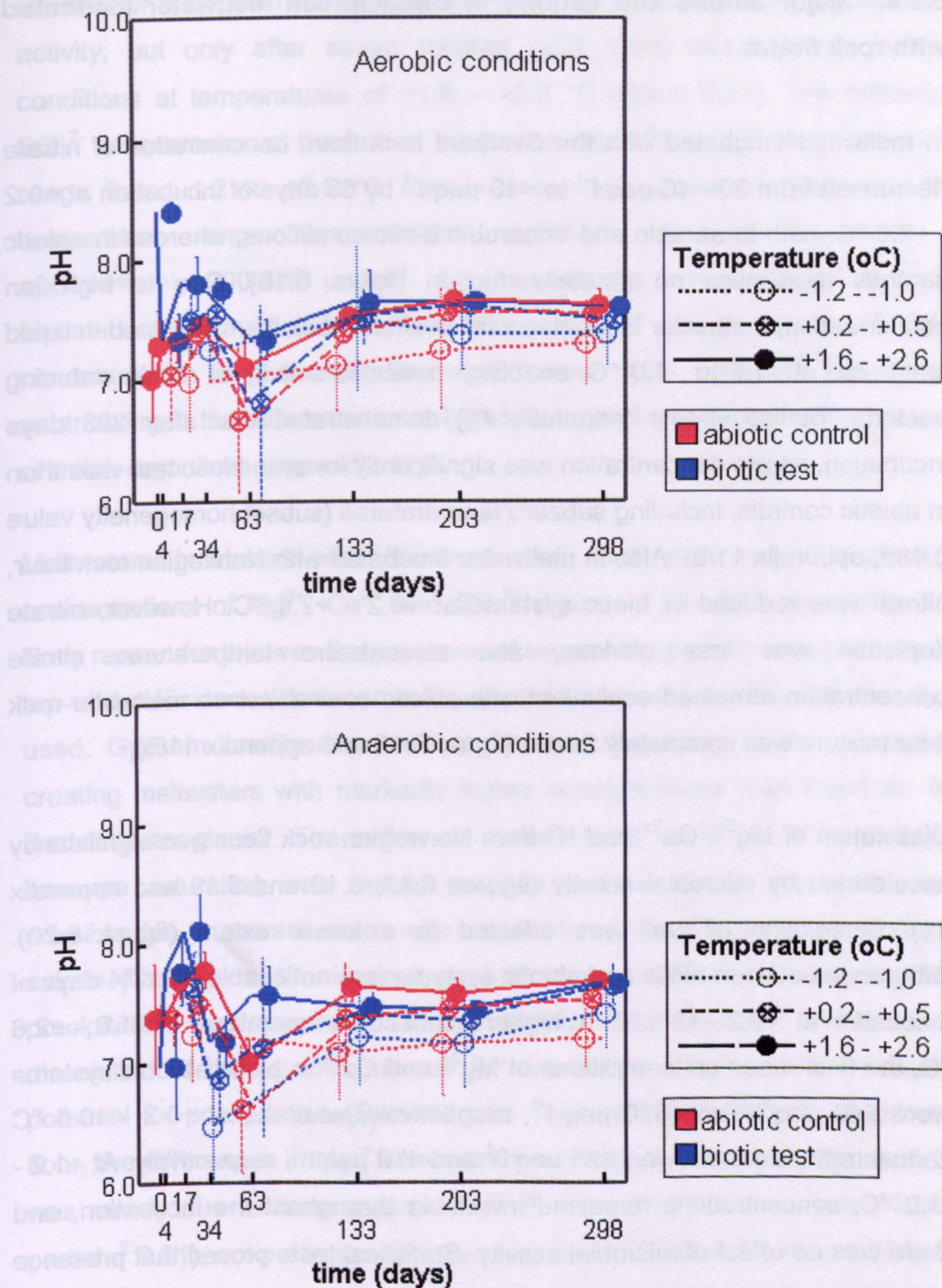


**Figure 6.14.** pH in Bødalsbreen meltwater incubated with rock flour from Finsterwalderbreen, Svalbard in aerobic and anaerobic conditions at a range of temperatures. Lines show the mean values and error bars show 95% confidence intervals for the means of the three replicates ( $n=3$ ). (●) = biotic test at +1.6 - +2.6 °C; (⊗) = biotic test at +0.2 - +0.5 °C; (○) = biotic test at -1.2 - -1.0 °C; (●) = abiotic control at +1.6 - +2.6 °C; (⊗) = abiotic control at +0.2 - +0.5 °C; (○) = abiotic control at -1.2 - -1.0 °C.



#### **6.2.8. Major anions and cations in Bødalsbreen meltwater incubated with rock flours**

In meltwater incubated with the Svalbard rock flour, concentration of nitrate decreased from 30 - 40  $\mu\text{eq l}^{-1}$  to  $<10 \mu\text{eq l}^{-1}$  by 63 days of incubation at +0.2 - +2.6 °C, both in aerobic and anaerobic biotic conditions, whereas in abiotic controls there was no nitrate reduction (figure 6.16). Due to high ion concentration, meltwater incubated with Svalbard rock flour remained in liquid state also at -1.2 to -1.0 °C, enabling metabolic activity of nitrate reducing bacteria. Statistical test (appendix 11) demonstrated that after 203 days incubation, nitrate concentration was significantly lower in biotic test vials than in abiotic controls, including subzero temperatures (subset homogeneity value 0.985, appendix 11/8). Also in meltwater incubated with Norwegian rock flour, nitrate was reduced in biotic systems at +0.2 - +2.6 °C. However, nitrate depletion was less obvious, and at subzero temperatures nitrate concentration remained equivalent with abiotic controls, since meltwater-rock flour mixture was completely frozen (figure 6.15 and appendix 11/5).

Dissolution of  $\text{Mg}^{2+}$ ,  $\text{Ca}^{2+}$  and  $\text{K}^{+}$  from Norwegian rock flour was significantly accelerated by microbial activity (figures 6.17, 6.18 and 6.19 and appendix 11). Dissolution of  $\text{Na}^{+}$  was affected to a lesser extent (figure 6.20). Difference between biotic and abiotic systems was noticeable after 34 days of incubation at +0.2 - +2.6 °C. At higher incubation temperatures of +1.6 – +2.6 °C, the final mean concentrations of  $\text{Mg}^{2+}$  and  $\text{Ca}^{2+}$  in biotic aerobic systems were 340  $\mu\text{eq l}^{-1}$  and 670  $\mu\text{eq l}^{-1}$ , respectively, whereas at +0.2 - +0.5 °C concentrations were lower, 225  $\mu\text{eq l}^{-1}$  and 470  $\mu\text{eq l}^{-1}$ , respectively. At -1.2 - -1.0 °C, concentrations remained invariable throughout the incubation, and there was no effect of microbial activity. Statistical tests proved that presence of viable micro-organisms and temperature had significant effect on concentrations of  $\text{Mg}^{2+}$ ,  $\text{Ca}^{2+}$  and  $\text{K}^{+}$ , and dissolution was comparable in aerobic and anaerobic conditions (appendix 11).  $\text{Na}^{+}$  concentration in anaerobic biotic system at +0.2 - +2.6 °C was significantly higher than in abiotic controls, and elevated concentration could be explained with interactions of higher temperature, microbial activity and anaerobic environment (appendix 11, partial  $r^2$  values 0.94, 0.83 and 0.54, respectively).



Release of  $\text{SO}_4^{2-}$  from Norwegian rock flour was also accelerated by microbial activity, but only after seven months (203 days) incubation in aerobic conditions at temperatures of  $+1.6 - +2.6$  °C (figure 6.21). The maximum  $\text{SO}_4^{2-}$  concentration at the end of incubation was  $670 \mu\text{eq l}^{-1}$ . At temperature range from  $-1.2$  to  $+0.5$  °C and in anaerobic conditions throughout the temperature range, concentration of  $\text{SO}_4^{2-}$  remained constantly of approximately  $200\text{-}300 \mu\text{eq l}^{-1}$ . Again, statistical test confirmed that the elevated concentration of  $\text{SO}_4^{2-}$  at  $+1.6 - +2.6$  °C differed significantly from concentrations in the other test and control vials, and that the factors contributing in the difference were higher temperature together with presence of micro-organisms (appendix 11).

Meltwaters incubated with Svalbard rock flour had exceptionally high concentrations of  $\text{Mg}^{2+}$ ,  $\text{Ca}^{2+}$  and  $\text{SO}_4^{2-}$  (figures 6.22, 6.23 and 6.26). The likely reason for this was the presence of secondary gypsum deposited on the top of the Finsterwalderbreen outwash plain and mixed within the rock flour used. Gypsum readily dissolved at the very beginning of the incubation, creating meltwaters with markedly higher concentrations than found at the Bødalsbreen glacier. Thereafter, no further trend could be seen, probably because saturation was rapidly reached and no further dissolution was possible due to oversaturation with respect to calcite. The saturation index of calcite ( $\text{CaCO}_3$ ) at the beginning of incubation was  $-0.08$ , showing that precipitation was possible.  $\text{SI} < 0$  indicates thermodynamic potential for dissolution of the specific mineral for dissolution, whereas  $\text{SI} > 0$  indicates potential for precipitation (Raiswell and Thomas 1984). With Svalbard rock flour, the differences in  $\text{Mg}^{2+}$  concentrations between subgroups (figure 6.22) was mainly due to temperature effect (F-value 54.40 and p-value  $< 0.005$ , partial  $r^2$  0.81), not presence of micro-organisms (F-value 12.79, p 0.001 and partial  $r^2$  0.33, appendix 11). After the initial release from freshly abraded fine mineral grains, concentrations of  $\text{Ca}^{2+}$  and  $\text{SO}_4^{2-}$  remained constant, and the presence of microbes in meltwater did not have an effect on concentrations (figures 6.23 and 6.26 and appendix 11). At time 203 days, variation of concentrations of  $\text{Ca}^{2+}$ ,  $\text{SO}_4^{2-}$ ,  $\text{K}^+$  and  $\text{Na}^+$  within subgroups was relatively wide, compared with differences between subgroups (appendix 11, F-value 9.38, 8.48, 7.59 and 1.26, respectively), and no obvious effect of interaction between temperature and microbial activity in concentrations was recorded.



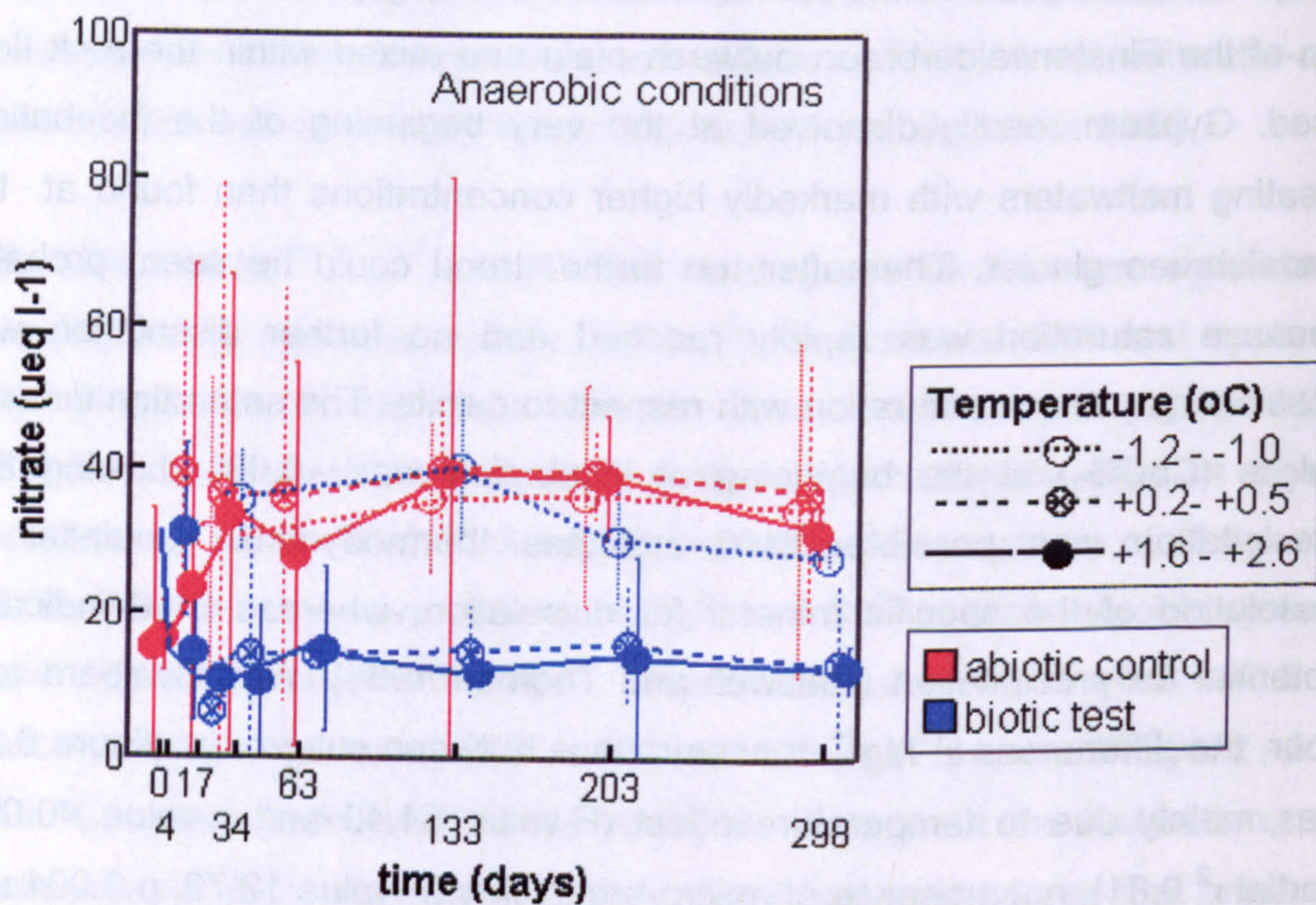
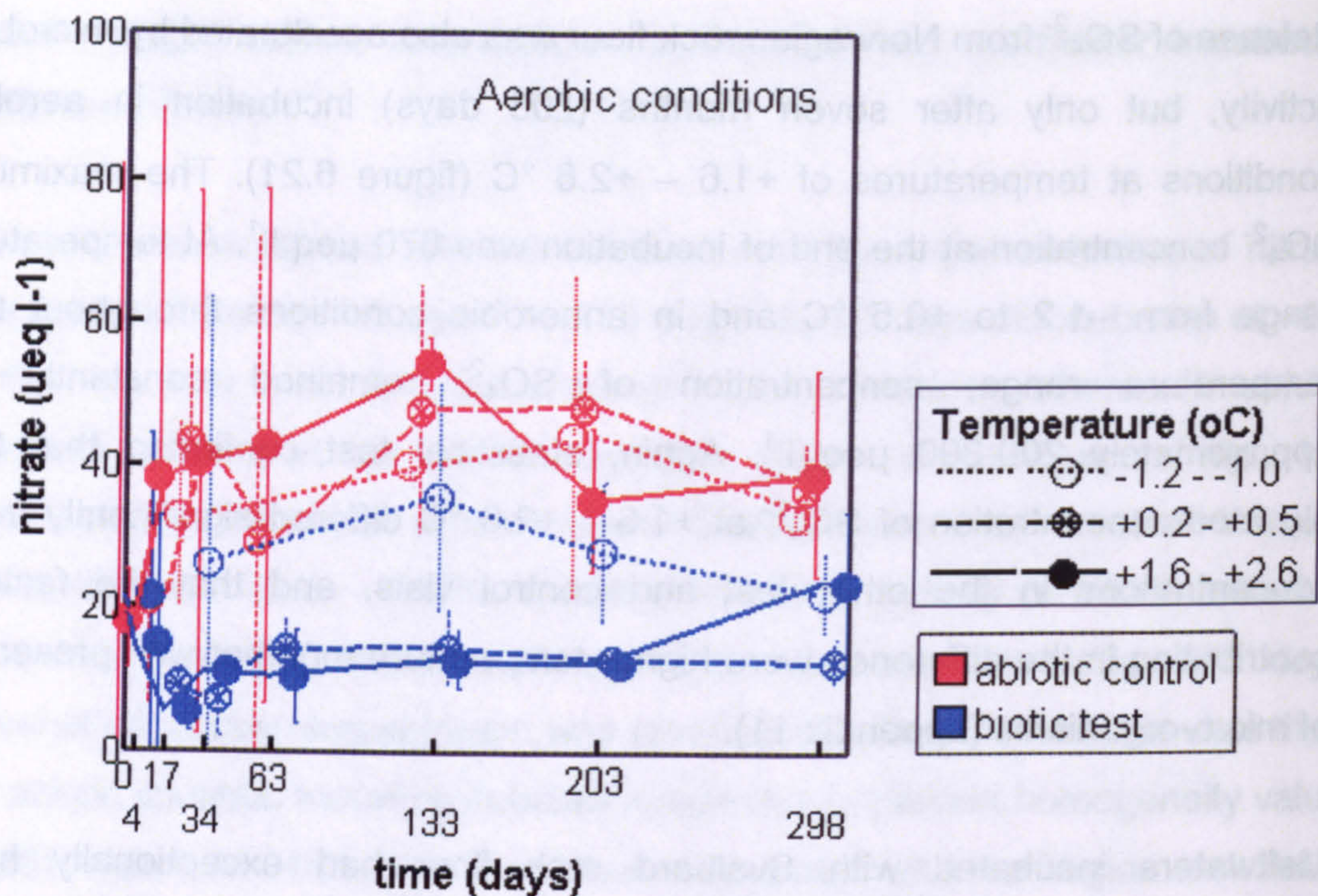


**Figure 6.15.** Nitrate concentrations in Bødalsbreen meltwater incubated with rock flour from Bødalsbreen, Norway in aerobic and anaerobic conditions at a range of temperatures. Lines show the mean values and error bars show 95% confidence intervals for the means of the three replicates ( $n=3$ ). (●) = biotic test at +1.6 - +2.6 °C; (⊗) = biotic test at +0.2 - +0.5 °C; (○) = biotic test at -1.2 - -1.0 °C; (●) = abiotic control at +1.6 - +2.6 °C; (⊗) = abiotic control at +0.2 - +0.5 °C; (○) = abiotic control at -1.2 - -1.0 °C.



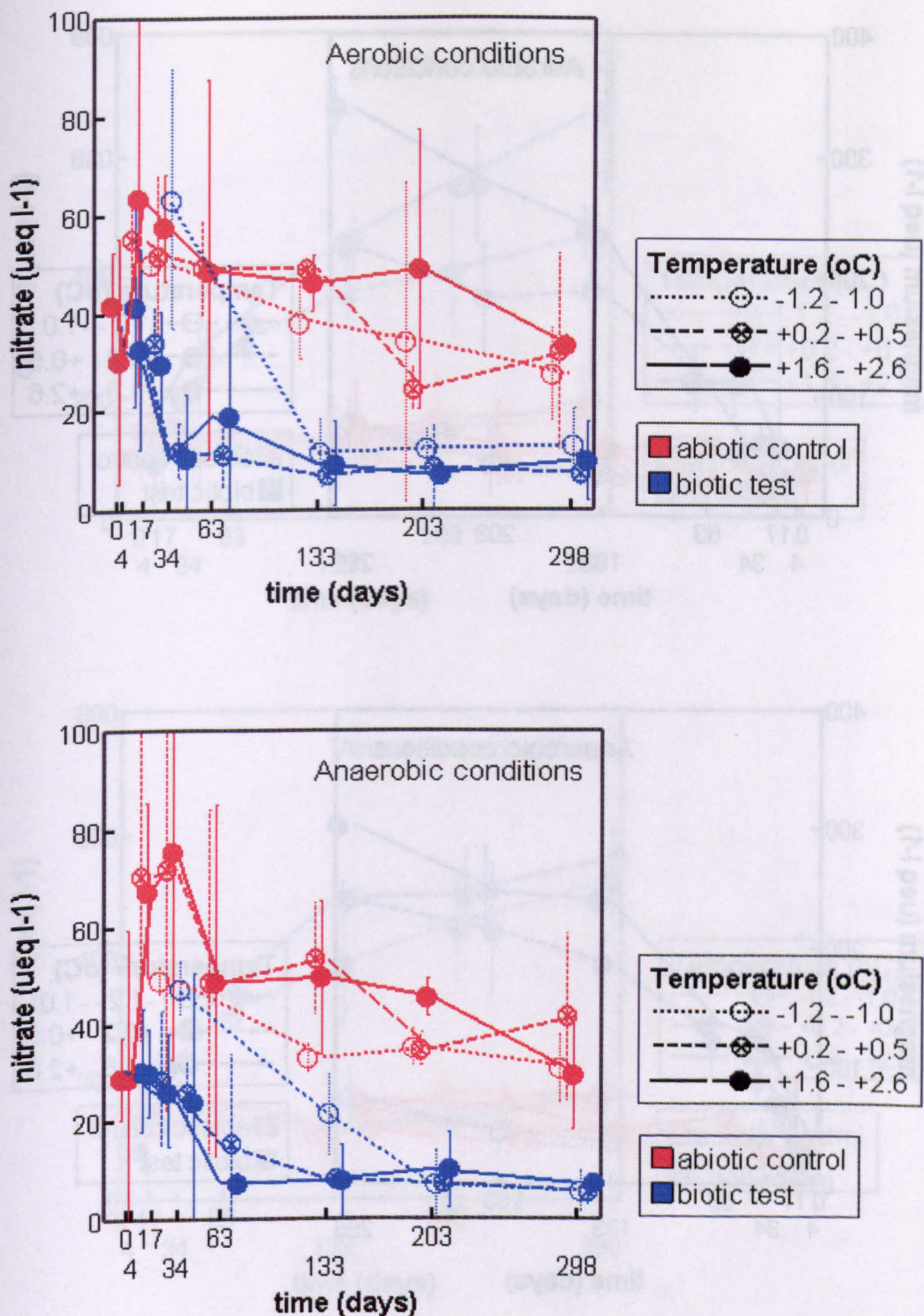


**Figure 6.16.** Nitrate concentrations in Bødalsbreen meltwater incubated with rock flour from Finsterwalderbreen, Svalbard in aerobic and anaerobic conditions at a range of temperatures. Lines show the mean values and error bars show 95% confidence intervals for the means of the three replicates ( $n=3$ ). ( $\bullet$ ) = biotic test at +1.6 - +2.6  $^{\circ}\text{C}$ ; ( $\otimes$ ) = biotic test at +0.2 - +0.5  $^{\circ}\text{C}$ ; ( $\circ$ ) = biotic test at -1.2 - -1.0  $^{\circ}\text{C}$ ; ( $\bullet$ ) = abiotic control at +1.6 - +2.6  $^{\circ}\text{C}$ ; ( $\otimes$ ) = abiotic control at +0.2 - +0.5  $^{\circ}\text{C}$ ; ( $\circ$ ) = abiotic control at -1.2 - -1.0  $^{\circ}\text{C}$ .



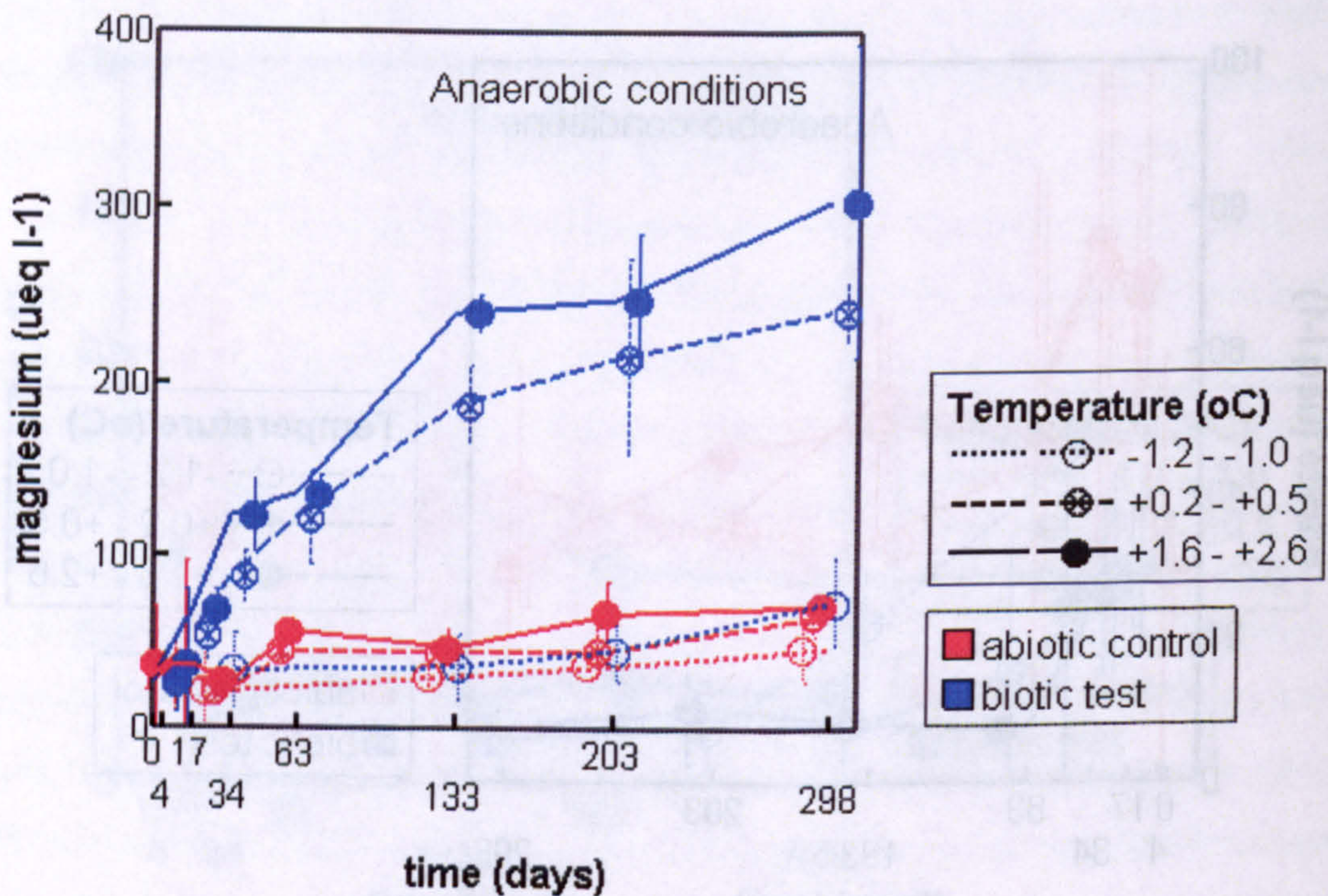
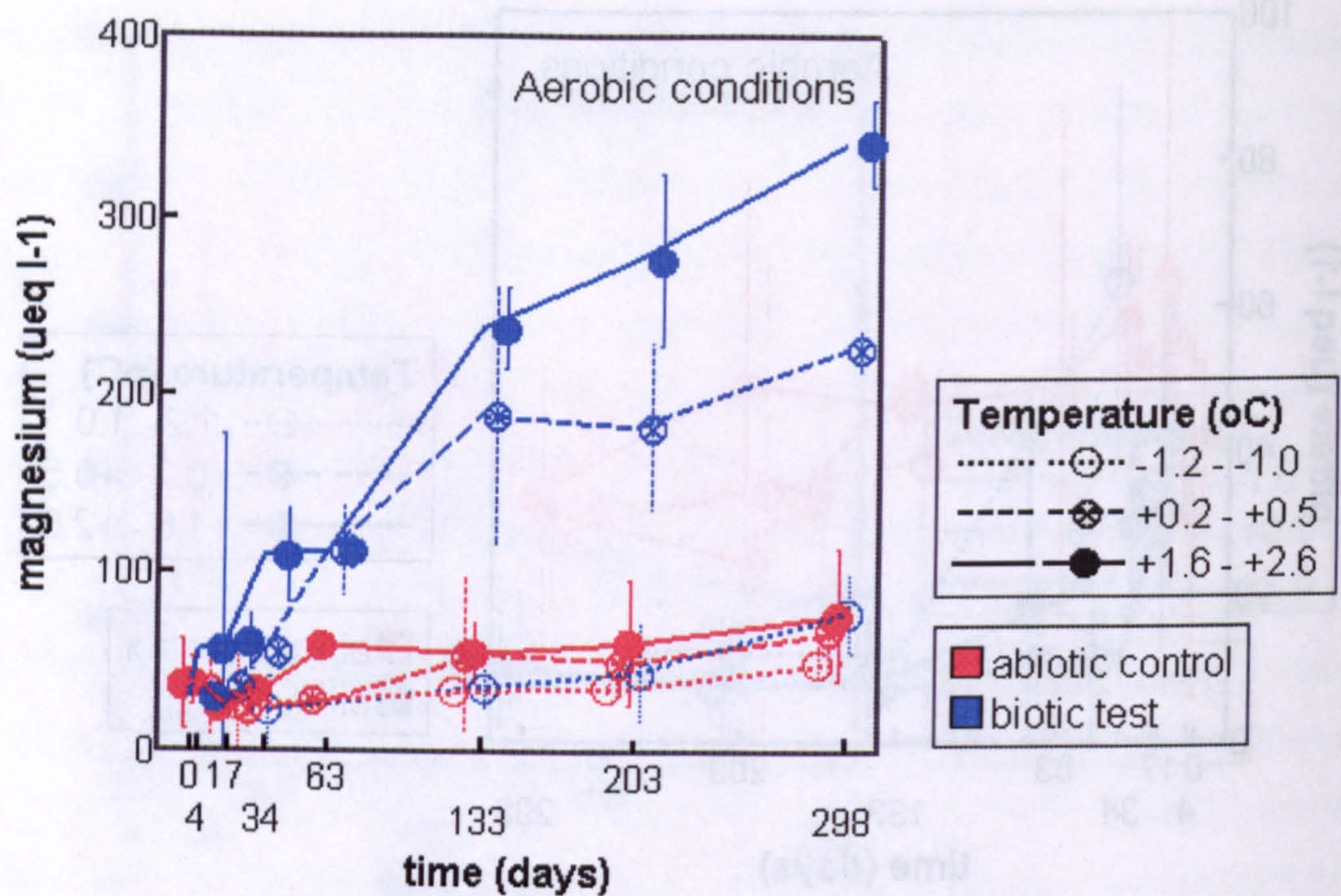


**Figure 6.17.** Magnesium concentrations in Bødalsbreen meltwater incubated with rock flour from Bødalsbreen, Norway in aerobic and anaerobic conditions at a range of temperatures. Lines show the mean values and error bars show 95% confidence intervals for the means of the three replicates ( $n=3$ ). (●) = biotic test at +1.6 - +2.6 °C; (⊗) = biotic test at +0.2 - +0.5 °C; (○) = biotic test at -1.2 - -1.0 °C; (●) = abiotic control at +1.6 - +2.6 °C; (⊗) = abiotic control at +0.2 - +0.5 °C; (○) = abiotic control at -1.2 - -1.0 °C.



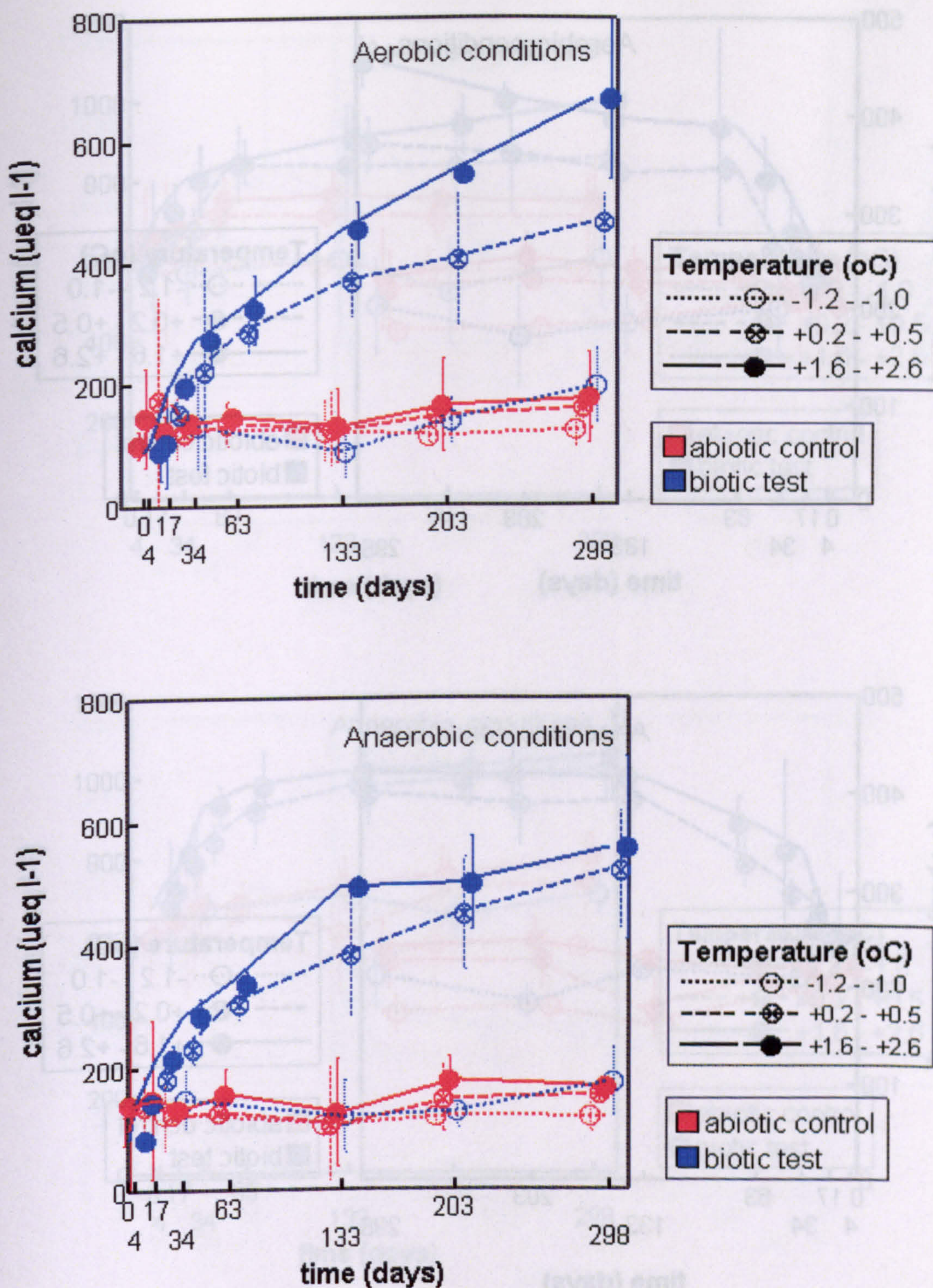


**Figure 6.18.** Calcium concentrations in Bødalsbreen meltwater incubated with rock flour from Bødalsbreen, Norway in aerobic and anaerobic conditions at a range of temperatures. Lines show the mean values and error bars show 95% confidence intervals for the means of the three replicates ( $n=3$ ). ( $\bullet$ ) = biotic test at +1.6 - +2.6  $^{\circ}\text{C}$ ; ( $\otimes$ ) = biotic test at +0.2 - +0.5  $^{\circ}\text{C}$ ; ( $\circ$ ) = biotic test at -1.2 - -1.0  $^{\circ}\text{C}$ ; ( $\bullet$ ) = abiotic control at +1.6 - +2.6  $^{\circ}\text{C}$ ; ( $\otimes$ ) = abiotic control at +0.2 - +0.5  $^{\circ}\text{C}$ ; ( $\circ$ ) = abiotic control at -1.2 - -1.0  $^{\circ}\text{C}$ .



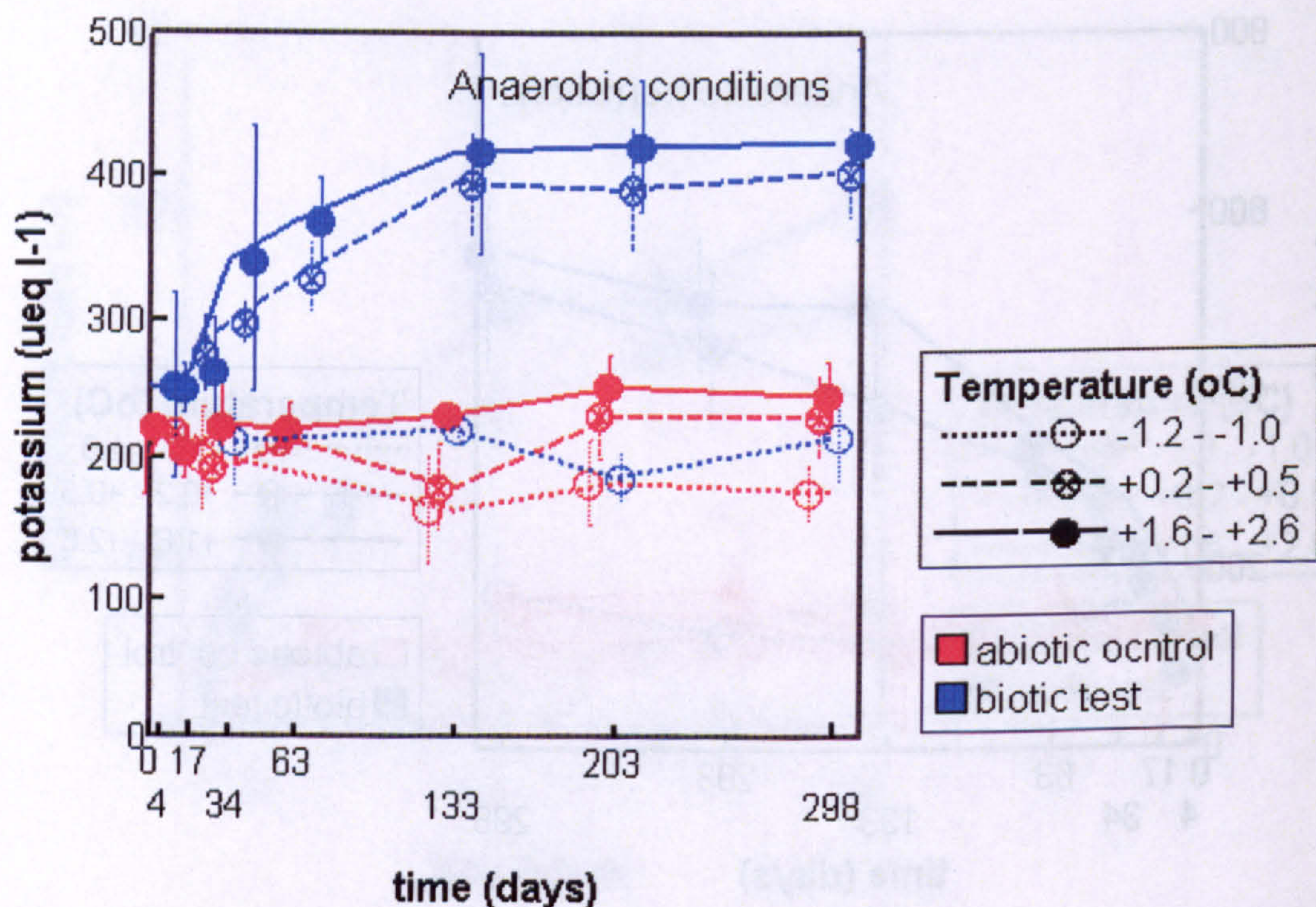
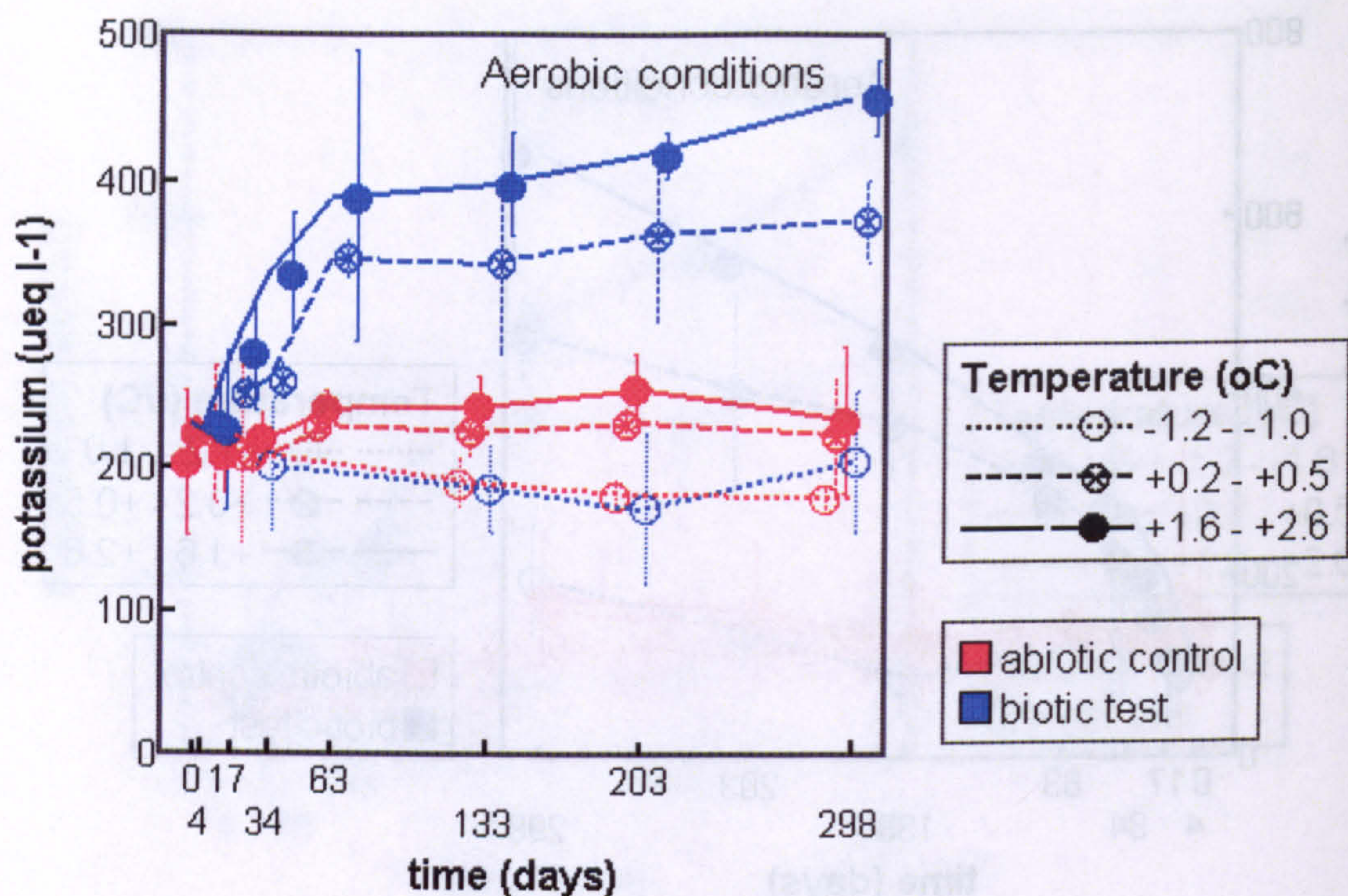


**Figure. 6.19.** Potassium concentrations in Bødalsbreen meltwater incubated with rock flour from Bødalsbreen, Norway in aerobic and anaerobic conditions at a range of temperatures. Lines show the mean values and error bars show 95% confidence intervals for the means of the three replicates ( $n=3$ ). (●) = biotic test at +1.6 - +2.6 °C; (⊗) = biotic test at +0.2 - +0.5 °C; (○) = biotic test at -1.2 - -1.0 °C; (●) = abiotic control at +1.6 - +2.6 °C; (⊗) = abiotic control at +0.2 - +0.5 °C; (○) = abiotic control at -1.2 - -1.0 °C.



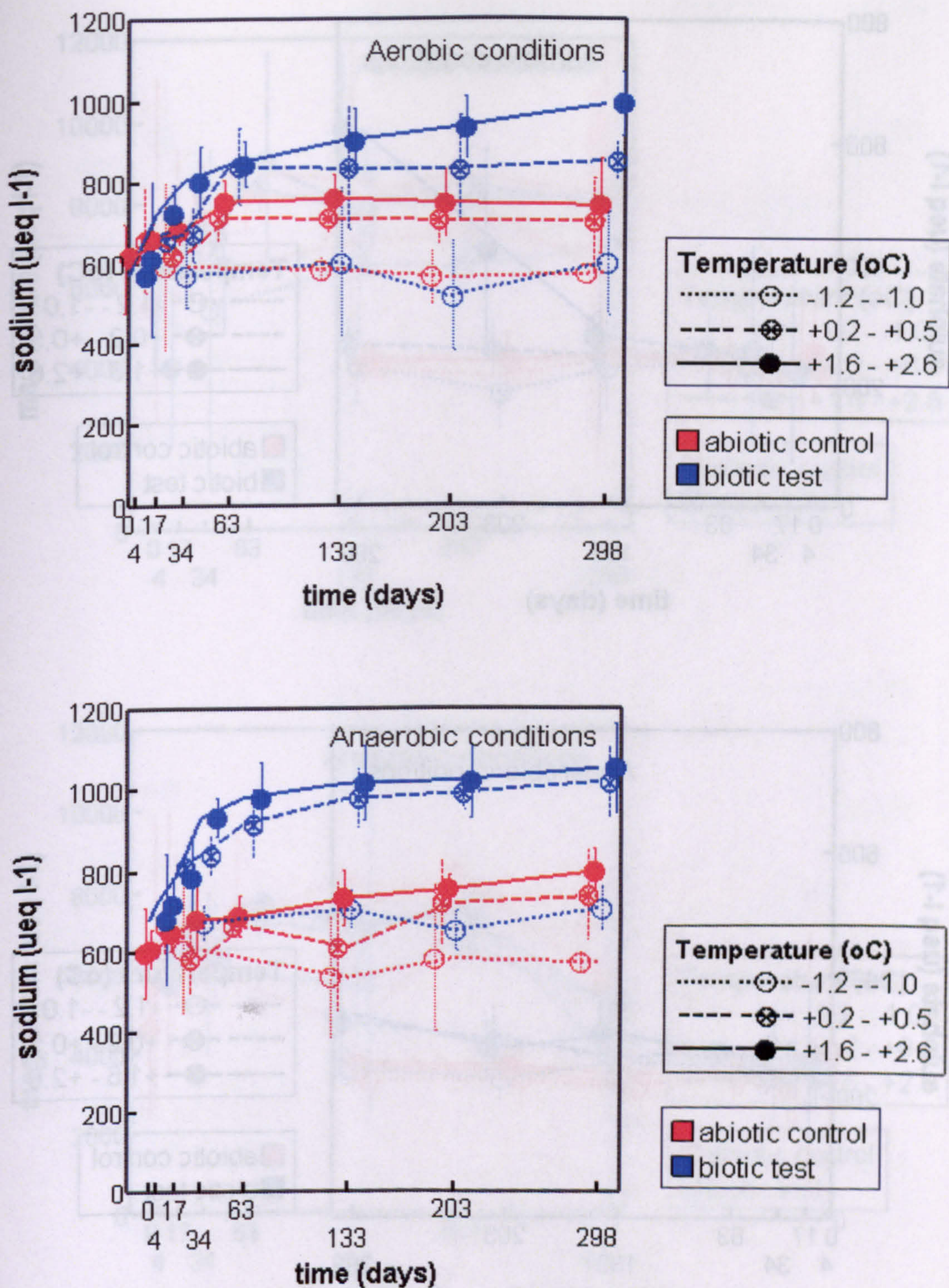


**Figure 6.20.** Sodium concentrations in Bødalsbreen meltwater incubated with rock flour from Bødalsbreen, Norway in aerobic and anaerobic conditions at a range of temperatures. Lines show the mean values and error bars show 95% confidence intervals for the means of the three replicates ( $n=3$ ). (●) = biotic test at +1.6 - +2.6 °C; (⊗) = biotic test at +0.2 - +0.5 °C; (○) = biotic test at -1.2 - -1.0 °C; (●) = abiotic control at +1.6 - +2.6 °C; (⊗) = abiotic control at +0.2 - +0.5 °C; (○) = abiotic control at -1.2 - -1.0 °C.



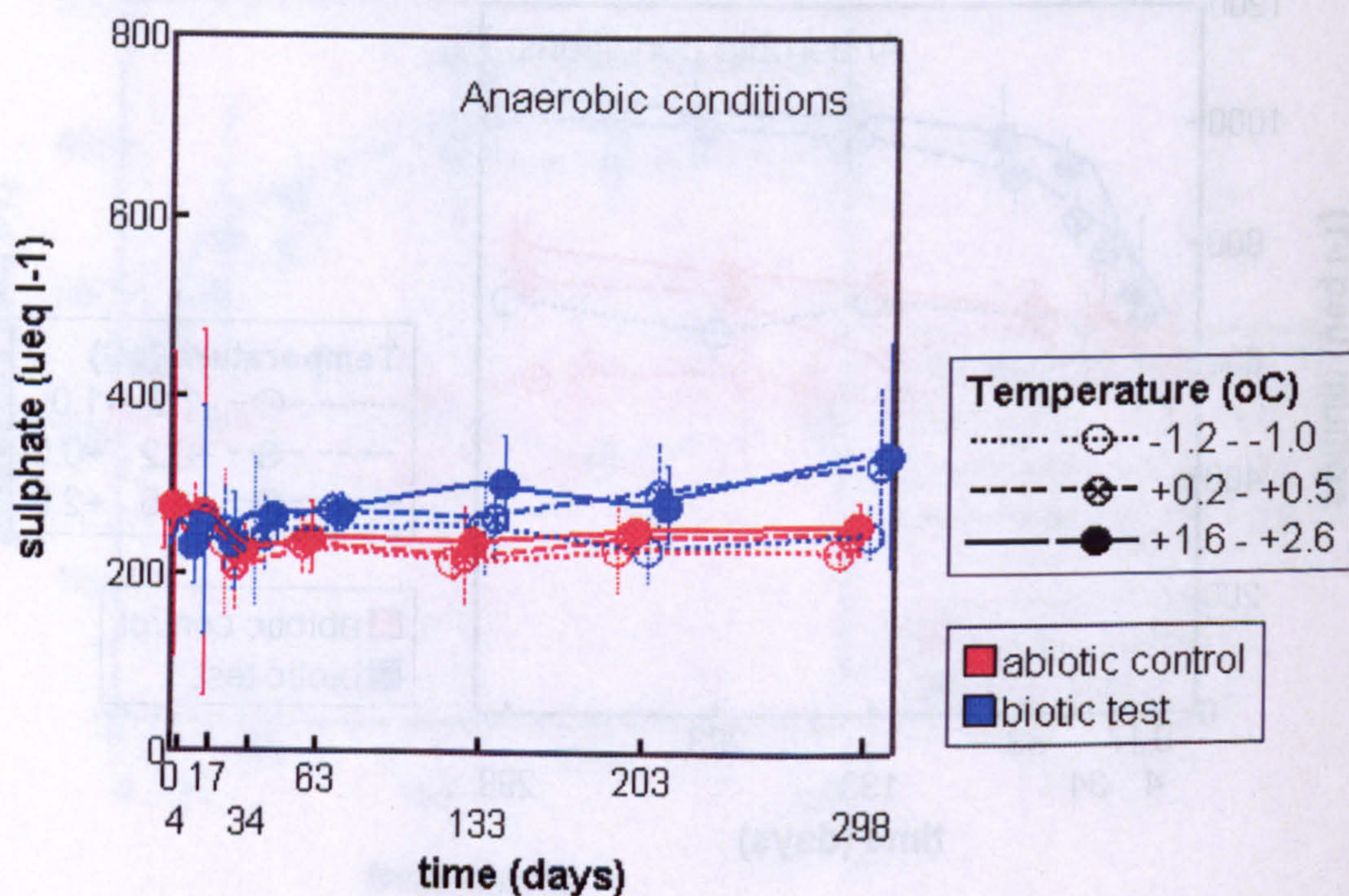
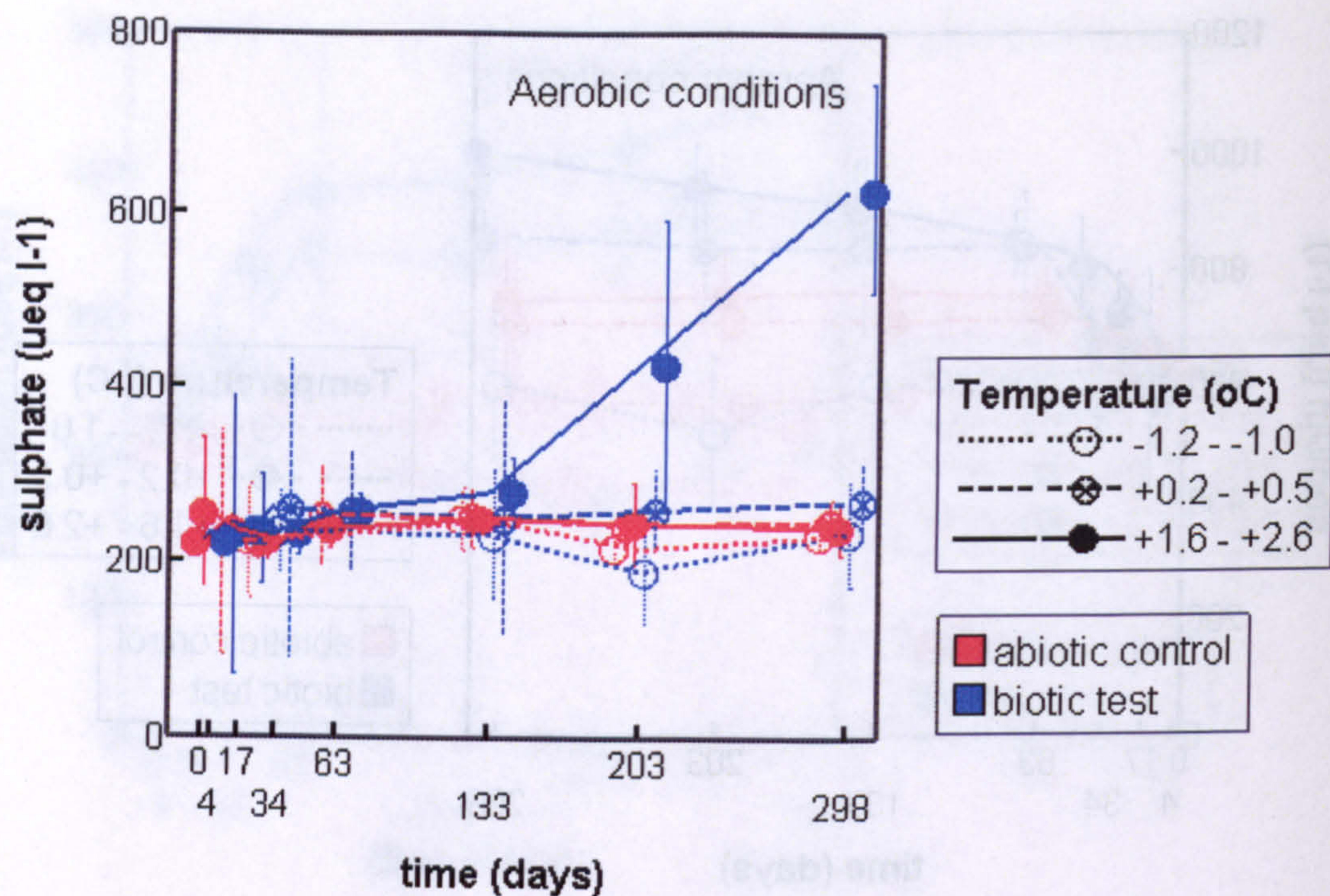


**Figure 6.21.** Sulphate concentrations in Bødalsbreen meltwater incubated with rock flour from Bødalsbreen, Norway in aerobic and anaerobic conditions at a range of temperatures. Lines show the mean values and error bars show 95% confidence intervals for the means of the three replicates ( $n=3$ ). (●) = biotic test at +1.6 - +2.6 °C; (⊗) = biotic test at +0.2 - +0.5 °C; (○) = biotic test at -1.2 - -1.0 °C; (●) = abiotic control at +1.6 - +2.6 °C; (⊗) = abiotic control at +0.2 - +0.5 °C; (○) = abiotic control at -1.2 - -1.0 °C.



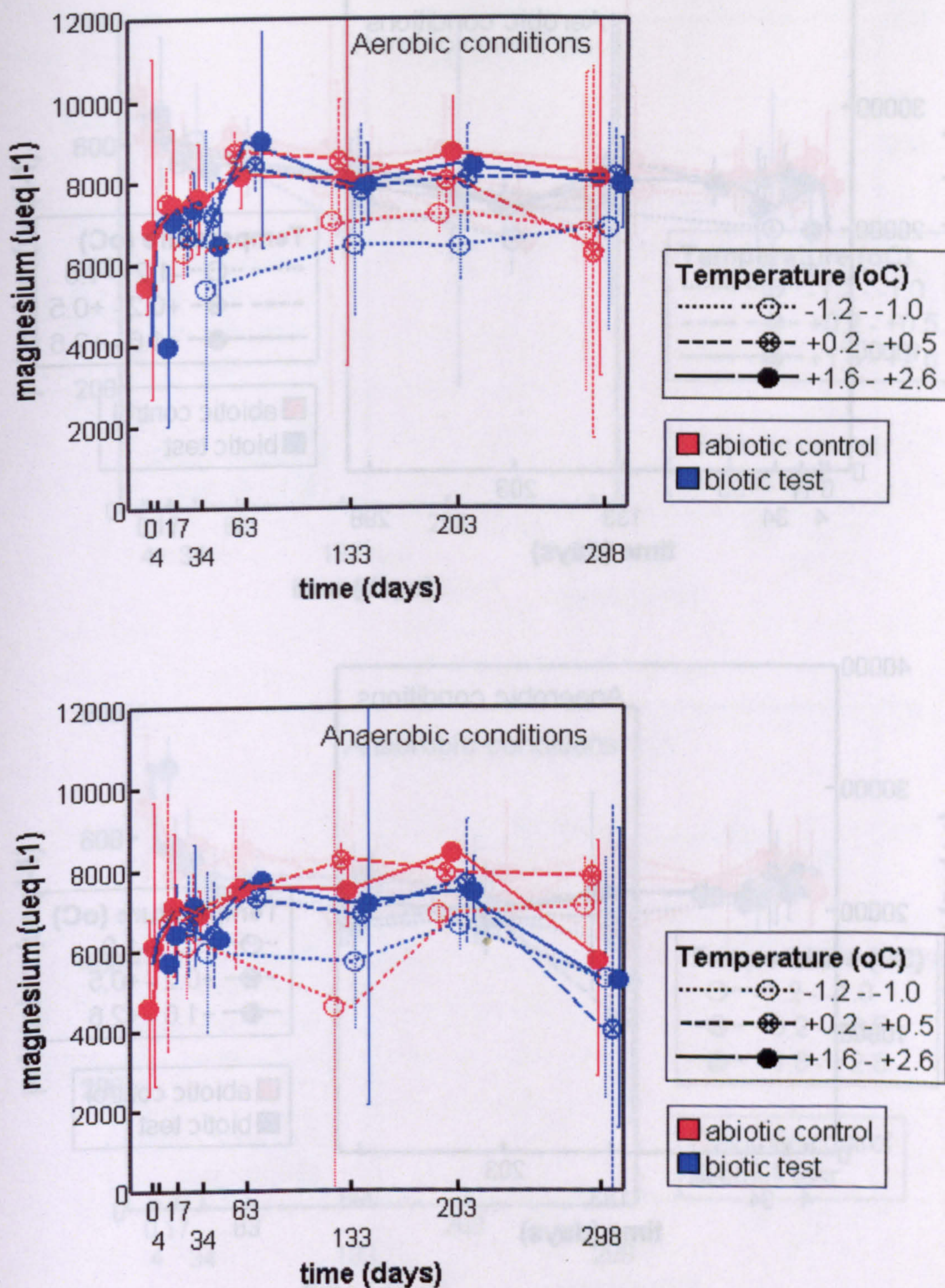


**Figure 6.22.** Magnesium concentrations in Bødalsbreen meltwater incubated with rock flour from Finsterwalderbreen, Svalbard in aerobic and anaerobic conditions at a range of temperatures. Lines show the mean values and error bars show 95% confidence intervals for the means of the three replicates ( $n=3$ ). (●) = biotic test at +1.6 - +2.6 °C; (⊗) = biotic test at +0.2 - +0.5 °C; (○) = biotic test at -1.2 - -1.0 °C; (●) = abiotic control at +1.6 - +2.6 °C; (⊗) = abiotic control at +0.2 - +0.5 °C; (○) = abiotic control at -1.2 - -1.0 °C.



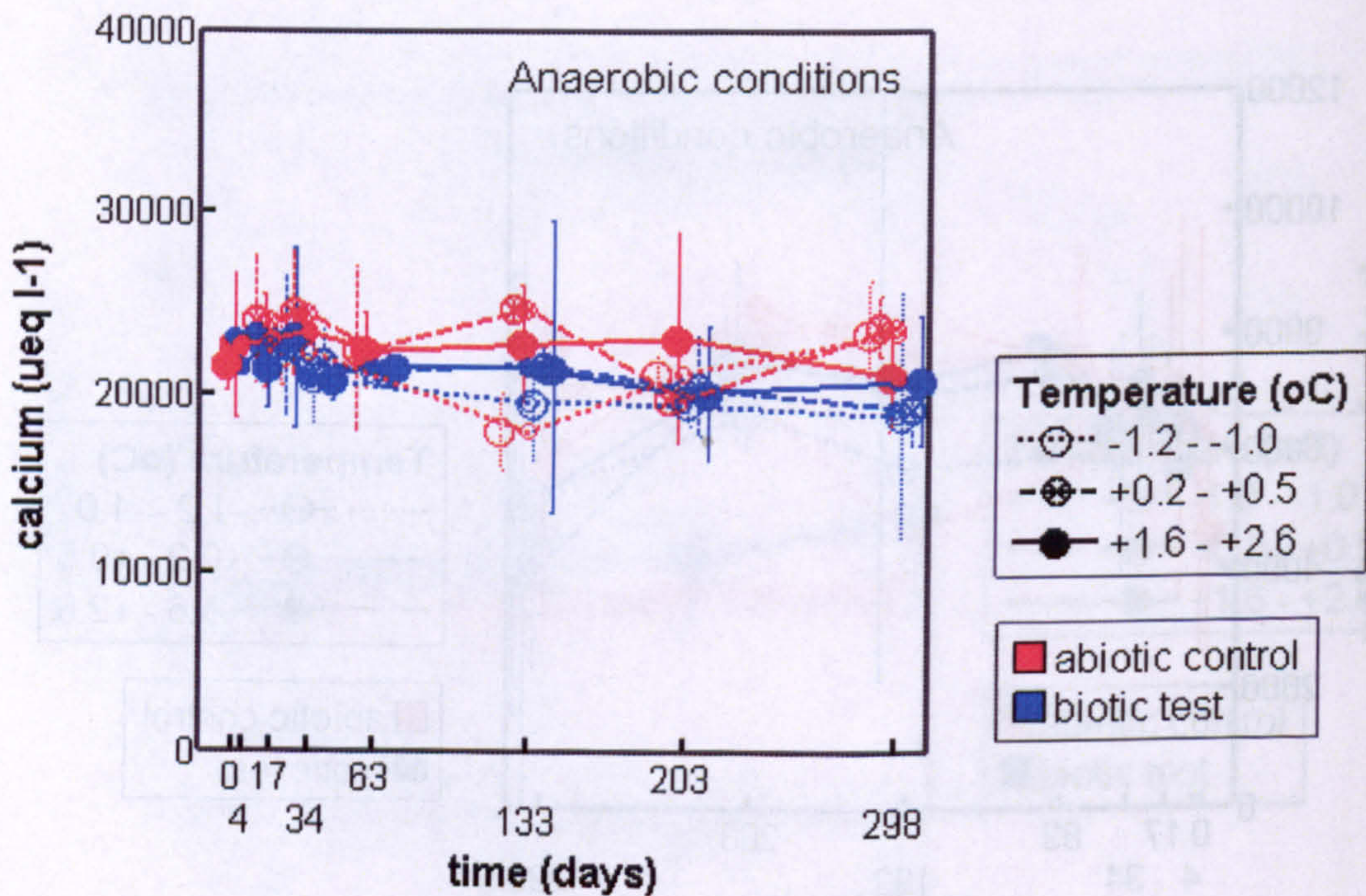
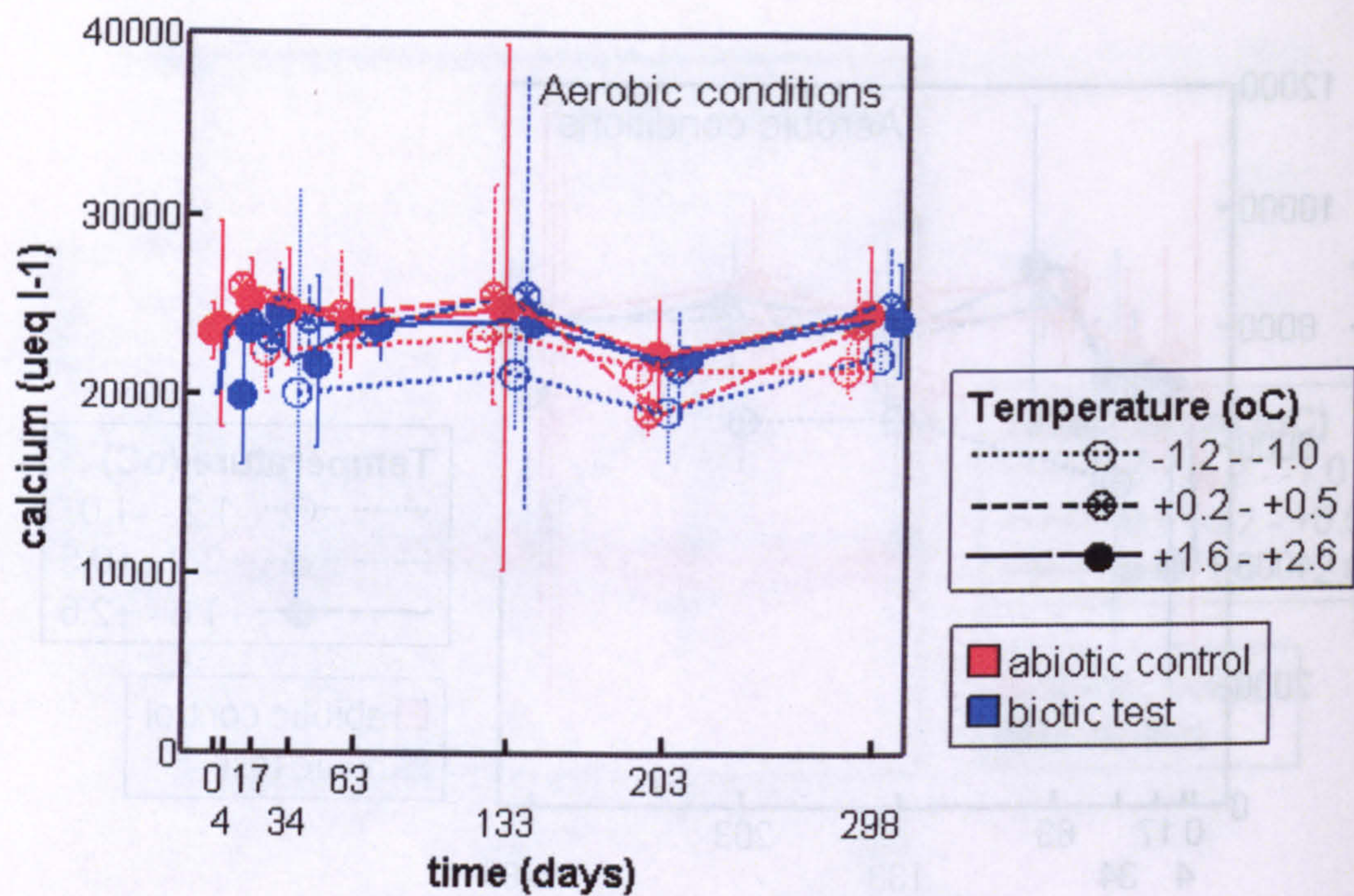


**Figure 6.23.** Calcium concentrations in Bødalsbreen meltwater incubated with rock flour from Finsterwalderbreen, Svalbard in aerobic and anaerobic conditions at a range of temperatures. Lines show the mean values and error bars show 95% confidence intervals for the means of the three replicates ( $n=3$ ). (●) = biotic test at +1.6 - +2.6 °C; (⊗) = biotic test at +0.2 - +0.5 °C; (○) = biotic test at -1.2 - -1.0 °C; (●) = abiotic control at +1.6 - +2.6 °C; (⊗) = abiotic control at +0.2 - +0.5 °C; (○) = abiotic control at -1.2 - -1.0 °C.



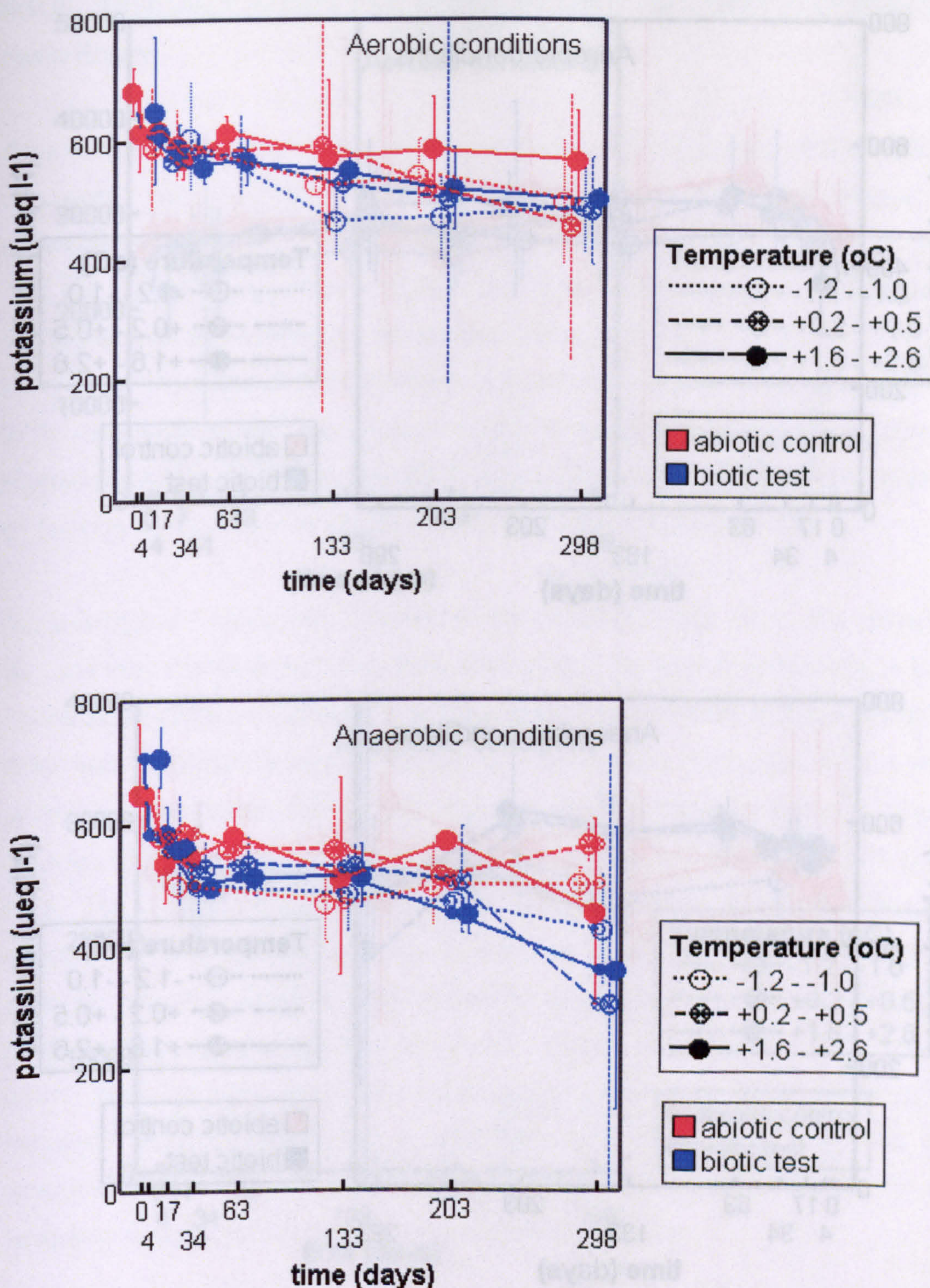


**Figure 6.24.** Potassium concentrations in Bødalsbreen meltwater incubated with rock flour from Finsterwalderbreen, Svalbard in aerobic and anaerobic conditions at a range of temperatures. Lines show the mean values and error bars show 95% confidence intervals for the means of the three replicates ( $n=3$ ). (●) = biotic test at +1.6 - +2.6 °C; (⊗) = biotic test at +0.2 - +0.5 °C; (○) = biotic test at -1.2 - -1.0 °C; (●) = abiotic control at +1.6 - +2.6 °C; (⊗) = abiotic control at +0.2 - +0.5 °C; (○) = abiotic control at -1.2 - -1.0 °C.



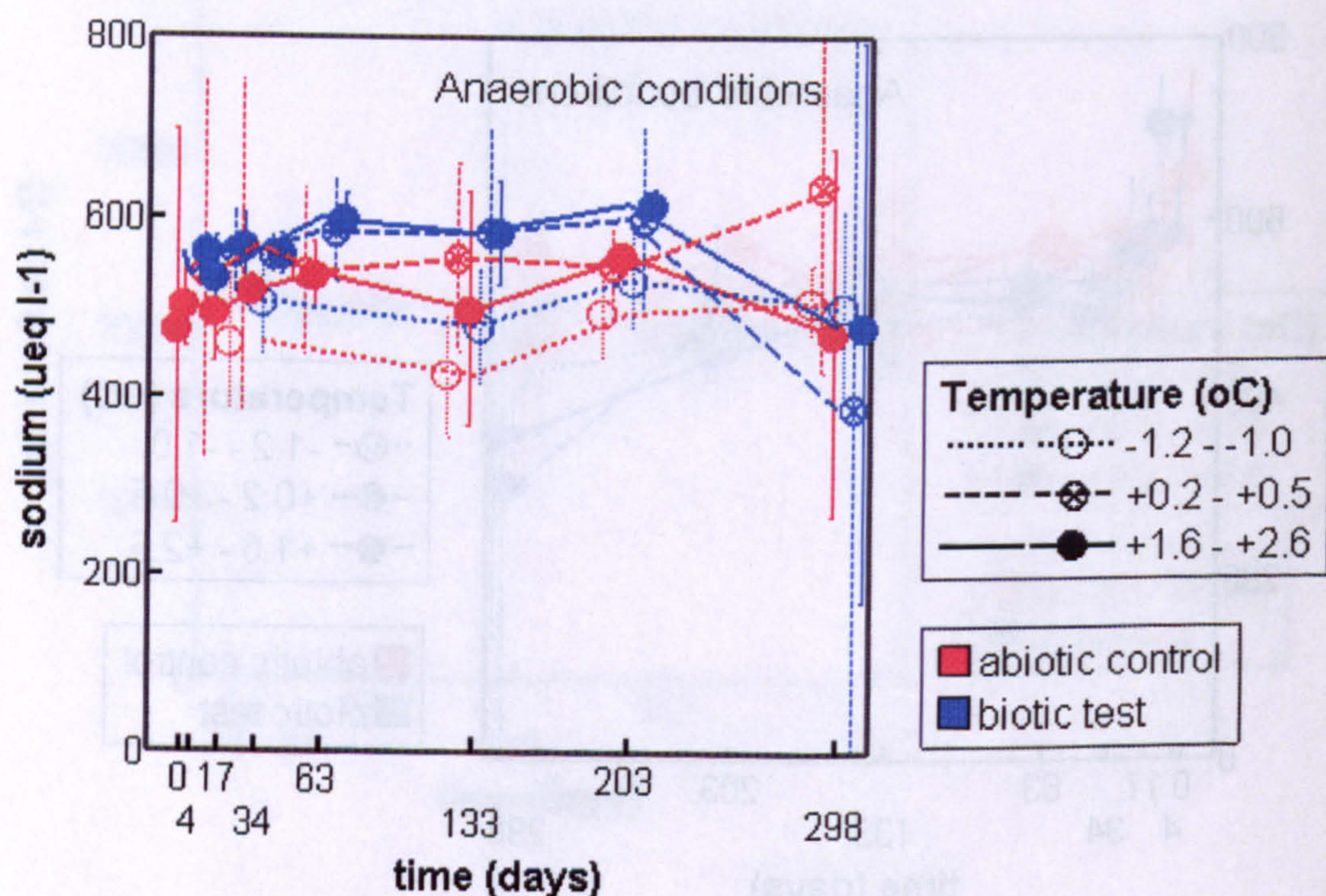
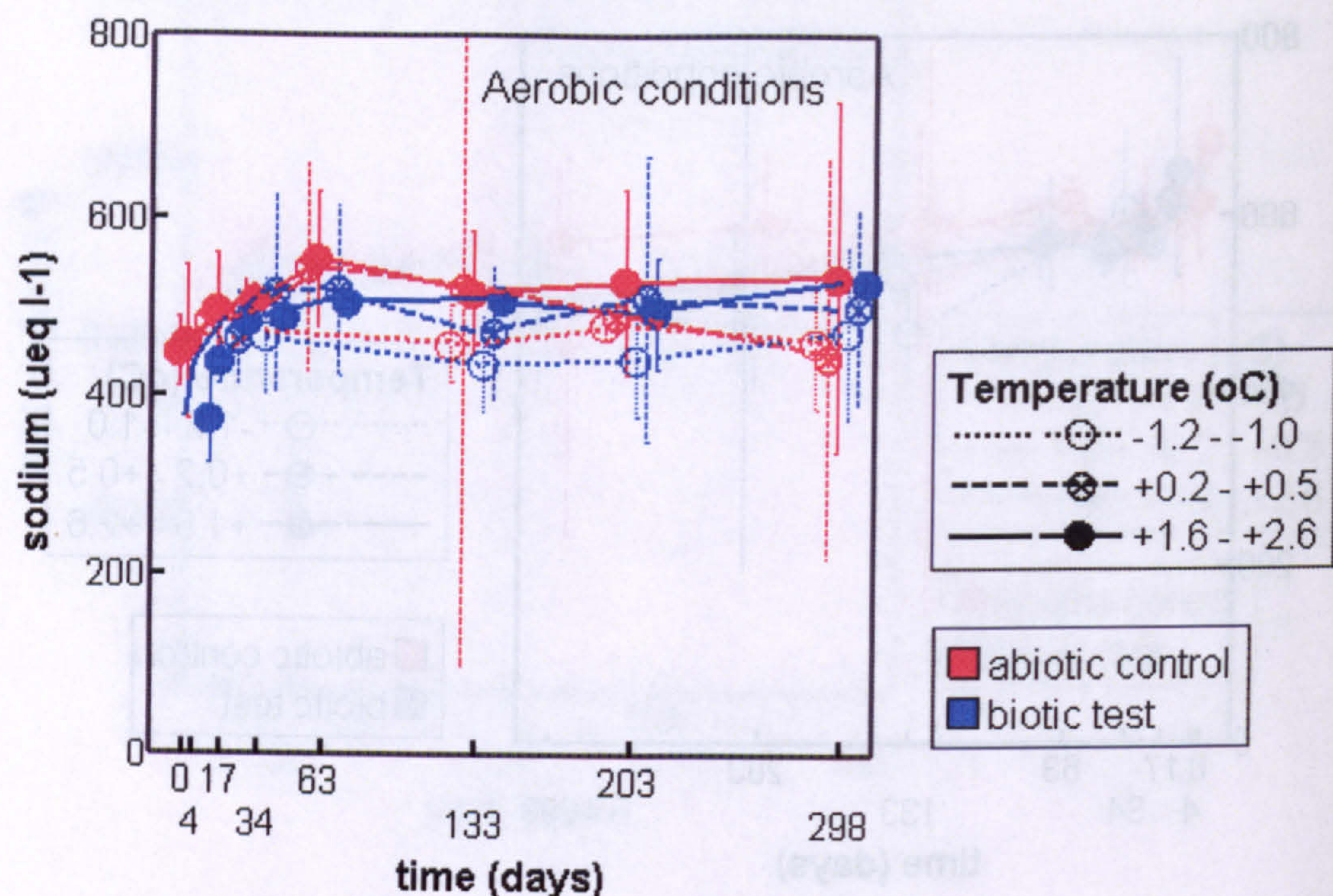


**Figure 6.25.** Sodium concentrations in Bødalsbreen meltwater incubated with rock flour from Finsterwalderbreen, Svalbard in aerobic and anaerobic conditions at a range of temperatures. Lines show the mean values and error bars show 95% confidence intervals for the means of the three replicates ( $n=3$ ). (●) = biotic test at +1.6 - +2.6 °C; (⊗) = biotic test at +0.2 - +0.5 °C; (○) = biotic test at -1.2 - -1.0 °C; (●) = abiotic control at +1.6 - +2.6 °C; (⊗) = abiotic control at +0.2 - +0.5 °C; (○) = abiotic control at -1.2 - -1.0 °C.



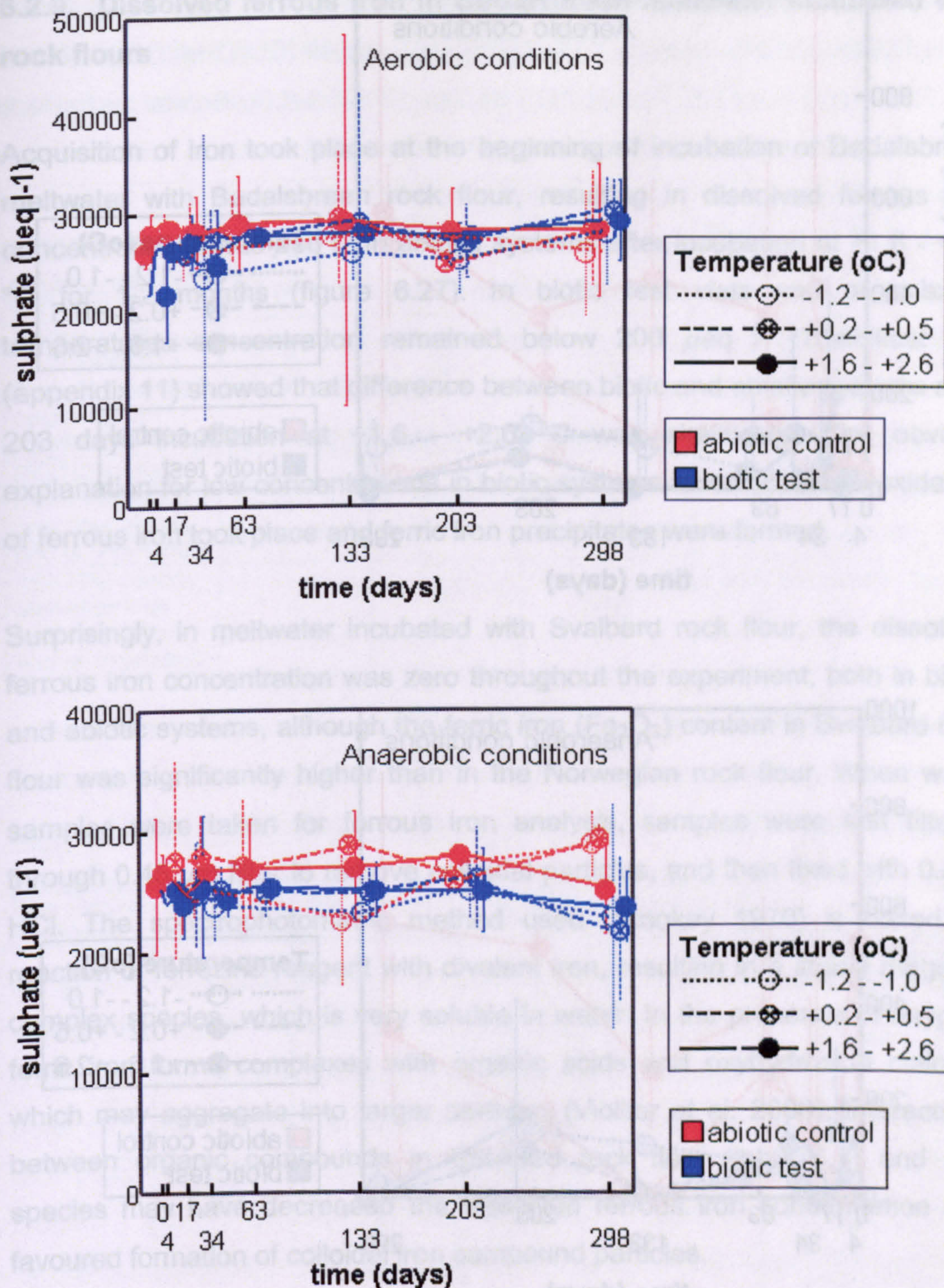


**Figure. 6.26.** Sulphate concentrations in Bødalsbreen meltwater incubated with rock flour from Finsterwalderbreen, Svalbard in aerobic and anaerobic conditions at a range of temperatures. Lines show the mean values and error bars show 95% confidence intervals for the means of the three replicates ( $n=3$ ). (●) = biotic test at +1.6 - +2.6 °C; (⊗) = biotic test at +0.2 - +0.5 °C; (○) = biotic test at -1.2 - -1.0 °C; (●) = abiotic control at +1.6 - +2.6 °C; (⊗) = abiotic control at +0.2 - +0.5 °C; (○) = abiotic control at -1.2 - -1.0 °C.



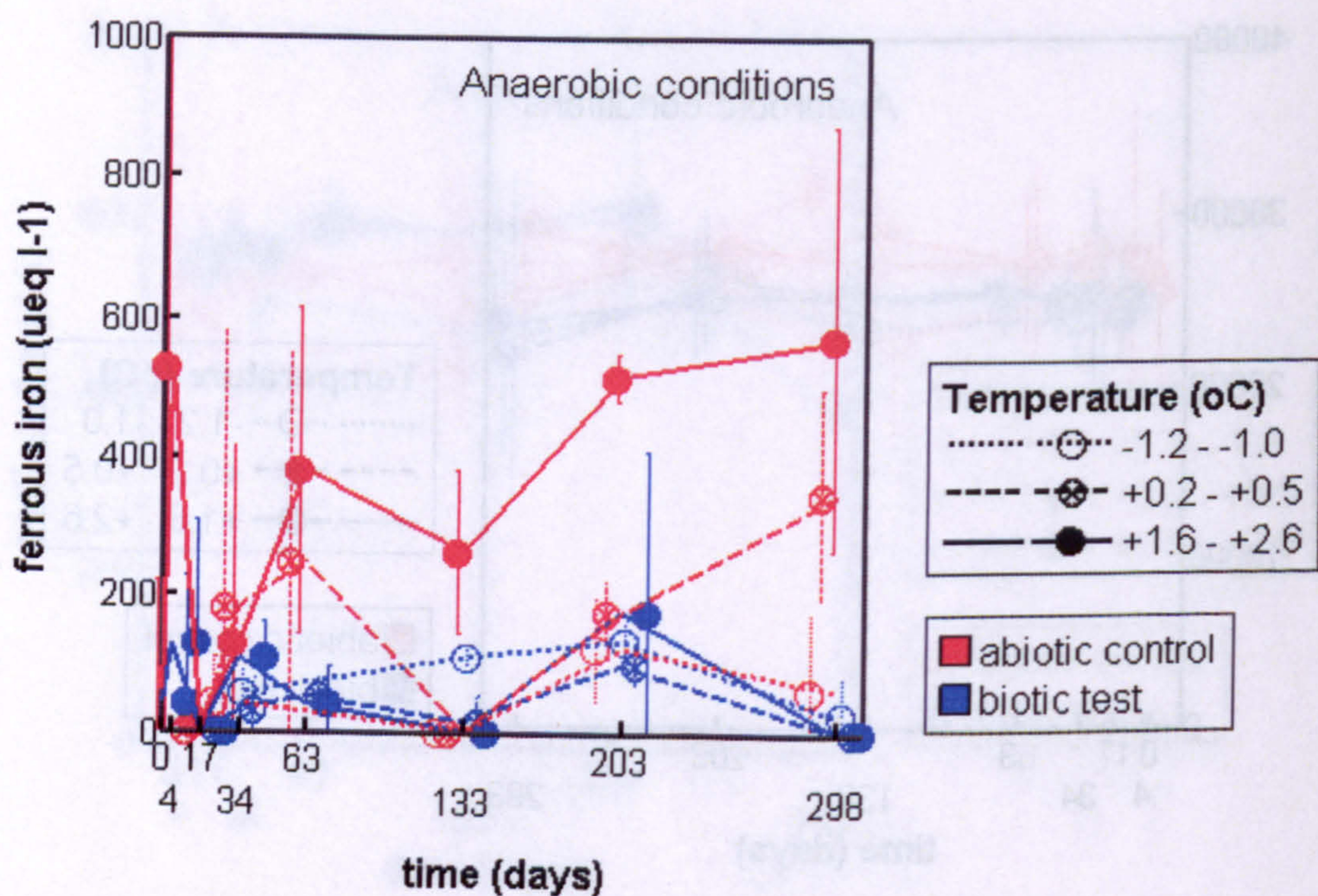
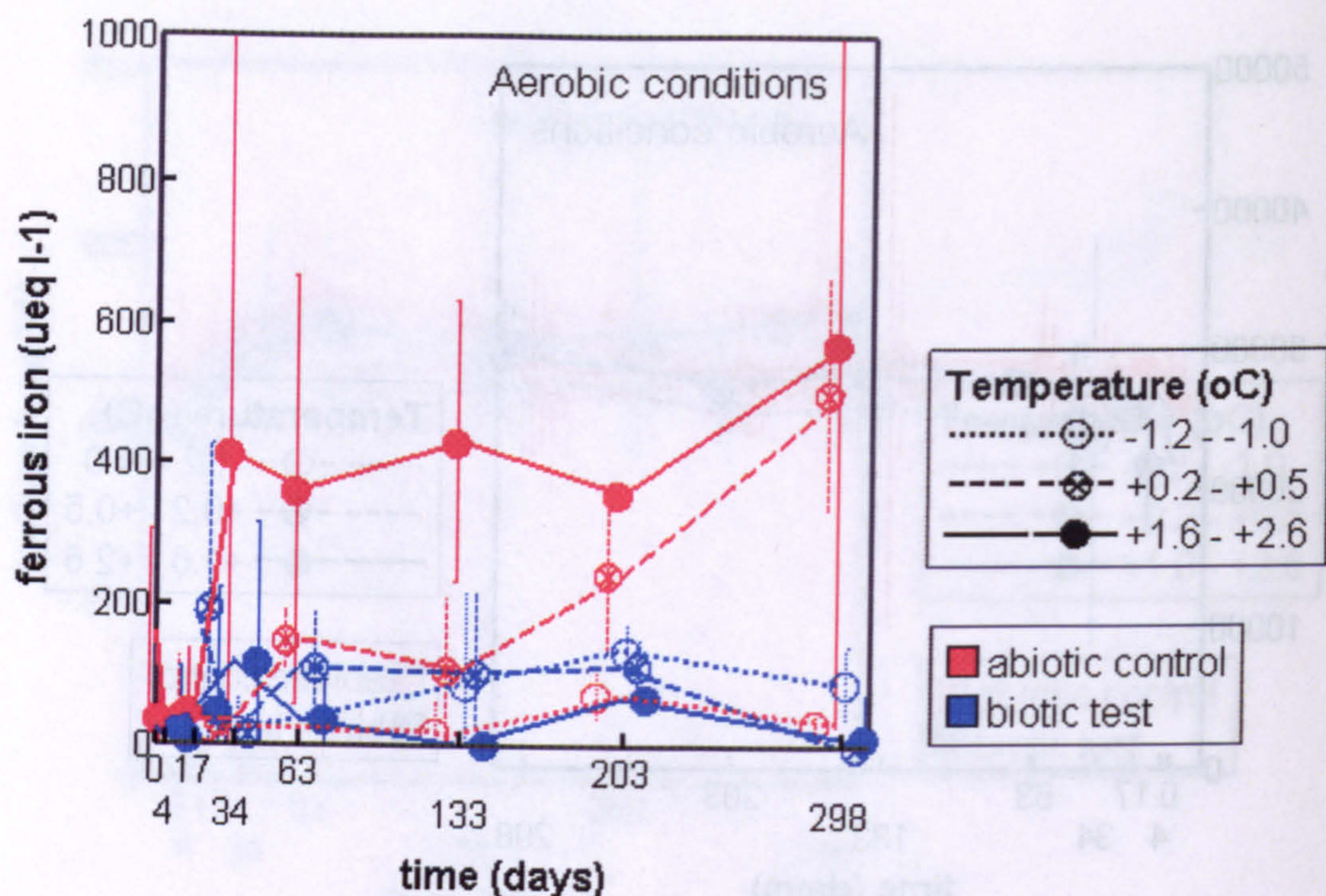


**Figure 6.27.** Dissolved ferrous iron concentrations in Bødalsbreen meltwater incubated with rock flour from Bødalsbreen, Norway in aerobic and anaerobic conditions at a range of temperatures. Lines show the mean values and error bars show 95% confidence intervals for the means of the three replicates ( $n=3$ ). ( $\bullet$ ) = biotic test at +1.6 - +2.6  $^{\circ}\text{C}$ ; ( $\otimes$ ) = biotic test at +0.2 - +0.5  $^{\circ}\text{C}$ ; ( $\circ$ ) = biotic test at -1.2 - -1.0  $^{\circ}\text{C}$ ; ( $\bullet$ ) = abiotic control at +1.6 - +2.6  $^{\circ}\text{C}$ ; ( $\otimes$ ) = abiotic control at +0.2 - +0.5  $^{\circ}\text{C}$ ; ( $\circ$ ) = abiotic control at -1.2 - -1.0  $^{\circ}\text{C}$ .



### **6.2.9. Dissolved ferrous iron in Bødalsbreen meltwater incubated with rock flours**

Acquisition of iron took place at the beginning of incubation of Bødalsbreen meltwater with Bødalsbreen rock flour, resulting in dissolved ferrous iron concentration of  $400 \mu\text{eq l}^{-1}$  in abiotic systems after incubation at  $+1.6 - +2.6$  °C for 1-2 months (figure 6.27). In biotic test vials and at subzero temperatures concentration remained below  $200 \mu\text{eq l}^{-1}$ . Statistical test (appendix 11) showed that difference between biotic and abiotic systems after 203 days incubation at  $+1.6 - +2.6$  °C was significant. The obvious explanation for low concentrations in biotic systems is that bacterial oxidation of ferrous iron took place and ferric iron precipitates were formed.

Surprisingly, in meltwater incubated with Svalbard rock flour, the dissolved ferrous iron concentration was zero throughout the experiment, both in biotic and abiotic systems, although the ferric iron ( $\text{Fe}_2\text{O}_3$ ) content in Svalbard rock flour was significantly higher than in the Norwegian rock flour. When water samples were taken for ferrous iron analysis, samples were first filtered through  $0.45 \mu\text{m}$  filter to remove colloidal particles, and then fixed with 0.5 M HCl. The spectrophotometric method used (Stookey 1970) is based on reaction of ferrozine reagent with divalent iron, resulting in a stable magenta complex species, which is very soluble in water. In the presence of oxygen, ferric iron forms complexes with organic acids and oxyhydroxide colloids, which may aggregate into larger particles (Viollier et al. 2000). Interactions between organic compounds in Svalbard rock flour (table 6.3) and iron species may have decreased the dissolved ferrous iron concentration and favoured formation of colloidal iron compound particles.

### **6.2.10. Organic acids in Bødalsbreen meltwater incubated with rock flours**

Organic acids present in Bødalsbreen meltwater at the beginning and the end of incubation were identified by high performance ion chromatography (Dionex DX600) gradient analysis, using KOH as an eluent and an AS11-HC separator column. Combined standard solution (table 4.3) was used to



analyse concentrations of monocarboxylic organic anions including lactate ( $\text{CH}_3\text{CH}(\text{OH})\text{COO}^-$ ), acetate ( $\text{CH}_3\text{COO}^-$ ), propionate ( $\text{CH}_3\text{CH}_2\text{COO}^-$ ), formate ( $\text{HCOO}^-$ ) and butyrate ( $\text{C}_3\text{H}_7\text{COO}^-$ ) (tables 6.7 and 6.8). Before mixing with rock flour, concentration of above mentioned organic acids in meltwater was zero. Simple organic acids in initially low DOC meltwater had likely been biodegraded by heterotrophic micro-organisms during storage at +2 °C (see chapter 6.2.1). However, instantly after mixing with the Norwegian rock flour, lactate, acetate and formate were released to meltwater (table 6.7). By the end of 298 days incubation period at +1.6 – +2.6 °C, acetate and formate were entirely utilized by microbes, and concentration of lactate had also markedly decreased. In abiotic controls, mineralisation of organic acids did not happen and concentrations had increased from values after the initial rapid release at time zero.

**Table 6.7.** Organic acids detected in Bødalsbreen meltwater incubated with the Norwegian rock flour. Figures presented are the mean values of the two replicates. Incubation for 298 days at temperature of +1.6 – +2.6 °C.

	Lactic acid ( $\mu\text{mol l}^{-1}$ )	Acetic acid ( $\mu\text{mol l}^{-1}$ )	Propionic acid ( $\mu\text{mol l}^{-1}$ )	Formic acid ( $\mu\text{mol l}^{-1}$ )	Glutaric acid ( $\mu\text{mol l}^{-1}$ )
Meltwater before mixing with rock flour	0	0	0	< 5	0
Meltwater after mixing with rock flour, at t=0 at the beginning of incubation	85	8	0	7	< 5
BIOTIC system, Meltwater with rock flour at the end of incubation	35	< 5	0	0	0
ABIOTIC control, Meltwater with rock flour at the end of incubation	114	48	0	50	20

Propionate was released into meltwater from the Svalbard rock flour, but there were no traces of lactate, acetate or formate (table 6.8). Again, in biotic systems propionate was biodegraded by the end of incubation, whereas in abiotic controls no removal occurred and the concentration of propionate was increasing. Butyrate was not found in any of the samples.



**Table 6.8.** Organic acids detected in Bødalsbreen meltwater incubated with the Svalbard rock flour. Figures presented are the mean values of the two replicates. Incubation for 298 days at temperature of +1.6 – +2.6 °C.

	Lactic acid ( $\mu\text{mol l}^{-1}$ )	Acetic acid ( $\mu\text{mol l}^{-1}$ )	Propionic acid ( $\mu\text{mol l}^{-1}$ )	Formic acid ( $\mu\text{mol l}^{-1}$ )	Glutaric acid ( $\mu\text{mol l}^{-1}$ )
Meltwater before mixing with rock flour	0	0	0	< 5	0
Meltwater after mixing with rock flour, at t=0 at the beginning of incubation	0	0	162	0	< 5
BIOTIC system, Meltwater with rock flour at the end of incubation	0	0	0	0	0
ABIOTIC control, Meltwater with rock flour at the end of incubation	0	0	330	0	< 5

High performance ion chromatography gradient analysis with combined standard solutions of major anions and monocarboxylic organic anions produced chromatographs including one unidentified peak between recorded nitrate and carbonate peaks. Based on the retention time and the fact that the unidentified peak was found in the same samples as the maximum concentrations of monocarboxylic acids, it was assumed that the unidentified peak may represent a dicarboxylic acid. Hence, the presence of a range of dicarboxylic organic acids, such as succinic acid ( $\text{HCOOHC}-\text{CHCOOH}$ ), maleic acid ( $\text{HOOCCH}(\text{OH})\text{CH}_2\text{COOH}$ ), glutaric acid ( $\text{HOOC}-\text{CH}_2\text{CH}_2\text{CH}_2\text{COOH}$ ), malonic acid ( $\text{HOOCCH}_2\text{COOH}$ ) and tartaric acid ( $\text{HOOCOHCH}-\text{CHOHCOOH}$ ), was also investigated. Both combined mixed standard solutions and single standards (blanks spiked with standard solution of one specific dicarboxylic acid) were used. No succinate, malate, malonate or tartrate were detected. Retention times of each tested standard dicarboxylic acids and the unidentified peak were compared, and the dicarboxylic acid showing the closest retention time was glutarate. In chromatographic analysis, glutarate single standard had a retention time of 32.57 min, glutarate in mixed standard solution had retention time of 32.58 – 32.70 min, and the unidentified peak had a retention time of 32.46 – 32.67



min. This particular dicarboxylic acid, most likely glutaric acid, was also released into meltwater from the Norwegian rock flour, and was entirely utilized by the end of incubation, whereas in the abiotic controls, concentration of glutarate increased up to  $20 \mu\text{mol l}^{-1}$ .



## **6.3. Weathering experiment with proglacial rock debris from Norway and Svalbard, and meltwater from Svalbard**

### **6.3.1. In situ and laboratory experiment conditions**

In the third weathering experiment, the aim was to investigate whether bacteria originating from different glacial and lithological environment of Svalbard, compared to Norway, are able to grow when incubated with Norwegian and Svalbard rock flours. Hence, grain size distribution, as well as elemental and mineralogical composition of the rock flours used was identical to those used in long-term weathering experiment (see chapter 6.2). In order to ensure that rock flours were sterile, they were dry heat sterilized once again at 120 °C for 8 hours, the day before starting the experiment.

Fresh meltwater from Midre Lovénbreen, Svalbard was used as a source of bacteria. The dissolved oxygen concentration at the time of sampling was 13 - 54 %-sat, and pH was 8.17 - 8.31. Meltwater samples were transported immediately after sampling from the field site to the laboratory. During transport, samples were stored at +2-+4 °C. The experiment was set up two days after sampling, following the similar procedure than with the second weathering experiment (see chapters 4.2.3.2 and 4.2.3.3). The biotic test vials and abiotic controls, both in duplicate, were incubated at +1.6 °C for 96 days.

### **6.3.2. Bacterial growth in Svalbard meltwater incubated with rock flours**

Growth of bacteria in Svalbard meltwater at +1.6 °C was indistinguishable, whether incubated with Norwegian or Svalbard rock flour (figure 6.28). In four weeks, the total number of bacteria increased from 4.5 log<sub>10</sub> cells ml<sup>-1</sup> to 8 log<sub>10</sub> cells ml<sup>-1</sup>. Bacterial population was still in the stationary phase at the end of 96 days of incubation, with the frequency of dividing and divided cells remaining around 10% until the end of the experiment.



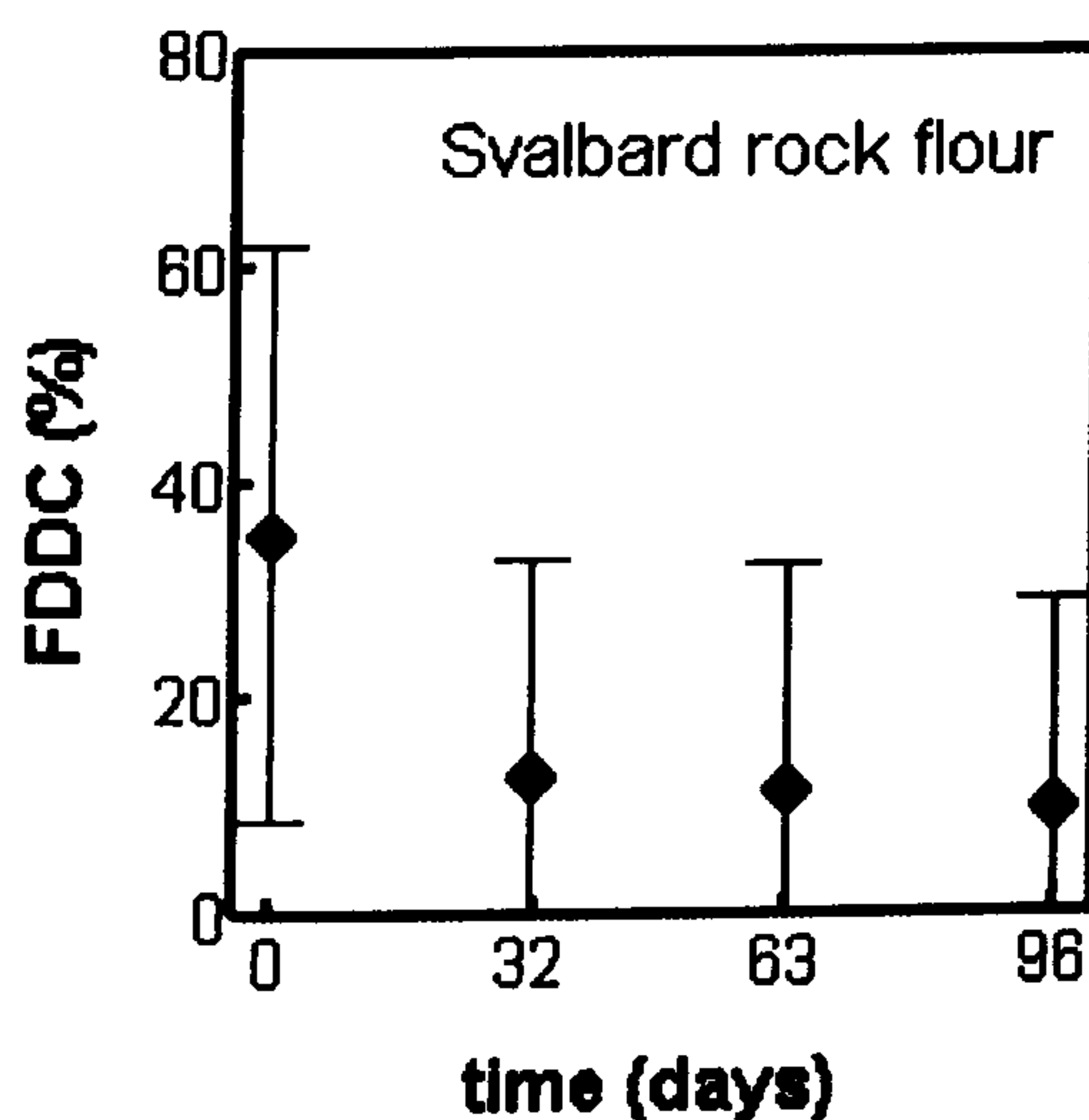
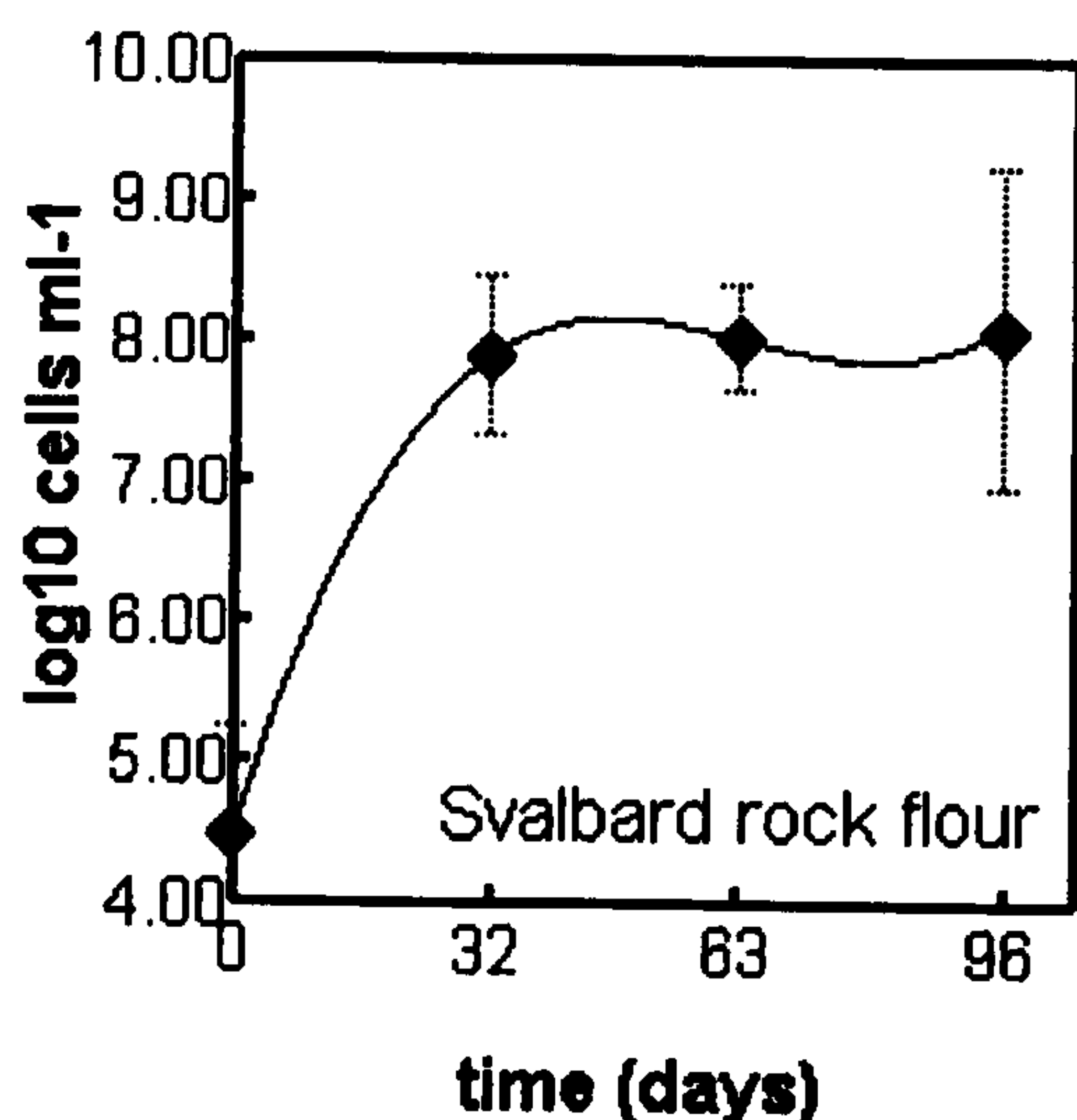
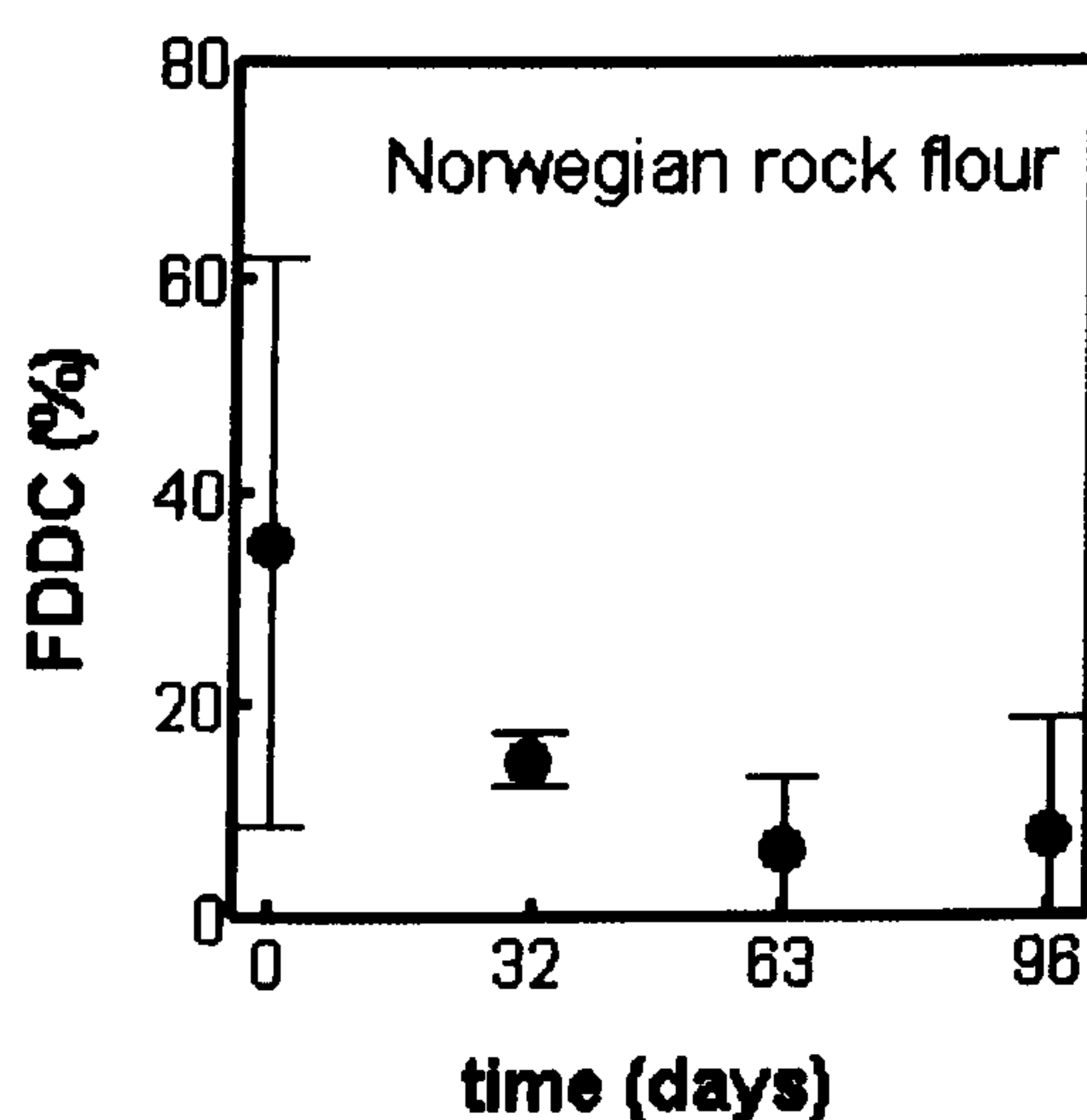
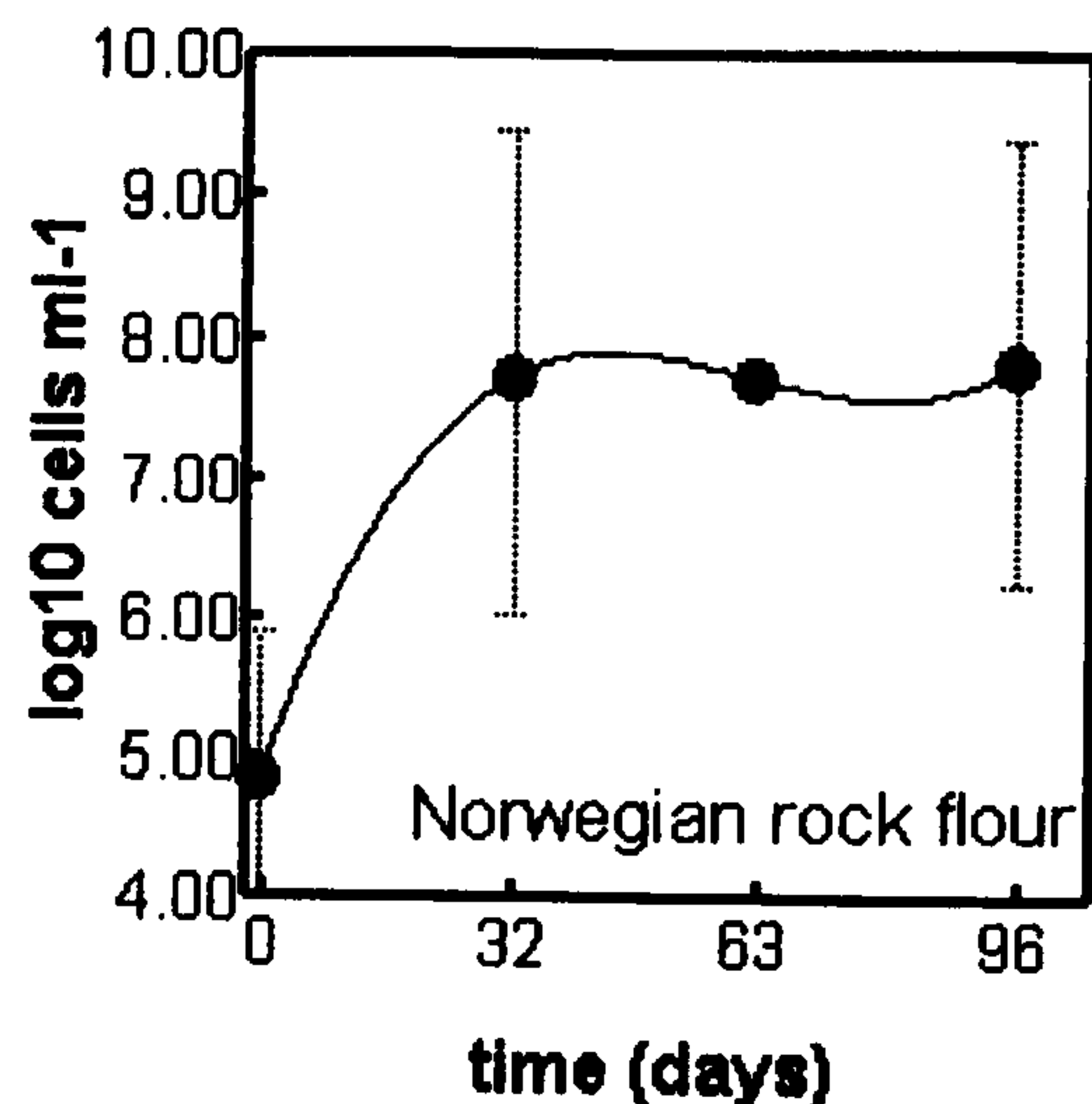


**Figure 6.28.** Growth curves of the total numbers of bacteria in meltwaters incubated at +1.6 °C with rock flours for 96 days, and frequency of dividing and divided cells (FDDC) over time. Subglacial meltwater taken from the Midre Lovénbreen glacier, Svalbard and rock flour from Bødalsbreen, Norway and Finsterwalderbreen, Svalbard. Lines with symbols show mean values and error bars show 95% confidence intervals for means of two replicates (n=2). (●) = Norwegian rock flour; (◆) = Svalbard rock flour.

### 6.3.3. Oxygen and methane in headspace

The oxygen content in the headspace decreased during the 96 days of incubation from the atmospheric value of 21 vol.% to 13 vol.% (when incubated with Norwegian rock flour) and 7 vol.% (when incubated with



Svalbard rock flour). Again, there was no methane production by the end of incubation.

#### 6.3.4. Dissolved oxygen and pH in Svalbard meltwater incubated with rock flours

The dissolved oxygen concentration in meltwater was  $0.30 - 0.50 \text{ mmol l}^{-1}$  throughout the experiment when incubated with Norwegian rock flour (figure 6.29). Changes, if any, were indistinguishable in biotic and abiotic vials (separate-variance test  $t$ -value =  $-1.138$  and  $p = 0.431$ ). Microbes in meltwater incubated with Svalbard rock flour utilised some of the oxygen, causing the final concentration of  $0.20 \text{ mmol l}^{-1}$ , but the difference between biotic and abiotic systems, however, was not significant ( $t = -7.857$ ,  $p = 0.081$ ).

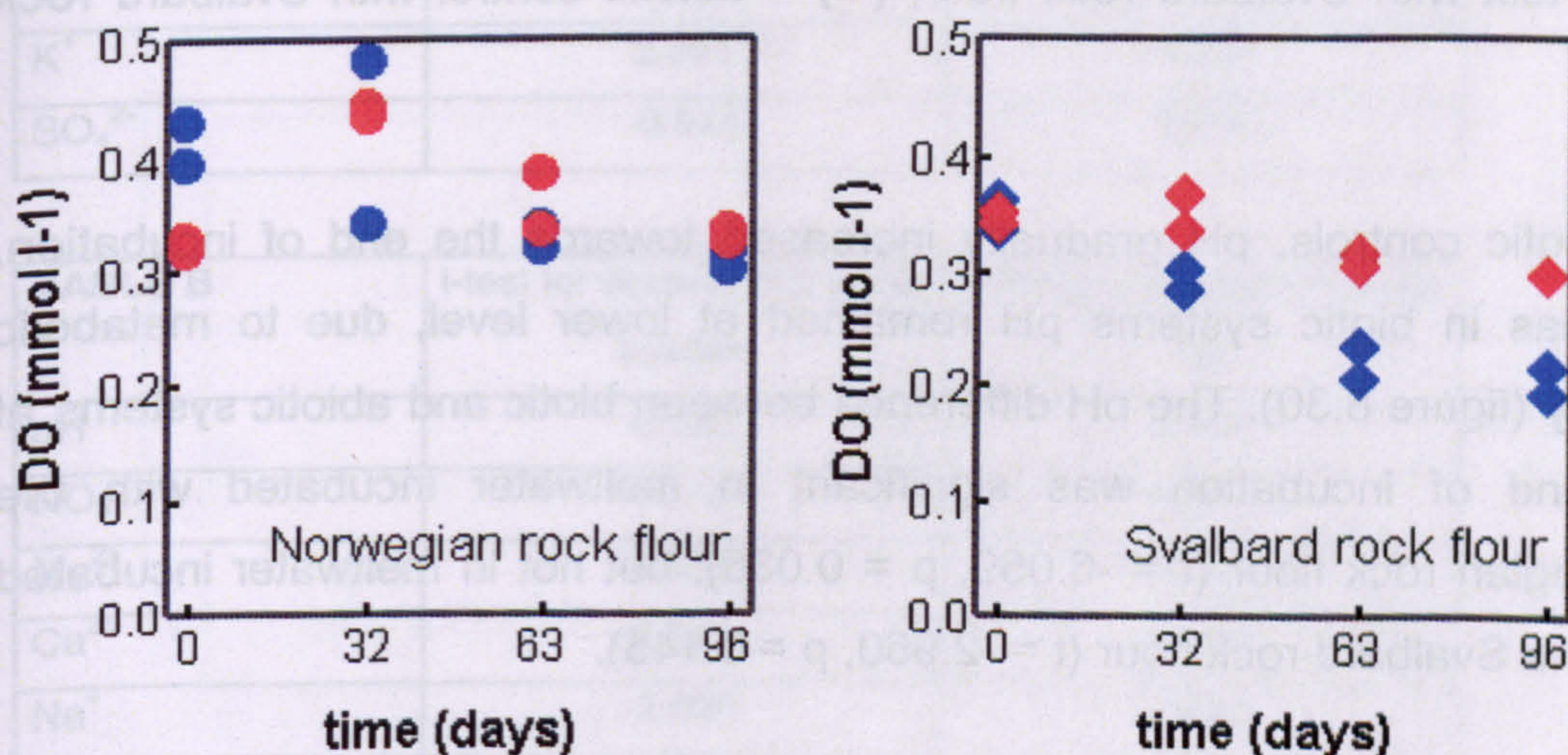


**Figure 6.29.** Dissolved oxygen concentrations in meltwaters incubated at  $+1.6 \text{ }^{\circ}\text{C}$  with rock flours for 96 days. Subglacial meltwater taken from the Midre Lovénbreen glacier, Svalbard and rock flour from Bødalsbreen, Norway and Finsterwalderbreen, Svalbard. Symbols show values of two replicates ( $n=2$ ). (●) = biotic test with Norwegian rock flour; (○) = abiotic control with Norwegian rock flour; (◆) = biotic test with Svalbard rock flour; (◇) = abiotic control with Svalbard rock flour.



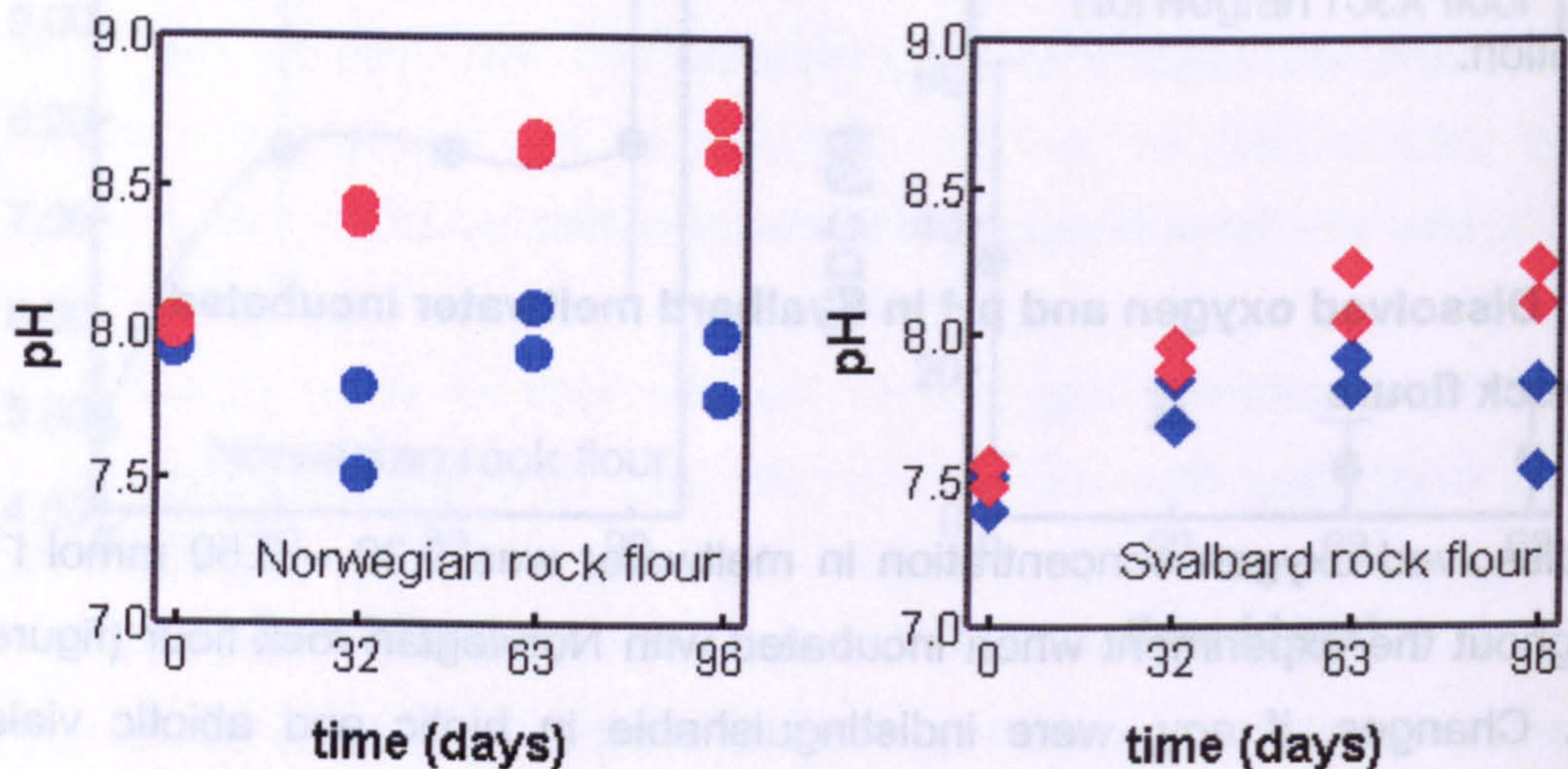


**Figure 6.30.** pH in meltwaters incubated at +1.6 °C with rock flours for 96 days. Subglacial meltwater taken from the Midre Lovénbreen glacier, Svalbard and rock flour from Bødalsbreen, Norway and Finsterwalderbreen, Svalbard. Symbols show values of two replicates ( $n=2$ ). (●) = biotic test with Norwegian rock flour; (●) = abiotic control with Norwegian rock flour; (◆) = biotic test with Svalbard rock flour; (◆) = abiotic control with Svalbard rock flour.

In abiotic controls, pH gradually increased towards the end of incubation, whereas in biotic systems pH remained at lower level, due to metabolic activity (figure 6.30). The pH difference between biotic and abiotic systems at the end of incubation was significant in meltwater incubated with the Norwegian rock flour ( $t = -6.059$ ,  $p = 0.038$ ), but not in meltwater incubated with the Svalbard rock flour ( $t = -2.960$ ,  $p = 0.145$ ).

#### 6.3.5. Major anions and cations in Svalbard meltwater incubated with rock flours

Nitrate concentrations during the initial stages of incubation were clearly higher in the meltwater incubated with the Svalbard rock flour (figure 6.31). In meltwater incubated with the Norwegian rock flour, the maximum nitrate concentration after the initial release was  $20 \mu\text{eq l}^{-1}$ , and no nitrate reduction was detected during 96 days of incubation. In the meltwater incubated with the Svalbard rock flour, nitrate concentration after 32 days of incubation was



50  $\mu\text{eq l}^{-1}$ , but from then on, concentration of nitrate in biotic systems decreased noticeably, almost to zero, due to activity of nitrate reducing bacteria. Difference between biotic and abiotic systems was significant after 63 days of incubation (table 6.9).

**Table 6.9.** Results of the separate-variance t-tests (equal variances not assumed) for equality of means (two replicates) of pH and major anions and cations in Midre Lovénbreen meltwater incubated at +1.6 °C with rock flours from Bødalsbreen, Norway (table A) and Finsterwalderbreen, Svalbard (table B). Comparisons between biotic tests and abiotic controls after 63 days of incubation.

TABLE A	t-test for equality of means t-value	t-test for equality of means p
pH	-7.761	0.065
NO <sub>3</sub> <sup>-</sup>	-0.763	0.557
Mg <sup>2+</sup>	34.276	0.005
Ca <sup>2+</sup>	40.746	0.013
Na <sup>+</sup>	0.650	0.597
K <sup>+</sup>	2.301	0.239
SO <sub>4</sub> <sup>2-</sup>	-0.944	0.494

TABLE B	t-test for equality of means t-value	t-test for equality of means p
pH	-2.562	0.163
NO <sub>3</sub> <sup>-</sup>	-46.739	0.001
Mg <sup>2+</sup>	0.098	0.934
Ca <sup>2+</sup>	0.821	0.525
Na <sup>+</sup>	-2.025	0.287
K <sup>+</sup>	-1.186	0.417
SO <sub>4</sub> <sup>2-</sup>	0.919	0.498

Accelerated dissolution of Mg<sup>2+</sup> and Ca<sup>2+</sup> from Norwegian rock flour was detected in biotic systems after two months incubation at +1.6 °C (figures 6.32 and 6.33 and table 6.9). The two months lag between the beginning of incubation and microbially accelerated dissolution of Mg<sup>2+</sup> and Ca<sup>2+</sup> was longer than when meltwater from the Bødalsbreen glacier in Norway was incubated with Norwegian rock flour, in which case increase elevated



concentrations were detected after one month's incubation at +0.2 - +2.6 °C (figure 6.17). The likely reason for this is the adaptation time that micro-organisms from the different glacial and lithological environment of Svalbard needed, before they became fully active in the new nutritional environment.

The rapid dissolution of high concentrations of  $Mg^{2+}$  and  $Ca^{2+}$  from Svalbard rock flour masked any potential impacts of microbial activity, and thus no differences between biotic and abiotic systems could be distinguished (figures 6.32 and 6.33 and table 6.9), despite the apparent activity of at least bacteria using nitrate as an electron acceptor (figure 6.31).

During the three months incubation at +1.6 °C, there was no sign of microbially mediated release of  $Na^+$ ,  $K^+$  or  $SO_4^{2-}$ , neither from the Norwegian rock flour nor the Svalbard rock flour (figures 6.34, 6.35 and 6.36 and table 6.9).

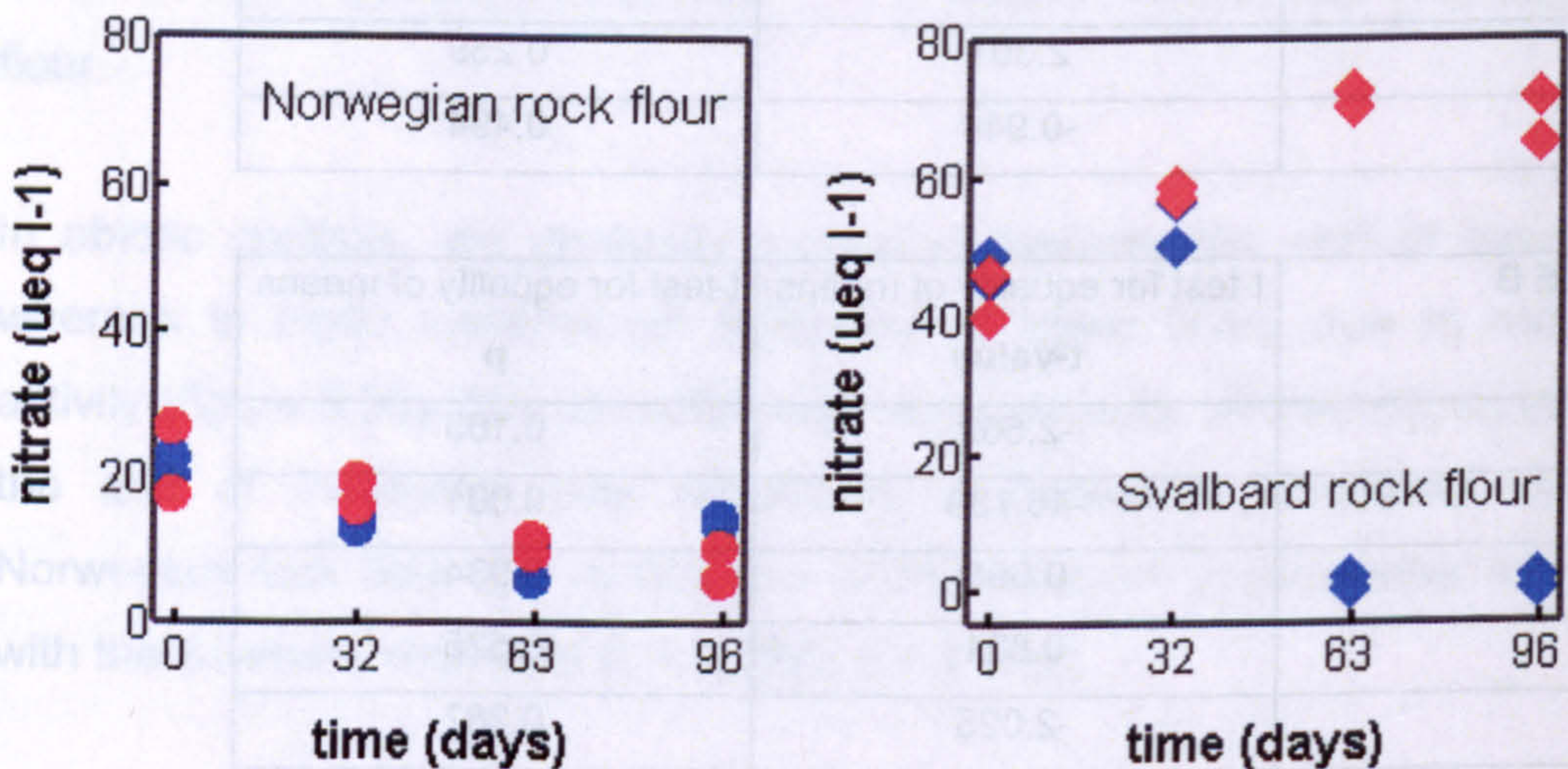


**Figure 6.31.** Nitrate concentrations in meltwaters incubated at +1.6 °C with rock flours for 96 days. Subglacial meltwater taken from the Midre Lovénbreen glacier, Svalbard and rock flour from Bødalsbreen, Norway and Finsterwalderbreen, Svalbard. Symbols show values of two replicates (n=2). (●) = biotic test with Norwegian rock flour; (●) = abiotic control with Norwegian rock flour; (◆) = biotic test with Svalbard rock flour; (◆) = abiotic control with Svalbard rock flour.



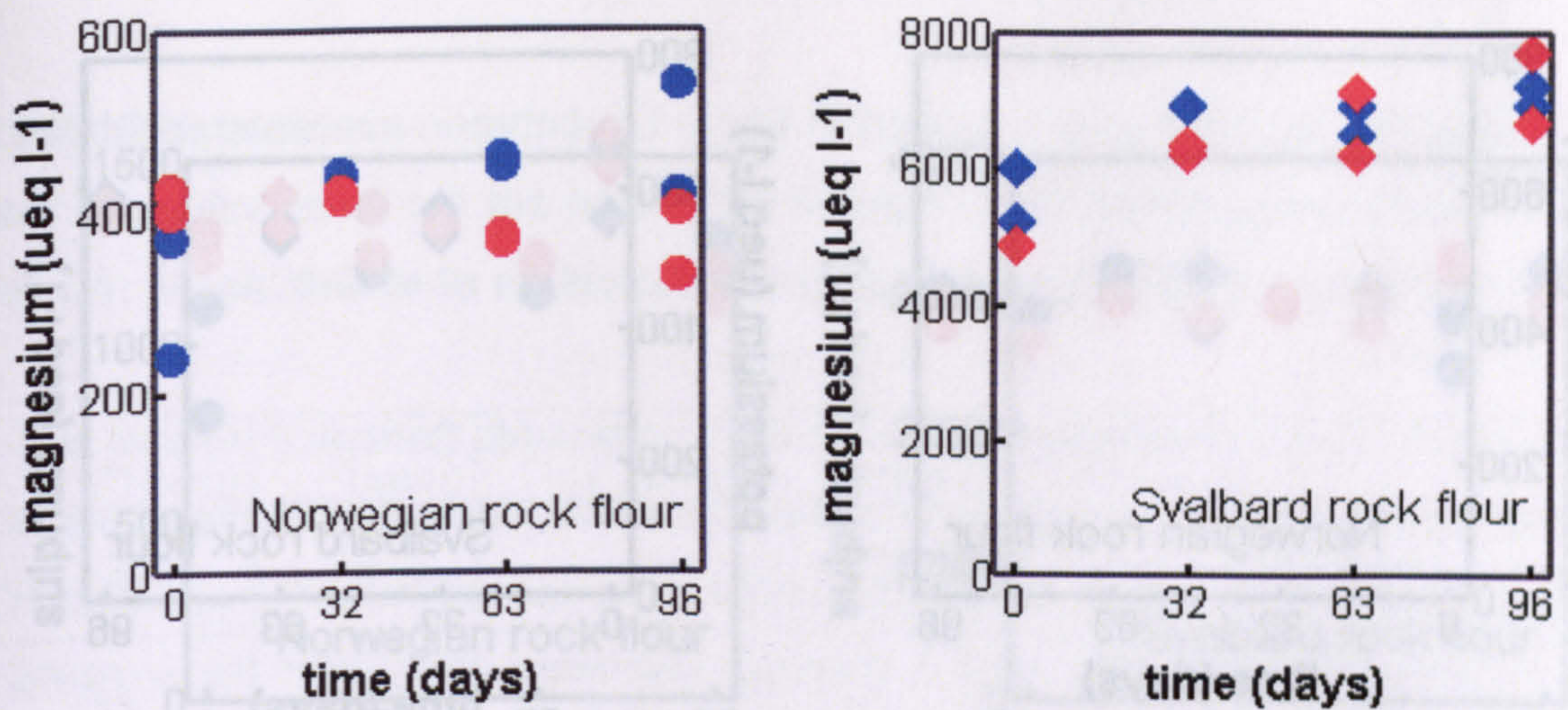


**Figure 6.32.** Magnesium concentrations in meltwaters incubated at +1.6 °C with rock flours for 96 days. Subglacial meltwater taken from the Midre Lovénbreen glacier, Svalbard and rock flour from Bødalsbreen, Norway and Finsterwalderbreen, Svalbard. Symbols show values of two replicates (n=2). (●) = biotic test with Norwegian rock flour; (●) = abiotic control with Norwegian rock flour; (◆) = biotic test with Svalbard rock flour; (◆) = abiotic control with Svalbard rock flour.

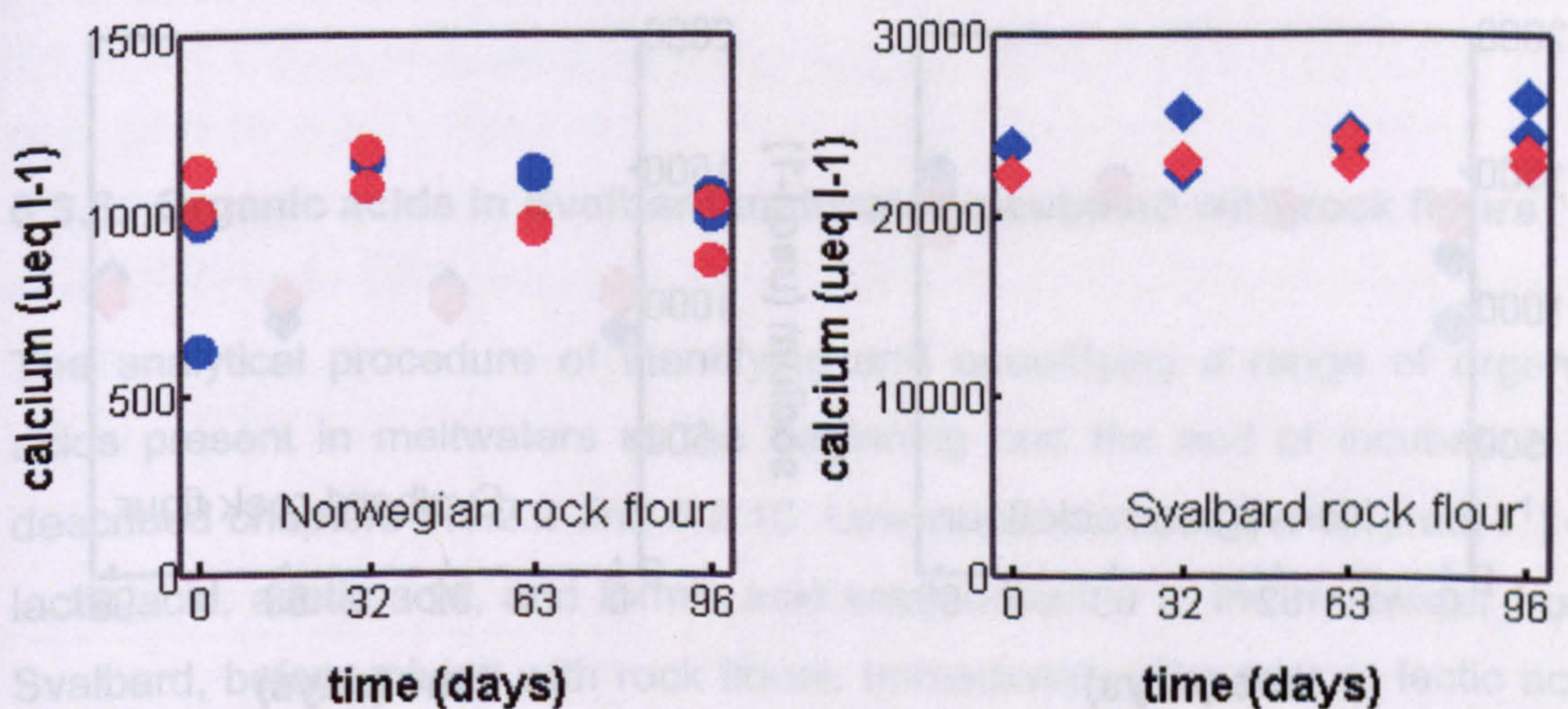


**Figure 6.33.** Calcium concentrations in meltwaters incubated at +1.6 °C with rock flours for 96 days. Subglacial meltwater taken from the Midre Lovénbreen glacier, Svalbard and rock flour from Bødalsbreen, Norway and Finsterwalderbreen, Svalbard. Symbols show values of two replicates (n=2). (●) = biotic test with Norwegian rock flour; (●) = abiotic control with Norwegian rock flour; (◆) = biotic test with Svalbard rock flour; (◆) = abiotic control with Svalbard rock flour.



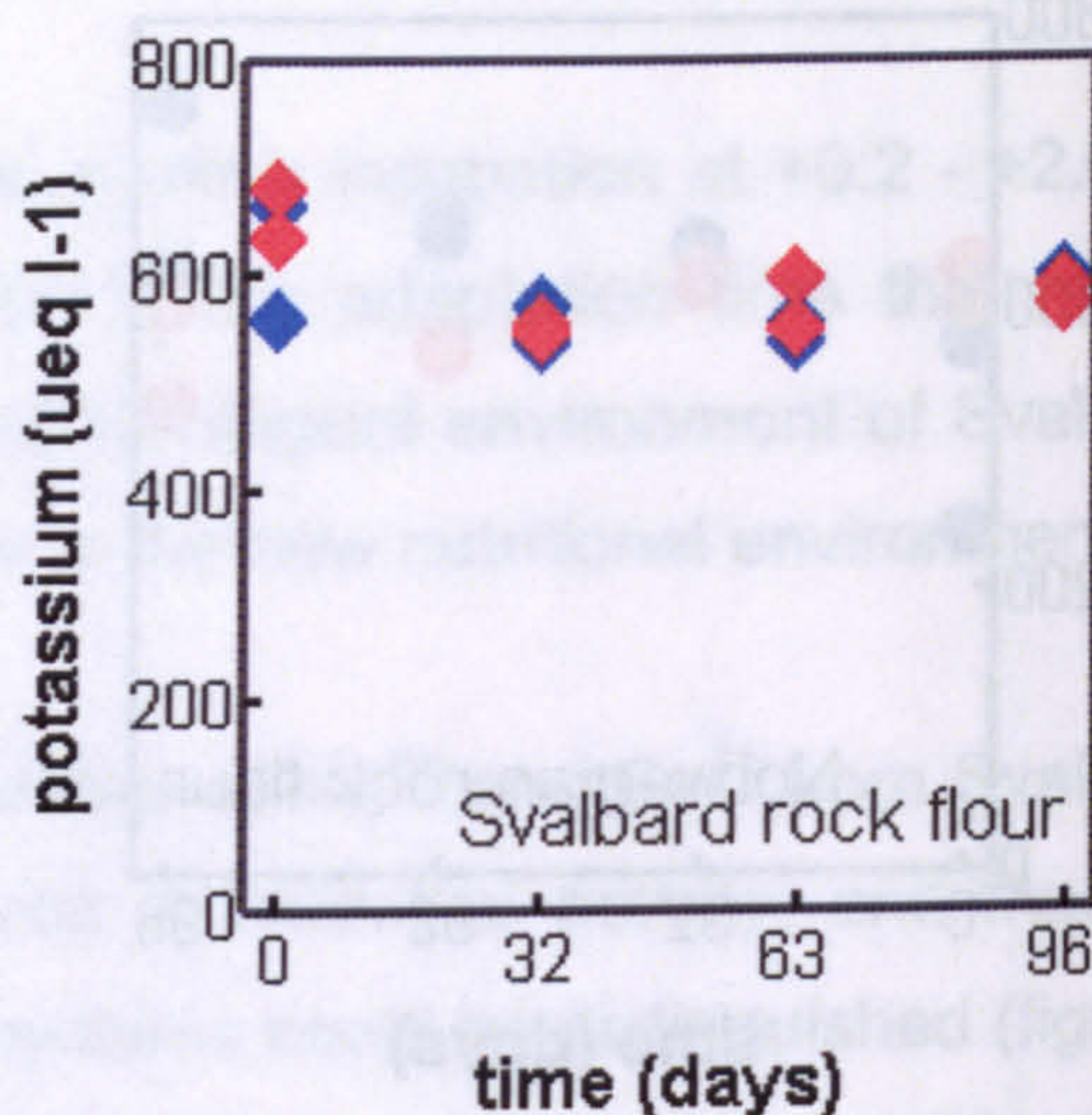
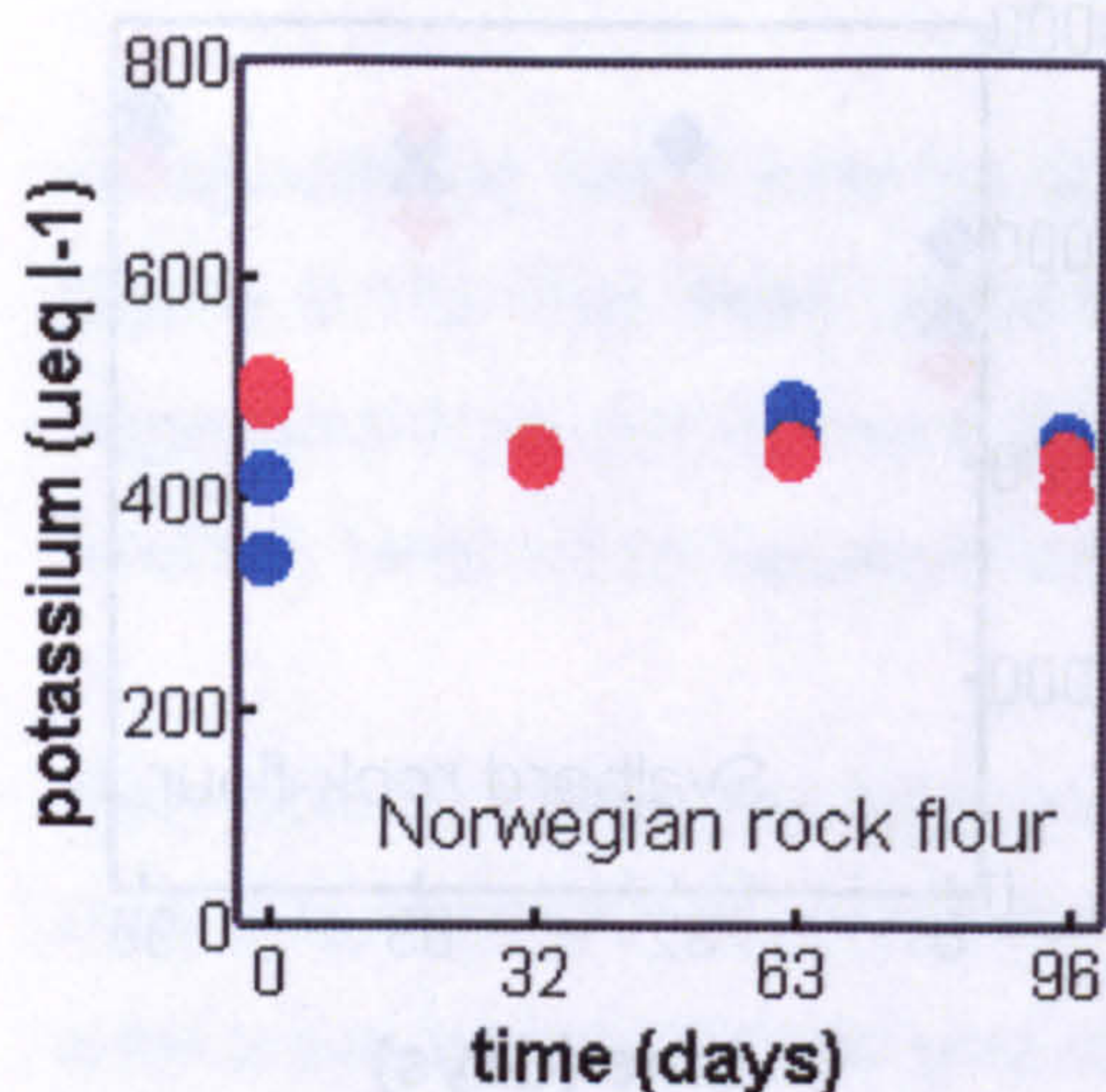


**Figure 6.34.** Potassium concentrations in meltwaters incubated at +1.6 °C with rock flours for 96 days. Subglacial meltwater taken from the Midre Lovénbreen glacier, Svalbard and rock flour from Bødalsbreen, Norway and Finsterwalderbreen, Svalbard. Symbols show values of two replicates (n=2). (●) = biotic test with Norwegian rock flour; (●) = abiotic control with Norwegian rock flour; (◆) = biotic test with Svalbard rock flour; (◆) = abiotic control with Svalbard rock flour.

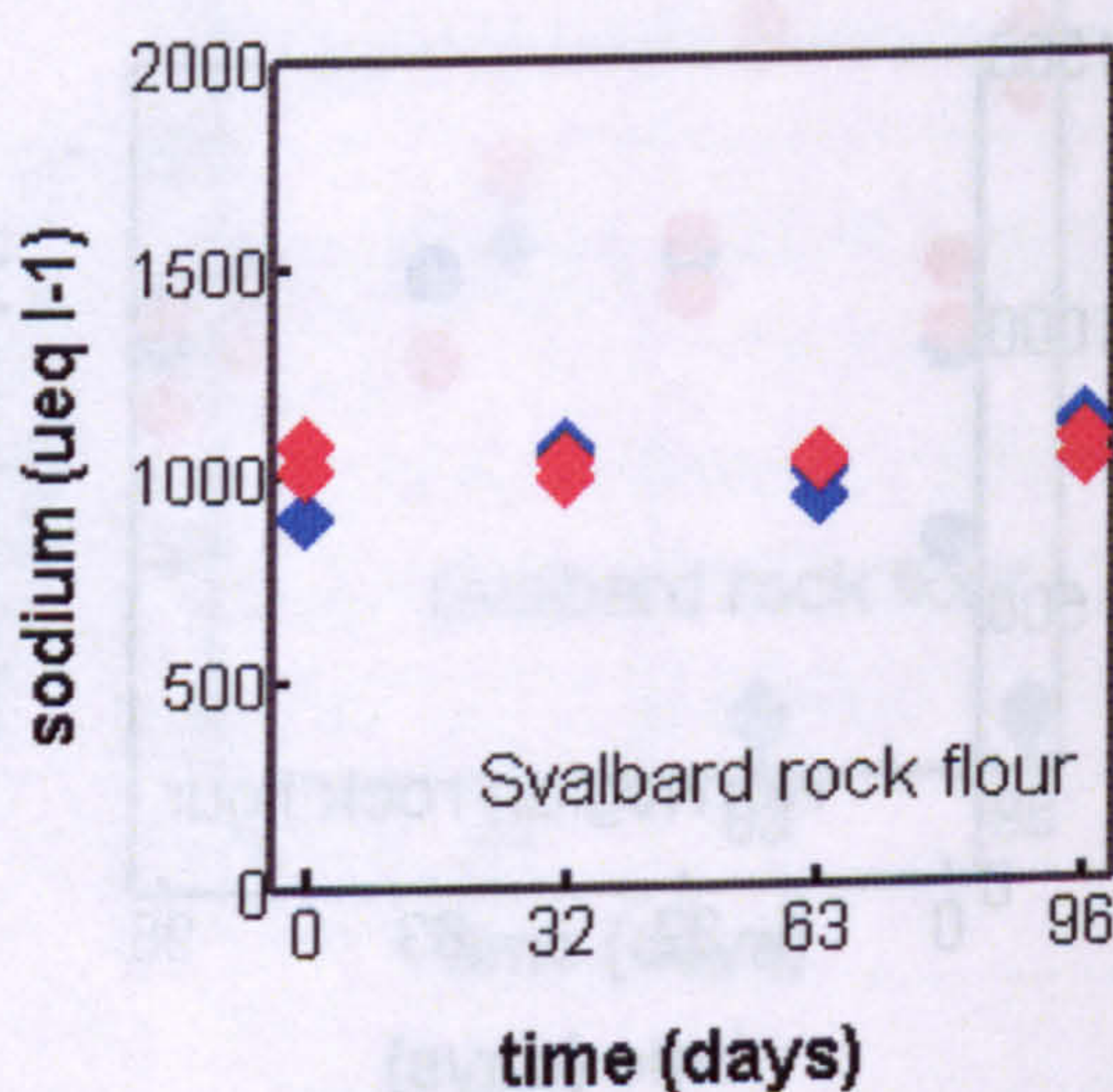
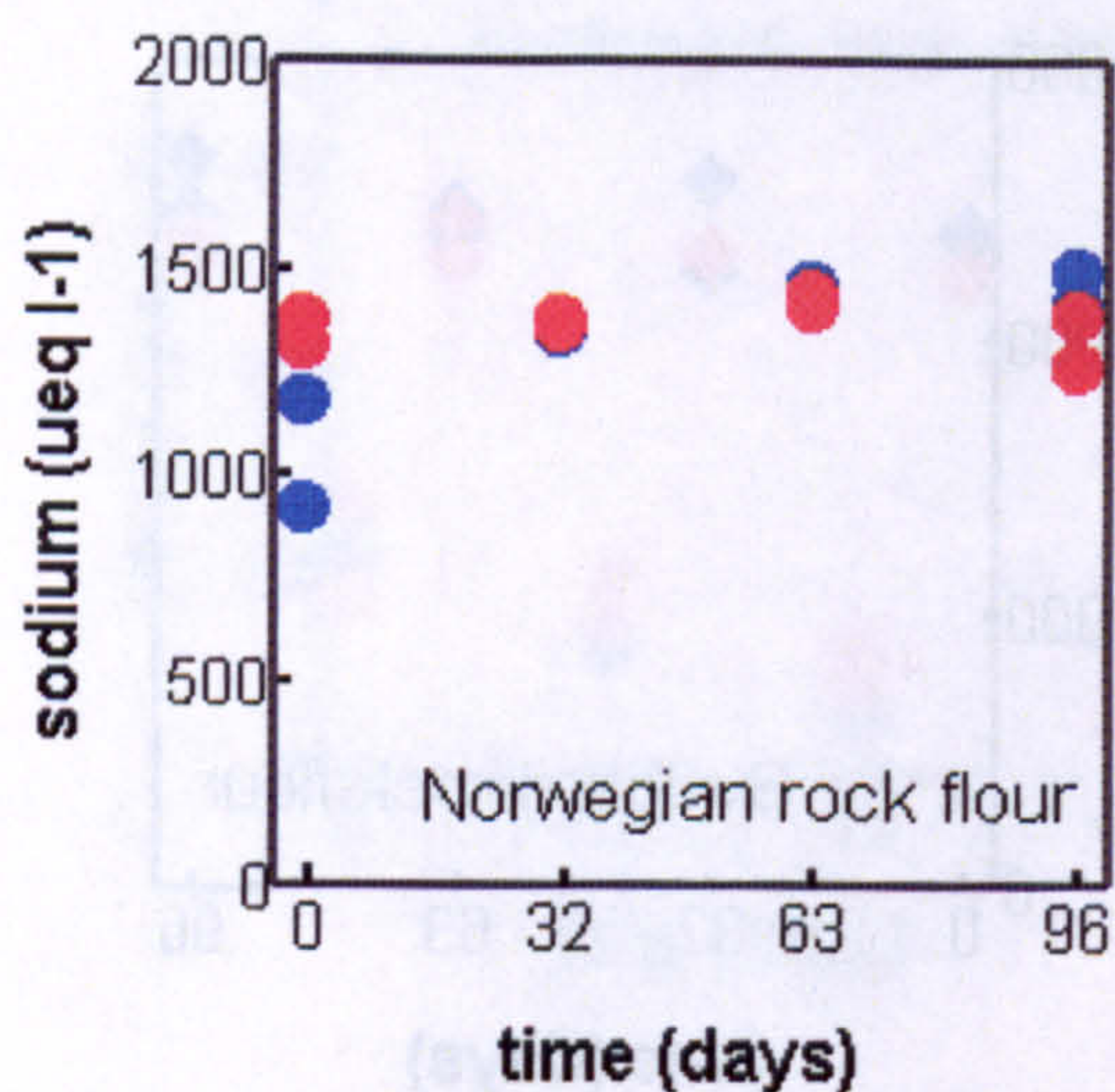


**Figure 6.35.** Sodium concentrations in meltwaters incubated at +1.6 °C with rock flours for 96 days. Subglacial meltwater taken from the Midre Lovénbreen glacier, Svalbard and rock flour from Bødalsbreen, Norway and Finsterwalderbreen, Svalbard. Symbols show values of two replicates (n=2). (●) = biotic test with Norwegian rock flour; (●) = abiotic control with Norwegian rock flour; (◆) = biotic test with Svalbard rock flour; (◆) = abiotic control with Svalbard rock flour.



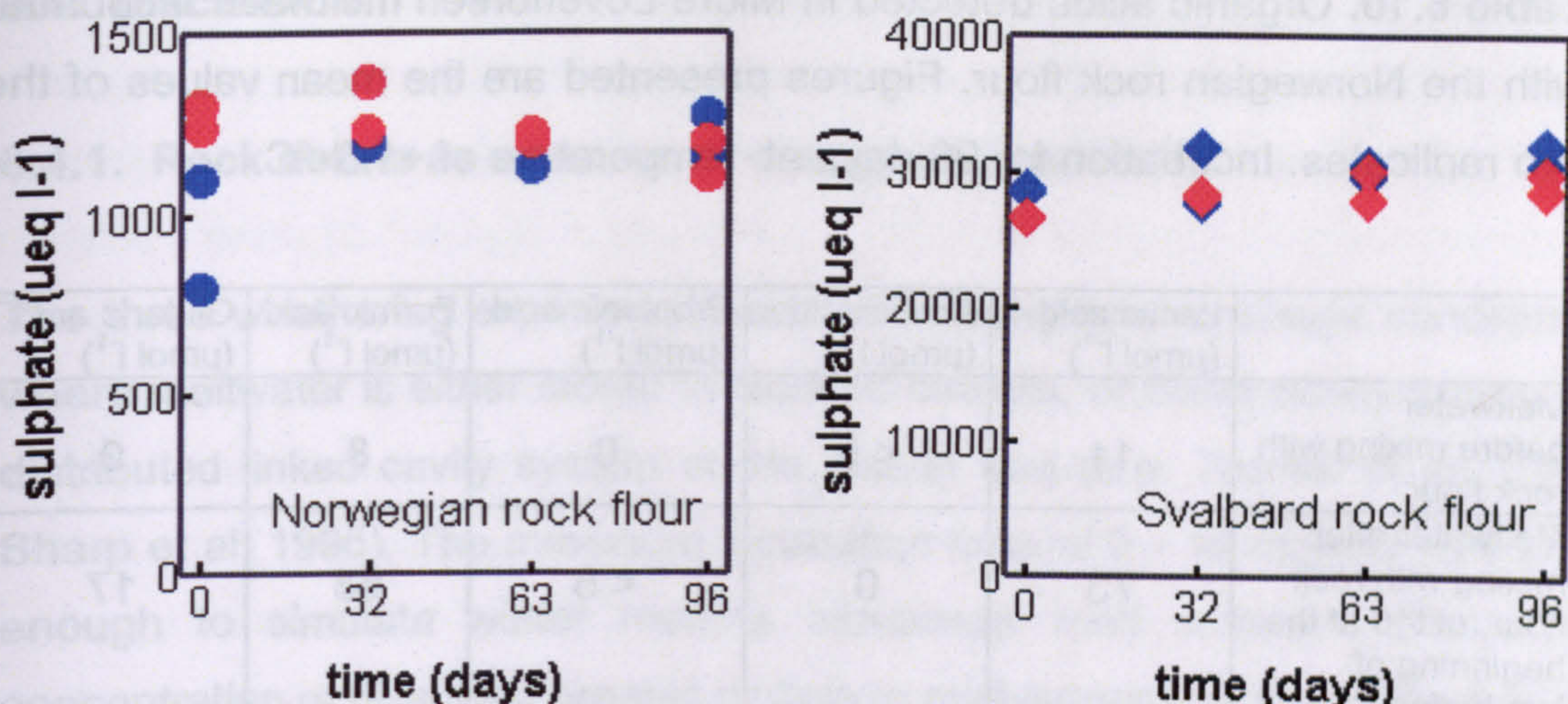


**Figure 6.36.** Sulphate concentrations in meltwaters incubated at +1.6 °C with rock flours for 96 days. Subglacial meltwater taken from the Midre Lovénbreen glacier, Svalbard and rock flour from Bødalsbreen, Norway and Finsterwalderbreen, Svalbard. Symbols show values of two replicates ( $n=2$ ). (●) = biotic test with Norwegian rock flour; (●) = abiotic control with Norwegian rock flour; (◆) = biotic test with Svalbard rock flour; (◆) = abiotic control with Svalbard rock flour.

#### 6.3.6. Organic acids in Svalbard meltwater incubated with rock flours

The analytical procedure of identifying and quantifying a range of organic acids present in meltwaters at the beginning and the end of incubation is described chapters 4.3.2.2 and 6.2.10. Low concentrations ( $\leq 10 \mu\text{mol l}^{-1}$ ) of lactic acid, acetic acid, and formic acid were detected in the meltwater from Svalbard, before mixing with rock flours. Immediately after mixing, lactic acid and formic acid were released from the Norwegian rock flour (table 6.10), and propionate was released from the Svalbard rock flour (table 6.11). Microbes utilised all the formate and propionate available in three months, whereas there was no consumption of lactate. In sterile control conditions, the concentrations of organic acids increased. Similarly, glutarate, which was present only in meltwater incubated with the Norwegian rock flour, was entirely used by microbes in three months. (As described in the chapter 6.2.10., identification of glutarate was merely a tentative result, not to be taken as a confirmed quantitative result).



**Table 6.10.** Organic acids detected in Midre Lovénbreen meltwater incubated with the Norwegian rock flour. Figures presented are the mean values of the two replicates. Incubation for 96 days at temperature of +1.6 °C.

	Lactic acid ( $\mu\text{mol l}^{-1}$ )	Acetic acid ( $\mu\text{mol l}^{-1}$ )	Propionic acid ( $\mu\text{mol l}^{-1}$ )	Formic acid ( $\mu\text{mol l}^{-1}$ )	Glutaric acid ( $\mu\text{mol l}^{-1}$ )
Meltwater before mixing with rock flour	11	< 5	0	8	0
Meltwater after mixing with rock flour, at t=0 at the beginning of incubation	73	0	< 5	68	17
BIOTIC system, Meltwater with rock flour at the end of incubation	75	0	0	0	0
ABIOTIC control, Meltwater with rock flour at the end of incubation	108	0	5	98	28

**Table 6.11.** Organic acids detected in Midre Lovénbreen meltwater incubated with the Svalbard rock flour. Figures presented are the mean values of the two replicates. Incubation for 96 days at temperature of +1.6 °C.

	Lactic acid ( $\mu\text{mol l}^{-1}$ )	Acetic acid ( $\mu\text{mol l}^{-1}$ )	Propionic acid ( $\mu\text{mol l}^{-1}$ )	Formic acid ( $\mu\text{mol l}^{-1}$ )	Glutaric acid ( $\mu\text{mol l}^{-1}$ )
Meltwater before mixing with rock flour	11	< 5	0	8	0
Meltwater after mixing with rock flour, at t=0 at the beginning of incubation	0	0	250	0	0
BIOTIC system, Meltwater with rock flour at the end of incubation	0	0	0	0	0
ABIOTIC control, Meltwater with rock flour at the end of incubation	0	0	332	0	0



## 6.4. Discussion

### 6.4.1. Rock debris as a source of energy and nutrients

The three weathering experiments simulated subglacial drainage conditions, where meltwater is either stored in isolated cavities, or flows slowly through a distributed linked cavity system at the glacier bed (e.g. Tranter et al. 1993, Sharp et al. 1995). The maximum incubation time of 3 - 10 months was long enough to simulate winter months inbetween melt seasons. Since the concentration of dissolved organic carbon in meltwaters was low (from 6 to 12  $\mu\text{mol l}^{-1}$  in Bødalsbreen, Norway, from 400 to 450  $\mu\text{mol l}^{-1}$  in Midre Lovénbreen, Svalbard), the main potential source of energy and nutrients for bacteria in meltwater was assumed to be the freshly comminuted rock flour, including reduced inorganic compounds and organic carbon mixed within rock debris .

The first weathering experiment at +7 °C was conducted with coarse-grained proglacial rock debris (approximately 40 weight-% of grains > 500  $\mu\text{m}$ , figures 6.1 and 6.2) and early melt season meltwater, with a rock debris-meltwater ratio of 0.10 g  $\text{ml}^{-1}$ . Rock debris was mainly composed of silicates rich in quartz and feldspars, and had an organic carbon content of 0.03% (table 6.1), thus potentially releasing organic carbon to meltwater with hypothetical maximum dissolved organic carbon concentration of 2.5  $\mu\text{mol ml}^{-1}$ . Compared with the DOC concentration of 0.012  $\mu\text{mol ml}^{-1}$  in the Bødalsbreen meltwater that was used in the experiment, rock debris provided superior source of organic carbon for heterotrophic micro-organisms. The *in situ* -temperature of the micro-organisms attached to mineral grains ranged from +2.8 to +8.8 °C (chapter 6.1.1). When this mixed population of microbes was incubated in oligotrophic meltwater - rock debris mixture, bacteria were able to grow, most likely deriving nutrients from rock debris. After two weeks, the total number of bacteria in meltwater was above 7.0  $\log_{10}$  cells  $\text{ml}^{-1}$  (figure 6.3). Comparable numbers of total bacteria have been found from Alpine glaciers in debris rich ice (7.0  $\log_{10}$  cells  $\text{ml}^{-1}$ ) and melt-out till (7.2  $\log_{10}$  cells  $\text{ml}^{-1}$ ), with a sediment content of 1.14 g  $\text{ml}^{-1}$  and organic carbon content of 0.3% (Sharp et al. 1999).



The second weathering experiment was conducted at a temperature range from  $-1.2\text{ }^{\circ}\text{C}$  to  $+2.6\text{ }^{\circ}\text{C}$ , equivalent to *in situ*-temperatures in subglacial meltwater streams (Brown et al. 1994a, Skidmore et al. 2000). Fine-grained rock flour with a grain size  $\leq 300\text{ }\mu\text{m}$  was used (figure 6.9). Fine sediment particles with fresh mineral surfaces are better than coarse sandy sediment as a microbial substrate (Gilichinsky et al. 1995). The sediment content after mixing rock flour and meltwater was  $1.00\text{ g ml}^{-1}$ . The maximum suspended sediment concentration observed in a proglacial bulk stream in an Alpine warm-based glacier was only  $0.004\text{ g ml}^{-1}$  (Brown et al. 1994a), and in a high Arctic cold-based glacier  $0.016\text{ g ml}^{-1}$  (Hodgkins et al. 1998). However, at the ice-till interface, where a deformable bed is composed largely of fine-grained sediments, rock debris to meltwater ratios can be several orders of magnitude higher, especially in lenses of water-laid sorted sediments within the till (Walder and Fowler, 1994).

In the second weathering experiment, two types of rock flours from proglacial outwash plains in Norway and Svalbard, with different elemental and mineralogical composition and nutrient content, were used to study the impact of microbial growth and activity on chemical weathering. Again, due to initially low dissolved organic carbon concentration in the Bødalsbreen meltwater, the main potential source of energy and nutrients for micro-organisms was rock flour mixed with the meltwater (tables 6.4, 6.5 and 6.12). Rock flour from the Svalbard proglacial outwash plain was expected to be superior as a carbon and energy source, due to the higher content of nutrients (table 6.12). Nevertheless, the bacterial population which originated from the Norwegian meltwater gained a higher total number of cells ( $7.25\text{ log}_{10}\text{ cells ml}^{-1}$  in 17 days) when incubated with the Norwegian rock flour (figure 6.10). When incubated with the Svalbard rock flour, growth started after a lag phase of several weeks and population density at its highest was  $7.00\text{ log}_{10}\text{ cells ml}^{-1}$ . Apparently the bacteria needed time to adapt to an environment which differed greatly from their original oligotrophic habitat. As stated by Vishnivetskaya et al (2000), micro-organisms which have been exposed to low temperature and starvation for long periods may not survive a sudden change to an environment rich in nutrients. The stress caused by a dramatic change can inhibit recovery of a fraction of microbial population. Moreover, incubation with Svalbard rock flour instantly resulted in relatively high solute



concentrations, especially  $\text{Mg}^{2+}$ ,  $\text{Ca}^{2+}$  and  $\text{SO}_4^{2-}$  (figures 6.22, 6.23 and 6.26) representing another cause of stress and requiring additional halotolerance. Salinity, however, did not inhibit growth and activity of all the microbes present, since, for example, microbial nitrate respiration took place even at  $-1^\circ\text{C}$  (figure 6.16). Psychrophilic and halophilic denitrifying bacteria growing in an environment of low dissolved carbon but high salt concentration have earlier been isolated from an ice-covered Antarctic lake (Ward and Priscu, 1997).

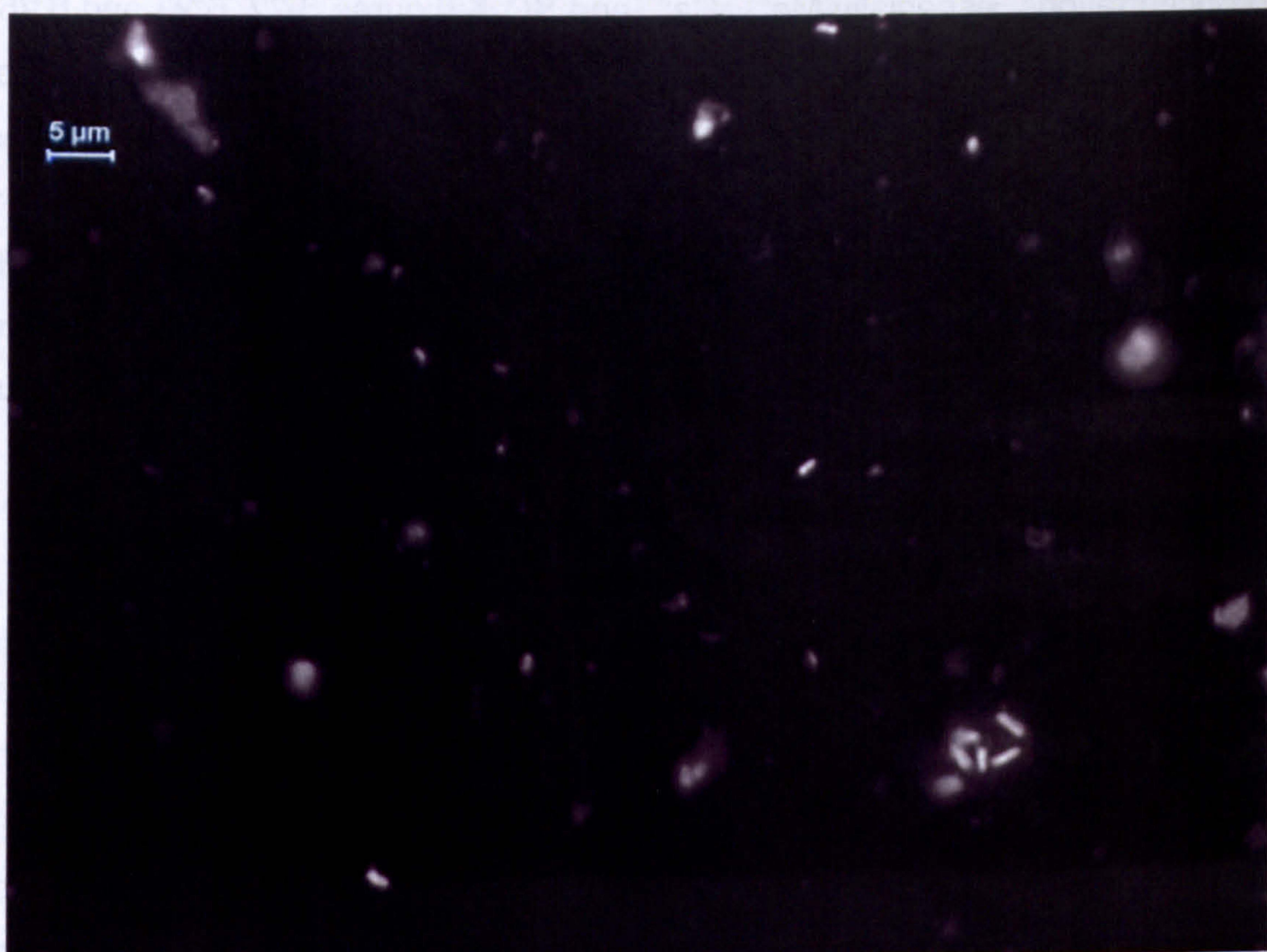
**Table 6.12.** Basic nutrients in the rock flours from the proglacial outwash plains in Norway and Svalbard.

	Norway	Svalbard
loss of ignition at $980^\circ\text{C}$ (%)	0.4	7.2
organic carbon (%)	0.01	0.70
nitrogen (%)	0.00	0.04
phosphorus (%)	0.15	0.15
ferric iron (%)	1.89	3.23

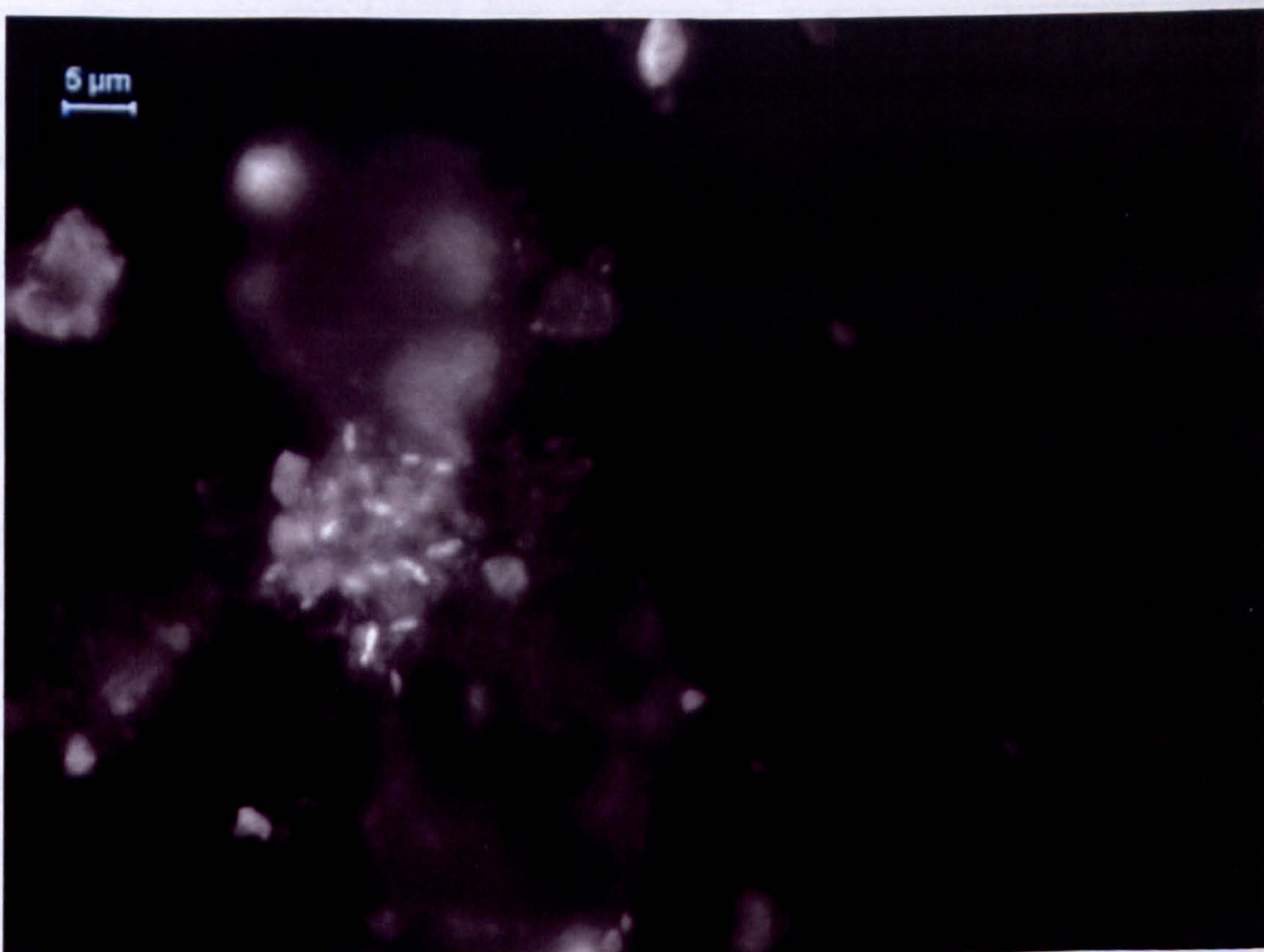
Although the total numbers of bacterial cells were lower in the meltwater incubated with the Svalbard rock flour, the morphology and size of the growing cells revealed the positive effect of nutrients. When incubated with the Norwegian rock flour, the size of coccus or rod shaped cells ranged from  $0.5$  to  $2\ \mu\text{m}$ , whereas when the Svalbard rock flour was used, the size of rod shaped cells was  $1 - 3\ \mu\text{m}$  (figure 6.37).

The third weathering experiment with fresh meltwater from Svalbard did not show any difference in the total number of bacteria when incubated with Norwegian and Svalbard rock flours at  $+1.6^\circ\text{C}$  (figure 6.28). However, reduction of nitrate from  $50\ \mu\text{eq l}^{-1}$  to zero (figure 6.31) indicated that anaerobic nitrate reducing bacteria became active only when incubated with Svalbard rock flour. Microbes had to adapt to a new lithological and nutritional environment, and therefore microbially accelerated dissolution of  $\text{Mg}^{2+}$  and  $\text{Ca}^{2+}$  from the Norwegian rock flour initiated after a lag phase of two months.





(A)



(B)

**Figure 6.37.** Images of bacteria cells growing in meltwater incubated with (a) Norwegian rock flour and (b) Svalbard rock flour.



#### **6.4.2. Carboxylic acids as a source of carbon**

Carboxylic acids in soil and natural waters may be derived from decomposition of plants and animal residues (Prapaipong et al. 1999). Norwegian and Svalbard rock debris samples were taken from the surface of the proglacial outwash plain. Decomposition of phototrophic algae is thus the likely source of mono- and dicarboxylic acids released from the Norwegian rock flour. The other potential source of carboxylic acids in the Svalbard rock flour was polymerised molecules with carboxyl groups originating from shales. Although the rock flours were heated at 120 °C before mixing with meltwater, some of the carboxylic acids did not decompose, but were released to meltwater immediately after mixing with rock flours (tables 6.7, 6.8, 6.10 and 6.11). Before mixing, only a residue of formic acid was detected in the Norwegian meltwater, whereas in the Svalbard meltwater, also lactic acid and acetic acid were found. This was concurrent with the fact that the total dissolved organic carbon concentration in the Svalbard meltwater was initially 35 times as high as in the Norwegian meltwater. Moreover, the weathering experiment with the Svalbard meltwater was set up two days after sampling the meltwater (chapter 6.3.1), whereas the Norwegian meltwater was stored at +2 °C before starting the experiment (chapter 6.2.1) and therefore concentrations of organic acids in the meltwater had likely been reduced by slow biodegradation.

In permanently cold marine sediments, sulphate reducers, which use acetate, propionate, lactate, butyrate and hydrogen as their carbon and energy sources (Parkes et al. 1989), are responsible for up to 50% of the organic carbon remineralization (Jørgensen 1982; Nedwell et al. 1993). Culturable anaerobic heterotrophic bacteria which used nitrate or sulphate as an electron acceptor (SRB-medium based on Postgate 1984 and NRB-medium based on Cragg et al. 1990) were present in subglacial drainage systems in all the glaciers studied in Greenland, Norway and Svalbard (see chapter V). In the subsequent weathering experiments, bacteria in subglacial meltwaters from Norway and Svalbard were active at +0.2 - +2.6 °C and utilised formate, acetate and propionate as substrates (tables 6.7, 6.8, 6.10 and 6.11), and O<sub>2</sub> or NO<sub>3</sub> as an electron acceptor (figures 6.5, 6.11, 6.15, 6.16 and 6.31).



### 6.4.3. Solute acquisition accelerated by microbial activity

After two weeks at the incubation temperature of +7 °C, the exponential growth phase of the mixed bacterial population in meltwater was over (figure 6.3), and nitrate-reducing bacteria were utilising nitrate in meltwater (figure 6.5 and table 6.13). At this point, the microbial production of organic ligands was not adequate to decrease the pH of meltwater (figure 6.4) but through some other mechanism microbial activity accelerated dissolution of  $\text{Mg}^{2+}$  (figure 6.6). After three months, slightly elevated concentration of  $\text{SO}_4^{2-}$  was detected in the biotic systems (figure 6.8). This timescale (table 6.13) is consistent with findings by Bennett et al. (2001), which confirmed biological weathering of silicates after three months at *in situ*-temperature in an aquifer in Minnesota (presumably +6 - +8 °C). At the lower temperature of +0.2 - +2.6 °C, nitrate concentration was reduced after four weeks (figures 6.15 and 6.16 and table 6.13). Rock flour was fine-grained and provided plenty of fresh and reactive mineral surfaces for attaching micro-organisms (table 6.13). Microbial activity resulted in elevated concentrations of  $\text{Mg}^{2+}$  and  $\text{Ca}^{2+}$  (figures 6.17 and 6.19 and table 6.13) and later  $\text{K}^+$  and  $\text{Na}^+$  (figures 6.19 and 6.20). After seven months, the impact of microbial activity on concentration of  $\text{SO}_4^{2-}$  was obvious (figure 6.21). Interestingly, bacteria were not able to speed up dissolution of  $\text{SO}_4^{2-}$  at +0.2 to +0.5 °C, but only at +1.6 to +2.6 °C, whereas the impact on the release of major cations was equal at both incubation temperatures. Rapid acquisition of  $\text{Mg}^{2+}$ ,  $\text{Ca}^{2+}$  and  $\text{HCO}_3^-$  with respect to  $\text{SO}_4^{2-}$  has been detected also in subglacial meltwaters from an Alpine glacier which contains trace amounts of carbonate in the bedrock (Tranter et al. 2002). In addition, Brown et al. (1994) have postulated that the release of sulphate through oxidation of sulphides in sediments is a slow process, possible only in subglacial waters with a long residence time at the glacier bed. This is concurrent with the results of our weathering experiment, showing that sulphate was released into the water several months later than major cations.



**Table 6.13.** Incubation times needed at a range of temperatures to detect the first signs of impact of microbial activity on solute concentrations in the meltwater mixed with the rock flour originating from quartzo-feldspathic gneiss from Bødalsbreen, Norway .

Incubation temperature and grain size * In rock flour °C	NO <sub>3</sub> <sup>-</sup> reduction	Accelerated dissolution of Mg <sup>2+</sup> and Ca <sup>2+</sup>	Accelerated dissolution of K <sup>+</sup> and Na <sup>+</sup>	Accelerated dissolution of SO <sub>4</sub> <sup>2-</sup>
+ 7.0 °C grain size 100-1000 µm	2 weeks	2 weeks (Mg <sup>2+</sup> )	> 14 weeks	> 14 weeks
+ 1.6 - +2.6 °C grain size 10-300 µm	4 weeks	4 weeks	4 weeks	> 19 weeks
+0.2 - +0.5 °C grain size 10-300 µm	4 weeks	4 weeks	4 weeks	no impact detected
-1.2 - -1.0 °C grain size 10-300 µm	no impact detected	no impact detected	no impact detected	no impact detected

\* Effect of grain size distribution on solute acquisition has to be considered, since surface area exposed to solution increases as particle size decreases.

Microbial activity accelerated the release of both alkali elements (K<sup>+</sup>, Na<sup>+</sup>) and earth alkaline elements (Mg<sup>2+</sup>, Ca<sup>2+</sup>) (table 6.14), but the dissolution rate of K<sup>+</sup> and Na<sup>+</sup> was slower than that of Mg<sup>2+</sup> and Ca<sup>2+</sup> (table 6.13). Prompt increase in Ca<sup>2+</sup> and Mg<sup>2+</sup> concentrations was likely to be the result of microbial activity stimulating enhanced carbonate dissolution, whereas slower release of Mg<sup>2+</sup> and Ca<sup>2+</sup> was linked with biological weathering of silicates (table 6.6). Rapid and simultaneous release of Mg<sup>2+</sup> and Ca<sup>2+</sup> indicates that the source mineral may have been dolomite. The Ca/Mg ratio (by weight) of dolomitic carbonate rocks varies from <10 to 90 (Hitchon et al. 1999). Elevated K<sup>+</sup> and Na<sup>+</sup> concentrations may have arisen because of ion exchange of some of the divalent ions back onto the silicate mineral particles, or because the microbial respiration stimulated micro-regions of lower pH.

In the biotic aerobic system with the Norwegian rock flour, there was a relatively good linear regression between (Ca<sup>2+</sup>+ Mg<sup>2+</sup>) and SO<sub>4</sub><sup>2-</sup>, with an r<sup>2</sup>



value of 0.62, whereas in sterile conditions there was no correlation (figure 6.38(a)). The scatterplot of  $\text{Ca}^{2+}+\text{Mg}^{2+}$  versus  $\text{SO}_4^{2-}$ , however, shows that concentrations did not increase steadily and concurrently, and the sources of solutes were different minerals and various weathering processes. First carbonates and silicates were weathered, resulting in release of cations, and much later sulphides were oxidised by chemolithotrophic micro-organisms. At the end of 300 days incubation,  $\text{Na}^+$ ,  $\text{Ca}^{2+}$  and  $\text{SO}_4^{2-}$  were the main ions in the meltwater. The dominance of these solutes could also be seen in the proglacial bulk stream in Bødalsbreen during early melt season, circumstances the laboratory experiments were designed to simulate (table 6.14). The differences in the overall concentrations between samples from the laboratory experiment and the field site are due to dilution with icemelt at Bødalsbreen.

**Table 6.14.** The major cations and anions in Bødalsbreen meltwater  
**(a)** after 300 days of laboratory incubation in aerobic conditions with microbes deriving energy and nutrients from the rock flour at +1.6 to +2.6 °C ; **(b)** after 300 days abiotic incubation with the rock flour (sterile controls) at +1.6 to +2.6 °C and **(c)** after a long residence time in the subglacial drainage system (sampling at the early melt season from the bulk meltwater stream). Comparison of equality of means between biotic (a) and abiotic (b) systems with the pooled-variance t-test.

	(a) laboratory incubation with rock flour (mean ± SD $\mu\text{eq l}^{-1}$ , n=3)	(b) laboratory incubation sterile control (mean ± SD $\mu\text{eq l}^{-1}$ , n=3)	(c) early melt season sample from the field site ( $\mu\text{eq l}^{-1}$ )	pooled- variance t-test  t-value	pooled- variance t- test  p
$\text{Ca}^{2+}$	670 ± 53	176 ± 30	92	14.074	< 0.001
$\text{Mg}^{2+}$	342 ± 9	77 ± 15	14	26.128	< 0.001
$\text{K}^+$	457 ± 10	233 ± 21	9	16.913	< 0.001
$\text{Na}^+$	991 ± 31	742 ± 48	47	7.535	0.002
$\text{SO}_4^{2-}$	624 ± 48	237 ± 13	62	13.556	< 0.001
$\text{NO}_3^-$	24 ± 4	39 ± 6	9	-3.734	0.020
$\text{Cl}^-$	198 ± 10	210 ± 50	50	-0.400	0.709
pH	7.5 ± 0.01	7.6 ± 0.05	6.3	-4.801	0.034



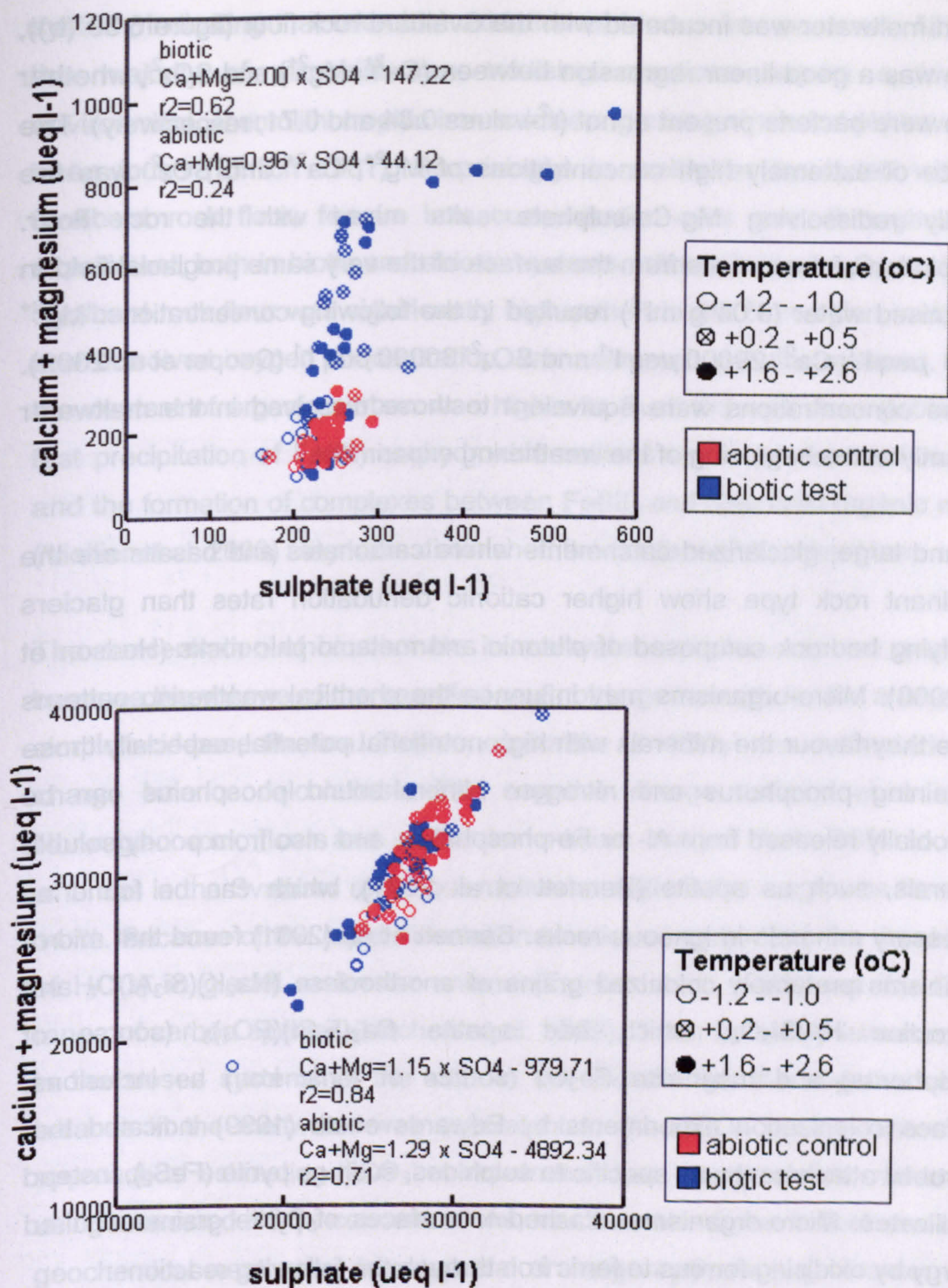
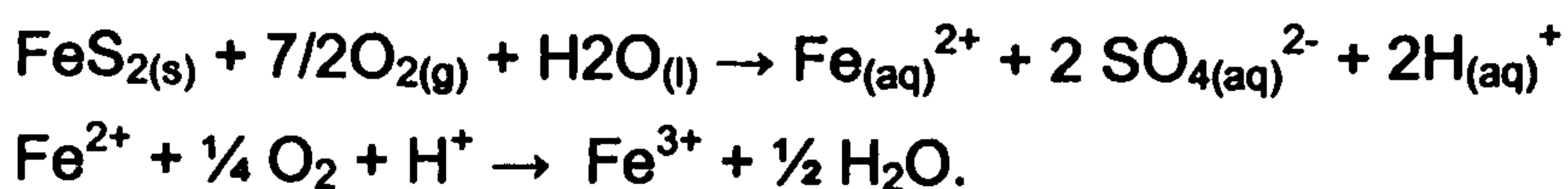


**Figure 6.38.** Scatterplot of  $\text{Ca}^{2+}$  and  $\text{Mg}^{2+}$  versus  $\text{SO}_4^{2-}$  in meltwaters incubated with (a) Norwegian rock flour and (b) Svalbard rock flour at a range of temperatures ( $n=24$ ). (●) = biotic test at +1.6 - +2.6 °C; (⊗) = biotic test at +0.2 - +0.5 °C; (○) = biotic test at -1.2 - -1.0 °C; (●) = abiotic control at +1.6 - +2.6 °C; (⊗) = abiotic control at +0.2 - +0.5 °C; (○) = abiotic control at -1.2 - -1.0 °C.



When meltwater was incubated with the Svalbard rock flour (figure 6.38 (b)), there was a good linear regression between  $(\text{Ca}^{2+} + \text{Mg}^{2+})$  and  $\text{SO}_4^{2-}$ , whether there were bacteria present or not ( $r^2$ -values 0.84 and 0.71, respectively). The source of extremely high concentrations of  $\text{Mg}^{2+}$ ,  $\text{Ca}^{2+}$  and  $\text{SO}_4^{2-}$  was the rapidly redissolving Mg-Ca-sulphate salts mixed with the rock flour. Dissolution of these salts from the surface of the very same proglacial field in de-ionised water ( $0.04 \text{ g ml}^{-1}$ ) resulted in the following concentrations:  $\text{Mg}^{2+}$   $1500 \mu\text{eq l}^{-1}$ ;  $\text{Ca}^{2+}$   $29000 \mu\text{eq l}^{-1}$  and  $\text{SO}_4^{2-}$   $30000 \mu\text{eq l}^{-1}$  (Cooper et al. 2002). These concentrations were equivalent to those dissolved in the meltwater instantly at the beginning of the weathering experiment.

By and large, glacierized catchments where carbonates and basalts are the dominant rock type show higher cationic denudation rates than glaciers overlying bedrock composed of plutonic and metamorphic rocks (Hodson et al. 2000). Micro-organisms may influence the chemical weathering patterns since they favour the minerals with high nutritional potential, especially those containing phosphorus and nitrogen. Mineral-bound phosphorus can be microbially released from Al- or Fe-phosphates, and also from poorly soluble minerals, such as apatite (Bennett et al. 2001), which can be found as accessory minerals in igneous rocks. Bennett et al. (2001) found that micro-organisms preferably colonized grains of anorthoclase  $(\text{Na}_2\text{K})(\text{Si}_3\text{Al})\text{O}_8$  and microcline  $\text{KAlSi}_3\text{O}_8$ , which had apatite  $\text{Ca}_5(\text{F,Cl})(\text{PO}_4)_3$  (source of phosphorus) and magnetite  $\text{Fe}_3\text{O}_4$  (source of ferric iron) as inclusions. Surface colonization experiments by Edwards et al. (1999) indicated that microbial attachment was specific to sulphides, such as pyrite ( $\text{FeS}_2$ ), instead of silicates. Micro-organisms attached to surfaces of pyrite grains acquired energy by oxidising ferrous to ferric iron through the following reactions:



In the pores of the rock flour in our experiment, presence of anoxic micro-niches was possible, despite the overall solution remained oxic. Acquisition of iron from the Norwegian rock flour took place at the beginning of the experiment (figure 6.27). After this, the concentration of dissolved ferrous iron increased in sterile controls, whereas no ferrous iron was detected in biotic



system, indicating that microbial oxidation of ferrous iron occurred. Although the majority of microbial iron oxidising reactions require a low pH environment, chemolithotrophic iron oxidisers growing at neutral pH have also been found (Ehrlich 1981). Surprisingly, in meltwater incubated with the Svalbard rock flour, ferrous iron concentration was zero throughout the experiment, both in biotic and abiotic systems, although the  $\text{Fe}_2\text{O}_3$  content in Svalbard rock flour was significantly higher than in the Norwegian rock flour, and dissolved oxygen concentration was near zero in biotic systems. Since the content of organic carbon was higher in Svalbard rock flour (table 6.5), fast precipitation of Fe(III) oxyhydroxide colloids in the presence of oxygen, and the formation of complexes between Fe(III) and dissolved organic matter (Viollier et al. 2000) may have diminished the content of dissolved iron.

The concentration of bicarbonate in meltwater samples was not analysed, because the volume of the samples was not large enough for the analysis by simple acid-base titration. The concentration of  $\text{HCO}_3^-$  was estimated using charge balance calculations. The negative charge balance error in the Norwegian rock flour and meltwater mixture ranged from 36% to 51%, whereas in the Svalbard rock flour-meltwater system the range was from 5 to 14 %. Because of the rapid dissolution kinetics of carbonate, the dominance of  $\text{HCO}_3^-$  in glacial meltwater anions (Tranter et al. 1993) and the Eh-pH range of carbon species (Hitchon et al. 1999), it can be safely assumed that in the closed systems of the vials in our experiment, the negative charge balance in the meltwater was equivalent to the  $\text{HCO}_3^-$  concentration. This approach of estimating  $\text{HCO}_3^-$  concentration from charge deficit, rather than using measured  $\text{HCO}_3^-$  concentrations, has been used also in field studies on geochemical weathering in subglacial drainage systems (e.g. Tranter et al. 2002).

Hydrogen ions used in weathering processes of minerals are mainly derived from the dissolution and dissociation of  $\text{CO}_2$ , but transfer of  $\text{CO}_2$  across the gas-liquid interface is normally slower than weathering and dissolution reactions. The  $p(\text{CO}_2)$  value gives information on the degree to which the chemical weathering environment is in equilibrium with atmospheric  $\text{CO}_2$  (Tranter et al. 2002). Low  $p(\text{CO}_2)$  values indicate chemical evolution in a



closed system, where rates of CO<sub>2</sub> consumption by weathering exceed renewal by CO<sub>2</sub> solution (Raiswell and Thomas 1984).

**Table 6.15.** Partial pressure of carbon dioxide  $p(\text{CO}_2)$  in the rock flour-meltwater mixture at the beginning and the end of incubation at +1.6 to +2.6 °C. Figures show the mean values and standard deviations of the three replicates. Calculations based on the following equation:  $\log p(\text{CO}_2) = \log(\text{HCO}_3^-) - \text{pH} + p\text{KCO}_2 + p\text{K}_1$ , where  $p\text{KCO}_2 = 1.12$  and  $p\text{K}_1 = 6.58$ .

	Norway biotic start	Norway biotic end	Norway abiotic start	Norway abiotic end	Svalbard biotic start	Svalbard biotic end	Svalbard abiotic start	Svalbard abiotic end
$\log_{10}p(\text{CO}_2)$	-5.34	-2.57	-4.32	-3.04	-3.23	-2.35	-1.74	-2.21
	$\pm 0.02$	$\pm 0.02$	$\pm 0.09$	$\pm 0.07$	$\pm 0.13$	$\pm 0.02$	$\pm 0.11$	$\pm 0.14$

At the very beginning of incubation, the headspace was filled with air, and also the air from the pores in the rock flour was released to the aqueous system. During the experiment, access of atmospheric CO<sub>2</sub> to the sealed vials was inhibited, and the only potential source of CO<sub>2</sub> was microbial respiration. If the system at the beginning of the experiment had been in equilibrium with the atmosphere,  $p(\text{CO}_2)$  value would have been 10<sup>-3.5</sup> bars. However, mixing with the Norwegian rock flour caused lowering of  $p(\text{CO}_2)$  (table 6.15) to the level typical for closed-system conditions found in the subglacial meltwaters (Raiswell and Thomas 1984, Thomas and Raiswell 1984). Also, according to Tranter et al. (1993), low  $p(\text{CO}_2)$  values are common when large supply of reactive, comminuted rock is brought into contact with relatively pure water. Mixing with the Svalbard rock flour resulted in higher  $p(\text{CO}_2)$  value, most likely due to rapid oxidation of sulphides which generated acidity and produced H<sup>+</sup> to the solution. During the incubation, in the biotic systems with both Norwegian and Svalbard rock flours,  $p(\text{CO}_2)$  was elevated by microbial activity, producing CO<sub>2</sub> and exceeding the consumption of protons needed in weathering processes.



## **CHAPTER VII CONCLUSIONS**

### **7.1. Presence of microbial populations in meltwaters**

The focus of this research was the presence and activity of microbial populations in glacial drainage systems, especially in subglacial meltwaters. The three field sites represented glaciers with different characteristics: a warm-based ice cap with several outlet glaciers in a maritime climate in Norway, a subarctic polythermal-based inland ice sheet in Greenland, and a polythermal-based valley glacier in a High Arctic climate in Svalbard. Lithologies ranged from Precambrian metamorphic gneisses and quartzites to Carboniferous and Permian sedimentary rocks.

Bacterial populations growing at +2 °C – including culturable nitrate- and sulphate-reducing bacteria - were found in subglacial meltwaters from the Greenland Ice Sheet, the Jostedalsbreen ice cap in Norway and the Midre Lovénbreen valley glacier in Svalbard. The total number of bacteria ranged from 3.40 – 4.63 log<sub>10</sub> cells ml<sup>-1</sup> (from 2.51×10<sup>3</sup> to 4.27×10<sup>4</sup> cells ml<sup>-1</sup>), giving lower numbers than in surface waters on average (10<sup>6</sup> cells ml<sup>-1</sup> in lake waters and 10<sup>4</sup> - 10<sup>6</sup> cells ml<sup>-1</sup> in oceans) (Kjelleberg et al. 1993b), and also lower densities of bacterial cells than in Alpine valley glaciers, where the total number of bacterial cells in meltwaters ranged from 4.72 to 5.74 log<sub>10</sub>cells ml<sup>-1</sup> (Sharp et al. 1999). When changes in discharge rates in meltwater streams were considered, the total microbial biomass in the main meltwater streams from early to mid-melt season in the Manitsoq glacier (Greenland) and the Bødalsbreen glacier (Norway) ranged from 10.50 to 11.16 log<sub>10</sub> cells s<sup>-1</sup> and from 10.28 to 10.73 log<sub>10</sub> cells s<sup>-1</sup>, respectively. Although meltwaters were more diluted with snow and ice melt in the mid-melt season, enhanced flushing of the subglacial sediments increased the total microbial biomass at both glaciers.

All the meltwaters studied had very low suspended sediment concentrations (ranging from 0.003 g l<sup>-1</sup> to 0.94 g l<sup>-1</sup>). Unattached bacterial cells detected in subglacial meltwaters represented only a small proportion of the total number of cells in rock flours at the base of glaciers. Nevertheless, there is likely to be a constant exchange of microbes between the attached and unattached



communities (Madsen and Ghiorse 1993) at the ice-till interface. Therefore, unattached and attached communities probably represented overlapping components of an entire microbial community in the subglacial drainage system. Some of the bacterial cells detected in meltwaters were ultramicrobacteria, with coccus-shaped cells smaller than 0.5  $\mu\text{m}$ . Ultramicrobacteria, which have shrunk in size to 0.1 – 0.5  $\mu\text{m}$  due to starvation, become non-attachable, and they can remain in a state of suspended animation for very prolonged periods of time (Cullimore 1993). In the subglacial drainage systems, bacteria have to cope with a combined stress of starvation and low temperature, which explains the presence of unattached ultramicrobacteria in meltwaters. This may partly explain why the total number of bacteria did not correlate positively with suspended sediment concentration in meltwaters, as expected (Sharp et al. 1999).

The different size and thermal regime of the glaciers did not have an effect on the total number of bacterial cells. Also, despite the vast difference in concentration of dissolved organic carbon between Svalbard meltwater (407 – 453  $\mu\text{M}$ ) and Greenland and Norway early melt season meltwaters (22-52  $\mu\text{M}$  and 12-16  $\mu\text{M}$ , respectively), response of the total number of bacteria was not parallel. Significantly higher numbers of bacteria in meltwaters were discovered at the very early phase of melt season, when melting was minimal and no meltwater streams had formed yet. Hence, meltwater represented pure subglacial water, stored for several months in subglacial cavities. The long contact time with the rock flour favoured growth of bacterial populations, and no dilution with snow and ice melt scarce in bacteria was occurring.

## **7.2. Temperature characteristics of bacteria in meltwaters**

Although the *in situ* –temperature at the base of the glacier is continuously ca. 0 °C (Skidmore et al. 2000) and in subglacial meltwater streams from +0.5 to +2.5 °C (Brown et al. 1994a), the mixed populations of bacteria from subglacial drainage systems were active at a wide temperature range, from subzero to +31 °C. Sulphate-reducing bacteria in the subglacial drainage systems were adapted for activity at constantly low temperatures from 0 °C to +4 °C, but their optimum temperature varied from +10 to +32 °C. After 25



weeks of incubation, the activity of sulphate-reducing bacteria was detected also at the subzero temperature of  $-0.6\text{ }^{\circ}\text{C}$ . Estimated doubling times of bacterial populations in enrichment cultures, which had lactate and acetate as substrates, ranged from 3 days at  $+7\text{ }^{\circ}\text{C}$  and  $+12\text{ }^{\circ}\text{C}$  (cultures from Svalbard) to 12 days at  $+16\text{ }^{\circ}\text{C}$  (cultures from Norway).

Obligate anaerobic bacteria, such as sulphate-reducing bacteria, were present in the meltwaters throughout the melt season from April to August. Active sulphate-reducing bacteria were detected only in meltwaters dominated by waters from the subglacial drainage system, which demonstrates that there was no oxygen or only a limited amount of oxygen present in subglacial cavities. The dominance of psychrophilic, psychrotolerant or mesophilic bacteria changed from the pre-melt season to the late melt season. Interestingly, temporal changes in the dominance of psychrophilic and mesophilic micro-organisms was not identical in the Manitsog glacier in Greenland and the Jostedalsgreen ice cap in Norway. In Greenland, sulphate reduction activity in the early melt season meltwater was dominated by mesophilic and psychrotolerant organisms with an optimum temperature of  $+25\text{ }^{\circ}\text{C}$ , whereas in Norway during the early melt season true psychrophiles and psychrotrophs with an optimum temperature of  $+13$  to  $+16\text{ }^{\circ}\text{C}$  were dominant. Differences in climate, bedrock topography and glacier morphology between the two glaciers had an impact on the development of the drainage systems and this may have had an effect on the temperature characteristics of early melt season sulphate-reducing bacteria.

The morphology of bacterial cells in mixed cultures of sulphate-reducing bacteria changed, depending on the incubation temperature. In cultures at  $+4\text{ }^{\circ}\text{C}$ , coccus-shaped cells about  $1\text{ }\mu\text{m}$  in diameter grew in clusters, whereas at  $+25\text{ }^{\circ}\text{C}$ , populations of spirillum-shaped and filamentous cells were dominant. The length of spirillum-shaped cells was approximately  $3\text{ }\mu\text{m}$ . Also, rod-shaped cells,  $\sim 2\text{ }\mu\text{m}$  in length, grew at  $+25\text{ }^{\circ}\text{C}$ . This demonstrates that at different temperatures, only a specific proportion of the mixed microbial population was growing, while the others were in a no-growth state or in a starvation-survival state.



### **7.3. Growth and activity of subglacial microbial populations**

Microbes originating from subglacial drainage systems were active at the temperature range from +0.2 °C to +2.6 °C, when incubated with proglacial rock flours without any additional substrates. As a source of energy and nutrients, they used organic acids released from rock flours, and oxidation of reduced inorganic constituents, such as sulphide minerals. Oxygen or nitrate were utilised as electron acceptors. Presence of sulphate-reducing bacteria in meltwaters demonstrated that after oxidation of organic matter underneath the ice have driven conditions anoxic, sulphate is used as an electron acceptor.

Decomposition of biodegradable detritus and polymerised molecules with carboxyl groups originating from shales were the likely source of mono- and dicarboxylic acids in rock flours. Organic acids, such as formate, acetate, propionate were entirely utilised by micro-organisms in meltwaters, in conditions which simulated subglacial isolated cavities during winter months. The metabolic activity of heterotrophic bacteria produced carbon dioxide, which was a potential source of protons, enhancing accelerated chemical weathering reactions. Oxygen was consumed slowly, and after 10 months, there was still some oxygen left in headspace. Hence, conditions were not suitable for the survival of obligate anaerobic micro-organisms, such as sulphate-reducers and methanogens. No methane production was detected.

Bacterial populations grew better when incubated with rock flour from their original environment, resulting in 10-fold increase in total number of bacteria in 17 days, compared to rock flour with different mineralogical composition, although higher in nutritional value. Growth with the different mineralogical substrate started after a lag phase of 2 - 3 weeks, showing bacterial ability of adaptation to the different habitat.

Microbial activity accelerated the release of alkali elements ( $K^+$ ,  $Na^+$ ) and earth alkaline elements ( $Mg^{2+}$ ,  $Ca^{2+}$ ), as well as sulphate ( $SO_4^{2-}$ ) from rock flours. Prompt increase in  $Ca^{2+}$  and  $Mg^{2+}$  concentrations was likely to be the result of microbial activity stimulating enhanced dolomitic carbonate dissolution, whereas slower increase in  $Mg^{2+}$  and  $Ca^{2+}$  concentrations was



linked with biological weathering of silicates. Elevated  $K^+$  and  $Na^+$  concentrations may have arisen because of ion exchange of some of the divalent ions back onto the silicate mineral particles, or because the microbial respiration stimulated micro-regions of lower pH. Sulphide oxidation was markedly slower process than biological weathering of silicates, and more than 19 weeks incubation was needed until oxidation of sulphides initiated. Microbes responsible for sulphide oxidation were active only at  $+1.6 - +2.6$  °C, whereas the impact of microbial activity on weathering of carbonates and silicates was indistinguishable at the temperature range from  $+0.2$  to  $+2.6$  °C. Unsurprisingly, low oxygen contents inhibited sulphate formation because oxidation of sulphides was limited. Alkali and earth alkaline elements were released to the same degree both in aerobic and anaerobic conditions. The results of the weathering experiments demonstrated that both chemoorganotrophic and chemolithotrophic bacteria are able to grow in simulated subglacial conditions, similar to those in distributed drainage systems. Their potential activity in subglacial cavities during winter months can accelerate chemical weathering rates. As a result, microbial activity has a marked impact on major ion concentrations in meltwaters, causing 1.3 to 4.4 times as high concentrations as in abiotic conditions. This effect is detected especially in the early melt season, when discharge is low and dilution of subglacial meltwater with snow and ice melt is minimal.







## REFERENCES

Abyzov, S.S. 1993. Microorganisms in the Antarctic Ice. In: Friedmann, E.I. Antarctic Microbiology. Wiley-Liss Inc, New York. p. 265-295.

Abyzov, S.S., Mitskevich, I.N. and Poglazova, M.N. 1998. Microflora of the Deep Glacier Horizons of Central Antarctica. *Microbiology*, Vol.67, No.4, p. 451-458.

Aghajari, N., Feller, G., Gerday, C. and Haser, R. 1998. Structures of the psychrophilic *Alteromonas haloplanctis*  $\alpha$ -amylase give insights into cold adaptation at a molecular level. *Structure*, Vol. 6, p. 1503-1516.

Amy, P.S., Pauling, C. and Morita, R.Y. 1983. Recovery from nutrient starvation by a marine *Vibrio* sp. *Applied and Environmental Microbiology*, Vol. 45, p. 1685-1690.

Austrheim H. & Mørk, M.B.E. 1988. The lower continental crust of the Caledonian mountain chain: evidence from former deep crustal sections in western Norway. In: Kristoffersen Y. (ed.). Progress in studies of the lithosphere in Norway. Proceedings of a meeting reporting progress in Norwegian research in the International Lithosphere Programme, held at Sundvollen, Norway, 12-13 November 1987. Norges Geologiske Undersøkelse, special publication no.3. p. 102-113.

Barnes S., Bradbrook S., Cragg B., Marchesi J.R., Weightman A.J., Fry J.C., Parkes R.J. 1998. Isolation of Sulfate-Reducing Bacteria From Deep Sediment Layers of the Pacific Ocean. *Geomicrobiology Journal*, Vol. 15, p. 67-83.

Battersby, N.S. 1988. Sulphate-Reducing Bacteria. In: Austin, B. (Ed.). Methods in Aquatic Bacteriology. John Wiley & Sons Ltd. ISBN 047191651X. p. 269-299.

Bennett, P.C., Rogers, J.R., Choi, W.J. and Hiebert, F.K. 2001. Silicates, Silicate Weathering, and Microbial Ecology. *Geomicrobiology Journal*, Vol. 18, p. 3-19.



Bennett, P.C., Engel, A.S. and Rogers, J.R. 2002. Microbes, Microbial Ecology, and the Mineral Surface. Abstracts of the William Smith Meeting, Geological Society, London, 22-23 October 2002.

Bickerton R.W. and Matthews J.A. 1993. 'Little Ice Age' variations of outlet glaciers from the Jostedalsbreen ice-cap, southern Norway: a regional lichenometric-dating study of ice-marginal moraine sequences and their climatic significance. *Journal of Quaternary Science*, Vol. 8, no.1, p. 45-66.

Bish, D.L & Reynolds Jr., R.C. 1989. Sample preparation for X-ray diffraction. *Reviews in Mineralogy* Vol.20. Mineralogical Society of America. p. 73-99.

Boulton, G.S. 1974. Processes and patterns of glacial erosion. In: Oates, R.D. (ed.), *Glacial Geomorphology*, State University, New York. p. 41-87.

Brown G.H., Sharp M.J., Tranter M., Gurnell A.M. and Nienow P.W. 1994a. Impact of post-mixing chemical reactions on the major ion chemistry of bulk meltwaters draining the Haut Glacier D'Arolla, Valais, Switzerland. *Hydrological Processes*, Vol.8, p. 465-480.

Brown G.H., Tranter M., Sharp M.J., Davies T.D. and Tsiouris S. 1994b. Dissolved oxygen variations in Alpine glacial meltwaters. *Earth Surface Processes and Landforms*, Vol. 19, p. 247-253.

Brown G.H., Tranter M. and Sharp M.J. 1996. Experimental investigations of the weathering of suspended sediment by Alpine glacial meltwater. *Hydrological Processes*, Vol. 10, p. 579-597.

Brown, G.H. 2002. Glacier meltwater hydrochemistry. *Applied Geochemistry*, Vol. 17, p. 855-833.

Campen, R.K., Sowers, T. and Alley, R.B. 2003. Evidence of microbial consortia metabolising within a low-latitude mountain glacier. *Geology*, Vol. 31, No. 3, p. 231-234.



Carpenter, E.J., Lin, S. and Capone, D.G. 2000. Bacterial Activity in South Pole Snow. *Applied and Environmental Microbiology*, Vol. 66, No.10, p. 4514-4517.

Christner, B.C., Mosley-Thompson, E., Thompson, L.G., Zagorodnov, V., Sandman, K. and Reeve, J.N. 2000. Recovery and Identification of Viable Bacteria Immured in Glacial Ice. *Icarus*, Vol. 144, p. 479-485.

Cline, J.D. 1969. Spectrophotometric determination of hydrogen sulphide in natural waters. *Limnology and Oceanography*, Vol. 14, p. 454-458.

Cooper, R.J., Wadham, J.L., Tranter, M., Hodgkins, R. and Peters, N.E. 2002. Groundwater hydrochemistry in the active layers of the proglacial zone, Finsterwalderbreen, Svalbard. *Journal of Hydrology*, Vol. 269, p. 208-223.

Cragg, B.A., Parkes, R.J., Fry, J.C., Herbert, R.A., Wimpenny, J.W.T. and Getliff, J.M. 1990. Bacterial biomass and activity profiles within deep sediment layers. *Proceedings of the Ocean Drilling Program, Scientific Results*, Vol. 112, p. 607-619.

Cullimore, D.R. 1993. *Practical Manual of Groundwater Microbiology*. Lewis Publishers. 412 p.

Dallmann W.K., Hjelle A., Ohta Y., Salvigsen O., Bjornerud M.G., Hauser E.C., Maher H.D. and Craddock C. 1990. Geological map of Svalbard 1:100,000, Sheet B11G Van Keulenfjorden. Norsk Polarinstitut, Oslo. 58 p. ISBN 82-90307-68-3.

Deming, J.W. 2002. Psychrophiles and polar regions. *Current opinion in Microbiology*, Vol. 5, p. 301-309.

Dionex Corporation. 1996. Introduction to the Dionex DX500 chromatography systems. Document No. 034892., revision 02.



DSMZ - Deutsche Sammlung von Mikroorganismen und Zellkulturen GmbH.  
German Collection of Microorganisms and Cell Cultures.

Duckworth, O.W. and Martin, S.T. 2001. Surface complexation and dissolution of hematite by C1 – C6 dicarboxylic acids at pH=5.0. *Geochimica et Cosmochimica Acta*, Vol. 65, p. 4289-4301.

Edwards, K.J., Goebel, B.M., Rodgers, T.M., Schrenk, M.O., Gihring, T.M., Cardona, M.M., Hu, B., McGuire, M.M., Hamers, R.J., Pace, N.R., Banfield, J.F. 1999. Geomicrobiology of Pyrite (FeS<sub>2</sub>) Dissolution: Case Study at Iron Mountain, California. *Geomicrobiology Journal*, Vol. 16, p. 155-179.

Ehrlich, H.L. 1981. Geomicrobiology. New York: Marcel Dekker.

Escher A. and Watt W.S. 1976. Summary of the geology of Greenland. In: Escher A. and Watt W.S. (eds.). Geology of Greenland. The Geological Survey of Greenland. ISBN 87-980404-0-5. p. 10-16.

Escher A., Sørensen K & Zeck H.P. 1976. Nagssugtoqidian mobile belt in West Greenland. In: Escher A. and Watt W.S. (eds.). Geology of Greenland. The Geological Survey of Greenland. ISBN 87-980404-0-5. p. 77-95.

European Standard EN 25814:1992. Water quality – Determination of dissolved oxygen – Electrochemical probe method (ISO 5814:1990).

Faure, G. 1998. Principles and Applications of Geochemistry. Prentice-Hall, Inc.

Feller, G., Narinx, E., Arpigny, J.L., Aittaleb, M., Baise, E., Genicot, S. and Gerday, C. 1996. Enzymes from psychrophilic organisms. *FEMS Microbiology Reviews*, Vol. 18, p. 189-202.

Feller, G. and Gerday, C. 1997. Psychrophilic enzymes: molecular basis of cold adaptation. *CMLS Cellular and Molecular Life Sciences*, Vol. 53, p. 830-841.



Feller, G., Arpigny, J.L., Narinx, E. and Gerday, C. 1997. Molecular Adaptations of Enzymes from Psychrophilic Organisms. *Comparative Biochemistry and Physiology*, Vol. 118A, No. 3, p. 495-499.

Fish, S.A., Shepherd, T.J., McGenity, T.J., Grant, W.D. 2002. Recovery of 16S ribosomal RNA gene fragments from ancient halite. *Nature*, Vol. 417, p. 432-436.

Fleming K.M., Dowdeswell J.A., Oerlemans J. 1997. Modelling the mass balance of northwest Spitsbergen glaciers and responses to climate change. *Annals of Glaciology*, Vol. 24, p. 203-210.

Flint, R.F. 1971. *Glacial and Quaternary Geology*, John Wiley and Sons, New York, 892 p.

Fountain, A.G. and Walder, J.S. 1998. Water flow through temperate glaciers. *Reviews of Geophysics*, Vol. 36, p. 299-328.

Friedmann, E.I. 1982. Endolithic microorganisms in the antarctic cold desert. *Science*, Vol. 215, p. 1045-1053.

Fristrup B. 1966. *The Greenland Ice Cap*. International Science publishers, Copenhagen. 312 p.

Fry, J.C. 1988. Determination of biomass. In: Austin, B. (ed.). *Methods in aquatic bacteriology*: Chichester, John Wiley and Sons. p. 27-72.

Gerday, C., Aittaleb, M., Arpigny, J.L., Baise, E., Chessa, J-P., Garsoux, G., Petrescu, I. and Feller, G. 1997. Psychrophilic enzymes: a thermodynamic challenge. *Biochimica et Biophysica*, Vol. 1342, p. 119-131.

Gerday, C., Aittaleb, M., Bentahir, M., Chessa, J-P., Claverie, P., Collins, T., D'Amico, S., Dumont, J., Garsoux, G., Georlette, D., Hoyoux, A., Lonhienne, T., Meuwis, M-A. and Feller, G. 2000. Cold-adapted enzymes: from fundamentals to biotechnology. *Trends in Biotechnology*, Vol. 18, p. 103-107.



Gilichinsky, D.A., Wagener, S. and Vishnevetskaya, T.A. 1995. Permafrost microbiology: Permafrost and Periglacial Processes, Vol. 6, p. 281-291.

Glasser N.F. and Hambrey M.J. 2001. Styles of sedimentation beneath Svalbard valley glaciers under changing dynamic and thermal regimes. *Journal of the Geological Society*, Vol. 158, no.4, p. 697-707.

Glasser N.F. and Hambrey M.J. 2002.  $\delta D$ - $\delta^{18}O$  relationships on a polythermal valley glacier: Midtre Lovénbreen, Svalbard. *Polar Research* Vol. 21, p. 123-131.

Gounot, A.M. 2001. Ecology of psychrophilic and psychrotrophic microorganisms in cold and frozen soils. In: Paepe, R. and Melnikov, V. (eds.). Permafrost Response on Economic Development, Environmental Security and Natural Resources. Proceedings of the NATO Advanced Research Workshop on Permafrost Response on Economic Development, Environmental Security and Natural Resources, Novosibirsk, Russia, 12-16 November 1998. p. 543-551.

Grust K., Käß W. & Nienow P. 2002. Lithium chloride as a tracer in glacier hydrology. Manuscript. Unpublished.

Herbert, R.A. 1986. The Ecology and Physiology of Psychrophilic Microorganisms. . In: Herbert, R.A. and Codd, G.A. (eds.). Microbes in Extreme Environments. Society for General Microbiology, Harcourt Brace Jovanovich Publishers, p. 1-23.

Hitchon, B., Perkins, E.H. and Gunter, W.D. 1999. Introduction to Ground Water Geochemistry. Geoscience Publishing Ltd. 310 p.

Hjelle A. 1993. Geology of Svalbard. Polarhåndbok no. 7. Norsk Polarinstitutt, Oslo. 162 p. ISBN 82-7666-057-6.



Hodgkins, R., Tranter, M. and Dowdeswell, J.A. 1997. Solute provenance, transport and denudation in a High Arctic glacierized catchment. *Hydrological Processes*, Vol. 11, p. 1813-1832.

Hodgkins, R., Tranter, M. and Dowdeswell, J.A. 1998. The hydrochemistry of runoff from a 'cold-based' glacier in the High Arctic (Scott Turnerbrean, Svalbard). In: Sharp, M., Richards, K.S. and Tranter, M. Glacier hydrology and hydrochemistry. John Wiley and Sons Ltd. p. 47-63.

Hodson A., Tranter M. & Vatne G. 2000. Contemporary rates of chemical denudation and atmospheric CO<sub>2</sub> sequestration in glacier basins: an Arctic perspective. *Earth Surface Processes and Landforms* 25(13), p. 1447-1471.

Holmquist, L. and Kjelleberg, S. 1993. Changes in viability, respiratory activity and morphology of the marine *Vibrio* sp. strain S14 during starvation of individual nutrients and subsequent recovery. *FEMS Microbiology Ecology*, Vol.12 (4), p. 215-224.

Isaksen, M.F. and Jørgensen, B.B. 1994. Thermophilic sulphate-reducing bacteria in cold marine sediment. *FEMS Microbial Ecology* Vo. 14, p. 1-8.

Isaksen, M.F. and Jørgensen, B.B. 1996. Adaptation of Psychrophilic and Psychrotrophic Sulfate-Reducing Bacteria to Permanently Cold Marine Environments. *Applied and Environmental Microbiology*, Vol. 62 (2), p. 408-414.

Jenkins, R. 1989. Modern Powder Diffraction - Instrumentation. *Reviews in Mineralogy* Vol.20. Mineralogical Society of America. p. 19-37.

Jobin Yvon/Emission Spectrometry Department. 1989. The Spectrometer JY 24 Sequential ICP. User Manual number 31 088 152.

Jones I.W. 2002. The Role of Terrestrial Ice in Global Geochemical Cycles. A dissertation submitted to the University of Bristol, Department of Geography.



Junge, K., Eicken, H. and Deming, J.H.W. 2001. An Arctic wintertime study of sea-ice bacteria: abundance, activity and diversity at *in situ* temperatures of –2 to –20 °C. Abstract N-201 of the American Society for Microbiology 101<sup>st</sup> Annual Meeting, 2001 May 20-24, Orlando, Florida.

Jørgensen, B.B. 1982. Mineralization of organic matter in the sea bed – the role of sulphate reduction. *Nature*, Vol. 296, p. 643-645.

Karl, D.M., Bird, D.F., Björkman, K., Houlihan, T., Shackelford, R. and Tupas, L. 1999. Microorganisms in the Accreted Ice of Lake Vostok, Antarctica. *Science*, Vol. 286, p. 2144-2147.

Khlebnikova, G.M., Gilichinsky, D.A., Fedorov-Davydov, D.C., Vorobyova, E.A. 1990. Quantitative evaluation of microorganisms in permafrost deposits and buried soils. *Microbiology*, Vol. 59, p. 106-112.

Kjelleberg, S., Albertson, N., Flärdh, K., Holmquist, L., Jouper-Jaan, Å., Marouga, R., Östling, J., Svenblad, B. & Weichart, D. 1993a. How do non-differentiating bacteria adapt to starvation? *Antonie van Leeuwenhoek*, Vol. 63, p. 333-341.

Kjelleberg, S., Flärdh, K.B.G., Nyström, T. & Moriarty, D.J.W. 1993b. Growth limitation and starvation of bacteria. In: Ford, T.E. (Ed.). *Aquatic Microbiology – An ecological approach*. Blackwell Scientific Publications. p. 289-320.

Kjøllmoen B (Ed.). 2001. Glaciological investigations in Norway in 2000. The Norwegian Water Resources and Energy Directorate (NVE). Report No 2. ISBN 82-410-0453-2. 122 p.

Knoblauch, C. and Jørgensen, B.B. 1999. Effect of temperature on sulphate reduction, growth rate and growth yield in five psychrophilic sulphate-reducing bacteria from Arctic sediments. *Environmental Microbiology*, Vol.1, No. 5, p. 457-467.



Knoblauch, C., Sahm, K. and Jørgensen, B.B. 1999. Psychrophilic sulfate-reducing bacteria isolated from permanently cold Arctic marine sediments: description of *Desulfofrigus oceanense* gen.nov., sp. nov., *Desulfofrigus fragile* sp. nov., *Desulfofaba gelida* gen. nov., sp. nov., *Desulfotalea psychrophila* gen. nov., sp. nov. and *Desulfotalea arctica* sp. nov. *International Journal of Systematic Bacteriology*, Vol. 49, p. 1631-1643.

Krumholz, L.R., McKinley, J.P., Ulrich, G.A. and Suflita, J.M. 1997. Confined subsurface microbial communities in Cretaceous rock. *Nature*, Vol. 386, p. 64-66.

Lafrenière, M.J. and Sharp M.J. The concentration and spectrofluorometric properties of Dissolved Organic Carbon in surface waters: interpreting the flow routing of runoff and DOC sources in glacial and non-glacial catchments. *Arctic, Antarctic and Alpine Research*. In press (submitted December 2002).

Langdahl, B.R. and Ingvorsen, K. 1997. Temperature characteristics of bacterial iron solubilisation and  $^{14}\text{C}$  assimilation in naturally exposed sulfide ore material at Citronen Fjord, North Greenland (83 °N), *FEMS Microbiology Ecology*, Vol. 23, p. 275-283.

Liestøl O. 1990. Glaciers in Kongsfjorden area. *Norsk Polarinstitutt Årbok* 1989, p. 51-61.

Madigan, M.T., J.M.Martinko and J.Parker (eds.).1997. Brock Biology of Microorganisms. Eight edition. 986 p.

Madsen, E.L. and Ghiorse, W.C. 1993. Groundwater microbiology: subsurface ecosystem processes. . In: Ford, T.E. (Ed.). Aquatic Microbiology – An ecological approach. Blackwell Scientific Publications. p. 167-213.

Malvern Instruments Inc. Mastersizer Reference Manual.



Morgan, P. and Dow, C.S. 1986. Bacterial Adaptation for Growth in Low Nutrient Environments. *In*: Herbert, R.A. and Codd, G.A. (eds.). *Microbes in Extreme Environments*. Society for General Microbiology, Harcourt Brace Jovanovich Publishers, p. 187-214.

Morita, R.Y. 1975. Psychrophilic bacteria. *Bacteriological Reviews*, Vol. 39, p. 144-167.

Morita, R.Y. 1986. Starvation and Miniaturisation of Heterotrophs, with Special Emphasis on Maintenance of the Starved Viable State. . *In*: Herbert, R.A. and Codd, G.A. (eds.). *Microbes in Extreme Environments*. Society for General Microbiology, Harcourt Brace Jovanovich Publishers, p. 111-130.

Morita, R.Y. 1988. Bioavailability of energy and its relationship to growth and starvation survival in nature. *Canadian Journal of Microbiology*, Vol. 34, p. 436-441.

Morita, R.Y. 2000. Is H<sub>2</sub> the Universal Energy Source for Long-Term Survival? *Microbial Ecology*, Vol. 38, p. 307-320.

Mulvaney, R., Wolff, E.W. and Oates, K. 1988. Sulphuric acid at grain boundaries in Antarctic ice. *Nature*, Vol. 331, p. 247-249.

Nedwell, D.B. 1989. Benthic microbial activity in an Antarctic coastal sediment at Signy Island, South Orkney Islands. *Estuarine Coastal and Shelf Science*, Vol. 28, p. 507-516.

Nedwell, D.B. 1999. Effect of low temperature on microbial growth: lowered affinity for substrates limits growth at low temperature. *FEMS Microbiology Ecology*, Vol. 30, p. 101-111.

Nedwell, D.B., Walker, T.R., Ellis-Evans, J.C. and Clarke, A. 1993. Measurements of seasonal rates and annual budgets of organic carbon fluxes in an Antarctic coastal environment at Signy Island, South Orkney Islands, suggest



a broad balance between production and decomposition. *Applied and Environmental Microbiology*, Vol. 59, p. 3989-3995.

Newell, S.Y. and Fallon, R.D. 1982. Bacterial Productivity in the Water Column and Sediments of the Georgia (USA) Coastal Zone: Estimates via Direct Counting and Parallel Measurement of Thymidine Incorporation. *Microbial Ecology*, Vol. 8, p. 33-46.

Nienow, P.W., Sharp, M.J., Willis, I.C. 1998. Seasonal changes in the morphology of the subglacial drainage system, Haut Glacier d'Arolla, Switzerland, *Earth Surface Processes and Landforms*, Vol. 23, p. 825-843.

Nienow, P., Sharp, M., Boon, S., Bingham, R. and Heppenstall, K. (Accepted subject to revision). Supraglacial drainage processes on High Arctic glaciers: implications for subglacial hydrology and ice dynamics. *Journal of Geophysical Research*.

Norris, J.R. and Ribbons, D.W. (eds.). 1969. Methods in Microbiology. Volume 1. Academic Press. London and New York.

Norske statens kartverk. 1995. Jostedalsbreen. Målestokk 1:100 000. Best.nr.2229.

Novitsky, J.A. and Morita, R.Y. 1976. Morphological characterization of small cells resulting from nutrient starvation of a psychrophilic marine vibrio. *Applied and Environmental Microbiology*, Vol. 32, p. 617-622.

Novitsky, J.A. and Morita, R.Y. 1977. Survival of a Psychrophilic Marine Vibrio Under Long-Term Nutrient Starvation. *Applied and Environmental Microbiology*, Vol. 33 p. 635-641.

Nuttall A-M, Hagen J.O., Dowdeswell J. 1997. Quiescent-phase changes in velocity and geometry of Finsterwalderbreen, a surge-type glacier in Svalbard. *Annals of Glaciology*., Vol. 24, p. 249-254.



- Oerlemans J. 1992. Climate sensitivity of glaciers in southern Norway: application of an energy-balance model to Nigardsbreen, Hellstugubreen and Alfotbreen. *Journal of Glaciology*, Vol. 38, no. 129, p. 223-232.
- Oerlemans J. 1997. A flowline model for Nigardsbreen, Norway: projection of future glacier length based on dynamic calibration with the historic record. *Annals of Glaciology*., Vol. 24, p. 382-389.
- Oftedahl C. 1980. Geology of Norway. Norges geologiske undersøkelse, NGU Nr.356, Bulletin 54. Contributions tot he 26th International Geological Congress in Paris - July 1980. ISBN 82-00-31392-1. 128 p.
- Oppenheimer, C.H. 1970. Temperature. In: Kinne, O. (ed.). *Microbial Ecology*, Vol. 1, p. 347-361. Wiley, New York.
- Palmisano, A.C. and Garrison, D.L. 1993. Microorganisms in Antarctic Sea Ice. In: Friedmann, E.I. *Antarctic Microbiology*. Wiley-Liss Inc, New York. p. 167-218.
- Parkes, R.J., Gibson, G.R., Mueller-Harvey, I., Buckingham, W.J. & Herbert, R.A. 1989. Determination of the substrates for sulphate-reducing bacteria within marine and estuarine sediments with different rates of sulphate reduction. *Journal of Gen.Microbiology*, Vol. 135, p. 175-187.
- Parkes, R.J. 2000. A case of bacterial immortality? *Nature*, Vol. 407, p. 844-845.
- Patterson, W.S.B. 1994. *The Physics of Glaciers*, 3<sup>rd</sup> edition. Pergamon, Exeter.
- Philips Analytical Customer Support. 1989. PW1800 Automatic Powder Diffractometer System. Operation Manual, 890120 Third Edition. Nederlandse Philips Bedrijven b.v., The Netherlands.
- Postgate J.R. 1984. *The sulfate-reducing bacteria*. Cambridge: Cambridge University Press.



Prapaipong, P., Shock, E.L. and Koretsky, C.M. 1999. Metal-organic complexes in geochemical processes: Temperature dependence of the standard thermodynamic properties of aqueous complexes between metal cations and dicarboxylate ligands. *Geochimica et Cosmochimica Acta*, Vol. 63, p. 2547-2577.

Price, P.B. 2000. A habitat for psychrophiles in deep Antarctic ice. *PNAS National Academy of Science Proceedings*, Vol. 97, No. 3, p. 1247-1251.

Priscu, J.C., Adams, E.E., Lyons, W.B., Voytek, M.A., Mogk, D.W., Brown, R.L., McKay, C.P., Takacs, C.D., Welch, K.A., Wolf, C.F., Kirshtein, J.D. 1999. Geomicrobiology of Subglacial Ice Above Lake Vostok, Antarctica. *Science*, Vol. 286, p. 2141-2144.

Raiswell, R. 1984. Chemical models of solute acquisition in glacial melt waters. *Journal of Glaciology*, Vol. 30, p. 49-57.

Raiswell, R. and Thomas, A.G. 1984. Solute acquisition in glacial melt waters. I. Fjallsjökull (South-East Iceland): Bulk melt water with closed-system characteristics. *Journal of Glaciology*, Vol. 30, p. 35-43.

Reynolds Jr., R.C. 1989. Principles of powder diffraction. *Reviews in Mineralogy Mineralogical Society of America*, Vol. 20. p. 1-17.

Richards, K., Sharp, M., Arnold, N., Gurnell, A., Clark, M., Tranter, M., Nienow, P., Brown, G., Willis, I. and Lawson, W. 1996. An integrated approach to modelling hydrology and water quality in glacierized catchments. *Hydrological Processes*, Vol. 10, p. 479-508.

Rippin, D. 2001. The Hydrology and Dynamics of Polythermal Glaciers: Midre Lovénbreen, Svalbard. PhD thesis submitted to the University of Cambridge, St.John's College. 362 p.



- Rippin, D., Willis, I., Arnold, N., Hodson, A., Moore, J., Kohler, J. and Bjornsson, H. 2003. Changes in geometry and subglacial drainage of Midre Lovénbreen, Svalbard, determined from digital elevation models. *Earth Surface Processes and Landforms*, Vol. 28, p. 273-298.
- Rivkina, E., Gilichinsky, D., Wagener, S., Tiedje, J. and McGrath, J. 1998. Biogeochemical Activity of Anaerobic Micro-organisms From Buried Permafrost Sediments. *Geomicrobiology*, Vol. 15, p. 187-193.
- Rothschild, L.J. and Mancinelli, R.L. 2001. Life in extreme environments. *Nature*, Vol. 409, p. 1092-1101.
- Russell, N.J. 1990. Cold adaptation of microorganisms. *Philosophical Transactions of the Royal Society of London*, Vol. B326, p. 595-611.
- Russell, N.J. 1997. Psychrophilic Bacteria – Molecular Adaptations of Membrane Lipids. *Comparative Biochemistry and Physiology*. Vol. 118A, No. 3, p. 489-493.
- Sagemann, J., Jørgensen, B.B., Greeff, O. 1998. Temperature Dependence and Rates of Sulfate Reduction in Cold Sediments of Svalbard, Arctic Ocean. *Geomicrobiology Journal*, Vol. 15, No.2, p. 85-100.
- Sagemann, J., Bale, S.J., Briggs, D.E.G and Parkes, R.J. 1999. Controls on the formation of authigenic minerals in association with decaying organic matter: An experimental approach. *Geochimica et Cosmochimica Acta*, Vol. 63, No.7/8, p. 1083-1095.
- Sahm, K., Knoblauch, C. and Amann, R. 1999. Phylogenetic Affiliation and Quantification of Psychrophilic Sulfate-Reducing Isolates in Marine Arctic Sediments. *Applied and Environmental Microbiology*, Vol. 65, p. 3976-3981.
- Sattler, B., Puxbaum, H., Psenner, R. 2001. Bacterial growth in supercooled cloud droplets. *Geophysical Research Letters*, Vol. 28, p. 239-242.



Sharp R.P. 1988. *Living Ice - Understanding Glaciers and Glaciation*. Cambridge University Press. ISBN 0-521-33009-2. 225 p.

Sharp, M., Brown, G.H., Tranter, M., Willis, I.C. and Hubbard, B. 1995. Comments on the use of chemically based mixing models in glacier hydrology. *Journal of Glaciology*, Vol. 41, p. 241-246.

Sharp M., Parkes J., Cragg B., Fairchild I.J., Lamb H. and Tranter M. 1999. Widespread bacterial populations at glacier beds and their relationship to rock weathering and carbon cycling. *Geology*, Vol. 27, no.2, p. 107-110.

Shi, T., Reeves, R.H., Gilichinsky, D.A. and Friedmann, E.I. 1997. Characterization of Viable Bacteria from Siberian Permafrost by 16S rDNA Sequencing. *Microbial Ecology*, Vol. 33, p. 169-179.

Sigler, W.V. and Zeyer, J. 2002. Microbial Diversity and Activity along the Forefields of Two Receding Glaciers. *Microbial Ecology*, Vol. 43, p. 397-407.

Skidmore, M.L. and Sharp, M.J. 1999. Drainage system behaviour of a High Arctic polythermal glacier. *Annals of Glaciology*, Vol. 28, p. 209-215.

Skidmore, M.L., Foght, J.M. and Sharp, M.J. 2000a. Microbial Life beneath a High Arctic Glacier. *Applied and Environmental Microbiology*, Vol. 66, No. 8, p. 3214-3220.

Skidmore, M., Foght, J., Sharp, M., Parkes, J. and Tranter, M. 2000b. Subglacial Microbiology and Chemical Weathering. Goldschmidt 2000, September 3<sup>rd</sup>-8<sup>th</sup>, 2000, Oxford, UK, Journal of Conference Abstracts, Vol. 5, p. 932.

Slazóki, I., Somogyi, A., Braun, M. & Tóth, A. 1999. Investigation of Geochemical Composition of Lake Sediments Using ED-XRF and ICP-AES Techniques. *X-Ray Spectrometry*, Vol. 28, p. 399-405.



Souchez, R., Janssens, L., Lemmens, M. & Stauffer, B. 1995. Very low oxygen concentration in basal ice from Summit, Central Greenland. *Geophysical Research Letters*, Vol. 22, No. 15, p. 2001-2004.

SPECTRO Analytical Instruments. 1999. Documentation SPECTRO X-LAB. Manual Version 1/99.

Stookey, L.L. 1970. Ferrozine - A New Spectrophotometric Reagent for Iron. *Analytical Chemistry*, Vol. 42, No. 7, p. 779-781.

Sugden, D.E. and John, B.S. 1976. *Glaciers and Landscape*. Edward Arnold, London, 376 p.

Sullivan, C.W. and Palmisano, A.C. 1984. Sea ice microbial communities: distribution, abundance, and diversity of ice bacteria in McMurdo Sound, Antarctica in 1980. *Applied and Environmental Microbiology*, Vol. 47, p. 788-795.

Thomas, A.G. and Raiswell, R. 1984. Solute acquisition in glacial melt waters. II. Argentière (French Alps): Bulk melt waters with open-system characteristics. *Journal of Glaciology*, Vol. 30, p. 44-48.

Tranter, M., Brown, G., Raiswell, R., Sharp, M. and Gurnell, A. 1993. A conceptual model of solute acquisition by Alpine glacial meltwaters. *Journal of Glaciology*, Vol. 39, p. 573-581.

Tranter, M., Brown, G.H., Hodson, A., Gurnell, A.M., Sharp, M.J. 1994. Variations in nitrate concentration of glacial runoff in Alpine and sub-Polar environments, IAMAP/IAHS Joint International Meeting, 11-23 July 1993, Yokohama, Japan, *International Association of Hydrological Sciences Publications*, Vol. 223, p. 299-311.

Tranter, M., Brown, G.H., Hodson, A., Gurnell, A.M., Sharp, M.J. 1996. Hydrochemistry as an indicator of subglacial drainage system structure: a



comparison of Alpine and Sub-Polar environments. *Hydrological Processes*, Vol. 10, p. 541-556.

Tranter, M., Sharp, M.J., Brown, G.H., Willis, I.C., Hubbard, B.P., Nielsen, M.K., Smart, C.C., Gordon, S., Tulley, M. and Lamb, H.R. 1997. Variability in the chemical composition of *in situ* subglacial meltwaters. *Hydrological Processes*, Vol. 11, p. 59-77.

Tranter, M., Sharp, M.J., Lamb, H.R., Brown, G.H., Hubbard, B.P. and Willis, I.C. 2002. Geochemical weathering at the bed of Haut Glacier d'Arolla, Switzerland – a new model. *Hydrological Processes*, Vol. 16, p. 959-993.

Viollier, E., Inglett, P.W., Hunter, K., Roychoudhury, A.N. and Van Cappellen, P. 2000. The ferrozine method revisited: Fe(II)/Fe(III) determination in natural waters. *Applied Geochemistry*, Vol. 15, p. 785-790.

Vishnivetskaya, T., Kathariou, S., McGrath, J., Gilichinsky, D. and Tiedje, J.M. 2000. Low-temperature recovery strategies for the isolation of bacteria from ancient permafrost sediments. *Extremophiles*, Vol. 4, p. 165-173.

Vishniac, H.S. 1993. The Microbiology of Antarctic Soils. In: Friedmann, E.I. Antarctic Microbiology. Wiley-Liss Inc, New York. p. 297-341.

Vorobyova, E., Minkovsky, N., Mamukelashvili, A., Zvyagintsev, D., Soina, V., Polanskaya, L. and Gilichinsky, D. 2001. Micro-organisms and Biomarkers in Permafrost. In: Paepe, R. and Melnikov, V. (eds.). Permafrost Response on Economic Development, Environmental Security and Natural Resources. Proceedings of the NATO Advanced Research Workshop on Permafrost Response on Economic Development, Environmental Security and Natural Resources, Novosibirsk, Russia, 12-16 November 1998. p. 527-541.

Vreeland, R.H., Rosenzweig, W.D., Powers, D.W. 2000. Isolation of a 250 million-year-old halotolerant bacterium from a primary salt crystal. *Nature*, Vol. 407, p. 897-900.



Wadham J.L. 1997. The Hydrochemistry of a High Arctic Polythermal-based Glacier: Finsterwalderbreen, Svalbard. PhD thesis submitted to the University of Bristol, Department of Geography. 297 p.

Wadham J.L., Hodson A.J., Tranter M. and Dowdeswell J.A. 1997. The rate of chemical weathering beneath a quiescent, surge-type, polythermal based glacier, southern Spitsbergen. *Annals of Glaciology*., Vol. 24, p.27-31.

Wadham, J.L., Hodson, A.J., Tranter, M. and Dowdeswell, J.A. 1998. The hydrochemistry of meltwaters draining a polythermal-based, high Arctic glacier, south Svalbard: I. The ablation season. *Hydrological Processes*, Vol. 12, p. 1825-1849.

Wadham, J.L., Tranter, M. and Dowdeswell, J.A. 2000. Hydrochemistry of meltwaters draining a polythermal-based, high-Arctic glacier, south Svalbard: II. Winter and early Spring. *Hydrological Processes*, Vol. 14, p. 1767-1786.

Wadham J.L., Hodgkins R., Cooper R.J. and Tranter M. 2001. Evidence for seasonal subglacial outburst events at a polythermal glacier, Finsterwalderbreen, Svalbard. *Hydrological Processes*. Vol.15, p. 2259-2280.

Walder, J.S. and Fowler, A. 1994. Channelized subglacial drainage over a deformable bed. *Journal of Glaciology*, Vol. 40, p. 3-15.

Ward, B.B. and Priscu, J.C. 1997. Detection and characterization of denitrifying bacteria from a permanently ice-covered Antarctic Lake. *Hydrobiologia*, Vol. 347, p. 57-68.

Weidick A. 1976. Glaciation and the Quaternary of Greenland. . In: Escher A. and Watt W.S. (eds.). *Geology of Greenland*. The Geological Survey of Greenland. ISBN 87-980404-0-5. p. 431-458.



Weidick A., Bøggild C.E. and Knudsen N.T. 1992. Glacier inventory and atlas of West Greenland. Grønlands Geologiske Undersøgelse, Rapport 158. 194 p.

Welker, J.M., Fahnestock, J.T., Henry, G.H.R., O'dea, K.W. and Piper, R.E. 2002. Microbial Activity Discovered in Previously Ice-entobed Arctic Ecosystems. *EOS, Transactions, American Geophysical Union*, Vol. 83, p. 281-284.

Wellsbury, P. 1992. Uncoupling of bacterial productivity and organic carbon mineralisation in coastal marine, estuarine and freshwater sediments. PhD-thesis submitted to the University of Dundee, Department of Biological Sciences. 161 p.

Wellsbury P., Herbert R.A. and Parkes R.J. 1996. Bacterial activity and production in near surface estuarine and freshwater sediments. *FEMS Microbiology Ecology*, Vol. 19, p. 203-214.

Willerslev, E., Hansen, A.J., Christensen, B., Steffensen, J.P. and Arctander, P. 1999. Diversity of Holocene life forms in fossil glacier ice. *Proceedings of the National Academy of Sciences of the United States of America*, Vol, 96, p. 8017-8021.

Woorward, J., Sharp, M. and Arendt, A. 1997. The influence of superimposed-ice formation on the sensitivity of glacier mass balance to climate change. *Annals of Glaciology*, Vol. 24, p. 186-190.

Ødegård R.S., Hagen J.O. and Hamran S.-E. 1997. Comparison of radio-echo sounding (30 -1000 MHz) and high resolution borehole temperature measurements at Finsterwalderbreen, southern Spitsbergen, Svalbard. *Annals of Glaciology.*, Vol. 24, p. 262-267.







## **APPENDICES**

- 1** Glossary of Glaciology;
- 2** Results of statistical tests with the total numbers of bacteria in meltwaters from Greenland;
- 3** Growth of cultures of sulphate-reducing bacteria from meltwater in the Manitsog glacier in the early (June 1999) and late (August 1999) melt season in the thermal gradient incubator;
- 4** Semilogarithmic graph method used for estimating the doubling times of sulphate reducing bacteria in the thermal gradient experiments;
- 5** Results of statistical tests with the total numbers of bacteria in meltwaters from four outlet glaciers of the Jostedalsbreen ice cap, Norway, in the early melt season and mid-melt season;
- 6** Growth of cultures of sulphate-reducing bacteria from meltwater in the Jostedalsbreen ice cap in the early melt season (Kjenndalsbreen, June 2000) and in the mid-melt season (Bergsetbreen, July 2000) in the thermal gradient incubator;
- 7** Results of statistical tests with the total numbers of bacteria in meltwaters from the Midre Løvenbreen glacier, Svalbard, in April-May 2001 and 2002;
- 8** Growth of cultures of sulphate-reducing bacteria from meltwater in the Midre Løvenbreen glacier before the actual melt season (May 2001) in the thermal gradient incubator;
- 9** Results of statistical tests with the total numbers of bacteria in meltwaters at the beginning of the melt season from Greenland (1999), Norway (2000) and Svalbard (2001 and 2002);
- 10** Results of nonparametric correlation tests between the total numbers of bacteria and suspended sediment concentrations in meltwaters from Greenland (1999), Norway (2000) and Svalbard (2001 and 2002);
- 11** Results of statistical tests (two-way ANOVA with interactions and Tukey's HSD-test) with data from the long-term weathering experiment with proglacial rock debris from Norway and Svalbard, and meltwater from Norway.







## **APPENDIX 1: GLOSSARY OF GLACIOLOGY**

*All the definitions of the terms, if not otherwise mentioned, taken from Sharp R.P. 1988. Living Ice - Understanding Glaciers and Glaciation.*

### **accumulation area**

part of a glacier's surface over which more snow is deposited than is ablated each year

### **cirque glacier**

small glacier lying wholly within a cirque. Cirque is steep-walled, gentle-floored, semicircular topographic hollow created by glacial excavation high in mountainous areas.

### **cold-based glacier**

glacier which is below the pressure melting temperature throughout the ice (synonym: polar glacier)

### **crevasse**

deep, steeply inclined, open fracture created in brittle surficial ice of a flowing glacier undergoing extension

### **ground moraine**

more or less continuous mantle of till with gently undulating surface; deposited principally under an ice sheet or along the edge of a steadily receding glacier.

### **ice cap**

sheet of glacier ice, of less than 50 000 km<sup>2</sup>, capping an upland and spreading out radially

### **ice carapace**

sheet of ice covering upper part of a high, isolated peak.



**ice dome**

a dome-shaped surface feature in the marginal area of the inland ice sheet with its own firn area and almost radial movement (Weidick et al. 1992)

**ice lobe**

tongue-shaped mass of glacier ice projecting from a larger body, usually a sheet, cap or carapace.

**icing**

see naled ice

**(inland) ice sheet**

very large, thick sheet of glacier ice, covering areas greater than 50 000 km<sup>2</sup>, largely submerging the subglacial topography, and flowing generally outward in all directions. According to Weidick et al. (1992), the main feature of the inland ice is a form which, apart from a narrow marginal zone, is independent of the subglacial topography.

**kame terrace**

thread of glaciofluvial material deposited along the margin of a glacier

**marginal moraine**

moraine formed along the margin of an ice sheet, cap, or lobe, not appropriately described as lateral or terminal

**moulin**

roughly cylindrical, near-vertical hole up to 30 m deep in a glacier's surface

**naled ice**

proglacial feature of layers of sheetlike mass of ice in front of a polythermal (or rarely a cold-based) glacier; forms when wintertime subglacial runoff freezes rapidly after reaching sub-zero air temperature at the ice margin (synonyms icing, aufeis) (Wadham 1997)



**outlet glacier**

ice stream or lobe normally flowing rapidly outward from a larger body of ice, usually a sheet or cap

**outwash plain**

broad, gently sloping plain of outwashed glaciofluvial debris

**polythermal-based glacier**

glacier with the areas of both warm-based and cold-based ice, ice thickness dictating the extent of the warm-based component (Wadham 1997). As the glacier grows thicker through accumulation on the surface, ice within the glacier in the deeper layers melts because of the increased pressure.

**pressure melting**

melting of ice where pressure is great enough to lower its melting point below the ambient temperature

**rock flour**

fresh, clay- and silt-sized rock and mineral particles ground by glacial abrasion

**subglacial**

the realm beneath a glacier

**subpolar glacier**

glacier with accumulation areas at melting point, whereas the ice in the tongue is frozen to the ground (Liestøl 1990)

**superimposed ice**

layer(s) of cold ice at the base of snowpack, at the surface of a glacier; prevents percolation of surface meltwater; often formed in the accumulation areas of high Arctic glacier (Ødegård et al. 1997, Wadham 1997)



**superglacial/supraglacial**

on the top surface of a glacier

**surge**

relatively short-lived episode of greatly accelerated flow within a glacier

**temperate glacier**

at the pressure melting temperature of ice throughout (synonym warm-based glacier)

**terminal moraine**

outermost end moraine deposited during a major episode of glacier advance

**valley glacier**

glacier flowing down a valley, the catchment in most cases well defined, and glacier tongue partly or wholly filling a valley. Transitional types to cirque glaciers occur (Weidick et al. 1992)

**valley train**

long, narrow accumulation of outwash material extending downstream from the stabilized front of a valley glacier

**warm-based glacier**

at the pressure melting temperature of ice throughout (synonym: temperate glacier)



**APPENDIX 2. Results of statistical tests with the total numbers of bacteria in meltwaters from the Manitsoq glacier and the Akuliarusiarssuk glacier in Greenland.**

- 1 = subglacial meltwater from the Manitsoq glacier in the early melt season (22 June 1999);**
- 2 = debris poor supraglacial meltwater from the Manitsoq glacier in the early melt season (22 June 1999);**
- 3 = debris rich supraglacial meltwater from the Manitsoq glacier in the early melt season (22 June 1999);**
- 4 = subglacial meltwater from the Manitsoq glacier in the mid-melt season (24 July 1999);**
- 5 = debris poor supraglacial meltwater from the Manitsoq glacier in the mid-melt season (24 July 1999);**
- 6 = subglacial meltwater from the Manitsoq glacier in the late melt season (15 August 1999);**
- 7 = subglacial meltwater from the Akuliarusiarssuk glacier in the mid-melt season (27 July 1999);**
- 8 = supraglacial meltwater from the Akuliarusiarssuk glacier in the mid-melt season (27 July 1999).**



Descriptives

AODC

	N	Mean	Std. Deviation	Std. Error	95% Confidence Interval for Mean		Minimum	Maximum
					Lower Bound	Upper Bound		
1,00	3	37433,33	14819,21784	8555,879	620,3554	74246,3112	20418,00	47512,00
2,00	3	4450,3333	599,88110	346,34151	2960,1461	5940,5206	3927,00	5105,00
3,00	3	16594,67	4530,85360	2615,890	5339,4024	27849,9310	11387,00	19633,00
4,00	3	10645,33	2515,04917	1452,064	4397,6048	16893,0618	8377,00	13350,00
5,00	3	4188,3333	599,77190	346,27847	2698,4173	5678,2493	3534,00	4712,00
6,00	3	8507,3333	5612,61662	3240,446	-5435,1793	22449,8459	2356,00	13350,00
7,00	3	8376,6667	2266,67716	1308,667	2745,9285	14007,4049	7068,00	10994,00
8,00	3	2617,6667	817,53430	472,00365	586,7989	4648,5345	1963,00	3534,00
Total	24	11601,71	11921,30095	2433,425	6567,7844	16635,6322	1963,00	47512,00

Test of Homogeneity of Variances

AODC

Levene Statistic	df1	df2	Sig.
8,473	7	16	,000

ANOVA

AODC

	Sum of Squares	df	Mean Square	F	Sig.
Between Groups	2,70E+09	7	385674207,7	10,845	,000
Within Groups	5,69E+08	16	35561320,08		
Total	3,27E+09	23			

AODC

Tukey HSD<sup>a</sup>

GROUPCOD	N	Subset for alpha = .05	
		1	2
8,00	3	2617,6667	37433,33
5,00	3	4188,3333	
2,00	3	4450,3333	
7,00	3	8376,6667	
6,00	3	8507,3333	
4,00	3	10645,33	
3,00	3	16594,67	
1,00	3		
Sig.		,145	1,000

Means for groups in homogeneous subsets are displayed.

a. Uses Harmonic Mean Sample Size = 3,000.



Multiple Comparisons

Dependent Variable: AODC  
Tukey HSD

(I) GROUPCOD	(J) GROUPCOD	Mean Difference (I-J)	Std. Error	Sig.	95% Confidence Interval	
					Lower Bound	Upper Bound
1,00	2,00	32983,0000*	4869,040	,000	16125,6511	49840,3489
	3,00	20838,6667*	4869,040	,010	3981,3178	37696,0155
	4,00	26788,0000*	4869,040	,001	9930,6511	43645,3489
	5,00	33245,0000*	4869,040	,000	16387,6511	50102,3489
	6,00	28926,0000*	4869,040	,000	12068,6511	45783,3489
	7,00	29056,6667*	4869,040	,000	12199,3178	45914,0155
	8,00	34815,6667*	4869,040	,000	17958,3178	51673,0155
2,00	1,00	-32983,000*	4869,040	,000	-49840,3489	-16125,6511
	3,00	-12144,3333	4869,040	,265	-29001,6822	4713,0155
	4,00	-6195,0000	4869,040	,896	-23052,3489	10662,3489
	5,00	262,0000	4869,040	1,000	-16595,3489	17119,3489
	6,00	-4057,0000	4869,040	,988	-20914,3489	12800,3489
	7,00	-3926,3333	4869,040	,990	-20783,6822	12931,0155
	8,00	1832,6667	4869,040	1,000	-15024,6822	18690,0155
3,00	1,00	-20838,667*	4869,040	,010	-37696,0155	-3981,3178
	2,00	12144,3333	4869,040	,265	-4713,0155	29001,6822
	4,00	5949,3333	4869,040	,914	-10908,0155	22806,6822
	5,00	12406,3333	4869,040	,244	-4451,0155	29263,6822
	6,00	8087,3333	4869,040	,710	-8770,0155	24944,6822
	7,00	8218,0000	4869,040	,695	-8639,3489	25075,3489
	8,00	13977,0000	4869,040	,145	-2880,3489	30834,3489
4,00	1,00	-26788,000*	4869,040	,001	-43645,3489	-9930,6511
	2,00	6195,0000	4869,040	,896	-10662,3489	23052,3489
	3,00	-5949,3333	4869,040	,914	-22806,6822	10908,0155
	5,00	6457,0000	4869,040	,876	-10400,3489	23314,3489
	6,00	2138,0000	4869,040	1,000	-14719,3489	18995,3489
	7,00	2268,6667	4869,040	1,000	-14588,6822	19126,0155
	8,00	8027,6667	4869,040	,717	-8829,6822	24885,0155
5,00	1,00	-33245,000*	4869,040	,000	-50102,3489	-16387,6511
	2,00	-262,0000	4869,040	1,000	-17119,3489	16595,3489
	3,00	-12406,333	4869,040	,244	-29263,6822	4451,0155
	4,00	-6457,0000	4869,040	,876	-23314,3489	10400,3489
	6,00	-4319,0000	4869,040	,983	-21176,3489	12538,3489
	7,00	-4188,3333	4869,040	,986	-21045,6822	12669,0155
	8,00	1570,6667	4869,040	1,000	-15286,6822	18428,0155
6,00	1,00	-28926,000*	4869,040	,000	-45783,3489	-12068,6511
	2,00	4057,0000	4869,040	,988	-12800,3489	20914,3489
	3,00	-8087,3333	4869,040	,710	-24944,6822	8770,0155
	4,00	-2138,0000	4869,040	1,000	-18995,3489	14719,3489
	5,00	4319,0000	4869,040	,983	-12538,3489	21176,3489
	7,00	130,6667	4869,040	1,000	-16726,6822	16988,0155
	8,00	5889,6667	4869,040	,918	-10967,6822	22747,0155
7,00	1,00	-29056,667*	4869,040	,000	-45914,0155	-12199,3178
	2,00	3926,3333	4869,040	,990	-12931,0155	20783,6822
	3,00	-8218,0000	4869,040	,695	-25075,3489	8639,3489
	4,00	-2268,6667	4869,040	1,000	-19126,0155	14588,6822
	5,00	4188,3333	4869,040	,986	-12669,0155	21045,6822
	6,00	-130,6667	4869,040	1,000	-16988,0155	16726,6822
	8,00	5759,0000	4869,040	,926	-11098,3489	22616,3489
8,00	1,00	-34815,667*	4869,040	,000	-51673,0155	-17958,3178
	2,00	-1832,6667	4869,040	1,000	-18690,0155	15024,6822
	3,00	-13977,000	4869,040	,145	-30834,3489	2880,3489
	4,00	-8027,6667	4869,040	,717	-24885,0155	8829,6822
	5,00	-1570,6667	4869,040	1,000	-18428,0155	15286,6822
	6,00	-5889,6667	4869,040	,918	-22747,0155	10967,6822
	7,00	-5759,0000	4869,040	,926	-22616,3489	11098,3489

\*. The mean difference is significant at the .05 level.



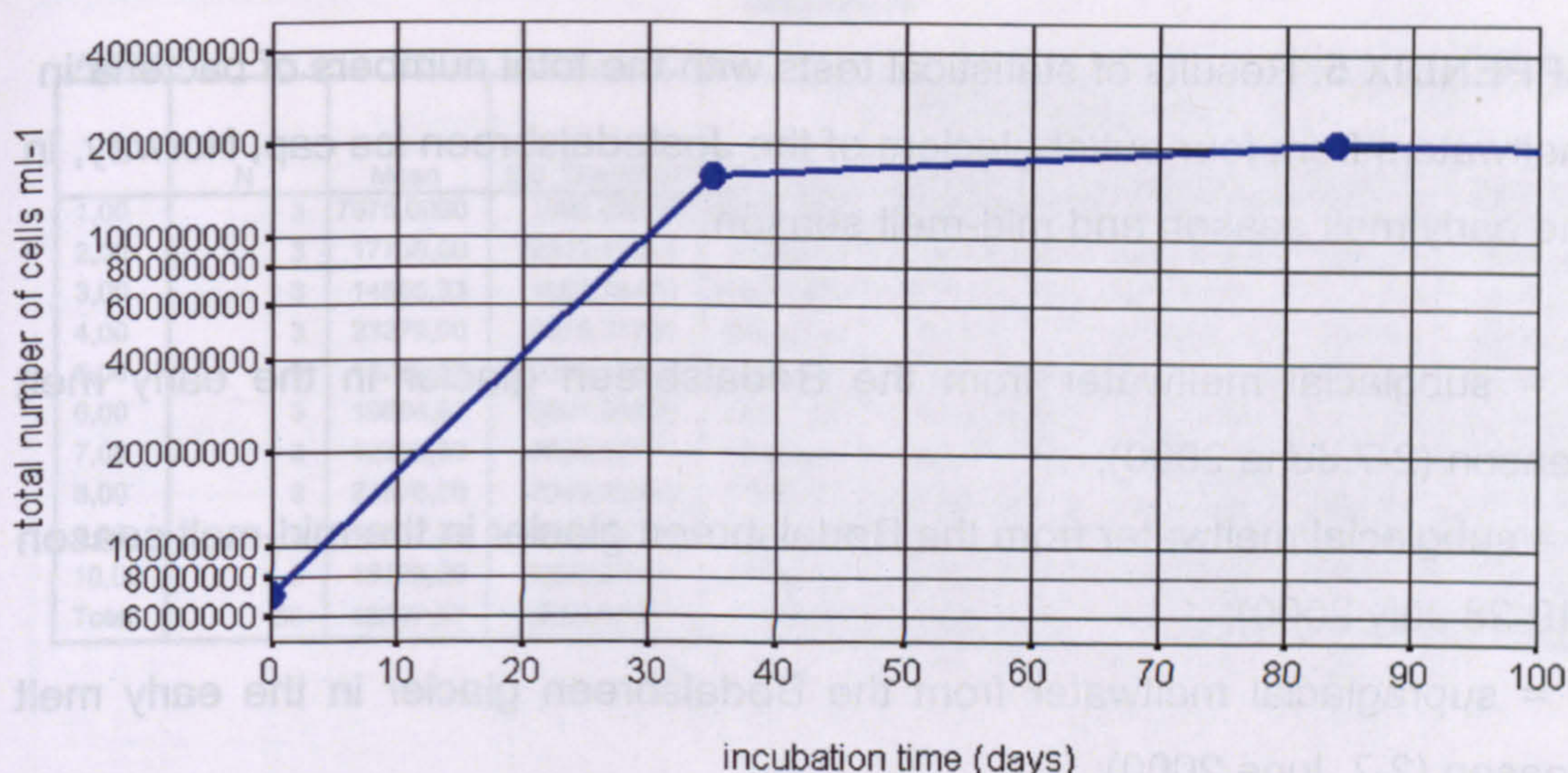
**APPENDIX 3.** Growth of cultures of sulphate-reducing bacteria from meltwater in the Manitsoq Glacier in the early (June 1999) and late (August 1999) melt season in the thermal gradient incubator. 0=no sign of growth; 1=culture turning cloudy, dark grey precipitates, growth; 2=black precipitates, strong growth; p=medium turned pink due to oxygen contamination during inoculation at the beginning of the experiment or sampling after 5 weeks.

Incubation time						
early	1 w	2 w	3 w	4 w	5 w	7 w
0.0 °C	0	0	0	0	0	1
+2.1 °C	0	0	1	1	2	2
+4.2 °C	0	1	2	2	2	2
+6.3 °C	0	1	2	2	2	2
+8.4 °C	0	2	2	2	2	2
+10.5 °C	0	2	2	2	2	2
+12.6 °C	0	2	2	2	2	2
+14.7 °C	0	2	2	2	2	2
+16.8 °C	2	2	2	2	2	2
+18.9 °C	1	2	2	2	2	2
+21.0 °C	0	2	2	2	2	2
+23.1 °C	0	2	2	2	2	2
+25.2 °C	0	0	2	2	2	2
+27.3 °C	0	0	2	2	2	2
+29.4 °C	0	0	2	2	2	2
+31.5 °C	0	0	0	0	0	0
+33.6 °C	0	0	0	0	0	0
+35.7 °C	0	0	0	0	0	0
+37.8 °C	0	0	0	0	0	0 (p)
+39.9 °C	0	0	0	0	0	0
+42.0 °C	0	0	0 (p)	0 (p)	0 (p)	0 (p)

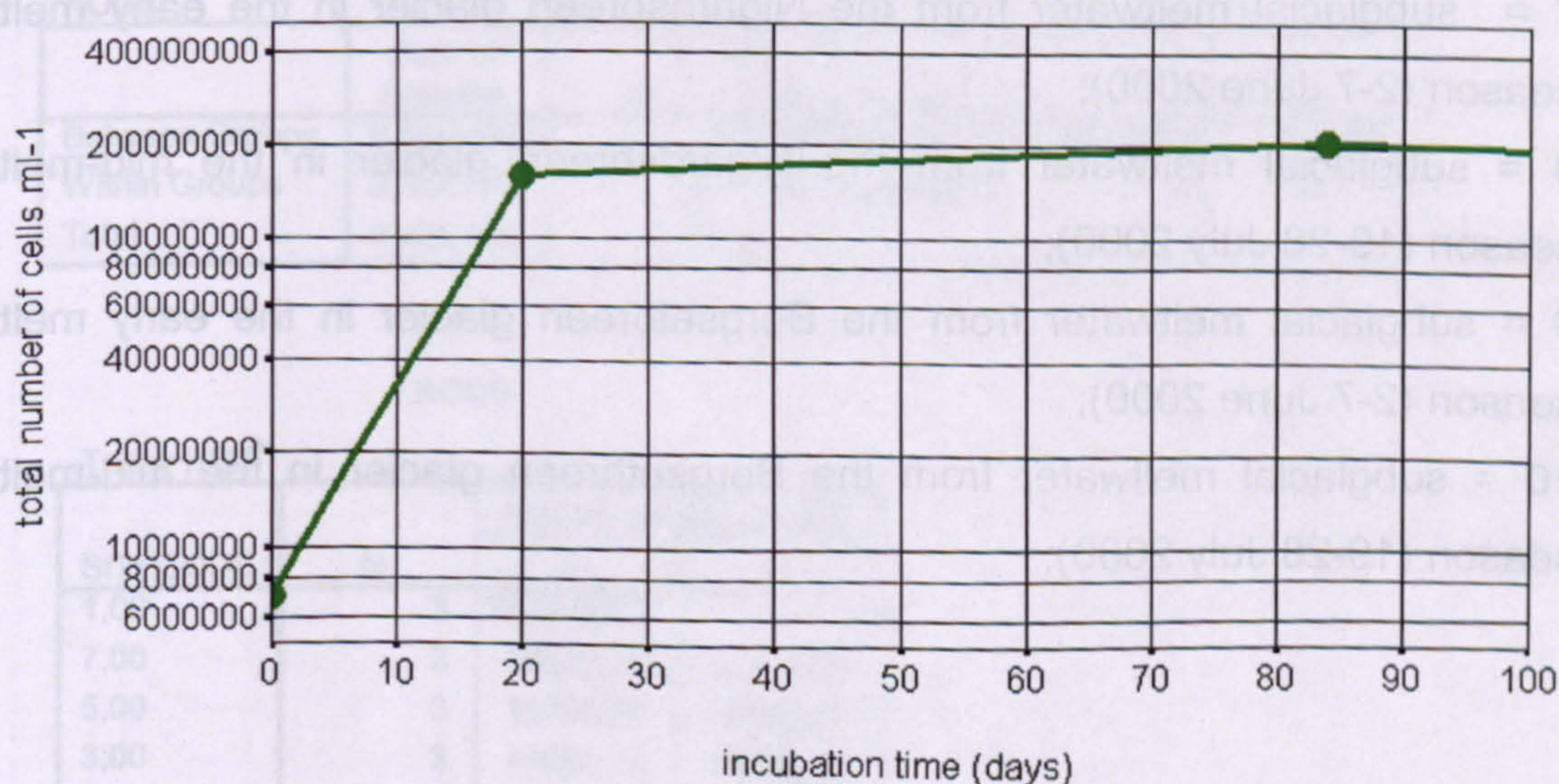
late	1 w	2 w	3 w	4 w	5 w	7 w
0.0 °C	0	0	0	0	0	0
+2.1 °C	0	0	0	0	1	2
+4.2 °C	0	0	2	2	2	2
+6.3 °C	0	2	2	2	2	2
+8.4 °C	0	2	2	2	2	2
+10.5 °C	1	2	2	2	2	2
+12.6 °C	1	2	2	2	2	2
+14.7 °C	2	2	2	2	2	2
+16.8 °C	2	2	2	2	2	2
+18.9 °C	2	2	2	2	2	2
+21.0 °C	2	2	2	2	2	2
+23.1 °C	2	2	2	2	2	2
+25.2 °C	0	0	0	0	0	0
+27.3 °C	0	1	2	2	2	2
+29.4 °C	0	0	0	0	0	0
+31.5 °C	0	0	0	0	0	0
+33.6 °C	0	0	0	0	0	0
+35.7 °C	0	0	0	0	0	0 (p)
+37.8 °C	0	0	0	0	0	0
+39.9 °C	0	0	0	0 (p)	0 (p)	0 (p)
+42.0 °C	0	0	0	0	0	0



**APPENDIX 4.** Semilogarithmic graph method used for estimating the doubling times of sulphate reducing bacteria in the thermal gradient experiments.



**Example 1.** Doubling time of the total number of cells in culture of sulphate-reducing bacteria from the Manitsog Glacier in the early melt season during exponential growth, at incubation temperature of +4 °C. Increase in total number of bacteria from  $1.0 \times 10^7$  to  $2.0 \times 10^7$  cells ml<sup>-1</sup> from t=4 days to t= 11.5 days → doubling time 7.5 days.



**Example 2.** Estimated minimum doubling time of the total number of cells in culture of sulphate-reducing bacteria from the Manitsog Glacier in the early melt season during exponential growth, at incubation temperature of +4 °C. Based on the assumption that stationary phase was reached after 20 days, instead of > 35 days. Increase in total number of bacteria from  $1.0 \times 10^7$  to  $2.0 \times 10^7$  cells ml<sup>-1</sup> from t=3 days to t= 7 days → doubling time 4 days.



**APPENDIX 5.** Results of statistical tests with the total numbers of bacteria in meltwaters from four outlet glaciers of the Jostedalsbreen ice cap, Norway, in the early melt season and mid-melt season.

1 = subglacial meltwater from the Bødalsbreen glacier in the early melt season (2-7 June 2000);

2 = subglacial meltwater from the Bødalsbreen glacier in the mid-melt season (19-28 July 2000);

3 = supraglacial meltwater from the Bødalsbreen glacier in the early melt season (2-7 June 2000);

4 = supraglacial meltwater from the Bødalsbreen glacier in the mid-melt season (19-28 July 2000);

5 = subglacial meltwater from the Kjenndalsbreen glacier in the early melt season (2-7 June 2000);

6 = subglacial meltwater from the Kjenndalsbreen glacier in the mid-melt season (19-28 July 2000);

7 = subglacial meltwater from the Nigardsbreen glacier in the early melt season (2-7 June 2000);

8 = subglacial meltwater from the Nigardsbreen glacier in the mid-melt season (19-28 July 2000);

9 = subglacial meltwater from the Bergsetbreen glacier in the early melt season (2-7 June 2000);

10 = subglacial meltwater from the Bergsetbreen glacier in the mid-melt season (19-28 July 2000);



Descriptives

AODC								
	N	Mean	Std. Deviation	Std. Error	95% Confidence Interval for Mean		Minimum	Maximum
					Lower Bound	Upper Bound		
1,00	3	7575,0000	1698,02856	980,35725	3356,8632	11793,1368	5644,00	8835,00
2,00	3	17735,00	2342,13514	1352,232	11916,8138	23553,1862	16099,00	20418,00
3,00	3	14855,33	1586,76474	916,11905	10913,5912	18797,0755	13154,00	18295,00
4,00	3	23279,00	5015,37765	2895,630	10820,1112	35737,8888	18651,00	28608,00
5,00	3	14790,00	6212,45491	3586,763	-642,5935	30222,5935	9424,00	21596,00
6,00	3	19894,67	5891,09806	3401,227	5260,3678	34528,9655	13939,00	25719,00
7,00	3	12303,33	3859,10771	2228,057	2716,7783	21889,8883	7853,00	14725,00
8,00	3	22578,00	2040,35585	1178,000	17509,4751	27646,5249	21400,00	24934,00
9,00	3	15837,33	5417,15740	3127,597	2380,3683	29294,2983	11780,00	21989,00
10,00	3	18128,00	3322,27497	1918,116	9875,0114	26380,9886	15314,00	21793,00
Total	30	16697,57	5699,92061	1040,658	14569,1813	18825,9520	5644,00	28608,00

Test of Homogeneity of Variances

AODC			
Levene Statistic	df1	df2	Sig.
1,367	9	20	,267

ANOVA

AODC					
	Sum of Squares	df	Mean Square	F	Sig.
Between Groups	6,05E+08	9	67180587,19	3,980	,005
Within Groups	3,38E+08	20	16877923,53		
Total	9,42E+08	29			

AODC

Tukey HSD <sup>a</sup>			
SITECODE	N	Subset for alpha = .05	
		1	2
1,00	3	7575,0000	
7,00	3	12303,33	12303,33
5,00	3	14790,00	14790,00
3,00	3	14855,33	14855,33
9,00	3	15837,33	15837,33
2,00	3	17735,00	17735,00
10,00	3	18128,00	18128,00
6,00	3		19894,67
8,00	3		22578,00
4,00	3		23279,00
Sig.		,108	,085

Means for groups in homogeneous subsets are displayed.

a. Uses Harmonic Mean Sample Size = 3,000.



Multiple Comparisons

Dependent Variable: AODC  
Tukey HSD

(I) SITECODE	(J) SITECODE	Mean Difference (I-J)	Std. Error	Sig.	95% Confidence Interval	
					Lower Bound	Upper Bound
1,00	2,00	-10160,000	3354,392	,136	-22038,2654	1718,2654
	3,00	-7280,3333	3354,392	,506	-19158,5987	4697,9321
	4,00	-15704,000*	3354,392	,004	-27582,2654	-3825,7346
	5,00	-7215,0000	3354,392	,516	-19093,2654	4663,2654
	6,00	-12319,667*	3354,392	,038	-24197,9321	-441,4013
	7,00	-4728,3333	3354,392	,910	-18606,5987	7149,9321
	8,00	-15003,000*	3354,392	,007	-26881,2654	-3124,7346
	9,00	-8262,3333	3354,392	,343	-20140,5987	3615,9321
	10,00	-10553,000	3354,392	,106	-22431,2654	1325,2654
2,00	1,00	10160,0000	3354,392	,136	-1718,2654	22038,2654
	3,00	2879,6667	3354,392	,996	-8998,5987	14757,9321
	4,00	-5544,0000	3354,392	,808	-17422,2654	6334,2654
	5,00	2945,0000	3354,392	,996	-8933,2654	14823,2654
	6,00	-2159,6667	3354,392	1,000	-14037,9321	9718,5987
	7,00	5431,6667	3354,392	,824	-8446,5987	17309,9321
	8,00	-4843,0000	3354,392	,696	-16721,2654	7035,2654
	9,00	1897,6667	3354,392	1,000	-9980,5987	13775,9321
	10,00	-393,0000	3354,392	1,000	-12271,2654	11485,2654
3,00	1,00	7280,3333	3354,392	,506	-4597,9321	19158,5987
	2,00	-2879,6667	3354,392	,996	-14757,9321	8998,5987
	4,00	-8423,6667	3354,392	,319	-20301,9321	3454,5987
	5,00	85,3333	3354,392	1,000	-11812,9321	11943,5987
	6,00	-5039,3333	3354,392	,876	-16917,5987	6838,9321
	7,00	2552,0000	3354,392	,988	-9328,2654	14430,2654
	8,00	-7722,6667	3354,392	,428	-19600,9321	4155,5987
	9,00	-982,0000	3354,392	1,000	-12860,2654	10896,2654
	10,00	-3272,6667	3354,392	,991	-15150,9321	8605,5987
4,00	1,00	15704,0000*	3354,392	,004	3825,7346	27582,2654
	2,00	5544,0000	3354,392	,808	-8334,2654	17422,2654
	3,00	8423,6667	3354,392	,319	-3454,5987	20301,9321
	5,00	8489,0000	3354,392	,310	-3389,2654	20367,2654
	6,00	3384,3333	3354,392	,988	-8493,9321	15262,5987
	7,00	10975,6667	3354,392	,085	-902,5987	22853,9321
	8,00	701,0000	3354,392	1,000	-11177,2654	12579,2654
	9,00	7441,6667	3354,392	,476	-4436,5987	19319,9321
	10,00	5151,0000	3354,392	,862	-6727,2654	17029,2654
5,00	1,00	7215,0000	3354,392	,516	-4663,2654	19093,2654
	2,00	-2945,0000	3354,392	,996	-14823,2654	8933,2654
	3,00	-65,3333	3354,392	1,000	-11943,5987	11812,9321
	4,00	-8489,0000	3354,392	,310	-20367,2654	3389,2654
	6,00	-5104,6667	3354,392	,868	-16982,9321	6773,5987
	7,00	2486,6667	3354,392	,999	-9391,5987	14364,9321
	8,00	-7788,0000	3354,392	,417	-19666,2654	4090,2654
	9,00	-1047,3333	3354,392	1,000	-12925,5987	10830,9321
	10,00	-3338,0000	3354,392	,989	-15216,2654	8540,2654
6,00	1,00	12319,6667*	3354,392	,038	441,4013	24197,9321
	2,00	2159,6667	3354,392	1,000	-9718,5987	14037,9321
	3,00	5039,3333	3354,392	,876	-6838,9321	16917,5987
	4,00	-3384,3333	3354,392	,988	-15262,5987	8493,9321
	5,00	5104,6667	3354,392	,868	-6773,5987	16982,9321
	7,00	7591,3333	3354,392	,450	-4266,9321	19469,5987
	8,00	-2683,3333	3354,392	,996	-14561,5987	9194,9321
	9,00	4057,3333	3354,392	,962	-7820,9321	15935,5987
	10,00	1766,6667	3354,392	1,000	-10111,5987	13644,9321
7,00	1,00	4728,3333	3354,392	,910	-7149,9321	16606,5987
	2,00	-5431,6667	3354,392	,824	-17309,9321	6446,5987
	3,00	-2552,0000	3354,392	,996	-14430,2654	9328,2654
	4,00	-10975,667	3354,392	,085	-22853,9321	902,5987
	5,00	-2486,6667	3354,392	,999	-14364,9321	9391,5987
	6,00	-7591,3333	3354,392	,450	-19469,5987	4266,9321
	8,00	-10274,667	3354,392	,127	-22152,9321	1603,5987
	9,00	-3534,0000	3354,392	,984	-15412,2654	8344,2654
	10,00	-5824,6667	3354,392	,764	-17702,9321	6053,5987
8,00	1,00	15003,0000*	3354,392	,007	3124,7346	26881,2654
	2,00	4843,0000	3354,392	,896	-7035,2654	16721,2654
	3,00	7722,6667	3354,392	,428	-4155,5987	19600,9321
	4,00	-701,0000	3354,392	1,000	-12579,2654	11177,2654
	5,00	7788,0000	3354,392	,417	-4090,2654	19666,2654
	6,00	2683,3333	3354,392	,996	-9194,9321	14561,5987
	7,00	10274,6667	3354,392	,127	-1603,5987	22162,9321
	9,00	6740,6667	3354,392	,603	-6137,5987	18618,9321
	10,00	4450,0000	3354,392	,935	-7426,2654	16328,2654
9,00	1,00	8262,3333	3354,392	,343	-3615,9321	20140,5987
	2,00	-1897,6667	3354,392	1,000	-13775,9321	9980,5987
	3,00	982,0000	3354,392	1,000	-10896,2654	12860,2654
	4,00	-7441,6667	3354,392	,476	-19319,9321	4436,5987
	5,00	1047,3333	3354,392	1,000	-10830,9321	12925,5987
	6,00	-4057,3333	3354,392	,962	-15935,5987	7820,9321
	7,00	3534,0000	3354,392	,984	-8344,2654	15412,2654
	8,00	-6740,6667	3354,392	,603	-18618,9321	5137,5987
	10,00	-2290,6667	3354,392	,999	-14168,9321	9587,5987
10,00	1,00	10553,0000	3354,392	,106	-1325,2654	22431,2654
	2,00	393,0000	3354,392	1,000	-11485,2654	12271,2654
	3,00	3272,6667	3354,392	,991	-8605,5987	15150,9321
	4,00	-5151,0000	3354,392	,862	-17029,2654	6727,2654
	5,00	3338,0000	3354,392	,989	-8540,2654	15216,2654
	6,00	-1766,6667	3354,392	1,000	-13644,9321	10111,5987
	7,00	5824,6667	3354,392	,764	-6053,5987	17702,9321
	8,00	-4450,0000	3354,392	,935	-16328,2654	7426,2654
	9,00	2290,6667	3354,392	,999	-6587,5987	14168,9321

\*. The mean difference is significant at the .05 level.



**APPENDIX 6.** Growth of cultures of sulphate-reducing bacteria from meltwater in the Jostedalsbreen ice cap in the early melt season (Kjenndalsbreen, June 2000) and in the mid-melt season (Bergsetbreen, July 2000) in the thermal gradient incubator. 0=no sign of growth; 1=culture turning cloudy, dark grey precipitates, growth; 2=black precipitates, strong growth; p=medium turned pink due to oxygen contamination during inoculation at the beginning of the experiment or sampling after 5 weeks.

Incubation time					
Kjenndals- breen	1 w	2 w	3 w	4 w	5 w
- 0.6 °C	0	0	0	0	0
+1.3 °C	0	0	0	0	0
+3.1 °C	0	0	0	0	0
+5.0 °C	0	0	1	1	2
+6.9 °C	0	1	2	2	2
+9.2 °C	0	1	2	2	2
+11.5 °C	1	2	2	2	2
+13.8 °C	1	2	2	2	2
+16.1 °C	2	2	2	2	2
+18.3 °C	2	2	2	2	2
+20.5 °C	2	2	2	2	2
+22.7 °C	2	2	2	2	2
+24.9 °C	2	2	2	2	2
+27.2 °C	2	2	2	2	2
+29.3 °C	2	2	2	2	2
+31.4 °C	0	0	0	0	0
+33.5 °C	0	0	0	0	0
+35.7 °C	0	0	0	0	0
+37.8 °C	0	0	0	0	0
+39.9 °C	0	0	0	0	0

Bergset- breen	1 w	2 w	3 w	4 w	5 w
- 0.6 °C	0	0	0	0	0
+1.3 °C	0	0	0	0	0
+3.1 °C	0	0	0	0	1
+5.0 °C	0	0	1	1	1
+6.9 °C	0	0	1	1	2
+9.2 °C	0	1	2	2	2
+11.5 °C	1	2	2	2	2
+13.8 °C	2	2	2	2	2
+16.1 °C	2	2	2	2	2
+18.3 °C	0	0	0	0	0
+20.5 °C	2	2	2	2	2 (p)
+22.7 °C	2	2	2	2	2
+24.9 °C	2	2	2	2	2
+27.2 °C	2	2	2	2	2
+29.3 °C	2	2	2	2	2
+31.4 °C	2	2	2	2	2
+33.5 °C	2	2	2	2	2
+35.7 °C	0	0	0	0	0
+37.8 °C	0	0	0	0	0
+39.9 °C	0	0 (p)	0 (p)	0 (p)	0 (p)



**APPENDIX 7. Results of statistical tests with the total numbers of bacteria in meltwaters from the Midre Løvenbreen glacier, Svalbard, in April-May 2001 and 2002.**

1 = subglacial meltwater from the Midre Løvenbreen glacier before the actual melt season in May 2001, outflow 1, replicate A

2 = subglacial meltwater from the Midre Løvenbreen glacier before the actual melt season in May 2001, outflow 1, replicate B

3 = subglacial meltwater from the Midre Løvenbreen glacier before the actual melt season in April 2002, outflow 1

4 = subglacial meltwater from the Midre Løvenbreen glacier before the actual melt season in April 2002, outflow 2

5 = subglacial meltwater from the Midre Løvenbreen glacier before the actual melt season in April 2002, outflow 3

6 = subglacial meltwater from the Midre Løvenbreen glacier before the actual melt season in April 2002, outflow 4



Descriptives

AODC

	N	Mean	Std. Deviation	Std. Error	95% Confidence Interval for Mean		Minimum	Maximum
					Lower Bound	Upper Bound		
1,00	3	10863,33	2162,96217	1248,787	5490,2374	16236,4292	8638,00	12958,00
2,00	3	15706,00	1178,00000	680,11862	12779,6858	18632,3142	14528,00	16884,00
3,00	3	36517,00	4964,28615	2866,132	24185,0296	48848,9704	31805,00	41700,00
4,00	3	37459,67	4947,50001	2856,440	25169,3953	49749,9380	32512,00	42407,00
5,00	3	21910,33	6742,30601	3892,672	5161,5167	38659,1500	15549,00	28978,00
6,00	3	44056,33	11854,73097	6844,332	14607,5491	73505,1176	30392,00	51595,00
Total	18	27752,11	13690,75104	3226,941	20943,8608	34560,3614	8638,00	51595,00

Test of Homogeneity of Variances

AODC

Levene Statistic	df1	df2	Sig.
3,512	5	12	,035

ANOVA

AODC

	Sum of Squares	df	Mean Square	F	Sig.
Between Groups	2,70E+09	5	540812129,8	13,454	,000
Within Groups	4,82E+08	12	40196886,56		
Total	3,19E+09	17			

AODC

Tukey HSD<sup>a</sup>

SAMPCODE	N	Subset for alpha = .05		
		1	2	3
1,00	3	10863,33		
2,00	3	15706,00		
5,00	3	21910,33	21910,33	
3,00	3		36517,00	36517,00
4,00	3		37459,67	37459,67
6,00	3			44056,33
Sig.		,333	,090	,695

Means for groups in homogeneous subsets are displayed.

a. Uses Harmonic Mean Sample Size = 3,000.



Multiple Comparisons

Dependent Variable: AODC

Tukey HSD

(I) SAMPCODE	(J) SAMPCODE	Mean Difference (I-J)	Std. Error	Sig.	95% Confidence Interval	
					Lower Bound	Upper Bound
1,00	2,00	-4842,6667	5176,671	,929	-22230,6955	12545,3621
	3,00	-25653,667*	5176,671	,003	-43041,6955	-8265,6379
	4,00	-26596,333*	5176,671	,003	-43984,3621	-9208,3045
	5,00	-11047,000	5176,671	,333	-28435,0288	6341,0288
	6,00	-33193,000*	5176,671	,000	-50581,0288	-15804,9712
2,00	1,00	4842,6667	5176,671	,929	-12545,3621	22230,6955
	3,00	-20811,000*	5176,671	,016	-38199,0288	-3422,9712
	4,00	-21753,667*	5176,671	,012	-39141,6955	-4365,6379
	5,00	-6204,3333	5176,671	,830	-23592,3621	11183,6955
	6,00	-28350,333*	5176,671	,002	-45738,3621	-10962,3045
3,00	1,00	25653,6667*	5176,671	,003	8265,6379	43041,6955
	2,00	20811,0000*	5176,671	,016	3422,9712	38199,0288
	4,00	-942,6667	5176,671	1,000	-18330,6955	16445,3621
	5,00	14606,6667	5176,671	,121	-2781,3621	31994,6955
	6,00	-7539,3333	5176,671	,695	-24927,3621	9848,6955
4,00	1,00	26596,3333*	5176,671	,003	9208,3045	43984,3621
	2,00	21753,6667*	5176,671	,012	4365,6379	39141,6955
	3,00	942,6667	5176,671	1,000	-16445,3621	18330,6955
	5,00	15549,3333	5176,671	,090	-1838,6955	32937,3621
	6,00	-6596,6667	5176,671	,793	-23984,6955	10791,3621
5,00	1,00	11047,0000	5176,671	,333	-6341,0288	28435,0288
	2,00	6204,3333	5176,671	,830	-11183,6955	23592,3621
	3,00	-14606,667	5176,671	,121	-31994,6955	2781,3621
	4,00	-15549,333	5176,671	,090	-32937,3621	1838,6955
	6,00	-22146,000*	5176,671	,011	-39534,0288	-4757,9712
6,00	1,00	33193,0000*	5176,671	,000	15804,9712	50581,0288
	2,00	28350,3333*	5176,671	,002	10962,3045	45738,3621
	3,00	7539,3333	5176,671	,695	-9848,6955	24927,3621
	4,00	6596,6667	5176,671	,793	-10791,3621	23984,6955
	5,00	22146,0000*	5176,671	,011	4757,9712	39534,0288

\*. The mean difference is significant at the .05 level.



**APPENDIX 8.** Growth of cultures of sulphate-reducing bacteria from meltwater in the Midre Løvenbreen glacier before the actual melt season (May 2001) in the thermal gradient incubator. 0=no sign of growth; 1=culture turning cloudy, dark grey precipitates, growth; 2=black precipitates, strong growth; p=medium turned pink due to oxygen contamination during inoculation at the beginning of the experiment or sampling after 2.5 weeks, 5 weeks or 12 weeks.

SV 1A	Incubation time						
	1 w	2 w	3 w	5 w	7 w	9 w	12 w
- 0.6 °C	0	1	1 (p)	0 (p)	0 (p)	0 (p)	0 (p)
+1.3 °C	0	1	1	1	1	2	2
+3.1 °C	1	2	2	2	2	2	2
+5.0 °C	1	2	2	2	2	2	2
+6.9 °C	1	2	2	2	2	2	2
+9.2 °C	1	2	2	2	2	2	2
+11.5 °C	0 (p)	0 (p)	0 (p)	0 (p)	0 (p)	0 (p)	0 (p)
+13.8 °C	2	2	2	2 (p)	1 (p)	1 (p)	1 (p)
+16.1 °C	0 (p)	0 (p)	0 (p)	0 (p)	0 (p)	0 (p)	0 (p)
+18.3 °C	0 (p)	0 (p)	0 (p)	0 (p)	0 (p)	0 (p)	0 (p)
+20.5 °C	1	2	2	2	2	2	2
+22.7 °C	1	2	2	2	2	2	2
+24.9 °C	0	0	0 (p)	0 (p)	0 (p)	0 (p)	0 (p)
+27.2 °C	0	0	0 (p)	0 (p)	0 (p)	0 (p)	0 (p)
+29.3 °C	1	1	1	1	1	1	1 (p)
+31.4 °C	0 (p)	0 (p)	0 (p)	0 (p)	0 (p)	0 (p)	0 (p)
+33.5 °C	0 (p)	0 (p)	0 (p)	0 (p)	0 (p)	0 (p)	0 (p)
+35.7 °C	0	0	0 (p)	1	1	1	2
+37.8 °C	0	0	0	0	1	1	2
+39.9 °C	0	0	0 (p)	0	1	1	2

SV 1B	Incubation time						
	1 w	2 w	3 w	5 w	7 w	9 w	12 w
- 0.6 °C	0	1	1	1	1 (p)	0 (p)	0 (p)
+1.3 °C	0	0	0	0	1	1	2
+3.1 °C	1	1	1	2	2	2	0 (p)
+5.0 °C	1	2	2	2	2	2	2
+6.9 °C	1	2	2	2	2	2	2
+9.2 °C	0 (p)	0 (p)	0 (p)	0 (p)	2	2 (p)	2 (p)
+11.5 °C	2	2	2	2	2	2	2
+13.8 °C	2	2	2	2	2	2	2
+16.1 °C	2	2	2	2 (p)	0 (p)	0 (p)	0 (p)
+18.3 °C	1 (p)	2	2	2	2	2	2
+20.5 °C	1 (p)	2	2	2	1 (p)	0 (p)	0 (p)
+22.7 °C	1	2	1 (p)	0 (p)	0 (p)	0 (p)	0 (p)
+24.9 °C	0	0	0 (p)	0 (p)	0 (p)	0 (p)	0 (p)
+27.2 °C	0	0	0 (p)	0 (p)	0 (p)	0 (p)	0 (p)
+29.3 °C	0	0	0	0	0	1	1
+31.4 °C	0	0	0	0	0	1	1
+33.5 °C	0	0	0 (p)	0 (p)	0 (p)	0 (p)	0 (p)
+35.7 °C	0	0	0	0	1	1	2
+37.8 °C	0	0	0	0	1	1	2 (p)
+39.9 °C	0	0	0	0	1	1	2



**APPENDIX 9.** Results of statistical tests with the total numbers of bacteria in meltwaters at the beginning of the melt season from Greenland (1999), Norway (2000) and Svalbard (2001 and 2002).

- 1 = subglacial meltwater from the Manitsoq glacier, Greenland in 1999;
- 2 = subglacial meltwater from the Jostedalsbreen ice cap, Norway in 2000;
- 3 = subglacial meltwater from the Midre Løvenbreen glacier, Svalbard in 2001;
- 4 = subglacial meltwater from the Midre Løvenbreen glacier, Svalbard in 2002.

**Descriptives**

AODC

	N	Mean	Std. Deviation	Std. Error	95% Confidence Interval for Mean		Minimum	Maximum
					Lower Bound	Upper Bound		
1,00	3	27014,00	10419,00000	6015,412	1131,7692	52896,2308	16595,00	37433,00
2,00	3	14310,00	1815,23800	1048,028	9800,6988	18819,3012	12303,00	15837,00
3,00	3	16159,67	5537,45540	3197,051	2403,8649	29915,4685	10863,00	21910,00
4,00	3	39344,33	4107,57402	2371,509	29140,5538	49548,1129	36517,00	44056,00
Total	12	24207,00	11747,17502	3391,117	16743,2011	31670,7989	10863,00	44056,00

**Test of Homogeneity of Variances**

AODC

Levene Statistic	df1	df2	Sig.
1,381	3	8	,317

**ANOVA**

AODC

	Sum of Squares	df	Mean Square	F	Sig.
Between Groups	1,20E+09	3	399728292,2	10,032	,004
Within Groups	3,19E+08	8	39846556,67		
Total	1,52E+09	11			



AODC

Tukey HSD<sup>a</sup>

SITECODE	N	Subset for alpha = .05	
		1	2
2,00	3	14310,00	27014,00 39344,33
3,00	3	16159,67	
1,00	3	27014,00	
4,00	3		
Sig.		,141	,156

Means for groups in homogeneous subsets are displayed.  
a. Uses Harmonic Mean Sample Size = 3,000.

Multiple Comparisons

Dependent Variable: AODC  
Tukey HSD

		Mean Difference (I-J)	Std. Error	Sig.	95% Confidence Interval	
(I) SITECODE	(J) SITECODE				Lower Bound	Upper Bound
1,00	2,00	12704,0000	5154,064	,141	-3801,1258	29209,1258
	3,00	10854,3333	5154,064	,230	-5650,7924	27359,4591
	4,00	-12330,333	5154,064	,156	-28835,4591	4174,7924
2,00	1,00	-12704,000	5154,064	,141	-29209,1258	3801,1258
	3,00	-1849,6667	5154,064	,983	-18354,7924	14655,4591
	4,00	-25034,333*	5154,064	,006	-41539,4591	-8529,2076
3,00	1,00	-10854,333	5154,064	,230	-27359,4591	5650,7924
	2,00	1849,6667	5154,064	,983	-14655,4591	18354,7924
	4,00	-23184,667*	5154,064	,009	-39689,7924	-6679,5409
4,00	1,00	12330,3333	5154,064	,156	-4174,7924	28835,4591
	2,00	25034,3333*	5154,064	,006	8529,2076	41539,4591
	3,00	23184,6667*	5154,064	,009	6679,5409	39689,7924

\*. The mean difference is significant at the .05 level.



**APPENDIX 10.** Results of nonparametric correlation tests between the total numbers of bacteria and suspended sediment concentrations in meltwaters from Greenland (1999), Norway (2000) and Svalbard (2001 and 2002).

Greenland

Correlations			AODC	SSC
Spearman's rho	AODC	Correlation Coefficient	1,000	,329
		Sig. (2-tailed)	.	,117
		N	24	24
	SSC	Correlation Coefficient	,329	1,000
		Sig. (2-tailed)	,117	.
		N	24	24

Norway

Correlations			AODC	SSC
Spearman's rho	AODC	Correlation Coefficient	1,000	,218
		Sig. (2-tailed)	.	,247
		N	30	30
	SSC	Correlation Coefficient	,218	1,000
		Sig. (2-tailed)	,247	.
		N	30	30

Svalbard

Correlations			AODC	SSC
Spearman's rho	AODC	Correlation Coefficient	1,000	,430
		Sig. (2-tailed)	.	,075
		N	18	18
	SSC	Correlation Coefficient	,430	1,000
		Sig. (2-tailed)	,075	.
		N	18	18



**APPENDIX 11.** Results of statistical tests (two-way ANOVA with interactions and Tukey's HSD-test) with data from the long-term weathering experiment with proglacial rock debris from Norway and Svalbard, and meltwater from Norway.

Statistical tests were run with the data gathered at incubation time of 203 days. This incubation time of 6-7 months represented time equivalent to winter period inbetween melt seasons in glaciated areas, and simulated slow reactions occurring in subglacial isolated cavities.

### Subgroups in the experiment

- 1 = biotic test in aerobic conditions at +1.6 - +2.6 °C;
- 2 = biotic test in aerobic conditions at +0.2 - +0.5 °C;
- 3 = biotic test in aerobic conditions at -1.2 - -1.0 °C;
- 4 = abiotic control in aerobic conditions at +1.6 - +2.6 °C;
- 5 = abiotic control in aerobic conditions at +0.2 - +0.5 °C;
- 6 = abiotic control in aerobic conditions at -1.2 - -1.0 °C;
- 7 = biotic test in anaerobic conditions at +1.6 - +2.6 °C;
- 8 = biotic test in anaerobic conditions at +0.2 - +0.5 °C;
- 9 = biotic test in anaerobic conditions at -1.2 - -1.0 °C;
- 10 = abiotic control in anaerobic conditions at +1.6 - +2.6 °C;
- 11 = abiotic control in anaerobic conditions at +0.2 - +0.5 °C;
- 12 = abiotic control in anaerobic conditions at -1.2 - -1.0 °C;

### Fixed factors

BACCON = viable micro-organisms present (in biotic tests) or not (in abiotic controls)

TEMPERAT = incubation temperature

AERANAER = aerobic conditions or anaerobic conditions

### Dependent variables

pH, dissolved oxygen,  $\text{NO}_3^-$ ,  $\text{Mg}^{2+}$ ,  $\text{Ca}^{2+}$ ,  $\text{K}^+$ ,  $\text{Na}^+$ ,  $\text{SO}_4^{2-}$ ,  $\text{Fe}^{2+}$ .



Bødalsbreen meltwater incubated with rock flour from Bødalsbreen, Norway  
in aerobic and anaerobic conditions at a range of temperatures

Tests of Between-Subjects Effects

Dependent Variable: PH

Source	Type III Sum of Squares	df	Mean Square	F	Sig.	Partial Eta Squared	Noncent. Parameter	Observed Power <sup>a</sup>
Corrected Model	,584 <sup>b</sup>	9	,065	3,253	,009	,530	29,280	,927
Intercept	2005,547	1	2005,547	100508,2	,000	1,000	100508,215	1,000
BACCON * TEMPERAT	,123	2	,061	3,078	,063	,191	6,157	,543
BACCON * AERANAER	,000	1	,000	,014	,907	,001	,014	,051
TEMPERAT * AERANAER	,006	2	,003	,153	,859	,012	,306	,071
BACCON	,240	1	,240	12,033	,002	,316	12,033	,916
TEMPERAT	,176	2	,088	4,416	,022	,254	8,832	,709
AERANAER	,039	1	,039	1,938	,176	,069	1,938	,268
Error	,519	26	,020					
Total	2006,650	36						
Corrected Total	1,103	35						

- a. Computed using alpha = ,05  
b. R Squared = ,530 (Adjusted R Squared = ,367)

Tests of Between-Subjects Effects

Dependent Variable: DOMMOLL

Source	Type III Sum of Squares	df	Mean Square	F	Sig.	Partial Eta Squared	Noncent. Parameter	Observed Power <sup>a</sup>
Corrected Model	,293 <sup>b</sup>	9	,033	42,898	,000	,937	386,078	1,000
Intercept	1,756	1	1,756	2316,853	,000	,989	2316,853	1,000
BACCON * TEMPERAT	,037	2	,019	24,650	,000	,655	49,300	1,000
BACCON * AERANAER	,057	1	,057	75,397	,000	,744	75,397	1,000
TEMPERAT * AERANAER	,003	2	,001	1,777	,189	,120	3,554	,337
BACCON	,066	1	,066	86,711	,000	,769	86,711	1,000
TEMPERAT	,020	2	,010	13,150	,000	,503	26,299	,994
AERANAER	,110	1	,110	144,817	,000	,848	144,817	1,000
Error	,020	26	,001					
Total	2,068	36						
Corrected Total	,312	35						

- a. Computed using alpha = ,05  
b. R Squared = ,937 (Adjusted R Squared = ,915)

Tests of Between-Subjects Effects

Dependent Variable: NITRATE

Source	Type III Sum of Squares	df	Mean Square	F	Sig.	Partial Eta Squared	Noncent. Parameter	Observed Power <sup>a</sup>
Corrected Model	5433,912 <sup>b</sup>	9	603,768	28,490	,000	,908	258,410	1,000
Intercept	31616,882	1	31616,882	1491,907	,000	,983	1491,907	1,000
BACCON * TEMPERAT	539,328	2	269,664	12,725	,000	,495	25,449	,993
BACCON * AERANAER	91,048	1	91,048	4,296	,048	,142	4,296	,514
TEMPERAT * AERANAER	59,125	2	29,563	1,395	,266	,097	2,790	,272
BACCON	4177,321	1	4177,321	197,115	,000	,883	197,115	1,000
TEMPERAT	557,080	2	278,540	13,143	,000	,503	26,287	,994
AERANAER	10,008	1	10,008	,472	,498	,018	,472	,102
Error	550,999	26	21,192					
Total	37601,793	36						
Corrected Total	5984,911	35						

- a. Computed using alpha = ,05  
b. R Squared = ,908 (Adjusted R Squared = ,876)



Tests of Between-Subjects Effects

Dependent Variable: MAGNESIU

Source	Type III Sum of Squares	df	Mean Square	F	Sig.	Partial Eta Squared	Noncent. Parameter	Observed Power <sup>a</sup>
Corrected Model	281281,758 <sup>b</sup>	9	31253,528	136,108	,000	,979	1224,957	1,000
Intercept	425673,995	1	425673,995	1853,773	,000	,986	1853,773	1,000
BACCON * TEMPERAT	58398,130	2	29198,065	127,155	,000	,907	254,310	1,000
BACCON * AERANAER	1,528	1	1,528	,007	,936	,000	,007	,051
TEMPERAT * AERANAER	921,925	2	460,963	2,007	,155	,134	4,015	,378
BACCON	127835,972	1	127835,972	556,714	,000	,955	556,714	1,000
TEMPERAT	94124,205	2	47062,103	204,951	,000	,940	409,903	1,000
AERANAER	1,996	1	1,996	,009	,928	,000	,009	,051
Error	5970,269	26	229,626					
Total	712926,021	36						
Corrected Total	287252,026	35						

- a. Computed using alpha = ,05  
b. R Squared = ,979 (Adjusted R Squared = ,972)

Tests of Between-Subjects Effects

Dependent Variable: CALCIUM

Source	Type III Sum of Squares	df	Mean Square	F	Sig.	Partial Eta Squared	Noncent. Parameter	Observed Power <sup>a</sup>
Corrected Model	927667,181 <sup>b</sup>	9	103074,131	156,980	,000	,982	1412,820	1,000
Intercept	2324694,945	1	2324694,945	3540,468	,000	,993	3540,468	1,000
BACCON * TEMPERAT	188858,395	2	94429,197	143,814	,000	,917	287,628	1,000
BACCON * AERANAER	306,928	1	306,928	,467	,500	,018	,467	,101
TEMPERAT * AERANAER	2305,029	2	1152,515	1,755	,193	,119	3,511	,334
BACCON	418734,527	1	418734,527	637,725	,000	,961	637,725	1,000
TEMPERAT	317412,466	2	158706,233	241,707	,000	,949	483,413	1,000
AERANAER	49,835	1	49,835	,076	,785	,003	,076	,058
Error	17071,775	26	656,607					
Total	3269433,901	36						
Corrected Total	944738,956	35						

- a. Computed using alpha = ,05  
b. R Squared = ,982 (Adjusted R Squared = ,976)

Tests of Between-Subjects Effects

Dependent Variable: POTASSIU

Source	Type III Sum of Squares	df	Mean Square	F	Sig.	Partial Eta Squared	Noncent. Parameter	Observed Power <sup>a</sup>
Corrected Model	311049,992 <sup>b</sup>	9	34561,110	186,900	,000	,985	1682,101	1,000
Intercept	2690329,685	1	2690329,685	14548,810	,000	,998	14548,810	1,000
BACCON * TEMPERAT	51549,323	2	25774,661	139,385	,000	,915	278,769	1,000
BACCON * AERANAER	591,535	1	591,535	3,199	,085	,110	3,199	,406
TEMPERAT * AERANAER	301,351	2	150,675	,815	,454	,059	1,630	,174
BACCON	95679,574	1	95679,574	517,418	,000	,952	517,418	1,000
TEMPERAT	162522,712	2	81261,356	439,447	,000	,971	878,893	1,000
AERANAER	405,498	1	405,498	2,193	,151	,078	2,193	,297
Error	4807,855	26	184,918					
Total	3006187,533	36						
Corrected Total	315857,847	35						

- a. Computed using alpha = ,05  
b. R Squared = ,985 (Adjusted R Squared = ,980)



Tests of Between-Subjects Effects

Dependent Variable: SODIUM

Source	Type III Sum of Squares	df	Mean Square	F	Sig.	Partial Eta Squared	Noncent. Parameter	Observed Power <sup>a</sup>
Corrected Model	903218,311 <sup>b</sup>	9	100357,590	67,760	,000	,959	609,837	1,000
Intercept	20304308,9	1	20304308,91	13709,106	,000	,998	13709,106	1,000
BACCON * TEMPERAT	81506,650	2	40753,325	27,516	,000	,679	55,032	1,000
BACCON * AERANAER	27865,074	1	27865,074	18,814	,000	,420	18,814	,987
TEMPERAT * AERANAER	2672,991	2	1336,496	,902	,418	,065	1,805	,189
BACCON	187852,882	1	187852,882	126,835	,000	,830	126,835	1,000
TEMPERAT	559046,641	2	279523,321	188,729	,000	,936	377,458	1,000
AERANAER	44274,072	1	44274,072	29,893	,000	,535	29,893	1,000
Error	38508,130	26	1481,082					
Total	21246035,4	36						
Corrected Total	941726,441	35						

- a. Computed using alpha = ,05  
b. R Squared = ,959 (Adjusted R Squared = ,945)

Tests of Between-Subjects Effects

Dependent Variable: SULPHATE

Source	Type III Sum of Squares	df	Mean Square	F	Sig.	Partial Eta Squared	Noncent. Parameter	Observed Power <sup>a</sup>
Corrected Model	99683,739 <sup>b</sup>	9	11075,971	9,304	,000	,763	83,735	1,000
Intercept	2382296,142	1	2382296,142	2001,149	,000	,987	2001,149	1,000
BACCON * TEMPERAT	21219,965	2	10609,983	8,912	,001	,407	17,825	,955
BACCON * AERANAER	2289,986	1	2289,986	1,924	,177	,069	1,924	,267
TEMPERAT * AERANAER	17102,694	2	8551,347	7,183	,003	,356	14,366	,903
BACCON	15471,504	1	15471,504	12,996	,001	,333	12,996	,934
TEMPERAT	43128,690	2	21564,345	18,114	,000	,582	36,228	1,000
AERANAER	470,900	1	470,900	,396	,535	,015	,396	,093
Error	30952,070	26	1190,464					
Total	2512931,952	36						
Corrected Total	130635,809	35						

- a. Computed using alpha = ,05  
b. R Squared = ,763 (Adjusted R Squared = ,681)

Tests of Between-Subjects Effects

Dependent Variable: FERROUS

Source	Type III Sum of Squares	df	Mean Square	F	Sig.	Partial Eta Squared	Noncent. Parameter	Observed Power <sup>a</sup>
Corrected Model	570107,873 <sup>b</sup>	9	63345,319	110,923	,000	,975	998,303	1,000
Intercept	1214656,371	1	1214656,371	2126,956	,000	,988	2126,956	1,000
BACCON * TEMPERAT	190582,418	2	95291,209	166,862	,000	,928	333,724	1,000
BACCON * AERANAER	635,855	1	635,855	1,113	,301	,041	1,113	,174
TEMPERAT * AERANAER	46705,436	2	23352,718	40,892	,000	,759	81,785	1,000
BACCON	144602,865	1	144602,865	253,211	,000	,907	253,211	1,000
TEMPERAT	175045,698	2	87522,849	153,259	,000	,922	306,518	1,000
AERANAER	12535,601	1	12535,601	21,951	,000	,458	21,951	,995
Error	14848,008	26	571,077					
Total	1799612,253	36						
Corrected Total	584955,881	35						

- a. Computed using alpha = ,05  
b. R Squared = ,975 (Adjusted R Squared = ,966)



NITRATE

Tukey HSD<sup>a</sup>

GROUPCOD	N	Subset for alpha = .05			
		1	2	3	4
1,00	3	12,3757			
2,00	3	13,0502			
7,00	3	13,8792			
8,00	3	15,6113	15,6113		
3,00	3		27,9745	27,9745	
9,00	3			30,2883	
4,00	3			35,2288	35,2288
12,00	3			36,3550	36,3550
10,00	3			38,8583	38,8583
11,00	3			39,6557	39,6557
6,00	3				44,1125
5,00	3				48,2333
Sig.		,999	,074	,108	,051

Means for groups in homogeneous subsets are displayed.

a. Uses Harmonic Mean Sample Size = 3,000.

SULPHATE

Tukey HSD<sup>a</sup>

GROUPCOD	N	Subset for alpha = .05			
		1	2	3	4
3,00	3	187,6672			
6,00	3	213,3492	213,3492		
9,00	3	227,8142	227,8142	227,8142	
12,00	3	228,4375	228,4375	228,4375	
5,00	3	240,2779	240,2779	240,2779	
4,00	3	242,8383	242,8383	242,8383	
11,00	3	243,6814	243,6814	243,6814	
10,00	3	250,5000	250,5000	250,5000	
2,00	3	257,0188	257,0188	257,0188	
7,00	3		278,9585	278,9585	
8,00	3			292,3770	
1,00	3				424,0177
Sig.		,069	,101	,112	1,000

Means for groups in homogeneous subsets are displayed.

a. Uses Harmonic Mean Sample Size = 3,000.



Bødalsbreen meltwater incubated with rock flour from Finsterwalderbreen,  
Svalbard in aerobic and anaerobic conditions at a range of temperatures

Tests of Between-Subjects Effects

Dependent Variable: PH

Source	Type III Sum of Squares	df	Mean Square	F	Sig.	Partial Eta Squared	Noncent. Parameter	Observed Power <sup>a</sup>
Corrected Model	1,090 <sup>b</sup>	9	,121	12,111	,000	,807	108,997	1,000
Intercept	1998,388	1	1998,388	199924,2	,000	1,000	99924,239	1,000
BACCON * TEMPERAT	,030	2	,015	1,511	,240	,104	3,021	,292
BACCON * AERANAER	,043	1	,043	4,273	,049	,141	4,273	,512
TEMPERAT * AERANA	,002	2	,001	,123	,884	,009	,247	,067
BACCON	,002	1	,002	,160	,692	,006	,160	,067
TEMPERAT	,792	2	,396	39,598	,000	,753	79,196	1,000
AERANAER	,221	1	,221	22,099	,000	,459	22,099	,995
Error	,260	26	,010					
Total	1999,737	36						
Corrected Total	1,349	35						

- a. Computed using alpha = ,05  
b. R Squared = ,807 (Adjusted R Squared = ,741)

Tests of Between-Subjects Effects

Dependent Variable: DOMMOLL

Source	Type III Sum of Squares	df	Mean Square	F	Sig.	Partial Eta Squared	Noncent. Parameter	Observed Power <sup>a</sup>
Corrected Model	,197 <sup>b</sup>	9	,022	15,844	,000	,846	142,596	1,000
Intercept	,354	1	,354	256,104	,000	,908	256,104	1,000
BACCON * TEMPERAT	,004	2	,002	1,276	,296	,089	2,551	,252
BACCON * AERANAER	,060	1	,060	43,392	,000	,625	43,392	1,000
TEMPERAT * AERANAER	,002	2	,001	,757	,479	,055	1,513	,164
BACCON	4,016E-05	1	4,016E-05	,029	,866	,001	,029	,053
TEMPERAT	,125	2	,063	45,193	,000	,777	90,387	1,000
AERANAER	,007	1	,007	4,723	,039	,154	4,723	,553
Error	,036	26	,001					
Total	,588	36						
Corrected Total	,233	35						

- a. Computed using alpha = ,05  
b. R Squared = ,846 (Adjusted R Squared = ,792)

Tests of Between-Subjects Effects

Dependent Variable: NITRATE

Source	Type III Sum of Squares	df	Mean Square	F	Sig.	Partial Eta Squared	Noncent. Parameter	Observed Power <sup>a</sup>
Corrected Model	8438,312 <sup>b</sup>	9	937,590	29,665	,000	,911	266,987	1,000
Intercept	19013,896	1	19013,896	601,597	,000	,959	601,597	1,000
BACCON * TEMPERAT	485,697	2	242,848	7,684	,002	,371	15,367	,921
BACCON * AERANAER	32,467	1	32,467	1,027	,320	,038	1,027	,164
TEMPERAT * AERANAER	74,011	2	37,006	1,171	,326	,083	2,342	,234
BACCON	7322,000	1	7322,000	231,667	,000	,899	231,667	1,000
TEMPERAT	518,532	2	259,266	8,203	,002	,387	16,406	,938
AERANAER	5,606	1	5,606	,177	,677	,007	,177	,069
Error	821,749	26	31,606					
Total	28273,956	36						
Corrected Total	9260,061	35						

- a. Computed using alpha = ,05  
b. R Squared = ,911 (Adjusted R Squared = ,881)



Tests of Between-Subjects Effects

Dependent Variable: MAGNESIU

Source	Type III Sum of Squares	df	Mean Square	F	Sig.	Partial Eta Squared	Noncent. Parameter	Observed Power <sup>a</sup>
Corrected Model	17780152,0 <sup>b</sup>	9	1975572,444	15,133	,000	,840	136,197	1,000
Intercept	2120654614	1	2120654614	16244,302	,000	,998	16244,302	1,000
BACCON * TEMPERAT	504947,057	2	252473,528	1,934	,165	,130	3,868	,384
BACCON * AERANAER	43240,083	1	43240,083	,331	,570	,013	,331	,086
TEMPERAT * AERANAER	538858,602	2	269429,301	2,064	,147	,137	4,128	,386
BACCON	1669059,440	1	1669059,440	12,785	,001	,330	12,785	,931
TEMPERAT	14203357,3	2	7101678,637	54,399	,000	,807	108,798	1,000
AERANAER	820689,537	1	820689,537	6,287	,019	,195	6,287	,675
Error	3394237,625	26	130547,601					
Total	2141829003	36						
Corrected Total	21174389,6	35						

- a. Computed using alpha = ,05
- b. R Squared = ,840 (Adjusted R Squared = ,784)

Tests of Between-Subjects Effects

Dependent Variable: CALCIUM

Source	Type III Sum of Squares	df	Mean Square	F	Sig.	Partial Eta Squared	Noncent. Parameter	Observed Power <sup>a</sup>
Corrected Model	55187283,0 <sup>b</sup>	9	6131920,338	4,788	,001	,624	43,095	,990
Intercept	1,547E+10	1	1,547E+10	12080,303	,000	,998	12080,303	1,000
BACCON * TEMPERAT	24016103,3	2	12008051,64	9,377	,001	,419	18,754	,963
BACCON * AERANAER	4131649,084	1	4131649,084	3,226	,084	,110	3,226	,409
TEMPERAT * AERANAER	655966,020	2	327983,010	,256	,776	,019	,512	,086
BACCON	4342705,200	1	4342705,200	3,391	,077	,115	3,391	,426
TEMPERAT	21809099,9	2	10904549,93	8,515	,001	,396	17,031	,946
AERANAER	231759,600	1	231759,600	,181	,674	,007	,181	,069
Error	33295197,7	26	1280584,527					
Total	1,556E+10	36						
Corrected Total	88482480,7	35						

- a. Computed using alpha = ,05
- b. R Squared = ,624 (Adjusted R Squared = ,493)

Tests of Between-Subjects Effects

Dependent Variable: POTASSIU

Source	Type III Sum of Squares	df	Mean Square	F	Sig.	Partial Eta Squared	Noncent. Parameter	Observed Power <sup>a</sup>
Corrected Model	46939,586 <sup>b</sup>	9	5215,510	8,460	,000	,745	76,142	1,000
Intercept	9517664,206	1	9517664,206	15438,849	,000	,998	15438,849	1,000
BACCON * TEMPERAT	9356,842	2	4678,421	7,589	,003	,369	15,178	,916
BACCON * AERANAER	2,840	1	2,840	,005	,946	,000	,005	,050
TEMPERAT * AERANAER	2539,128	2	1269,564	2,059	,148	,137	4,119	,365
BACCON	23748,860	1	23748,860	38,524	,000	,597	38,524	1,000
TEMPERAT	7794,857	2	3897,428	6,322	,006	,327	12,644	,860
AERANAER	3497,061	1	3497,061	5,673	,025	,179	5,673	,631
Error	16028,349	26	616,475					
Total	9580632,141	36						
Corrected Total	62967,935	35						

- a. Computed using alpha = ,05
- b. R Squared = ,745 (Adjusted R Squared = ,657)



Tests of Between-Subjects Effects

Dependent Variable: SODIUM

Source	Type III Sum of Squares	df	Mean Square	F	Sig.	Partial Eta Squared	Noncent. Parameter	Observed Power <sup>a</sup>
Corrected Model	83921,656 <sup>b</sup>	9	9324,628	11,312	,000	,797	101,806	1,000
Intercept	9904824,094	1	9904824,094	12015,631	,000	,998	12015,631	1,000
BACCON * TEMPERAT	2082,012	2	1041,006	1,263	,300	,089	2,526	,250
BACCON * AERANAER	10229,458	1	10229,458	12,409	,002	,323	12,409	,924
TEMPERAT * AERANAER	1030,669	2	515,334	,625	,543	,046	1,250	,143
BACCON	2031,790	1	2031,790	2,465	,129	,087	2,465	,327
TEMPERAT	26230,363	2	13115,181	15,910	,000	,550	31,820	,999
AERANAER	42317,365	1	42317,365	51,336	,000	,664	51,336	1,000
Error	21432,535	26	824,328					
Total	10010178,3	36						
Corrected Total	105354,191	35						

- a. Computed using alpha = ,05  
b. R Squared = ,797 (Adjusted R Squared = ,726)

Tests of Between-Subjects Effects

Dependent Variable: SULPHATE

Source	Type III Sum of Squares	df	Mean Square	F	Sig.	Partial Eta Squared	Noncent. Parameter	Observed Power <sup>a</sup>
Corrected Model	48079792,4 <sup>b</sup>	9	5342199,158	4,824	,001	,615	41,617	,988
Intercept	2,542E+10	1	2,542E+10	21999,491	,000	,999	21999,491	1,000
BACCON * TEMPERAT	19583081,3	2	9791540,630	8,475	,001	,395	16,951	,945
BACCON * AERANAER	367497,404	1	367497,404	3,780	,063	,127	3,780	,465
TEMPERAT * AERANAER	979147,404	2	489573,702	1,722	,198	,117	3,444	,328
BACCON	480166,245	1	480166,245	7,340	,012	,220	7,340	,742
TEMPERAT	10049347,8	2	5024673,885	4,349	,023	,251	8,699	,702
AERANAER	620552,338	1	620552,338	1,403	,247	,051	1,403	,207
Error	30037660,0	26	1155294,616					
Total	2,549E+10	36						
Corrected Total	78117452,4	35						

- a. Computed using alpha = ,05  
b. R Squared = ,615 (Adjusted R Squared = ,482)

NITRATE

Tukey HSD<sup>a</sup>

GROUPCOD	N	Subset for alpha = .05			
		1	2	3	4
9,00	3	7,0585			
1,00	3	7,1201			
8,00	3	7,3360			
2,00	3	8,4158			
7,00	3	10,1014	10,1014		
3,00	3	12,2904	12,2904		
5,00	3		24,5128	24,5128	
6,00	3			34,1559	34,1559
11,00	3			34,9551	34,9551
12,00	3			35,1002	35,1002
10,00	3				45,7073
4,00	3				49,0283
Sig.		,985	,099	,438	,080

Means for groups in homogeneous subsets are displayed.

- a. Uses Harmonic Mean Sample Size = 3,000.

